frontiers | Research Topics

Oral neutrophils - the good, the bad, and the ugly

Edited by
Ljubomir Vitkov, Martin Herrmann and Jasmin Knopf

Published in
Frontiers in Immunology

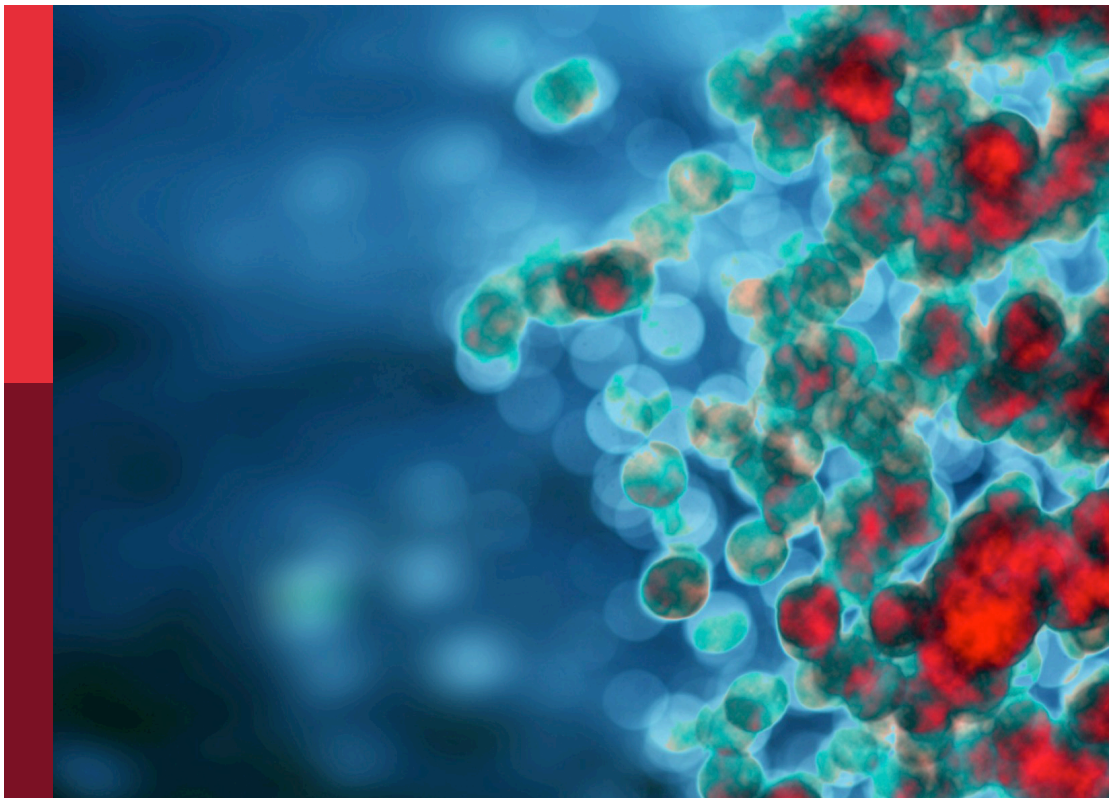

ISSN 1664-8714
ISBN 978-2-8325-2644-6
DOI 10.3389/978-2-8325-2644-6

About Frontiers

Frontiers is more than just an open access publisher of scholarly articles: it is a pioneering approach to the world of academia, radically improving the way scholarly research is managed. The grand vision of Frontiers is a world where all people have an equal opportunity to seek, share and generate knowledge. Frontiers provides immediate and permanent online open access to all its publications, but this alone is not enough to realize our grand goals.

Frontiers journal series

The Frontiers journal series is a multi-tier and interdisciplinary set of open-access, online journals, promising a paradigm shift from the current review, selection and dissemination processes in academic publishing. All Frontiers journals are driven by researchers for researchers; therefore, they constitute a service to the scholarly community. At the same time, the *Frontiers journal series* operates on a revolutionary invention, the tiered publishing system, initially addressing specific communities of scholars, and gradually climbing up to broader public understanding, thus serving the interests of the lay society, too.

Dedication to quality

Each Frontiers article is a landmark of the highest quality, thanks to genuinely collaborative interactions between authors and review editors, who include some of the world's best academicians. Research must be certified by peers before entering a stream of knowledge that may eventually reach the public - and shape society; therefore, Frontiers only applies the most rigorous and unbiased reviews. Frontiers revolutionizes research publishing by freely delivering the most outstanding research, evaluated with no bias from both the academic and social point of view. By applying the most advanced information technologies, Frontiers is catapulting scholarly publishing into a new generation.

What are Frontiers Research Topics?

Frontiers Research Topics are very popular trademarks of the *Frontiers journals series*: they are collections of at least ten articles, all centered on a particular subject. With their unique mix of varied contributions from Original Research to Review Articles, Frontiers Research Topics unify the most influential researchers, the latest key findings and historical advances in a hot research area.

Find out more on how to host your own Frontiers Research Topic or contribute to one as an author by contacting the Frontiers editorial office: frontiersin.org/about/contact

Oral neutrophils - the good, the bad, and the ugly

Topic editors

Ljubomir Vitkov — University of Salzburg, Austria

Martin Herrmann — University Hospital Erlangen, Germany

Jasmin Knopf — University Medical Centre Mannheim, University of Heidelberg, Germany

Citation

Vitkov, L., Herrmann, M., Knopf, J., eds. (2023). *Oral neutrophils - the good, the bad, and the ugly*. Lausanne: Frontiers Media SA. doi: 10.3389/978-2-8325-2644-6

Table of contents

frontiers | Frontiers in Immunology

TYPE Editorial
PUBLISHED 24 May 2023
DOI 10.3389/fimmu.2023.1225210

OPEN ACCESS

EDITED AND REVIEWED BY
Francesca Granucci,
University of Milano-Bicocca, Italy

*CORRESPONDENCE
Ljubomir Vitkov
lvitkov@yahoo.com

†These authors have contributed equally to this work

RECEIVED 18 May 2023
ACCEPTED 19 May 2023
PUBLISHED 24 May 2023

CITATION
Vitkov L, Herrmann M and Knopf J (2023) Editorial: Oral neutrophils - the good, the bad, and the ugly.
Front. Immunol. 14:1225210.
doi: 10.3389/fimmu.2023.1225210

Editorial: Oral neutrophils - the good, the bad, and the ugly

Ljubomir Vitkov[1,2,3*†], Martin Herrmann[4,5†] and Jasmin Knopf[4,5,6†]

[1]Clinic of Operative Dentistry, Periodontology and Preventive Dentistry, Saarland University, Homburg, Germany, [2]Department of Environment & Biodiversity, University of Salzburg, Salzburg, Austria, [3]Department of Dental Pathology, University of East Sarajevo, East Sarajevo, Bosnia and Herzegovina, [4]Department of Internal Medicine 3 - Rheumatology and Immunology, Friedrich-Alexander-University Erlangen-Nürnberg (FAU) and Universitätsklinikum Erlangen, Erlangen, Germany, [5]Deutsches Zentrum für Immuntherapie (DZI), Friedrich-Alexander-University Erlangen-Nürnberg and Universitätsklinikum Erlangen, Erlangen, Germany, [6]Department of Pediatric Surgery, University Medical Centre Mannheim, University of Heidelberg, Mannheim, Germany

KEYWORDS

dysbiosis, systemic low-grade inflammation, innate immunity, dysregulated immunity, maladaptive trained immunity

Editorial on the Research Topic
Oral neutrophils - the good, the bad, and the ugly

1 Introduction

Historically, all oral mucosa diseases due to non-specific symbiotic flora have been considered topical diseases. In the last two decades, this vision has been embodied by the idea of dysbiosis. However, the concept of dysbiosis as a pathogenic factor became very controversial in the last decade (1). Otherwise, the host microbiome is presently seen as the normal environment of the host, whereby both are in state of symbiosis and permanent interactions. The host controls its symbionts and if this fails, disease or even host death may occur. The control on symbionts is accomplished by both innate and adaptive immunity. In the oral mucosa the major defenders of the innate immune system are neutrophils and neutrophil extracellular traps (NETs). So, non-specific oral mucosa inflammation is caused by the symbiont flora when the innate immunity is dysregulated, due to either inborn immune defects, or acquired ones. In both cases, these immune defects can affect neutrophils. The former are characterised by insufficiency or lack of neutrophils in gingiva (2, 3) or by reduced NET formation on oral mucosal surfaces (4, 5), the latter by heavy neutrophil infiltration (6) and neutrophil hyper-responsiveness (7, 8). Over the last ten years, the conception of trained immunity (TI) has been developed (9, 10) and the inadequate host response has been denoted maladaptive TI (11). TI confers partial "autonomy" on neutrophils that does not underlie the direct control of adaptive immunity and dysregulated TI can harm gingiva and periodontium (12). The maladaptive TI, which is epigenetically encoded in haematopoietic stem and progenitor cells (HSPCs), causes neutrophil hyper-responsiveness. The latter dysregulates their immune response, which underlies the pathogenesis of periodontitis with late-onset. Transfusion of HSPCs, which are responsible for TI, from mice with ligature-induced periodontitis into healthy animals causes periodontitis, even without dysbiosis (8). Periodontitis with late-onset affects more than 60% of humans (13) and represent the largest share of all oral mucosal diseases. Periodontitis, its pathogenesis, the role of neutrophils, NETs

and maladaptive TI has been reviewed by Vitkov et al. The neutrophil proneness to form NETs on mucosal surfaces as well as NET roles, detection, and visualisation have been described by Li et al.

2 Interconnection between oral disorders and other diseases

As periodontitis is a systemic low-grade inflammatory (LGI) disease (12, 14), implications can be expected in other organs. Irwandi et al. discussed the contribution of periodontitis to the onset, progression, and complications of atherosclerotic cardiovascular diseases. In addition, infectious diseases characterised by overproduction of NETs, like COVID-19 (15), are also aggravated in periodontitis (16), and is caused by maladaptive TI (17). Heterogeneity of neutrophils and inflammatory responses in patients with COVID-19 and healthy controls have been studied by Xu et al., Hornigold et al. reported the age-related decline in the resistance of mice to bacterial infection and in LPS/TLR4 pathway-dependent neutrophil responses. The implications of this senescence-related decline in responsiveness may contribute to exacerbating the transient bacteraemia associated with periodontitis (12). Tang et al. demonstrated that in acute stress the enriched transcripts were mainly related to inflammation, defence, wounding, wound healing, complement activation and pro-inflammatory cytokine production. Additionally, the concentration of IL-1b, IL-6 and neutrophil number in peripheral blood increased significantly after acute stress, indicating the immunity transition into an inflammatory state. In sum, acute stress led to rapid mobilisation of the immune system. The body presented an inflammatory state dominated by an innate immune response represented by neutrophils. These findings suggest that stress may be an important contributor to onset and progression of periodontitis. Siddiqui et al. studied the periodontal neuropeptide Substance P (SP) and its role on host responses and bone loss in ligature-induced periodontitis. Deletion of tachykinin precursor 1 (Tac1), a gene encodes SP, or treatment of gingiva with SP antagonist significantly reduced bone loss in ligature-induced periodontitis. Ligature-induced recruitment of leukocytes, including neutrophils, and increase in cytokines leading to bone loss in periodontium was significantly lower in Tac1 knockout mice. Furthermore, intragingival injection of SP, but not neurokinin A, induced a vigorous inflammatory response and osteoclast activation in alveolar bone and facilitated bone loss in ligature-induced periodontitis. These data suggest that the periodontal innervation, in particular SP, plays a significant role in regulating host responses and bone resorption in ligature-induced periodontitis.

3 Treatment strategies

With immunological advances, a number of treatment strategies have been introduced to combat neutrophil inflammatory responses and to reverse maladaptive TI. This enables geroscientific strategies for periodontal rejuvenation and periodontal bone restoration (18). Another treatment possibility in periodontitis might be suppression of NET formation. As summarised by Liu et al., therapies targeting NETs can be segmented into two categories: degradation/destabilization of NETs, and the inhibition of NETs formation. Due to adverse side effects, most treatment options are not justified for the treatment of periodontitis.

In patients with antithrombotic prophylaxis employing low molecular weight heparins, a possible benefit for periodontitis can be expected, as they reportedly reduce NETs formation and dissociate histones from the chromatin backbone of NETs, as resumed by Liu et al. However, any clinical studies on low molecular weight heparins in periodontitis are lacking. Irwandi et al. summarised that novel and targeted approaches to manipulate neutrophil numbers and functions are warranted within the context of the treatment of periodontitis and also to mitigate its potential impact on other LGI disease. However, manipulation of neutrophil numbers is no mild treatment option, as demonstrated by Hebeda et al. neutrophil depletion promotes a higher frequency of monocytes, natural killers, and T regulatory cells, and lower frequency of cytotoxic T cells in the blood.

Additional completely new treatment approaches have been reported. Li et al. studied inhibition effects of taurine on bacteria-induced NADPH oxidase-dependent neutrophil extracellular traps via TAK1/MAPK signalling pathways. Chen et al. analysed how the ginsenoside Rg5 counteracts NETosis and inflammatory response in neutrophils via the adenosine diphosphate receptor P2RY12 on the platelet surface, which may pave the road for its clinical application in inflammatory disorders. Cxcr2 plays a crucial role in phagocytic ability, reactive oxygen species production, F-actin and α-tubulin levels, and phosphorylation of ERK1/2 and p38 MAPK, impaired PI3K-AKT, NF-κB, TGFβ and IFNγ pathways. Therefore, Cxcr2 blockers might also be a possible option to attenuate the neutrophil hyper-responsiveness seen in periodontitis Delobel et al.

4 Conclusion

Recently, the attention in mucosal inflammatory disease has been shifted from the topical to systemic point of view i.e., from the concept of dental biofilm dysbiosis to that of dysregulated immunity. The oral dysbiosis appears to be rather a corollary phenomenon of dysregulated immunity. The neutrophils and NETs play a crucial role in the mucosal inflammatory diseases. Reversing the maladaptive TI and geroscientific strategies may aid in oral mucosal rejuvenation and even reversion of periodontal bone loses, as recently demonstrated in experimental animals. The prophylaxis and treatment perspectives of oral mucosal pathology particularly periodontology largely depends on the progress in neutrophil immunology.

Author contributions

All authors listed have made a substantial, direct and intellectual contribution to the work, and approved it for publication.

Conflict of interest

The authors declare that the research was conducted in the absence of any commercial or financial relationships that could be construed as a potential conflict of interest.

Publisher's note

References

1. Lee JY, Tsolis RM, Bäumler AJ. The microbiome and gut homeostasis. *Science* (2022) 377(6601):eabp9960. doi: 10.1126/science.abp9960

2. Silva LM, Brenchley L, Moutsopoulos NM. Primary immunodeficiencies reveal the essential role of tissue neutrophils in periodontitis. *Immunol Rev* (2019) 287 (1):226–35. doi: 10.1111/imr.12724

3. Silva LM, Doyle AD, Greenwell-Wild T, Dutzan N, Tran CL, Abusleme L, et al. Fibrin is a critical regulator of neutrophil effector function at the oral mucosal barrier. *Science* (2021) 374(6575):eabl5450. doi: 10.1126/science.abl5450

4. Sørensen OE, Clemmensen SN, Dahl SL, Østergaard O, Heegaard NH, Glenthøj A, et al. Papillon-lefèvre syndrome patient reveals species-dependent requirements for neutrophil defenses. *J Clin Invest* (2014) 124(10):4539–48. doi: 10.1172/JCI76009

5. Vitkov L, Hartl D, Minnich B, Hannig M. Janus-faced neutrophil extracellular traps in periodontitis. *Front Immunol* (2017) 8:1404. doi: 10.3389/fimmu.2017.01404

6. Williams DW, Greenwell-Wild T, Brenchley L, Dutzan N, Overmiller A, Sawaya AP, et al. Human oral mucosa cell atlas reveals a stromal-neutrophil axis regulating tissue immunity. *Cell* (2021) 184(15):4090–104 e15. doi: 10.1016/j.cell.2021.05.013

7. Matthews JB, Wright HJ, Roberts A, Ling-Mountford N, Cooper PR, Chapple ILC. Neutrophil hyper-responsiveness in periodontitis. *J Dental Res* (2007) 86(8):718–22. doi: 10.1177/154405910708600806

8. Li X, Wang H, Yu X, Saha G, Kalafati L, Ioannidis C, et al. Maladaptive innate immune training of myelopoiesis links inflammatory comorbidities. *Cell* (2022) 185 (10):1709–27 e18. doi: 10.1016/j.cell.2022.03.043

9. Goodridge HS, Ahmed SS, Curtis N, Kollmann TR, Levy O, Netea MG, et al. Harnessing the beneficial heterologous effects of vaccination. *Nat Rev Immunol* (2016) 16(6):392–400. doi: 10.1038/nri.2016.43

10. Netea MG, Giamarellos-Bourboulis EJ, Domínguez-Andrés J, Curtis N, van Crevel R, van de Veerdonk FL, et al. Trained immunity: a tool for reducing susceptibility to and the severity of SARS-CoV-2 infection. *Cell* (2020) 181(5):969–77. doi: 10.1016/j.cell.2020.04.042

11. Hajishengallis G, Li X, Divaris K, Chavakis T. Maladaptive trained immunity and clonal hematopoiesis as potential mechanistic links between periodontitis and inflammatory comorbidities. *Periodontol 2000* (2022) 89(1):215–30. doi: 10.1111/prd.12421

12. Vitkov L, Muñoz LE, Knopf J, Schauer C, Oberthaler H, Minnich B, et al. Connection between periodontitis-induced low-grade endotoxemia and systemic diseases: neutrophils as protagonists and targets. *Int J Mol Sci* (2021) 22(9):4647. doi: 10.3390/ijms22094647

13. Trindade D, Carvalho R, Machado V, Chambrone L, Mendes JJ, Botelho J. Prevalence of periodontitis in dentate people between 2011 and 2020: a systematic review and meta-analysis of epidemiological studies. *J Clin Periodontol* (2023) 50 (5):604–26. doi: 10.1111/jcpe.13769

14. Hajishengallis G, Chavakis T. Local and systemic mechanisms linking periodontal disease and inflammatory comorbidities. *Nat Rev Immunol* (2021) 21 (7):426–40. doi: 10.1038/s41577-020-00488-6

15. Ackermann M, Anders HJ, Bilyy R, Bowlin GL, Daniel C, De Lorenzo R, et al. Patients with COVID-19: in the dark-NETs of neutrophils. *Cell Death Differ* (2021) 28 (11):3125–39. doi: 10.1038/s41418-021-00805-z

16. Marouf N, Cai W, Said KN, Daas H, Diab H, Chinta VR, et al. Association between periodontitis and severity of COVID-19 infection: a case-control study. *J Clin Periodontol* (2021) 48(4):483–91. doi: 10.1111/jcpe.13435

17. Vitkov L, Knopf J, Krunić J, Schauer C, Schoen J, Minnich B, et al. Periodontitis-derived dark-NETs in severe covid-19. *Front Immunol* (2022) 13:872695. doi: 10.3389/fimmu.2022.872695

18. An JY, Kerns KA, Ouellette A, Robinson L, Morris HD, Kaczorowski C, et al. Rapamycin rejuvenates oral health in aging mice. *Elife* (2020) 9:e54318. doi: 10.7554/eLife.54318

frontiers in Immunology

REVIEW
published: 24 November 2021
doi: 10.3389/fimmu.2021.788766

Neutrophils Orchestrate the Periodontal Pocket

Ljubomir Vitkov[1,2], Luis E. Muñoz[3,4], Janina Schoen[3,4], Jasmin Knopf[3,4], Christine Schauer[3,4], Bernd Minnich[1], Martin Herrmann[3,4†] and Matthias Hannig[2†]*

[1] Vascular & Exercise Biology Unit, Department of Biosciences, University of Salzburg, Salzburg, Austria, [2] Clinic of Operative Dentistry, Periodontology and Preventive Dentistry, Saarland University, Homburg, Germany, [3] Department of Internal Medicine 3 - Rheumatology and Immunology, Friedrich-Alexander-University Erlangen-Nürnberg (FAU) and Universitätsklinikum Erlangen, Erlangen, Germany, [4] Deutsches Zentrum für Immuntherapie (DZI), Friedrich-Alexander-University Erlangen-Nürnberg and Universitätsklinikum Erlangen, Erlangen, Germany

The subgingival biofilm attached to tooth surfaces triggers and maintains periodontitis. Previously, late-onset periodontitis has been considered a consequence of dysbiosis and a resultant polymicrobial disruption of host homeostasis. However, a multitude of studies did not show "healthy" oral microbiota pattern, but a high diversity depending on culture, diets, regional differences, age, social state etc. These findings relativise the aetiological role of the dysbiosis in periodontitis. Furthermore, many late-onset periodontitis traits cannot be explained by dysbiosis; e.g. age-relatedness, attenuation by anti-ageing therapy, neutrophil hyper-responsiveness, and microbiota shifting by dysregulated immunity, yet point to the crucial role of dysregulated immunity and neutrophils in particular. Furthermore, patients with neutropenia and neutrophil defects inevitably develop early-onset periodontitis. Intra-gingivally injecting lipopolysaccharide (LPS) alone causes an exaggerated neutrophil response sufficient to precipitate experimental periodontitis. Vice versa to the surplus of LPS, the increased neutrophil responsiveness characteristic for late-onset periodontitis can effectuate gingiva damage likewise. The exaggerated neutrophil extracellular trap (NET) response in late-onset periodontitis is blameable for damage of gingival barrier, its penetration by bacteria and pathogen-associated molecular patterns (PAMPs) as well as stimulation of Th17 cells, resulting in further neutrophil activation. This identifies the dysregulated immunity as the main contributor to periodontal disease.

Keywords: dysbiosis, dysregulated immunity, NET formation, caspase 4, caspase 11, bacterial membrane vesicles, outer membrane vesicles

OPEN ACCESS

Edited by:
Claudia Ida Brodskyn, Gonçalo Moniz Institute (IGM), Brazil

Reviewed by:
Ana Carolina Morandini, Augusta University, United States
Francisco Mesa, University of Granada, Spain

****Correspondence:***
Matthias Hannig
matthias.hannig@uks.eu

†These authors share senior authorship

Specialty section:
This article was submitted to Molecular Innate Immunity, a section of the journal Frontiers in Immunology

Received: *03 October 2021*
Accepted: *08 November 2021*
Published: *24 November 2021*

Citation:
Vitkov L, Muñoz LE, Schoen J, Knopf J, Schauer C, Minnich B, Herrmann M and Hannig M (2021) Neutrophils Orchestrate the Periodontal Pocket. Front. Immunol. 12:788766. doi: 10.3389/fimmu.2021.788766

Abbreviations: BMVs, bacterial membrane vesicles; CGD, chronic granulomatous disease; DAMPs, damage-associated molecular pattern; DOAJ, directory of open access journals; EPS, extracellular polymeric substances; FcR, Fc receptor; GCF, gingival crevicular fluid; NADPH, Nicotinamide adenine dinucleotide phosphate; HSPC, hematopoietic stem and progenitor cells; IgA, Immunoglobulin A; LPS, lipopolysaccharide; NETs, neutrophil extracellular traps; NOD-like, nucleotide-binding oligomerisation-like; OMVs, outer membrane vesicles; PAMPs, pathogen-associated molecular patterns; PAR2, protease activated receptor 2; Plg, plasminogen; PRRs, pattern recognition receptors; RIG-I, retinoic acid-inducible gene I; TLR, toll-like receptor; TNF, tumour necrosis factor.

INTRODUCTION

Periodontitis is a collective term for disorders of the tooth supporting tissues with various aetiologies (1). In general, the most frequently forms of periodontitis can be divided into two main categories triggered by (I) the biofilm attached to the outer tooth surface and (II) by dental pulp necrosis, respectively (1). The latter is also denoted "endodontic-periodontal lesions" (1) and is also a subject of endodontology. The most frequent form of biofilm-triggered periodontitis is the late-onset, formerly referred to as "chronic periodontitis". The quite common denoting "late-onset" is not a diagnosis, but just tagging the periodontal disorders, which are an age-related condition occurring in humans after the age of 30 (2–4). Late-onset periodontitis is characterised by the formation of a periodontal pocket, a pathological formation of a duct-like space (periodontal crevice) between the pocket epithelium and the subgingival biofilm attached to the tooth root (5). The subgingival biofilm continuously disperses planktonic bacteria, pathogen-associated molecular patterns (PAMPs), and periodontal pathogenic bacteria (6). These afflict the epithelium in order to get internalised and PAMPs impair the epithelial barrier (7). The crevice is filled with the gingival crevicular fluid (GCF) and is where the periodontal pathogens are initially encountered by the first line of host defence, the crevicular neutrophils and the humoral components of innate and adaptive immunity (8). Late-onset periodontitis is characterised by the inability to efficiently control subgingival biofilm (9), damage of the host tooth supporting tissues (5) and transmigration of periodontal pathogens into blood circulation (10). That the late-onset periodontitis is triggered by subgingival dental biofilm is beyond doubt. One may argue that the dental biofilm is also the cause for this disease, or at least the dysbiosis of the subgingival dental biofilm. Currently, some observations relativise the etiological role of subgingival dysbiosis: (I) the age-association of late-onset periodontitis in susceptible individuals and (II) the neutrophil hyper-responsiveness in late-onset periodontitis, (III) the responsiveness of biofilm-induced periodontitis to anti-ageing therapy (11–13) and (IV) a microbiota shift by dysregulated immunity (14, 15).

The aim of this review was to investigate the role of neutrophils in periodontal disease. We consider the factors responsible for resistance, induction, clearance failure and maintenance of this disease and discuss the role of neutrophils in its aetiopathogenesis.

PERIODONTITIS PATHOLOGY

Maintenance of tissue homeostasis is imperative to host survival. This fundamental process relies on a complex and coordinated set of innate and adaptive responses that calibrates responses against self, food, commensals, and pathogens (16). In health, homeostasis between gingiva and microbiota exists, i.e. the microbiota is controlled by the immunity (17) (**Figure 1**). In patients with neutropenia and defects of leukocyte adhesion early-onset periodontitis inevitably develops (18). Similarly, dysregulating the immunity *via* intra-gingival application of lipopolysaccharide results in experimental periodontitis without the contribution of any additional bacterial pathogens (19, 20). Patients with late-onset periodontitis have systemic low-grade inflammation and neutrophil hyper-responsiveness (21–25). Taken together, all forms of periodontitis are characterised with either neutrophil defects or dysregulated immunity, in particular neutrophil dysregulation. Periodontitis is not a consequence of basic alteration of the oral microbiota, but rather of the inability of the host immunity to resolve chronic inflammation (26, 27). The capacity of certain bacteria to act as a commensal or pathogen is highly dependent on the host immune conditions (28).

The development of a periodontal pocket marks the point of no return to homeostasis. The pocket reflects an impairment of the innate immunity to control the subgingival microbiota, as this pathological structure provides anaerobic conditions and

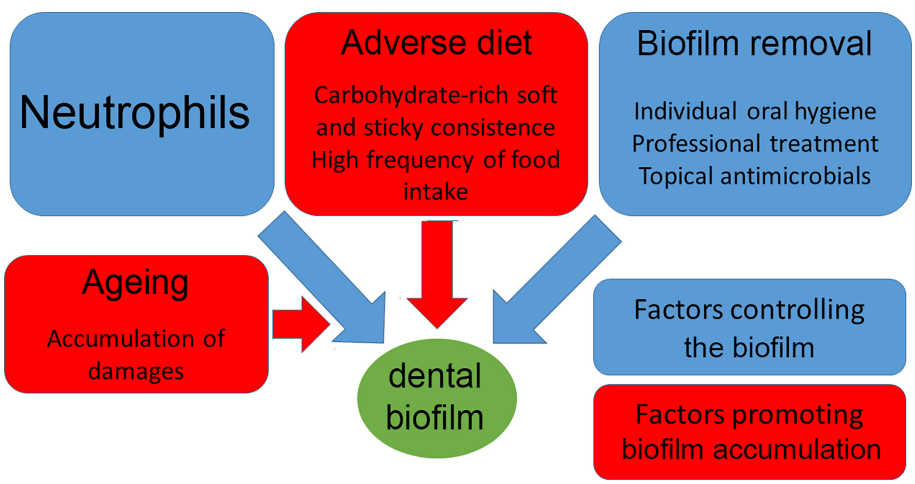

FIGURE 1 | Relationship between host and dental biofilm.

mechanical protection for the accumulation of subgingival biofilm. It hampers the GCF flow through the prolonged duct-like crevice and facilitates the accumulation of PAMPs, proteases and is accompanied by an excess of reactive oxygen species (ROS). The periodontal inflammation can temporarily be suppressed by antimicrobials that reduce the dental biofilm (29), but not on permanent basis. Conservatively treated periodontal sites are subject to recolonization with a microbiota similar to that prior to therapy. The degree and speed of recolonization depends on the treatment protocol and the distribution patterns of periodontal microorganisms elsewhere in the oral cavity. It is further influenced by the quality of the patient's oral hygiene (29). Nevertheless, the surgical elimination of periodontal pocket does not eliminate the proneness to relapse and does not substantially alter the microbiota (30). Albeit the sulcular microbiota in orally healthy subjects has been considered symbiotic, the differences between oral symbiotic and dysbiotic microbiota remain elusive (26, 27). The symbiosis between the microbiota and its mammalian host encompasses various forms of relationships, and how members of the microbiota interact with their host can be highly contextual with the same microbe developing as mutualist, commensal, or pathogens according to the genetic landscape and immunity of the host (16, 28). Increased inflammation in periodontitis is not associated with a distinct microbiome; it rather corresponds with higher dental biofilm biomass (31). Indeed, the higher biofilm biomass produces more PAMPs, hence a stronger inflammatory response and more host damages, as the lipopolysaccharide (LPS)-induced experimental periodontitis shows (19, 20). These findings support the alternative notion that the microbiota shift is due to dysregulated immunity (14, 15). Indeed, neutrophil hyper-responsiveness has been reported in late-onset periodontitis (21–25). The neutrophil hyper-responsiveness remains in edentulous patients with a history of late-onset periodontitis (21–23, 25), despite the disappearance of the bacteraemia after teeth exfoliation (32). Its control by the immune response is obviously insufficient in periodontitis-susceptible modern humans, who also have dissimilar diet and lifestyle than their pre-modern ancestors (33). The role of dental biofilm overgrowth is crucial (29), but it appears to be the consequence of dysregulated immunity (27); the aberrant responsiveness of neutrophils in periodontal disease supports this possibility (21–25). Lastly, the majority of modern people over 30 years remain periodontitis resistant (34).

Human beings are domestic beings seemingly eluding the "natural selection" and some of their evolutionary adaptations, like oral hygiene and professional dental treatment are artificial. The same applies to the pets. In comparison, advanced late-onset periodontitis has not been reported in wild-living Mammalia. Periodontitis completely lacks in rhinoceros (35), or is rare in marmosets (36). In wild-living apes, only occasional and mild forms of periodontitis have been reported (37).

DENTAL BIOFILM

Biofilm Basics

Biofilms are aggregates of interface-associated sessile bacteria, Candida, and viruses (38), all embedded within a matrix of extracellular polymeric substances (EPS) (39–41). Horizontal transfer of EPS genes (42) plays an important role in the multi-species consortia of dental biofilm (43, 44). Each oral biofilm consists of five main components: (I) bacteria, (II) bacterial membrane vesicles (BMVs), (III) macromolecules like proteases and toxins, (IV) immune cell and their remnants, all encapsulated by (V) EPS. The biofilm EPS offers protection from the surrounding environment and provides certain advantages to the embedded sessile bacterial community that planktonic bacteria do not possess (45). Biofilms go through a life cycle of planktonic cell attachment to an interface, micro-colony formation, biofilm maturation, and finally dissemination (46). Each phase of this circle is characterised by distinct bacterial phenotype. Thus, the biofilm is a complex microbial community characterised by attributes not seen in planktonic bacteria: (I) primitive homeostasis and metabolic cooperativity (47) (II) cell-to-cell signalling (39) (III) essentially higher resistance to antibiotics (48) (IV) dissemination by dispersion (49) (V) detachment of bacteria (50–52) and last not least (VI) resistance to the host defence (40). Thus, many oral pathogens are protected from crevicular neutrophils within the bulky dental biofilm and can rely on nutrition from ingredients of GCF diffusing through the EPS. Thereby, the gingivitis is beneficial to the biofilm, as the first host response of gingivitis involves increased flow rate of the GCF (53). The role of dental biofilm is beyond doubt, as its removal efficiently prevents gingivitis and periodontitis. Importantly, even a short-term biofilm accumulation is sufficient to induce gingival inflammation (53). Dental biofilm is a *conditio sine qua non* for biofilm-induced periodontitis (29). In individuals without gingivitis and periodontitis, biofilm might be partly removed *via* mastication, but the artificial biofilm destruction, i.e. teeth brushing, is by far more efficient (54). The abundance of carbohydrates and the soft consistency of the diet in post-industrial revolution societies lead to biofilm overgrowth as mechanical biofilm destruction is insufficient and carbohydrates foster biofilm accumulation (55). Surviving some biofilm parts enables the biofilm maturing. This is characterised by phenotype transition into the so-called state of persisters, bacteria highly resistant to antibiotics and neutrophil killing (see § 3.3). Both persisters and EPS hinder neutrophil killing and prevent destruction of the biofilm by crevicular neutrophils (56). Modern humans attempt to compensate for this failed biofilm removal by targeting dental biofilm through oral hygiene and professional treatment. These are the new evolutionary strategies of the post-industrial age. However, only susceptible individuals are affected by periodontal disease; most humans, i.e. nearly 60%, are resistant and remain periodontally healthy lifelong (34). This fact suggests the existence of unknown immune mechanisms, able to completely protect orally healthy individuals from oral microbiota.

Heritability of Oral Microbiota and Shift Due to Diet

Oral microbiota is primarily inherited from caregivers (17). Genetic studies in twins have shown that host-related microbial communities depend on both host genetics and environmental factors (57). Oral microbiome similarity increases with shared host

genotypes. Highly heritable oral taxa have been identified, although most of the variation of the oral microbiome has been determined by environmental factors (57). These findings indicate that the hosts control almost half of their oral microbiota. The remaining half differs due to differences in diet, lifestyle and environment (29) and hence are "independent" of the host genotype. From the microbiologic perspective, the environment shapes the microbiota (17). The environment of supragingival biofilm microbiota is determined by both host and diet. That of subgingival biofilm predominantly by host, as the subgingival effects of diet are minor However, a discrimination between supragingival and subgingival biofilm has been rarely reported in oral microbiome studies (31). Subgingival biofilm is found in the gingival sulcus of people without and in the pocket of people with periodontal disease. Discrimination between supragingival and subgingival biofilm in fossils of individuals without periodontitis is not possible and only partly feasible in living animals for technical reasons. The fact that no discrimination has been reported in studies on fossils and animals (33, 58) strongly suggests that the examined biofilm was either supragingival or mixed, thus limiting the usefulness of these studies on oral microbiome concerning periodontitis.

With the establishment of the agricultural and industrial lifestyle and diet alteration, there was a shift in the oral microbiota and the number of oral pathogens increased, especially of *Porphyromonas gingivalis (P. gingivalis)* (33). However, not only the carbohydrate-rich Neolithic diet, but also the low chewing resistance leads to the formation of biofilm. The importance of the mechanical destruction of dental biofilm in modern humans is beyond doubt and they solve this problem artificially, at least in part, by brushing teeth, flossing and professional oral hygiene (59).

Planktonic Bacteria and Biofilm Differ

A fraction of biofilm bacteria evolves into persister cells that are genetically nearly identical, but phenotypically distinct from their parent cells. Persisters are metabolically inert, replicate slowly, modulate the toxin-antitoxin system, upregulate DNA repair and anti-oxidative machinery, have enhanced phosphate metabolism, and exhibit unresponsiveness towards minimal inhibitory concentrations of antibiotics (60). Drug treatment normally kills planktonic cells and the majority of biofilm cells. Nevertheless, EPS and drug tolerant persisters remains unharmed. The latter repopulate the biofilm, disseminate into planktonic forms and start a new cycle of biofilm development (60–62). This perpetuates diseases caused by biofilm forming pathogenic microorganisms. For this reason, the biofilm is considered of "pseudo-organismic nature" (27). Therefore, new strategies aiming at EPS destruction have been introduced (41).

IMMUNITY DYSREGULATION AS INSTIGATOR OF PERIODONTITIS

Many features of periodontitis appear to be unrelated to the composition of oral microbiota. They can be used to examine to what extent the oral microbiota determines development and maintenance of periodontitis.

Heritability of Periodontitis: Dysbiosis as a Consequence of Immune Deficiency

The genetic backdrop of all forms of early-onset periodontitis is based on inborn neutrophil defects (18, 63) or on other inborn genetic defects leading to neutrophil activation (64). The concomitant dysbiosis in early-onset periodontitis is hence a consequence of inborn immune deficiency. The genetic predisposition of late-onset periodontitis is beyond doubt (65). However, the association of genetic polymorphisms in PAMP-sensing and PAMP-signalling genes with the microbiota composition has been detailed studied only in gut. Importantly, host cells sense bacteria *via* their PAMPs by pattern recognition receptors (PRRs) (66–73). PRRs include several families of receptors: toll-like receptors (TLRs), nucleotide-binding oligomerisation-like (NOD-like) receptors, RIG-I-like receptors, and C-type lectin receptors. Thus, gut dysbiosis has been demonstrated in studies on knockout TLRs in mice (67). Nod2-deficient mice showed an increased load of commensal resident bacteria, a reduced ability to prevent intestinal colonisation by pathogenic bacteria (69, 70), and an increased susceptibility to bacterial infections (71). Inflammasome-deficient mice have an impaired host/microbiome interaction causing an increased intestinal inflammation (66, 72, 73). A locus containing the Irak4 gene, a kinase that activates the nuclear factor-kB pathway in TLR-and T cell receptor-signalling pathways is associated with certain bacterial species (74). Several bacteria are associated with the locus that contains the Irak3 gene, another regulator of TLR-signalling pathway (75). Consistent findings have been observed for the association of PRR genes with microbiome composition and microbiome-associated disease (76). So, single-nucleotide polymorphisms in the NOD1 gene are associated with bacterial pathways and gene groups specific for *E. coli* (68). Genetic variants in NOD2 are strongly associated with Crohn's disease, an inflammatory condition of the gut associated with dysbiosis (77, 78)]. Carriership of the NOD2 genetic risk for Crohn's disease is associated with an increased relative abundance of Enterobacteriaceae (77). An increased risk of periodontitis among patients with Crohn's disease has been well established (63, 78).

The host genetic backdrop of dysbiosis indicates that it is in many cases a consequence of immune defects respectively dysregulation. In addition, the inability to transfer oral pathogens within the family (79) or the merely transient effect of a single oral microbiota transplant in dogs (80), supports the concept that the dysbiosis of dental biofilm is a result of the dysregulated host immunity and not vice versa. Neither microbiota transplantation (80) nor probiotics have any effect on periodontitis (81) and gingival inflammation (82).

Ageing. Periodontitis as a Common Mammalian Age-Related Disease

Postnatal development of an individual is followed by a "middle" period of relative stability, when changes in physical and cognitive function are small and only detectable by very sensitive tools or challenging tests. During that period, most

individuals in the population are free of diseases (83). This also applies to people who develop late-onset periodontitis over the age of 30 (2–4). Underneath this apparent stability, several compensatory and homeostatic mechanisms continuously operate to preserve the biochemical balance and prevent phenotypic derangements, as well as functional decline (84). These mechanisms are initially effective and provide a robust homeostasis, but start to fade later in life. Ageing is a complex process involving various mechanisms that lead to the accumulation of subcellular, cellular and intercellular damages as well as other age-related deleterious changes, together representing the organisms' "deleteriomes" (85). Unrepaired damage accumulates beyond the functional threshold (84). On the molecular level, the most precise biomarker of ageing is based on DNA methylation profiling and is known as the "epigenetic clock" (86).

Periodontitis is a common mammalian disease affecting humans, non-human primates (87), ruminants (88, 89), rodents (11, 90), and pets (91, 92). Periodontitis has been reported in Palaeolithic, Mesolithic, Neolithic and post-industrial revolution humans (93). An important question is, whether the prevalence of periodontitis increases in Neolithic and post-industrial revolution or just the average human longevity. This question cannot be answered without doubt. The synchronous increase of average human longevity and the accompanying increase in prevalence of periodontitis creates the impression of genuine increase in prevalence in post-industrial humans. This has been mainly explained as a consequence of altered diet and lifestyle (33). However, the accumulation of somatic mutations dysregulates the immunity and results in a plethora of age-related diseases (94), which become flashier with the lifespan increase in both humans (34) and domestic mammalians (90) during the post-industrial revolution. The prevalence increase of late-onset periodontitis underlies the same kinetics. It can be deduced that anti-aging therapies should alleviate periodontal disease. Indeed, the good responsiveness of periodontitis to anti-ageing therapies (11–13) scrutinise the role of dysbiosis in periodontitis and highlights the role of dysregulated immunity. On cellular level, *Porphyromonas gingivalis* causes *in vitro* cell senescence, which is reversed by anti-ageing treatment (95).

Dysbiosis and Immunity

The capacity of certain bacteria to act as a commensal or pathogen is highly dependent on the host immune conditions, genetic predispositions, and coinfections (28). The host poses a complex regulatory system, involving epithelial cells, IgA, AMPs, and an array of innate and adaptive immune cells to control the composition and distribution of the microbiota (16). Thus, periodontitis heritability, ageing relatedness and neutrophil hyper-responsiveness (10) are consequences of immunity dysregulation. This underscores the role of immunity and enables a new perspective on periodontal disease, independently of the dysbiosis tenet. The common definition of dysbiosis is an imbalance between beneficial and harmful microorganisms (96–98). This requires the existence of "healthy" microbiota in healthy individuals that can be used as a reference pattern for differentiation between health and disease. However, a "healthy" microbiota pattern has never been established (99, 100). Especially in oral microbiota, where the diversity is very high (101), and strongly differs depending on culture, diets, regional differences, age, social state etc. The lack of "healthy" oral microbiota relativises the pathogenic role of oral dysbiosis. Recently, the dysbiosis in general (but not the oral one) has been hypothesised to be a consequence of the dysregulated immunity (14, 15, 102), and a new environmental concept of microbiota regulation by the host as its environment has been established (16, 17, 28). In knocked out $CXCR2^{-/-}$ mice, which are characterised by the absence of gingival neutrophils, the oral microbiome undergoes a significant shift in total load and composition as compared to that of wild type $CXCR2^{+/+}$ mice with normal levels of neutrophil recruitment into the gingival tissues. This dysbiosis in $CXCR2^{-/-}$ mice is accompanied by a significant increase in periodontal bone pathology (103). However, transfer of the oral microbiome of $CXCR2^{-/-}$ mice into germ free $CXCR2^{+/+}$ mice led to restoration of the microbiome to the wild type $CXCR2^{+/+}$ composition and the absence of pathology. These data demonstrate that the composition of the oral microbiome is governed to a significant extent by the genetically determined immunity of the host organism (103).

DYSREGULATED IMMUNITY

Neutrophil Functions in Gingiva

Neutrophils play a central role in the control of bacterial infections. Neutrophils are also the effector immune cells responsible for the antimicrobial defence in the gingiva and the first defenders to face the bacterial invasion. Thus, the tissue neutrophil density increases at least 150-fold in the first 4 h after intradermal inoculation of healthy rabbits with *E. coli*, since a certain neutrophil density is required to counter bacterial invasion (104). The indispensable role of neutrophils in periodontal health is evident from development of early-onset periodontitis in patients with neutropenia and with defects of leukocyte adhesion (18). Neutrophils do not recognise individual pathogens or pathogen species, but just danger signals, (I) chemokines, (II) cytokines, (III) immune complexes, (IV) PAMPs, (V) damage-associated molecular patterns (DAMPs), (VI) C3a or 5a, and (VII) complement C3 and C4 and their derivatives (105). Intra-gingivally injecting LPS is sufficient to cause experimental periodontitis and is routinely used as animal model (19, 20). Vice versa to the surplus of PAMPs, the increased PMN responsiveness characteristic for late-onset periodontitis (21–24) may effectuate the same result. Thus, neutrophils can turn from bacterial defender into tissue devastators independently from the bacterial challenge (105, 106). In particular, components of exaggerated NETs harm and even kill epithelial cells (107) and promote tissue damage (108, 109).

Trained Immunity: Neutrophil Hyper-Responsiveness and NET Aggregation

The neutrophil hyper-responsiveness in late-onset periodontitis is also an aspect of dysregulated immunity (21–25); it persists in edentulous patients with a history of periodontitis (21–23, 25).

Certain microbial challenges promote the response of myeloid cell populations to subsequent infections either with the same or with other pathogens. This phenomenon involves changes in the cell epigenetic and transcription, and is referred to as "trained immunity" (110). It acts *via* modulation of hematopoietic stem and progenitor cells (HSPCs). A main driver of modulation is the sustained low level transfer of lipopolysaccharides from the periodontal pocket to the peripheral blood. Dysregulated trained immunity misleads the neutrophils to a non-resolving inflammatory state with elevated and reduced levels of inflammatory and homeostatic mediators, respectively (111). In general, trained neutrophils are prone to increased NET formation (112, 113). The neutrophil hyper-response aims to destroy the pocket pathogens, but they appear to be resistant to NET killing (114). So, bystander damages, due to the surplus of NET proteases and histones, are responsible for lessening the epithelial barrier and formation of ulceration (see §4.4). Both sorts of epithelial damage compromise the gingiva defence. Thus, the exaggerated NET formation in late-onset periodontitis (115) may also be a result of trained immunity. Trained immunity gives neutrophils a partial "autonomy" that does not underlie the direct control of adaptive immunity (10).

NET Response in Periodontitis

Dental biofilms communicate with the crevicular neutrophils *via* soluble excretions of dental biofilms, mostly PAMPs, recognised by neutrophil surface receptors (116). However, in periodontitis neutrophil toll-like receptors (TLRs) may be degraded by the increased concentrations of crevicular neutrophil proteases (117–121). Interestingly, when neutrophils are stimulated *in vitro* with oral pathogens, TLR inhibitors have no effect on ROS and NET release (114); this indicates that TLRs are not involved in the activation of crevicular neutrophil. An alternative bacterial recognition takes place *via* outer membrane vesicles (OMVs) (122). These are endocytosed by neutrophils and activate caspase-4/11 (123). Gram negative bacteria prevail in subgingival biofilms. Thus, the main share of BMVs from dental biofilm in periodontitis are OMVs that are heavily loaded with LPS (122). OMVs are released into the GCF by bacterial biofilms during normal cell growth without affecting cell viability; but growth conditions have a profound effect on the release of OMVs (124, 125). Two main mechanisms are responsible for bacterial and OMV dissemination from biofilms: (I) bacterial dispersion, an active process controlled by various biofilm-intrinsic mechanisms, like *quorum sensing* (49) and (II) detachment, a passive process driven by mechanical forces (46). During mastication and hygiene procedures, subgingival dental biofilms are exposed by a pump-like action of the periodontal pocket. It is accompanied by bacterial translocation, a clear indication of a biofilm detachment (50–52). Indeed, free LPS is recognised by membrane-borne TLR4 and induces NET formation *via* the MEK/ERK pathway (126); this is similar to the action of PMA (127) and activates several transcriptional nuclear factors. OMVs function as vehicles that deliver LPS into the cytosol. When endocytosed, OMVs release LPS from the early endosomal compartments into the cytosol (122). The host is thus capable of TLR4-independent cytosolic recognition of LPS (128, 129). Inflammatory caspases, namely murine caspase-11 and human caspase-4 and caspase-5 serve as receptors for cytosolic LPS (130). The latter also induces caspase 4/5/11-dependent cleavage of gasdermin D (GSDMD) and thus promotes suicidal NET formation, whereas caspase 1 is not activated (123). Otherwise, NET induced by canonical stimulants proceed caspases-independently but share the morphological features of NET formation induced by caspase-4/5/11/GSDMD signalling (123).

Another possibility to trigger NET formation when TLRs are proteolytically degraded involves the cleavage of the protease activated receptor (PAR2) on neutrophils surfaces, e.g. by gingipain. Importantly, NETs formed in this way are deficient in antibacterial activity (131), hence it is evident that the PAR2-based responses do not orchestrate the host's defence but drive gingival damage (131).

Neutrophil-Induced Gingival Damages

Hyper-responsive neutrophils and in particular exaggerated NET formation cause tissue damage (108). Abundant crevicular neutrophils and NETs overload the pocket with neutrophil-derived proteases (118, 120, 132) and cause epitheliopathy *via* Oncostatin M (133). This correlates with the epithelial ulceration in periodontitis (5, 134). NET-derived components such as histones (107, 135–137) and myeloperoxidase (MPO) (107) are cytotoxic to epithelial cells; neutrophil proteases damage and even kill epithelial cells. High NET levels reportedly suppress keratinocyte proliferation, delay wound closure (138, 139) and chronifies ulcers. In contrast, aggNETs proteolytically inactivate several soluble pro-inflammatory mediators over time (140). Neutrophil activation due to plasminogen (Plg) deficiency causes periodontitis in both humans (known as ligneous periodontitis) (141) and $Plg^{-/-}$ mice (64). The neutrophil activation in Plg deficiency is effected *via* fibrin polymer binding motif recognisable by the integrin αmβ2 (CD11b/CD18) (142) and results in exaggerated NET formation in $Plg^{-/-}$ mice. The exaggerated NET formation effectuates heavy periodontitis, which can be suppressed by DNase I in a mouse model (64). Exaggerated NET formation is concomitant with heavy purulent periodontitis (6).

Gingival homeostasis does not require oxidative burst, as periodontitis occasionally occurs in patients with chronic granulomatous disease (CGD), a rare primary immunodeficiency that affects the innate immune system. It is caused by mutations in any of the four genes encoding the subunits of the superoxide generating phagocyte NADPH oxidase; CGD displays no or very low levels of enzyme activity (143). Some isolated cases of periodontitis have been reported in CGD patients (144–146). A survey on 368 CGD patients has reported just nine cases of gingivitis or periodontitis (147). However, excess of ROS characterises periodontitis-related neutrophil hyper-responsiveness (21–25). Consequently, the deleterious effects of ROS on host tissues (148) are boosted in periodontitis. NETs entrap oral bacteria, but do not kill them (114). Thus, the surplus of both ROS and proteases in periodontitis harms the host, a clear indication of dysregulated immunity.

Neutrophil Orchestration by Gingiva and the Adaptive Immunity

Oral epithelial cells are sentinel cells provided with a multitude of PRRs and upon PAMP stimulation produce interleukins (ILs), in particular IL-8 (149). IL-8 is mostly recognised *via* the neutrophil chemokine receptor CXCR2, which play a crucial role for the neutrophil recruitment into periodontal crevice (150). After penetrating the epithelial barrier, lipopolysaccharides mount a strong inflammatory response of gingival fibroblasts *via* their surface-expressed TLR-4 (151). In periodontitis, there is extensive inferred communication between stromal and immune cells (152). Of interest and consistent with pathways upregulated in disease, stromal and epithelial cells appeared to promote adhesion of immune cells, while fibroblasts displayed a potential toward recruitment of inflammatory cells. Gene-expression signatures indicate an active role for stromal cells in the recruitment of immune cells to the site of disease (152). Fibroblasts are particularly transcriptionally active in the production of chemokines. Fibroblasts expressed a broad array of chemokine ligands exclusive in their potential to recruit neutrophils (CXCL1, 2, 5, 8) as well as chemokines with the potential of recruiting several types of leukocytes, e.g. CXCL12, CXCL13, CCL19. Taken together, these data suggest that stromal cells utilize intercellular signalling to drive immune cell recruitment and tissue transmigration in periodontitis (152) (152).Though the gingival inflammatory response is dominated by neutrophils (153), the entire immune response is involved. Within the crevice, IgA binds to neutrophil Fc-alpha receptors; thus the adaptive immunity guides the neutrophil response (154–156). Once the adaptive immunity has developed, the neutrophil response in periodontitis is orchestrated by Th17 cells (32, 157).

CONCLUSION

Dental biofilms are aggregates of tooth surface-associated sessile bacteria. They are characterised by phenotype transition of a few bacteria into the so-called state of persisters, cells highly resistant to antibiotics and neutrophil killing. Both persisters and EPS hinder neutrophil killing and prevent destruction of the subgingival biofilm by crevicular neutrophils. Each microbiota depends on environmental factors, so host-related microbiota depends on host genetics and immunity. Ageing of persons developing late-onset periodontitis is a complex process involving various mechanisms that lead to the accumulation of subcellular, cellular, intercellular and other deleterious changes of immunity. Due to neutrophil defects or immunity dysregulation, both a shift in oral microbiota and periodontal damage occur, the homeostasis between host and microbiota is disbalanced and the latter is no more under the complete control of immunity. The inability of immunity to control the biofilm results in biofilm overgrowth and increased number of periodontal pathogens. As a consequence of dysregulated trained immunity, the neutrophils become hyper-responsive. The neutrophil hyper-response is aimed to destroy the pocket pathogens, but they appear to be resistant to NET killing, so gingiva damage occurs, due to the excess of NET proteases and histones. The last two are blameable for damages of epithelial barrier, its penetration by bacteria and PAMPs as well as the stimulation of Th17 cells, resulting in further neutrophil activation and host tissue damage.

AUTHOR CONTRIBUTIONS

Conceptualization and writing—original draft preparation, LV. Writing—review and editing, LV, MH, MHa, JK, LM, SJ, and CS. Funding acquisition, MHa and MH. All authors have read and agreed to the published version of the manuscript.

FUNDING

This research was supported by the German Research Foundation (DFG) Grants No. 2886 PANDORA B3; SCHA 2040/1-1; CRC1181(C03); TRR241(B04), by the EU H2020-FETOPEN-2018-2019-2020-01; 861878 "NeutroCure", and by the Volkswagen-Stiftung (Grant 97744).

ACKNOWLEDGMENTS

We acknowledge support by the Deutsche Forschungsgemeinschaft (DFG, German Research Foundation) and Saarland University within the funding program Open Access Publishing.

REFERENCES

1. Papapanou PN, Sanz M, Buduneli N, Dietrich T, Feres M, Fine DH, et al. Periodontitis: Consensus Report of Workgroup 2 of the 2017 World Workshop on the Classification of Periodontal and Peri-Implant Diseases and Conditions: Classification and Case Definitions for Periodontitis. *J Periodontol* (2018) 89:S173–82. doi: 10.1002/JPER.17-0721
2. Persson GR. Dental Geriatrics and Periodontitis. *Periodontol 2000* (2017) 74 (1):102–15. doi: 10.1111/prd.12192
3. Ebersole JL, Dawson DA, Emecen Huja P, Pandruvada S, Basu A, Nguyen L, et al. Age and Periodontal Health—Immunological View. *Curr Oral Health Rep* (2018) 5(4):229–41. doi: 10.1007/s40496-018-0202-2
4. Billings M, Holtfreter B, Papapanou PN, Mitnik GL, Kocher T, Dye BA. Age-Dependent Distribution of Periodontitis in Two Countries: Findings From NHANES 2009 to 2014 and SHIP-TREND 2008 to 2012. *J Periodontol* (2018) 89:S140–58. doi: 10.1002/JPER.17-0670
5. Bosshardt DD. The Periodontal Pocket: Pathogenesis, Histopathology and Consequences. *Periodontol 2000* (2018) 76(1):43–50. doi: 10.1111/prd.12153
6. Vitkov L, Klappacher M, Hannig M, Krautgartner WD. Extracellular Neutrophil Traps in Periodontitis. *J Periodontal Res* (2009) 44(5):664–72. doi: 10.1111/j.1600-0765.2008.01175.x
7. Vitkov L, Krautgartner WD, Hannig M. Bacterial Internalization in Periodontitis. *Oral Microbiol Immunol* (2005) 20(5):317–21. doi: 10.1111/j.1399-302X.2005.00233.x

8. Vitkov L, Klappacher M, Hannig M, Krautgartner WD. Neutrophil Fate in Gingival Crevicular Fluid. *Ultrastruct Pathol* (2010) 34(1):25–30. doi: 10.3109/01913120903419989
9. Loos BG, Van Dyke TE. The Role of Inflammation and Genetics in Periodontal Disease. *Periodontol 2000* (2020) 83(1):26–39. doi: 10.1111/prd.12297
10. Vitkov L, Muñoz LE, Knopf J, Schauer C, Oberthaler H, Minnich B, et al. Connection Between Periodontitis-Induced Low-Grade Endotoxemia and Systemic Diseases: Neutrophils as Protagonists and Targets. *Int J Mol Sci* (2021) 17:4647. doi: 10.3390/ijms22094647
11. An JY, Kerns KA, Ouellette A, Robinson L, Morris HD, Kaczorowski C, et al. Rapamycin Rejuvenates Oral Health in Aging Mice. *eLife* (2020) 9:e54318. doi: 10.7554/eLife.54318
12. Bhattarai G, Poudel SB, Kook S-H, Lee J-C. Resveratrol Prevents Alveolar Bone Loss in an Experimental Rat Model of Periodontitis. *Acta Ultrastruct* (2016) 29:398–408. doi: 10.1016/j.actbio.2015.10.031
13. Corrêa MG, Pires PR, Ribeiro FV, Pimentel SP, Cirano FR, Napimoga MH, et al. Systemic Treatment With Resveratrol Reduces the Progression of Experimental Periodontitis and Arthritis in Rats. *PloS One* (2018) 13(10): e0204414. doi: 10.1371/journal.pone.0204414
14. Litvak Y, Byndloss MX, Tsolis RM, Bäumler AJ. Dysbiotic Proteobacteria Expansion: A Microbial Signature of Epithelial Dysfunction. *Curr Opin Microbiol* (2017) 39:1–6. doi: 10.1016/j.mib.2017.07.003
15. Tiffany CR, Bäumler AJ. Dysbiosis: From Fiction to Function. *Am J Physiol Gastrointest Liver Physiol* (2019) 317(5):G602–g8. doi: 10.1152/ajpgi.00230.2019
16. Belkaid Y, Harrison OJ. Homeostatic Immunity and the Microbiota. *Immunity* (2017) 46(4):562–76. doi: 10.1016/j.immuni.2017.04.008
17. Shaw L, Ribeiro ALR, Levine AP, Pontikos N, Balloux F, Segal AW, et al. The Human Salivary Microbiome Is Shaped by Shared Environment Rather Than Genetics: Evidence From a Large Family of Closely Related Individuals. *mBio* (2017) 8(5):e01237–17. doi: 10.1128/mBio.01237-17
18. Silva LM, Brenchley L, Moutsopoulos NM. Primary Immunodeficiencies Reveal the Essential Role of Tissue Neutrophils in Periodontitis. *Immunol Rev* (2019) 287(1):226–35. doi: 10.1111/imr.12724
19. Garcia de Aquino S, Manzolli Leite FR, Stach-Machado DR, Francisco da Silva JA, Spolidorio LC, Rossa C. Signaling Pathways Associated With the Expression of Inflammatory Mediators Activated During the Course of Two Models of Experimental Periodontitis. *Life Sci* (2009) 84(21):745–54. doi: 10.1016/j.lfs.2009.03.001
20. de Almeida Brandão D, Spolidorio LC, Johnson F, Golub LM, Guimarães-Stabili MR, Rossa C Jr. Dose-Response Assessment of Chemically Modified Curcumin in Experimental Periodontitis. *J Periodontol* (2019) 90(5):535–45. doi: 10.1002/jper.18-0392
21. Fredriksson MI, Gustafsson AK, Bergström KG, Åsman BE. Constitutionally Hyperreactive Neutrophils in Periodontitis. *J Periodontol* (2003) 74(2):219–24. doi: 10.1902/jop.2003.74.2.219
22. Gustafsson A, Ito H, Asman B, Bergstrom K. Hyper-Reactive Mononuclear Cells and Neutrophils in Chronic Periodontitis. *J Clin Periodontol* (2006) 33 (2):126–9. doi: 10.1111/j.1600-051X.2005.00883.x
23. Matthews JB, Wright HJ, Roberts A, Cooper PR, Chapple ILC. Hyperactivity and Reactivity of Peripheral Blood Neutrophils in Chronic Periodontitis: Neutrophil Hyperactivity and Reactivity in Chronic Periodontitis. *Clin Exp Immunol* (2006) 147(2):255–64. doi: 10.1111/j.1365-2249.2006.03276.x
24. Matthews JB, Wright HJ, Roberts A, Ling-Mountford N, Cooper PR, Chapple IL. Neutrophil Hyper-Responsiveness in Periodontitis. *J Dent Res* (2007) 86(8):718–22. doi: 10.1177/154405910708600806
25. Johnstone AM, Koh A, Goldberg MB. Glogauer M. A Hyperactive Neutrophil Phenotype in Patients With Refractory Periodontitis. *J Periodontol* (2007) 78(9):1788–94. doi: 10.1902/jop.2007.070107
26. Hajishengallis G, Lamont RJ. Dancing With the Stars: How Choreographed Bacterial Interactions Dictate Nososymbiocity and Give Rise to Keystone Pathogens, Accessory Pathogens, and Pathobionts. *Trends Microbiol* (2016) 24(6):477–89. doi: 10.1016/j.tim.2016.02.010
27. Hajishengallis G, Lamont RJ. Polymicrobial Communities in Periodontal Disease: Their Quasi-Organismal Nature and Dialogue With the Host. *Periodontol 2000* (2021) 86(1):210–30. doi: 10.1111/prd.12371
28. Zheng D, Liwinski T, Elinav E. Interaction Between Microbiota and Immunity in Health and Disease. *Cell Res* (2020) 30(6):492–506. doi: 10.1038/s41422-020-0332-7
29. Mombelli A. Microbial Colonization of the Periodontal Pocket and Its Significance for Periodontal Therapy. *Periodontol 2000* (2018) 76(1):85–96. doi: 10.1111/prd.12147
30. Levy RM, Giannobile WV, Feres M, Haffajee AD, Smith C, Socransky SS. The Effect of Apically Repositioned Flap Surgery on Clinical Parameters and the Composition of the Subgingival Microbiota: 12-Month Data. *Int J Periodontics Restor Dent* (2002) 22(3):209–19.
31. Abusleme L, Dupuy AK, Dutzan N, Silva N, Burleson JA, Strausbaugh LD, et al. The Subgingival Microbiome in Health and Periodontitis and Its Relationship With Community Biomass and Inflammation. *Isme J* (2013) 7 (5):1016–25. doi: 10.1038/ismej.2012.174
32. Tsukasaki M, Komatsu N, Nagashima K, Nitta T, Pluemsakunthai W, Shukunami C, et al. Host Defense Against Oral Microbiota by Bone-Damaging T Cells. *Nat Commun* (2018) 9(1):701. doi: 10.1038/s41467-018-03147-6
33. Adler CJ, Dobney K, Weyrich LS, Kaidonis J, Walker AW, Haak W, et al. Sequencing Ancient Calcified Dental Plaque Shows Changes in Oral Microbiota With Dietary Shifts of the Neolithic and Industrial Revolutions. *Nat Genet* (2013) 45(4):450–5. doi: 10.1038/ng.2536
34. Eke PI, Borgnakke WS, Genco RJ. Recent Epidemiologic Trends in Periodontitis in the USA. *Periodontol 2000* (2020) 82(1):257–67. doi: 10.1111/prd.12323
35. Pasicka E, Nowakowski D, Bendrey R, Melnyk OP. A Model for Dental Age Verification Using Ultrastructural Imaging for Modern and Fossil Representatives of the Rhinocerotidae Family. *Animals* (2021) 11(3):910. doi: 10.3390/ani11030910
36. Hershkovitz P. Dental and Periodontal Diseases and Abnormalities in Wild-Caught Marmosets (Primates — Callithricidae). *Am J Phys Anthropol* (1970) 32(3):377–94. doi: 10.1002/ajpa.1330320308
37. Dean MC, Jones ME, Pilley JR. The Natural History of Tooth Wear, Continuous Eruption and Periodontal Disease in Wild Shot Great Apes. *J Hum Evol* (1992) 22(1):23–39. doi: 10.1016/0047-2484(92)90027-7
38. Jakubovics NS, Goodman SD, Mashburn-Warren L, Stafford GP, Cieplik F. The Dental Plaque Biofilm Matrix. *Periodontol 2000* (2021) 86(1):32–56. doi: 10.1111/prd.12361
39. Goo E, An JH, Kang Y, Hwang I. Control of Bacterial Metabolism by Quorum Sensing. *Trends Microbiol* (2015) 23(9):567–76. doi: 10.1016/j.tim.2015.05.007
40. Kumar A, Alam A, Rani M, Ehtesham NZ, Hasnain SE. Biofilms: Survival and Defense Strategy for Pathogens. *Int J Med Microbiol* (2017) 307(8):481–9. doi: 10.1016/j.ijmm.2017.09.016
41. Farkash Y, Feldman M, Ginsburg I, Steinberg D, Shalish M. Polyphenols Inhibit Candida Albicans and Streptococcus Mutans Biofilm Formation. *Dent J (Basel)* (2019) 7(2):42. doi: 10.3390/dj7020042
42. Wang L, Wang Y, Li Q, Tian K, Xu L, Liu G, et al. Exopolysaccharide, Isolated From a Novel Strain Bifidobacterium Breve Lw01 Possess an Anticancer Effect on Head and Neck Cancer - Genetic and Biochemical Evidences. *Front Microbiol* (2019) 10:1044. doi: 10.3389/fmicb.2019.01044
43. Zijnge V, van Leeuwen MB, Degener JE, Abbas F, Thurnheer T, Gmür R, et al. Oral Biofilm Architecture on Natural Teeth. *PloS One* (2010) 5(2): e9321. doi: 10.1371/journal.pone.0009321
44. Wake N, Asahi Y, Noiri Y, Hayashi M, Motooka D, Nakamura S, et al. Temporal Dynamics of Bacterial Microbiota in the Human Oral Cavity Determined Using an *In Situ* Model of Dental Biofilms. *NPJ Biofilms Microbiomes* (2016) 2(1):16018. doi: 10.1038/npjbiofilms.2016.18
45. Blackledge MS, Worthington RJ, Melander C. Biologically Inspired Strategies for Combating Bacterial Biofilms. *Curr Opin Pharmacol* (2013) 13(5):699–706. doi: 10.1016/j.coph.2013.07.004
46. Krsmanovic M, Biswas D, Ali H, Kumar A, Ghosh R, Dickerson AK. Hydrodynamics and Surface Properties Influence Biofilm Proliferation. *Adv Colloid Interface Sci* (2021) 288:102336. doi: 10.1016/j.cis.2020.102336
47. Stoodley P, Sauer K, Davies DG, Costerton JW. Biofilms as Complex Differentiated Communities. *Annu Rev Microbiol* (2002) 56(1):187–209. doi: 10.1146/annurev.micro.56.012302.160705
48. Costerton JW, Lewandowski Z, Caldwell DE, Korber DR, Lappin-Scott HM. Microbial Biofilms. *Annu Rev Microbiol* (1995) 49(1):711–45. doi: 10.1146/annurev.mi.49.100195.003431
49. Rumbaugh KP, Sauer K. Biofilm Dispersion. *Nat Rev Microbiol* (2020) 18 (10):571–86. doi: 10.1038/s41579-020-0385-0

50. Lockhart PB, Brennan MT, Sasser HC, Fox PC, Paster BJ, Bahrani-Mougeot FK. Bacteremia Associated With Toothbrushing and Dental Extraction. *Circulation* (2008) 117(24):3118–25. doi: 10.1161/CIRCULATIONAHA.107.758524
51. Crasta K, Daly CG, Mitchell D, Curtis B, Stewart D, Heitz-Mayfield LJA. Bacteraemia Due to Dental Flossing. *J Clin Periodontol* (2009) 36(4):323–32. doi: 10.1111/j.1600-051X.2008.01372.x
52. Tomás I, Diz P, Tobías A, Scully C, Donos N. Periodontal Health Status and Bacteraemia From Daily Oral Activities: Systematic Review/Meta-Analysis. *J Clin Periodontol* (2012) 39(3):213–28. doi: 10.1111/j.1600-051X.2011.01784.x
53. Zhang J, Kashket S, Lingström P. Evidence for the Early Onset of Gingival Inflammation Following Short-Term Plaque Accumulation: Plaque and Early Onset of Inflammation. *J Clin Periodontol* (2002) 29(12):1082–5. doi: 10.1034/j.1600-051X.2002.291206.x
54. Rubido S, García-Caballero L, Abeleira MT, Limeres J, García M, Diz P. Effect of Chewing an Apple on Dental Plaque Removal and on Salivary Bacterial Viability. *PloS One* (2018) 13(7):e0199812. doi: 10.1371/journal.pone.0199812
55. Martinon P, Fraticelli L, Giboreau A, Dussart C, Bourgeois D, Carrouel F. Nutrition as a Key Modifiable Factor for Periodontitis and Main Chronic Diseases. *J Clin Med* (2021) 10(2):197. doi: 10.3390/jcm10020197
56. Shapira L, Tepper P, Steinberg D. The Interactions of Human Neutrophils With the Constituents of an Experimental Dental Biofilm. *J Dent Res* (2000) 79(10):1802–7. doi: 10.1177/00220345000790101201
57. Gomez A, Espinoza JL, Harkins DM, Leong P, Saffery R, Bockmann M, et al. Host Genetic Control of the Oral Microbiome in Health and Disease. *Cell Host Microbe* (2017) 22(3):269–78.e3. doi: 10.1016/j.chom.2017.08.013
58. Fellows Yates JA, Velsko IM, Aron F, Posth C, Hofman CA, Austin RM, et al. The Evolution and Changing Ecology of the African Hominid Oral Microbiome. *Proc Natl Acad Sci USA* (2021) 118(20):e2021655118. doi: 10.1073/pnas.2021655118
59. Puri S, Vasthare R, Munoli R. The Impact of Sibling Behavior on Oral Health: A Narrative Review. *J Int Soc Prev Community Dent* (2019) 9(2):106–11. doi: 10.4103/jispcd.JISPCD_349_18
60. Lewis K. Persister Cells, Dormancy and Infectious Disease. *Nat Rev Microbiol* (2007) 5(1):48–56. doi: 10.1038/nrmicro1557
61. Conlon BP, Rowe SE, Lewis K. Persister Cells in Biofilm Associated Infections. *Adv Exp Med Biol* (2015) 831:1–9. doi: 10.1007/978-3-319-09782-4_1
62. Keren I, Kaldalu N, Spoering A, Wang Y, Lewis K. Persister Cells and Tolerance to Antimicrobials. *FEMS Microbiol Lett* (2004) 230(1):13–8. doi: 10.1016/S0378-1097(03)00856-5
63. Mizuno N, Kume K, Nagatani Y, Matsuda S, Iwata T, Ouhara K, et al. Aggressive Periodontitis and NOD2 Variants. *J Hum Genet* (2020) 65(10):841–6. doi: 10.1038/s10038-020-0777-z
64. Silva LM, Doyle AD, Tran CL, Greenwell-Wild T, Dutzan N, Lum AG, et al. Fibrin Is a critical regulator of neutrophil effector function at mucosal barrier sites. *bioRxiv* (2021) 2021.01.15.426743. doi: 10.1101/2021.01.15.426743
65. Haworth S, Esberg A, Kuja-Halkola R, Lundberg P, Magnusson PKE, Johansson I. Using National Register Data to Estimate the Heritability of Periodontitis. *J Clin Periodontol* (2021) 48(6):756–64. doi: 10.1111/jcpe.13459
66. Elinav E, Strowig T, Kau Andrew L, Henao-Mejia J, Thaiss Christoph A, Booth Carmen J, et al. NLRP6 Inflammasome Regulates Colonic Microbial Ecology and Risk for Colitis. *Cell* (2011) 145(5):745–57. doi: 10.1016/j.cell.2011.04.022
67. Vijay-Kumar M, Aitken JD, Carvalho FA, Cullender TC, Mwangi S, Srinivasan S, et al. Metabolic Syndrome and Altered Gut Microbiota in Mice Lacking Toll-Like Receptor 5. *Science* (2010) 328(5975):228–31. doi: 10.1126/science.1179721
68. Bonder MJ, Kurilshikov A, Tigchelaar EF, Mujagic Z, Imhann F, Vila AV, et al. The Effect of Host Genetics on the Gut Microbiome. *Nat Genet* (2016) 48(11):1407–12. doi: 10.1038/ng.3663
69. Petnicki-Ocwieja T, Hrncir T, Liu Y-J, Biswas A, Hudcovic T, Tlaskalova-Hogenova H, et al. Nod2 Is Required for the Regulation of Commensal Microbiota in the Intestine. *Proc Natl Acad Sci* (2009) 106(37):15813–8. doi: 10.1073/pnas.0907722106
70. Rehman A, Sina C, Gavrilova O, Häsler R, Ott S, Baines JF, et al. Nod2 Is Essential for Temporal Development of Intestinal Microbial Communities. *Gut* (2011) 60(10):1354–62. doi: 10.1136/gut.2010.216259
71. Kobayashi KS, Chamaillard M, Ogura Y, Henegariu O, Inohara N, Nuñez G, et al. Nod2-Dependent Regulation of Innate and Adaptive Immunity in the Intestinal Tract. *Science* (2005) 307(5710):731–4. doi: 10.1126/science.1104911
72. Henao-Mejia J, Elinav E, Jin C, Hao L, Mehal WZ, Strowig T, et al. Inflammasome-Mediated Dysbiosis Regulates Progression of NAFLD and Obesity. *Nature* (2012) 482(7384):179–85. doi: 10.1038/nature10809
73. Nordlander S, Pott J, Maloy KJ. NLRC4 Expression in Intestinal Epithelial Cells Mediates Protection Against an Enteric Pathogen. *Mucosal Immunol* (2014) 7(4):775–85. doi: 10.1038/mi.2013.95
74. Org E, Parks BW, Joo JW, Emert B, Schwartzman W, Kang EY, et al. Genetic and Environmental Control of Host-Gut Microbiota Interactions. *Genome Res* (2015) 25(10):1558–69. doi: 10.1101/gr.194118.115
75. Benson AK, Kelly SA, Legge R, Ma F, Low SJ, Kim J, et al. Individuality in Gut Microbiota Composition Is a Complex Polygenic Trait Shaped by Multiple Environmental and Host Genetic Factors. *Proc Natl Acad Sci* (2010) 107(44):18933–8. doi: 10.1073/pnas.1007028107
76. Kurilshikov A, Wijmenga C, Fu J, Zhernakova A. Host Genetics and Gut Microbiome: Challenges and Perspectives. *Trends Immunol* (2017) 38(9):633–47. doi: 10.1016/j.it.2017.06.003
77. Knights D, Silverberg MS, Weersma RK, Gevers D, Dijkstra G, Huang H, et al. Complex Host Genetics Influence the Microbiome in Inflammatory Bowel Disease. *Genome Med* (2014) 6(12):107. doi: 10.1186/s13073-014-0107-1
78. Chi Y-C, Chen J-L, Wang L-H, Chang K, Wu C-L, Lin S-Y, et al. Increased Risk of Periodontitis Among Patients With Crohn's Disease: A Population-Based Matched-Cohort Study. *Int J Colorectal Dis* (2018) 33(10):1437–44. doi: 10.1007/s00384-018-3117-4
79. Petit MDA, Steenbergen TJM, Graaff J, Velden U. Transmission of Actinobacillus Actinomycetemcomitans in Families of Adult Periodontitis Patients. *J Periodontal Res* (1993) 28(5):335–45. doi: 10.1111/j.1600-0765.1993.tb01077.x
80. Beikler T, Bunte K, Chan Y, Weiher B, Selbach S, Peters U, et al. Oral Microbiota Transplant in Dogs With Naturally Occurring Periodontitis. *J Dental Res* (2021) 100(7):764–70. doi: 10.1177/0022034521995423
81. Ng E, Tay JRH, Ong MMA, Bostanci N, Belibasakis GN, Seneviratne CJ. Probiotic Therapy for Periodontal and Peri-Implant Health - Silver Bullet or Sham? *Benef Microbes* (2021) 12(3):215–30. doi: 10.3920/bm2020.0182
82. Liu J, Liu Z, Huang J, Tao R. Effect of Probiotics on Gingival Inflammation and Oral Microbiota: A Meta-Analysis. *Oral Dis* (2021) 1–10. doi: 10.1111/odi.13861
83. Blekhman R, Man O, Herrmann L, Boyko AR, Indap A, Kosiol C, et al. Natural Selection on Genes That Underlie Human Disease Susceptibility. *Curr Biol* (2008) 18(12):883–9. doi: 10.1016/j.cub.2008.04.074
84. Ferrucci L, Gonzalez-Freire M, Fabbri E, Simonsick E, Tanaka T, Moore Z, et al. Measuring Biological Aging in Humans: A Quest. *Aging Cell* (2020) 19(2):e13080. doi: 10.1111/acel.13080
85. Gladyshev VN. Aging: Progressive Decline in Fitness Due to the Rising Deleteriome Adjusted by Genetic, Environmental, and Stochastic Processes. *Aging Cell* (2016) 15(4):594–602. doi: 10.1111/acel.12480
86. Horvath S, Raj K. DNA Methylation-Based Biomarkers and the Epigenetic Clock Theory of Ageing. *Nat Rev Genet* (2018) 19(6):371–84. doi: 10.1038/s41576-018-0004-3
87. Maekawa T, Briones RA, Resuello RRG, Tuplano JV, Hajishengallis E, Kajikawa T, et al. Inhibition of Pre-Existing Natural Periodontitis in Non-Human Primates by a Locally Administered Peptide Inhibitor of Complement C3. *J Clin Periodontol* (2016) 43(3):238–49. doi: 10.1111/jcpe.12507
88. Borsanelli AC, Lappin DF, Viora L, Bennett D, Dutra IS, Brandt BW, et al. Microbiomes Associated With Bovine Periodontitis and Oral Health. *Vet Microbiol* (2018) 218:1–6. doi: 10.1016/j.vetmic.2018.03.016
89. Dvorak G, Reich K, Tangl S, Lill CA, Gottschalk-Baron M, Watzek G, et al. Periodontal Histomorphometry and Status of Aged Sheep Subjected to Ovariectomy, Malnutrition and Glucocorticoid Application. *Arch Oral Biol* (2009) 54(9):857–63. doi: 10.1016/j.archoralbio.2009.05.010

90. Liang S, Hosur KB, Domon H, Hajishengallis G. Periodontal Inflammation and Bone Loss in Aged Mice. *J Periodontal Res* (2010) 45:574–8. doi: 10.1111/j.1600-0765.2009.01245.x
91. Rodrigues MX, Bicalho RC, Fiani N, Lima SF, Peralta S. The Subgingival Microbial Community of Feline Periodontitis and Gingivostomatitis: Characterization and Comparison Between Diseased and Healthy Cats. *Sci Rep* (2019) 9(1):12340. doi: 10.1038/s41598-019-48852-4
92. Page RC, Schroeder HE. Spontaneous Chronic Periodontitis in Adult Dogs: A Clinical and Histopathological Survey. *J Periodontol* (1981) 52(2):60–73. doi: 10.1902/jop.1981.52.2.60
93. Eshed V, Gopher A, Hershkovitz I. Tooth Wear and Dental Pathology at the Advent of Agriculture: New Evidence From the Levant. *Am J Phys Anthropol* (2006) 130(2):145–59. doi: 10.1002/ajpa.20362
94. Vijg J, Dong X. Pathogenic Mechanisms of Somatic Mutation and Genome Mosaicism in Aging. *Cell* (2020) 182(1):12–23. doi: 10.1016/j.cell.2020.06.024
95. Elsayed R, Elashiry M, Liu Y, El-Awady A, Hamrick M, Cutler CW. Porphyromonas Gingivalis Provokes Exosome Secretion and Paracrine Immune Senescence in Bystander Dendritic Cells. *Front Cell Infect Microbiol* (2021) 11:669989. doi: 10.3389/fcimb.2021.669989
96. Tamboli CP, Neut C, Desreumaux P, Colombel JF. Dysbiosis in Inflammatory Bowel Disease. *Gut* (2004) 53(1):1–4. doi: 10.1136/gut.53.1.1
97. Mazmanian SK, Round JL, Kasper DL. A Microbial Symbiosis Factor Prevents Intestinal Inflammatory Disease. *Nature* (2008) 453(7195):620–5. doi: 10.1038/nature07008
98. Bäumler AJ, Sperandio V. Interactions Between the Microbiota and Pathogenic Bacteria in the Gut. *Nature* (2016) 535(7610):85–93. doi: 10.1038/nature18849
99. Consortium THMP. Structure, Function and Diversity of the Healthy Human Microbiome. *Nature* (2012) 486(7402):207–14. doi: 10.1038/nature11234
100. consortium tiHirN. The Integrative Human Microbiome Project. *Nature* (2019) 569(7758):641–8. doi: 10.1038/s41586-019-1238-8
101. Lloyd-Price J, Mahurkar A, Rahnavard G, Crabtree J, Orvis J, Hall AB, et al. Strains, Functions and Dynamics in the Expanded Human Microbiome Project. *Nature* (2017) 550(7674):61–6. doi: 10.1038/nature23889
102. Byndloss MX, Litvak Y, Bäumler AJ. Microbiota-Nourishing Immunity and Its Relevance for Ulcerative Colitis. *Inflammation Bowel Dis* (2019) 25 (5):811–5. doi: 10.1093/ibd/izz004
103. Hashim A, Alsam A, Payne MA, Aduse-Opoku J, Curtis MA, Joseph S. Loss of Neutrophil Homing to the Periodontal Tissues Modulates the Composition and Disease Potential of the Oral Microbiota. *Infect Immun* (2021) 89(12):e0030921. doi: 10.1128/iai.00309-21
104. Li Y, Karlin A, Loike JD, Silverstein SC. Determination of the Critical Concentration of Neutrophils Required to Block Bacterial Growth in Tissues. *J Exp Med* (2004) 200(5):613–22. doi: 10.1084/jem.20040725
105. Chen GY, Nuñez G. Sterile Inflammation: Sensing and Reacting to Damage. *Nat Rev Immunol* (2010) 10(12):826–37. doi: 10.1038/nri2873
106. Kruger P, Saffarzadeh M, Weber ANR, Rieber N, Radsak M, von Bernuth H, et al. Neutrophils: Between Host Defence, Immune Modulation, and Tissue Injury. *PloS Pathog* (2015) 11(3):e1004651. doi: 10.1371/journal.ppat.1004651
107. Saffarzadeh M, Juenemann C, Queisser MA, Lochnit G, Barreto G, Galuska SP, et al. Neutrophil Extracellular Traps Directly Induce Epithelial and Endothelial Cell Death: A Predominant Role of Histones. *PloS One* (2012) 7 (2):e32366. doi: 10.1371/journal.pone.0032366
108. Castanheira FVS, Kubes P. Neutrophils and NETs in Modulating Acute and Chronic Inflammation. *Blood* (2019) 133(20):2178–85. doi: 10.1182/blood-2018-11-844530
109. Carmona-Rivera C, Carlucci PM, Goel RR, James E, Brooks SR, Rims C, et al. Neutrophil Extracellular Traps Mediate Articular Cartilage Damage and Enhance Cartilage Component Immunogenicity in Rheumatoid Arthritis. *JCI Insight* (2020) 5(13):e139388. doi: 10.1172/jci.insight.139388
110. Netea MG, Domínguez-Andrés J, Barreiro LB, Chavakis T, Divangahi M, Fuchs E, et al. Defining Trained Immunity and Its Role in Health and Disease. *Nat Rev Immunol* (2020) 20(6):375–88. doi: 10.1038/s41577-020-0285-6
111. Geng S, Zhang Y, Lee C, Li L. Novel Reprogramming of Neutrophils Modulates Inflammation Resolution During Atherosclerosis. *Sci Adv* (2019) 5(2):eaav2309. doi: 10.1126/sciadv.aav2309
112. Hamam, Palaniyar. Post-Translational Modifications in NETosis and NETs-Mediated Diseases. *Biomolecules* (2019) 9(8):369. doi: 10.3390/biom9080369
113. Hamam H, Khan M, Palaniyar N. Histone Acetylation Promotes Neutrophil Extracellular Trap Formation. *Biomolecules* (2019) 9(1):32. doi: 10.3390/biom9010032
114. Hirschfeld J, White PC, Milward MR, Cooper PR, Chapple ILC. Modulation of Neutrophil Extracellular Trap and Reactive Oxygen Species Release by Periodontal Bacteria. *Infect Immun* (2017) 85(12):1404. doi: 10.1128/IAI.00297-17
115. Vitkov L, Hartl D, Minnich B, Hannig M. Janus-Faced Neutrophil Extracellular Traps in Periodontitis. *Front Immunol* (2017) 8:1404. doi: 10.3389/fimmu.2017.01404
116. Abbas AK, Lichtman AH, Pillai S, Baker DL, Baker A. *Cellular and Molecular Immunology. Ninth Edition Ed* Vol. 2018. Philadelphia, PA: Elsevier (2018). p. 565.
117. Armitage GC, Jeffcoat MK, Chadwick DE, Taggart EJ, Numabe Y, Landis JR, et al. Longitudinal Evaluation of Elastase as a Marker for the Progression of Periodontitis. *J Periodontol* (1994) 65(2):120–8. doi: 10.1902/jop.1994.65.2.120
118. Mäntylä P, Stenman M, Kinane DF, Tikanoja S, Luoto H, Salo T, et al. Gingival Crevicular Fluid Collagenase-2 (MMP-8) Test Stick for Chair-Side Monitoring of Periodontitis: MMP-8 Test in Monitoring Periodontitis. *J Periodontal Res* (2003) 38(4):436–9. doi: 10.1034/j.1600-0765.2003.00677.x
119. Sorsa T, Tervahartiala T, Leppilahti J, Hernandez M, Gamonal J, Tuomainen AM, et al. Collagenase-2 (MMP-8) as a Point-of-Care Biomarker in Periodontitis and Cardiovascular Diseases. Therapeutic Response to Non-Antimicrobial Properties of Tetracyclines. *Pharmacol Res* (2011) 63(2):108–13. doi: 10.1016/j.phrs.2010.10.005
120. Sorsa T, Gursoy UK, Nwhator S, Hernandez M, Tervahartiala T, Leppilahti J, et al. Analysis of Matrix Metalloproteinases, Especially MMP-8, in Gingival Crevicular Fluid, Mouthrinse and Saliva for Monitoring Periodontal Diseases. *Periodontol 2000* (2016) 70(1):142–63. doi: 10.1111/prd.12101
121. Domon H, Nagai K, Maekawa T, Oda M, Yonezawa D, Takeda W, et al. Neutrophil Elastase Subverts the Immune Response by Cleaving Toll-Like Receptors and Cytokines in Pneumococcal Pneumonia. *Front Immunol* (2018) 9:732. doi: 10.3389/fimmu.2018.00732
122. Vanaja Sivapriya K, Russo Ashley J, Behl B, Banerjee I, Yankova M, Deshmukh Sachin D, et al. Bacterial Outer Membrane Vesicles Mediate Cytosolic Localization of LPS and Caspase-11 Activation. *Cell* (2016) 165 (5):1106–19. doi: 10.1016/j.cell.2016.04.015
123. Chen KW, Monteleone M, Boucher D, Sollberger G, Ramnath D, Condon ND, et al. Noncanonical Inflammasome Signaling Elicits Gasdermin D–dependent Neutrophil Extracellular Traps. *Sci Immunol* (2018) 3(26): eaar6676. doi: 10.1126/sciimmunol.aar6676
124. Sutterlin HA, Shi H, May KL, Miguel A, Khare S, Huang KC, et al. Disruption of Lipid Homeostasis in the Gram-Negative Cell Envelope Activates a Novel Cell Death Pathway. *Proc Natl Acad Sci USA* (2016) 113 (11):E1565–74. doi: 10.1073/pnas.1601375113
125. Nagakubo T, Nomura N, Toyofuku M. Cracking Open Bacterial Membrane Vesicles. *Front Microbiol* (2020) 10:3026. doi: 10.3389/fmicb.2019.03026
126. Papayannopoulos V. Neutrophil Extracellular Traps in Immunity and Disease. *Nat Rev Immunol* (2018) 18(2):134–47. doi: 10.1038/nri.2017.105
127. Hakkim A, Fuchs TA, Martinez NE, Hess S, Prinz H, Zychlinsky A, et al. Activation of the Raf-MEK-ERK Pathway Is Required for Neutrophil Extracellular Trap Formation. *Nat Chem Biol* (2011) 7(2):75–7. doi: 10.1038/nchembio.496
128. Hagar JA, Powell DA, Aachoui Y, Ernst RK, Miao EA. Cytoplasmic LPS Activates Caspase-11: Implications in TLR4-Independent Endotoxic Shock. *Science* (2013) 341(6151):1250–3. doi: 10.1126/science.1240988
129. Kayagaki N, Wong MT, Stowe IB, Ramani SR, Gonzalez LC, Akashi-Takamura S, et al. Noncanonical Inflammasome Activation by Intracellular LPS Independent of TLR4. *Science* (2013) 341(6151):1246–9. doi: 10.1126/science.1240248
130. Shi J, Zhao Y, Wang Y, Gao W, Ding J, Li P, et al. Inflammatory Caspases Are Innate Immune Receptors for Intracellular LPS. *Nature* (2014) 514 (7521):187–92. doi: 10.1038/nature13683
131. Bryzek D, Ciaston I, Dobosz E, Gasiorek A, Makarska A, Sarna M, et al. Triggering NETosis *via* Protease-Activated Receptor (PAR)-2 Signaling as a Mechanism of Hijacking Neutrophils Function for Pathogen Benefits. *PloS Pathog* (2019) 15(5):e1007773. doi: 10.1371/journal.ppat.1007773

132. Figueredo CMS, Fischer RG, Gustafsson A. Aberrant Neutrophil Reactions in Periodontitis. *J Periodontol* (2005) 76(6):951–5. doi: 10.1902/jop.2005.76.6.951
133. An S, Raju I, Surenkhuu B, Kwon J-E, Gulati S, Karaman M, et al. Neutrophil Extracellular Traps (NETs) Contribute to Pathological Changes of Ocular Graft-vs.-Host Disease (oGVHD) Dry Eye: Implications for Novel Biomarkers and Therapeutic Strategies. *Ocular Surf* (2019) 17(3):589–614. doi: 10.1016/j.jtos.2019.03.010
134. WHO. Epidemiology, Etiology, and Prevention of Periodontal Diseases. Report of a WHO Scientific Group. *World Health Organ Tech Rep Ser* (1978) 621):1–60.
135. Allam R, Scherbaum CR, Darisipudi MN, Mulay SR, Hägele H, Lichtnekert J, et al. Histones From Dying Renal Cells Aggravate Kidney Injury *via* TLR2 and TLR4. *J Am Soc Nephrol* (2012) 23(8):1375–88. doi: 10.1681/ASN.2011111077
136. Wei Z, Wang J, Wang Y, Wang C, Liu X, Han Z, et al. Effects of Neutrophil Extracellular Traps on Bovine Mammary Epithelial Cells *In Vitro*. *Front Immunol* (2019) 10:1003. doi: 10.3389/fimmu.2019.01003
137. Knopf J, Leppkes M, Schett G, Herrmann M, Muñoz LE. Aggregated NETs Sequester and Detoxify Extracellular Histones. *Front Immunol* (2019) 10:2176. doi: 10.3389/fimmu.2019.02176
138. Wong SL, Demers M, Martinod K, Gallant M, Wang Y, Goldfine AB, et al. Diabetes Primes Neutrophils to Undergo NETosis, Which Impairs Wound Healing. *Nat Med* (2015) 21(7):815–9. doi: 10.1038/nm.3887
139. Tonello S, Rizzi M, Migliario M, Rocchetti V, Renò F. Low Concentrations of Neutrophil Extracellular Traps Induce Proliferation in Human Keratinocytes *via* NF-kB activation. *J Dermatol Sci* (2017) 88(1):110–6. doi: 10.1016/j.jdermsci.2017.05.010
140. Podolska MJ, Mahajan A, Hahn J, Knopf J, Maueröder C, Petru L, et al. Treatment With DNases Rescues Hidden Neutrophil Elastase From Aggregated NETs. *J Leuk Biol* (2019) 106(6):1359–66. doi: 10.1002/JLB.3AB0918-370R
141. MacPherson M, Pho M, Cox J, Armstrong J, Darling MR, McCord C. Ligneous Gingivitis Secondary to Plasminogen Deficiency: A Multidisciplinary Diagnostic Challenge. *Oral Surg Oral Med Oral Pathol Oral Radiol* (2020) 130(3):e87–95. doi: 10.1016/j.oooo.2019.12.014
142. Luyendyk JP, Schoenecker JG, Flick MJ. The Multifaceted Role of Fibrinogen in Tissue Injury and Inflammation. *Blood* (2019) 133(6):511–20. doi: 10.1182/blood-2018-07-818211
143. Heyworth PG, Cross AR, Curnutte JT. Chronic Granulomatous Disease. *Curr Opin Immunol* (2003) 15(5):578–84. doi: 10.1016/s0952-7915(03)00109-2
144. Cohen MS, Leong PA, Simpson DM. Phagocytic Cells in Periodontal Defense. Periodontal Status of Patients With Chronic Granulomatous Disease of Childhood. *J Periodontol* (1985) 56(10):611–7. doi: 10.1902/jop.1985.56.10.611
145. Buduneli N, Baylas H, Aksu G, Kutukculer N. Prepubertal Periodontitis Associated With Chronic Granulomatous Disease. *J Clin Periodontol* (2001) 28(6):589–93. doi: 10.1034/j.1600-051x.2001.028006589.x
146. Dar-Odeh NS, Hayajneh WA, Abu-Hammad OA, Hammad HM, Al-Wahadneh AM, Bulos NK, et al. Orofacial Findings in Chronic Granulomatous Disease: Report of Twelve Patients and Review of the Literature. *BMC Res Notes* (2010) 3:37. doi: 10.1186/1756-0500-3-37
147. Winkelstein JA, Marino MC, Johnston RB Jr, Boyle J, Curnutte J, Gallin JI, et al. Chronic Granulomatous Disease. Report on a National Registry of 368 Patients. *Med (Baltimore)* (2000) 79(3):155–69. doi: 10.1097/00005792-200005000-00003
148. Chapple IL, Matthews JB. The Role of Reactive Oxygen and Antioxidant Species in Periodontal Tissue Destruction. *Periodontol 2000* (2007) 43:160–232. doi: 10.1111/j.1600-0757.2006.00178.x
149. Chang AM, Kantrong N, Darveau RP. Maintaining Homeostatic Control of Periodontal Epithelial Tissue. *Periodontol 2000* (2021) 86(1):188–200. doi: 10.1111/prd.12369
150. Greer A, Irie K, Hashim A, Leroux BG, Chang AM, Curtis MA, et al. Site-Specific Neutrophil Migration and CXCL2 Expression in Periodontal Tissue. *J Dent Res* (2016) 95(8):946–52. doi: 10.1177/0022034516641036
151. Uehara A, Takada H. Functional TLRs and NODs in Human Gingival Fibroblasts. *J Dent Res* (2007) 86(3):249–54. doi: 10.1177/154405910708600310
152. Williams DW, Greenwell-Wild T, Brenchley L, Dutzan N, Overmiller A, Sawaya AP, et al. Human Oral Mucosa Cell Atlas Reveals a Stromal-Neutrophil Axis Regulating Tissue Immunity. *Cell* (2021) 184(15):4090–104.e15. doi: 10.1016/j.cell.2021.05.013
153. Landzberg M, Doering H, Aboodi GM, Tenenbaum HC, Glogauer M. Quantifying Oral Inflammatory Load: Oral Neutrophil Counts in Periodontal Health and Disease. *J Periodontal Res* (2015) 50(3):330–6. doi: 10.1111/jre.12211
154. Aleyd E, Al M, Tuk CW, van der Laken CJ, van Egmond M. IgA Complexes in Plasma and Synovial Fluid of Patients With Rheumatoid Arthritis Induce Neutrophil Extracellular Traps *via* Fcαri. *J Immunol* (2016) 197(12):4552–9. doi: 10.4049/jimmunol.1502353
155. Aleyd E, Heineke MH, van Egmond M. The Era of the Immunoglobulin A Fc Receptor Fcαri; Its Function and Potential as Target in Disease. *Immunol Rev* (2015) 268(1):123–38. doi: 10.1111/imr.12337
156. Aleyd E, van Hout MWM, Ganzevles SH, Hoeben KA, Everts V, Bakema JE, et al. IgA Enhances NETosis and Release of Neutrophil Extracellular Traps by Polymorphonuclear Cells *via* Fcα Receptor I. *J Immunol* (2014) 192(5):2374–83. doi: 10.4049/jimmunol.1300261
157. Dutzan N, Abusleme L. T Helper 17 Cells as Pathogenic Drivers of Periodontitis. In: Belibasakis GN, Hajishengallis G, Bostanci N, Curtis MA, editors. *Oral Mucosal Immunity and Microbiome*, vol. 1197. Cham: Springer International Publishing (2019). p. 107–17.

Conflict of Interest: The authors declare that the research was conducted in the absence of any commercial or financial relationships that could be construed as a potential conflict of interest.

Publisher's Note: All claims expressed in this article are solely those of the authors and do not necessarily represent those of their affiliated organizations, or those of the publisher, the editors and the reviewers. Any product that may be evaluated in this article, or claim that may be made by its manufacturer, is not guaranteed or endorsed by the publisher.

frontiers | Frontiers in Immunology

REVIEW
published: 07 July 2022
doi: 10.3389/fimmu.2022.915081

The Roles of Neutrophils Linking Periodontitis and Atherosclerotic Cardiovascular Diseases

*Rizky A. Irwandi[1], Scott T. Chiesa[2], George Hajishengallis[3], Venizelos Papayannopoulos[4], John E. Deanfield[2] and Francesco D'Aiuto[1]**

[1] Periodontology Unit, UCL Eastman Dental Institute, University College London, London, United Kingdom, [2] UCL Institute of Cardiovascular Science, University College London, London, United Kingdom, [3] Department of Basic & Translational Sciences, Laboratory of Innate Immunity & Inflammation, Penn Dental Medicine, University of Pennsylvania, Philadelphia, PA, United States, [4] Antimicrobial Defense Laboratory, The Francis Crick Institute, London, United Kingdom

Inflammation plays a crucial role in the onset and development of atherosclerosis. Periodontitis is a common chronic disease linked to other chronic inflammatory diseases such as atherosclerotic cardiovascular disease (ASCVD). The mechanistic pathways underlying this association are yet to be fully understood. This critical review aims at discuss the role of neutrophils in mediating the relationship between periodontitis and ASCVD. Systemic inflammation triggered by periodontitis could lead to adaptations in hematopoietic stem and progenitor cells (HSPCs) resulting in trained granulopoiesis in the bone marrow, thereby increasing the production of neutrophils and driving the hyper-responsiveness of these abundant innate-immune cells. These alterations may contribute to the onset, progression, and complications of atherosclerosis. Despite the emerging evidence suggesting that the treatment of periodontitis improves surrogate markers of cardiovascular disease, the resolution of periodontitis may not necessarily reverse neutrophil hyper-responsiveness since the hyper-inflammatory re-programming of granulopoiesis can persist long after the inflammatory inducers are removed. Novel and targeted approaches to manipulate neutrophil numbers and functions are warranted within the context of the treatment of periodontitis and also to mitigate its potential impact on ASCVD.

Keywords: neutrophils, systemic inflammation, trained immunity, innate immune memory, periodontitis, periodontal disease, atherosclerosis, atherosclerotic cardiovascular disease

OPEN ACCESS

Edited by:
Martin Herrmann, University Hospital Erlangen, Germany

Reviewed by:
Mallary Greenlee-Wacker, Central Michigan University, United States
Katherine C. MacNamara, Albany Medical College, United States

***Correspondence:**
Francesco D'Aiuto
f.daiuto@ucl.ac.uk

Specialty section:
This article was submitted to Molecular Innate Immunity, a section of the journal Frontiers in Immunology

Received: *07 April 2022*
Accepted: *13 June 2022*
Published: *07 July 2022*

Citation:
Irwandi RA, Chiesa ST, Hajishengallis G, Papayannopoulos V, Deanfield JE and D'Aiuto F (2022) The Roles of Neutrophils Linking Periodontitis and Atherosclerotic Cardiovascular Diseases. Front. Immunol. 13:915081. doi: 10.3389/fimmu.2022.915081

INTRODUCTION

Atherosclerotic cardiovascular disease (ASCVD) consists of a group of disorders that affect the heart and blood vessels (1) and include coronary heart disease, cerebrovascular disease, and peripheral vascular disease (2). ASCVD is a major cause of global mortality and a leading contributor to disability as it causes 18.6 million deaths and contributes to 34.4 million people living with disability in 2019 (3). Although its pathogenesis, progression, and complications comprise multiple complex processes, inflammation plays a key role in each stage of the disease (4).

Periodontitis is a common chronic inflammatory disease caused by oral microbial dysbiosis. The onset and progression of the disease could span over decades and is influenced by genetic and environmental factors. This prevalent oral disease is characterized by progressive destruction of hard and soft tissues supporting the tooth, including the periodontal ligament and alveolar bone (5). Untreated periodontitis leads inevitably not only to tooth loss but also to masticatory impairment and negative influences on the quality of life of a patient (6). Like ASCVD, periodontitis is a major public health concern as it affects over half of the population of the world (7) and 5–15% of the global population presents a severe form of the disease (8), causing increased costs of oral healthcare (9).

The evidence linking periodontitis to systemic diseases has previously focused on the findings that periodontal bacteria and their endotoxins disseminate physically through the blood circulation (10, 11). However, periodontitis also triggers systemic inflammation, indicated by an increased level of C-reactive protein (CRP), TNFα, IL-1β, and IL-6 in the serum of patients (2). Because of chronic inflammation occurring at the periodontium, endotoxemia, bacteremia, and systemic inflammation are collectively implicated in numerous systemic diseases, including atherosclerotic cardiovascular disease (ASCVD) (12–14).

Neutrophils are the most abundant inflammatory cells in humans and the first-line defense against infection in the innate-arm of the immune system. They are derived from the myeloid differentiation lineage of hematopoietic stem cells (HSCs) in the bone marrow. Upon detection of pathogens, neutrophils capture and destroy invading pathogens *via* phagocytosis and intracellular degradation, degranulation, and the formation of neutrophil extracellular traps (NETs) (15). Moreover, the emerging evidence over the past decade reveals that neutrophils are involved in chronic inflammation and are implicated in chronic inflammatory disorders, including periodontitis and ASCVD (16–20). Periodontitis appears to be associated with hyper-responsive neutrophils (21–23), which might, at least in part, be attributed to the notion that oral disease could influence hematopoietic tissue activity and trained immunity (12). Trained immunity represents a non-specific memory in innate immune cells that is induced by earlier encounters with infectious or inflammatory stimuli and which promotes increased immune responses to future challenges with the same or different stimuli (24, 25). Meanwhile, in ASCVD, neutrophils contribute to different stages and clinical manifestations of atherosclerosis (26) and literature also suggests that inflammation-adapted hematopoietic stem and progenitor cells (HSPCs) may contribute to the disease pathogenesis (27–29). As such, recent consensus between the European Federation of Periodontology and the World Heart Federation includes neutrophil hyper-responsiveness as one of the mechanisms to explain the epidemiological association between periodontitis and ASCVD (2).

Mechanisms linking periodontitis to ASCVD and the effect of periodontitis treatment in improving the surrogate markers of ASCVD in an attempt to show causal interactions between the two diseases have been extensively explored (2, 14). However, the causal mechanistic pathways between these two common non-communicable diseases are yet to be fully understood. In this review, we aim to critically address the role of neutrophils in linking periodontitis to ASCVD. Systemic inflammation triggered by different causes, including periodontitis, may drive inflammatory adaptation of HSPCs and trained granulopoiesis in the bone marrow, resulting in increased production of neutrophils with a hyper-responsive phenotype (12, 30). This systemic inflammation-driven modification of granulopoiesis can contribute to atherosclerosis in a stage-dependent manner. However, although the periodontitis treatment successfully achieves the resolution of the periodontal tissue site and improves surrogate markers of ASCVD, studies reveal that the hyper-responsive function in neutrophils may persist (23, 31). Therefore, novel approaches to target neutrophils by manipulating their numbers and functions are warranted in periodontitis treatment and to mitigate its impact on ASCVD.

THE LINK BETWEEN PERIODONTITIS AND ASCVD

The impact of the treatment of periodontitis on cardiovascular outcomes and surrogate markers of ASCVD has been extensively explored. Patients with periodontitis exhibit an increased risk of coronary and cerebrovascular events compared with periodontally healthy individuals. These findings may not apply to the whole population as influenced by the demographic characteristics, individuals, studies, and case definition of periodontitis (2, 32). In the ARIC study on 6736 dentate participants with 299 incidents of ischemic stroke, it was revealed that seven periodontal profile classes, that were used to assess the participants were associated with an increased risk of cardioembolic and thrombotic stroke subtypes compared with periodontally healthy participants. The assessment in this study was based on seven tooth-clinical parameters, resulting in seven different periodontal profile classes, and the greater class indicates a more severe form of periodontitis (33). Lastly, based on the 1999–2010 Taiwanese National Health Insurance Research Database involving 393,745 patients with periodontitis and 393,745 non-periodontitis individuals, there was a significantly increased incidence of arterial fibrillation in patients with periodontitis compared with controls (34). The findings from all studies had been adjusted for a wide range of potential confounders, indicating that periodontitis is an independent risk factor for an increased risk of ASCVD events.

Treatment of periodontitis may influence the progression of ASCVD. The study involving 511,630 periodontitis patients and 208,713 individuals without periodontitis from The Longitudinal Database of Taiwan's National Health Insurance demonstrated that patients receiving dental prophylaxis had a lower hazard ratio of acute myocardial infarction compared to periodontally healthy controls, suggesting an almost 10% reduction in the risk of a new ASCVD event (35). These improvements were not observed across all types of periodontitis and controls, suggesting

a difference in host susceptibility and response even after the treatment of peridontitis when looking at future incidence of ASCVD events (36).

Consistent evidence suggests that periodontitis is associated with higher blood pressure and endothelial dysfunction (2, 37–39). A recent review and subsequent meta-analysis of intervention studies confirmed that the management of periodontitis can be a novel non-drug approach for the treatment of hypertension. The evidence is still inconclusive as to whether the treatment of periodontitis influences blood pressure even in the absence of hypertension (40). The basis of this improvement in vascular function could be linked to the effect of the treatment of periodontitis in improving endothelial function as assessed by flow-mediated dilation (FMD) (41–44). A possible mechanism by which local periodontal treatment improves endothelial function in periodontitis patients is endothelial nitric oxide synthase/nitric oxide (eNOS/NO) activation. NO is mainly produced by eNOS in endothelial cells and induces the relaxation of smooth muscle cells (45, 46). Meanwhile, IL-6, TNFα, IL-1β, and CRP directly reduced eNOS at both mRNA and protein levels in human endothelial cells (47–49). As a result, NO bioavailability in the serum is reduced, leading to endothelial dysfunction and periodontitis is associated with this surrogate marker of ASCVD (50, 51). Hepatocytes are the major producers of CRP triggered by IL-6 and IL-1β stimulation, while TNFα also upregulates CRP production in human coronary artery smooth muscle cells (52–55). A recent meta-analysis reveals a progressive CRP level reduction up to 6 months in patients with periodontitis following effective treatment (37). This was also associated with a reduction of reduced serum IL-6, TNFα, and IL-1β in patients with periodontitis compared to baseline (56–59). Collectively, these findings suggest that reduced levels of CRP, IL-6, TNFα, and IL-1β after treatment of periodontitis could restore eNOS activity and NO bioavailability, resulting in improved endothelial dysfunction.

PERIODONTITIS AS A TRIGGER OF SYSTEMIC INFLAMMATION

Periodontitis and ASCVD share similar hallmarks of inflammatory mechanisms (60), genetic (2, 61), and common risk factors (62). However, a significant body of evidence supports an independent association between periodontitis and ASCVD following adjustment for confounders and shared risk factors (63, 64). This independent association can be explained by the capability of periodontitis to trigger a low-grade but consistent systemic inflammation, which may contribute to the development of ASCVD (65). Patients with periodontitis exhibit an elevated level of systemic pro-inflammatory mediators, which include CRP, TNFα, IL-1β, IL-6, as well as increased neutrophil numbers in the blood (2, 14, 66–69). A retrospective study involving 60,174 participants revealed that even after the adjustment of confounders, participants with periodontitis were 1.59 times more likely to have ASCVD (63). Previously, an 8-year prospective cohort study involving 11,869 participants also showed that those reporting poor oral hygiene had an enhanced risk of CVD events as well as an elevated level of CRP and fibrinogen in the serum (70).

Systemic inflammation triggered by periodontitis potentially occurs because of bacterial dissemination or periodontal tissue-derived inflammatory mediator leakage into the blood circulation. The ulceration of the epithelium owing to local periodontal inflammation along with the support of its rich vascularization may provide greater access for bacteria and their endotoxins such as lipopolysaccharides (LPS) to the circulation, leading to bacteremia (13). This event has been reported in patients with periodontitis during mastication, toothbrushing, and dental scaling (10, 11). Bacteremia would induce inflammatory alterations in the endothelium, which include enhanced expression of adhesion molecules and the production of pro-inflammatory cytokines. With regard to the spillover of inflammatory mediators into the bloodstream, this can affect vascular tissues as well as other distant organs, including the liver, which then may initiate an acute-phase response (14).

INFLAMMATION AND NEUTROPHILS: IMPLICATIONS FOR ATHEROSCLEROSIS

Atherosclerosis is a cause of myocardial infarction, ischemic cardiomyopathy, and ischemic stroke that contribute to most deaths in the population worldwide (4). Arterial wall damage due to blood lipid profile imbalance, oscillating shear stress, and pro-inflammatory mediators initiates this underlying ASCVD pathology. The subsequent processes are endothelial cell activation in arterial tissue, myeloid cell adhesion to the endothelium, and infiltration into the arterial intima (26). At the late stage of atherosclerosis, inflammatory cell accumulation, lipoprotein deposition, and cellular debris buildup are responsible for the arterial plaque formation followed by the plaque instability leading to atherosclerotic plaque rupture. Atherosclerosis is a decades-long process with many stages of evolution, and evidence suggests that neutrophils are involved in different stages of atherosclerosis (**Figure 1**) (26).

The onset of atherosclerosis is characterized by endothelial dysfunction, which induces neutrophil recruitment to the endothelium. Specifically, the dysfunction up-regulates the expression of various endothelial cell adhesion molecules, including E-selectin, P-selectin, and intracellular adhesion molecule-1 (ICAM-1) (71). Platelets then deliver CCL5, the primary ligand of CCR5 on the endothelium and promote cathepsin G secretion by neutrophils, resulting in the firm adhesion to and accumulation of the cells in the endothelium (72, 73). Furthermore, neutrophils aggravate endothelial dysfunction by secreting reactive oxygen species (ROS), azurocidin, proteinase 3, cathelicidin, and cathepsin G in the arterial lumen (26, 74). ROS and proteases activate and dysregulate the endothelial cell layer and degrade the underlying extracellular matrix, enabling leukocyte infiltration and low-density lipoprotein (LDL) extravasation (26). Azurocidin also contributes to increasing endothelial

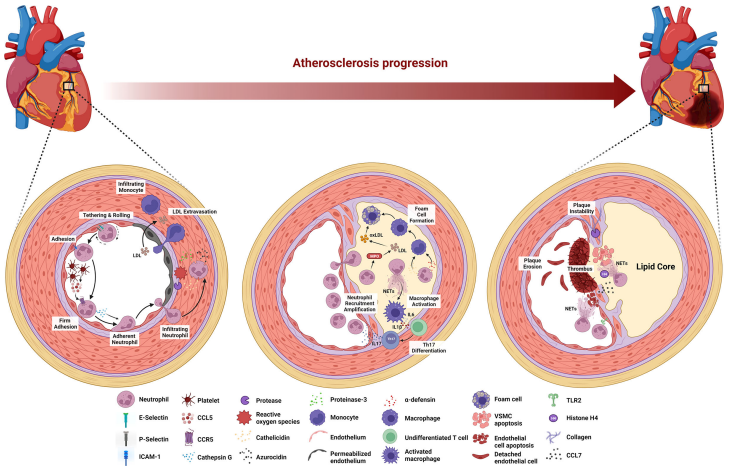

FIGURE 1 | Stage-dependent role of neutrophils in atherosclerosis. During the early stage of atherosclerosis, upregulation of E-selectin, P-selectin, and ICAM-1 induces neutrophil recruitment. Platelet-derived CCL5 activates neutrophils to release cathepsin G, leading to the firm adhesion to and accumulation of neutrophils in the endothelium. ROS and proteases secreted by neutrophils activate and dysregulate the endothelial cell layer and degrade the underlying extracellular matrix, resulting in monocyte infiltration and LDL extravasation. Neutrophils secrete MPO that mediates LDL oxidation and promotes foam cell formation. Cathelicidin- and α-defensin-derived neutrophils activate macrophages towards pro-inflammatory state, while NETs stimulate macrophage to release IL-6 and IL-1β that promote Th17 differentiation followed by the amplification of neutrophil recruitment. At the late stage of atherosclerosis, activated VSMCs induce neutrophil chemotaxis and release CCL7 to stimulate NETs. Histone H4-derived from NETs induces VSMC lysis and the secretion of proteases by neutrophils degrades collagen and lyses VSMCs, leading to the plaque instability. Neutrophils contribute to plaque erosion through NET release as well as colocalization with TLR2 of endothelial cells to induce endothelial cell stress and apoptosis.

permeability (26, 74–76), whereas azurocidin, proteinase 3, cathelicidin, α-defensin, and cathepsin G all promote myeloid cell recruitment and facilitate monocyte entry into the atherosclerotic lesions (74, 77–82).

The progression of the lesion continues following the aggravation of endothelial dysfunction by neutrophils, where macrophage activation and foam cell formation occur in the arterial intima. Neutrophil-derived granule proteins, cathelicidin, and α-defensin activate macrophages toward a pro-inflammatory state (M1 macrophage phenotype). Neutrophils also secrete myeloperoxidase (MPO) to generate oxygen radicals that oxidize apolipoprotein B, a protein structure in LDL (82). Subsequently, macrophages take up this oxidized LDL (oxLDL), resulting in foam cell formation (83). Moreover, NETs stimulate macrophages by turning on transcription factors encoding IL-6 and IL-1β. These cytokines promote the differentiation of Th17 cells, which in turn amplify neutrophil recruitment in the lesion (84). At this stage, because of sustained myeloid cell recruitment and foam cell generation, the atheroma becomes pronounced.

In the late stage of atherosclerosis, neutrophils destabilize the atherosclerotic plaque. Mechanistically, activated vascular smooth muscle cells (VSMCs) in advanced atherosclerotic lesions induce neutrophil chemotaxis and secrete CCL7, which stimulates NET release. One of the NET cytotoxic components, histone H4, disrupts the integrity of the VSMC plasma membrane, leading to cell lysis (85). Moreover, endotoxemia in a mouse model of atherosclerosis revealed that leukotriene B4-induced neutrophil recruitment to atherosclerotic plaques induces collagen degradation and VSMC lysis, leading to the feature of plaque instability (86). In eroded human plaques, neutrophils colocalized with toll-like receptor 2 of endothelial cells, and an *in vitro* experiments showed that co-culture of neutrophils with endothelial cells potentiates endothelial stress and apoptosis, resulting in endothelial cell detachment followed by luminal endothelial cell desquamation (plaque erosion) (19). Lastly, NETs are also involve during endothelial erosion as the disruption of NETs by either peptidyl arginine deiminase 4 (PAD4) gene knockout or DNase I treatment in atherosclerotic mice attenuates endothelial disintegration and endothelial cell apoptosis (87).

Neutrophils play dual roles, which are both adverse and favorable for cardiac tissue repair following myocardial infarction (**Figure 2A**). Tissue necrosis/ischemia post-acute myocardial infarction releases alarmins and inflammatory signals that attract neutrophils to the site of infarction (88). Activated neutrophils secrete ROS, proteases, NETs, and IL-1β. Granulopoiesis stimulated by IL-1β leads to neutrophil accumulation in the injured site, which is harmful to the remodeling of the ischemic area, resulting in eventual heart failure (89, 90). Following neutrophil accumulation, monocytes and monocyte-derived macrophages infiltrate the infarcted site to phagocytose cell debris and apoptotic neutrophils, activating cardiac repair (88). Intriguingly, neutrophils also contribute to this cardiac healing as their damage-associated molecular patterns (DAMPs), such as neutrophil gelatinase-associated lipocalin (NGAL) and S100A8/A9, stimulate macrophages to shift toward reparative phenotypes (91, 92). These anti-inflammatory macrophages aid in the resolution of inflammation (88). Neutrophils also secrete annexin A1, which stimulates pro-angiogenic macrophage polarization. These macrophage phenotypes release vascular endothelial growth factor A (VEGFA) to support angiogenesis in the ischemic site of

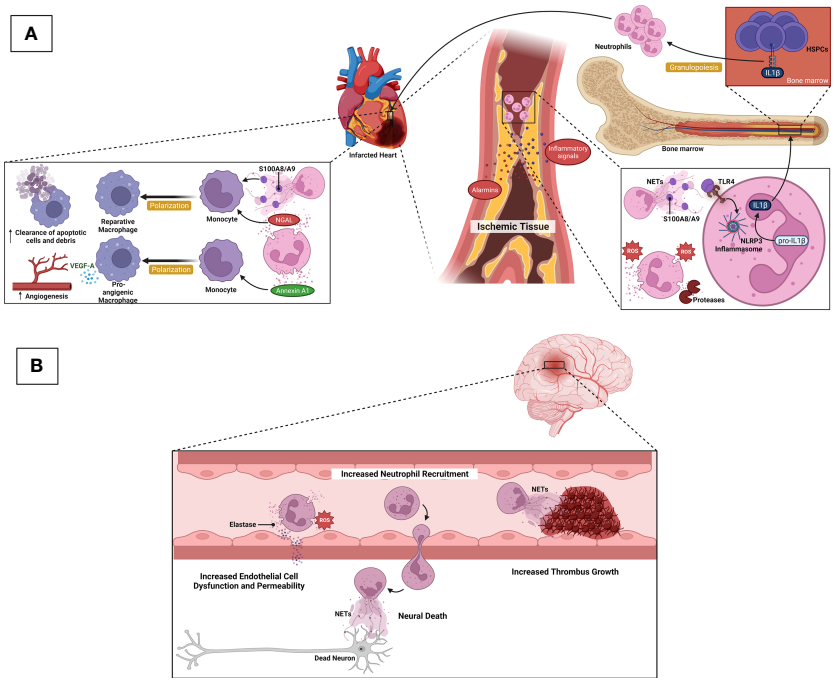

FIGURE 2 | Neurophils in ASCVD complications. **(A)** After acute myocardial infarction, ischemic/necrotic tissues release alarmins and inflammatory signals to induce neutrophil recruitment. Activated neutrophils secrete ROS, proteases, and NETs. S100A8/A9-derived from NETs induces IL-1β release following NLRP3 inflammasome priming in naïve neutrophils. IL-1β reaches the bone marrow to stimulate granulopoiesis leading to the amplification of neutrophil production and accumulation, which in turn, detriments the ischemic heart and eventual heart failure. During cardiac tissue repair, NGAL and S100A8/A9 stimulate macrophages to shift towards reparative phenotypes, resulting in increased clearance of apoptotic cells/debris. Neutrophils also secrete Annexin A1 to favor the shift of macrophages towards pro-angiogenic phenotypes that release VEGFA to promote angiogenesis in the ischemic site of cardiac tissue. **(B)** Following ischemic stroke, dying neurons attract neutrophils to the ischemic area, and neutrophil ROS and elastase promote endothelial cell dysfunction and vascular permeability. NETs contribute to thrombus growth, thereby increasing stroke volume. Neutrophils also promote neuronal cell death that is likely mediated by NETs.

the myocardium (93). Besides cardiac tissue repair, neutrophils aggravate other atherosclerosis complications, namely, ischemic stroke (**Figure 2B**). Following an episode of ischemic stroke, dying neurons attract neutrophils to the area to release ROS and elastase to enhance endothelial cell dysfunction and permeability. NETs promote thrombus growth, thereby increasing stroke volume. Finally, neutrophils increase neuronal cell death in a process that is likely to involve NETs (26, 94).

IMPACT OF PERIODONTITIS-INDUCED SYSTEMIC INFLAMMATION ON BONE MARROW ACTIVITY AND SUBSEQUENT CIRCULATING NEUTROPHIL ALTERATIONS: PLAUSIBLE MECHANISMS

Modulation of HSPCs in the Bone Marrow: A Key Role for Periodontitis-Induced Systemic Inflammation

Trained immunity can be initiated in the bone marrow *via* sustained epigenetic, metabolic, and transcriptional adaptations in HSPCs, leading to enhanced myeloid-biased differentiation and production of increased numbers of trained myeloid cells, including neutrophils (trained myelopoiesis/granulopoiesis) (95, 96). This training is based on the ability of HSPCs to sense numerous inflammatory cues in response to hematopoietic stress such as systemic inflammation (12, 96). HSPCs can directly sense pathogen-associated molecular patterns (PAMPs), such as LPS, *via* their pattern recognition receptors (PRRs), such as toll-like receptors (for example, TLR-4 for sensing LPS). Regarding the direct mechanism, in the context of periodontitis-induced bacteremia, it could be envisioned that systemically disseminated periodontal pathogens or their products (for example, LPS or lipopeptides) may also reach the bone marrow, resulting in innate immune training of HSPCs. However, indirect activation relies on specialized cells residing in either the peripheral tissue or bone marrow to affect the hematopoietic system through the release of cytokines (97, 98).

In addition to direct sensing of pathogens, cytokines and growth factors derived from both the bone marrow niche and peripheral tissue can mediate indirect adaptation of HSPCs (97, 98). IL-1β promotes myeloid differentiation and self-renewal of HSPCs as chronic administration of this cytokine elevates the number of myeloid-bias HSPCs. This is also consistent with the recent finding that enhanced myelopoiesis of HSPCs in a mouse model of β-glucan or experimental periodontitis-induced trained

immunity is mediated by IL-1β (95, 99). TNFα exhibits different actions in HSPCs as it promotes both the survival and myeloid differentiation of HSCs while inducing the apoptosis of myeloid progenitors (100). The increased level of IL-6 in the bone marrow niche promotes myelopoiesis, indicated by an elevated number of multipotent progenitors (MPPs) and common myeloid progenitors (CMPs) (101). Type 1 IFN mediates trained granulopoiesis in mice following β-glucan treatment resulting in the production of neutrophils with an enhanced ROS-dependent anti-tumor phenotype (102). IFNγ promotes HSC self-renewal and myeloid differentiation in a mouse model of repeated *Mycobacterium avium* infection (103). Granulocyte colony-stimulating factor (G-CSF) is a key growth factor that drives granulopoiesis. Specifically, G-CSF produced by monocytes in the bone marrow niche is responsible for HSPC mobilization from the bone marrow to the circulation (104). Moreover, in emergency granulopoiesis, G-CSF promotes the expansion and granulocyte lineage specification of granulocyte-monocyte progenitors (GMPs) (105).

Systemic inflammation, indicated by elevated levels of TNFα, IL-1β, IL-6, and IFNγ in the serum, is clinically present in patients with periodontitis (66, 67). Plasma IFNα, a type 1 IFN, is also higher in periodontitis patients compared to healthy controls (106). However, the role of type 1 IFN-mediated trained granulopoiesis in inducing hyper-responsive neutrophils in periodontitis patients needs to be addressed experimentally. Recent evidence indicates an increased level of serum G-CSF in ligature-induced periodontitis mice (107). Fibroblasts in the periodontal tissue contribute to the release of G-CSF during periodontal inflammation, resulting in the promotion of granulopoiesis (108). Based on the cumulative evidence of the effect of cytokines and growth factors on HSPCs and the abovementioned clinical studies, it could be shown that periodontitis-associated systemic inflammation may modulate HSPCs toward trained granulopoiesis (**Table 1**). This notion was recently confirmed in a preclinical model. Specifically, it was shown that ligature-induced periodontitis (LIP)-associated systemic inflammation leads to maladaptive innate immune training in the bone marrow (i.e., generating inflammatory memory) and the generation of increased numbers of hyper-responsive neutrophils; these populate oral and non-oral tissues and promote the emergence of inflammatory comorbidities, as exemplified by the periodontitis-arthritis axis (99). This is consistent with available clinical observations as outlined below. Intriguingly, the transplantation of bone marrow from LIP-subjected mice to healthy recipient mice resulted in increased severity of arthritis in the latter, as compared with the transplantation of bone marrow from periodontally healthy mice (99). The implication of this finding (if a similar phenomenon is confirmed in humans) is that clinicians should take inflammatory memory in the bone marrow into consideration when selecting appropriate donors for hematopoietic transplantation (99).

Indeed, the notion that periodontitis might trigger an adaptation of HSPCs is supported by clinical imaging studies using ^{18}F-fluorodeoxyglucose positron emission tomography/computed tomography (^{18}F-FDG-PET/CT). One study revealed that periodontal inflammation was associated with hematopoietic activity in the bone marrow and arterial inflammation. Furthermore, the authors used mediation path analysis to show that the relationship between periodontal and arterial inflammation was significantly mediated by bone marrow activity (109). More recently, another study using the same cohort of 304 participants as the aforementioned study showed that periodontal inflammation (as determined by ^{18}F-FDG-PET/CT) is independently correlated with not only increased arterial inflammation but also increased an risk of future cardiovascular events (64). Additionally, another study harnessing the same imaging technique also reported a trend for increased periodontal inflammation and femur bone marrow activity in patients with periodontitis (relative to controls), albeit no differences were observed in vascular inflammation between the two groups (110). The lack of clear differences in this study is likely attributed (a) to the small sample size (14 participants as opposed to >300 participants in the above-discussed studies) and (b) to the fact that participants with severe periodontal disease were under supportive periodontal therapy, which could have mitigated inflammation and associated parameters, including surrogate markers of ASCVD (discussed below) (110). Moreover, the control group also included individuals with mild periodontitis, which could also impact systemic inflammation and hematopoietic tissue activity, thus reducing potential differences compared with the experimental group.

Alteration of Circulating Neutrophils in Periodontitis and its Putative Effect on Atherosclerosis

Patients with periodontitis exhibit elevated numbers of neutrophils and altered phenotypes presenting hyper-reactive features in cellular functions (discussed below) (21–23, 68, 69,

TABLE 1 | Summary of circulating molecules that are elevated in periodontitis and involved in hematopoietic tissue adaptation.

No.	Molecules	Action on hematopoietic tissue adaptation	References
1.	IL-1β	Promotes myeloid differentiation and self-renewal of HSPCs	(95, 97–99)
2.	TNF-α	Promotes survival of HSPCs and myeloid differentiation Induces myeloid progenitor apoptosis	(100)
3.	IL-6	Enhances myelopoiesis by elevating MPPs and CMPs	(101)
4.	Type 1 IFN	Mediates trained granulopoiesis with hyper-responsive neutrophils	(102)
5.	IFN-γ	Promotes HSC self-renewal and myeloid differentiation	(103)
6.	G-CSF	Drives granulopoiesis Promotes GMP expansion and granulocyte lineage specification	(104) (105)

110–117). These include increased levels of ROS production in response to fMLP, PMA, or periodontal pathogens (21–23, 102, 111–115), elevated TNFα production following stimulation with the periodontal pathogen, *Fusobacterium nucleatum*, *in vitro* (116), and elevated neutrophil elastase levels linked to periodontal tissue destruction (117, 118). The systemic effect of this alteration has been recently confirmed in an experimental study with mice and experimental periodontitis that exhibited hyper-inflammatory neutrophil response following the exposure to secondary peritonitis compared with mice without periodontitis (119).

These altered features in neutrophils present a hallmark of trained myelopoiesis, which includes increased numbers of myeloid cells with enhanced inflammatory responsiveness (24, 95). As such, these changes may implicate the response of future inflammatory stimuli that drive certain pathological processes such as atherosclerosis.

Neutrophils that are increased in number and hyper-responsiveness due to periodontitis can contribute to any stage of this ASCVD pathology. Further research should address this hypothesis experimentally. However, it is still interesting to speculate that periodontitis-induced neutrophil alteration contributes to the association between periodontitis and ASCVD because of several clinical studies that support this notion. An elevated number of neutrophils in peripheral blood may increase the risk of ASCVD in periodontitis patients because neutrophil counts from peripheral blood are positively correlated with ASCVD risk (120, 121). Moreover, periodontitis patients consistently present with endothelial dysfunction, which is a key feature of ASCVD (2). This disturbed vascular function and elevated neutrophil ROS production triggered by periodontitis can aggravate the initiation of atherosclerosis. The latter may also potentiate the progression of atherosclerosis, particularly in oxidizing LDL. Hyper-responsiveness of neutrophils characterized by excessive production of neutrophil elastase and ROS in periodontitis patients could also contribute to the late stage of atherosclerosis as both hyper-reactive features induce endothelial apoptosis, resulting in endothelial desquamation (plaque erosion), fibrous cap thinning and plaque ruptures. Finally, whereas the production of NETs by circulating neutrophils has been shown to be comparable between patients with periodontitis and healthy controls, plasma NET degradation was lower in patients with periodontitis than in controls, suggesting an impaired NET degradation process in the plasma of periodontitis patients (122). This impairment might favor atherosclerosis complications, especially in post-ischemic stroke where NET accumulation promotes thrombus formation and expands stroke volume. In this context, a case-control study revealed that periodontitis was an independent predictor of poor outcome in post-ischemic stroke patients (123).

IMPACT OF PERIODONTITIS TREATMENT ON NEUTROPHILS

Whereas the treatment of periodontitis improves the surrogate markers of ASCVD, its long-term cardiovascular-protective effect is uncertain. A reduction of several serum inflammatory markers that is expected to reduce the risk of ASCVD is not observed in serum IFNγ and IL-10 because both markers remain unchanged following periodontitis treatment (40). As these markers are predominantly generated and released into blood circulation by inflammatory cells, it is interesting to speculate that while successful treatment indeed achieves the resolution of periodontal inflammation, circulating inflammatory cells still retain their periodontitis-induced altered phenotypes. The latter is supported by clinical studies that investigated the functions of peripheral blood-derived neutrophils and monocytes in periodontitis patients after the treatment. The hyper-responsiveness of these myeloid cells persisted as the levels of cytokines produced by the cells in response to pathogen or LPS stimulation were comparable between neutrophils from patients before and after periodontal treatment (31, 116). Similarly, a longitudinal study on the circulating neutrophil profiles of patients with periodontitis showed that neutrophils (as a proportion of total cells isolated from peripheral blood of periodontitis patients) did not change between baseline (before treatment) and after 3-, 6-, and 12-month post-periodontitis treatment (124). The retained neutrophil phenotypes might be because of the trained myelopoiesis induced by periodontitis-triggered systemic inflammation. In murine experiments, long-lasting changes in myelopoiesis were observed following either microbial- or sterile-induced inflammation (29, 95). Similarly, a recent report shows that upon the LIP resolution, HSPCs in the bone marrow retain a myeloid differentiation bias (99).

TARGETING NEUTROPHILS AS A NOVEL THERAPEUTIC APPROACH: DUAL BENEFIT ON PERIODONTITIS AND ASCVD

The targeted therapeutic approach for ASCVD has been established by focusing on the reduction of inflammation (**Table 2**). The first clinical trial, CANTOS, in an attempt to close the gap between pre-clinical studies and clinical practice, provided evidence that reducing inflammation could be relevant to treating atherosclerosis in humans. In this trial, the anti-IL-1β antibody, Canakinumab, was administered subcutaneously to individuals with a sustained acute myocardial infarction. The trial revealed a significant reduction in the rates of recurrent cardiovascular events, hospitalization for heart failure, and heart failure-associated death (125, 126). However, the adverse event in the group receiving Canakinumab was more significant death due to infection or sepsis compared to the placebo group (125). Moreover, oral administration of colchicine in patients with a recent myocardial infarction significantly reduces the risk of ischemic cardiovascular events (127). The benefits of colchicine were also observed in patients with chronic coronary disease (128). Unfortunately, patients in the colchicine group showed higher incidents of pneumonia and non-cardiovascular-caused death than those in the placebo group (127, 128). Other clinical studies on targeting inflammation in ASVD treatment have been

TABLE 2 | Summary of clinical trials.

No.	Name of drug	Mechanism of action	Phase	Identifier (Trial registration)	Outcome
1.	Canakinumab	Binds to IL-1β resulting in blocking the interaction between IL-1β and IL-1 receptor	Phase 3	NCT01327846	Reduction in cardiovascular events, hospitalization for heart failure, and heart failure-associated death Emergence of death due to sepsis
2.	Colchicine	Prevents microtubule formation resulting in tubulin disruption	Phase 3	NCT02551094	Reduction in ischemic cardiovascular events Increase in pneumonia
3.	Metoprolol	Attenuates neutrophil migration and infiltration by impairing the neutrophil-platelet interaction that is crucial during early phases of neutrophil recruitment	Phase 4	NCT01311700	Reduction of infarct size Improvement of cardiac function
4.	AZD5069 (a CXCR2 antagonist)	Prevents neutrophil recruitment to the site of inflammation	Phase 1 Phase 2	NCT01480739 ISRCTN48328178	No adverse events and safety concerns Currently on going
5.	AMY-101 (a complement C3 inhibitor)	Inhibits downstream activation of the anaphylatoxin C3a and C5a receptors	Phase 2a	NCT03694444	Reduction in gingival inflammation Reduction of MMP-8 and MMP-9 levels in gingival crevicular fluids

reviewed elsewhere (129). These clinical trials indicate that therapies with alternative strategies are required to achieve outcomes in which the benefits outweigh the risks.

Besides the necessity of different strategies to reduce the risk–benefit ratio, a refined understanding of the potential role of periodontitis-induced neutrophil alteration in the pathology of ASCVD and its retained phenotypes following successful periodontitis treatment highlights the importance of selectively targeting neutrophils during the treatment of periodontitis. This therapeutic approach is warranted to mitigate the potential impact of periodontitis on ASCVD. The main endpoint of this intervention is to either manipulate the number of neutrophils and/or their functional activities. We only discuss the approaches to block neutrophil recruitment and prevent NET-driven inflammation, while other neutrophil-targeted therapeutics have been extensively reviewed elsewhere (130).

While the results of neutrophil recruitment blockage are promising in preclinical studies, clinical trials exhibit unsuccessful outcomes due to the redundancy of signals during neutrophil recruitment and off-target effects caused by receptor cross-linking. Recent studies have provided strategies for overcoming such difficulties. The combined inhibition of several endothelial cell molecules interrupts redundant signals that recruit neutrophils (131). Intravenous injection of nanoparticles carrying small interfering RNAs (siRNAs) that target endothelial adhesion molecules including ICAM-1, E-, P-selectin, and vascular cellular adhesion molecule-1 (VCAM-1) decreased leukocyte recruitment to ischemic myocardium in a mouse model of post-myocardial infarction (131). Moreover, specific blockage of neutrophils that traffic to certain vascular tissue requires a refined understanding of recruitment patterns at particular sites (16). A neutrophil granule protein, cathepsin G promotes myeloid cell adhesion to only arterial but not microvascular tissue (73). Indeed, antibody-assisted cathepsin G neutralization in an atherosclerotic mouse model specifically alleviated neutrophil recruitment to the carotid artery, resulting in reduced atherosclerotic plaque size. However, a similar treatment did not affect neutrophil adhesion in lung microcirculation following an LPS-induced lung inflammation model in mice (73). Furthermore, the elucidation of heteromeric interactions between neutrophil-derived human neutrophil peptide-1 (HNP1) and platelet-borne CCL5 that must stimulate monocyte adhesion *via* CCR5 ligation allows the design of a peptide that can disturb these neutrophil–platelet interactions. This specifically designed short peptide alleviated inflammation in a mouse model of myocardial infarction (20). Finally, inducing endogenous inhibitors in leukocytes can overcome integrin activation by chemokine, thereby suppressing myeloid cell adhesion. For example, growth differentiation factor-15 (GDF-15) and annexin A1 inhibit chemokine-induced β2 integrin activation and subsequently reduce neutrophil recruitment in a mouse model of chronic inflammation (72, 132). Moreover, recombinant developmental endothelial locus-1 (DEL-1), the first identified endogenous inhibitor of the leukocyte adhesion cascade (133), inhibited neutrophil recruitment in mouse and non-human primate models (17, 134).

Important roles of NETs in both atherosclerosis progression (atherogenesis, plaque destabilization and erosion) and complication (atherothrombosis) stand out as a potential therapeutic target to manipulate cardiovascular inflammation. Peptidyl arginine deiminase 4 (PAD4) citrullinates histone to disrupt electrostatic bonds in nucleosomes, decondensing chromatin that leads to NET release (135). Cl-amidine, a PAD inhibitor administered intravenously in an atherosclerotic mouse model, prevented NET formation, leading to reduced atherosclerotic lesion area and thrombosis (136). However, the mechanism of NETosis in mice is different from that in humans as *ex vivo* experiments of human neutrophils showed that PMA-induced NETosis of the cells was not affected following the PAD4 inhibitor, Cl-amidine (137). Meanwhile, DNase 1 treatment might be considered to mitigate ASCVD complications like

thrombosis due to NET deposition in the vascular lumen. This notion is supported by a study where the treatment protected mice from deep vein thrombosis following an inferior vena cava stenosis model (138). A reduction in lesion size was also observed in an atherosclerosis mouse model after DNase injections (84). In humans, DNAse 1 treatment to eliminate NET deposition might need a combination with other substances, as DNAse 1 alone was not adequate to degrade NETs *in vitro* (139). Lastly, NET chromatin can stimulate macrophages by activating AIM2 inflammation, causing the release of IL-8 and IL-1β in atherosclerotic lesions. The use of an AIM2 inhibitor could also attenuate ASCVD complications because reduced plaque vulnerability through the thickening of the fibrous cap was observed in an atherosclerotic mouse model after the treatment of an AIM2 inhibitor (140). ApoE-deficient mice on a 6-week high fat diet and injected with anti-chromatin antibodies also showed a reduced plaque area per lumen, suggesting the potential of chromatin blockage to hinder atherosclerosis (141). The use of substances to block NETs in humans should be implemented with caution because studies about the pro-inflammatory features of NETs in humans are still conflicting, as *in vitro* NET clearance by human macrophages did not induce pro-inflammatory cytokines (139), but NET transfection to mouse macrophages did (142).

Targeting neutrophils as an approach to mitigate the potential impact of periodontitis on ASCVD is appealing considering the numerous efforts outlined previously. This targeted strategy can not only have direct effects on ASCVD but also reduce periodontitis, which triggers inflammation that primes neutrophils for ASCVD pathology. However, safety and specificity issues are challenges that need to be solved as neutrophils interact with other myeloid lineages (130). The solution to the former concern is that the intervention should consider the therapeutic window, where the attenuation of the inflammatory process mediated by neutrophils does not interfere with neutrophil capacity during host defense (130). Recent studies revealed that the use of antibodies to inhibit NET-derived histones reduced the amplification of NET-induced inflammation rather than completely blocking NETosis or inflammation (141). Few studies have presented strategies to obtain the specificity to therapeutically target neutrophils. For example, the conjugation of siRNA targeting Bruton's tyrosine kinase (BTK) to the F(ab')2 fragment of an anti-neutrophil monoclonal antibody specifically targeted alveolar neutrophils in an acute lung injury mouse model. This treatment was administered locally using a technique called intranasal instillation (143). Meanwhile, others harness nanoparticle technology to enhance specificity. One of them reported that neutrophils adhered to activated endothelium-engulfed albumin nanoparticles carrying piceatannol, leading to the inactivation of these adherent neutrophils and consequently preventing vascular inflammation (144). Additionally, another report exhibited lipid-based nanoparticles that were successfully incorporated with identified peptides that interact with the neutrophil-specific surface marker, CD177 (145).

A clinical trial targeting neutrophils to lower ASCVD risk is still lacking. However, two randomized clinical trials reported that metoprolol provides a cardio-protective effect following acute myocardial infarction, which is one of the atherosclerosis complications (**Table 2**). Specifically, intravenous administration of metoprolol reduced infarct size and improved cardiac function in patients with acute myocardial infarction (146, 147). Studies using a myocardial infarct mouse model revealed the mechanism of this protection in which metoprolol attenuates neutrophil migration and infiltration by impairing the neutrophil–platelet interaction that is crucial during early phases of neutrophil recruitment (148, 149). Another drug candidate, AZD5069, a CXCR2 antagonist, could be a potent drug candidate in treating patients with advanced atherosclerotic lesions. CXCR2 is a chemokine receptor 2 in neutrophils that regulates neutrophil migration, and the inhibition of this receptor successfully prevents neutrophil recruitment to the site of inflammation (150). No adverse effects on neutrophil function were observed, and no safety concerns were raised in participants receiving oral administration of AZD5069 (151). The CICADA trial was proposed to investigate the effect of a CXCR2 antagonist (administered orally) on coronary flow, structure, and function in patients with coronary heart disease (152).

Mechanical intervention in periodontitis management with adjunctive neutrophil-targeted therapeutic approach could also provide benefit in reducing periodontal-induced systemic inflammation that can implicate all stages of atherosclerosis. A phase IIa clinical trial of the complement C3 inhibitor, AMY-101, summarized in **Table 2**, shows promising results in reducing local inflammation in periodontal tissue (153). The pharmacological blockade of the central complement component, C3, inhibits downstream activation of the anaphylatoxin C3a and C5a receptors (C3aR and C5aR, respectively), which induce inflammatory bone loss in a preclinical model (154). C5aR and TLR2 coactivation in neutrophils contribute to oral microbiota dysbiosis leading to overt periodontal inflammation and subsequent periodontal tissue destruction (155). Local injection of AMY-101 to the gingiva reduced gingival inflammation without adverse events, warranting phase III clinical trials for further investigation (153, 156). Importantly, AMY-101 significantly reduced the gingival crevicular levels of MMP-8 and MMP-9 (152), which are the major neutrophil-derived proteases and are considered biomarkers of periodontal tissue destruction (157). Meanwhile, other local neutrophil-targeted treatments, including resolvin E1, developmental endothelial locus-1, and milk fat globule epidermal growth factor 8, are still in pre-clinical studies. These proteins reduce neutrophil recruitment to the site of inflammation and prevent animal models of ligature-induced periodontitis (134, 158, 159). Additionally, resolving E1 also promotes neutrophil apoptosis and its clearance (efferocytosis), resulting in the resolution of periodontal inflammation (157). Focusing on the termination of periodontitis may prevent its systemic impact, which is heightened systemic inflammation. These strategies of local intervention potentially further improve

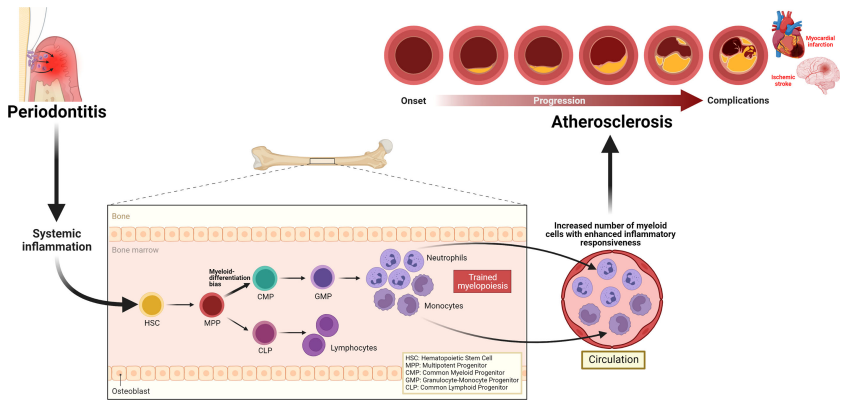

FIGURE 3 | Periodontitis-induced systemic inflammation, inflammatory modulation of bone marrow progenitor cells, and implications for atherosclerosis. Periodontitis triggers systemic inflammation, which causes inflammatory modulation of hematopoietic stem and progenitor cells, resulting in a trained myelopoiesis. In turn, as a hallmark of trained myelopoiesis, an increased number of myeloid cells, including neutrophils with enhanced inflammatory responsiveness, may contribute to all stages of the ASCVD pathology, atherosclerosis.

the current periodontal treatment in providing a sustained protection to cardiovascular health.

CONCLUSION

Periodontitis triggers systemic inflammation which could modulate hematopoietic tissue activity in the bone marrow, resulting in trained myelopoiesis. Clinical studies demonstrating increased numbers as well as enhanced inflammatory responsiveness in neutrophils back this notion. The evidence of persistent elevated neutrophil numbers and their altered phenotypes, despite the resolution of periodontitis following local treatment, also supports the speculation that periodontitis-induced systemic inflammation can induce long-term myelopoiesis bias, a hallmark of innate immune training in the bone marrow. The quantitative and qualitative alterations in neutrophils may contribute to all stages of the ASCVD pathology, atherosclerosis (**Figure 3**). Although clinical intervention studies suggest that periodontal therapy improves surrogate markers of ASCVD, the long-term effects of this oral treatment to maintain such improvement and convincing evidence that successful periodontitis treatment can reduce the risk or incidence of ASCVD are yet to be investigated. Meanwhile, targeting neutrophils is warranted to improve local periodontal therapy, eliminate periodontitis effectively, that can reduce periodontitis-triggered systemic inflammation and reverse the periodontitis-induced neutrophil changes. Such targeted approaches can be harnessed as a direct treatment for ASCVD and indirect intervention of the disease through the reduction of heightened systemic inflammation triggered by periodontitis.

AUTHOR CONTRIBUTIONS

RI wrote the original draft. RI, SC, GH, VP, JD, and FD provided critical revisions to the article. All authors listed have made a substantial, direct, and intellectual contribution to the work and approved it for publication.

FUNDING

This work was undertaken at the UCL Biomedical Research Centre which receives funding from the UK National Institute for Health and Care Research. GH receives a grant from the US National Institutes of Health (DE031206). RI receives funding from the Indonesia Endowment Fund for Education (S-1692/LPDP.4/2019 —LPDP—Indonesia Scholarship). The figures were created using Biorender.com

REFERENCES

1. Ellulu MS, Patimah I, Khaza'ai H, Rahmat A, Abed Y, Ali F. Atherosclerotic Cardiovascular Disease: A Review of Initiators and Protective Factors. *Inflammopharmacology* (2016) 24(1):1–10. doi: 10.1007/s10787-015-0255-y
2. Sanz M, Marco del Castillo A, Jepsen S, Gonzalez-Juanatey JR, D'Aiuto F, Bouchard P, et al. Periodontitis and Cardiovascular Diseases: Consensus Report. *J Clin Periodontol* (2020) 47(3):268–88. doi: 10.5334/gh.400
3. Roth GA, Mensah GA, Johnson CO, Addolorato G, Ammirati E, Baddour LM, et al. Global Burden of Cardiovascular Diseases and Risk Factors, 1990–2019: Update From the GBD 2019 Study. *J Am Coll Cardiol* (2020) 76 (25):2982–3021. doi: 10.1016/j.jacc.2020.11.010
4. Libby P. The Biology of Atherosclerosis Comes Full Circle: Lessons for Conquering Cardiovascular Disease. *Nat Rev Cardiol* (2021) 18(10):683–4. doi: 10.1038/s41569-021-00609-1
5. Kinane DF, Stathopoulou PG, Papapanou PN. Periodontal Diseases. *Nat Rev Dis Primers* (2017) 3(1):17038. doi: 10.1038/nrdp.2017.38
6. Graziani F, Music L, Bozic D, Tsakos G. Is Periodontitis and Its Treatment Capable of Changing the Quality of Life of a Patient? *Br Dent J* (2019) 227 (7):621–5. doi: 10.1038/s41415-019-0735-3

7. Kassebaum N, Bernabé E, Dahiya M, Bhandari B, Murray C, Marcenes W. Global Burden of Severe Periodontitis in 1990-2010: A Systematic Review and Meta-Regression. *J Dent Res* (2014) 93(11):1045–53. doi: 10.1177/0022034514552491
8. Dye BA. Global Periodontal Disease Epidemiology. *Periodontol 2000* (2012) 58(1):10–25. doi: 10.1111/j.1600-0757.2011.00413.x
9. Baehni P, Tonetti M. Group 1 of the European Workshop on Periodontology. Conclusions and Consensus Statements on Periodontal Health, Policy and Education in Europe: A Call for Action–Consensus View 1: Consensus Report of the 1st European Workshop on Periodontal Education. *Eur J Dent Educ* (2010) 14:2–3. doi: 10.1111/j.1600-0579.2010.00619.x
10. Geerts SO, Nys M, De Mol P, Charpentier J, Albert A, Legrand V, et al. Systemic Release of Endotoxins Induced by Gentle Mastication: Association With Periodontitis Severity. *J Periodontol* (2002) 73(1):73–8. doi: 10.1902/jop.2002.73.1.73
11. Forner L, Larsen T, Kilian M, Holmstrup P. Incidence of Bacteremia After Chewing, Tooth Brushing and Scaling in Individuals With Periodontal Inflammation. *J Clin Periodontol* (2006) 33(6):401–7. doi: 10.1111/j.1600-051X.2006.00924.x
12. Hajishengallis G, Chavakis T. Local and Systemic Mechanisms Linking Periodontal Disease and Inflammatory Comorbidities. *Nat Rev Immunol* (2021) 21(7):426–40. doi: 10.1038/s41577-020-00488-6
13. Konkel JE, O'Boyle C, Krishnan S. Distal Consequences of Oral Inflammation. *Front Immunol* (2019) 10:1403. doi: 10.3389/fimmu.2019.01403
14. Schenkein HA, Papapanou PN, Genco R, Sanz M. Mechanisms Underlying the Association Between Periodontitis and Atherosclerotic Disease. *Periodontol 2000* (2020) 83(1):90–106. doi: 10.1111/prd.12304
15. Rosales C. Neutrophil: A Cell With Many Roles in Inflammation or Several Cell Types? *Front Physiol* (2018) 9:113. doi: 10.3389/fphys.2018.00113
16. Soehnlein O, Steffens S, Hidalgo A, Weber C. Neutrophils as Protagonists and Targets in Chronic Inflammation. *Nat Rev Immunol* (2017) 17(4):248–61. doi: 10.1038/nri.2017.10
17. Eskan MA, Jotwani R, Abe T, Chmelar J, Lim J-H, Liang S, et al. The Leukocyte Integrin Antagonist Del-1 Inhibits IL-17-Mediated Inflammatory Bone Loss. *Nat Immunol* (2012) 13(5):465–73. doi: 10.1038/ni.2260
18. Dutzan N, Kajikawa T, Abusleme L, Greenwell-Wild T, Zuazo CE, Ikeuchi T, et al. A Dysbiotic Microbiome Triggers T(H)17 Cells to Mediate Oral Mucosal Immunopathology in Mice and Humans. *Sci Transl Med* (2018) 10(463):eaat0797. doi: 10.1126/scitranslmed.aat0797
19. Quillard T, Araújo HA, Franck G, Shvartz E, Sukhova G, Libby P. TLR2 and Neutrophils Potentiate Endothelial Stress, Apoptosis and Detachment: Implications for Superficial Erosion. *Eur Heart J* (2015) 36(22):1394–404. doi: 10.1093/eurheartj/ehv044
20. Alard J-E, Ortega-Gomez A, Wichapong K, Bongiovanni D, Horckmans M, Megens RT, et al. Recruitment of Classical Monocytes Can be Inhibited by Disturbing Heteromers of Neutrophil HNP1 and Platelet Ccl5. *Sci Transl Med* (2015) 7(317):317ra196–317ra196. doi: 10.1126/scitranslmed.aad5330
21. Matthews J, Wright H, Roberts A, Cooper P, Chapple I. Hyperactivity and Reactivity of Peripheral Blood Neutrophils in Chronic Periodontitis. *Clin Exp Immunol* (2007) 147(2):255–64. doi: 10.1111/j.1365-2249.2006.03276.x
22. Matthews J, Wright H, Roberts A, Ling-Mountford N, Cooper P, Chapple I. Neutrophil Hyper-Responsiveness in Periodontitis. *J Dent Res* (2007) 86(8):718–22. doi: 10.1177/154405910708600806
23. Ling MR, Chapple IL, Matthews JB. Neutrophil Superoxide Release and Plasma C-Reactive Protein Levels Pre-And Post-Periodontal Therapy. *J Clin Periodontol* (2016) 43(8):652–8. doi: 10.1111/jcpe.12575
24. Netea MG, Domínguez-Andrés J, Barreiro LB, Chavakis T, Divangahi M, Fuchs E, et al. Defining Trained Immunity and Its Role in Health and Disease. *Nat Rev Immunol* (2020) 20(6):375–88. doi: 10.1038/s41577-020-0285-6
25. Kaufmann E, Sanz J, Dunn JL, Khan N, Mendonça LE, Pacis A, et al. BCG Educates Hematopoietic Stem Cells to Generate Protective Innate Immunity Against Tuberculosis. *Cell* (2018) 172(1-2):176–90. doi: 10.1016/j.cell.2017.12.031
26. Silvestre-Roig C, Braster Q, Ortega-Gomez A, Soehnlein O. Neutrophils as Regulators of Cardiovascular Inflammation. *Nat Rev Cardiol* (2020) 17(6):327–40. doi: 10.1038/s41569-019-0326-7
27. Chavakis T, Wielockx B, Hajishengallis G. Inflammatory Modulation of Hematopoiesis: Linking Trained Immunity and Clonal Hematopoiesis With Chronic Disorders. *Ann Rev Physiol* (2021) 84:183–207. doi: 10.1146/annurev-physiol-052521-013627
28. Bekkering S, Arts RJW, Novakovic B, Kourtzelis I, van der Heijden C, Li Y, et al. Metabolic Induction of Trained Immunity Through the Mevalonate Pathway. *Cell* (2018) 172(1-2):135–46. doi: 10.1016/j.cell.2017.11.025
29. Christ A, Günther P, Lauterbach MAR, Duewell P, Biswas D, Pelka K, et al. Western Diet Triggers NLRP3-Dependent Innate Immune Reprogramming. *Cell* (2018) 172(1-2):162–75. doi: 10.1016/j.cell.2017.12.013
30. Poller WC, Nahrendorf M, Swirski FK. Hematopoiesis and Cardiovascular Disease. *Circ Res* (2020) 126(8):1061–85. doi: 10.1161/CIRCRESAHA.120.315895
31. Radvar M, Tavakkol-Afshari J, Bajestan MN, Naseh MR, Arab HR. The Effect of Periodontal Treatment on IL-6 Production of Peripheral Blood Monocytes in Aggressive Periodontitis and Chronic Periodontitis Patients. *Iran J Immunol* (2008) 5(2):100–6.
32. Dietrich T, Sharma P, Walter C, Weston P, Beck J. The Epidemiological Evidence Behind the Association Between Periodontitis and Incident Atherosclerotic Cardiovascular Disease. *J Periodontol* (2013) 84(4 Suppl):S70–84. doi: 10.1902/jop.2013.134008
33. Sen S, Giamberardino LD, Moss K, Morelli T, Rosamond WD, Gottesman RF, et al. Periodontal Disease, Regular Dental Care Use, and Incident Ischemic Stroke. *Stroke* (2018) 49(2):355–62. doi: 10.1161/STROKEAHA.117.018990
34. Chen D-Y, Lin C-H, Chen Y-M, Chen H-H. Risk of Atrial Fibrillation or Flutter Associated With Periodontitis: A Nationwide, Population-Based, Cohort Study. *PLoS One* (2016) 11(10):e0165601. doi: 10.1371/journal.pone.0165601
35. Lee Y-L, Hu H-Y, Chou P, Chu D. Dental Prophylaxis Decreases the Risk of Acute Myocardial Infarction: A Nationwide Population-Based Study in Taiwan. *Clin Interv Aging* (2015) 10:175–82. doi: 10.2147/CIA.S67854
36. Holmlund A, Lampa E, Lind L. Poor Response to Periodontal Treatment May Predict Future Cardiovascular Disease. *J Dent Res* (2017) 96(7):768–73. doi: 10.1177/0022034517701901
37. Machado V, Botelho J, Escalda C, Hussain SB, Luthra S, Mascarenhas P, et al. Serum C-Reactive Protein and Periodontitis: A Systematic Review and Meta-Analysis. *Front Immunol* (2021) 12:706432. doi: 10.3389/fimmu.2021.706432
38. Muñoz Aguilera E, Suvan J, Buti J, Czesnikiewicz-Guzik M, Barbosa Ribeiro A, Orlandi M, et al. Periodontitis is Associated With Hypertension: A Systematic Review and Meta-Analysis. *Cardiovasc Res* (2020) 116(1):28–39. doi: 10.1093/cvr/cvz201
39. Muñoz Aguilera E, Suvan J, Orlandi M, Miró Catalina Q, Nart J, D'Aiuto F. Association Between Periodontitis and Blood Pressure Highlighted in Systemically Healthy Individuals: Results From a Nested Case-Control Study. *Hypertension* (2021) 77(5):1765–74. doi: 10.1161/HYPERTENSIONAHA.120.16790
40. Sharma S, Sridhar S, Mcintosh A, Messow C-M, Aguilera EM, Del Pinto R, et al. Periodontal Therapy and Treatment of Hypertension–Alternative to the Pharmacological Approach. A Systematic Review and Meta-Analysis. *Pharmacol Res* (2021) 166:105511. doi: 10.1016/j.phrs.2021.105511
41. Orlandi M, Suvan J, Petrie A, Donos N, Masi S, Hingorani A, et al. Association Between Periodontal Disease and Its Treatment, Flow-Mediated Dilatation and Carotid Intima-Media Thickness: A Systematic Review and Meta-Analysis. *Atherosclerosis* (2014) 236(1):39–46. doi: 10.1016/j.atherosclerosis.2014.06.002
42. Tonetti MS, D'Aiuto F, Nibali L, Donald A, Storry C, Parkar M, et al. Treatment of Periodontitis and Endothelial Function. *N Engl J Med* (2007) 356(9):911–20. doi: 10.1056/NEJMoa063186
43. D'Aiuto F, Gkranias N, Bhowruth D, Khan T, Orlandi M, Suvan J, et al. Systemic Effects of Periodontitis Treatment in Patients With Type 2 Diabetes: A 12 Month, Single-Centre, Investigator-Masked, Randomised Trial. *Lancet Diabetes Endocrinol* (2018) 6(12):954–65. doi: 10.1016/S2213-8587(18)30038-X
44. Czesnikiewicz-Guzik M, Osmenda G, Siedlinski M, Nosalski R, Pelka P, Nowakowski D, et al. Causal Association Between Periodontitis and Hypertension:Evidence From Mendelian Randomization and a

Randomized Controlled Trial of Non-Surgical Periodontal Therapy. *Eur Heart J* (2019) 40(42):3459–70. doi: 10.1093/eurheartj/ehz646
45. Stuehr DJ. Mammalian Nitric Oxide Synthases. *Biochim Biophys Acta* (1999) 1411(2-3):217–30. doi: 10.1016/s0005-2728(99)00016-x
46. Palmer RM, Ferrige AG, Moncada S. Nitric Oxide Release Accounts for the Biological Activity of Endothelium-Derived Relaxing Factor. *Nature* (1987) 327(6122):524–6. doi: 10.1038/327524a0
47. Yoshizumi M, Perrella MA, Burnett JCJr., Lee ME. Tumor Necrosis Factor Downregulates an Endothelial Nitric Oxide Synthase mRNA by Shortening Its Half-Life. *Circ Res* (1993) 73(1):205–9. doi: 10.1161/01.res.73.1.205
48. Bhagat K, Vallance P. Inflammatory Cytokines Impair Endothelium-Dependent Dilatation in Human Veins. *In Vivo Circ* (1997) 96(9):3042–7. doi: 10.1161/01.cir.96.9.3042
49. Venugopal SK, Devaraj S, Yuhanna I, Shaul P, Jialal I. Demonstration That C-Reactive Protein Decreases eNOS Expression and Bioactivity in Human Aortic Endothelial Cells. *Circulation* (2002) 106(12):1439–41. doi: 10.1161/01.cir.0000033116.22237.f9
50. Clapp BR, Hingorani AD, Kharbanda RK, Mohamed-Ali V, Stephens JW, Vallance P, et al. Inflammation-Induced Endothelial Dysfunction Involves Reduced Nitric Oxide Bioavailability and Increased Oxidant Stress. *Cardiovasc Res* (2004) 64(1):172–8. doi: 10.1016/j.cardiores.2004.06.020
51. Higashi Y, Goto C, Jitsuiki D, Umemura T, Nishioka K, Hidaka T, et al. Periodontal Infection is Associated With Endothelial Dysfunction in Healthy Subjects and Hypertensive Patients. *Hypertension* (2008) 51 (2):446–53. doi: 10.1161/HYPERTENSIONAHA.107.101535
52. Baumann M, Baumann H, Fey G. Molecular Cloning, Characterization and Functional Expression of the Rat Liver Interleukin 6 Receptor. *J Biol Chem* (1990) 265(32):19853–62. doi: 10.1016/S0021-9258(17)45451-2
53. Nesbitt JE, Fuller GM. Differential Regulation of Interleukin-6 Receptor and Gp130 Gene Expression in Rat Hepatocytes. *Mol Biol Cell* (1992) 3(1):103–12. doi: 10.1091/mbc.3.1.103
54. Calabró P, Willerson JT, Yeh ET. Inflammatory Cytokines Stimulated C-Reactive Protein Production by Human Coronary Artery Smooth Muscle Cells. *Circulation* (2003) 108(16):1930–2. doi: 10.1161/01.CIR.0000096055.62724.C5
55. Zhang D, Jiang SL, Rzewnicki D, Samols D, Kushner I. The Effect of Interleukin-1 on C-Reactive Protein Expression in Hep3B Cells is Exerted at the Transcriptional Level. *Biochem J* (1995) 310(Pt 1):143–8. doi: 10.1042/bj3100143
56. Zhou QB, Xia WH, Ren J, Yu BB, Tong XZ, Chen YB, et al. Effect of Intensive Periodontal Therapy on Blood Pressure and Endothelial Microparticles in Patients With Prehypertension and Periodontitis: A Randomized Controlled Trial. *J Periodontol* (2017) 88(8):711–22. doi: 10.1902/jop.2017.160447
57. Shimada Y, Komatsu Y, Ikezawa-Suzuki I, Tai H, Sugita N, Yoshie H. The Effect of Periodontal Treatment on Serum Leptin, Interleukin-6, and C-Reactive Protein. *J Periodontol* (2010) 81(8):1118–23. doi: 10.1902/jop.2010.090741
58. Türer ÇC, Durmuş D, Balli U, Güven B. Effect of Non-Surgical Periodontal Treatment on Gingival Crevicular Fluid and Serum Endocan, Vascular Endothelial Growth Factor-A, and Tumor Necrosis Factor-Alpha Levels. *J Periodontol* (2017) 88(5):493–501. doi: 10.1902/jop.2016.160279
59. Vijayakumar S, Koshi E, Sadasivan A, Indhuja RS, Vallabhan CG. Effect of Nonsurgical Periodontal Therapy on Serum Levels of Interleukin-1β and Interleukin-8 in Smokers and Nonsmokers With Chronic Periodontitis. *J Pharm Bioallied Sci* (2020) 12(Suppl 1):S313–s8. doi: 10.4103/jpbs.JPBS_93_20
60. Paul O, Arora P, Mayer M, Chatterjee S. Inflammation in Periodontal Disease: Possible Link to Vascular Disease. *Front Physiol* (2021) 14:609614. doi: 10.3389/fphys.2020.609614
61. Loos BG, Van Dyke TE. The Role of Inflammation and Genetics in Periodontal Disease. *Periodontol 2000* (2020) 83(1):26–39. doi: 10.1111/prd.12297
62. Herrera D, Molina A, Buhlin K, Klinge B. Periodontal Diseases and Association With Atherosclerotic Disease. *Periodontol 2000* (2020) 83 (1):66–89. doi: 10.1111/prd.12302
63. Beukers NG, van der Heijden GJ, van Wijk AJ, Loos BG. Periodontitis is an Independent Risk Indicator for Atherosclerotic Cardiovascular Diseases Among 60 174 Participants in a Large Dental School in the Netherlands. *J Epidemiol Community Health* (2017) 71(1):37–42. doi: 10.1136/jech-2015-206745
64. Van Dyke TE, Kholy KE, Ishai A, Takx RA, Mezue K, Abohashem SM, et al. Inflammation of the Periodontium Associates With Risk of Future Cardiovascular Events. *J Periodontol* (2021) 92(3):348–58. doi: 10.1002/JPER.19-0441
65. Moutsopoulos NM, Madianos PN. Low-Grade Inflammation in Chronic Infectious Diseases: Paradigm of Periodontal Infections. *Ann N Y Acad Sci* (2006) 1088:251–64. doi: 10.1196/annals.1366.032
66. Górska R, Gregorek H, Kowalski J, Laskus-Perendyk A, Syczewska M, Madaliński K. Relationship Between Clinical Parameters and Cytokine Profiles in Inflamed Gingival Tissue and Serum Samples From Patients With Chronic Periodontitis. *J Clin Periodontol* (2003) 30(12):1046–52. doi: 10.1046/j.0303-6979.2003.00425.x
67. Loos BG, Craandijk J, Hoek FJ, PMWv D, van der Velden U. Elevation of Systemic Markers Related to Cardiovascular Diseases in the Peripheral Blood of Periodontitis Patients. *J Periodontol* (2000) 71(10):1528–34. doi: 10.1902/jop.2000.71.10.1528
68. Botelho J, Machado V, Hussain SB, Zehra SA, Proença L, Orlandi M, et al. Periodontitis and Circulating Blood Cell Profiles: A Systematic Review and Meta-Analysis. *Exp Hematol* (2021) 93:1–13. doi: 10.1016/j.exphem.2020.10.001
69. Irwandi RA, Kuswandani SO, Harden S, Marletta D, D'Aiuto F. Circulating Inflammatory Cell Profiling and Periodontitis: A Systematic Review and Meta-Analysis. *J Leukoc Biol* (2022) 111(5):1069–96. doi: 10.1002/JLB.5RU1021-524R
70. de Oliveira C, Watt R, Hamer M. Toothbrushing, Inflammation, and Risk of Cardiovascular Disease: Results From Scottish Health Survey. *BMJ* (2010) 27:340. doi: 10.1136/bmj.c2451
71. Zarbock A, Ley K. Mechanisms and Consequences of Neutrophil Interaction With the Endothelium. *Am J Pathol* (2008) 172(1):1–7. doi: 10.2353/ajpath.2008.070502
72. Drechsler M, de Jong R, Rossaint J, Viola JR, Leoni G, Wang JM, et al. Annexin A1 Counteracts Chemokine-Induced Arterial Myeloid Cell Recruitment. *Circ Res* (2015) 116(5):827–35. doi: 10.1161/CIRCRESAHA.116.305825
73. Ortega-Gomez A, Salvermoser M, Rossaint J, Pick R, Brauner J, Lemnitzer P, et al. Cathepsin G Controls Arterial But Not Venular Myeloid Cell Recruitment. *Circulation* (2016) 134(16):1176–88. doi: 10.1161/CIRCULATIONAHA.116.024790
74. Soehnlein O. Multiple Roles for Neutrophils in Atherosclerosis. *Circ Res* (2012) 110(6):875–88. doi: 10.1161/CIRCRESAHA.111.257535
75. Di Gennaro A, Kenne E, Wan M, Soehnlein O, Lindbom L, Haeggström JZ. Leukotriene B4-Induced Changes in Vascular Permeability Are Mediated by Neutrophil Release of Heparin-Binding Protein (HBP/CAP37/azurocidin). *FASEB J* (2009) 23(6):1750–7. doi: 10.1096/fj.08-121277
76. Rasmuson J, Kenne E, Wahlgren M, Soehnlein O, Lindbom L. Heparinoid Sevuparin Inhibits Streptococcus-Induced Vascular Leak Through Neutralizing Neutrophil-Derived Proteins. *FASEB J* (2019) 33(9):10443–52. doi: 10.1096/fj.201900627R
77. Chertov O, Ueda H, Xu LL, Tani K, Murphy WJ, Wang JM, et al. Identification of Human Neutrophil-Derived Cathepsin G and Azurocidin/CAP37 as Chemoattractants for Mononuclear Cells and Neutrophils. *J Exp Med* (1997) 186(5):739–47. doi: 10.1084/jem.186.5.739
78. Taekema-Roelvink MEJ, Kooten CV, Kooij SV, Heemskerk E, Daha MR. Proteinase 3 Enhances Endothelial Monocyte Chemoattractant Protein-1 Production and Induces Increased Adhesion of Neutrophils to Endothelial Cells by Upregulating Intercellular Cell Adhesion Molecule-1. *J Am Soc Nephrol* (2001) 12(5):932–40. doi: 10.1681/ASN.V125932
79. De Y, Chen Q, Schmidt AP, Anderson GM, Wang JM, Wooters J, et al. LL-37, the Neutrophil Granule- and Epithelial Cell-Derived Cathelicidin, Utilizes Formyl Peptide Receptor-Like 1 (FPRL1) as A Receptor to Chemoattract Human Peripheral Blood Neutrophils, Monocytes, and T Cells. *J Exp Med* (2000) 192(7):1069–74. doi: 10.1084/jem.192.7.1069
80. Chaly YV, Paleolog EM, Kolesnikova TS, Tikhonov II, EV P, Voitenok NN. Neutrophil Alpha-Defensin Human Neutrophil Peptide Modulates

Cytokine Production in Human Monocytes and Adhesion Molecule Expression in Endothelial Cells. *Eur Cytokine Netw* (2000) 11(2):257–66.
81. Sun R, Iribarren P, Zhang N, Zhou Y, Gong W, Cho EH, et al. Identification of Neutrophil Granule Protein Cathepsin G as A Novel Chemotactic Agonist for the G Protein-Coupled Formyl Peptide Receptor. *J Immunol* (2004) 173 (1):428–36. doi: 10.4049/jimmunol.173.1.428
82. Carr AC, McCall MR, Frei B. Oxidation of LDL by Myeloperoxidase and Reactive Nitrogen Species: Reaction Pathways and Antioxidant Protection. *Arterioscler Thromb Vasc Biol* (2000) 20(7):1716–23. doi: 10.1161/01.atv.20.7.1716
83. Bekkering S, Quintin J, Joosten LA, van der Meer JW, Netea MG, Riksen NP. Oxidized Low-Density Lipoprotein Induces Long-Term Proinflammatory Cytokine Production and Foam Cell Formation *via* Epigenetic Reprogramming of Monocytes. *Arterioscler Thromb Vasc Biol* (2014) 34 (8):1731–8. doi: 10.1161/ATVBAHA.114.303887
84. Warnatsch A, Ioannou M, Wang Q, Papayannopoulos V. Neutrophil Extracellular Traps License Macrophages for Cytokine Production in Atherosclerosis. *Science* (2015) 17:349(6245):316–20. doi: 10.1126/science.aaa8064
85. Silvestre-Roig C, Braster Q, Wichapong K, Lee EY, Teulon JM, Berrebeh N, et al. Externalized Histone H4 Orchestrates Chronic Inflammation by Inducing Lytic Cell Death. *Nature* (2019) 569(7755):236–40. doi: 10.1038/s41586-019-1167-6
86. Mawhin MA, Tilly P, Zirka G, Charles AL, Slimani F, Vonesch JL, et al. Neutrophils Recruited by Leukotriene B4 Induce Features of Plaque Destabilization During Endotoxaemia. *Cardiovasc Res* (2018) 114 (12):1656–66. doi: 10.1093/cvr/cvy130
87. Franck G, Mawson TL, Folco EJ, Molinaro R, Ruvkun V, Engelbertsen D, et al. Roles of PAD4 and NETosis in Experimental Atherosclerosis and Arterial Injury: Implications for Superficial Erosion. *Circ Res* (2018) 123 (1):33–42. doi: 10.1161/CIRCRESAHA.117.312494
88. Gopalkrishna S, Johnson J, Jaggers RM, Dahdah A, Murphy AJ, Hanssen NM, et al. Neutrophils in Cardiovascular Disease: Warmongers, Peacemakers or Both? *Cardiovasc Res* (2021), cvab302. doi: 10.1093/cvr/cvab302
89. Nagareddy PR, Sreejit G, Abo-Aly M, Jaggers RM, Chelvarajan L, Johnson J, et al. NETosis is Required for S100A8/A9-Induced Granulopoiesis After Myocardial Infarction. *Arterioscler Thromb Vasc Biol* (2020) 40(11):2805–07. doi: 10.1161/ATVBAHA.120.314807
90. Sreejit G, Abdel-Latif A, Athmanathan B, Annabathula R, Dhyani A, Noothi SK, et al. Neutrophil-Derived S100A8/A9 Amplify Granulopoiesis After Myocardial Infarction. *Circulation* (2020) 141(13):1080–94. doi: 10.1161/CIRCULATIONAHA.119.043833
91. Horckmans M, Ring L, Duchene J, Santovito D, Schloss MJ, Drechsler M, et al. Neutrophils Orchestrate Post-Myocardial Infarction Healing by Polarizing Macrophages Towards a Reparative Phenotype. *Eur Heart J* (2017) 14;38(3):187–97. doi: 10.1093/eurheartj/ehw002
92. Marinković G, Koenis DS, de Camp L, Jablonowski R, Graber N, de Waard V, et al. S100A9 Links Inflammation and Repair in Myocardial Infarction. *Circ Res* (2020) 14;127(5):664–76. doi: 10.1161/CIRCRESAHA.120.315865
93. Ferraro B, Leoni G, Hinkel R, Ormanns S, Paulin N, Ortega-Gomez A, et al. Pro-Angiogenic Macrophage Phenotype to Promote Myocardial Repair. *J Am Coll Cardiol* (2019) 18;73(23):2990–3002. doi: 10.1016/j.jacc.2019.03.503
94. Allen C, Thornton P, Denes A, McColl BW, Pierozynski A, Monestier M, et al. Neutrophil Cerebrovascular Transmigration Triggers Rapid Neurotoxicity Through Release of Proteases Associated With Decondensed DNA. *J Immunol* (2012) 189(1):381–92. doi: 10.4049/jimmunol.1200409
95. Mitroulis I, Ruppova K, Wang B, Chen LS, Grzybek M, Grinenko T, et al. Modulation of Myelopoiesis Progenitors Is an Integral Component of Trained Immunity. *Cell* (2018) 172(1-2):147–61.e12. doi: 10.1016/j.cell.2017.11.034
96. Chavakis T, Mitroulis I, Hajishengallis G. Hematopoietic Progenitor Cells as Integrative Hubs for Adaptation to and Fine-Tuning of Inflammation. *Nat Immunol* (2019) 20(7):802–11. doi: 10.1038/s41590-019-0402-5
97. King KY, Goodell MA. Inflammatory Modulation of HSCs: Viewing the HSC as a Foundation for the Immune Response. *Nat Rev Immunol* (2011) 11 (10):685–92. doi: 10.1038/nri3062
98. Manz MG, Boettcher S. Emergency Granulopoiesis. *Nat Rev Immunol* (2014) 14(5):302–14. doi: 10.1038/nri3660
99. Li X, Wang H, Yu X, Saha G, Kalafati L, Ioannidis C, et al. Maladaptive Innate Immune Training of Myelopoiesis Links Inflammatory Comorbidities. *Cell* (2022) 185(10):1709–27.e18. doi: 10.1016/j.cell.2022.03.043
100. Yamashita M, Passegué E. TNF-α Coordinates Hematopoietic Stem Cell Survival and Myeloid Regeneration. *Cell Stem Cell* (2019) 25(3):357–72.e7. doi: 10.1016/j.stem.2019.05.019
101. Schürch CM, Riether C, Ochsenbein AF. Cytotoxic CD8+ T Cells Stimulate Hematopoietic Progenitors by Promoting Cytokine Release From Bone Marrow Mesenchymal Stromal Cells. *Cell Stem Cell* (2014) 3;14(4):460–72. doi: 10.1016/j.stem.2014.01.002
102. Kalafati L, Kourtzelis I, Schulte-Schrepping J, Li X, Hatzioannou A, Grinenko T, et al. Innate Immune Training of Granulopoiesis Promotes Anti-Tumor Activity. *Cell* (2020) 183(3):771–85.e12. doi: 10.1016/j.cell.2020.09.05
103. Matatall KA, Jeong M, Chen S, Sun D, Chen F, Mo Q, et al. Chronic Infection Depletes Hematopoietic Stem Cells Through Stress-Induced Terminal Differentiation. *Cell Rep* (2016) 17(10):2584–95. doi: 10.1016/j.celrep.2016.11.031
104. Christopher MJ, Rao M, Liu F, Woloszynek JR, Link DC. Expression of the G-CSF Receptor in Monocytic Cells is Sufficient to Mediate Hematopoietic Progenitor Mobilization by G-CSF in Mice. *J Exp Med* (2011) 208(2):251–60. doi: 10.1084/jem.20101700
105. Hérault A, Binnewies M, Leong S, Calero-Nieto FJ, Zhang SY, Kang Y-A, et al. Myeloid Progenitor Cluster Formation Drives Emergency and Leukaemic Myelopoiesis. *Nature* (2017) 544(7648):53–8. doi: 10.1038/nature21693
106. Wright HJ, Matthews JB, Chapple IL, Ling-Mountford N, Cooper PR. Periodontitis Associates With a Type 1 IFN Signature in Peripheral Blood Neutrophils. *J Immunol* (2008) 181(8):5775–84. doi: 10.4049/jimmunol.181.8.5775
107. Yu H, Zhang T, Lu H, Ma Q, Zhao D, Sun J, et al. Granulocyte Colony-Stimulating Factor (G-CSF) Mediates Bone Resorption in Periodontitis. *BMC Oral Health* (2021) 21(1):299. doi: 10.1186/s12903-021-01658-1
108. Hajishengallis G, Chavakis T, Hajishengallis E, Lambris JD. Neutrophil Homeostasis and Inflammation: Novel Paradigms From Studying Periodontitis. *J Leukoc Biol* (2015) 98(4):539–48. doi: 10.1189/jlb.3VMR1014-468R
109. Ishai A, Osborne MT, El Kholy K, Takx RA, Ali A, Yuan N, et al. Periodontal Disease Associates With Arterial Inflammation *via* Potentiation of a Hematopoietic-Arterial Axis. *JACC Cardiovasc Imaging* (2019) 12(11 Pt 1):2271–73. doi: 10.1016/j.jcmg.2019.05.015
110. Noz MP, Plachokova AS, Smeets EM, Aarntzen EH, Bekkering S, Vart P, et al. An Explorative Study on Monocyte Reprogramming in the Context of Periodontitis. *In Vitro In Vivo Front Immunol* (2021) 12:69522. doi: 10.3389/fimmu.2021.69522
111. Fredriksson MI. Effect of Priming in Subpopulations of Peripheral Neutrophils From Patients With Chronic Periodontitis. *J Periodontol* (2012) 83(9):1192–9. doi: 10.1902/jop.2012.110584
112. Johnstone AM, Koh A, Goldberg MB, Glogauer M. A Hyperactive Neutrophil Phenotype in Patients With Refractory Periodontitis. *J Periodontol* (2007) 78(9):1788–94. doi: 10.1902/jop.2007.070107
113. Kim KY, Kim M-K, Choi YS, Kim YC, A-r Jo, Rhyu I-C, et al. A Hyperactive Neutrophil Phenotype in Aggresive Periodontitis. *Int J Oral Biol* (2013) 37 (2):69–75.
114. Dias IH, Chapple IL, Milward M, Grant MM, Hill E, Brown J, et al. Sulforaphane Restores Cellular Glutathione Levels and Reduces Chronic Periodontitis Neutrophil Hyperactivity in Vitro. *PLoS One* (2013) 8(6): e66407. doi: 10.1371/journal.pone.0066407
115. Žilinskas J, Žekonis J, Žekonis G, Šadzevičienė R, Sapragonienė M, Navickaitė J, et al. Inhibition of Peripheral Blood Neutrophil Oxidative Burst in Periodontitis Patients With a Homeopathic Medication Traumeel s. *Med Sci Monit* (2011) 17(5):Cr284–91. doi: 10.12659/msm.881769
116. Ling MR, Chapple IL, Matthews JB. Peripheral Blood Neutrophil Cytokine Hyper-Reactivity in Chronic Periodontitis. *Innate Immun* (2015) 21(7):714–25. doi: 10.1177/1753425915589387

117. Figueredo C, Gustafsson A, Åsman B, Bergström K. Expression of Intracellular Elastase Activity in Peripheral Neutrophils From Patients With Adult Periodontitis. *J Clin Periodontol* (2000) 27(8):572–7. doi: 10.1034/j.1600-051x.2000.027008572.x
118. Guentsch A, Puklo M, Preshaw PM, Glockmann E, Pfister W, Potempa J, et al. Neutrophils in Chronic and Aggressive Periodontitis in Interaction With Porphyromonas Gingivalis and Aggregatibacter Actinomycetemcomitans. *J Periodontal Res* (2009) 44(3):368–77. doi: 10.1111/j.1600-0765.2008.01113.x
119. Fine N, Chadwick JW, Sun C, Parbhakar KK, Khoury N, Barbour A, et al. Periodontal Inflammation Primes the Systemic Innate Immune Response. *J Dent Res* (2021) 100(3):318–25. doi: 10.1177/0022034520963710
120. Welsh C, Welsh P, Mark PB, Celis-Morales CA, Lewsey J, Gray SR, et al. Association of Total and Differential Leukocyte Counts With Cardiovascular Disease and Mortality in the UK Biobank. *Arterioscler Thromb Vasc Biol* (2018) 38(6):1415–23. doi: 10.1161/ATVBAHA.118.310945
121. Lassale C, Curtis A, Abete I, van der Schouw YT, Verschuren WM, Lu Y. Elements of the Complete Blood Count Associated With Cardiovascular Disease Incidence: Findings From the EPIC-NL Cohort Study. *Sci Rep* (2018) 8(1):3290. doi: 10.1038/s41598-018-21661-x
122. White P, Sakellari D, Roberts H, Risafi I, Ling M, Cooper P, et al. Peripheral Blood Neutrophil Extracellular Trap Production and Degradation in Chronic Periodontitis. *J Clin Periodontol* (2016) 43(12):1041–9. doi: 10.1111/jcpe.12628
123. Leira Y, Rodríguez-Yáñez M, Arias S, López-Dequidt I, Campos F, Sobrino T, et al. Periodontitis as a Risk Indicator and Predictor of Poor Outcome for Lacunar Infarct. *J Clin Periodontol* (2019) 46(1):20–30. doi: 10.1111/jcpe.13032
124. Medara N, Lenzo JC, Walsh KA, Reynolds EC, O'Brien-Simpson NM, Darby IB. Peripheral Neutrophil Phenotypes During Management of Periodontitis. *J Periodontal Res* (2021) 56(1):58–68. doi: 10.1111/jre.12793
125. Ridker PM, Everett BM, Thuren T, MacFadyen JG, Chang WH, Ballantyne C, et al. Antiinflammatory Therapy With Canakinumab for Atherosclerotic Disease. *N Engl J Med* (2017) 377(12):1119–31. doi: 10.1056/NEJMoa1707914
126. Everett BM, Cornel JH, Lainscak M, Anker SD, Abbate A, Thuren T, et al. Anti-Inflammatory Therapy With Canakinumab for the Prevention of Hospitalization for Heart Failure. *Circulation* (2019) 139(10):1289–99. doi: 10.1161/CIRCULATIONAHA.118.038010
127. Tardif J-C, Kouz S, Waters DD, Bertrand OF, Diaz R, Maggioni AP, et al. Efficacy and Safety of Low-Dose Colchicine After Myocardial Infarction. *N Engl J Med* (2019) 381(26):2497–505. doi: 10.1056/NEJMoa1912388
128. Nidorf SM, Fiolet ATL, Mosterd A, Eikelboom JW, Schut A, Opstal TSJ, et al. Colchicine in Patients With Chronic Coronary Disease. *N Engl J Med* (2020) 383(19):1838–47. doi: 10.1056/NEJMoa2021372
129. Soehnlein O, Libby P. Targeting Inflammation in Atherosclerosis — From Experimental Insights to the Clinic. *Nat Rev Drug Discov* (2021) 20(8):589–610. doi: 10.1038/s41573-021-00198-1
130. Németh T, Sperandio M, Mócsai A. Neutrophils as Emerging Therapeutic Targets. *Nat Rev Drug Discovery* (2020) 19(4):253–75. doi: 10.1038/s41573-019-0054-z
131. Sager HB, Dutta P, Dahlman JE, Hulsmans M, Courties G, Sun Y, et al. RNAi Targeting Multiple Cell Adhesion Molecules Reduces Immune Cell Recruitment and Vascular Inflammation After Myocardial Infarction. *Sci Transl Med* (2016) 8(342):342ra80. doi: 10.1126/scitranslmed.aaf1435
132. Kempf T, Zarbock A, Widera C, Butz S, Stadtmann A, Rossaint J, et al. GDF-15 is an Inhibitor of Leukocyte Integrin Activation Required for Survival After Myocardial Infarction in Mice. *Nat Med* (2011) 17(5):581–8. doi: 10.1038/nm.2354
133. Choi EY, Orlova VV, Fagerholm SC, Nurmi SM, Zhang L, Ballantyne CM, et al. Regulation of LFA-1-Dependent Inflammatory Cell Recruitment by Cbl-B and 14-3-3 Proteins. *Blood* (2008) 111(7):3607–14. doi: 10.1182/blood-2007-07-103077
134. Shin J, Maekawa T, Abe T, Hajishengallis E, Hosur K, Pyaram K, et al. DEL-1 Restrains Osteoclastogenesis and Inhibits Inflammatory Bone Loss in Nonhuman Primates. *Sci Transl Med* (2015) 7(307):307ra155. doi: 10.1126/scitranslmed.aac5380
135. Papayannopoulos V. Neutrophil Extracellular Traps in Immunity and Disease. *Nat Rev Immunol* (2018) 18(2):134–47. doi: 10.1038/nri.2017.105
136. Knight JS, Luo W, O'Dell AA, Yalavarthi S, Zhao W, Subramanian V, et al. Peptidylarginine Deiminase Inhibition Reduces Vascular Damage and Modulates Innate Immune Responses in Murine Models of Atherosclerosis. *Circ Res* (2014) 114(6):947–56. doi: 10.1161/CIRCRESAHA.114.303312
137. Kenny EF, Herzig A, Krüger R, Muth A, Mondal S, Thompson PR, et al. Diverse Stimuli Engage Different Neutrophil Extracellular Trap Pathways. *Elife* (2017) 6:e24437. doi: 10.7554/eLife.24437
138. Brill A, Fuchs T, Savchenko A, Thomas G, Martinod K, De Meyer S, et al. Neutrophil Extracellular Traps Promote Deep Vein Thrombosis in Mice. *J Thromb Haemost* (2012) 10(1):136–44. doi: 10.1111/j.1538-7836.2011.04544.x
139. Farrera C, Fadeel B. Macrophage Clearance of Neutrophil Extracellular Traps is a Silent Process. *J Immunol* (2013) 191(5):2647–56. doi: 10.4049/jimmunol.1300436
140. Paulin N, Viola JR, Maas SL, de Jong R, Fernandes-Alnemri T, Weber C, et al. Double-Strand DNA Sensing Aim2 Inflammasome Regulates Atherosclerotic Plaque Vulnerability. *Circulation* (2018) 138(3):321–3. doi: 10.1161/CIRCULATIONAHA.117.033098
141. Tsourouktsoglou TD, Warnatsch A, Ioannou M, Hoving D, Wang Q, Papayannopoulos V. Histones, DNA, and Citrullination Promote Neutrophil Extracellular Trap Inflammation by Regulating the Localization and Activation of TLR4. *Cell Rep* (2020) 31(5):107602. doi: 10.1016/j.celrep.2020.107602
142. Apel F, Andreeva L, Knackstedt LS, Streeck R, Frese CK, Goosmann C, et al. The Cytosolic DNA Sensor cGAS Recognizes Neutrophil Extracellular Traps. *Sci Signal* (2021) 14(673):eaax7942. doi: 10.1126/scisignal.aax7942
143. Krupa A, Fol M, Rahman M, Stokes KY, Florence JM, Leskov IL, et al. Silencing Bruton's Tyrosine Kinase in Alveolar Neutrophils Protects Mice From LPS/Immune Complex-Induced Acute Lung Injury. *Am J Physiol Lung Cell Mol Physiol* (2014) 307(6):L435–48. doi: 10.1152/ajplung.00234.2013
144. Wang Z, Li J, Cho J, Malik AB. Prevention of Vascular Inflammation by Nanoparticle Targeting of Adherent Neutrophils. *Nat Nanotechnol* (2014) 9(3):204–10. doi: 10.1038/nnano.2014.17
145. Miettinen HM, Gripentrog JM, Lord CI, Nagy JO. CD177-Mediated Nanoparticle Targeting of Human and Mouse Neutrophils. *PLoS One* (2018) 13(7):e0200444. doi: 10.1371/journal.pone.0200444
146. Ibanez B, Macaya C, Sánchez-Brunete V, Pizarro G, Fernández-Friera L, Mateos A, et al. Effect of Early Metoprolol on Infarct Size in ST-Segment-Elevation Myocardial Infarction Patients Undergoing Primary Percutaneous Coronary Intervention: The Effect of Metoprolol in Cardioprotection During an Acute Myocardial Infarction (METOCARD-CNIC) Trial. *Circulation* (2013) 128(14):1495–503. doi: 10.1161/CIRCULATIONAHA.113.003653
147. Pizarro G, Fernández-Friera L, Fuster V, Fernández-Jiménez R, García-Ruiz JM, García-Álvarez A, et al. Long-Term Benefit of Early Pre-Reperfusion Metoprolol Administration in Patients With Acute Myocardial Infarction: Results From the METOCARD-CNIC Trial (Effect of Metoprolol in Cardioprotection During an Acute Myocardial Infarction). *J Am Coll Cardiol* (2014) 63(22):2356–62. doi: 10.1016/j.jacc.2014.03.014
148. García-Prieto J, Villena-Gutiérrez R, Gómez M, Bernardo E, Pun-García A, García-Lunar I, et al. Neutrophil Stunning by Metoprolol Reduces Infarct Size. *Nat Commun* (2017) 8:14780. doi: 10.1038/ncomms14780
149. Clemente-Moragón A, Gómez M, Villena-Gutiérrez R, Lalama DV, García-Prieto J, Martínez F, et al. Metoprolol Exerts a Non-Class Effect Against Ischaemia-Reperfusion Injury by Abrogating Exacerbated Inflammation. *Eur Heart J* (2020) 41(46):4425–40. doi: 10.1093/eurheartj/ehaa733
150. Herz J, Sabellek P, Lane TE, Gunzer M, Hermann DM, Doeppner TR. Role of Neutrophils in Exacerbation of Brain Injury After Focal Cerebral Ischemia in Hyperlipidemic Mice. *Stroke* (2015) 46(10):2916–25. doi: 10.1161/STROKEAHA.115.010620
151. Jurcevic S, Humfrey C, Uddin M, Warrington S, Larsson B, Keen C. The Effect of a Selective CXCR2 Antagonist (AZD5069) on Human Blood Neutrophil Count and Innate Immune Functions. *Br J Clin Pharmacol* (2015) 80(6):1324–36. doi: 10.1111/bcp.12724
152. Joseph JP, Reyes E, Guzman J, O'Doherty J, McConkey H, Arri S, et al. CXCR2 Inhibition - a Novel Approach to Treating CoronAry Heart DiseAse (CICADA): Study Protocol for a Randomised Controlled Trial. *Trials* (2017) 18(1):473. doi: 10.1186/s13063-017-2210-2

153. Hasturk H, Hajishengallis G, Lambris JD, Mastellos DC, Yancopoulou D. Phase IIa Clinical Trial of Complement C3 Inhibitor AMY-101 in Adults With Periodontal Inflammation. *J Clin Invest* (2021) 131(23):e152973. doi: 10.1172/JCI152973
154. Hajishengallis G, Liang S, Payne MA, Hashim A, Jotwani R, Eskan MA, et al. Low-Abundance Biofilm Species Orchestrates Inflammatory Periodontal Disease Through the Commensal Microbiota and Complement. *Cell Host Microbe* (2011) 10(5):497–506. doi: 10.1016/j.chom.2011.10.006
155. Maekawa T, Krauss JL, Abe T, Jotwani R, Triantafilou M, Triantafilou K, et al. Porphyromonas Gingivalis Manipulates Complement and TLR Signaling to Uncouple Bacterial Clearance From Inflammation and Promote Dysbiosis. *Cell Host Microbe* (2014) 15(6):768–78. doi: 10.1016/j.chom.2014.05.012
156. Hajishengallis G, Hasturk H, Lambris JD. C3-Targeted Therapy in Periodontal Disease: Moving Closer to the Clinic. *Trends Immunol* (2021) 42(10):856–64. doi: 10.1016/j.it.2021.08.001
157. Räisänen IT, Lähteenmäki H, Gupta S, Grigoriadis A, Sahni V, Suojanen J, et al. An aMMP-8 Point-Of-Care and Questionnaire Based Real-Time Diagnostic Toolkit for Medical Practitioners. *Diagnostics (Basel)* (2021) 11 (4):711. doi: 10.3390/diagnostics11040711
158. Lee CT, Teles R, Kantarci A, Chen T, McCafferty J, Starr JR, et al. Resolvin E1 Reverses Experimental Periodontitis and Dysbiosis. *J Immunol* (2016) 197 (7):2796–806. doi: 10.4049/jimmunol.1600859
159. Kajikawa T, Meshikhes F, Maekawa T, Hajishengallis E, Hosur KB, Abe T, et al. Milk Fat Globule Epidermal Growth Factor 8 Inhibits Periodontitis in Non-Human Primates and Its Gingival Crevicular Fluid Levels Can Differentiate Periodontal Health From Disease in Humans. *J Clin Periodontol* (2017) 44(5):472–83. doi: 10.1111/jcpe.12707

Conflict of Interest: The authors declare that the research was conducted in the absence of any commercial or financial relationships that could be construed as a potential conflict of interest.

Publisher's Note: All claims expressed in this article are solely those of the authors and do not necessarily represent those of their affiliated organizations, or those of the publisher, the editors and the reviewers. Any product that may be evaluated in this article, or claim that may be made by its manufacturer, is not guaranteed or endorsed by the publisher.

frontiers | Frontiers in Immunology

TYPE Mini Review
PUBLISHED 05 August 2022
DOI 10.3389/fimmu.2022.974821

OPEN ACCESS

EDITED BY
Markus H. Hoffmann,
University of Lübeck, Germany

REVIEWED BY
Mohammed Merza,
Hawler Medical University, Iraq
Christian Maueröder,
VIB-UGent Center for Inflammation Research (IRC), Belgium

*CORRESPONDENCE
Cong Qiao
qiaocong@hrbmu.edu.cn

SPECIALTY SECTION
This article was submitted to Inflammation, a section of the journal Frontiers in Immunology

RECEIVED 21 June 2022
ACCEPTED 18 July 2022
PUBLISHED 05 August 2022

CITATION
Li H, Zhao L, Wang Y, Zhang M-C and Qiao C (2022) Roles, detection, and visualization of neutrophil extracellular traps in acute pancreatitis. *Front. Immunol.* 13:974821. doi: 10.3389/fimmu.2022.974821

Roles, detection, and visualization of neutrophil extracellular traps in acute pancreatitis

Hongxuan Li[1], Lingyu Zhao[2], Yueying Wang[3], Meng-Chun Zhang[4] and Cong Qiao[2]*

[1]Department of General Surgery, The First Affiliated Hospital of Harbin Medical University, Harbin, China, [2]Department of Pathology, Harbin Medical University, Harbin, China, [3]Department of Pathology, The First Affiliated Hospital of Harbin Medical University, Harbin, China, [4]Department of Pharmacology, Harbin Medical University, Harbin, China

Neutrophil extracellular traps (NETs) are produced in large quantities at the site of inflammation, and they locally capture and eliminate various pathogens. Thus, NETs quickly control the infection of pathogens in the body and play vital roles in immunity and antibacterial effects. However, evidence is accumulating that NET formation can exacerbate pancreatic tissue damage during acute pancreatitis (AP). In this review, we describe the research progress on NETs in AP and discuss the possibility of NETs as potential therapeutic targets. In addition, since the current detection and visualization methods of NET formation are not uniform and the selection of markers is still controversial, a synopsis of these issues is provided in this review.

KEYWORDS

neutrophil extracellular traps, acute pancreatitis, multicolor immunofluorescence, citrullinated histone 3, peptidylarginine deiminase 4

Introduction

Acute pancreatitis (AP) begins with cellular injury and endoplasmic reticulum stress due to premature activation of digestive enzymes in acinar cells (1–5). The associated processes include converting trypsinogen to trypsin by lysosomal hydrolase cathepsin B (3, 6) and then degrading trypsin by cathepsin L (6–8). Subsequently, protease activation cascade induces cell death, releasing danger molecules known as damage-associated molecular patterns (DAMPs), and eventually activating the immune system (3, 7). In this process, the intensity of the immune response determines the possibility of systemic complications and disease severity (9–11). After the onset of AP, neutrophils are the first set of leukocytes that infiltrate the pancreatic tissue, directly inducing the activation of

intracellular proteases, promoting necrotic cell death, and occluding the acinar lumen leading to pancreatic damage (9, 12–15). An avalanche of research reports indicates that the aggregation of neutrophils in pancreatic tissues is a key factor in the development of AP. Mechanistically, this is because neutrophils infiltrating the pancreatic tissue can aggravate tissue damage by releasing reactive oxygen species (ROS) (13), enzymes (such as elastase and matrix metalloproteinase-9) (16, 17) and tumor necrosis factor-α (TNFα) (12, 18).

There is growing evidence that the web-like structures released by neutrophils, the neutrophil extracellular traps (NETs), can promote pancreatic tissue damage in AP (19–21). However, presently, the available detection and visualization methods of NET formation are not uniform. Due to the different stimulation of neutrophils, histone H3 may not be citrullinated during the NET formation, so the use of citrullinated histone H3 (citH3) or peptidylarginine deiminase 4 (PAD4) as a marker for NETs remains controversial (22, 23). In addition, given the diversity of AP models, the effect of different stimuli on markers may also be one of the controversial factors. Therefore, in this article, we review the research progress between NETs and AP along with the detection and visualization methods, and selection of markers underlying NET formation.

Mechanisms of NET formation

NETs are web-like structures with decondensed chromatin fragments as the skeleton and wrapped in histones, proteases, granules, and cytoplasmic proteins (24). Based on recommendations published by experts in this field, the term "NET formation" is used to describe the process by which neutrophils produce and release NETs (25).Currently, there are two known pathways for NET formation. The first is the cell death pathway known as lytic NET formation, which begins with nuclear delobulation and the disassembly of the nuclear envelope and continues until the loss of cell polarization, chromatin decondensation, and plasma membrane rupture. The second is non-lytic NET formation, which can occur independently of cell death and involves the secretory excretion of nuclear chromatin that is accompanied by the release of granular proteins through degranulation (26). According to the literature, non-lytic NET formation occurs within minutes of exposure to *Staphylococcus aureus*, during which there is no cell death (27, 28). In addition to this, P-selectin/P-selectin glycoprotein ligand-1 mediates neutrophil-platelet interaction (29, 30) and activated platelets can promote non-lytic NET formation through high mobility group protein B1 (HMGB1)/receptor for advanced glycation end products (31). In view of the peculiarity of the non-lytic NET formation, most of the current studies are conducted in lytic NET formation background.

In the NET formation pathway, the process from ROS generation to chromatin decondensation is the core mechanism. However, it is noteworthy that the inhibition of leukocyte signal inhibitory receptor 1 prevented NET formation without affecting ROS (32). Due to various stimuli, calcium ions are released from the endoplasmic reticulum into the cytoplasm, resulting in an increase in the production of ROS through the NADPH oxidase complex, which in turn activates the protein kinase C or RAF-MEK-MAPK pathway, resulting in NET formation (23, 33, 34). In the aforementioned process, one of the most important ways is to stimulate myeloperoxidase (MPO) through the generated ROS to activate neutrophil elastase (NE) and facilitate the transfer of NE from the azurophilic granules to the nucleus. NE transferred to the nucleus can destroy chromatin packaging by hydrolyzing histones, and then MPO binds to chromatin and synergizes with NE to cause chromatin decondensation (35). However, one study found that inhibiting the enzymatic activity of MPO only delayed NET formation, but did not prevent NET formation (36). NE plays a more important role in this process because NE needs to bind to F-actin filaments in the cytoplasm and degrade them before entering the nucleus to drive chromatin decondensation (37). In addition, the results of the *in vitro* studies showed that NE is sufficient to disintegrate the nucleus (35). Therefore, in the MPO-NE pathway, compared with MPO, the effect of NE activity on NET formation may be more important. In addition to the MPO-NE pathway, another well-studied pathway related to chromatin decondensation is PAD4-driven histone citrullination (38, 39). It has been found that the activation of PAD4 requires a reducing environment (40), but the inhibition of NADPH oxidase still reduces the occurrence of PAD4-driven histone citrullination (24, 26). This is because hydrogen peroxide and ROS generated by NADPH oxidase activation are sufficient to activate PAD4 (41–43). However, ROS production was not eliminated by the inhibition of NADPH oxidase, possibly due to increased mitochondrial ROS production (44). In addition, NADPH oxidase is negatively regulated by active PAD4 (45).

Role of NETs in acute pancreatitis

Many recent studies have shown that NETs may play a pivotal role in the development of AP (19–21). Elimination of NET formation by injecting DNase I into mice effectively reduced CXCL2 production and neutrophil recruitment in inflamed pancreatic tissue (19). The results showed that NETs themselves may play a role as chemotactic signals, or NETs stimulated the release of related chemokines. In addition, the results of the *in vitro* studies showed that histones (histones 2A, 2B, 3, and 4) in NETs can regulate STAT3 activity and trypsin

activation in acinar cells, and their effects on acinar cells are similar to cerulein (19). Emphatically, the formation of NETs is partially dependent on the ROS production. For instance, a study found that c-Abl kinase can promote ROS production and NET formation. This process is accompanied by the increased expression of citH3. Concurrently, inhibition of c-Abl kinase can reduce inflammation and tissue damage in AP (46). ROS can induce autophagy (47) and NET formation is dependent on autophagy (48). Researchers have found that when specific inhibitors for autophagy were injected into mice that NET formation was also inhibited, and this was due to the expression of PAD4, and consequently the severity and survival rates for AP were improved (21). Citrullination of histones is usually driven by PAD4, as described previously. Therefore, a study demonstrated the role of PAD4 in reducing NET formation in pancreatic tissue of severe acute pancreatitis (SAP) by the oral administration of Cl-amidine, a specific inhibitor of PAD4, and the construction of PAD4 knockout (PAD4−/−) mice (21), respectively. In addition, the inhibition of PAD4 expression reduces pathological inflammation and tissue damage in the inflamed pancreas (20). In fact, a recent study also found that the injection of protectin D1 into mice can effectively inhibit the expression of PAD4, thereby reducing NET formation and improving AP (49). Furthermore, the premise of NET formation is the accumulation of neutrophils in pancreatic tissues, where the release of DAMPs plays an important role. The results of the studies found that extracellular cold-inducible RNA-binding protein (eCIRP) and complement C3 can act as DAMPs to promote neutrophil accumulation in pancreatic tissues, which, in turn, leads to NET formation and pancreatic tissue injuries (50, 51). Concurrently, eCIRP is also a component of NETs and can induce acinar cells to secrete amylase by binding to the TLR4 complex in the acinar cell membrane (50). This result suggests that NETs themselves may function as DAMPs or chemotactic signals to some extent. NETs can also be formed by responding to extracellular HMGB1 and histones in a TLR4- and TLR9-dependent manner (26). The results show that HMGB1 can cause pancreatic tissue injury by activating NET formation, but the specific mechanism of activation is not clear (52). To date, the most comprehensive research has shown that IL-17A promotes the accumulation of neutrophils in the pancreatic duct, and bicarbonate ions and calcium carbonate crystals in the pancreatic juice stimulate the accumulated neutrophils to form aggregated NETs (aggNETs), which can then occlude the pancreatic duct, inducing pancreatitis. Notably, the study also found that no intraductal aggNETs were found in cerulein-induced AP, and disease progression in this experimental animal model was independent of PAD4 (53). Based on the above results, further studies found that both low pH and high carbon dioxide/bicarbonate ratio reduced the ability of neutrophils to release NETs (54). Usually, bicarbonate can effectively increase pH, which can then increase the calcium influx, mitochondrial ROS generation, PAD4 activity, and histone 4 cleavage, thereby promoting NET formation (55, 56). Therefore, the alkaline environment provided by pancreatic juice might provide better mechanistic insight into the etiology of AP. In addition, studies have found that platelet particles in plasma samples from patients with AP can significantly promote NET formation, and the level of platelet particles is positively correlated with the severity of AP (57). In summary, reducing NET formation is an effective strategy to improve pancreatic tissue injury in AP, but the relevant mechanisms need to be further explored. Figure 1 summarizes the potential mechanisms of NET formation in AP.

Detection and visualization of NETs in pancreatic tissues of AP

Numerous studies have reported using immunofluorescence staining is often used as a method to detect NET formation in tissue samples (58–60). This is because NET formation is characterized by the co-localization of extracellular DNA, nuclear proteins and granular (or cytoplasmic) proteins, which are significantly separated and relatively fixed from the nucleus in resting neutrophils (61). One study tested diverse antigen retrieval methods and various combinations of commercially available antibodies, and it was found that NETs in the tissue could be best detected when using a mild antigen retrieval protocol and a combination of the NE and histone H3 antibodies (62). In existing studies, the available detection and visualization methods of NET formation in pancreatic tissues of AP are not consistent. In some studies, researchers used scanning and transmission electron microscopies combined with immuno-double-gold labeling technique to detect NET formation, using citH3 or histone2B as the marker of NETs and elastase as a marker of neutrophils (19, 20, 50, 51). Because it is difficult to identify neutrophils from cell morphology by scanning electron microscopy, transmission electron microscopy combined with immuno-double-gold labeling technique can make up for the deficiency of the former. The advantage of this technique is that the pretreatment steps have little effect on the microstructure, and the gold particles have high electron density, which make them clearly distinguishable from other immune products under the electron microscope. In addition, some researchers use immunofluorescence staining to detect NET formation. In this process, they chose citH3 as the marker of NETs, MPO or Ly-6G as the marker of neutrophils (21, 49), or directly chose SYTOX Green dye-labeled extracellular DNA as the marker of NET formation (52). In view of the fact that most of the aforementioned studies focused on the histone citrullination in chromatin driven by PAD4, which depolymerizes the chromatin and promotes NET formation, it is reliable to use citH3 as a marker in the detection of NET

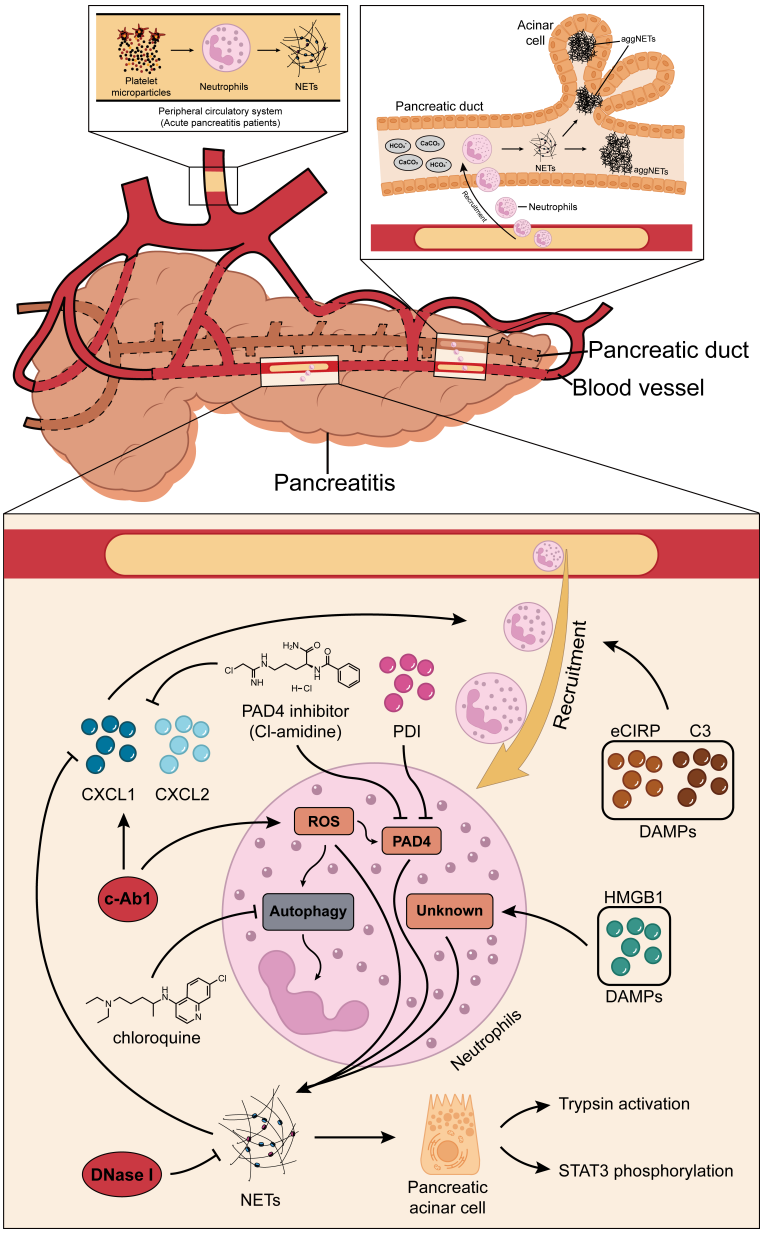

FIGURE 1
Roles of NETs in AP. NETs may inherently function as chemotactic signals to induce the recruitment of neutrophils, or they may stimulate the release of related chemokines (CXCL1 and CXCL2). c-Abl kinase, eCIRP, HMGB1, protectin D1, and complement C3 promote NET formation through the PAD4-driven histone citrullination pathway. Autophagy is also thought to play a role in the NET formation in AP. IL-17A promotes the accumulation of neutrophils in the pancreatic duct, and the bicarbonate ions and calcium carbonate crystals in the pancreatic juice will then stimulate the accumulated neutrophils to generate aggregated NETs and these can occlude the pancreatic duct, inducing pancreatitis. In addition, platelet microparticles can significantly promote NET formation. NETs, neutrophil extracellular traps; AP, acute pancreatitis; CXCL1, C-X-C motif chemokine ligand 1; CXCL2, C-X-C motif chemokine ligand 2; eCIRP, extracellular cold-inducible RNA-binding protein; HMGB1, high mobility group protein 1; PAD4, peptidylarginine deiminase 4.

formation. However, considering the different stimuli in the construction of AP mouse model, we cannot rule out the possibility that NETs are produced by other ways or histone citrullination driven by PAD4 is not the main pathway; thus, if citH3 is used as the sole marker, it may lead to a potential deviation. Therefore, further studies may be needed to discuss the selection of NETs-related markers and the relationship between NETs and AP. A summary of the advantages and disadvantages of each technique based on the corresponding AP mouse model is provided in Table 1.

TABLE 1 Detection and visualization of NETs in pancreatic tissues.

AP models	Detection method	Marker selection	Advantages	Possible problems
Taurocholate (19, 20, 50, 51)	Transmission electron microscopy + Immuno-double-gold labeling	NET-marker: citH3 or Histone 2B Neutrophils-marker: Elastase	The preprocessing steps have less effect on the microstructure; The gold particles have a high electron density, which are clearly distinguishable from other immune products under the electron microscope.	citH3 independent pathways are not detected.
Taurocholate (46); Careulein (52)	Western Blot	NET-marker: citH3 or PAD4		Do not provide the required subcellular resolution; Do not readily allow simultaneous localization of two antigens.
Taurocholate (52); L-arginine (19)	SYTOX Green staining	NET-marker: Extracellular DNA		Poor stability and toxicity; Cannot differentiate between necrotic and NET-cells.
Careulein (49); Pancreatic duct ligation (49); L-arginine (21)	Immunofluorescence staining	NET-marker: citH3 Neutrophils-marker: MPO or Ly-6G	Provide the required subcellular resolution; Allow simultaneous localization of two antigens.	citH3 independent pathways are not detected.

NETs, neutrophil extracellular traps; AP, acute pancreatitis; citH3, citrullinated histone H3; PAD4, peptidylarginine deiminase 4; MPO, myeloperoxidase; Ly-6G, lymphocyte antigen 6 complex locus G6D.

Discussion

An overwhelming number of studies have found that NETs can contribute to inflammation and injury of organs in mice with AP, and thus may be used as a target to reduce pancreatic tissue injuries and inflammation in patients with AP. However, there are a few issues that deserve further discussion, as outlined below. First, are there any other pathways, aside from PAD4-driven histone citrullination pathway, that are involved in the occurrence and development of AP? If so, which one is the main pathway? For now, this issue remains open for exploration in future studies. Second, most studies, including AP, used citH3 as the sole marker of NETs (59, 63), but the use of citH3 or PAD4 as a marker of NETs is controversial (22, 23). Although the detection of citH3 is considered a minimum requirement for the identification of NET formation, quantification biases caused by citH3-independent pathways should also be considered. To address this, co-staining analysis of multiple pathway-related markers should be conducted to visualize NET formation in pancreatic tissues. The components of NETs include MPO and NE: in the resting neutrophils, they do coexist in granules, and their localization with the nucleus is relatively fixed. However, after NET formation, due to chromatin depolymerization and nuclear membrane rupture, the positions of MPO, NE and nuclear DNA become unclear, and the original relatively fixed positions are dismantled, resulting in residual mixing of nucleus, cytoplasm, and granules, which provides conditions for the co-localization of the three. Therefore, a comprehensive visual qualitative analysis of co-staining of MPO, NE and citH3 by immunofluorescence may provide a more comprehensive assessment of NET formation, but further research and discussion are needed in quantitative aspects. Furthermore, it is worth noting that while NET-enriched area can be quite spacious, NETs can be significantly less stretched and contain only a few neutrophils in dense tissue, as in myocarditis (61, 64). Therefore, it is crucial to show the colocalization of nuclear and granular components more clearly by immunofluorescence staining. With the advent of multiple fluorescence immunohistochemicals, this issue can be successfully addressed. A third issue is that of generalizability. Invasive interventions are rarely performed in the early stages of SAP and the optimal timing of invasive interventions is still unclear (65), making it difficult to obtain human pancreatic tissue samples. Currently, only blood samples from patients can be tested for NET formation, and there is still a lack of effective detection methods of NET formation in human pancreatic tissue samples. This limitation is difficult to overcome. Finally, as a fourth issue, we want to remark on an interesting outlook. The premise of NET formation in AP is the accumulation of neutrophils in pancreatic tissues, it is also possible that there are neutrophil subsets with different molecular signatures during pancreatitis. Furthermore, these subsets may respond differently to environmental challenges that subsequently affect their polarization and activation. With the advent of single-cell sequencing technology, combined with analyses based on the technology of cytometry by time-of-flight (CyTOF) mass spectrometry (66, 67), the heterogeneity of neutrophils can be better elucidated. At the same time, this could

also provide more directions for follow-up studies on neutrophils that produce NETs with different phenotypes and functions. Taken together, the related research progress is still limited, although these data suggest that NETs have a therapeutic potential in AP.

Author contributions

HL and CQ developed the concept and design. HL and LZ analyzed the data. HL and CQ wrote the manuscript. LZ, YW, M-CZ, and CQ provided critical discussion, supervised the study, and edited the manuscript. All authors reviewed the paper. All authors contributed to the article and approved the submitted version.

Funding

This work was supported by a grant from the Innovation Foundation of Higher Education of Heilongjiang Province (Grant No.900204).

Acknowledgments

We would like to thank Editage (www.editage.cn) for English language editing.

Conflict of interest

The authors declare that the research was conducted in the absence of any commercial or financial relationships that could be construed as a potential conflict of interest.

Publisher's note

References

1. Lerch MM, Saluja AK, Dawra R, Ramarao P, Saluja M, Steer ML. Acute necrotizing pancreatitis in the opossum: earliest morphological changes involve acinar cells. *Gastroenterology* (1992) 103(1):205–13. doi: 10.1016/0016-5085(92)91114-j

2. Mayerle J, Sendler M, Hegyi E, Beyer G, Lerch MM, Sahin-Toth M. Genetics, cell biology, and pathophysiology of pancreatitis. *Gastroenterology* (2019) 156(7):1951–68.e1. doi: 10.1053/j.gastro.2018.11.081

3. Sendler M, Maertin S, John D, Persike M, Weiss FU, Kruger B, et al. Cathepsin b activity initiates apoptosis *via* digestive protease activation in pancreatic acinar cells and experimental pancreatitis. *J Biol Chem* (2016) 291(28):14717–31. doi: 10.1074/jbc.M116.718999

4. Kereszturi E, Szmola R, Kukor Z, Simon P, Weiss FU, Lerch MM, et al. Hereditary pancreatitis caused by mutation-induced misfolding of human cationic trypsinogen: a novel disease mechanism. *Hum Mutat* (2009) 30(4):575–82. doi: 10.1002/humu.20853

5. Lukas J, Pospech J, Oppermann C, Hund C, Iwanov K, Pantoom S, et al. Role of endoplasmic reticulum stress and protein misfolding in disorders of the liver and pancreas. *Adv Med Sci* (2019) 64(2):315–23. doi: 10.1016/j.advms.2019.03.004

6. Halangk W, Lerch MM, Brandt-Nedelev B, Roth W, Ruthenbuerger M, Reinheckel T, et al. Role of cathepsin b in intracellular trypsinogen activation and the onset of acute pancreatitis. *J Clin Invest* (2000) 106(6):773–81. doi: 10.1172/JCI9411

7. Talukdar R, Sareen A, Zhu H, Yuan Z, Dixit A, Cheema H, et al. Release of cathepsin b in cytosol causes cell death in acute pancreatitis. *Gastroenterology* (2016) 151(4):747–58.e5. doi: 10.1053/j.gastro.2016.06.042

8. Lerch MM, Saluja AK, Dawra R, Saluja M, Steer ML. The effect of chloroquine administration on two experimental models of acute pancreatitis. *Gastroenterology* (1993) 104(6):1768–79. doi: 10.1016/0016-5085(93)90658-y

9. Sendler M, Weiss FU, Golchert J, Homuth G, van den Brandt C, Mahajan UM, et al. Cathepsin b-mediated activation of trypsinogen in endocytosing macrophages increases severity of pancreatitis in mice. *Gastroenterology* (2018) 154(3):704–18.e10. doi: 10.1053/j.gastro.2017.10.018

10. Sendler M, van den Brandt C, Glaubitz J, Wilden A, Golchert J, Weiss FU, et al. NLRP3 inflammasome regulates development of systemic inflammatory response and compensatory anti-inflammatory response syndromes in mice with acute pancreatitis. *Gastroenterology* (2020) 158(1):253–69.e14. doi: 10.1053/j.gastro.2019.09.040

11. Glaubitz J, Wilden A, van den Brandt C, Weiss FU, Broker BM, Mayerle J, et al. Experimental pancreatitis is characterized by rapid T cell activation, Th2 differentiation that parallels disease severity, and improvement after CD4(+) T cell depletion. *Pancreatology* (2020) 20(8):1637–47. doi: 10.1016/j.pan.2020.10.044

12. Sendler M, Dummer A, Weiss FU, Kruger B, Wartmann T, Scharffetter-Kochanek K, et al. Tumour necrosis factor alpha secretion induces protease activation and acinar cell necrosis in acute experimental pancreatitis in mice. *Gut* (2013) 62(3):430–9. doi: 10.1136/gutjnl-2011-300771

13. Gukovskaya AS, Vaquero E, Zaninovic V, Gorelick FS, Lusis AJ, Brennan ML, et al. Neutrophils and NADPH oxidase mediate intrapancreatic trypsin activation in murine experimental acute pancreatitis. *Gastroenterology* (2002) 122(4):974–84. doi: 10.1053/gast.2002.32409

14. Mayerle J, Schnekenburger J, Kruger B, Kellermann J, Ruthenburger M, Weiss FU, et al. Extracellular cleavage of e-cadherin by leukocyte elastase during acute experimental pancreatitis in rats. *Gastroenterology* (2005) 129(4):1251–67. doi: 10.1053/j.gastro.2005.08.002

15. Perides G, Weiss ER, Michael ES, Laukkarinen JM, Duffield JS, Steer ML. TNF-alpha-dependent regulation of acute pancreatitis severity by ly-6C(hi) monocytes in mice. *J Biol Chem* (2011) 286(15):13327–35. doi: 10.1074/jbc.M111.218388

16. Wang HH, Tang AM, Chen L, Zhou MT. Potential of sivelestat in protection against severe acute pancreatitis-associated lung injury in rats. *Exp Lung Res* (2012) 38(9-10):445–52. doi: 10.3109/01902148.2012.721860

17. Awla D, Abdulla A, Syk I, Jeppsson B, Regner S, Thorlacius H. Neutrophil-derived matrix metalloproteinase-9 is a potent activator of trypsinogen in acinar cells in acute pancreatitis. *J Leukoc Biol* (2012) 91(5):711–9. doi: 10.1189/jlb.0811443

18. Gukovskaya AS, Gukovsky I, Zaninovic V, Song M, Sandoval D, Gukovsky S, et al. Pancreatic acinar cells produce, release, and respond to tumor necrosis factor-alpha. role in regulating cell death and pancreatitis. *J Clin Invest* (1997) 100(7):1853–62. doi: 10.1172/JCI119714

19. Merza M, Hartman H, Rahman M, Hwaiz R, Zhang E, Renstrom E, et al. Neutrophil extracellular traps induce trypsin activation, inflammation, and tissue damage in mice with severe acute pancreatitis. *Gastroenterology* (2015) 149(7):1920–31.e8. doi: 10.1053/j.gastro.2015.08.026

20. Madhi R, Rahman M, Taha D, Morgelin M, Thorlacius H. Targeting peptidylarginine deiminase reduces neutrophil extracellular trap formation and

tissue injury in severe acute pancreatitis. *J Cell Physiol* (2019) 234(7):11850–60. doi: 10.1002/jcp.27874

21. Murthy P, Singhi AD, Ross MA, Loughran P, Paragomi P, Papachristou GI, et al. Enhanced neutrophil extracellular trap formation in acute pancreatitis contributes to disease severity and is reduced by chloroquine. *Front Immunol* (2019) 10:28. doi: 10.3389/fimmu.2019.00028

22. Kenny EF, Herzig A, Kruger R, Muth A, Mondal S, Thompson PR, et al. Diverse stimuli engage different neutrophil extracellular trap pathways. *Elife* (2017) 6:e24437. doi: 10.7554/eLife.24437

23. Gupta AK, Giaglis S, Hasler P, Hahn S. Efficient neutrophil extracellular trap induction requires mobilization of both intracellular and extracellular calcium pools and is modulated by cyclosporine a. *PLoS One* (2014) 9(5):e97088. doi: 10.1371/journal.pone.0097088

24. Jorch SK, Kubes P. An emerging role for neutrophil extracellular traps in noninfectious disease. *Nat Med* (2017) 23(3):279–87. doi: 10.1038/nm.4294

25. Boeltz S, Amini P, Anders HJ, Andrade F, Bilyy R, Chatfield S, et al. To NET or not to NET:current opinions and state of the science regarding the formation of neutrophil extracellular traps. *Cell Death Differ* (2019) 26(3):395–408. doi: 10.1038/s41418-018-0261-x

26. Papayannopoulos V. Neutrophil extracellular traps in immunity and disease. *Nat Rev Immunol* (2018) 18(2):134–47. doi: 10.1038/nri.2017.105

27. Pilsczek FH, Salina D, Poon KK, Fahey C, Yipp BG, Sibley CD, et al. A novel mechanism of rapid nuclear neutrophil extracellular trap formation in response to staphylococcus aureus. *J Immunol* (2010) 185(12):7413–25. doi: 10.4049/jimmunol.1000675

28. Yipp BG, Petri B, Salina D, Jenne CN, Scott BN, Zbytnuik LD, et al. Infection-induced NETosis is a dynamic process involving neutrophil multitasking in vivo. *Nat Med* (2012) 18(9):1386–93. doi: 10.1038/nm.2847

29. Etulain J, Martinod K, Wong SL, Cifuni SM, Schattner M, Wagner DD. P-selectin promotes neutrophil extracellular trap formation in mice. *Blood* (2015) 126 (2):242–6. doi: 10.1182/blood-2015-01-624023

30. Rossaint J, Kuhne K, Skupski J, Van Aken H, Looney MR, Hidalgo A, et al. Directed transport of neutrophil-derived extracellular vesicles enables platelet-mediated innate immune response. *Nat Commun* (2016) 7:13464. doi: 10.1038/ncomms13464

31. Maugeri N, Campana L, Gavina M, Covino C, De Metrio M, Panciroli C, et al. Activated platelets present high mobility group box 1 to neutrophils, inducing autophagy and promoting the extrusion of neutrophil extracellular traps. *J Thromb Haemost* (2014) 12(12):2074–88. doi: 10.1111/jth.12710

32. Van Avondt K, van der Linden M, Naccache PH, Egan DA, Meyaard L. Signal inhibitory receptor on leukocytes-1 limits the formation of neutrophil extracellular traps, but preserves intracellular bacterial killing. *J Immunol* (2016) 196(9):3686–94. doi: 10.4049/jimmunol.1501650

33. Fuchs TA, Abed U, Goosmann C, Hurwitz R, Schulze I, Wahn V, et al. Novel cell death program leads to neutrophil extracellular traps. *J Cell Biol* (2007) 176(2):231–41. doi: 10.1083/jcb.200606027

34. Hakkim A, Fuchs TA, Martinez NE, Hess S, Prinz H, Zychlinsky A, et al. Activation of the raf-MEK-ERK pathway is required for neutrophil extracellular trap formation. *Nat Chem Biol* (2011) 7(2):75–7. doi: 10.1038/nchembio.496

35. Papayannopoulos V, Metzler KD, Hakkim A, Zychlinsky A. Neutrophil elastase and myeloperoxidase regulate the formation of neutrophil extracellular traps. *J Cell Biol* (2010) 191(3):677–91. doi: 10.1083/jcb.201006052

36. Metzler KD, Fuchs TA, Nauseef WM, Reumaux D, Roesler J, Schulze I, et al. Myeloperoxidase is required for neutrophil extracellular trap formation: implications for innate immunity. *Blood* (2011) 117(3):953–9. doi: 10.1182/blood-2010-06-290171

37. Metzler KD, Goosmann C, Lubojemska A, Zychlinsky A, Papayannopoulos V. A myeloperoxidase-containing complex regulates neutrophil elastase release and actin dynamics during NETosis. *Cell Rep* (2014) 8(3):883–96. doi: 10.1016/j.celrep.2014.06.044

38. Rohrbach AS, Slade DJ, Thompson PR, Mowen KA. Activation of PAD4 in NET formation. *Front Immunol* (2012) 3:360. doi: 10.3389/fimmu.2012.00360

39. Wang Y, Wysocka J, Sayegh J, Lee YH, Perlin JR, Leonelli L, et al. Human PAD4 regulates histone arginine methylation levels *via* demethylimination. *Science* (2004) 306(5694):279–83. doi: 10.1126/science.1101400

40. Damgaard D, Bjorn ME, Steffensen MA, Pruijn GJ, Nielsen CH. Reduced glutathione as a physiological co-activator in the activation of peptidylarginine deiminase. *Arthritis Res Ther* (2016) 18(1):102. doi: 10.1186/s13075-016-1000-7

41. Li P, Li M, Lindberg MR, Kennett MJ, Xiong N, Wang Y. PAD4 is essential for antibacterial innate immunity mediated by neutrophil extracellular traps. *J Exp Med* (2010) 207(9):1853–62. doi: 10.1084/jem.20100239

42. DeSouza-Vieira T, Guimaraes-Costa A, Rochael NC, Lira MN, Nascimento MT, Lima-Gomez PS, et al. Neutrophil extracellular traps release induced by leishmania: role of PI3Kgamma, ERK, PI3Ksigma, PKC, and [Ca2+]. *J Leukoc Biol* (2016) 100(4):801–10. doi: 10.1189/jlb.4A0615-261RR

43. Neeli I, Radic M. Opposition between PKC isoforms regulates histone deimination and neutrophil extracellular chromatin release. *Front Immunol* (2013) 4:38. doi: 10.3389/fimmu.2013.00038

44. Douda DN, Khan MA, Grasemann H, Palaniyar N. SK3 channel and mitochondrial ROS mediate NADPH oxidase-independent NETosis induced by calcium influx. *Proc Natl Acad Sci U S A* (2015) 112(9):2817–22. doi: 10.1073/pnas.1414055112

45. Eghbalzadeh K, Georgi L, Louis T, Zhao H, Keser U, Weber C, et al. Compromised anti-inflammatory action of neutrophil extracellular traps in PAD4-deficient mice contributes to aggravated acute inflammation after myocardial infarction. *Front Immunol* (2019) 10:2313. doi: 10.3389/fimmu.2019.02313

46. Madhi R, Rahman M, Morgelin M, Thorlacius H. C-abl kinase regulates neutrophil extracellular trap formation, inflammation, and tissue damage in severe acute pancreatitis. *J Leukoc Biol* (2019) 106(2):455–66. doi: 10.1002/JLB.3A0618-222RR

47. Filomeni G, De Zio D, Cecconi F. Oxidative stress and autophagy: the clash between damage and metabolic needs. *Cell Death Differ* (2015) 22(3):377–88. doi: 10.1038/cdd.2014.150

48. Bhattacharya A, Wei Q, Shin JN, Abdel Fattah E, Bonilla DL, Xiang Q, et al. Autophagy is required for neutrophil-mediated inflammation. *Cell Rep* (2015) 12 (11):1731–9. doi: 10.1016/j.celrep.2015.08.019

49. Wu Z, Lu G, Zhang L, Ke L, Yuan C, Ma N, et al. Protectin D1 decreases pancreatitis severity in mice by inhibiting neutrophil extracellular trap formation. *Int Immunopharmacol* (2021) 94:107486. doi: 10.1016/j.intimp.2021.107486

50. Linders J, Madhi R, Rahman M, Morgelin M, Regner S, Brenner M, et al. Extracellular cold-inducible RNA-binding protein regulates neutrophil extracellular trap formation and tissue damage in acute pancreatitis. *Lab Invest* (2020) 100(12):1618–30. doi: 10.1038/s41374-020-0469-5

51. Linders J, Madhi R, Morgelin M, King BC, Blom AM, Rahman M. Complement component 3 is required for tissue damage, neutrophil infiltration, and ensuring NET formation in acute pancreatitis. *Eur Surg Res* (2020) 61(6):163–76. doi: 10.1159/000513845

52. Wu X, Yang Z, Wang H, Zhao Y, Gao X, Zang B. High-mobility group box protein-1 induces acute pancreatitis through activation of neutrophil extracellular trap and subsequent production of IL-1beta. *Life Sci* (2021) 286:119231. doi: 10.1016/j.lfs.2021.119231

53. Leppkes M, Maueroder C, Hirth S, Nowecki S, Gunther C, Billmeier U, et al. Externalized decondensed neutrophil chromatin occludes pancreatic ducts and drives pancreatitis. *Nat Commun* (2016) 7:10973. doi: 10.1038/ncomms10973

54. Maueroder C, Mahajan A, Paulus S, Gosswein S, Hahn J, Kienhofer D, et al. Menage-a-Trois: The ratio of bicarbonate to CO2 and the pH regulate the capacity of neutrophils to form NETs. *Front Immunol* (2016) 7:583. doi: 10.3389/fimmu.2016.00583

55. Naffah de Souza C, Breda LCD, Khan MA, de Almeida SR, Camara NOS, Sweezey N, et al. Alkaline pH promotes NADPH oxidase-independent neutrophil extracellular trap formation: A matter of mitochondrial reactive oxygen species generation and citrullination and cleavage of histone. *Front Immunol* (2017) 8:1849. doi: 10.3389/fimmu.2017.01849

56. Khan MA, Philip LM, Cheung G, Vadakepeedika S, Grasemann H, Sweezey N, et al. Regulating NETosis: Increasing pH promotes NADPH oxidase-dependent NETosis. *Front Med (Lausanne)* (2018) 5:19. doi: 10.3389/fmed.2018.00019

57. Qi Q, Yang B, Li H, Bao J, Li H, Wang B, et al. Platelet microparticles regulate neutrophil extracellular traps in acute pancreatitis. *Pancreas* (2020) 49 (8):1099–103. doi: 10.1097/MPA.0000000000001631

58. Yang L, Liu Q, Zhang X, Liu X, Zhou B, Chen J, et al. DNA Of neutrophil extracellular traps promotes cancer metastasis *via* CCDC25. *Nature* (2020) 583 (7814):133–8. doi: 10.1038/s41586-020-2394-6

59. Silvestre-Roig C, Braster Q, Wichapong K, Lee EY, Teulon JM, Berrebeh N, et al. Externalized histone H4 orchestrates chronic inflammation by inducing lytic cell death. *Nature* (2019) 569(7755):236–40. doi: 10.1038/s41586-019-1167-6

60. Byrd AS, Carmona-Rivera C, O'Neil LJ, Carlucci PM, Cisar C, Rosenberg AZ, et al. Neutrophil extracellular traps, b cells, and type I interferons contribute to immune dysregulation in hidradenitis suppurativa. *Sci Transl Med* (2019) 11(508): eaav5908. doi: 10.1126/scitranslmed.aav5908

61. Abu-Abed U, Brinkmann V. Immunofluorescent detection of NET components in paraffin-embedded tissue. *Methods Mol Biol* (2020) 2087:415–24. doi: 10.1007/978-1-0716-0154-9_24

62. Brinkmann V, Abu Abed U, Goosmann C, Zychlinsky A. Immunodetection of NETs in paraffin-embedded tissue. *Front Immunol* (2016) 7:513. doi: 10.3389/fimmu.2016.00513

63. Knight JS, Luo W, O'Dell AA, Yalavarthi S, Zhao W, Subramanian V, et al. Peptidylarginine deiminase inhibition reduces vascular damage and modulates

innate immune responses in murine models of atherosclerosis. *Circ Res* (2014) 114 (6):947–56. doi: 10.1161/CIRCRESAHA.114.303312

64. Weckbach LT, Grabmaier U, Uhl A, Gess S, Boehm F, Zehrer A, et al. Midkine drives cardiac inflammation by promoting neutrophil trafficking and NETosis in myocarditis. *J Exp Med* (2019) 216(2):350–68. doi: 10.1084/jem.20181102

65. Boxhoorn L, Voermans RP, Bouwense SA, Bruno MJ, Verdonk RC, Boermeester MA, et al. Acute pancreatitis. *Lancet* (2020) 396(10252):726–34. doi: 10.1016/S0140-6736(20)31310-6

66. Radermecker C, Sabatel C, Vanwinge C, Ruscitti C, Marechal P, Perin F, et al. Locally instructed CXCR4(hi) neutrophils trigger environment-driven allergic asthma through the release of neutrophil extracellular traps. *Nat Immunol* (2019) 20(11):1444–55. doi: 10.1038/s41590-019-0496-9

67. Zhu YP, Eggert T, Araujo DJ, Vijayanand P, Ottensmeier CH, Hedrick CC. CyTOF mass cytometry reveals phenotypically distinct human blood neutrophil populations differentially correlated with melanoma stage. *J Immunother Cancer* (2020) 8(2):e000473. doi: 10.1136/jitc-2019-000473

frontiers | Frontiers in Immunology

TYPE Original Research
PUBLISHED 12 August 2022
DOI 10.3389/fimmu.2022.918476

OPEN ACCESS

EDITED BY
Clifford Taggart,
Queen's University Belfast,
United Kingdom

REVIEWED BY
Girish S Kesturu,
Tumkur University, India
Ryan Brown,
Queen's University Belfast,
United Kingdom

*CORRESPONDENCE
Xiaojun Wu
xiaojunwu320@126.com
Zhengtao Wang
ztwang@shutcm.edu.cn

SPECIALTY SECTION
This article was submitted to Inflammation, a section of the journal Frontiers in Immunology

RECEIVED 12 April 2022
ACCEPTED 21 July 2022
PUBLISHED 12 August 2022

CITATION
Chen Z, Wang G, Xie X, Liu H, Liao J, Shi H, Chen M, Lai S, Wang Z and Wu X (2022) Ginsenoside Rg5 allosterically interacts with $P2RY_{12}$ and ameliorates deep venous thrombosis by counteracting neutrophil NETosis and inflammatory response. *Front. Immunol.* 13:918476. doi: 10.3389/fimmu.2022.918476

Ginsenoside Rg5 allosterically interacts with $P2RY_{12}$ and ameliorates deep venous thrombosis by counteracting neutrophil NETosis and inflammatory response

Ziyu Chen[1], Gaorui Wang[1], Xueqing Xie[1], Heng Liu[2], Jun Liao[2], Hailian Shi[1], Min Chen[3], Shusheng Lai[3], Zhengtao Wang[1]* and Xiaojun Wu[1]*

[1]Shanghai Key Laboratory of Compound Chinese Medicines, The Ministry of Education (MOE) Key Laboratory for Standardization of Chinese Medicines, The State Administration of TCM (SATCM) Key Laboratory for New Resources and Quality Evaluation of Chinese Medicine, Institute of Chinese Materia Medica, Shanghai University of Traditional Chinese Medicine, Shanghai, China, [2]School of Life Science and Technology, Shanghai Tech University, Shanghai, China, [3]Guangxi Key Laboratory of Comprehensive Utilization Technology of Pseudo-Ginseng, Wuzhou, China

Background: Deep venous thrombosis (DVT) highly occurs in patients with severe COVID-19 and probably accounted for their high mortality. DVT formation is a time-dependent inflammatory process in which NETosis plays an important role. However, whether ginsenoside Rg5 from species of *Panax* genus could alleviate DVT and its underlying mechanism has not been elucidated.

Methods: The interaction between Rg5 and $P2RY_{12}$ was studied by molecular docking, molecular dynamics, surface plasmon resonance (SPR), and molecular biology assays. The preventive effect of Rg5 on DVT was evaluated in inferior vena cava stasis–induced mice, and immunocytochemistry, Western blot, and calcium flux assay were performed in neutrophils from bone marrow to explore the mechanism of Rg5 in NETosis *via* $P2RY_{12}$.

Results: Rg5 allosterically interacted with $P2RY_{12}$, formed stable complex, and antagonized its activity *via* residue E188 and R265. Rg5 ameliorated the formation of thrombus in DVT mice; accompanied by decreased release of Interleukin (IL)-6, IL-1β, and tumor necrosis factor-α in plasma; and suppressed neutrophil infiltration and neutrophil extracellular trap (NET) release. In lipopolysaccharide- and platelet-activating factor–induced neutrophils, Rg5 reduced inflammatory responses *via* inhibiting the activation of ERK/NF-κB signaling pathway while decreasing cellular Ca^{2+} concentration, thus reducing the activity and expression of peptidyl arginine deiminase 4 to prevent NETosis. The inhibitory effect on neutrophil activity was dependent on $P2RY_{12}$.

Conclusions: Rg5 could attenuate experimental DVT by counteracting NETosis and inflammatory response in neutrophils *via* $P2RY_{12}$, which may pave the road for its clinical application in the prevention of DVT-related disorders.

KEYWORDS

deep venous thrombosis, ginsenoside Rg5, $P2RY_{12}$, neutrophil extracellular traps, inflammation

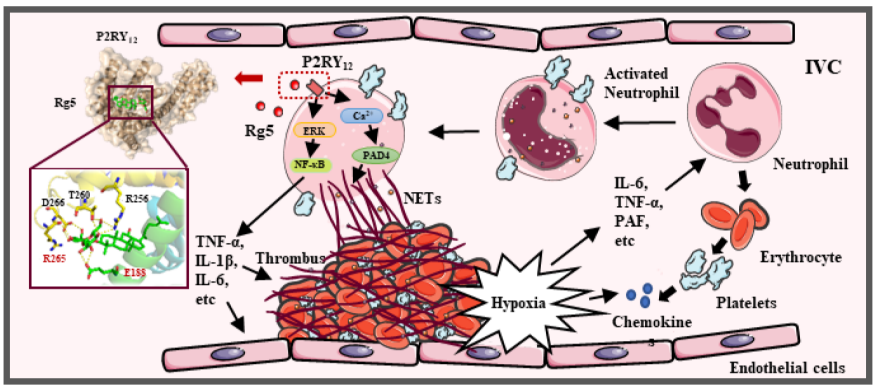

GRAPHICAL ABSTRACT

Introduction

Deep venous thrombosis (DVT) belongs to venous thromboembolic disorder and is the leading cause of pulmonary embolism, which eventually contributes to heart failure and even sudden death (1). DVT is generally characterized by abnormal coagulation of blood in deep veins of lower leg and thigh; however, it may occur in upper limb deep veins, visceral veins, and vena cava (2). DVT highly occurs in long-term sedentary people and post-surgery patients (3). Recently, clinical studies have found an association between high mortality in patients with COVID-19 and DVT (4). The clinical diagnosis of DVT mainly depends on clinical risk score, serum D-dimer, and color Doppler ultrasound. Anticoagulants such as Aspirin, antiplatelet drugs, Rivaroxaban, and low molecular–weight heparin are common clinical treatment for the prevention of DVT (5). Unfortunately, all of these treatments carry a remarkable risk of bleeding (6). Therefore, it is still urgent to develop effective antithrombotic drugs with less side effects to slow down the occurrence of DVT.

Neutrophils play an import role in thrombosis. Together with platelets, neutrophils are the first cells mobilized to the injury/infection sites to limit the dissemination of microbial infection by promoting blood coagulation. However, dysregulation or excessive stimulation may contribute to thrombotic processes (7). Neutrophils release neutrophil extracellular traps (NETs) upon excessive stimulation, a process called NETosis, which promotes thrombosis by forming a scaffold for adhesion of platelets, erythrocytes, and platelet adhesion molecules (8). NETs are extracellular, web-like structures mainly composed of decondensed chromatin and granule proteins such as histones, neutrophil elastase, myeloperoxidase (MPO), calprotectin, cathelicidins, defensins, and actin (9). When activated by Ca^{2+}, peptidyl arginine deiminase 4 (PAD4) catalyzes the conversion of histone arginine to citrulline, resulting in the decondensation of heterochromatin and prompting NET formation. Preventing NETosis can decrease thrombogenicity, which may be beneficial for thrombosis prevention and become a promising therapy target for DVT (10).

$P2RY_{12}$, as an adenosine diphosphate (ADP) receptor on the platelet surface, is a key player in platelet activation and a vital target of antithrombotic drugs such as Clopidogrel, Praugrel, and Ticagrelor (11). Upon activation by ADP, $P2RY_{12}$ is coupled to the G_{i2} protein, and its activation inhibits adenylate cyclase activity, thereby reducing the intracellular cyclic adenosine monophosphate (cAMP) level. In addition, G_{i2} signaling gives rise to the activation of Phosphatidylinositol 3-kinase/protein kinase B (PI3K/AKT) pathway, which leads to a significant increase of granule release and platelet aggregation (12, 13), suggesting that dense granule release, procoagulant activity, and thrombosis are dependent on $P2RY_{12}$ activation (14, 15). Interestingly, $P2RY_{12}$ is expressed not only on the surface of

platelets but also on several immune cells, including eosinophils, monocytes, macrophages, lymphocytes dendritic cells, and mast cells, which are involved in the inflammatory process of many diseases (16). Studies have shown that the $P2RY_{12}$ plays an important role in early DVT formation (17), and $P2RY_{12}$ inhibitor Clopidogrel, Ticagrelor, or Prasugrel can restrain platelet-leukocyte interaction (18–20). Although a study has demonstrated the reduction of platelet-leukocyte aggregation and NETs by Ticagrelor in patients with pneumonia (21), the direct relationship between $P2RY_{12}$ and NETosis has not been elucidated yet.

Species of *Panax* genus, including *Panax ginseng* C.A. Meyer, *Panax notoginseng* (Burkill) F.H. Chen, and *Panax quinquefolius* L., are precious Chinese herbal medicines with beneficial effects in reinforcing immunity and reducing fatigue. Ginsenoside Rg5 (Figure 2A) is one of the natural saponins in *P. ginseng* and *P. notoginseng*, which has multiple pharmacological activities, such as anti-cancer, anti-inflammation, anti-diabetes, anti-obesity, neuroprotection, and cardioprotection (22). However, whether Rg5 could benefit DVT therapy has not been elucidated yet. In the present study, we firstly identified that Rg5 might bind to $P2RY_{12}$ by molecular docking, which was confirmed by molecular dynamics (MD) simulation, surface plasmon resonance (SPR), and site mutation analysis. Furthermore, in DVT model mice, we found that Rg5 could attenuate thrombosis, which might be exerted by inhibiting NETosis through preventing NET release and inflammatory response by antagonizing $P2RY_{12}$. These findings may pave the road for the clinical application of Rg5 in the prevention of DVT.

Materials and methods

Chemicals

Ginsenoside Rg5 (Cat# BP1651, purity > 95%) was purchased from Biopurify Phytochemicals, Ltd. (Chengdu, China). Rivaroxaban (Cat# MB1878, purity > 98%) was obtained from Meilun Biotechnology Co., Ltd. (Dalian, China). Platelet-activating factor (PAF) (Cat# GC14535) was provided by GlpBio Technology, Inc. (CA, USA). Lipopolysaccharide (LPS) from *Escherichia coli* 0111:B4 was obtained from Sigma-Aldrich Company (MO, USA). 2-Methylthioadenosine diphosphate (2MesADP) trisodium salt was purchased from Tocris Bioscience (MN, USA). n-Dodecyl-β-D-Maltopyranoside (DDM) (Cat# D310) was bought from Anatrace (OH, USA).

Antibodies

Antibodies against AKT (Cat# T55561F), phospho-AKT-Ser473 (Cat# T40067F), phospho-ERK1 (T202/Y204) + ERK2 (T185) (Cat# T40072F), p44/42 MAPK (ERK1/2) (Cat# T40071F), and GAPDH (Cat# M20006F) were purchased from Abmart (Shanghai, China). Nuclear factor-kappa B (NF-kB) (Cat# 8242S), p-NF-κB-Ser536 (Cat# 3033L), and β-actin (Cat# 12413) antibodies were obtained from Cell Signaling Technology (C.S.T.) Co. (MA, USA). Anti-PAD4 antibody (Cat# ab214810) and anti-Histone H3 (citrulline R2 + R8 + R17) antibody (Cat# ab5103) were purchased from Abcam (Cambridge, England). Anti-MPO antibody (Cat# GB11224) was purchased from Servicebio (Wuhan, China).

Animals

Wide-type C57BL/6 male mice (25 ± 2 g) were provided by Shanghai Sippe-Bk Lab Animal Co., Ltd. and were adapted for 1 week before use. $P2RY_{12}$-knockout (KO) mice were kindly provided by Dr. Jun-ling Liu from Ruijin Hospital, Shanghai Jiaotong University School of Medicine (Shanghai, China), and genotyped as described previously (23). All mice received humane care and were kept in a standard environment with a 12/12-h cyclic lighting schedule (lights on at 07:00 am) in the Laboratory Animal Center of Shanghai University of Traditional Chinese Medicine (SHUTCM, Shanghai, China). The temperature and humidity were maintained at 25 ± 2°C and 45 ± 5%, respectively.

Bone marrow neutrophils preparation

BMNs from the femur and tibia of wild type (WT) or $P2RY_{12}$-KO mice were prepared according to the instruction of the Mouse Bone Marrow Neutrophil Extraction Kit (Solarbio, Beijing, China).

DNA content detection

BMNs were seeded in 24-well plate at 2×10^6/ml per well and treated with PBS or 6.25, 12.5, and 18.75 μM Rg5 for 2 h followed by stimulation of LPS (20 μg/ml) or 50 μM PAF for 30 min. Then, the cells were collected for Western blot analysis, and cell-free supernatant was collected for further analysis. DNA content in supernatant was measured by using Quant-iT PicoGreen dsDNA Reagent and Kits (Invitrogen, CA, USA). The concentration of DNA released by neutrophils treated with 0.3% Triton was set as 100%, and the relative proportion of cell-free DNA (cfDNA) concentration in each sample was calculated by comparing with the former.

ELISA assay

Serum or medium concentrations of D-dimer, IL-6, IL-1β, tumor necrosis factor-α (TNF-α) and citrullinated histones 3

(CitH3) were measured by using respective ELISA kits (Lengton Bioscience, Shanghai, China). The absorbance was detected at 450 or 570 nm on a microplate reader (FlexStation 3, Molecular Devices, CA, USA).

Immunocytochemistry

To examine the effect of Rg5 on the formation of NETs, the BMNs were seeded in 24-well plates with coverslips pre-coated with poly-D-lysine. After treatment of 18.75 μM Rg5 for 2 h followed by stimulation of LPS (5 μg/ml) or 20 μM PAF for 3 h, the cells were fixated by 4% Paraformaldehyde (PFA) for 10 min. Consequently, the cells were blocked with 5% donkey serum for 1 h and incubated overnight with antibody against CitH3 (1:1,000) at 4°C, followed by Alexa 488–conjugated secondary antibody (1:800). Finally, the coverslips were mounted on slides with mounting medium containing Diamidinyl phenyl indole (DAPI) in the dark. The microscopy images were captured by Olympus slide scanner (VS120, Japan) and analyzed by ImageJ (version 1.46r).

Molecular docking and consensus analysis

The $P2RY_{12}$–antagonist complex structure (Protein Data Bank Code: 4NTJ) was obtained to predict the potential binding mode of Rg5 with $P2RY_{12}$. As described previously (24), AutoDock Vina (version 1.1.2), Maestro (version 11.4, Schrödinger, LLC, New York, NY, 2021), and molecular operating environment (MOE, Chemical Computing Group, version 2019.0101) softwares were used to calculate the binding capability of Rg5 and other compounds. The exponential consensus ranking (ECR) analysis (25) was used to assign a rank to each ligand based on the molecular docking score provided by different docking programs to combine the results of multiple docking programs.

$P2RY_{12}$ protein expression and purification

$P2RY_{12}$ protein were expressed and purified as described previously (26) and concentrated to approximately 1 mg/ml for further usage.

Surface plasmon resonance

The binding affinity between Rg5 and $P2RY_{12}$ was measured using Biacore T200 (GE healthcare, MA, USA). $P2RY_{12}$ protein was immobilized on the chip in the presence of 1× HEPES Buffered Saline-EDTA P20 (HBS-EP) with 0.03% DDM buffer (pH 7.4) by using the His Capture Kit (GE healthcare, MA, USA). Various concentrations of Rg5 (0.098, 0.195, 0.391, 0.781, 0.562, and 3.125 μM) or Ticagrelor (0.031, 0.062, 0.125, 0.25, 0.5, and 1 μM) dissolved in 5% DMSO were passed at 30 μl/min for 120 s over the $P2RY_{12}$ protein, followed by a dissociation step of 120 s. The Equilibrium dissociation constant (KD) value was obtained by fitting the data to a steady state affinity model using Biacore T200 Evaluation Software (version 3.0).

Molecular dynamics simulations

The stable MD trajectory of the $P2RY_{12}$–Rg5, $P2RY_{12}$–Ticagrelor, or $P2RY_{12}$–Aspirin complex was estimated by the Molecular mechanics/poisson-boltzmann surface area (MM/PBSA) technique implemented in AMBER14 as described previously (27). The MM/PBSA method combined molecular mechanics and continuous solvent model was used to predict the binding free energy of $P2RY_{12}$ protein and ligands.

$P2RY_{12}$ signaling transduction detection

CHO-$P2RY_{12}$ cells overexpressing $P2RY_{12}$ were cultured in Dulbecco's modified eagle medium (DMEM) high-glucose medium containing 10% fetal bovine serum at 37°C. To examine the inhibitory effect of Rg5 against $P2RY_{12}$ signaling, CHO-$P2RY_{12}$ cells were seeded at a density of 1×10^5 cells per well in six-well plates for 24 h and serum-starved for 12 h. Then, the cells were treated with Rg5 (3.125, 6.25, 12.5, 25, and 50 μM) for 2 h followed by stimulation of 2MesADP (100 nM) for 5 min. Afterward, the cells were collected for further Western blot analysis.

$P2RY_{12}$ site mutation

The coding sequence of P2RY12 (Homo sapiens, Gene ID: 64805) was cloned into PCMV6 vector and site-directed mutated by using the Mut Express II Fast Mutagenesis Kit (Vazyme, Nanjing, China). The primers (Generay Biotech, Shanghai, China) were listed as follows: P2RY12_E188A mutation (forward, 5′- GTCTGGCATGC GATAGTAAATTACATCTGTC-3′; reverse, 5′- GTAATTTAC TATCGCATGCCAGACTAGACCG-3′), P2RY12_R265A mutation (forward, 5′- CAAACCGCTGATGTCTTTGACTGCA CTGCTGAA-3′; reverse, 5′- GACATCAGCGGTTTGGCTCAGGG TGTAAGGAATT-3′), P2RY12_D266A mutation (forward, 5′- A CCCGGGCGGTCTTTGACTGCACTGCTGAAAATA -3′; reverse, 5′- AAAGACCGCCCGGGTTTGGCTCAGGGTGTAA -3′), and P2RY12_R265A and D266A mutation (forward, 5′- CTGAGC CAAACCGCTGCGGTCTTTGACTGC -3′; reverse, 5′- GTGCAGTCAAAGACCGCAGCGGTTTGGCTC -3′). Plasmid

was extracted according to the steps in the EndoFree Midi Kit (Cwbiotech, Taizhou, China) and transfected into CHO cells for 12 h by Tecfect DNA transfection reagent (TEYE Co, Shanghai, China). CHO cells were cultured and treated under the same conditions as CHO-$P2RY_{12}$ cells, which were collected for further Western blot analysis.

Western blot analysis

The methods of protein samples preparation and Western blot analysis were described previously (28). After incubation in primary antibodies (1:1,000) and secondary antibody (1:5,000), the protein bands were visualized by using the ECL Enhanced Kit (ABclonal Technology, Wuhan, China). The photographs were taken and analyzed by using Tanon 5200 Multi (Shanghai, China).

Inferior vena cava stasis-induced DVT

DVT model was established as described previously (29). In brief, the IVC caudal to the left renal vein was ligated for 12 h to achieve stasis induction of thrombosis. None of the mice showed any bleeding during surgery.

Drug administration

A total of 48 mice were randomly divided into six groups: (1) Sham group; (2) DVT group; (3) Rg5 of 1.25 mg/kg + DVT group; (4) Rg5 of 2.5 mg/kg + DVT group; (5) Rg5 of 5 mg/kg + DVT group; and (6) Rivaroxaban of 0.3 mg/kg + DVT group. Rg5 is dissolved in saline containing 2% ethanol for injection, and Rivaroxaban was dissolved in a special solution (Polyethylene glycol/Saline/Glycerin = 996 g/100 g/60g). Rg5 or Rivaroxaban was intravenously given at 15 min prior to thrombus induction. IVC of mice in sham group was separated without ligation. After the formation of DVT, arterial blood was collected immediately and mixed with 10% sodium citrate for anticoagulation followed by centrifugation at 3,000 rpm for 15 min to obtain the plasma. The IVC between the left renal vein and the iliac crest bifurcation was separated, whose length and wet weight were measured. Afterward, the IVC was fixed by 4% PFA for further hematoxylin and eosin (HE) staining and immunohistochemistry.

Histopathology and immunohistochemistry

For HE staining, the 5-μm-thick sections were dewaxed and stained by HE as described previously (30). For immunohistochemistry, the sections were deparaffinzed and rehydrated, followed by antigen retrieval as described elsewhere (31). After deactivation of endogenous peroxidase with H_2O_2, they were blocked with 3% Bull serum albumin (BSA) and incubated with the anti-MPO antibody (1:2,000) and the secondary antibody (1:200). The immuno-reactive cells were visualized after Diaminobenzidine (DAB) chromogenic reaction. Finally, the images were captured by Olympus slide scanner (VS120, Japan) and analyzed by ImageJ (version 1.46r).

Calcium flux assay

Calcium flux in BMNs was monitored by using the Screen Quest^{TM} Calbryte-520 Probenecid-Free and Wash-Free Calcium Assay Kit (AAT Bioquest, CA, USA). In brief, BMNs were seeded at 2×10^6 cells/ml in 96-well plate. After Rg5 (18.75 μM) treatment for 2 h, BMNs were loaded with Calbryte 520 AM dye for 45 min. Then, the cells were stimulated with PAF (20 μM) and monitored immediately on a fluorescence microplate reader (FlexStation 3, Molecular Devices, CA, USA) with excitation wavelength at 490 nm and emission wavelength at 525 nm at 37°C for 60 min.

PAD4 activity assay

BMNs were stimulated with PAF (20 μM) for 3 h after pre-treated with Rg5 (18.75 μM) for 2 h. Then, the cells were collected and lysed to extract the proteins, which were incubated with 10 mM ethyl N-benzoyl-L-argininate hydrochloride (BAEE) at 37°C for 10 min. The ammonia content produced through the enzymatic hydrolysis of BAEE by PAD4 was measured according to the procedure described by the manufacturer (Blood Ammonia Content Detection Kit). Finally, the absorbance was measured at 630 nm on a microplate reader (FlexStation 3).

Statistical analysis

The data were presented as mean ± SEM to describe the differences among multiple groups. Differences among groups were analyzed by one-way ANOVA with Dunnett's analysis ($n \geq 4$) and Kruskal–Wallis test ($n = 3$) using GraphPad Prism 5.0. The value of $P < 0.05$ was considered statistically significant.

Results

$P2RY_{12}$ actively participated in NETosis

Because whether $P2RY_{12}$ is involved in NETosis has not been elucidated yet, we firstly investigated its role in NETosis. As shown

in Figure 1A, PAF dose-dependently induced the production of cfDNA in both WT and P2RY$_{12}$-KO neutrophils. However, when stimulated with the same dose of PAF, higher than 50 μM, P2RY$_{12}$-KO neutrophils produced significantly less cfDNA than WT neutrophils ($P < 0.05$, $P < 0.001$). Similarly, when stimulated at the concentration higher than 20 μg/ml, LPS also induced much more release of cfDNA in WT neutrophils than that in P2RY$_{12}$-KO neutrophils ($P < 0.01$ and $P < 0.001$). After PAF or LPS stimulation, much more NETs in reticular structure, which were mainly composed of DNA and CitH3 derived from chromatin depolymerization in the nucleus, were released from WT neutrophils than that from P2RY$_{12}$-KO neutrophils (Figure 1B, $P < 0.01$). Moreover, PAF-induced remarkably increased production of inflammatory factors, such as IL-6, IL-1β, and TNF-α in WT neutrophils (Figure 1C, $P < 0.05$); by contrast, it induced slight increment of IL-6, IL-1β, and TNF-α in P2RY$_{12}$-KO neutrophils. Similarly, LPS induced more release of inflammatory cytokines in WT neutrophils than that in P2RY$_{12}$-KO neutrophils (Figure 1D). These results implicated that P2RY$_{12}$ is critical for the NETosis and inflammatory response in neutrophils.

Rg5 allosterically bound to P2RY$_{12}$ and antagonized its activity

As aforementioned, P2RY$_{12}$ is important for neutrophil activation, particularly NETosis, we next carried out virtual screening by using ECR strategy, which was adopted to better describe the comprehensive binding affinity of the P2RY$_{12}$–ligand complex predicted by Autodock Vina, Glide, and MOE softwares. We used ranking values rather than docking scores in subsequent docking analyses. According to the ranking results, the binding affinity between Rg5 and P2RY$_{12}$ was similar to that between Ticagrelor and P2RY$_{12}$ (Table 1). To further investigate

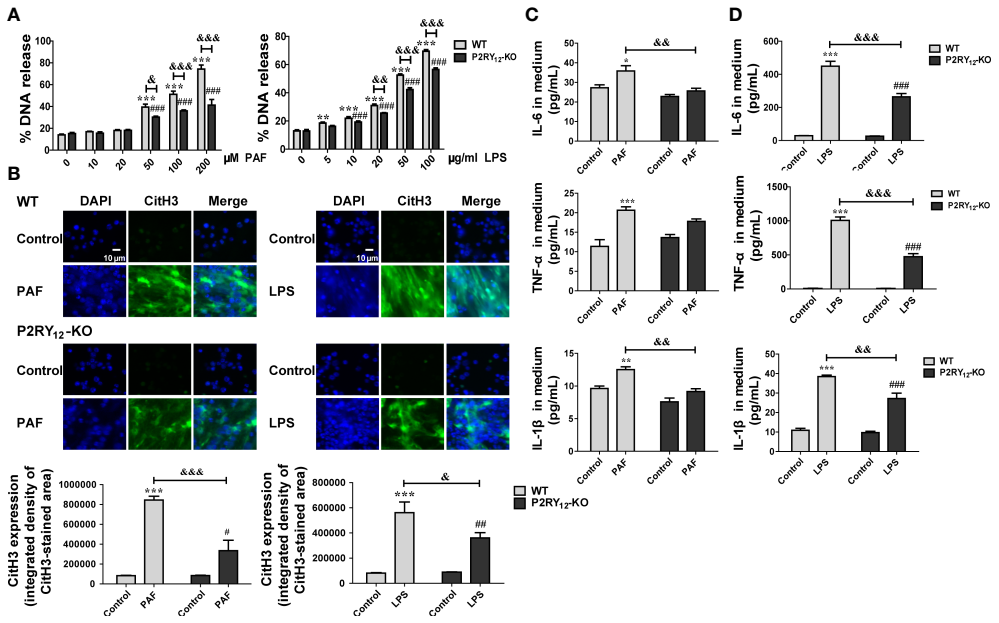

FIGURE 1
Effects of P2RY$_{12}$ on PAF and LPS-induced NET release and inflammatory responses. **(A)** Different concentrations of PAF or LPS induced the release of cfDNA from WT or P2RY$_{12}$-KO neutrophils (n = 4). **(B)** Immunofluorescent staining and statistical analysis of CitH3 and DAPI staining of WT or P2RY$_{12}$-KO neutrophils induced by PAF and LPS, respectively (n = 4). **(C, D)** Release of IL-6, IL-1β, and TNF-α in medium of WT or P2RY$_{12}$-KO neutrophils induced by PAF and LPS, respectively (n = 4). All the data are shown as the mean ± SEM. *$P < 0.05$, **$P < 0.01$, ***$P < 0.001$ vs. WT control; $^{\#\#\#}P < 0.001$ vs. P2RY$_{12}$-KO Control; $^{\&}P < 0.05$, $^{\&\&}P < 0.01$, $^{\&\&\&}P < 0.001$, WT vs. P2RY$_{12}$-KO. #P < 0.05, ##P < 0.01.

TABLE 1 Ranking results of Rg5, Ticagrelor, and Aspirin binding to P2RY$_{12}$.

Receptor	Ligand	Rank
P2RY$_{12}$	Rg5	0.684
	Ticagrelor	0.701
	Aspirin	0.525

the stability of Rg5 binding to $P2RY_{12}$, MD analysis was performed. As shown in Figure 2B, the electrostatic interaction (ΔE_{ele}) between Rg5 and $P2RY_{12}$ was higher than that between Ticagrelor and $P2RY_{12}$, and the total free energy (ΔG_{Tot}) of Rg5 was also slightly higher than that of Ticagrelor. In addition, as shown in Figure 2C, compared with the stable state of Ticagrelor in $P2RY_{12}$, although the complex of Rg5 and $P2RY_{12}$ fluctuated before 25 ns, it quickly leveled off later; and Aspirin remained in a state of fluctuation in $P2RY_{12}$. The Root mean square deviation (RMSD) trajectories of Rg5 and Pocket also fluctuated slightly at the beginning but became stable later on. To confirm the direct interaction, we conducted SPR assay. As shown in Figure 2D, Rg5 dose-dependently bound to $P2RY_{12}$ with a KD of 0.33 μM, which was similar to that of Ticagrelor (0.102 μM). These results suggested that Rg5 could bind to $P2RY_{12}$ steadily and affect the activity of the latter. On this premise, we used CHO-$P2Y_{12}$-OE cells to explore whether the binding of Rg5 to $P2RY_{12}$ could interfere the downstream signaling of the latter. As demonstrated in Figure 2E, Rg5 itself had no effect on $P2RY_{12}$ signaling, but it inhibited 2MesADP-induced phosphorylation of AKT and ERK in a dose-dependent manner, suggesting the antagonic effect of Rg5 on $P2RY_{12}$.

To find out the exact binding sites, we first carried out molecular docking analysis of Rg5 and $P2RY_{12}$. As shown in Figures 3A, B, Rg5 was predicted to interact with $P2RY_{12}$ at amino acid residues E188, R256, T260, R265, and D266. Furthermore, energy decomposition of amino acid residues based on MM/PBSA free energy calculation showed that amino acid residues S101, E188, R256, R265, and D266 were important in the binding process of Rg5 and $P2RY_{12}$ (Figure 3C). Because R256 was reported to play a pivotal role for the binding of ADP with $P2RY_{12}$, and the mutation of R256 weakened the activation of $P2RY_{12}$ by ADP, we chose E188, R265, and D266 for site-directed mutagenesis. As shown in Figure 3D, a series of $P2RY_{12}$ variants were generated and overexpressed in CHO cells followed by activation of 2MesADP. However, Rg5 still could antagonize 2MesADP-induced phosphorylation of AKT and ERK unless E188 and R265 was simultaneously mutated into alanine. According to the docking results in Figure 3D, there were two main binding modes of Rg5 in $P2RY_{12}$ mutants. As shown in Figure 3E, Rg5 mainly bound to two extracellular pockets, which were separated by residues Y105 and K280. Pocket 2 was the binding site of Rg5 in the WT conformation, E188A mutant, and E188A and R265A mutant of $P2RY_{12}$; whereas in other mutants, Rg5 bound to the more advantageous Pocket 1.

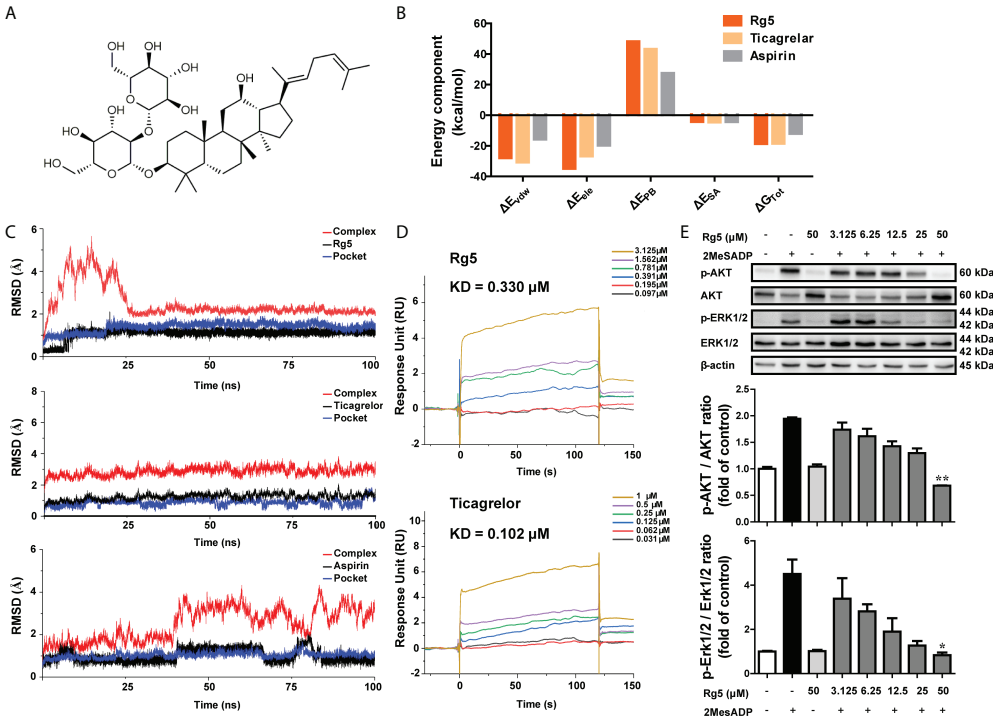

FIGURE 2
Interaction between Rg5 and $P2RY_{12}$. **(A)** Chemical structure for Rg5. **(B)** Comparison of binding free energy between Rg5, Ticagrelor, and Aspirin binding to $P2RY_{12}$. ΔE_{vdw}, van der Waals energy; ΔE_{ele}, electrostatic energy; ΔE_{PB}, Poisson–Boltzmann energy; ΔE_{SA}, nonpolar energy; ΔG_{Tot}, total binding free energy. **(C)** Stability analysis of Rg5, Ticagrelor, and Aspirin binding to $P2RY_{12}$. **(D)** SPR analyses of Rg5 and Ticagrelor binding to $P2RY_{12}$. **(E)** Protein expression and phosphorylation levels of AKT (n = 3) and ERK (n = 3). All the data are shown as the mean ± SEM. $^{*}P < 0.05$, $^{**}P < 0.01$ vs. 2MesADP group.

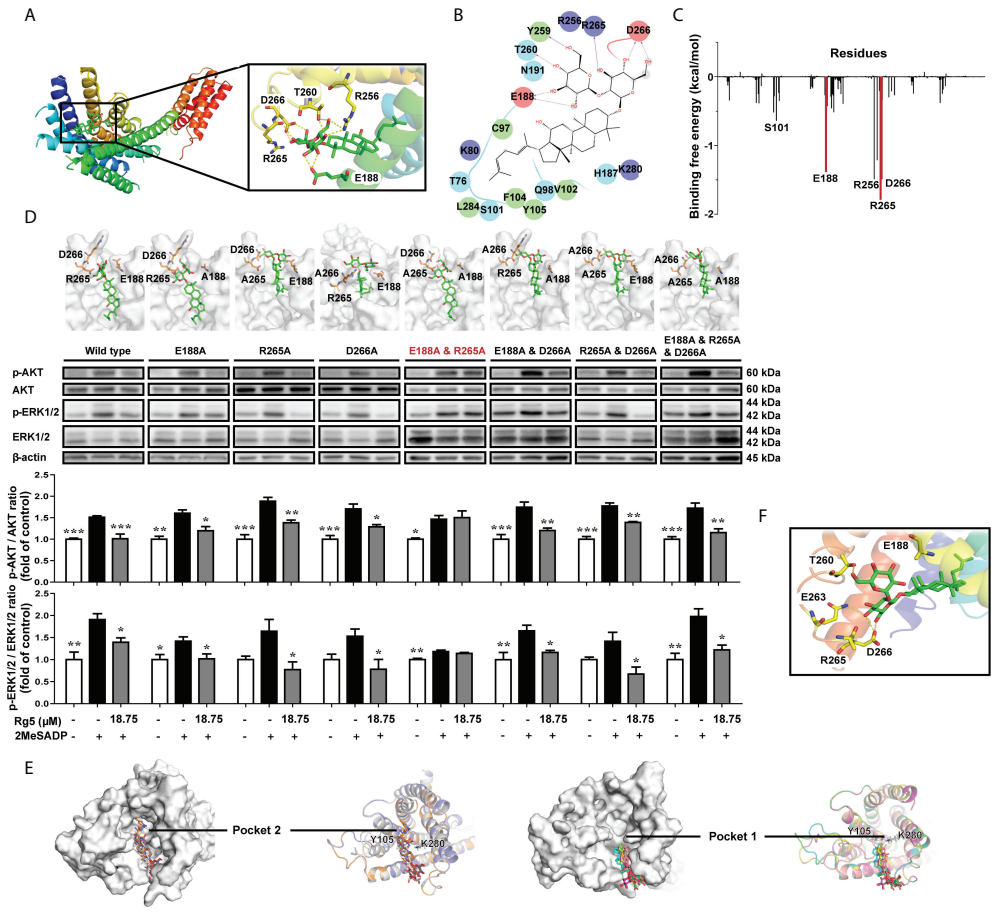

FIGURE 3
Interaction sites of Rg5 with $P2RY_{12}$. **(A)** $P2RY_{12}$ and Rg5 complex structure, and binding pocket with Rg5. **(B)** Two-dimensional interaction map of interactions between Rg5 and $P2RY_{12}$. **(C)** Energy decomposition of amino acid residues in $P2RY_{12}$ and Rg5 based on MM/PBSA free energy calculation. **(D)** Structures of $P2RY_{12}$ mutation variants with Rg5 bound were shown in the upper panel, and Western blot analysis in the lower panel displayed the protein expression and phosphorylation levels of AKT (n = 4) and ERK (n = 4). All the data are shown as the mean ± SEM. $^{*}P < 0.05$, $^{**}P < 0.01$, $^{***}P < 0.001$ vs. 2MesADP group. **(E)** Hypothetical binding modes of Rg5 to $P2RY_{12}$ mutation variants obtained by molecular docking. The binding conformation of Rg5 in each $P2RY_{12}$ mutant were colored as follows: white, original; slate, E188A; orange, E188A and R265A; magenta, R165A; pink, D266A; cyan, E188A and D266A; yellow, R265A and D266A; green, E188A and R265A and D266A. **(F)** A view of the P2RY12 mutant/Rg5 complex.

The interaction between Rg5 and binding pocket in Figure 3F showed the absence of hydrogen bonding with E188 and R265 in the interaction of Rg5 and E188A and R265A mutant, which resulted in the weakened binding effect of Rg5 to $P2RY_{12}$. Ranking results in Table 2 also verified that the E188A and R265A mutant had the weakest affinity with Rg5, suggesting that E188 and R265 play an important role in the interaction between Rg5 and $P2RY_{12}$.

TABLE 2 Ranking results of Rg5 binding to $P2RY_{12}$ mutation variants.

Mutation	Rank
E188A	0.647
R265A	0.635
D266A	0.631
E188A and R265A	0.626
E188A and D266A	0.633
R265A and D266A	0.656
E188A and R265A andD266A	0.649

Rg5 reduced thrombosis and inflammatory response in DVT model mice

As shown in Figure 4, IVC ligation caused significant thrombosis in mice (Figure 4A). Accordingly, the wet weight and length of thrombus in the DVT group mice were increased markedly, compared with the sham group ($P < 0.001$). Rg5 pretreatment, especially at dosages of 2.5 and 5 mg/kg, significantly reduced thrombus formation ($P < 0.05$ or $P <$

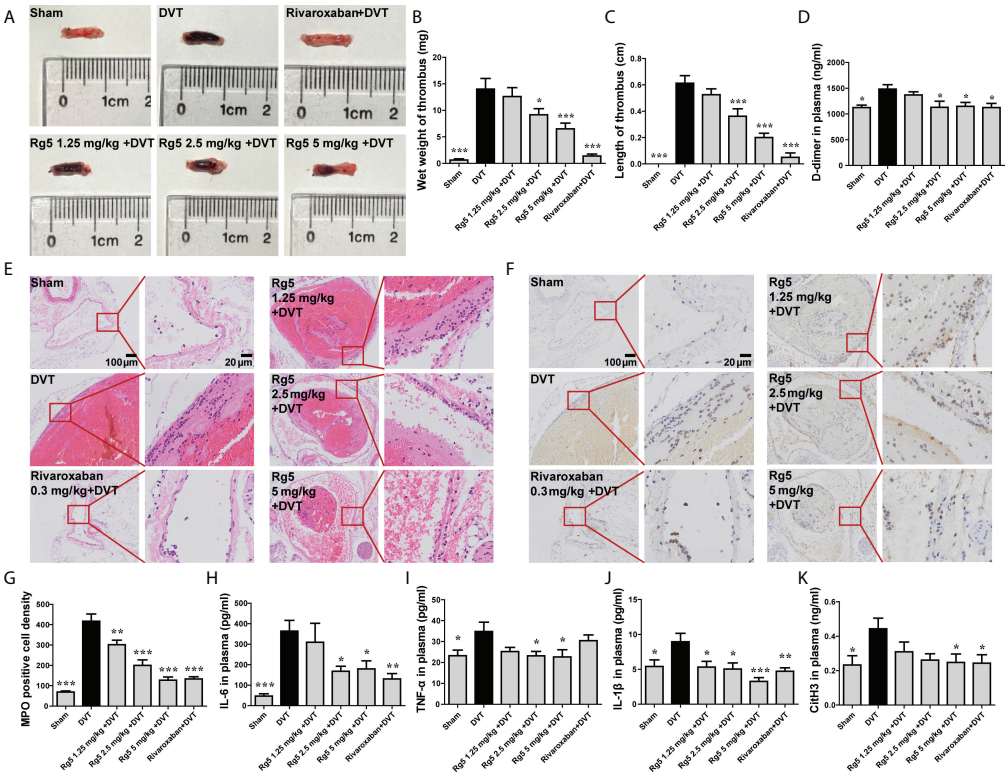

FIGURE 4
Effect of Rg5 administration on thrombosis and inflammation in DVT mice. **(A)** Morphology of venous thrombosis. **(B, C)** Thrombus wet weight and length (n = 8). **(D)** Plasma D-dimer content (n = 7). **(E)** HE staining of inferior vena cava. **(F)** MPO immunohistochemical staining of inferior vena cava. **(G)** MPO positive cell density (n = 6). **(H–K)** Plasma contents of IL-6, IL-1β, TNF-α, and CitH3 (n = 7). Data are shown as the mean ± SEM. *$P < 0.05$, **$P < 0.01$, ***$P < 0.001$ vs. DVT group.

0.001). Meanwhile, Rg5 pretreatment at higher dosages suppressed the plasma D-dimer content in DVT mice (Figure 4D, $P < 0.05$). Similarly, the positive control drug, Rivaroxiban (0.3 mg/kg), also attenuated thrombus formation, as well as the plasma D-dimer content in DVT mice. These results demonstrated that Rg5 could prevent thrombosis in deep vein. On the other hand, DVT is closely relevant to thrombophlebitis. As shown in Figure 4E, much more inflammatory cells infiltrated in the veins of DVT mice compared with the sham mice. Moreover, MPO staining exposed that most of the accumulated inflammatory cells were neutrophils (Figure 4F). After pretreatment of Rg5, the infiltration of inflammatory cells including neutrophils in vein was reduced ($P < 0.01$ or $P < 0.001$). Rg5 treatment (2.5 and 5 mg/kg) also significantly inhibited the release of inflammatory cytokines IL-6, TNF-α, and IL-1β in plasma (Figures 4H–J, $P < 0.05$ or $P < 0.001$). In addition, DVT is closely related to NETs produced by neutrophils. As the biomarker of NET formation, the content of citrullinated histone H3 (CitH3) was elevated after induction of DVT, which was significantly reduced after Rg5 (5 mg/kg) pre-administration (Figure 4K, $P < 0.05$). Interestingly, the positive drug, Rivaroxiban (0.3 mg/kg), could also suppress neutrophil infiltration and inflammatory response, as well as CitH3 expression. These results suggested that Rg5 could inhibit NET release and inflammatory response in mice.

Rg5 inhibited NETosis depending on $P2RY_{12}$

On the premise that Rg5 had no effect on neutrophils viability (Figure 5A), we first investigated whether Rg5 had an inhibitory effect on NETosis induced by PAF or LPS. As shown in Figure 5B, Rg5 pre-treatment significantly reduced the chromatin depolymerization and the expression of CitH3 in PAF-induced WT neutrophils ($P < 0.001$). However, in PAF-induced $P2RY_{12}$-KO neutrophils, Rg5 did not show the same effect. Similar results were found in LPS-induced WT and $P2RY_{12}$-KO neutrophils (Figure 5C). In addition, Rg5 treatment dose-dependently reduced cfDNA release and inflammatory factor production in culture medium of WT neutrophils induced by PAF and LPS (Figures 5D, E).

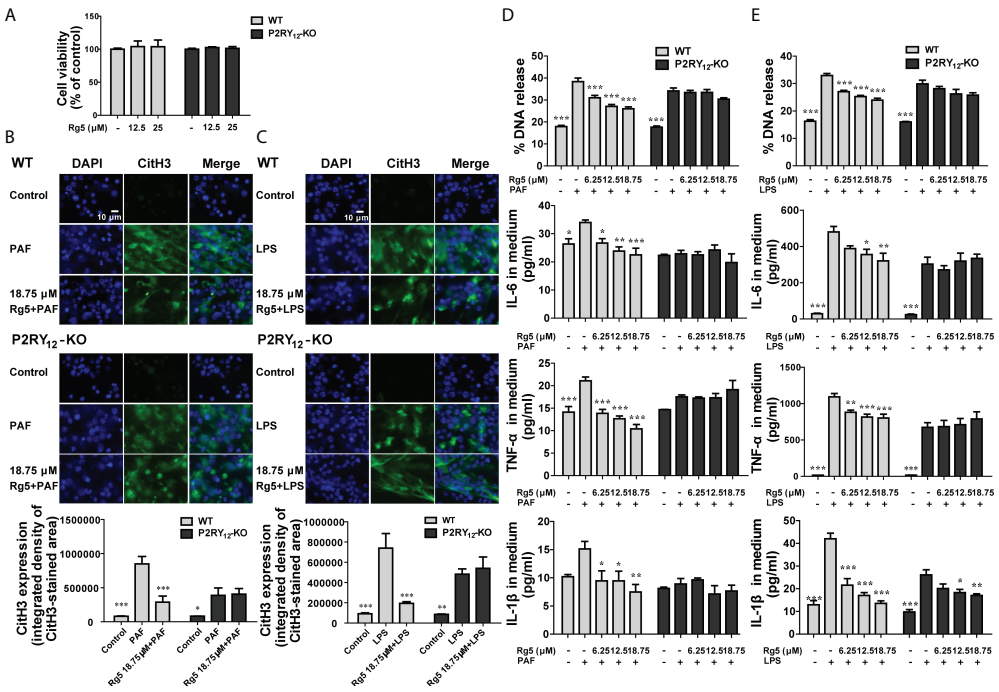

FIGURE 5
Effects of Rg5 on PAF or LPS-induced release of NETs and inflammatory factors in WT or $P2RY_{12}$-KO neutrophils. **(A)** Effect of Rg5 on WT or $P2RY_{12}$-KO neutrophils viability (n = 4). **(B, C)** Immunofluorescent staining and statistical analysis of CitH3 in WT or $P2RY_{12}$-KO neutrophils stimulated by PAF or LPS. (n = 6). **(D, E)** DNA concentration (n = 4) and IL-6, IL-1β, and TNF-α concentrations (n = 4) in the medium of WT or $P2RY_{12}$-KO neutrophils stimulated by PAF or LPS. All the data are shown as the mean ± SEM. $^*P < 0.05$, $^{**}P < 0.01$, $^{***}P < 0.001$ vs. PAF or LPS group.

However, in PAF-induced $P2RY_{12}$-KO neutrophils, Rg5 pre-treatment at 18.75 μM slightly suppressed the cfDNA release, whereas it could not inhibit further inflammatory factor release (Figure 5D). Similarly, in LPS-induced $P2RY_{12}$-KO neutrophils, Rg5 still showed slight inhibitory effects on the production of IL-1β (Figure 5E). These results suggested that Rg5 inhibited NETosis mainly through $P2RY_{12}$.

Rg5 attenuated LPS or PAF-induced activation of PAD4 and ERK/NF-κB signaling pathway in neutrophils *via* $P2RY_{12}$

As PAD4 plays an important role in NETosis, we next examined whether Rg5 could influence the activity of PAD4 and whether this action was dependent on $P2RY_{12}$. As shown in Figure 6A, Rg5 treatment significantly reduced PAF-induced calcium flux. In contrast, Rg5 could not further mitigate PAF-induced calcium flux in $P2RY_{12}$-KO neutrophils (Figure 6A). In terms of PAD4 expression, 18.75 μM Rg5 treatment significantly mitigated the increase of PAD4 induced by PAF in WT neutrophils (Figure 6B, $P < 0.05$). Accordingly, the catalytic activity of PAD4 in WT neutrophils was suppressed by Rg5, compared with PAF group cells (Figure 6C, $P < 0.01$ or $P < 0.001$). When $P2RY_{12}$ was deleted, Rg5 displayed no effect on the expression and activity of PAD4 in neutrophils. These results implicated that Rg5 suppressed PAF-induced elevation of PAD4 in neutrophils through $P2RY_{12}$. Thereby, we investigated whether Rg5 could regulate the signaling pathway associated with inflammatory cytokine production and whether this effect was dependent on $P2RY_{12}$. As shown in Figure 6D, PAF-induced a marked rise in the phosphorylation of ERK and NF-κB, which could be counteracted by Rg5 treatment ($P < 0.05$, $P < 0.01$, or $P < 0.001$). PAF could also induce the phosphorylation of ERK and NF-κB in $P2RY_{12}$-KO neutrophils. However, Rg5 treatment did not suppress the activated ERK and NF-κB in $P2RY_{12}$-KO cells. Similarly, Rg5 failed to inhibit LPS-activated ERK/NF-κB pathway in $P2RY_{12}$-KO neutrophils (Figure 6E). These results indicated that Rg5 suppressed the inflammatory pathway in neutrophils depending on $P2RY_{12}$.

Discussion and conclusions

In this study, we demonstrated that Rg5 inhibited signal transduction in neutrophils and reduced DVT formation by interacting with $P2RY_{12}$. On the one hand, Rg5 suppressed inflammatory response by inhibiting cytokine production

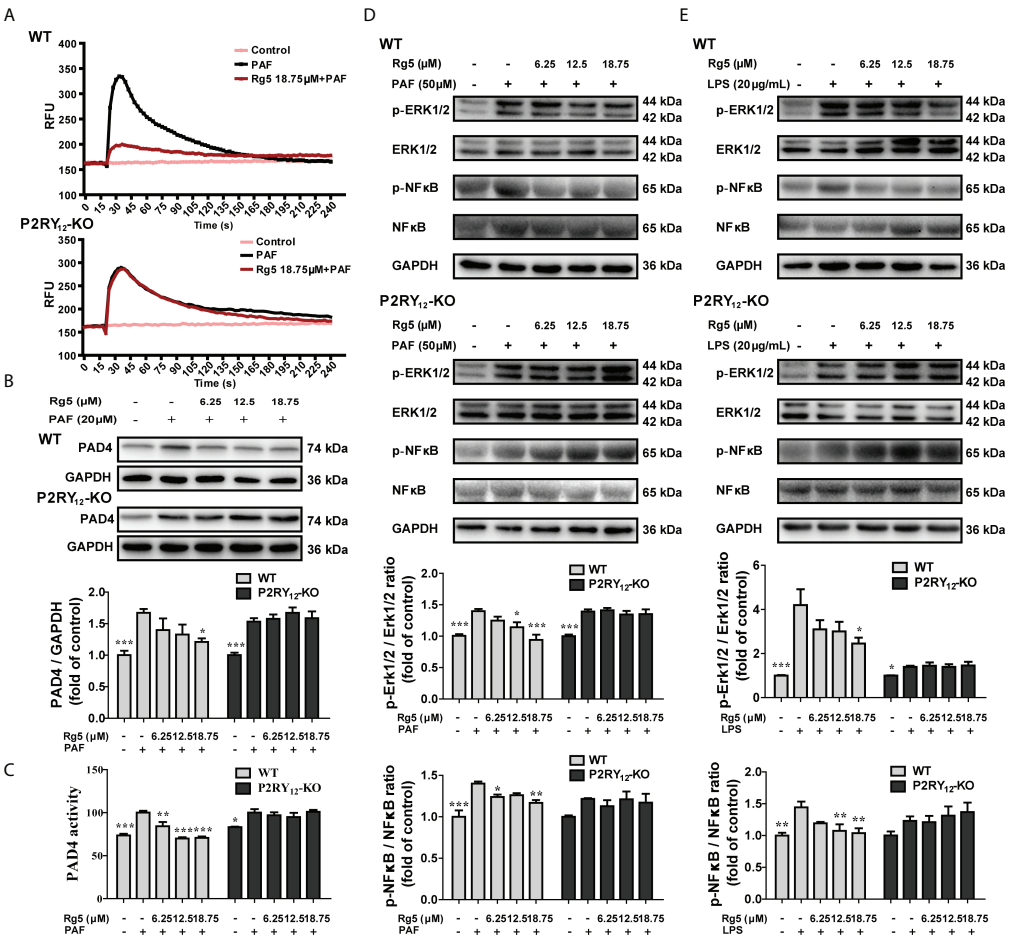

FIGURE 6
Effects of Rg5 on PAF or LPS-induced activation of PAD4 and ERK/NF-κB signaling pathway in WT or P2RY$_{12}$-KO neutrophils. **(A)** Calcium flux in WT or P2RY$_{12}$-KO neutrophils stimulated by PAF (n = 3). **(B)** Protein expression of PAD4 in WT or P2RY$_{12}$-KO neutrophils stimulated by PAF (n = 5). **(C)** Activity of PAD4 in WT or P2RY$_{12}$-KO neutrophils stimulated by PAF (n = 4). **(D, E)** Western Blot results and statistical analysis of protein expression and phosphorylation levels of ERK (n = 5) and NF-κB (n = 5) in WT or P2RY$_{12}$-KO neutrophils stimulated by PAF or LPS. All the data are shown as the mean ± SEM. *P < 0.05, **P < 0.01, ***P < 0.001 vs. PAF or LPS group.

through ERK/NF-κB signaling pathway; on the other hand, it reduced NETosis by preventing intracellular calcium mobilization, leading to the loss of PAD4 activity. Our results suggested that Rg5 might be a promising candidate for the prevention of DVT by counteracting neutrophil activation through P2RY$_{12}$.

P2RY$_{12}$ has been shown as a drug target for the prevention of platelet aggregation for a long time and is also involved in inflammation. For instance, knockout of P2RY$_{12}$ or blocking of P2RY$_{12}$ with Clopidogrel significantly reduced the volume of venous thrombosis in mice (18, 32). Clopidogrel, Cangrelor, and Ticagrelor have been used widely in clinic for the treatment of thrombogenesis by acting as P2RY$_{12}$ antagonists, but some patients experienced side effects such as bleeding or recurrent ischemia (33). Interestingly, in our experiment, the injection of Rg5 could prolong the coagulation time compared with that of Cangrelor, but the bleeding time of Rg5 was shorter than that of Cangrelor (data not shown), suggesting that Rg5 might have less bleeding risk compared with Cangrelor. However, further research remains to be done in the future to confirm the effect.

Clopidogrel has been proven to inhibit the production of proinflammatory mediator in plasma, particularly IL-6, TNFα, and IL-1β, and reduce platelet–neutrophil interactions (18, 21, 34). However, whether P2RY$_{12}$ plays an important role in the activation of neutrophils has not been clearly elucidated. A recent report demonstrated that, in the sepsis model of P2RY$_{12}$-KO mice, there was no prominent increase of neutrophils in the serum and inflammation sites (35). However, there was no further investigation to disclose the underlying mechanism. In the present study, we demonstrated that both LPS and PAF stimulation enhanced inflammatory response and NET release in neutrophils; however, the effect of

which was weakened in $P2RY_{12}$-deficient neutrophils. These results implicated that $P2RY_{12}$ is important for NETosis.

Rg5 has been shown to have multiple pharmacological activities, including anti-inflammatory, antitumor, neuroprotective, and cardioprotective properties (21). However, up to date, there is no report that clearly clarifies the direct molecular target. In our virtual screening, we found that Rg5 showed strong affinity with $P2RY_{12}$, which was similar to Ticagrelor, a well-known $P2RY_{12}$ antagonist. To confirm the binding, we conducted SPR assay and MD simulation, respectively, which revealed that Rg5 could dose-dependently bind to $P2RY_{12}$ and form stable complex rapidly. Moreover, site-mutation analysis exposed that two amino acid residues E188 and R265, which did not directly interact with 2MesADP (36), were critical sites for the binding of Rg5 to $P2RY_{12}$ and activation of downstream signaling. The roles of these two amino acids have been mentioned in previous studies, both of which were related to the activation of $P2RY_{12}$ (37, 38). However, a study has also indicated that E188 and R265 were not the active sites for $P2RY_{12}$; they mainly affect the conformational states of the protein (26). In agreement with the conjecture, the $P2RY_{12}$ mutant constructed by homologous modeling suggested that the allosteric effect caused by mutations of E188 and R265 might account for the diminished antagonism of Rg5 to $P2RY_{12}$. These results robustly corroborated the direct binding and antagonic activity of Rg5 to $P2RY_{12}$.

Platelet aggregation and inflammation are related to the pathogenesis of DVT. During the occurrence of DVT in clinic, slow or restricted blood flow in veins leads to damage of venous endothelial cells due to hypoxia and further releases cytokines such as inflammatory factors, PAF, and chemokines, which induces the activation and aggregation of platelets and white blood cells. When systemic or local infection occurs, in addition to similar responses described above, platelets and leukocytes activate rapidly in response to direct pathogen stimulation, leading to a significantly increased risk of DVT (39). Activated platelets are recruited and transported to the venous wall where they attach directly to endothelial cells or to leukocytes to form heterogeneous aggregates, which is a critical step in DVT initiation (40). $P2RY_{12}$ inhibitors Ticagrelor and Clopidogrel have been shown to significantly reduce the formation of platelet–neutrophil or platelet–monocyte aggregates and improve systemic inflammatory responses (41). The process of thrombosis is usually accompanied by the transformation of acute inflammation to chronic inflammation, and inflammation is closely related to DVT (42, 43). Recent studies have found that inflammation factors like IL-6, IL-1, and TNF-α were elevated in both DVT patients and mice (44, 45) and activated platelets and coagulation system, which further promoted thrombosis (46, 47). Neutrophils are essential in the development of thrombotic inflammation in DVT. In the DVT mouse model, 1 h after inferior vena cava stenosis, white blood cells began to appear and adhere to the venous endothelium. Six hours later, white blood cells covered the entire endothelial surface, of which more than 80% were neutrophils and the remaining 20% were monocytes. Moreover, when neutrophils are eliminated, DVT formation will be inhibited, indicating that the importance of neutrophils in DVT occurrence cannot be ignored (48). Activated neutrophils release NETs, which were found in the plasma and thrombus of patients with DVT (49, 50). Although monocytes also release extracellular traps (51), studies showed that neutrophils were the source of these extracellular traps (48), and a large number of NETs were also found in the thrombosis model (52). Meanwhile, treatment with DNase 1, known to degrade NETs, reduced the frequency of thrombosis (53), indicating that neutrophils and NETs in DVT are functionally important. In this study, we found that Rg5 inhibits DVT formation by reducing the release of inflammatory cytokines and the expression of NET biomarker CitH3 in mice. We induced bacterial and aseptic inflammation *in vitro* with LPS and PAF, respectively, and found that Rg5 reduced the inflammatory response of neutrophils by inhibiting $P2RY_{12}$. This study focused only on the antagonistic effect of Rg5 against $P2RY_{12}$ of neutrophils, rather than that of the platelets or other blood cells, like monocytes. However, Rg5 has been reported to have a significant anti-platelet aggregation effect (54). Combined with the fact that Rg5 can inhibit the phosphorylation of AKT and ERK signals downstream of $P2RY_{12}$ and antagonize its activity, we speculate that Rg5 can inhibit platelet activation and platelet–white blood cell interaction by targeting $P2RY_{12}$. Therefore, we believe that Rg5 may be an ideal treatment option for DVT.

$P2RY_{12}$, as a member of the GPCR family, transmits signals mainly through two pathways: one modulates the cAMP level and PI3K/AKT pathway by binding to Gi protein, and the other influences Mitogen activated protein kinases (MAPK) signaling pathways such as ERK pathway by binding to β-arrestin or Gi protein (55). Previous studies have reported that the transcription and expression of inflammatory cytokines such as TNF-α, IL-1β, and IL-6 were related to the phosphorylation of NF-κB signal (56), which was affected by ERK pathway (57). PAD4 is highly expressed in neutrophil nuclei and relies on calcium mobilization to catalyze the conversion of several arginine sites on histones into citrulline (58), which plays an important role in the formation of NETs (59, 60). It has also been found that Rg5 can play an anti-inflammatory role by interfering NLRP3 signaling pathway and reducing inflammatory cytokines, whereas PAD4 also has the ability to upregulate NLRP3 inflammatory granules through post-transcription (61). Meanwhile, the activation of $P2RY_{12}$ by ADP is closely associated with NLRP3- and NF-κB–mediated inflammatory responses (62). Therefore, on the basis of the inhibitory effect of Rg5 on $P2RY_{12}$ activation in this study, the interference of Rg5 on NLRP3 signaling *via* $P2RY_{12}$ may also explain the inhibitory effect of Rg5 on neutrophil inflammation. In the present study, Rg5 was found to inhibit ERK/NF-κB activation and inflammatory factor production in neutrophils

induced by both LPS and PAF. Meanwhile, Rg5 restrained calcium influx, PAD4 activity, and NET release in PAF/LPS-induced neutrophils. However, in $P2RY_{12}$ deficiency neutrophils, the suppressive effects of Rg5 on the aforementioned parameters were diminished. These results implicated that Rg5 modulated ERK/NF-κB and cAMP/PAD4 signaling pathway in neutrophils depending on $P2RY_{12}$.

In summary, this study demonstrated that Rg5 as a natural $P2RY_{12}$ antagonist could inhibit NETosis during thrombosis to slow down the formation of DVT. Our study provides a theoretical basis for the clinical application of Rg5 for the prevention of DVT.

Data availability statement

The raw data supporting the conclusions of this article will be made available by the authors, without undue reservation.

Ethics statement

The animal study was reviewed and approved by Shanghai University of Traditional Chinese Medicine.

Author contribution

ZC, GW, and XX performed the experiments, analyzed the data, and wrote the paper. ZW and XW designed the study. HL, JL, and HS participated in its design and helped to draft the manuscript. MC and SL gave valuable suggestions about the study. All authors contributed to the article and approved the submitted version.

Funding

This work was supported by Shanghai Municipal Natural Science Foundation (22ZR1461100). Major International (Regional) Joint Research Project of NSFC (81920108033), Guangxi Science and Technology Base and Talent Special Project (Guike AD20297068).

Conflict of interest

The authors declare that the research was conducted in the absence of any commercial or financial relationships that could be construed as a potential conflict of interest.

Publisher's note

All claims expressed in this article are solely those of the authors and do not necessarily represent those of their affiliated organizations, or those of the publisher, the editors and the reviewers. Any product that may be evaluated in this article, or claim that may be made by its manufacturer, is not guaranteed or endorsed by the publisher.

References

1. Badireddy M, Mudipalli VR. Deep venous thrombosis prophylaxis. In: *StatPearls*. Treasure Island (FL: StatPearls Publishing (2021).

2. Bevis PM, Smith FC. Deep vein thrombosis. *Surg (Oxford)* (2016) 34:159–64. doi: 10.1016/j.mpsur.2016.02.001

3. Diana Yap FS, Ng ZY, Wong CY, Muhamad Saifuzzaman MK, Yang LB. Appropriateness of deep vein thrombosis (DVT) prophylaxis use among medical inpatients: a DVT risk alert tool (DRAT) study. *Med J Malaysia* (2019) 74:45–50.

4. Kollias A, Kyriakoulis KG, Lagou S, Kontopantelis E, Stergiou GS, Syrigos K. Venous thromboembolism in COVID-19: A systematic review and meta-analysis. *Vasc Med* (2021) 26:415–25. doi: 10.1177/1358863X21995566

5. Lichota A, Szewczyk EM, Gwozdzinski K. Factors affecting the formation and treatment of thrombosis by natural and synthetic compounds. *Int J Mol Sci* (2020) 21:7975. doi: 10.3390/ijms21217975

6. Weitz JI, Chan NC. Novel antithrombotic strategies for treatment of venous thromboembolism. *Blood* (2020) 135:351–9. doi: 10.1182/blood.2019000919

7. Pfeiler S, Stark K, Massberg S, Engelmann B. Propagation of thrombosis by neutrophils and extracellular nucleosome networks. *Haematologica* (2017) 102:206–13. doi: 10.3324/haematol.2016.142471

8. Fuchs TA, Brill A, Duerschmied D, Schatzberg D, Monestier M, Myers DD Jr, et al. Extracellular DNA traps promote thrombosis. *Proc Natl Acad Sci USA* (2010) 107:15880–5. doi: 10.1073/pnas.1005743107

9. Urban CF, Ermert D, Schmid M, Abu-Abed U, Goosmann C, Nacken W, et al. Neutrophil extracellular traps contain calprotectin, a cytosolic protein complex involved in host defense against candida albicans. *PloS Pathog* (2009) 5: e1000639. doi: 10.1371/journal.ppat.1000639

10. Papayannopoulos V. Neutrophil extracellular traps in immunity and disease. *Nat Rev Immunol* (2018) 18:134–47. doi: 10.1038/nri.2017.105

11. Qutub MA, Chong AY, So DY. Current evidence on platelet P2Y12 receptor inhibitors: Is there still a role for clopidogrel in 2015? *Can J Cardiol* (2015) 31:1481–4. doi: 10.1016/j.cjca.2015.04.019

12. Niu H, Chen X, Gruppo RA, Li D, Wang Y, Zhang L, et al. Integrin αIIb-mediated PI3K/Akt activation in platelets. *PloS One* (2012) 7:e47356. doi: 10.1371/journal.pone.0047356

13. Guidetti GF, Canobbio I, Torti M. PI3K/Akt in platelet integrin signaling and implications in thrombosis. *Adv Biol Regul* (2015) 59:36–52. doi: 10.1016/j.jbior.2015.06.001

14. Kim S, Kunapuli SP. P2Y12 receptor in platelet activation. *Platelets* (2011) 22:56–60. doi: 10.3109/09537104.2010.497231

15. Speich HE, Bhal V, Houser KH, Caughran AT, Lands LT, Houng AK, et al. Signaling *via* P2Y12 may be critical for early stabilization of platelet aggregates. *J Cardiovasc Pharmacol* (2014) 63:520–7. doi: 10.1097/FJC.0000000000000076

16. Mansour A, Bachelot-Loza C, Nesseler N, Gaussem P, Gouin-Thibault I. $P2Y_{12}$ inhibition beyond thrombosis: Effects on inflammation. *Int J Mol Sci* (2020) 21:1391. doi: 10.3390/ijms21041391

17. Guenther F, Herr N, Mauler M, Witsch T, Roming F, Hein L, et al. Contrast ultrasound for the quantification of deep vein thrombosis in living mice: effects of

enoxaparin and P2Y12 receptor inhibition. *J Thromb Haemost* (2013) 11:1154–62. doi: 10.1111/jth.12206

18. Wang XL, Deng HF, Li T, Miao SY, Xiao ZH, Liu MD, et al. Clopidogrel reduces lipopolysaccharide-induced inflammation and neutrophil-platelet aggregates in an experimental endotoxemic model. *J Biochem Mol Toxicol* (2019) 33:e22279. doi: 10.1002/jbt.22279

19. Rahman M, Gustafsson D, Wang Y, Thorlacius H, Braun OÖ. Ticagrelor reduces neutrophil recruitment and lung damage in abdominal sepsis. *Platelets* (2014) 25:257–63. doi: 10.3109/09537104.2013.809520

20. Judge HM, Buckland RJ, Sugidachi A, Jakubowski JA, Storey RF. The active metabolite of prasugrel effectively blocks the platelet P2Y12 receptor and inhibits procoagulant and pro-inflammatory platelet responses. *Platelets* (2008) 19:125–33. doi: 10.1080/09537100701694144

21. Sexton TR, Zhang G, Macaulay TE, Callahan LA, Charnigo R, Vsevolozhskaya OA, et al. Ticagrelor reduces thromboinflammatory markers in patients with pneumonia. *JACC Basic Transl Sci* (2018) 3:435–49. doi: 10.1016/j.jacbts.2018.05.005

22. Liu MY, Liu F, Gao YL, Yin JN, Yan WQ, Liu JG, et al. Pharmacological activities of ginsenoside Rg5 (Review). *Exp Ther Med* (2021) 22:840. doi: 10.3892/etm.2021.10272

23. Zheng F, Zhou Q, Cao Y, Shi H, Wu H, Zhang B, et al. P2Y12 deficiency in mouse impairs noradrenergic system in brain, and alters anxiety-like neurobehavior and memory. *Genes Brain Behav* (2019) 18:e12458. doi: 10.1111/gbb.12458

24. Liao Q, Chen Z, Tao Y, Zhang B, Wu X, Yang L, et al. An integrated method for optimized identification of effective natural inhibitors against SARS-CoV-2 3CLpro. *Sci Rep* (2021) 11:22796. doi: 10.1038/s41598-021-02266-3

25. Palacio-Rodríguez K, Lans I, Cavasotto CN, Cossio P. Exponential consensus ranking improves the outcome in docking and receptor ensemble docking. *Sci Rep* (2019) 9:5142. doi: 10.1038/s41598-019-41594-3

26. Zhang K, Zhang J, Gao ZG, Zhang D, Zhu L, Han GW, et al. Structure of the human P2Y12 receptor in complex with an antithrombotic drug. *Nature* (2014) 509:115–8. doi: 10.1038/nature13083

27. Miller BR3rd, McGee TD Jr, JM S, Homeyer N, Gohlke H, Roitberg AE. MMPBSA.py: An efficient program for end-state free energy calculations. *J Chem Theory Comput* (2012) 8:3314–21. doi: 10.1021/ct300418h

28. Xu Q, Chen Z, Zhu B, Wang G, Jia Q, Li Y, et al. A-type cinnamon procyanidin oligomers protect against 1-Methyl-4-Phenyl-1,2,3,6-Tetrahydropyridine-Induced neurotoxicity in mice through inhibiting the P38 mitogen-activated protein Kinase/P53/BCL-2 associated X protein signaling pathway. *J Nutr* (2020) 150:1731–7. doi: 10.1093/jn/nxaa128

29. Wrobleski SK, Farris DM, Diaz JA, Myers DD Jr, Wakefield TW. Mouse complete stasis model of inferior vena cava thrombosis. *J Vis Exp* (2011) 52:2738. doi: 10.3791/2738

30. Yang L, Xing F, Han X, Li Q, Wu H, Shi H, et al. Astragaloside IV regulates differentiation and induces apoptosis of activated CD4+ T cells in the pathogenesis of experimental autoimmune encephalomyelitis. *Toxicol Appl Pharmacol* (2019) 362:105–15. doi: 10.1016/j.taap.2018.10.024

31. Varma MR, Varga AJ, Knipp BS, Sukheepod P, Upchurch GR, Kunkel SL, et al. Neutropenia impairs venous thrombosis resolution in the rat. *J Vasc Surg* (2003) 38:1090–8. doi: 10.1016/S0741-5214(03)00431-2

32. Bird JE, Wang X, Smith PL, Barbera F, Huang C, Schumacher WA. A platelet target for venous thrombosis? P2Y1 deletion or antagonism protects mice from vena cava thrombosis. *J Thromb Thrombolysis* (2012) 34:199–207. doi: 10.1007/s11239-012-0745-3

33. Terrier J, Daali Y, Fontana P, Csajka C, Reny JL. Towards personalized antithrombotic treatments: Focus on P2Y12 inhibitors and direct oral anticoagulants. *Clin Pharmacokinet* (2019) 58:1517–32. doi: 10.1007/s40262-019-00792-y

34. Xiao Z, Théroux P. Clopidogrel inhibits platelet-leukocyte interactions and thrombin receptor agonist peptide-induced platelet activation in patients with an acute coronary syndrome. *J Am Coll Cardiol* (2004) 43:1982–8. doi: 10.1016/j.jacc.2003.10.071

35. Liverani E, Rico MC, Tsygankov AY, Kilpatrick LE, Kunapuli SP. P2Y12 receptor modulates sepsis-induced inflammation. *Arterioscler Thromb Vasc Biol* (2016) 36:961–71. doi: 10.1161/ATVBAHA.116.307401

36. Zhang J, Zhang K, Gao ZG, Paoletta S, Zhang D, Han GW, et al. Agonist-bound structure of the human P2Y12 receptor. *Nature* (2014) 509:119–22. doi: 10.1038/nature13288

37. Ignatovica V, Megnis K, Lapins M, Schiöth HB, Klovins J. Identification and analysis of functionally important amino acids in human purinergic 12 receptor using a saccharomyces cerevisiae expression system. *FEBS J* (2012) 279:180–91. doi: 10.1111/j.1742-4658.2011.08410.x

38. Schmidt P, Ritscher L, Dong EN, Hermsdorf T, Cöster M, Wittkopf D, et al. Identification of determinants required for agonistic and inverse agonistic ligand properties at the ADP receptor P2Y12. *Mol Pharmacol* (2013) 83:256–66. doi: 10.1124/mol.112.082198

39. Beristain-Covarrubias N, Perez-Toledo M, Thomas MR, Henderson IR, Watson SP, Cunningham AF. Understanding infection-induced thrombosis: Lessons learned from animal models. *Front Immunol* (2019) 10:2569. doi: 10.3389/fimmu.2019.02569

40. Diaz JA, Obi AT, Myers DD Jr, Wrobleski SK, Henke PK, Mackman N, et al. Critical review of mouse models of venous thrombosis. *Arterioscler Thromb Vasc Biol* (2012) 32:556–62. doi: 10.1161/ATVBAHA.111.244608

41. Thomas MR, Outteridge SN, Ajjan RA, Phoenix F, Sangha GK, Faulkner RE, et al. Platelet P2Y12 inhibitors reduce systemic inflammation and its prothrombotic effects in an experimental human model. *Arterioscler Thromb Vasc Biol* (2015) 35:2562–70. doi: 10.1161/ATVBAHA.115.306528

42. Branchford BR, Carpenter SL. The role of inflammation in venous thromboembolism. *Front Pediatr* (2018) 6:142. doi: 10.3389/fped.2018.00142

43. Vazquez-Garza E, Jerjes-Sanchez C, Navarrete A, Joya-Harrison J, Rodriguez D. Venous thromboembolism: thrombosis, inflammation, and immunothrombosis for clinicians. *J Thromb Thrombolysis* (2017) 44:377–85. doi: 10.1007/s11239-017-1528-7

44. Candido S, Lumera G, Barcellona G, Vetri D, Tumino E, Platania I, et al. Direct oral anticoagulant treatment of deep vein thrombosis reduces IL-6 expression in peripheral mono-nuclear blood cells. *Exp Ther Med* (2020) 20:237. doi: 10.3892/etm.2020.9367

45. Meng Y, Yin Q, Ma Q, Qin H, Zhang J, Zhang B, et al. FXII regulates the formation of deep vein thrombosis *via* the PI3K/AKT signaling pathway in mice. *Int J Mol Med* (2021) 47:87. doi: 10.3892/ijmm.2021.4920

46. Zhang Y, Zhang Z, Wei R, Miao X, Sun S, Liang G, et al. IL (Interleukin)-6 contributes to deep vein thrombosis and is negatively regulated by miR-338-5p. *Arterioscler Thromb Vasc Biol* (2020) 40:323–34. doi: 10.1161/ATVBAHA.119.313137

47. Bester J, Pretorius E. Effects of IL-1β, IL-6 and IL-8 on erythrocytes, platelets and clot viscoelasticity. *Sci Rep* (2016) 6:32188. doi: 10.1038/srep32188

48. von Brühl ML, Stark K, Steinhart A, Chandraratne S, Konrad I, Lorenz M, et al. Monocytes, neutrophils, and platelets cooperate to initiate and propagate venous thrombosis in mice *in vivo*. *J Exp Med* (2012) 209:819–35. doi: 10.1084/jem.20112322

49. Liu L, Zhang W, Su Y, Chen Y, Cao X, Wu J. The impact of neutrophil extracellular traps on deep venous thrombosis in patients with traumatic fractures. *Clin Chim Acta* (2021) 519:231–8. doi: 10.1016/j.cca.2021.04.021

50. van Montfoort ML, Stephan F, Lauw MN, Hutten BA, Van Mierlo GJ, Solati S, et al. Circulating nucleosomes and neutrophil activation as risk factors for deep vein thrombosis. *Arterioscler Thromb Vasc Biol* (2013) 33:147–51. doi: 10.1161/ATVBAHA.112.300498

51. Granger V, Faille D, Marani V, Noël B, Gallais Y, Szely N, et al. Human blood monocytes are able to form extracellular traps. *J Leukoc Biol* (2017) 102:775–81. doi: 10.1189/jlb.3MA0916-411R

52. Campos J, Ponomaryov T, De Prendergast A, Whitworth K, Smith CW, Khan AO, et al. Neutrophil extracellular traps and inflammasomes cooperatively promote venous thrombosis in mice. *Blood Adv* (2021) 5:2319–24. doi: 10.1182/bloodadvances.2020003377

53. Brill A, Fuchs TA, Savchenko AS, Thomas GM, Martinod K, De Meyer SF, et al. Neutrophil extracellular traps promote deep vein thrombosis in mice. *J Thromb Haemost* (2012) 10:136–44. doi: 10.1111/j.1538-7836.2011.04544.x

54. Lee JG, Lee YY, Kim SY, Pyo JS, Yun-Choi HS, Park JH. Platelet antiaggregating activity of ginsenosides isolated from processed ginseng. *Pharmazie* (2009) 64:602–4.

55. Cattaneo M. P2Y12 receptors: structure and function. *J Thromb Haemost* (2015) 13(Suppl 1):S10–S16. doi: 10.1111/jth.12952

56. Lawrence T. The nuclear factor NF-kappaB pathway in inflammation. *Cold Spring Harb Perspect Biol* (2009) 1:a001651. doi: 10.1101/cshperspect.a001651

57. Lu CH, Li KJ, Wu CH, Shen CY, Kuo YM, Hsieh SC, et al. The FcγRIII engagement augments PMA-stimulated neutrophil extracellular traps (NETs) formation by granulocytes partially *via* cross-talk between syk-ERK-NF-κB and PKC-ROS signaling pathways. *Biomedicines* (2021) 9:1127. doi: 10.3390/biomedicines9091127

58. Thiam HR, Wong SL, Qiu R, Kittisopikul M, Vahabikashi A, Goldman AE, et al. NETosis proceeds by cytoskeleton and endomembrane disassembly and PAD4-mediated chromatin decondensation and nuclear envelope rupture. *Proc Natl Acad Sci USA* (2020) 117:7326–37. doi: 10.1073/pnas.1909546117

59. Li P, Li M, Lindberg MR, Kennett MJ, Xiong N, Wang Y. PAD4 is essential for antibacterial innate immunity mediated by neutrophil extracellular traps. *J Exp Med* (2010) 207:1853–62. doi: 10.1084/jem.20100239

60. Tan C, Aziz M, Wang P. The vitals of NETs. *J Leukoc Biol* (2021) 110:797–808. doi: 10.1002/JLB.3RU0620-375R

61. Münzer P, Negro R, Fukui S, di Meglio L, Aymonnier K, Chu L, et al. NLRP3 inflammasome assembly in neutrophils is supported by PAD4 and promotes NETosis under sterile conditions. *Front Immunol* (2021) 12:683803. doi: 10.3389/fimmu.2021.683803

62. Suzuki T, Kohyama K, Moriyama K, Ozaki M, Hasegawa S, Ueno T, et al. Extracellular ADP augments microglial inflammasome and NF-κB activation *via* the P2Y12 receptor. *Eur J Immunol* (2020) 50:205–19. doi: 10.1002/eji.201848013

frontiers | Frontiers in Immunology

TYPE Original Research
PUBLISHED 24 August 2022
DOI 10.3389/fimmu.2022.888415

OPEN ACCESS

EDITED BY
Amiram Ariel,
University of Haifa, Israel

REVIEWED BY
Jamel El-Benna,
INSERM U1149 Centre de Recherche sur l'Inflammation, France
Sonja Vermeren,
University of Edinburgh, United Kingdom

*CORRESPONDENCE
Heidi C. E. Welch
heidi.welch@babraham.ac.uk

SPECIALTY SECTION
This article was submitted to Inflammation, a section of the journal Frontiers in Immunology

RECEIVED 02 March 2022
ACCEPTED 02 August 2022
PUBLISHED 24 August 2022

CITATION
Hornigold K, Chu JY, Chetwynd SA, Machin PA, Crossland L, Pantarelli C, Anderson KE, Hawkins PT, Segonds-Pichon A, Oxley D and Welch HCE (2022) Age-related decline in the resistance of mice to bacterial infection and in LPS/TLR4 pathway-dependent neutrophil responses. *Front. Immunol.* 13:888415. doi: 10.3389/fimmu.2022.888415

Age-related decline in the resistance of mice to bacterial infection and in LPS/TLR4 pathway-dependent neutrophil responses

Kirsti Hornigold[1], Julia Y. Chu[1], Stephen A. Chetwynd[1], Polly A. Machin[1], Laraine Crossland[1], Chiara Pantarelli[1], Karen E. Anderson[1], Phillip T. Hawkins[1], Anne Segonds-Pichon[2], David Oxley[3] and Heidi C. E. Welch[1]*

[1]Signalling Programme, The Babraham Institute, Cambridge, United Kingdom, [2]Bioinformatics Facility, The Babraham Institute, Cambridge, United Kingdom, [3]Proteomics Facility, The Babraham Institute, Cambridge, United Kingdom

Host defense against bacterial and fungal infections diminishes with age. In humans, impaired neutrophil responses are thought to contribute to this decline. However, it remains unclear whether neutrophil responses are also impaired in old mice. Here, we investigated neutrophil function in old mice, focusing on responses primed by lipopolysaccharide (LPS), an endotoxin released by gram-negative bacteria like *E. coli*, which signals through toll-like receptor (TLR) 4. We show that old mice have a reduced capacity to clear pathogenic *E. coli* during septic peritonitis. Neutrophil recruitment was elevated during LPS-induced but not aseptic peritonitis. Neutrophils from old mice showed reduced killing of *E. coli*. Their reactive oxygen species (ROS) production was impaired upon priming with LPS but not with GM-CSF/TNFα. Phagocytosis and degranulation were reduced in a partially LPS-dependent manner, whereas impairment of NET release in response to *S. aureus* was independent of LPS. Unexpectedly, chemotaxis was normal, as were Rac1 and Rac2 GTPase activities. LPS-primed activation of Erk and p38 Mapk was defective. PIP_3 production was reduced upon priming with LPS but not with GM-CSF/TNFα, whereas PIP_2 levels were constitutively low. The expression of 5% of neutrophil proteins was dysregulated in old age. Granule proteins, particularly cathepsins and serpins, as well as TLR-pathway proteins and membrane receptors were upregulated, whereas chromatin and RNA regulators were downregulated. The upregulation of CD180 and downregulation of MyD88 likely contribute to the impaired LPS signaling. In summary, all major neutrophil responses except chemotaxis decline with age in mice, particularly upon LPS priming. This LPS/TLR4 pathway dependence resolves previous controversy regarding effects of age on murine neutrophils and confirms that mice are an appropriate model for the decline in human neutrophil function.

KEYWORDS
aging, neutrophils, TLR4, proteomics, ROS, degranulation, phagocytosis, NETs

Introduction

Neutrophils provide the first line of innate host defense against bacterial and fungal infections (1), as well as playing roles in wound healing and cancer progression (2, 3). During inflammation and infections, neutrophils are rapidly recruited from the blood stream into the inflamed or infected tissue. They kill pathogens by phagocytosis, degranulation, reactive oxygen species (ROS) and neutrophil extracellular traps (NETs) (1).

Host defense against bacterial and fungal infections diminishes with age. In the elderly, infections are more likely to develop into dangerous diseases such as pneumonia and peritonitis, progress to sepsis, and cause death from sepsis (4, 5). In humans, the age-related decline in neutrophil function is thought to contribute to the decreased immunity against bacteria and fungi, although a causal relationship is hard to establish. The elderly have normal numbers of circulating neutrophils (6), but all major neutrophil responses are altered. ROS and NET production are impaired in response to a wide range of stimuli (7–10), chemotaxis is reduced under multiple conditions, and chemokinesis is impaired upon TNFα priming (8, 11). The reduced chemotaxis has been linked to constitutively increased PI3K activity, where inhibition of PI3Kγ or PI3Kδ restored migration speed and accuracy (11). Degranulation of azurophil granules seems increased in old age (11), whereas phagocytosis is decreased (12, 13). These altered neutrophil responses have largely been attributed to the increased inflammatory state associated with advanced age (inflamm-aging), where chronically increased levels of a range of inflammatory mediators perturb signaling pathways. Impairments in signaling through the inflammatory cytokines GM-CSF and TNFα, and through toll-like receptor (TLR) pathways, are commonly reported (14). For example, the GM-CSF-mediated delay in neutrophil apoptosis which occurs during inflammation and infections is reduced in the elderly (8), as is the TNFα-priming of chemokinesis and chemotaxis (11). Neutrophils from the elderly express normal levels of TLR1, TLR2 and TLR4 (6, 8, 10). However, the cell surface level of TLR1 is reduced, and the TLR1-mediated upregulation of Mac1, shedding of L-selectin and production of IL8 are impaired (6), as is the LPS-stimulated recruitment of TLR4 into lipid rafts (8).

In mice, immunity against bacterial and fungal pathogens declines with age just as in humans. For example, old mice are less able to clear *Staphylococcus aureus* from skin wounds, leading to delayed wound closure (15), or to resolve *Salmonella typhimurium* after oral infection, causing the colonization of multiple organs (16), or clear *Candida albicans* after intravenous infection, leading to high fungal tissue burden and mortality (17). Old mice also show increased mortality after infection with influenza or *Herpes simplex* virus, and neutrophil depletion revealed that these losses of antiviral immunity are neutrophil-dependent (18, 19). Considering these consistent reductions in the immunity of old mice to a range of pathogens, the effects of age on neutrophil recruitment to infected tissues are surprisingly varied. Neutrophil recruitment to the skin was reduced in old mice after *S. aureus* infection (15), whereas peritoneal recruitment was increased during *C. albicans* infection (20), and recruitment to the lung was delayed during infection with *Francisella tularensis* (21) but increased during influenza virus infection (19). When neutrophil recruitment was induced with various inflammatory mediators, the effects of aging were similarly inconsistent. Keratinocyte-derived chemokine (KC)-induced neutrophil recruitment to the skin was reduced in old mice (15), as was IL-1 induced recruitment to the cremaster muscle (22), whereas LPS-induced recruitment to the lung was increased (23). Therefore, the age-related decline in immunity is clearly not simply correlated with neutrophil recruitment, suggesting that neutrophil effector responses may be reduced in old age. However, reports on the effects of age on mouse neutrophil responses show great variability. ROS production was reduced in neutrophils from old mice upon stimulation with TLR2 ligands (24), but normal in response to the oxysterol 7KC (25). NETosis was reduced in neutrophils from old mice upon stimulation with TLR2 ligands (24), but increased upon mitochondrial oxidative stress (25). Furthermore, despite neutrophil transcriptome analysis showing altered expression of NETosis-related genes with age, including histones, PADI4 and elastase, PMA-induced NETosis was normal (26). Phagocytosis of yeast by neutrophils from old mice was reduced (27), whereas phagocytosis of *S. aureus* was normal (15). Transwell assays showed either normal or increased spontaneous migration of neutrophils from old mice,

Abbreviations: AUC, area under the curve; fMLP, formyl-methionyl-leucyl-phenylalanine; HPLC-MS, high-performance liquid-chromatography mass spectrometry; KC, keratinocyte-derived chemokine; LPS, lipopolysaccharide; NETs, neutrophil extracellular traps; PI3K, phosphoinositide 3 kinase; PMA, phorbol 12-myristate 13-acetate; PIP_3, phosphatidylinositol (3,4,5)-trisphosphate; PIP_2, phosphatidylinositol bisphosphate; ROS, reactive oxygen species; TLR, toll-like receptor; TNFα, tumor necrosis factor alpha.

but a loss of KC-induced chemotaxis (19, 28). These variabilities have led to the proposal that the age-related decline in murine neutrophil responses is too subtle and complex for mice to be a useful model for the decline in human neutrophil function (29).

Over recent years, research focus has therefore shifted from studying the influence of organismal age on neutrophil function to investigating the aging of individual neutrophils. This showed that neutrophils age between their release from the bone marrow into the circulation and their homeostatic clearance into tissues a few hours or at most days later. In both humans and mice, neutrophils freshly released into the circulation have high surface levels of L-selectin (CD62L) which decline over several hours, whereas aged neutrophils show increased CXCR4 surface levels before they are cleared from the blood (30–32). Fresh neutrophils are preferentially recruited to inflamed and infected organs to provide host defense, whereas the homeostatic clearance of aged neutrophils serves to protect against vascular inflammation and patrol for pathogens in the homing tissues (30). The mechanism underlying this neutrophil aging is that the cells become primed by signaling through TLRs during their time in the circulation (31, 32). Elegant experiments with germ-free mice have shown that the stimuli responsible for this priming are the TLR4 ligand LPS and TLR2 ligand peptidoglycan released by the gut microbiota (32). Unlike tissue recruitment however, the capacity of neutrophils to produce ROS and cytokines is unaltered throughout their aging in the circulation (30, 31).

Intrigued by the discrepancies between previous studies on neutrophil responses in old mice, we sought to revive research efforts into the effects of organismal age on neutrophil function, focusing on the priming pathways that had been implicated in aging human neutrophils. We found an age-related decline in murine neutrophil function that is largely dependent on the LPS/TLR4 signaling pathway, thus resolving some of the previous controversy.

Materials and methods

Materials

Kwik-Diff stain (9990700) was from Thermo Scientific Shandon. Reagents for priming neutrophils were LPS (*E. coli*-derived, Sigma, L3024), mouse TNFα (R&D Systems, 410-MT-010), and mouse GM-CSF (Peprotech, 315-03). Reagents for stimulating neutrophils included f-Met-Leu-Phe (fMLP, Sigma, F3506), C5a (Sigma, C5788), and phorbol 12-myristate 13-acetate (PMA, Sigma, P1585). Antibodies for western blotting were Rac1 (clone 23A8, Millipore, 05-389, 1:3000), Rac2 (Millipore, 07-604, 1:5,000), Irak4 (Cell Signaling Technology, 4363, 1:500), MyD88 (Cell Signaling Technology, 4283, 1:500), TLR4 (Cell Signaling Technology, 14358, 1:500), and Trif (Abcam, ab13810, 1:1,000). Antibodies for LPS/TLR4 pathway analysis were from Cell Signaling Technology: phospho-p38 Mapk Thr180/Tyr182 (9211, 1:1000), p38 Mapk (9212, 1:1000), phospho-p42/44 Erk Thr202/Tyr204 (9106, 1:1000), p42/44 Erk (9102, 1:1000), phospho-Akt Thr308 (9275, 1:5000), and Akt (9272, 1:1000). Antibodies for other applications are listed in the relevant sections below. Fc block (553141) was from BD Biosciences.

Mice

Male wild type mice on C57BL/6 genetic background at 8-10 weeks of age (young) and at 24 months of age (old) were compared directly in experiments. Mice were bred and group-housed (up to 5) in individually ventilated cages in the Babraham Institute Small Animal Facility that uses 12 h light/dark cycles with dusk and dawn settings, 52% room humidity (55 ± 10% range) and 20°C room temperature (19-21°C range), and were fed chow diet and water *ad libitum*. The C57BL/6 strain was originally purchased from Charles River (Margate, UK) and imported into the facility by embryo transfer. The unit has Specific Pathogen Free (SPF) status, monitored by quarterly testing of sentinels for 62 pathogens, exceeding current FELASA guidelines (33). Staff work in designated units, with showering-in, wearing of fresh autoclaved uniforms, gloves, hairnets and masks, and with a 48 h exclusion from other units. All materials are autoclaved or treated with vapourized hydrogen peroxide on import. The animal diet is sterilised to ≥25 Gy. Cages are opened in laminar flow cabinets. For infection with pathogenic *E. coli*, animals were housed in individually ventilated isocages in the Babraham Institute biosafety level 2 containment facility. Animal breeding and experiments were carried out with approval from the local Animal Welfare Ethical Review Body under the British Home Office Animal Scientific Procedures Act 1986.

Peritonitis

Pathogenic *E. coli* O18:K1 bacteria (34) were used to induce septic peritonitis as described (35). The bacteria were grown in a biosafety level 2 facility to mid-log phase in Luria broth (LB) at 37°C, 5% CO_2, pelleted, snap-frozen in PBS/20% glycerol and stored in aliquots at −80°C. Titers were determined by CFU count on blood agar plates. Prior to infection, a fresh aliquot of bacterial stock was thawed, washed in ice-cold Dulbecco's Phosphate Buffered Saline (DPBS) without Ca^{2+} and Mg^{2+} ($DPBS^{-}$, Sigma, D8537) by centrifugation at 10,000 × g for 2 min at 4°C, resuspended at 5×10^4 bacteria/ml in ice-cold $DPBS^{-}$, kept on ice and used within 1.5 h. To induce septic peritonitis, mice in a biosafety level 2 containment facility were injected *i.p.* with 200 µl of the *E. coli* suspension (1×10^4 bacteria per animal), or were mock-treated with $DPBS^{-}$, before being

returned to their home cages with food and water *ad libitum*. 3 h later, mice were euthanized by CO_2 asphyxiation, death confirmed by pithing, and peritoneal lavages performed by *i.p.* injection and aspiration of 8 mL $DPBS^{-}$, 5 mM EDTA. A second lavage was performed, pooled with the first, and samples stored on ice. An aliquot of the lavage fluid was taken for enumeration of bacteria, serially diluted in ice-cold $DPBS^{-}$, plated onto blood agar plates, cultured overnight at 37°C, 5% CO_2, and CFU counted on plates of comparable density (20-200 bacteria). The remaining lavage cells were pelleted at 450 x g for 10 min at 4°C, erythrocytes lysed by resuspending cells in 1 ml Geye's solution (130 mM NH_4Cl, 5 mM KCl, 780 µM Na_2HPO_4, 176 µM KH_2PO_4, 5.5 mM glucose, 1 mM $MgCl_2$, 280 µM $MgSO_4$, 1.54 mM $CaCl_2$, 13.4 mM $NaHCO_3$) and incubated at RT for 150 s, prior to the addition of 10 ml DPBS with Ca^{2+} and Mg^{2+} ($DPBS^{++}$, Thermo Fisher Scientific, 14040117) supplemented with 0.1% glucose and 4 mM $NaHCO_3$ ($DPBS^{++++}$). Leukocytes were centrifuged again and resuspended in 1 ml fixation buffer (Biolegend, 420801), incubated for 20 min at RT, washed again, and resuspended in 1 ml $DPBS^{++++}$. Aliquots of fixed cells were counted by hemocytometer and the rest cytospun onto glass coverslips, stained with Kwik-Diff and imaged on a Zeiss Microbeam system. Leukocytes were enumerated taking into account the lavage volume recovered.

Aseptic peritonitis experiments were done essentially as previously described (36). Mice were injected *i.p.* with 0.25 ml sterile 3% thioglycollate (TGC, Sigma, T9032) in H_2O, or were mock-treated with H_2O. 3 h later, mice were euthanized and peritoneal lavages performed and erythrocytes lysed as described above. Leukocytes were resuspended in 1.25 ml $DPBS^{++++}$. 1 ml of the sample was processed for flow cytometry by staining leukocytes with AF647-Cd11b (clone M1/70, BD Pharmingen, 557686, 1:800) and FITC-Gr1 (clone RB6-8C5, BD Pharmingen, 553126, 1:800) antibodies in $DPBS^{++++}$ with Fc block for 20 min on ice in the dark, washing in $DPBS^{++++}$, 5 mM EDTA and resuspension in 500 µl $DPBS^{++++}$ containing 1 µg/ml DAPI and 1.25 × 10^5 Spherotech ACBP-50-10 standard beads/ml (5.0-5.9 µm). Flow cytometry was carried out in a BD Biosciences LSRII flow cytometer, and FlowJo was used for data analysis. Neutrophils were identified by $Cd11b^{hi}$, $Gr1^{hi}$ staining and enumerated by taking into account the lavage volume recovered. The remaining lavage leukocytes were counted by hemocytometer and analyzed by Kwik-Diff staining of cytospins as an alternative method of identification. Both methods of quantification gave essentially the same results.

To induce peritonitis with LPS, mice were challenged *i.p.* with 250 ng LPS (Sigma) in 250 µl sterile saline, or were mock-treated with saline, and euthanized by CO_2 asphyxiation after 3 h. Peritoneal lavages were performed and lavage leukocytes analyzed by flow cytometry and Kwik-Diff staining of cytospins as described above.

Neutrophil purification

Mature primary neutrophils were freshly isolated each day by $Percoll^{PLUS}$ gradient at 4°C from mouse bone marrow using endotoxin-free reagents throughout, essentially as previously described (35). Mouse bone-marrow was flushed from femurs, tibias and pelvic bones with ice-cold Hank's Balanced Salt Solution without Ca^{2+} or Mg^{2+} ($HBSS^{-}$, Sigma H6648) supplemented with 15 mM HEPES, pH 7.4 (RT) (Sigma, H3784) and 0.25% fatty acid-free (FAF) BSA (Sigma, A8806) ($HBSS^{-++}$), triturated and filtered through a 40 µm cell strainer. 58% isotonic $Percoll^{PLUS}$ (GE Healthcare, 17544501) in $HBSS^{-++}$ was underlayed and samples spun at 1620 × g without brake for 30 min at 4°C. For mass spectrometric analysis of the neutrophil proteome, this gradient step was repeated once, by collecting the lower 5 ml and subjecting it to another $Percoll^{PLUS}$ gradient. After gradient centrifugation, the lower 5 ml were resuspended in 40 ml $HBSS^{-++}$ and centrifuged at 326 × g for 10 min at 4°C. Erythrocytes were lysed in Geye's solution for 3 min at RT. 10 volumes of ice-cold $HBSS^{-++}$ were added and cells sedimented again. Neutrophils were resuspended in ice-cold $DPBS^{++++}$ and kept on ice while aliquots were counted by hemocytometer and purity assessed by Kwik-Diff of cytospins. Preparations were >90% pure, except for mass spectrometric analysis where purity was 95-98% due to the use of a second density gradient. Neutrophils were sedimented again and resuspended in the buffer appropriate for the subsequent assay.

Killing of bacteria *in vitro*

The ability of isolated neutrophils to kill *E. coli* was measured essentially as described (35). *E. coli* DH5α bacteria (New England Biolabs, 2527) were grown in LB to logarithmic phase on the day of the experiment. Bacteria were enumerated by OD_{600}, sedimented, resuspended in ice-cold $DPBS^{++++}$ at 2.5 x 10^9/ml, opsonized with 50% mouse serum for 15 min at 37°C, washed in ice-cold $DPBS^{++++}$, resuspended in $DPBS^{++++}$ at 2.5 x 10^8/ml and kept on ice. Purified neutrophils were resuspended in $DPBS^{++++}$ at 2.5 x 10^7/ml and kept on ice. Neutrophils were then either primed with 1 µg/ml LPS for 90 min at 37°C, or kept on ice for 45 min and then primed with 20 ng/ml TNFα and 50 ng/ml GM-CSF for 45 min at 37°C, or were heat-killed at 55°C for 45 min as a negative control. Opsonized bacteria and heat-killed neutrophils were prewarmed to 37°C for 3 min prior to the assay. One volume of opsonized bacteria was added to 4 volumes of primed or dead neutrophils at a ratio of 2.5 bacteria per neutrophil, and samples were incubated at 37°C. Aliquots were removed after 30 and 120 min, diluted 1:20 in ice-cold LB, 0.05% saponin, and incubated on ice for 10 min with frequent vortexing. Serial dilutions were made in LB, and samples were plated onto LB agar and incubated overnight at 37°C. Bacterial

CFU in samples with live neutrophils were expressed as % of samples with heat-killed neutrophils.

ROS

ROS production was measured by luminol chemiluminescence assay in a Berthold MicroLumat Plus luminometer (Berthold Technologies), essentially as previously described (37). Purified bone-marrow derived neutrophils were resuspended at 5 × 10^6 cells/ml in ice-cold $DPBS^{++++}$ and primed with 5 ng/ml TNFα, 100 ng/ml GM-CSF, or with TNFα or GM-CSF alone where indicated, for 45 min at 37°C, or with 1 µg/ml LPS (E. coli LPS, Sigma, L3024) for 90 min at 37°C, with occasional flicking to prevent settling, or they were mock-primed in $DPBS^{++++}$ under the same conditions. Unprimed neutrophils were kept on ice and prewarmed to 37°C for 3 min prior to the assay. Stimuli (fMLP, C5a, PMA) were prepared as 2.5x stocks in $DPBS^{++++}$. Prior to the assay, an equal volume of prewarmed Detect buffer ($DPBS^{++++}$ containing 16 units/ml horseradish peroxidase (HRP, Sigma, P8375) and 120 µM luminol (Sigma-Aldrich, 123072)) was added to the prewarmed (primed, mock-primed or unprimed) neutrophils. The neutrophils/Detect mix was incubated for 3 min at 37°C, before 150 µl/well were dispensed into a prewarmed 96-well luminometer plate. 100 µl of prewarmed 2.5x stimulus in $DPBS^{++++}$, or $DPBS^{++++}$ control, was added either by automatic injection port (fMLP, C5a) or manually (PMA), and real-time ROS production was recorded at 37°C. Final assay concentrations were 1.5×10^6 neutrophils/ml and 3 µM fMLP, 25 nM C5a, or 500 nM PMA. ROS production was quantified by integrating the area under the curve (AUC) of the ROS response over 2 min for fMLP and C5a, or over 10 min for PMA.

Phagocytosis

Phagocytosis of *E. coli* was measured as follows. *E. coli* DH5α were grown in LB to logarithmic phase on the day of the experiment, enumerated by OD_{600}, sedimented, resuspended in ice-cold $DPBS^{++++}$ at 2.5 x 10^9/ml, and opsonized with IgG opsonising reagent (Molecular Probes, E2870) according to manufacturer's instructions. Purified bone marrow-derived neutrophils were resuspended at 1x10^7 cells/ml in $DPBS^{++++}$ and primed with 1 µg/ml LPS, or mock-primed with $DPBS^{++++}$, for 90 min at 37°C. 100 µl of neutrophils were allowed to adhere to glass coverslips in a 24-well plate for 15 min at 37°C, 5% CO_2. 100 µl of opsonised *E. coli* were added at a ratio of 25 bacteria per neutrophil, and samples were incubated for a further 120 min. Samples were fixed in 4% paraformaldehyde, PBS for 15 min at RT, washed twice in PBS, permeabilized in 0.1% Triton X-100/PBS for 10 min at RT and washed twice in PBS. Samples were stained with anti-rabbit IgG AF568 (Thermo Fisher Scientific, A11036, 1:400), FITC-Gr1 antibody (Thermo Fisher Scientific, RM3001, 1:500) and Hoechst 33342 DNA dye (Thermo Fisher Scientific 62294, 1:400), in PBS containing Fc block (1:100), for 40 min at RT, followed by three washes in PBS. Samples were mounted in ProLong Gold Antifade mountant (Life Technologies), imaged using a Zeiss Axio Imager D2 widefield system, and images were analyzed using ImageJ.

Phagocytosis of zymosan yeast particles was assayed essentially as described (35). Zymosan A particles (Molecular Probes, Z2894) were opsonised using IgG opsonising reagent (Molecular Probes, Z2850) according to the manufacturer's instructions and stored in $HBSS^{++++}$ at 4°C. Purified bone marrow-derived neutrophils were resuspended at 1 x10^7 cells/ml in $DPBS^{++++}$ and primed with 1 µg/ml LPS or mock-primed with $DPBS^{++++}$ for 90 min at 37°C. 100 µl neutrophils were then allowed to adhere to glass coverslips in a 24-well plate for 15 min at 37°C, 5% CO_2 before 100 µl opsonised zymosan particles were added at a ratio of 5 particles per neutrophil and samples incubated for a further 30 min at 37°C, 5% CO_2. Samples were fixed, permeabilized, stained, imaged, and images analyzed as described here above.

Degranulation

Degranulation of myeloperoxidase (MPO) from azurophil granules in response to stimulation with *E. coli* was measured as follows. *E. coli* DH5α were grown in LB to logarithmic phase on the day of the experiment, enumerated by OD_{600}, sedimented, and resuspended in ice-cold $DPBS^{++++}$ at 2.5 x 10^9/ml. Purified bone marrow-derived neutrophils were resuspended at 1.82 × 10^7/ml in $DPBS^{++++}$, and 1 x 10^6 cells were stimulated with *E. coli* (at a ratio of 12.5 bacteria per neutrophil), or were mock-stimulated with $DBPS^{++++}$. Either immediately (0' control), or after 3 h, the cells were pelleted at 326 × g for 10 min at 4°C, and the supernatant was removed and centrifuged at 10,000 × g for 1 min. Cell pellets were washed in $DPBS^{++++}$. The cleared supernatant and washed cell pellets were boiled in SDS-PAGE sample buffer for 5 min, and samples were analyzed by SDS-PAGE and western blotting with MPO antibody (R&D Systems, AF3667, 1:3000), followed by ImageJ analysis. The percentage of secreted MPO was calculated as % of the total MPO in the 0' cell pellet.

Gelatinase (MMP9) degranulation was measured by in-gel zymography essentially as described (38). Purified bone marrow-derived neutrophils were resuspended at 5 × 10^6/ml in $DPBS^{+++}$ and primed with 1 µg/ml LPS for 90 min at 37°C, or were mock-primed in $DPBS^{++++}$, or were kept unprimed on ice. Neutrophils (80 µl/well) were pipetted into a 96-well plate (Nunc; pre-blocked with 10% heat-inactivated fetal bovine serum, FBS) containing 20 µl 5x fMLP and cytochalasin B in $DPBS^{++++}$, or $DPBS^{++++}$ alone. Final concentrations were up to 1 µM fMLP and 10 µM cytochalasin B. Cells were incubated for 30 min at 37°C in 5% CO_2, and then centrifuged at 300 × g for 10 min at 4°C. 40 µl of the conditioned supernatant was mixed

with 20 µl 3x non-reducing SDS-PAGE sample buffer (160 mM Tris, pH 6.8, 8% SDS, 50% glycerol, bromophenol blue) at RT. 10 µl aliquots were separated by SDS-PAGE gel containing 0.067% gelatine B. Gels were equilibrated in 2.5% Triton X-100 for 30 min and in developing buffer (50 mM Tris, pH 7.5, 200 mM NaCl, 5 mM $CaCl_2$, 0.02% Triton X-100) overnight at RT, allowing the gelatinase to digest the gelatine in the gel. Gels were coomassie-stained and gelatinase activity analyzed by densitometry using ImageJ software.

Release of NETs

Release of NETs in response to stimulation with *E. coli* was measured exactly as described above for the degranulation of MPO (same samples used for both assays), except that samples were western blotted for citrullinated histone H3 (CitH3 antibody, Abcam ab5103, 1:4000). In addition, DNA in the cell pellets and supernatant was quantified by spectrometry.

NET production in response to stimulation with *Staphylococcus aureus* (*S. aureus, Wood 46*) was done essentially as described (35). *S. aureus* were subcultured in LB to logarithmic growth at 37°C, sedimented for 2 min at 12,000 x g, washed in Dulbecco's Modified Eagle Medium with Ca^{2+}, Mg^{2+} and 4.5 g/l glucose ($DMEM^{+++}$, Thermo Fisher Scientific, 31053) supplemented with 10 mM Hepes, pH 7.4 ($DMEM^{++}$/Hepes), and opsonized with 10% mouse serum for 30 min at 37°C. *S. aureus* were washed twice in $DMEM^{+++}$/Hepes following opsonization and resuspended at $5x10^7$ bacteria/ml in $DMEM^{+++}$/Hepes. Purified bone marrow-derived neutrophils were resuspended at $4x10^5$ cells/ml in $DMEM^{+++}$/Hepes containing 10% heat-inactivated FBS and primed with 1 µg/ml LPS or mock-primed for 90 min at 37°C. 250µl of cells were then seeded into each well of an 8-well chamber slide (µ-slide 8 well, 80826, ibidi) and allowed to adhere for 30 min at 37°C, 5% CO_2. Cells were treated with opsonised *S. aureus* at a ratio of 10 bacteria per neutrophil or mocked-treated with $DMEM^{++}$/Hepes/FBS for the indicated periods of time. 15 min before the end of the incubation period, the non-cell permeable DNA dye Sytox Green (Thermo Fisher Scientific, S7020, 0.1µM) and the cell permeable DNA dye Hoechst 33342 (Thermo Fisher Scientific, 62294) were added to cells and samples were live-imaged using a Nikon Eclipse Ti-E widefield system. Images were analyzed by ImageJ software, using phase contrast and DAPI stain to determine the total cell number and Sytox Green signal to enumerate cells with NETs.

Chemotaxis

Transwell chemotaxis assays were done essentially as described (37) using 3 µM-pore polycarbonate filters (Millipore, Millicell-PC, PITP01250) in ultra-low cluster 24-well tissue culture plates (Costar, 3473). Bone marrow was flushed into HBSS with Ca^{2+} and Mg^{2+} (Sigma, H8264), supplemented with 0.25% fatty acid-free BSA, and 15 mM Hepes, pH 7.5 at 37°C, all endotoxin-free ($HBSS^{++++}$), triturated, filtered through a 40 µm nylon cell strainer, counted by hemocytometer and adjusted to 5 x 10^6/ml. Cells were primed with 1 µg/ml LPS for 90 min, or with 20 ng/ml murine TNFα and 50 ng/ml GM-CSF for 45 min, or were mock-primed in $HBSS^{++++}$ for the same periods of time at 37°C. Cells were pipetted into transwell filters (400 µl/filter) in a 24-well plate containing $HBSS^{++++}$ (600 µl/well) in the presence or absence of 3 nM C5a or 1 µM fMLP, and were incubated for 40 min at 37°C. Cells remaining in the transwell were removed and replaced with 400 µl ice-cold $HBSS^{-++}$ containing 3 mM EDTA. 60 µl $HBSS^{-++}$ containing 30 mM EDTA was added to the bottom well and plates were incubated on iced metal trays for 15 min to detach cells. Transmigrated cells were collected from the bottom well, and in parallel to control cells that had not undergone chemotaxis, were centrifuged at 10,000 xg for 30 s and resuspended in ice-cold $HBSS^{-++}$. Cells were stained with FITC-Gr1 (clone RB6-8C5, BD Pharmingen, 553126, 1:800) and AF647-Cd11b (clone M1/70, BD Pharmingen, 557686, 1:800) antibodies in $HBSS^{-++}$ containing 1% Fc block and were analyzed using an LSR2 flow cytometer alongside Spherotech ACBP-50-10 standard beads. Neutrophils were identified by their $Gr1^{hi}/Cd11b^{hi}$ staining. Transmigrated neutrophils were compared to total neutrophils in control samples.

For Ibidi chamber chemotaxis assays, 6-channel ibidi slides (µ-slide VI 0.4, ibidi 80601) were coated with 20 µg/ml fibronectin-like poly-Arg-Gly-Asp peptide (pRGD, Sigma, F5022) or with 1 mg/ml fibrinogen in $DPBS^-$ for 1 h at RT and washed 3 times in $HBSS^{++++}$, and the wells and central chamber were filled with $HBSS^{++++}$. Isolated neutrophils were resuspended at 2 x 10^7/ml in HBSS $^{-++}$ and kept on ice until use. Cells were primed by adding 5 µl to 90 µl of $HBSS^{++++}$ supplemented with 1g/l glucose and containing 20 ng/ml TNF-alpha and 50 ng/ml GMCSF for 45 min at 37°C, or were mock-primed. Buffer was removed from both wells of the ibidi slide before adding the cells, leaving the central chamber full. 45 µl of primed or mock-primed cells were added into one well and 45 µl of liquid removed from the other to draw the cells through into the central chamber. The slide was inserted into the microscope housing, and cells were allowed to adhere for 20 min at 37°C. 5 µl of $HBSS^{-++}$ containing 10 µM fMLP, or other concentrations where indicated, and 5 x 10^6 carboxyl polystyrene beads (Bangs Laboratories, PC06N, 6.9 µm) was then added to one well and 5 µl of buffer removed from the other to create an fMLP gradient, or $HBSS^{-++}$ alone was used for mock-stimulation. The beads were used to locate the steepest part of the gradient where imaging was done. Neutrophils were live-imaged for 20 min every 10 s in a prewarmed Olympus

CellR microscope using the 20x objective. Cells were tracked manually using the chemotaxis and migration plugin of ImageJ software to quantify various parameters of cell speed and directionality as indicated. Responders were defined as cells that migrated at least their own cell-length over the 20 min observation period.

Cell surface receptor levels

Bone marrow cells were flushed with ice-cold $HBSS^{-++}$, filtered through 40 µm cell strainers, counted, pelleted at 326 × g for 10 min at 4°C, and resuspended in ice-cold $DPBS^{++++}$ at 4 × 10^7 cells/ml. 125 µl of cells were either kept on ice, or were primed with 20 ng/ml TNFα and 50 ng/ml GM-CSF, or with 1 µg/ml LPS, for 45 min at 37°C. Cells were sedimented at 10,000 × g for 30 s at 4°C, resuspended in Fc block (BD Biosciences, clone 2.4G2, 1:1000; for Mac1 and L-selectin) or in $DPBS^{++++}$ (for FcγRIII), and incubated on ice for 15 min. Cells were sedimented at 10,000 × g for 30 s, resuspended in ice-cold $DPBS^{++++}$ containing fixable viability dye (eBioscience, eFluor™ 780, 1:1000), antibodies for neutrophil markers Ly6G (Ly6G-BV510, BioLegend, clone 1A8, 1:500) and Mac1 (CD11b-AF647, BD Bioscience Clone M1/70, 1:1000), and PE-labelled antibodies for FcγRIII (CD16, BioLegend, clone S17014E, 1:100) or L-selectin (BD Biosciences clone MEL-14, 1:100), and were incubated on ice for 30 min. Cells were washed in ice-cold $HBSS^{-++}$, 1 mM EDTA, resuspended in 300 µl ice-cold $HBSS^{-++}$, 1 mM EDTA, and kept on ice. Flow cytometry was performed using a BioRad ZE5 flow cytometer, recording 20,000 neutrophils per sample. Neutrophils were identified by $Ly6G^{hi}$, $CD11b^{hi}$ staining, and the mean fluorescence intensity (mfi) of receptor levels on the neutrophil surface was quantitated using FlowJo.

Neutrophil proteomics

Neutrophils were isolated to 95-98% purity as described above with two consecutive $Percoll^{PLUS}$ gradients from the pelvic bone-marrow of 8 young (8 weeks) and 8 old (24 months) mice, in 4 independent experiments with 2 young and 2 old mice per experiment. Separately for each mouse, cells were resuspended at 2 x 10^7/ml in $DPBS^{++++}$, treated with the cell-permeable serine protease inhibitor diisopropyl-fluorophosphate (DFP, 7 mM, Sigma, D0879) for 10 min at RT, washed twice in $DPBS^{++++}$, sedimented for 30 s at 10,000 x g, and the cell pellets snap-frozen in liquid nitrogen and stored at -80°C prior to further processing. Proteins were solubilized and reduced in 6 M guanidine-HCl, 100 mM Tris, 10 mM DTT for 1 h at 50°C, then cooled and alkylated with 50 mM iodo-acetamide for 30 min in the dark. The alkylated proteins were precipitated with 4 volumes of acetone for 16 h at -20°C, then solubilized in 100 mM triethyl-ammonium bicarbonate, 6 M guanidine hydrochloride, and sequentially digested with Lys-C and trypsin (Promega) for 16 h at 30°C. The resulting peptides were labelled with tandem mass-tags using two sets of 8-plex reagents (Thermo Scientific). The two combined sets of 8 samples were each separated into 60 fractions by high-pH reverse phase HPLC. The major peptide-containing fractions were analyzed by LC-MS on an Orbitrap Fusion Lumos mass spectrometer, using an SPS-MS3 scan sequence. Proteins were identified from the mass spectrometry data by searching the Uniprot mouse proteome database using Mascott software (Matrix Science), and relative abundances of the identified proteins were determined using Proteome Discoverer software (Thermo Scientific). This identified 8001 proteins in total. Non-mouse derived proteins (e.g. human keratins, bovine serum albumin) were removed from the list, which left 7945. Only proteins detected in at least 4 old and 4 young mice were analyzed further, which left 7338. Statistical analysis of the relative protein abundances was done using R software to calculate differences between young and old by two-sided t-tests on log-transformed data, with Benjamini-Hochberg false-discovery rate correction for multiple comparisons of all 7338 quantified proteins. Proteins were assigned to one or more categories of protein class or signaling pathway using a combination of PANTHER pathway analysis (www.pantherdb.org) and manual curation.

LPS/TLR4 pathway activity

Purified bone marrow-derived neutrophils were resuspended at 1x10^7 cells/ml in $DPBS^{++++}$, primed with 1 µg/ml LPS or mock-primed with $DPBS^{++++}$ for 90 min at 37°C, and stimulated with pre-warmed fMLP (1 µM final) for one min. The reaction was stopped by addition of excess ice-cold PBS, followed by centrifugation at 12,000 x g for 10 s at 4°C. The cell pellet was lysed in lysis buffer (20 mM Tris [pH 7.5, 4°C], 150 mM NaCl, 1 mM EDTA, 1 mM EGTA, 1% Triton X100, 2.5 mM Na pyrophosphate, 1 mM β-glycerol-phosphate, 1 mM Na orthovanadate, 4 mM DTT, 0.1 mM PMSF, and 10 µg/ml of each aprotinin, pepstatin, antipain and leupeptin) for 10 min on ice with frequent vortexing. Debris was sedimented at 12,000 x g for 10 min at 4°C, and the lysates were boiled in SDS-PAGE sample buffer and subjected to SDS-PAGE and western blotting using antibodies for phosphorylated p38 Mapk, p42/44 Erk and Akt. Blots were stripped and reprobed with antibodies for total p38 Mapk, p42/44 Erk and Akt. Antibodies are listed in Materials. Blots were quantitated by ImageJ densitometry, and phospho-protein signals normalized to total-protein for each sample.

Western blots

To evaluate protein expression in neutrophils, total lysates were prepared from mature neutrophils isolated from bone marrow as described above, were treated with 7 mM DFP for 10 min at RT, and washed in $DPBS^{++++}$. Cells were sedimented or 30 s at 10.000 xg, resuspended in boiling 1.3 x SDS-PAGE sample buffer, and boiled for 5 min with repeated trituration through a 25 x G needle. Proteins were separated by SDS-PAGE, transferred onto PVDF, blocked and probed with the appropriate antibodies, and detected using ECL or ECL Prime (GE Healthcare). Where required, membranes were stripped in 25 mM glycine, pH 2.0, 1% SDS for 5 min at RT and reprobed with different antibodies. Protein loading was assessed by coommassie staining. Densitometric analysis of western blots was done manually using the wand tool of ImageJ software, essentially as described in 'www.sybil-fp7.eu/node/95', except that bands of interest were delineated on the ImageJ plots using two vertical lines through the whole gel, and background was subtracted from the equivalent areas of an empty lane, to avoid bias.

Rac activity

Rac activity was assessed by Pak-CRIB pull down, essentially as described (18). GST-Pak-CRIB bait was purified from bacterial culture as described (39) and stored in GST-FISH buffer (10% glycerol, 50 mM Tris pH 7.4, 100 mM NaCl, 1% NP-40, 2 mM $MgCl_2$, 2 mM DTT, 100 µM PMSF, and 10 µg/ml each of leupeptin, pepstatin A, aprotinin and antipain) at 4°C for up to one week. Purified bone marrow-derived neutrophils were resuspended at 1×10^7/ml in $DPBS^{++++}$ and pre-warmed for 3 min at 37°C. 200 µl aliquots were stimulated with 10 x fMLP (Sigma, F3506) at the indicated concentrations in $DPBS^{++++}$ for 10 s, or were mock-stimulated. The reaction was stopped by the addition of 1 ml of ice-cold GST-FISH buffer containing 1.2% NP-40 (to give a final concentration of 1% NP-40), and cells were lysed by incubation on ice for 2 min with frequent vortexing. Samples were centrifuged at 12,000 x g for 3 min at 2°C to sediment debris, the supernatant transferred into fresh precooled tubes, and 2% kept as a total lysate control. The remaining sample was incubated with GST-Pak-CRIB beads by end-over-end rotation for 15 min on ice. Samples were washed 5 times in GST-FISH buffer before adding boiling 1.3x SDS-PAGE sample buffer and boiling the samples for 5 min. To process total lysate samples, boiling 4x SDS-PAGE sample buffer was added to final 1.3x, and samples boiled for 5 min. GTP-Rac and total Rac were quantified by western blotting with Rac1 and Rac2 antibodies and densitometry using ImageJ.

PIP_3 and PIP_2 measurements

PIP_3 production by class I PI3K, and the amount of PIP_2 in the cell, were measured directly by lipid mass spectrometry (40). Isolated bone-marrow derived neutrophils were resuspended in $DPBS^{++++}$ at 7.4 x 10^6 per ml and primed with 1 µg/ml LPS for 90 min, or with 20 ng/ml murine TNFα and 50 ng/ml GM-CSF for 45 min, or mock-primed for the same periods of time in $DPBS^{++++}$ at 37°C. 1 x 10^6 cells were then stimulated for 10 s with 3 µM fMLP or 25 nM C5a, or were mock-stimulated in $DPBS^{++++}$. The reaction was stopped by the addition of 750 µl $CHCl_3$:MeOH (1:2). Synthetic deuterated stearoyl/arachidonoyl PIP_3 (10 ng) and $PI(4,5)P_2$ (100 ng) were added to each sample as internal standards. Lipids were extracted as previously described (41) and analyzed by high performance liquid chromatography-mass spectrometry (HPLC-MS) (40). The stearoyl/arachidonoyl species of PIP_2 and PIP_3 were quantitated, as they are the most abundant species of these lipids in neutrophils (40). For quantification, the area of the PIP_2 and PIP_3 peaks was integrated and compared to the relevant internal standard.

Data collection and statistical analysis

Sample size was determined using power calculations to yield 80% power, based on results of pilot experiments and on previously published data as referenced. Experiments were performed at least three times except where indicated. Sample size and numbers of independent experiments are detailed in Figure Legends. Within the parameters of group size and age, mice were selected for cohorts at random by the staff of the Small Animal Unit. Image analysis was performed in a blinded manner. Excel 2016 and GraphPad Prism 8.0 were used for tabulation, statistical analysis and plotting graphs, except for proteome analysis where R software was used. Data were tested for normality of distribution using Shapiro-Wilk test to determine if parametric or non-parametric statistical analysis was required. Where warranted by variance between groups, data were log-transformed prior to statistical analysis. Statistical outliers were identified using Tukey's test and removed from datasets. Other samples were only excluded when there was a known technical problem affecting the analysis. For the analysis of proteomics data, comparisons between the age groups were made by two-tailed unpaired Student's t-test. For all other data, two-way or three-way ANOVA was used to test for effects of interventions. Group sizes (n) are listed in figure legends. Effect size and variance are reported as group mean ± standard error. P-values reported for proteomics data are from t-tests with Benjamini-Hochberg false discovery rate correction for multiple comparisons, p-values reported for other data are

from multiplicity-adjusted Sidak's *post-hoc* comparisons. The threshold for statistical significance was set at $p<0.05$.

Results

Old mice have impaired immunity against *E. coli* infection and altered neutrophil recruitment during septic peritonitis

In humans, the incidence of bacterial peritonitis increases with age, associated with high mortality rates from sepsis (4). To investigate if antibacterial immunity wanes similarly in aging mice, we compared young (8-10 week-old) and old (24 months-old) mice. These mouse ages are equivalent to the human ages of 20 and 80 years, respectively (42). We tested the ability of the mice to clear pathogenic *E. coli* strain O18:K1 in an acute model of septic peritonitis. This model tests the early innate response (after 3 h) to an infection that would prove fatal to 75% of the mice within 36 h if left to progress (34). At the acute stage tested here, only neutrophils are recruited, to combat the infection together with resident peritoneal macrophages (35). Old mice showed a 4.6-fold reduction in their ability to clear the infection, despite constitutively having 6-fold more peritoneal leukocytes than young mice and double the leukocyte recruitment in response to the infection (Figure 1A). Hence, as for elderly humans, the innate immunity of mice to septic peritonitis decreases with age. This result reinforces previous reports showing reduced innate immunity of old mice to other types of bacterial and fungal infections (15–17).

To investigate neutrophil recruitment, we compared two peritonitis models, thioglycollate (TGC)-induced aseptic peritonitis and septic LPS-induced peritonitis. The latter recapitulates in part the *E.coli* infection, as LPS is the main endotoxin derived from gram-negative bacteria like *E.coli*, driving the inflammation that leads to sepsis. Neutrophil recruitment into the peritoneum was normal during aseptic peritonitis (Figure 1B) but increased in response to LPS (Figure 1C). Furthermore, peritoneal macrophage numbers were constitutively elevated in old mice, accounting for the high number of total peritoneal leukocytes (Figures 1B, C). Altogether, defective neutrophil recruitment and peritoneal macrophage numbers do not seem to underlie the impaired antibacterial immunity of old mice, suggesting functional defects in one or more of these cell lineages.

We tested the effector responses of isolated neutrophils from young and old mice. We chose to purify mature neutrophils from the bone-marrow, where a pool of mature cells is always stored for rapid release into the circulation in case of inflammation or infection. We reasoned that using these cells instead of peripheral neutrophils would minimize confounding effects from the neutrophil aging which occurs in the circulation.

Killing of *E. coli* is impaired in neutrophils from old mice

Following from the *in vivo* infection experiments, we tested the capacity isolated neutrophils from young and old mice to kill *E.coli*. We primed neutrophils before the assay, either with LPS or with GM-CSF and TNFα, in order to mimic inflammatory conditions. Priming sensitizes neutrophils to mount larger effector responses in response to stimuli, and is based on receptors stored on granules being upregulated to the neutrophil surface (43). Neutrophils from old mice had a reduced ability to kill bacteria, regardless of whether they were primed with LPS or with GM-CSF and TNFα. However, the defect in GM-CSF/TNFα-primed cells was overcome by prolonged incubation of neutrophils with the bacteria, whereas the defect in LPS-primed cells persisted (Figure 1D). Overall, the impaired clearance of *E.coli* infections *in vivo* in old age may stem from an age-dependent loss of killing capacity in neutrophils.

LPS-primed ROS production is impaired in neutrophils from old mice

ROS production is an important effector response in neutrophil-mediated immunity, so we tested the ability of isolated neutrophils from young and old mice to produce ROS. We primed neutrophils with LPS or with GM-CSF and TNFα, and stimulated them with the GPCR ligands and chemoattractants C5a, a component of the complement cascade, or fMLP, a peptide derived from bacterial proteins. Priming alone did not elicit ROS production, and in the absence of priming, C5a and fMLP induced only limited responses, as expected (Figures 2A-C). These data show that bone-marrow derived mature neutrophils from old mice are not pre-activated through effects of 'inflamm-aging'. In mock-primed cells, C5a-stimulated ROS was lower in old age than young, whereas fMLP-stimulated ROS was not, showing an impairment dependent on the GPCR pathway (Figures 2A-C). Pilot experiments using priming with GM-CSF and TNFα separately or combined showed additive effects on fMLP-stimulated ROS production (Supplemental Figure 1). Hence, we decided to combine GM-CSF/TNFα throughout the study and juxtapose them to LPS. LPS or GM-CSF/TNFα effectively primed the C5a- and fMLP-stimulated ROS production in young age, as expected ($p<0.0001$ in A and C, $p=0.0002$ in B). In old age, the LPS-primed response was reduced (Figures 2A, B), whereas the GM-CSF/TNFα-primed response was not (Figure 2C). Therefore, there is an age-related decline in GPCR-dependent ROS production, with a degree of selectivity for the LPS-primed response over GM-CSF/TNFα. We also tested receptor-independent ROS production by activating the NADPH oxidase with PMA. PMA-stimulated

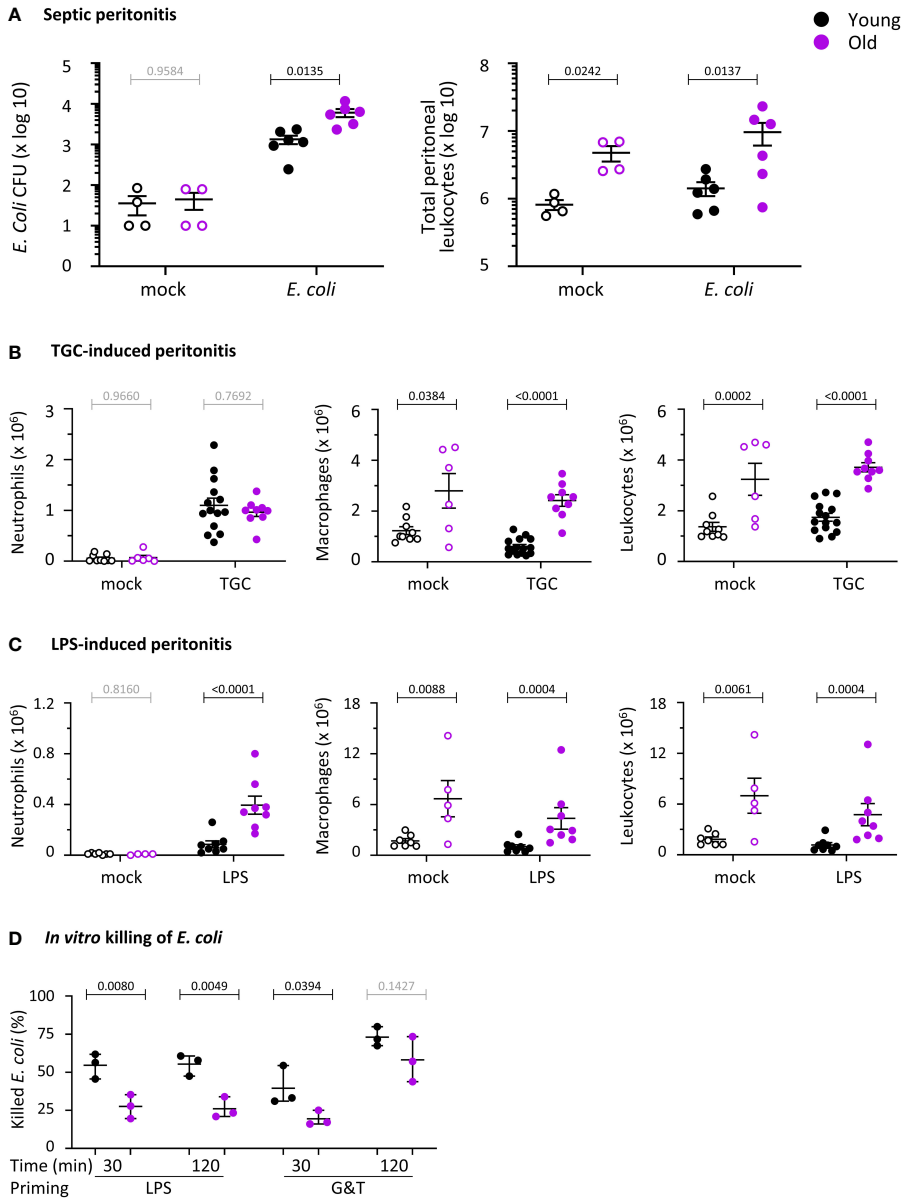

FIGURE 1
Hornigold K et al. Old mice have impaired immunity against *E. coli* infection and altered neutrophil recruitment, and the ability of their neutrophils to kill *E. coli* is reduced. **(A)** *E. coli*-induced septic peritonitis. Young (8-10 weeks, black symbols) and old (24 months, purple symbols) mice were infected *i.p.* with $1x10^4$ pathogenic *E. coli* O18:K1 (filled symbols), or were mock-infected (open symbols), and culled humanely 3 h later. Peritoneal lavages were performed and assessed for bacterial burden by bacterial culture and quantification of CFU. Lavage neutrophils and total leukocytes were quantified by microscopy. Data are mean ± SEM of mice pooled from 3 independent experiments, with 1-2 mock-infected and 1-3 infected mice/age/experiment. **(B)** Aseptic peritonitis. Young and old mice were challenged *i.p.* with 0.25 ml sterile 3% thioglycollate (TGC, filled symbols), or were mock-treated (open symbols), and culled 3 h later. Peritoneal lavages were assessed for numbers of peritoneal neutrophils, macrophages and total leukocytes by hemocytometer and microscopy of cytospins. Data are mean ± SEM, pooled from 5 independent experiments, with 1-3 mock-treated and 1-4 TGC-treated mice/age/experiment. **(C)** LPS-induced septic peritonitis. Young and old mice were challenged *i.p.* with 250 ng LPS in 0.25 ml saline (filled symbols), or were mock-treated with saline (open symbols), and culled 3 h later. Peritoneal lavages were assessed as in **(B)**. Data are mean ± SEM, pooled from 3 independent experiments, with 1-2 mock-treated and 2-3 LPS-treated mice/age/experiment; dots represent individual mice. Statistics in **(A-C)** are two-way ANOVA with Sidak's multiple comparisons test on log-transformed raw data; black p-values are significant, grey p-values non-significant. **(D)** *In vitro* killing of *E. coli*. Neutrophils purified from young (8-10 weeks, black symbols) and old (24 months, purple symbols) mice were primed with 1 µg/ml LPS or with 20 ng/ml TNFα and 50 ng/ml GM-CSF, as indicated, or were heat-killed as a negative control, and were incubated with serum-opsonised *E. coli* DH5α (ratio of 2.5 bacteria per neutrophil) at 37°C for 30 or 120 min. Bacterial killing by neutrophils was quantified by comparing CFU between samples containing live and heat-killed neutrophils. Data are mean ± SEM of 3 independent experiments; each dot represents the mean of one experiment. Statistics are three-way ANOVA with Sidak's multiple comparisons test; black p-values are significant, grey p-values non-significant.

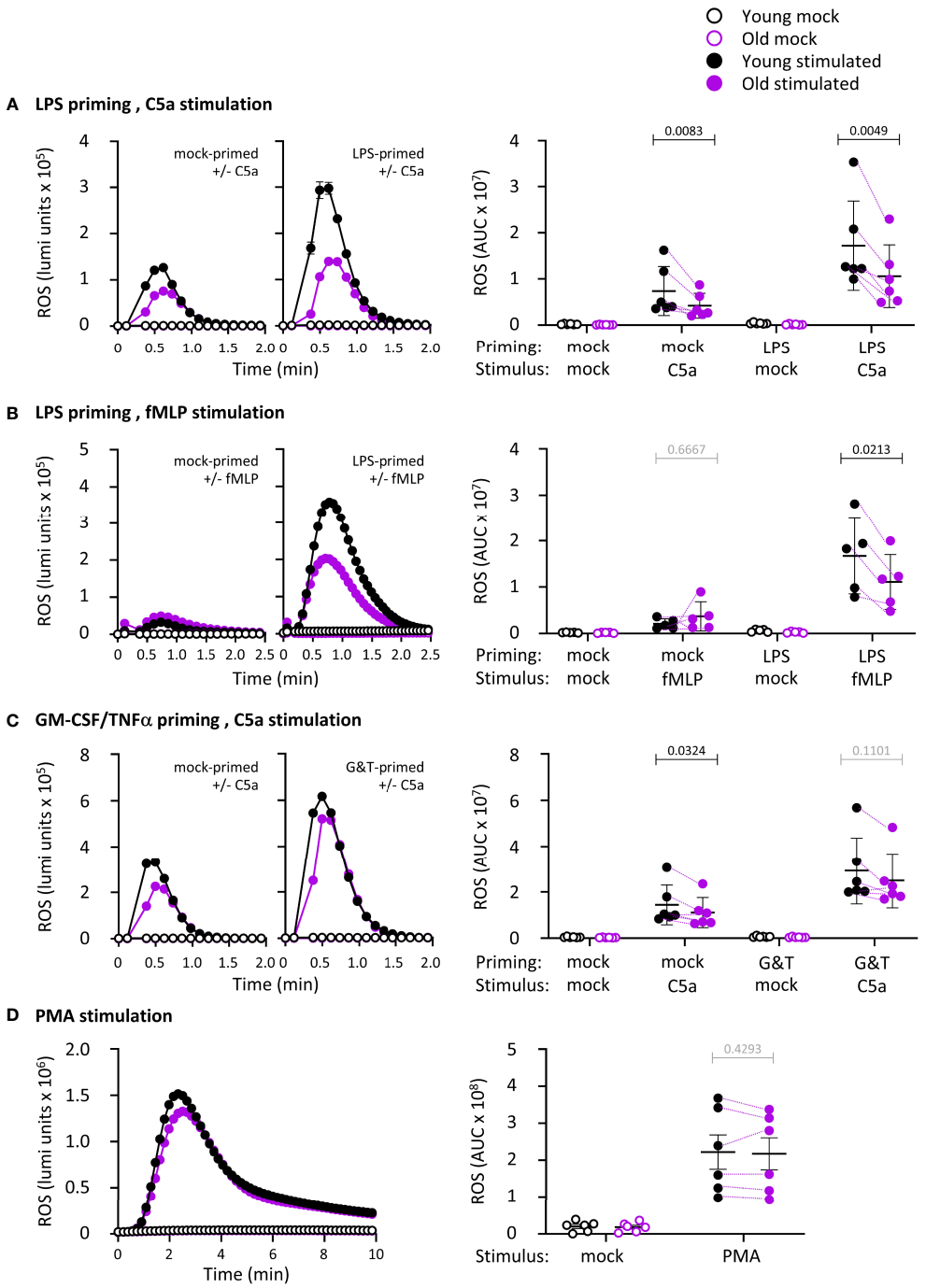

FIGURE 2
Hornigold K et al. LPS-primed ROS production is impaired in neutrophils from old mice. Isolated neutrophils from young (8-10 weeks, black symbols) and old (24 months, purple symbols) mice were primed with **(A, B)** 1 µg/ml LPS for 90 min or with **(C)** 100 ng/ml GM-CSF and 5 ng/ml TNFα for 45 min, or were mock-primed for the same periods of time, or **(D)** kept unprimed, prior to stimulation with **(A-C)** 25 nM C5a, **(B)** 3 µM fMLP or **(D)** 500 nM PMA (closed symbols), or mock-stimulation (open symbols), as indicated. ROS production was measured by real-time chemiluminescence assay with luminol and HRP for extra- and intracellular ROS. Left-hand panels show representative luminometer traces from one experiment; right-hand panels show the quantification as AUC. Data are mean ± SEM of 5-6 independent experiments, as indicated; each dot is the mean AUC from one experiment. Matched data are indicated by purple lines for stimulated cells. Statistics are two-way ANOVA with Sidak's multiple comparisons tests on log-transformed raw data, in A-C for chemoattractant-stimulated cells; black p-values are significant, grey p-values non-significant.

ROS production was equal in neutrophils from young and old mice, showing that the overall capacity of the NADPH oxidase complex is not affected by age (Figure 2D).

Phagocytosis is impaired in neutrophils from old mice, in part through effects of LPS

We tested the capacity of neutrophils from young and old mice to phagocytose either IgG-opsonized *E. coli* or IgG-opsonized zymosan yeast particles in the presence or absence of LPS priming. In the context of the *E. coli* experiments, LPS priming mimics the inflammatory conditions encountered by neutrophils prior to contact with the bacteria, and for the zymosan experiments, it mimics co-infection of fungus (yeast) and gram-negative bacteria (LPS). The overall number of *E. coli* or zymosan particles taken up by neutrophils from old mice was reduced in LPS-primed cells but not in mock-primed cells (Figures 3A, B). The number of particles inside phagocytosing neutrophils was no different between the ages or priming conditions, but the proportion of neutrophils capable of phagocytosing was diminished in old age, both in LPS- and mock-primed cells, and for both stimuli (Figures 3A, B). Hence, phagocytosis is impaired in neutrophils from old mice in a partly LPS-dependent manner.

Degranulation is impaired in neutrophils from old mice, in part through effects of LPS

We measured the ability of neutrophils from young and old mice to degranulate myeloperoxidase (MPO) from azurophil granules in response to *E. coli*, by western blotting cell pellets and cell supernatants for MPO. *E. coli* induced strong degranulation of MPO, which was higher in neutrophils from young mice than old, despite the total cellular content of MPO being the same between the ages (Figure 4A). Hence, degranulation of azurophil granules is impaired in old age.

We also measured the ability of neutrophils to degranulate gelatinase (MMP9) from gelatinase granules in response to fMLP, in the presence or absence of LPS priming, by using in-gel zymography to measure the secreted gelatinase activity (Figure 4B). Cytochalasin B, which depolymerizes the cortical actin ring of neutrophils thereby facilitating granule fusion with the plasma membrane, was used to test overall degranulation capacity. Stimulation of unprimed neutrophils with fMLP induced limited degranulation that was no different between the ages (Figure 4B). Mock-priming, which allows some vesicle trafficking, also resulted in limited degranulation, as expected (35). This was enhanced by fMLP stimulation in neutrophils from young mice but not old, showing there is a GPCR-dependent impairment (Figure 4B). LPS-priming induced robust degranulation in neutrophils from young but not old mice, showing there is also an LPS-dependent defect (Figure 4B). The LPS-primed response was not increased further by fMLP. The age-related defects in fMLP-stimulated mock-primed and LPS-primed cells were overcome by cytochalasin B treatment, demonstrating that LPS- and GPCR pathways were affected by age, rather than degranulation capacity overall. In contrast to LPS, GM-CSF/TNFα priming revealed no difference between the ages (data not shown). Hence, similar to ROS production and phagocytosis, neutrophils from old mice show both LPS-dependent and LPS-independent impairments in degranulation.

Release of NETs in response to *S. aureus* but not *E. coli* is impaired in neutrophils from old mice, independently of LPS

We measured the ability of neutrophils from young and old mice to release NETs in response to *E. coli*, using the same samples that were also tested for MPO degranulation (Figure 4A), by quantifying citrullination of histone H3 and the amount of DNA in cell pellets and cell supernatants. Unlike degranulation of MPO which was reduced in old age, extracellular release of DNA and citrullination of histone H3 were not affected by age under the same conditions (Figure 5A).

We also tested the ability of neutrophils to undergo *S. aureus*-induced NET release, in the presence or absence of LPS priming. *S. aureus* is a gram-positive bacterium, so in this context LPS priming was used to mimic co-infection with gram-negative bacteria. *S. aureus* induced robust NET formation which was stronger in neutrophils from young mice than old (Figure 5B). LPS priming alone hardly affected NET release, even when we used a species of LPS previously reported to induce NETs (data not shown) (44). LPS priming also had no major effect on *S. aureus*-induced NETs, meaning the response remained higher in cells from young than old mice (Figure 5B). Overall, neutrophils from old mice have a defect in NET release that depends on the type of bacteria but is independent of LPS. It should be noted that the defect was only observed after prolonged incubation (from 3 hours), which may explain why some previous studies failed to see the age-related impairment in NET release in mouse neutrophils.

Migration is normal in neutrophils from old mice

Our *in vivo* experiments showing altered neutrophil recruitment in old mice suggested that neutrophil migration may be affected. In addition, reduced chemotaxis of neutrophils from old mice was previously reported (15, 28). Hence, we investigated neutrophil migration. Using transwell assays, we

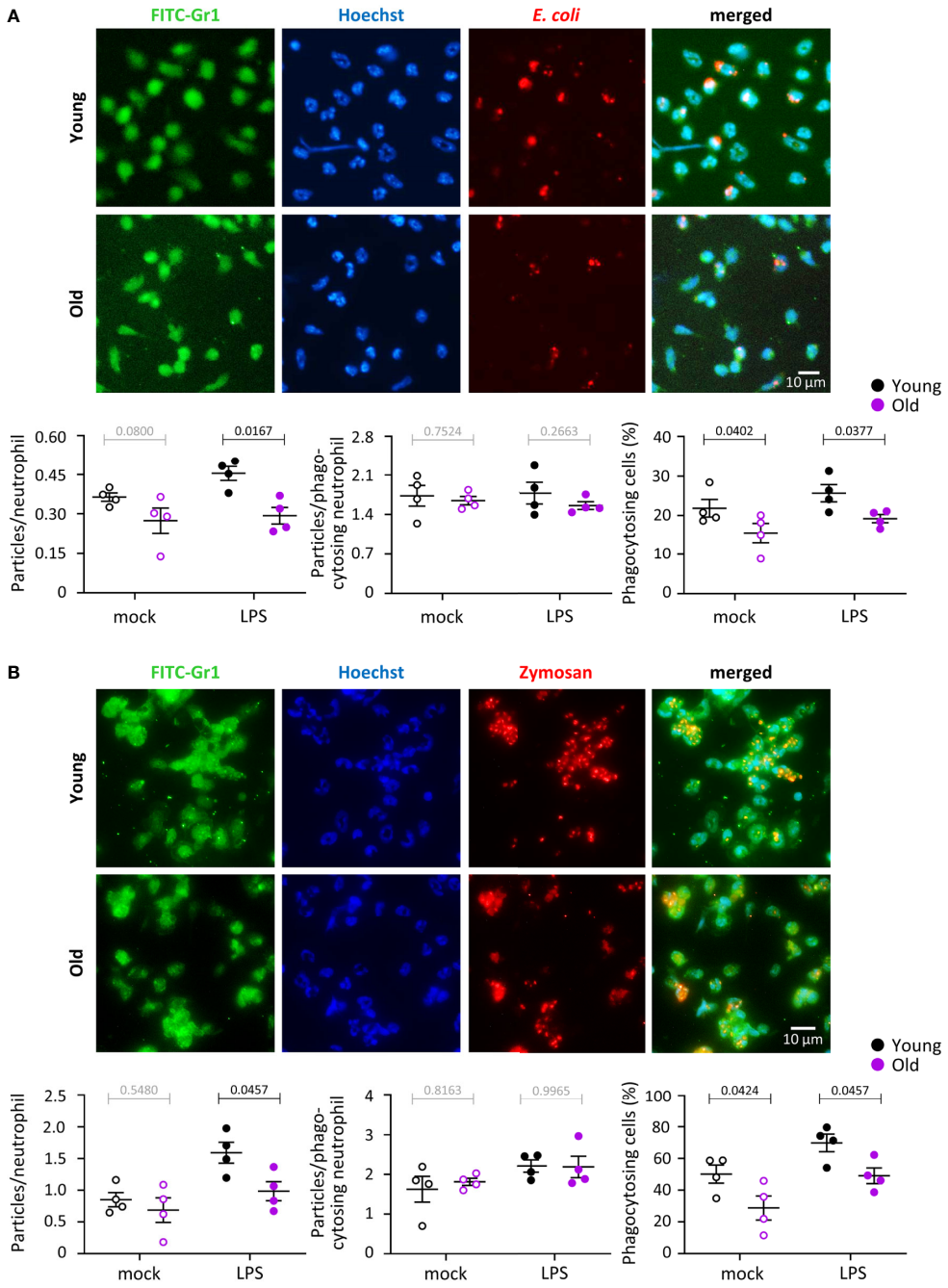

FIGURE 3
Hornigold K et al. Phagocytosis is impaired in neutrophils from old mice, in part through effects of LPS. Neutrophils from young (8-10 weeks, black symbols) and old (24 months, purple symbols) mice were primed with 1 µg/ml LPS for 90 min at 37°C (closed symbols), or were mock-primed (open symbols), and then plated onto glass coverslips for 15 min and stimulated either with IgG-opsonised *E. coli* (25 bacteria per neutrophil) for 120 min at 37°C **(A)**, or with IgG-opsonised zymosan yeast particles (5 particles per neutrophil) for 30 min at 37°C **(B)**. Cells were fixed, stained with FITC-Gr1 and AF568-IgG antibodies and Hoechst DNA dye, and assessed for the number of *E. coli* or zymosan particles within by widefield microscopy and ImageJ analysis. Representative images from one experiment are shown. Graphs in **(A)** and **(B)** show the quantification by ImageJ analysis for the number of particles per neutrophil overall (left panel), number of particles in neutrophils which had taken up at least one (middle panel), and proportion of phagocytosing neutrophils (right-hand panel). Data in **(A)** and **(B)** are mean ± SEM of 4 independent experiments; each dot represents the mean of one experiment. Statistics are two-way ANOVA with Sidak's multiple comparisons tests; black p-values are significant, grey p-values non-significant.

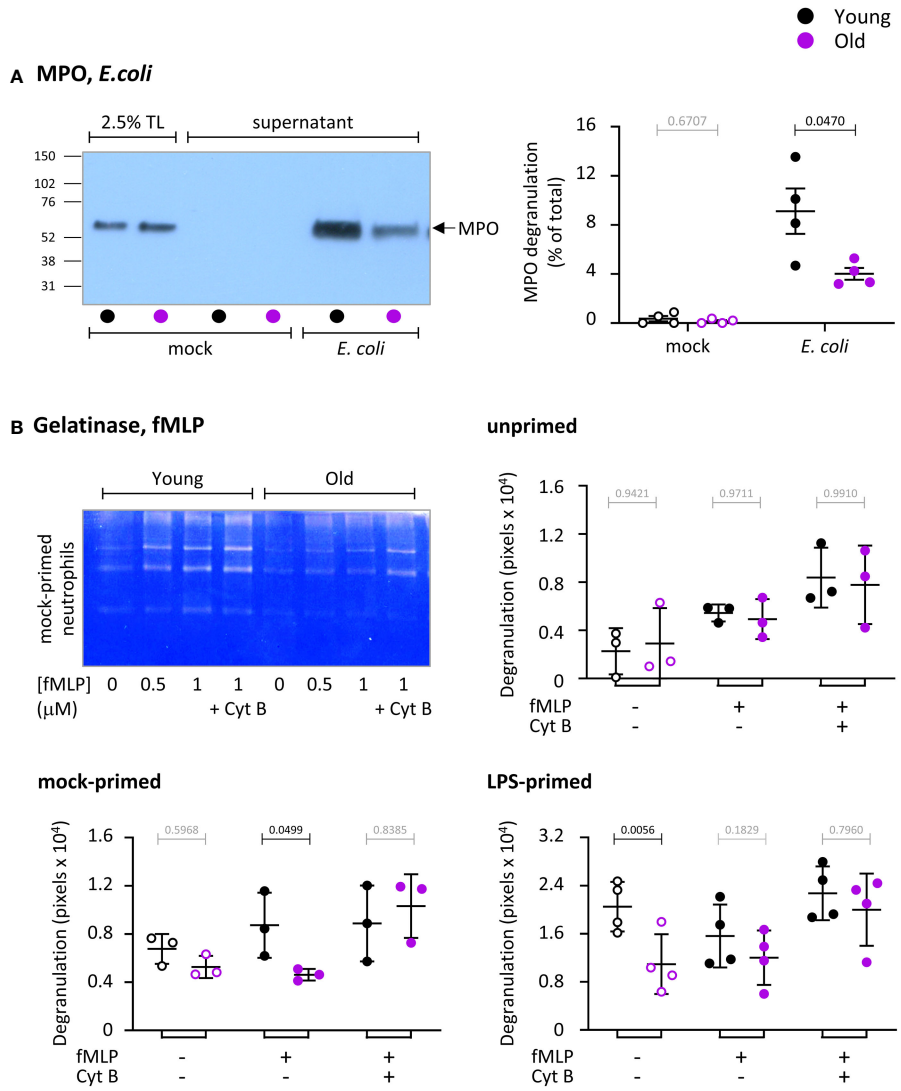

FIGURE 4
Hornigold K et al. Degranulation is impaired in neutrophils from old mice, in part through effects of LPS. **(A)** Degranulation of azurophil granules in response to *E.coli*. Neutrophils from young (8-10 weeks, black symbols) and old (24 months, purple symbols) mice were stimulated with *E. coli* (ratio of 12.5:1 bacteria/neutrophil; closed symbols), or were mock-stimulated with $DBPS^{++++}$ (open symbols), for 3 h at 37°C. Cell pellets and cell supernatants were collected and western blotted for the azurophil granule marker MPO. Degranulation was quantitated by comparing secreted MPO to total MPO in the 0' total lysate (TL) control. **(B)** Degranulation of gelatinase granules in response to fMLP. Neutrophils from young and old mice were kept unprimed on ice, or mock-primed at 37°C for 45 min, or primed with 1 µg/ml LPS for 90 min at 37°C, as indicated, and were then either mock-stimulated (open symbols), or stimulated with 1 µM fMLP, or with both 1 µM fMLP and 10 µM cytochalasin B (closed symbols) for 30 min at 37°C. Gelatinase activity released into the medium was analyzed by in-gel zymography. The representative coomassie-stained gel of mock-primed cells from one experiment shows the digestion of the gel by gelatinase as white areas. Quantification of gels was done by ImageJ densitometry. Data in **(A)** and **(B)** are mean ± SEM of 3-4 independent experiments, as indicated; each dot represents the mean of one experiment. Statistics are two-way ANOVA with Sidak's multiple comparisons tests on log-transformed raw data; black p-values are significant, grey p-values non-significant.

found no difference in spontaneous neutrophil migration or in chemotaxis to fMLP between young and old, regardless of whether the cells had been mock-primed, or primed with LPS or GM-CSF/TNFα (Figures 6A, B). To investigate the possibility of subtle defects in velocity or directionality, we used ibidi chamber chemotaxis assays, with an fMLP gradient ranging from 0 to 10 µM fMLP. Pilot experiments showed that these conditions elicited a clear chemotactic response without being saturating (Supplemental Figure 2). Nevertheless, neutrophils from old and young migrated equally well by all parameters tested (accumulated and Euclidian distance, velocity, straightness of path, directionality and % of responding cells), both during

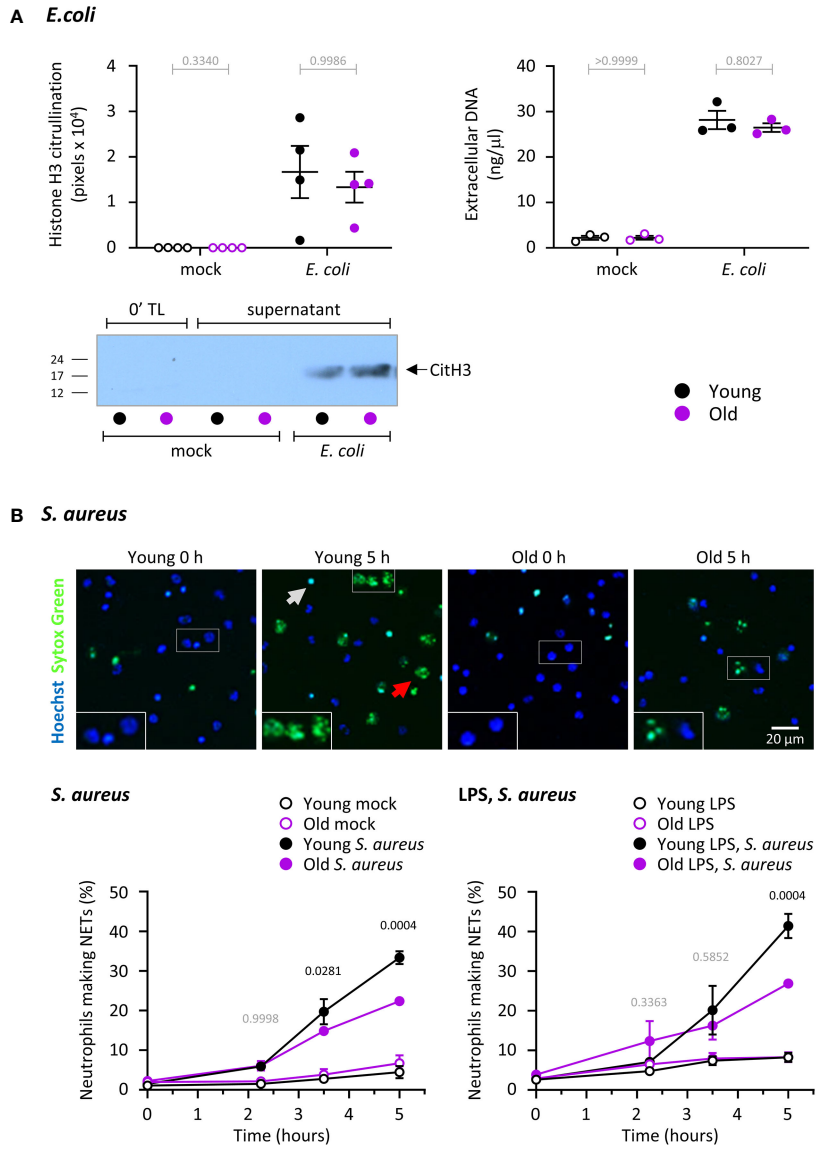

FIGURE 5
Hornigold K et al. NET release in response to *S. aureus* but not *E. coli* is impaired in neutrophils from old mice, independently of LPS. **(A)** NET release in response to *E. coli*. Release of DNA and citrullination of histone H3 were measured in the same samples as in Figure 4A to test NET release in neutrophils from young (8-10 weeks, black symbols) and old (24 months, purple symbols) mice in response to *E. coli*. DNA in cell pellets and cell supernatants was quantitated by spectrometry, and citrullinated H3 by western blotting. A representative blot from one experiment is shown. Data are mean ± SEM of 3-4 independent experiments, as indicated; each dot represents the mean of one experiment. Statistics (two-way ANOVA) revealed no differences between the ages (grey p-values). **(B)** NET release in response to *S. aureus*. Neutrophils from young and old mice were primed with 1 µg/ml LPS or mock-primed for 90 min at 37°C, seeded onto glass slides and allowed to adhere for 30 min at 37°C before stimulation with serum-opsonised *S. aureus* (10 bacteria per neutrophil; filled symbols), or mock stimulation (open symbols), for the indicated periods of time. Non-cell permeable Sytox Green and cell permeable Hoechst DNA dyes were added to samples 15 min before the end of incubation, and cells were live-imaged by widefield microscopy. **(A)** Representative images of mock-primed neutrophils from one experiment stimulated with *S. aureus* for the indicated lengths of time. The grey arrow indicates a dead cell, the red arrow a NET. **(B)** NETosis was quantify by ImageJ, using Sytox Green signal to identify NETs, and phase contrast and Hoechst signal to count total cells. Data are mean ± SEM of 7 independent experiments with mock-primed cells (left-hand panel) and 3 with LPS-primed cells (right-hand panel). Statistics are two-way ANOVA with Sidak's multiple comparisons test. P-values denote significant differences between *S. aureus*-stimulated cells from young and old mice; black p-values are significant, grey p-values non-significant.

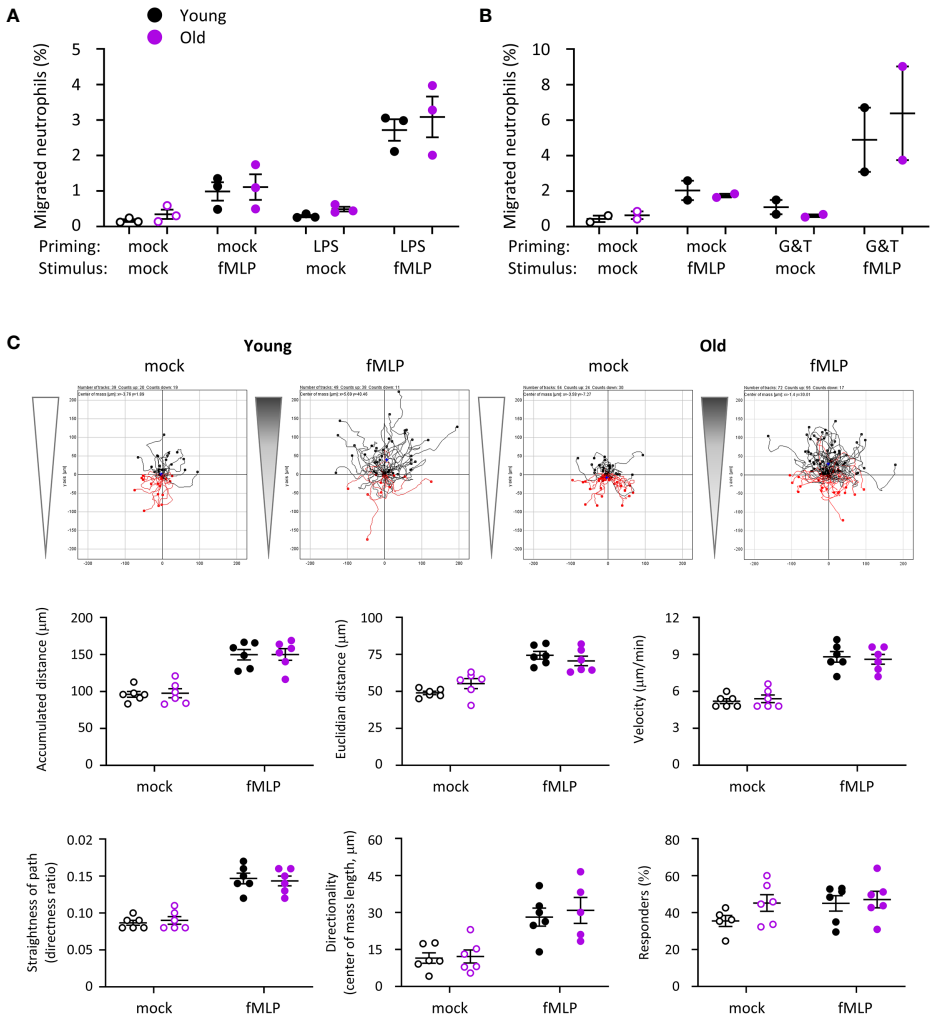

FIGURE 6
Hornigold K et al. Migration is normal in neutrophils from old mice. **(A, B)** Transwell assay. Bone marrow cells from young (8-10 weeks, black symbols) and old (24 months, purple symbols) mice were **(A)** primed with 1 µg/ml LPS or mock-primed for 90 min at 37°C, or **(B)** primed with 50 ng/ml GM-CSF and 20 ng/ml TNFα or mock-primed for 45 min, before placing them into the top well of transwell filters with 3 µM pores and stimulation with 1 µM fMLP, or mock-stimulation with buffer only, in the bottom well for 40 min at 37°C. Transmigrated and total neutrophils were quantitated by flow cytometry. Data are mean ± SEM of 3 independent experiments in **(A)** and 2 in **(B)**; each dot represents the mean of one experiment. **(C)** Ibidi chamber assays. Isolated neutrophils from young or old mice as in **(A)** were primed with 50 ng/ml GM-CSF and 20 ng/ml TNFα for 45 min and seeded into ibidi chambers coated with 20 µg/ml pRGD. Cells were allowed to adhere for 20 min at 37°C before establishing a gradient with 10 µM fMLP at one end of the chamber (filled symbols), or a mock-gradient with buffer only (open symbols), and neutrophils were live-imaged for 20 min (frames every 10 s) using an Olympus CellR microscope. Cells were tracked and migration quantitated using the 'chemotaxis and migration' plugin of ImageJ. Top panels show representative tracks from one experiment, other panels quantify the indicated parameters of cell speed and directionality obtained from ImageJ. Data are mean ± SEM of 6 independent experiments with tracks from 25-72 cells per condition in each experiment; each dot represents the mean of one experiment. Statistics in **(A)** and **(C)** were two-way ANOVA and revealed no differences between the ages.

random migration and chemotaxis to fMLP (Figure 6C). This was seem both when the neutrophils were plated on the fibrinonectin-like surface poly-RGD (Figure 6) or on fibrinogen, although there was a trend towards increased chemotaxis of mock-primed cells from old mice on fibrinogen (Supplemental Figure 3). Therefore, in contrast to our expectations, migration is normal in neutrophils from old mice. It appears that the increased neutrophil recruitment *in vivo* stems from LPS-dependent changes in the tissue environment rather than neutrophil-intrinsic migratory properties.

Neutrophils from old mice had constitutively reduced L-selectin and increased FcγRIII cell surface levels, whereas the cell surface level of Mac1 was low in both ages. Priming with GM-CSF/TNFα led to upregulation of Mac1 and shedding of L-selectin in both ages equally and overcame the altered FcγRIII level (Supplemental Figure 4). In contrast, LPS priming

increased the surface level of Mac1 and reduced L-selectin in neutrophils from old mice but not young, whereas it induced shedding of FcγRIII equally between the ages (Supplemental Figure 4). These data, together with the finding that LPS-treatment was able to prime fMLP-stimulated chemotaxis effectively (Figure 6A, p=0.0004), suggest that not the entire LPS signaling pathway, but only certain aspects of it are defective in neutrophils from old mice.

Age-related dysregulation of the neutrophil proteome

In order to begin to understand the origins of the functional impairments we observed, we compared the total proteomes of neutrophils from young and old mice using tandem mass-tag mass spectrometry. Overall, we identified murine 7943 proteins, and for 7338 of these we obtained enough data for a meaningful comparison between young and old (Supplemental Table 1). A surprisingly large number of proteins was not affected by age; only 361 proteins (5%) were expressed significantly differently, 207 higher in old age and 154 lower (Figure 7A, Supplemental Figure 5 and Supplemental Table 1). A heatmap of the 139 most deregulated proteins (p<0.01) shows that the age-related changes were consistent between the 8 mice tested per age-group (Figure 7B). Among the dysregulated proteins, chromatin and RNA regulators were noticeably downregulated, whereas proteases, protease inhibitors and cell surface receptors were enriched in in old age (Supplemental Figure 5). Also upregulated were immunoglobulins, but this is almost certainly an artefact caused by the homing of immunoglobulin-producing plasma cells into the bone marrow in old age (45). As expected from our ROS assays, the components of the NADPH oxidase were all expressed to normal amounts, which reinforces that LPS priming but not overall NADPH oxidase capacity is affected (Figure 7C). In contrast, many of the anti-pathogen proteins stored in granules (46–48) were among the most upregulated proteins in old age, particularly proteases from the cathepsin family and protease inhibitors from the serpin family (Figure 7D and Supplemental Figure 6). Hence the defect in bacterial clearance observed *in vivo* was not caused by a simple decline in granule protein expression; it seems more likely that granule proteins are upregulated in old age to compensate for the impaired degranulation. Of note, not all granule proteins were deregulated. For example, the marker proteins for the main granule populations, myeloperoxidase, lactoferrin and gelatinase, were all expressed at normal levels (Supplemental Figure 6), suggesting that bulk granulopoiesis is normal in old age, but some granule proteins are upregulated specifically.

We looked into the expression of signaling and cytoskeletal proteins in more detail. Among signaling proteins upregulated in old age were membrane receptors (9%, 11 out of 117 identified), phospholipid-modifying proteins (7%, 5/71) and proteins from the TLR signaling pathways (7%, 5/67) (Figure 7E, Supplemental Figures 7, 8). The deregulated membrane receptors comprised mainly Fc-receptors and integrins, but also the endosomal TLRs TLR7 and TLR9 (Supplemental Figure 8A). The phospholipid-modifying proteins comprised phosphoinositide kinases PI4K2a and phospholipases PLBD2, PLA2G15, PLD3 and PLD4 (Supplemental Figure 7A). PLD3 and PLD4 are of particular interest, as they were recently shown to not possess phospholipase activity, but rather to act as 5' exonucleases which metabolize pathogenic nucleic acids in endosomes, the substrates of TLR7 and TLR9 (49). Apart from TLR7, TLR9, PLD3 and PLD4, only one other protein relevant to TLR pathways, the CD180 antigen, was upregulated in old age by mass spectrometry (3-fold, p=0.0019) (Figure 7E and Supplemental Figure 7B). CD180 is a TLR-like transmembrane protein that binds to TLRs, inhibiting signaling through the TLR4, TLR7 and TLR9 pathways (50, 51). Remarkably few proteins from the GTPase pathways (3%, 9/339), protein kinases (3%, 6/224) and protein phosphatases (0%, 0/86), ubiquitin pathways (2%, 4/262) and cytoskeletal proteins (3%, 6/189) were deregulated (Supplemental Figures 8B–F and Supplemental Table 1).

Among the deregulated pathways, TLR4 signaling is particularly relevant here, seen that LPS priming of the ROS response, phagocytosis and degranulation was impaired in neutrophils from old mice. We failed to obtain enough data for TLR4, the LPS receptor, for quantification by mass spectrometry. However, western blotting showed that TLR4 expression was unaltered by age (Figure 7F), in agreement with earlier reports on human neutrophils (8, 10). In contrast, expression of the adaptor protein MyD88, a key mediator of the TLR4 pathway, was consistently lower in neutrophils from old than young mice by western blot (5-fold, p<0.0001) (Figure 7F). Irak4, an important kinase in the TLR4 pathway, was upregulated in old age (4-fold, p=0.0028), whereas the adaptor protein Trif was unchanged (Figure 7F). The data on MyD88 and Irak4 expression suggest that western blotting may be a more sensitive readout for age-dependent changes than the tandem mass-tag mass spectrometry, which required many more sample preparation steps. In any event, both the upregulation of the inhibitory CD180 and downregulation of MyD88 may be sufficient to explain the decline in LPS priming capacity in old age.

LPS/TLR4 pathway activity is impaired in neutrophils from old mice

To investigate the LPS/TLR4 pathway further, we tested the effects of LPS priming and fMLP stimulation on the activities of Erk, p38 Mapk and Akt in neutrophils from young and old mice by phospho-western blot. LPS priming alone significantly (p=0.0095) activated p38 Mapk in neutrophils from young

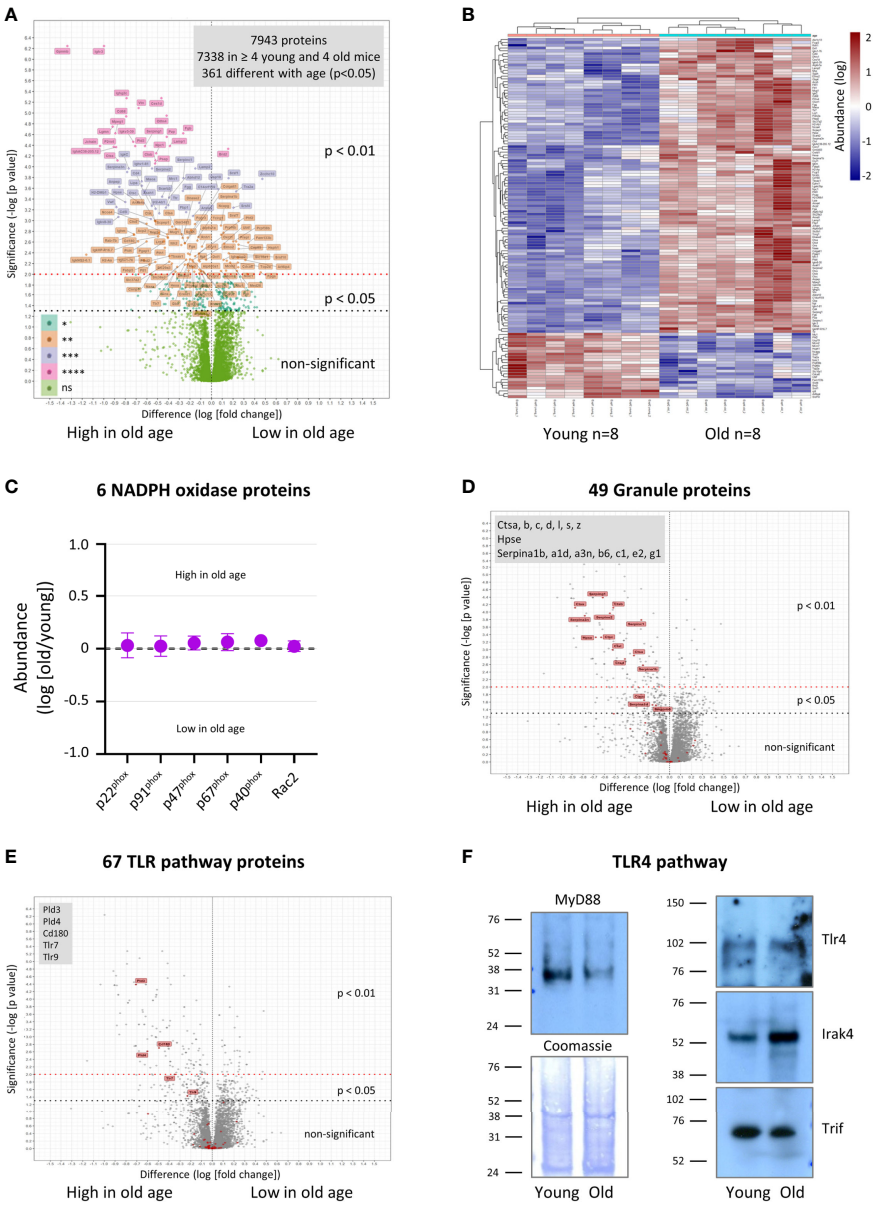

FIGURE 7
Hornigold K et al. Age-related dysregulation of the neutrophil proteome. Neutrophils were isolated to 95-98% purity from the bone-marrow of 8 young (8 weeks) and 8 old (24 months) mice, in 4 independent experiments with 2 young and 2 old mice per experiment, treated with the protease inhibitor DFP (7 mM) for 10 min at RT, washed twice, and frozen. Sample processing included protein digest and labeling with tandem mass-tags. Mass-tagged samples were combined, fractionated into 60 fractions, and analyzed by LC-MS mass spectrometry. Proteins were identified using Mascott software and their relative abundances determined using Proteome Discoverer software. **(A)** 7338 murine proteins were detected in at least 2 of 4 experiments (4 out of 8 mice per age) and analyzed using R software for differences in relative abundance between young and old. **(B)** Heatmap of proteins whose expression changed with p<0.01 between old and young mice. **(C-E)** Proteins were assigned to different classes and pathways by PANTHER pathway analysis and manual curation (see also Supplemental Figures 5–8 and Supplemental Table 1). **(C)** Proteins of the NADPH oxidase complex. **(D)** Granule-lumen proteins. **(E)** TLR pathway proteins. The 49 granule-lumen proteins **(D)** and 67 TLR pathway proteins **(E)** identified (red) are plotted in the context of all other proteins (grey). Deregulated granule lumen proteins **(D)** and TLR pathway proteins **(E)** are shown by red flags and listed in the grey boxes. **(A-E)** Abundances are expressed as log(old/young). Statistical significance was assessed by two-sided t-test of log(young) vs log(old) with Benjamini-Hochberg false discovery rate correction for multiple comparisons of all 7338 quantified proteins. **(F)** Neutrophils were isolated and DFP-treated as in **(A)**, lysed, and total lysates pooled (4 mice per pool per age) and western blotted for the indicated proteins of the LPS/TLR4 signaling pathway. Coomassie staining was used as loading control. Blots shown are representative from one of two pools per age-group.

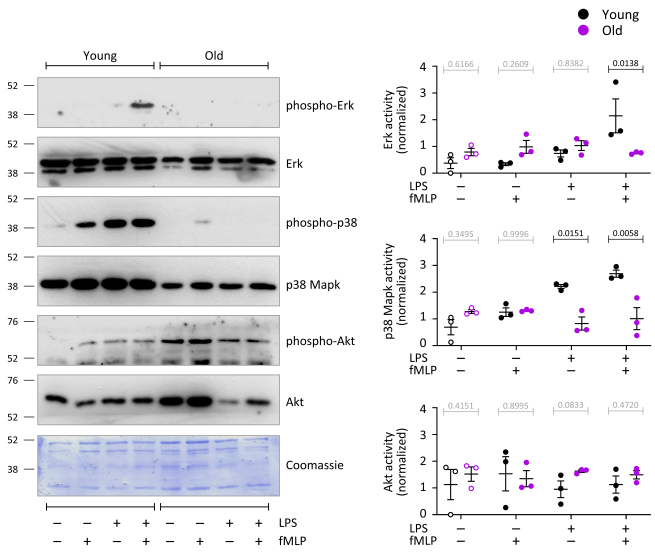

FIGURE 8
Hornigold K et al. LPS/TLR4 pathway activity is impaired in neutrophils from old mice. Neutrophils from young (8-10 weeks, black symbols) and old (24 months, purple symbols) mice were primed with 1 µg/ml LPS, or mock-primed with $DPBS^{++++}$, and stimulated with 1 µM fMLP for 1 min. Total cell lysates were western blotted using antibodies for phosphorylated p38 Mapk, p42/44 Erk and Akt. Blots were stripped and reprobed for total p38 Mapk, p42/44 Erk and Akt. Blots were quantitated by ImageJ densitometry, and phospho-protein signals normalized to total-protein for each sample. Representative blots, and a coomassie-stained membrane as total loading control, are shown. Data are mean ± SEM of 3 independent experiments; each dot represents the mean of one experiment. Statistics are two-way ANOVA with Sidak's multiple comparisons tests; black p-values are significant, grey p-values non-significant.

mice but not old (Figure 8). In mock-primed cells, fMLP stimulation (1 µM, 1 min) did not significantly activate any of the pathways. In contrast, in LPS-primed cells, fMLP stimulation led to robust further activation of p38 Mapk (p=0.0197) and induced the activation of Erk (p=0.0055), but only in neutrophils from young mice, not old (Figure 8). Akt was not significantly activated under the conditions tested here. Although there was a tendency for total protein levels of Erk and p38 Mapk to be higher in neutrophils from young mice than old, this did not reach significance throughout experiments. Together, these data show that LPS/TLR4 signaling through Erk and p38 Mapk is profoundly impaired in neutrophils from old mice.

PIP_3 production and PIP_2 levels are reduced in neutrophils from old mice

Production of the lipid second messenger PIP_3 by class 1 PI3Ks is required for chemoattractant-stimulated ROS production (52). Hence we measured PIP_3 in response to neutrophil stimulation with C5a or fMLP, either upon mock-priming or priming with LPS or GM-CSF/TNFα, using direct PIP_3 measurement by lipid mass spectrometry (40). No PIP_3 was detectable in mock-stimulated cells, even when cells were primed (Figures 9A–D). This was as expected (40), and confirms results from the ROS and degranulation assays showing that neutrophils from old mice are not pre-activated by inflamm-aging. Stimulation with C5a or fMLP induced rapid and robust PIP_3 production, which was lower in old than young after cells had been mock-primed for 90 min (Figures 9A–D). Priming with LPS or GM-CSF/TNFα increased fMLP-stimulated PIP_3 production, but had no effect on C5a-stimulated PIP_3, and the fMLP-stimulated response remained lower in LPS-primed cells from old mice (Figures 9A–D).

PIP_3 is produced by PI3K-mediated phosphorylation of the membrane phosphoinositide PIP_2. Hence, we analyzed the same lipid mass spectrometry samples further to see whether the impaired PIP_3 production might be caused by altered PIP_2 levels. Indeed, PIP_2 was constitutively reduced in neutrophils from old mice, and remained lower under all conditions tested (Figure 9E). Yet even after taking into account the ratio of PIP_3 to PIP_2, as is commonly done in PIP_3 mass-spectrometry (40, 41), neutrophils still showed the age-related reduction in fMLP-stimulated PIP_3, suggesting that it was not solely a consequence of lower substrate availability. Taking into account PIP_2, LPS-priming increased PIP_3 production only in the young, revealing an age-related LPS-priming defect independent of PIP_2 availability (Figure 9F). Hence, neutrophils from old mice show reduced fMLP-stimulated production of PIP_3 which is partially LPS-dependent, as well as having constitutively reduced levels of PIP_2. The reduced LPS-primed PIP_3 production might explain the impaired ROS response.

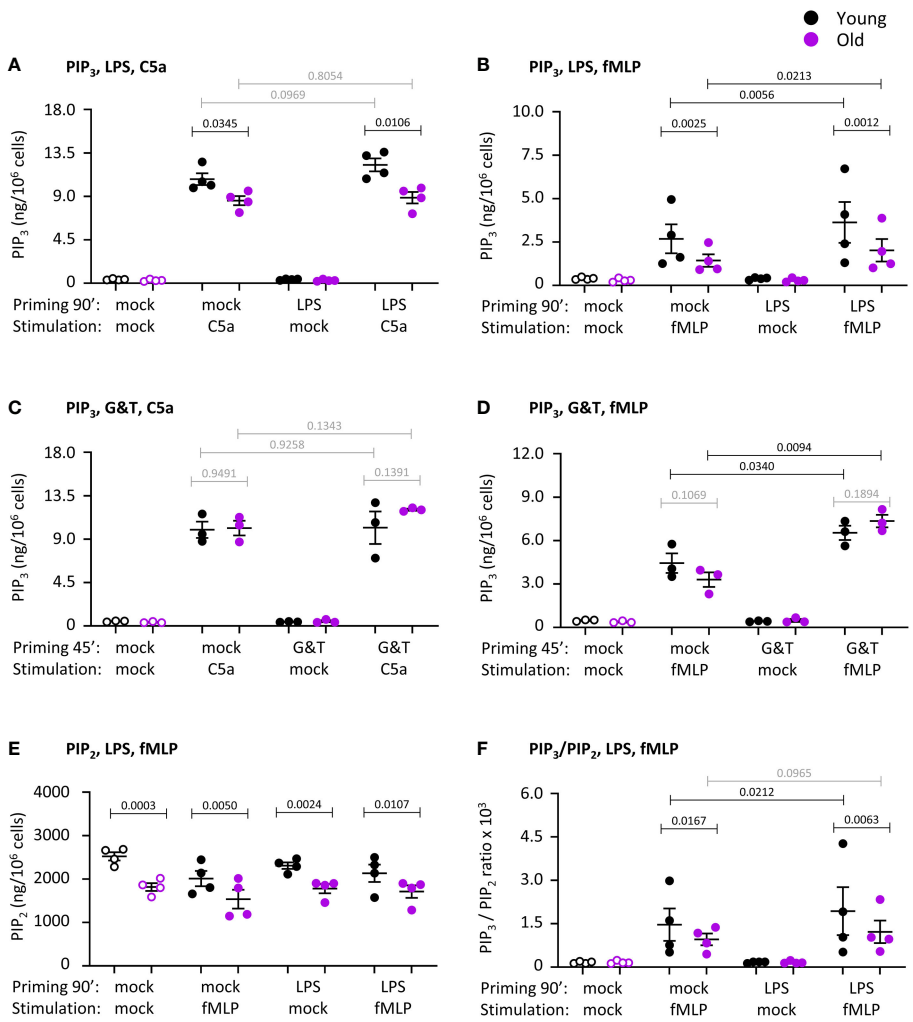

FIGURE 9
Hornigold K et al. PIP_3 production and PIP_2 levels are reduced in neutrophils from old mice. Neutrophils from young (8-10 weeks, black symbols) and old (24 months, purple symbols) mice were primed with 1 µg/ml LPS or mock-primed for 90 min **(A, B, E, F)**, or were primed with 50 ng/ml GM-CSF and 20 ng/ml murine TNFα or mock-primed for 45 min **(C, D)**, prior to stimulation with 25 nM C5a **(A, C)** or 3 µM fMLP **(B,D-F)**, or mock-stimulation, for 10 s. PIP_3 **(A-D)** and PIP_2 **(E)** were extracted and quantitated by lipid mass spectrometry using internal synthetic standards. Data in **(A, B, E, F)** are mean ± SEM of 4 independent experiments and data in **(C, D)** from 3; each dot represents the mean of one experiment. **(F)** Ratio of PIP_3 over PIP_2 from **(B)** and **(E)**. Statistics are two-way ANOVA with Sidak's multiple comparisons test, for chemoattractant-stimulated cells only in **(A–D, F)**; black p-values are significant, grey p-values non-significant.

Rac activity is normal in neutrophils from old mice

ROS production and migration require activation of the small GTPase Rac (53). Mouse neutrophils express two isoforms of Rac, Rac1 which confers directionality to migration, and Rac2 which confers the ability to migrate *per se* and is also required for ROS productions as an integral part of the NADPH oxidase complex. Seen that ROS production was impaired, we tested the activities of Rac1 and Rac2 in response to stimulation with C5a or fMLP, under mock-primed and LPS-primed conditions. Both Rac1 and Rac2 were robustly activated upon chemoattractant stimulation (p=0.0025 in A, p=0.0008 in B, p<0.0001 in D), but there was no difference between the ages. LPS priming had no effect on the activity of either Rac1 or Rac2 (Figure 10). Hence, as suggested by the normal migration properties of the neutrophils, the activities of Rac1 and Rac2 are not affected by age. These data imply furthermore that Rac activity is not related to the age-related decline in LPS-primed ROS production.

Discussion

Our study shows that old mice have lower resistance to bacterial infection, their neutrophils have a reduced ability to kill

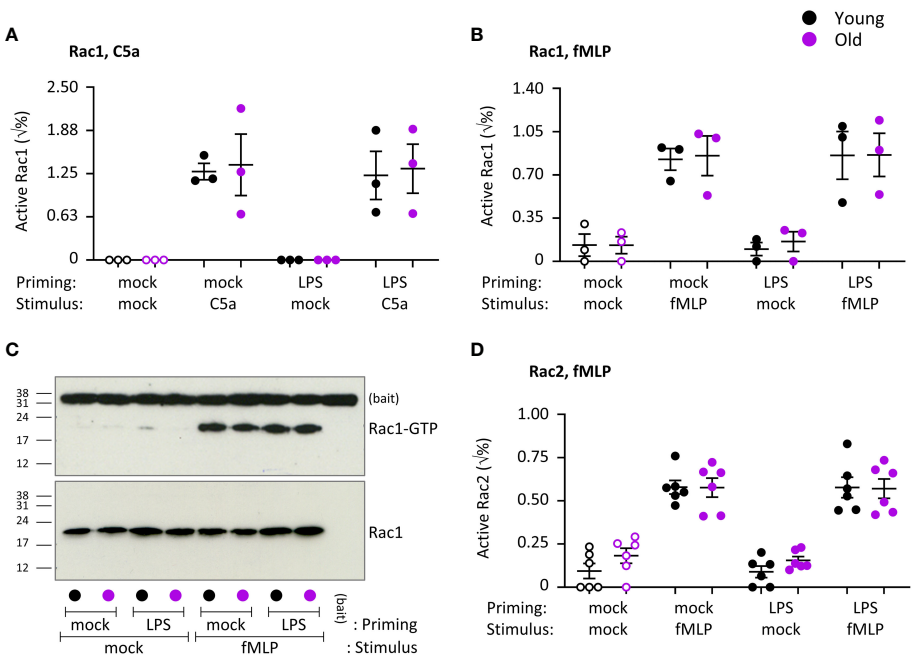

FIGURE 10
Hornigold K et al. Chemoattractant-stimulated Rac activity is normal in neutrophils from old mice. Neutrophils from young (8-10 weeks, black symbols) and old (24 months, purple symbols) mice were primed with 1 µg/ml LPS or mock-primed for 90 min, prior to stimulation for 10 s with 25 nM C5a **(A)** or 3 µM fMLP **(B-D)**, or mock-stimulation as indicated. Rac activity was assessed by Pak-CRIB pull down. GTP-Rac (active) and total Rac levels were analyzed by western blotting with Rac1 and Rac2 antibodies and quantified by densitometry using ImageJ. **(C)** Representative western blots from one experiment as in **(B)**. Data in **(A)** and **(B)** are mean ± SEM of 3 independent experiments and data in **(D)** of 6; each dot represents the mean of one experiment. Statistics were two-way ANOVA with Sidak's multiple comparisons test and showed no differences between ages.

bacteria, and all major neutrophil effector responses, with the notable exception of chemotaxis, are impaired, particularly in the context of LPS priming.

We showed that old mice have a lower capacity to clear pathogenic *E. coli* strain O18:K1 during an acute model of septic peritonitis. This infection model recapitulates the situation in humans, where the incidence of peritonitis increases with age to become a leading cause of mortality from sepsis for the elderly in intensive care units (4). Our data complement earlier reports on decreased immunity of old mice to cutaneous *S. aureus* infection (15), oral *S. typhimurium* infection and systemic *C. albicans* infection (17), showing that old mice have consistently reduced immunity to bacteria and fungi regardless of the infected organ. It would be valuable to perform a kinetic study in future to determine at which ages the immunity declines most.

In contrast to this consistent loss of innate immunity, the effects of age on neutrophil recruitment are much more varied, either reduced (15, 21, 22), or normal (54), or increased (19, 20) (23), depending on the affected organ and inflammatory or infectious agent. Congruently, we found that neutrophil recruitment was normal during aseptic peritonitis but elevated during LPS-induced peritonitis. The increased LPS-dependent recruitment is unlikely to be linked to the neutrophil-intrinsic defect in LPS priming, and more likely to systemically increased inflammatory chemokines/cytokines. A previous study used LPS to induce pulmonary neutrophil recruitment, which was also raised and accompanied by increased production of inflammatory cytokines (23), suggesting LPS may consistently increase recruitment in old mice regardless of the affected organ. A beautiful recent study used intravital microscopy to show that aberrant neutrophil trafficking in old mice is indeed caused by increased inflammatory cytokines in aged tissues rather than neutrophil-intrinsic defects (22). IL1β-stimulated neutrophil recruitment in the cremaster muscle of old mice was reduced due to increased reverse-transendothelial migration caused by mast cells in the aged tissue producing KC, leading to downregulation of the KC receptor CXCR2 on the neutrophil surface through agonist-induced internalization (22).

The finding by several studies that innate immunity declines in old mice regardless of effects on neutrophil recruitment (15, 17–20) suggested that neutrophil effector responses may be impaired. To study these effector responses, we required basal neutrophils that allowed us to induce specific pathways for priming and activation, which precluded the use of tissue-infiltrated neutrophils. We isolated mature neutrophils from the bone marrow rather than from peripheral blood in order to

minimize any age-dependent differences in the proportions of freshly released and senescent neutrophils. Indeed, the peripheral pool of neutrophils is more senescent in old mice than young (increased CXCR4 and lower L-selectin/CD62L on the cell surface), due to reduced efferocytosis of aged neutrophils by macrophages in old mice (55). As mentioned before, neutrophil aging occurs in the circulation through priming by factors such as LPS and peptidoglycans produced by the gut microbiota (32). Our bone marrow-derived neutrophils showed no evidence of being pre-primed when we assayed ROS production, degranulation or migration. The neutrophils from old mice did, however, show a reduction in L-selectin and increase in FcγRIII levels on their surface in the basal state (on ice), raising the possibility that they are partially primed. Alternative explanations that remain to be tested could be altered total levels or altered shedding of these proteins. The cell surface level of Mac1 was as low in basal neutrophils of both ages, as was the secretion of gelatinase granules (see below), arguing against a primed state in old age. Overall, it appears our approach effectively prevented confounding the effects of senescence and organismal age, but a more in-depth analysis of priming state may be required in the future.

ROS production by neutrophils from elderly humans is impaired in response to a range of priming agents and stimuli (7–10), whereas ROS production by neutrophils from old mice is more varied, either normal or reduced depending on stimulus (24, 25). PMA-stimulated ROS production is normal in neutrophils from both elderly humans (10) and old mice (our data), and all subunits of the NADPH oxidase are expressed at normal levels in old age, so aging clearly does not affect the NADPH oxidase itself but rather the upstream signaling pathways. The ROS response was normal upon priming with GM-CSF/TNFα, but impaired after LPS priming both upon stimulation with C5a and fMLP. Therefore, bone-marrow derived mouse neutrophils are a good model for the age-related decline in ROS production, particularly when associated with LPS priming. Human neutrophils are usually isolated from the periphery rather than the bone marrow, and like in mice, the peripheral population is more senescent ($CD62L^{lo}$) in old people than young from priming in the vasculature (56). The reduction in the GM-CSF primed ROS response that is commonly seen in elderly humans may therefore be a consequence of senescence rather than a neutrophil-intrinsic defect.

Phagocytosis is generally reduced in neutrophils from elderly humans (12, 13), whereas it was reported to be more variable in neutrophils from old mice, either reduced (27) or normal (15). Our assays showed an overall reduction in the phagocytosis of both *E. coli* and zymosan yeast particles. The number of *E. coli* or zymosan particles taken up was impaired in neutrophils from old mice after LPS priming, and there was also a decline in the proportion of phagocytosing neutrophils which was independent of LPS. This partial LPS dependence, together with the need to assess several parameters of phagocytosis to document a phenotype, may explain why some previous studies failed to observe an age-dependent decline in phagocytosis.

Neutrophil priming occurs through degranulation. The fusion of granules with the plasma membrane upregulates receptors stored on granules to the plasma membrane, readying the cell for stimulation, as well as causing the release of proteases and other anti-pathogen factors from the granule lumen into the extracellular space. Surprisingly little information on the effects of age on degranulation exists, both in human and mouse. The blood plasma of elderly humans contains more cleavage products of neutrophil elastase, an azurophil granule lumen protease, and neutrophils from elderly people have higher cell surface levels of CD63, a membrane protein stored on azurophil granules (11), and show higher elastase activity after phagocytosis of *S. pneumoniae* (57). However, the former may be a consequence of neutrophil senescence or death and the latter may reflect phagocytic capacity rather than degranulation. Direct degranulation assays with isolated neutrophils from the elderly have to our knowledge never been done. We show that, gelatinase release was low in basal neutrophils, with no difference between the ages. As the secretion of gelatinase granules is particularly sensitive to priming (46, 47), this further supports the notion that bone marrow-derived neutrophils from old mice are not primed. Neutrophils from old mice showed reduced degranulation of azurophil granules (induced by *E. coli*) as well as gelatinase granules (induced by LPS/fMLP), and the latter defect had again both LPS-dependent and LPS-independent elements. The overall capacity to degranulate was normal when depolymerization was forced with cytochalasin B. It seems possible that neutrophils from old mice are more reticent to depolymerize their cortical actin ring, making granule fusion harder. The age-related decrease in degranulation contrasted with the marked upregulation of granule lumen proteins from the cathepsin and serpin families. Hence, the decline in bacterial clearance *in vivo* is not caused by reduced expression of granule proteins. Evidently, the upregulation of cathepsins is insufficient to protect old mice during bacterial infection, but possibly the upregulation of serpins, which inhibit proteases, might contribute to the age-related decline in immunity. It would be of interest to investigate why cathepsins and serpins are selectively deregulated among granule proteins. In addition to these granule proteins, several other proteases and protease inhibitors were upregulated in old age. It would also be interesting to study the subcellular localizations of these proteins in the future.

NET release by neutrophils from elderly humans is impaired in response to many stimuli (7–10), whereas like the other neutrophil responses, this is reportedly more variable in neutrophils from old mice, either reduced upon stimulation with TLR2 ligands (24), normal after stimulation with PMA (26), or increased upon mitochondrial oxidative stress (25). We found normal NET release in response to *E. coli* in old age, but

reduced *S. aureus*-stimulated NETs. The lack of effect of age on *E. coli*-induced NET release suggests that the rapid killing of *E. coli* by young neutrophils, which was impaired in the old, was a consequence of responses such as phagocytosis and degranulation rather than NET release. LPS priming had hardly any effect, so this defect is independent of LPS. This was surprising, as ROS production is often strongly linked with NETs, and we saw an age-dependent decline in LPS-primed ROS production. However, NET release can also occur independently of ROS production, through mechanisms which remain incompletely understood (58). Our proteomic found no dysregulated expression of NETs-related proteins such as histones, PADI4 and elastase, in contrast to their previously reported up- or downregulated transcription (26), suggesting either that transcriptomics is a more sensitive readout or that protein production or stability overrides mRNA levels in these cases. Future work will be required to elucidate which NET pathways are impaired.

We showed that both random migration and fMLP-stimulated chemotaxis were normal in neutrophils from old mice, regardless of whether the cells were mock-primed or primed with LPS or GM-CSF/TNFα, both in transwell assays and in imaging-based ibidi assays on pRGD and fibrinogen surfaces. Therefore, the increased peritoneal neutrophil recruitment in response to LPS *in vivo* was clearly not a consequence of an altered intrinsic ability of neutrophils to migrate. Rather, our results support the recent study discussed above, which showed that altered neutrophil recruitment in old age is caused by extrinsic, tissue-derived factors (22). Other mouse studies reported normal or elevated spontaneous neutrophil migration, and reduced chemotaxis in old age (19, 28). Chemotaxis of neutrophils from elderly humans is also reduced, despite normal surface levels of major chemoattractant receptors (8, 11). We can only assume that the difference between our study and other mouse neutrophil studies is due to different assay conditions. However, we employed similar transwell assays and additionally the more sophisticated ibidi chamber, which if anything should have made it more likely to detect defects in migration. Using the ibidi assay under the same conditions, we could confidently detect differences in migration speed of 20% in other projects (unpublished observation), so assay sensitivity was not limiting. It is possible that the age-related impairment is specific to certain chemoattractants, as we employed fMLP, whereas as the previous studies used KC, despite the surface level of the KC receptor CXCR2 being reduced in neutrophils from old mice (19). We found altered cell surface levels of L-selectin and FcγRIII in neutrophils from old mice, and altered effects of LPS priming on Mac1 and L-selectin surface levels. It is therefore possible that more detailed future analysis of LPS-primed migration, particularly under shear-stress conditions, might reveal age-related defects.

Neutrophil proteomics had been done in multiple previous studies, mostly studies on subcellular fractions such as the various granule subsets, but also functional proteomics such as phosphoproteomics or changes associated with diurnal rhythms or neutrophil-dependent diseases such as chronic granulomatous disease or leukocyte adhesion deficiency (47, 48, 59, 60). One study compared the proteomes of neutrophils from newborn and adult humans, showing low abundance in newborns of proteins related to the proteasome, transendothelial migration and NETosis, as well as several granule proteins including elastase and myeloperoxidase (61). However, to our knowledge neutrophil proteomes have never been compared between young and old adults, neither in humans nor mice. A recent study compared transcriptomics, metabolomics and lipidomics of bone marrow-derived neutrophils from male and female old and young mice (26). Sex-differences outweighed age-differences, and age-dependent changes were seen only by transcriptomics but not metabolomics or lipidomics (26). Like our proteomic analysis, transcriptomics found chromatin regulators among the most downregulated genes in old age, associated with higher chromatin compaction. In addition, the mRNAs of several cell-cycle regulators were downregulated (26) which we did not see on the protein level, whereas we found reduced expression of many RNA regulators. Like our proteomics, the transcriptomics also detected the upregulation of several granule proteins in old age (26), but did not detect the increased levels of serpins. The transcriptomics also did not note any upregulation of membrane receptors, phospholipid-modifying or TLR pathway genes in old age. Overall however, the congruence between the two studies regarding chromatin regulators and granule proteases shows robust age-related changes.

Our proteomic analysis of the TLR pathways revealed an upregulation in old age of CD180, a transmembrane protein that inhibits signaling through TLR4 and other TLR pathways (50, 51). Furthermore, we found reduced expression of MyD88 by western blotting. MyD88 expression is also reduced in neutrophils from elderly humans (8). MyD88 confers one of the two major arms of the TLR4 signaling pathway, leading to the activation of NF-κB-responsive genes for the production of inflammatory cytokines (62). As CD180 and Myd88 are important regulators of the TLR4 pathway, their deregulation is likely to contribute to the impaired LPS priming in old age. It is important to note however that LPS-primed chemotaxis and shedding of FcγRIII were normal, meaning that not the entire LPS priming pathway is defective. Perhaps the MyD88-independent arm of the TLR4 pathway which is regulated by Trif (62) remains intact, as we found normal Trif levels. Moreover, aging will not only affect the expression but also the subcellular localization and activity of TLR4 pathway components. Evidence for this was seen in neutrophils from elderly humans, where the LPS-induced localization of TLR4 and Irak1 to lipid rafts is reduced (8). We demonstrate profoundly impaired activation of Erk and p38 Mapk in LPS-primed neutrophils from old mice. A more detailed future characterization of LPS/TLR4 signaling will be required to elucidate the mechanisms through which this pathway is impaired. Furthermore, our proteomics showed that

components of other TLR signaling pathways, notably the endosomal TLR7 and TLR9, as well as exonucleases PLD3 and PLD4 which metabolize substrates of endosomal TLRs (49), are among the most upregulated proteins in old age. Therefore, in addition to the TLR4 pathway, the effects of age on signaling through these endosomal TLRs would merit investigation.

We investigated the activity of class I PI3K, an important effector of the LPS/TLR4 pathway (63). PI3K activity was previously reported to be constitutively increased in neutrophils from elderly humans, and inhibition of PI3Kγ or PI3Kδ restored speed and accuracy during neutrophil chemotaxis (11). However, in that study PI3K activity was determined through phosphorylation of the regulatory PI3K subunit (11), an indirect proxy that can be a poor indicator of activity. We used direct lipid mass spectrometry to measure PI3K activity (40), which revealed a partially LPS-dependent reduction of chemoattractant-stimulated PIP_3 production. Hence, class I PI3K activity is reduced rather than increased in old age, both upon prolonged incubation of cells at 37°C and upon LPS priming, but not after GM-CSF/TNFα priming, which was unaffected. Furthermore, the neutrophil isoform PI3Kγ specifically determines the proportion of neutrophils that migrate by chemokinesis (64), whereas we only tested spontaneous migration and chemotaxis. In view of these PIP_3 results, it would be interesting to test chemokinesis.

The age-dependent loss of signaling through the LPS/TLR4 pathway is not specific to neutrophils. Loss of TLR4 and other TLR signaling pathways with age has also been shown in monocytes, macrophages and dendritic cells. Peritoneal or spleen-derived macrophages from old mice showed reduced production of inflammatory cytokines in response to LPS despite normal levels of TLR4, with reduced activation of $p38^{Mapk}$ and Jnk (65, 66). Similarly, LPS-induced maturation of dendritic cells is reduced in old mice (67, 68), and splenic dendritic cells produce less TNFα upon LPS stimulation despite normal TLR4 levels (67). Furthermore, peripheral blood monocytes showed reduced production of inflammatory cytokines in response to stimulation of TLR1/2, and lower TLR1 surface levels in old age (69), as well as impaired NF-κB activity in response to TLR5 ligands, despite higher TLR5 expression and TLR5-dependent activation of p38 Mapk and Erk (70). Hence, age-related impairments of TLR pathways are seen in the mouse throughout different types of innate immune cells. How the reduced TLR functions in each of these cell types contribute to the impaired innate immunity of old mice *in vivo*, however largely remains to be demonstrated.

Our study suggests that mice are an appropriate model for studying the age-related decline human neutrophil function, particularly regarding the impaired LPS/TLR4 pathway. Age-related impairments in ROS production, degranulation, phagocytosis and PIP_3 production were all partially LPS-dependent. This LPS/TLR4 pathway dependence resolves some of the previous controversy regarding the effects of age on murine neutrophils. No other study specified the use of endotoxin-free reagents, and only three recent papers (22, 24, 26) described the health status of the mice, specifying pathogen-controlled conditions. This suggests that neutrophils may have been in varying states of priming, especially in some older studies. Finally, the impaired ability to kill bacteria *in vitro* and reductions in neutrophil ROS production, phagocytosis, degranulation and NET formation that we demonstrated here may all contribute to the decline in antibacterial immunity *in vivo*. Future studies will need to evaluate the contribution of each neutrophil response to this impaired innate immunity through the use of genetic deficiencies, neutrophil depletion and pharmacological inhibitors.

Data availability statement

The proteomics data presented in this study are deposited in the PRIDE repository, accession number PXD035577.

Ethics statement

The animal study was reviewed and approved by the Babraham Institute Animal Welfare Ethical Review Body and the British Home Office.

Author contributions

KH, JYC, PAM, LC, SAC, CP, and DO devised, conducted and analyzed experiments. KEA and AS-P devised and analyzed experiments. PTH devised experiments. HCEW obtained funding, devised and analyzed experiments and wrote the paper. All authors contributed to the article and approved the submitted version.

Funding

PM is the recipient of a targeted PhD studentship from the BBSRC. SC is the recipient of a targeted PhD studentship from the MRC. CP was the recipient of a DTP PhD studentship from the BBSRC. This project was funded by Institute Strategic Programme Grant BB/P013384/1 from the BBSRC to the Signalling Programme at the Babraham Institute.

Acknowledgments

We thank the staff of the Babraham Biological Support Unit and the Imaging and Flow Cytometry facilities for their dedicated and highly skilled support.

Conflict of interest

The authors declare that the research was conducted in the absence of any commercial or financial relationships that could be construed as a potential conflict of interest.

Publisher's note

All claims expressed in this article are solely those of the authors and do not necessarily represent those of their affiliated organizations, or those of the publisher, the editors and the reviewers. Any product that may be evaluated in this article, or claim that may be made by its manufacturer, is not guaranteed or endorsed by the publisher.

Supplementary material

The Supplementary Material for this article can be found online at: https://www.frontiersin.org/articles/10.3389/fimmu.2022.888415/full#supplementary-material

References

1. Nauseef WM, Borregaard N. Neutrophils at work. *Nat Immunol* (2014) 15:602–11. doi: 10.1038/ni.2921

2. Ustyanovska Avtenyuk N, Visser N, Bremer E, Wiersma VR. The neutrophil: The underdog that packs a punch in the fight against cancer. *Int J Mol Sci* (2020) 21:7820. doi: 10.3390/ijms21217820

3. Wang J. Neutrophils in tissue injury and repair. *Cell Tissue Res* (2018) 371:531–9. doi: 10.1007/s00441-017-2785-7

4. Martin-Loeches I, Guia MC, Vallecoccia MS, Suarez D, Ibarz M, Irazabal M, et al. Risk factors for mortality in elderly and very elderly critically ill patients with sepsis: a prospective, observational, multicenter cohort study. *Ann Intensive Care* (2019) 9:26. doi: 10.1186/s13613-019-0495-x

5. Organisation WH. *Global report on the epidemiology and burden of sepsis: Current evidence, identifying gaps and future directions*. Geneva: World Health Organisation (2020) p. 1–56.

6. Qian F, Guo X, Wang X, Yuan X, Chen S, Malawista SE, et al. Reduced bioenergetics and toll-like receptor 1 function in human polymorphonuclear leukocytes in aging. *Aging* (2014) 6:131–9. doi: 10.18632/aging.100642

7. Tortorella C, Stella I, Piazzolla G, Simone O, Cappiello V, Antonaci S. Role of defective ERK phosphorylation in the impaired GM-CSF-induced oxidative response of neutrophils in elderly humans. *Mech Ageing Dev* (2004) 125:539–46. doi: 10.1016/j.mad.2004.06.001

8. Fulop T, Larbi A, Douziech N, Fortin C, Guerard KP, Lesur O, et al. Signal transduction and functional changes in neutrophils with aging. *Aging Cell* (2004) 3:217–26. doi: 10.1111/j.1474-9728.2004.00110.x

9. Braga PC, Sala MT, Dal Sasso M, Pecile A, Annoni G, Vergani C. Age-associated differences in neutrophil oxidative burst (chemiluminescence). *Exp Gerontol* (1998) 33:477–84. doi: 10.1016/S0531-5565(98)00012-6

10. Hazeldine J, Harris P, Chapple IL, Grant M, Greenwood H, Livesey A, et al. Impaired neutrophil extracellular trap formation: a novel defect in the innate immune system of aged individuals. *Aging Cell* (2014) 13:690–8. doi: 10.1111/acel.12222

11. Sapey E, Greenwood H, Walton G, Mann E, Love A, Aaronson N, et al. Phosphoinositide 3-kinase inhibition restores neutrophil accuracy in the elderly: toward targeted treatments for immunosenescence. *Blood* (2014) 123:239–48. doi: 10.1182/blood-2013-08-519520

12. Butcher SK, Chahal H, Nayak L, Sinclair A, Henriquez NV, Sapey E, et al. Senescence in innate immune responses: reduced neutrophil phagocytic capacity and CD16 expression in elderly humans. *J Leuk Biol* (2001) 70:881–6. doi: 10.1189/jlb.70.6.881

13. Alonso-Fernandez P, Puerto M, Mate I, Ribera JM, de la Fuente M. Neutrophils of centenarians show function levels similar to those of young adults. *J Am Geriatr Soc* (2008) 56:2244–51. doi: 10.1111/j.1532-5415.2008.02018.x

14. Lord JM, Butcher S, Killampali V, Lascelles D, Salmon M. Neutrophil ageing and immunesenescence. *Mech Ageing Dev* (2001) 122:1521–35. doi: 10.1016/S0047-6374(01)00285-8

15. Brubaker AL, Rendon JL, Ramirez L, Choudhry MA, Kovacs EJ. Reduced neutrophil chemotaxis and infiltration contributes to delayed resolution of cutaneous wound infection with advanced age. *J Immunol* (2013) 190:1746–57. doi: 10.4049/jimmunol.1201213

16. Ren Z, Gay R, Thomas A, Pae M, Wu D, Logsdon L, et al. Effect of age on susceptibility to salmonella typhimurium infection in C57BL/6 mice. *J Med Microbiol* (2009) 58:1559–67. doi: 10.1099/jmm.0.013250-0

17. Murciano C, Villamon E, Yanez A, O'Connor JE, Gozalbo D, Gil ML. Impaired immune response to candida albicans in aged mice. *J Med Microbiol* (2006) 55:1649–56. doi: 10.1099/jmm.0.46740-0

18. Stout-Delgado HW, Du W, Shirali AC, Booth CJ, Goldstein DR. Aging promotes neutrophil-induced mortality by augmenting IL-17 production during viral infection. *Cell Host Microbe* (2009) 6:446–56. doi: 10.1016/j.chom.2009.09.011

19. Kulkarni U, Zemans RL, Smith CA, Wood SC, Deng JC, Goldstein DR. Excessive neutrophil levels in the lung underlie the age-associated increase in influenza mortality. *Mucosal Immunol* (2019) 12:545–54. doi: 10.1038/s41385-018-0115-3

20. Murciano C, Yanez A, O'Connor JE, Gozalbo D, Gil ML. Influence of aging on murine neutrophil and macrophage function against candida albicans. *FEMS Immunol Med Microbiol* (2008) 53:214–21. doi: 10.1111/j.1574-695X.2008.00418.x

21. Mares CA, Ojeda SS, Li Q, Morris EG, Coalson JJ, Teale JM. Aged mice display an altered pulmonary host response to francisella tularensis live vaccine strain (LVS) infections. *Exp Gerontol* (2010) 45:91–6. doi: 10.1016/j.exger.2009.10.004

22. Barkaway A, Rolas L, Joulia R, Bodkin J, Lenn T, Owen-Woods C, et al. Age-related changes in the local milieu of inflamed tissues cause aberrant neutrophil trafficking and subsequent remote organ damage. *Immunity* (2021) 54:1–17. doi: 10.1016/j.immuni.2021.04.025

23. Ito Y, Betsuyaku T, Nasuhara Y, Nishimura M. Lipopolysaccharide-induced neutrophilic inflammation in the lungs differs with age. *Exp Lung Res* (2007) 33:375–84. doi: 10.1080/01902140701634843

24. Xu F, Zhang C, Zou Z, Fan EKY, Chen L, Li Y, et al. Aging-related Atg5 defect impairs neutrophil extracellular traps formation. *Immunology* (2017) 151:417–32. doi: 10.1111/imm.12740

25. Wang Y, Wang W, Wang N, Tall AR, Tabas I. Mitochondrial oxidative stress promotes atherosclerosis and neutrophil extracellular traps in aged mice. *Arterioscler Thromb Vasc Biol* (2017) 37:e99–e107. doi: 10.1161/ATVBAHA.117.309580

26. Lu RJ, Taylor S, Contrepois K, Kim M, Bravo JI, Ellenberger M, et al. Multi-omic profiling of primary mouse neutrophils predicts a pattern of sex and age-related functional regulation. *Nat Aging* (2021) 1:715–33. doi: 10.1038/s43587-021-00086-8

27. Sharma R, Kapila R, Haq MR, Salingati V, Kapasiya M, Kapila S. Age-associated aberrations in mouse cellular and humoral immune responses. *Aging Clin Exp Res* (2014) 26:353–62. doi: 10.1007/s40520-013-0190-y

28. Nomellini V, Brubaker AL, Mahbub S, Palmer JL, Gomez CR, Kovacs EJ. Dysregulation of neutrophil CXCR2 and pulmonary endothelial icam-1 promotes age-related pulmonary inflammation. *Aging Dis* (2012) 3:234–47.

29. Kovacs EJ, Palmer JL, Fortin CF, Fulop TJr., Goldstein DR, Linton PJ. Aging and innate immunity in the mouse: impact of intrinsic and extrinsic factors. *Trends Immunol* (2009) 30:319–24. doi: 10.1016/j.it.2009.03.012

30. Adrover JM, Del Fresno C, Crainiciuc G, Cuartero MI, Casanova-Acebes M, Weiss LA, et al. A neutrophil timer coordinates immune defense and vascular protection. *Immunity* (2019) 50:390–402.e310. doi: 10.1016/j.immuni.2019.01.002

31. Uhl B, Vadlau Y, Zuchtriegel G, Nekolla K, Sharaf K, Gaertner F, et al. Aged neutrophils contribute to the first line of defense in the acute inflammatory response. *Blood* (2016) 128:2327–37. doi: 10.1182/blood-2016-05-718999

32. Zhang D, Chen G, Manwani D, Mortha A, Xu C, Faith JJ, et al. Neutrophil ageing is regulated by the microbiome. *Nature* (2015) 525:528–32. doi: 10.1038/nature15367

33. FELASA working group on revision of guidelines for health monitoring of rodents and rabbits, Mähler Convenor M, Berard M, Feinstein R, Gallagher A, Illgen-Wilcke B, et al. FELASA recommendations for the health monitoring of mouse, rat, hamster, guinea pig and rabbit colonies in breeding and experimental units. *Lab Anim* (2014) 48:178–92. doi: 10.1177/0023677213516312

34. van 't Veer C, van den Pangaart PS, Kruijswijk D, Florquin S, de Vos AF, van der Poll T. Delineation of the role of toll-like receptor signaling during peritonitis by a gradually growing pathogenic escherichia coli. *J Biol Chem* (2011) 286:36603–18. doi: 10.1074/jbc.M110.189126

35. Pantarelli C, Pan D, Chetwynd S, Stark AK, Hornigold K, Machin P, et al. The GPCR adaptor protein norbin suppresses the neutrophil-mediated immunity of mice to pneumococcal infection. *Blood Adv* (2021) 5:3076–91. doi: 10.1182/bloodadvances.2020002782

36. Welch HC, Condliffe AM, Milne LJ, Ferguson GJ, Hill K, Webb LM, et al. P-Rex1 regulates neutrophil function. *Curr Biol* (2005) 15:1867–73. doi: 10.1016/j.cub.2005.09.050

37. Lawson C, Donald S, Anderson K, Patton D, Welch H. P-Rex1 and Vav1 cooperate in the regulation of fMLF-dependent neutrophil responses. *J Immunol* (2011) 186:1467–76. doi: 10.4049/jimmunol.1002738

38. Mocsai A, Abram CL, Jakus Z, Hu Y, Lanier LL, Lowell. CA. Integrin signaling in neutrophils and macrophages uses adaptors containing immunoreceptor tyrosine-based activation motifs. *Nat Immunol* (2006) 7:1326–33. doi: 10.1038/ni1407

39. Johnsson AE, Dai Y, Nobis M, Baker MJ, McGhee EJ, Walker S, et al. The rac-FRET mouse reveals tight spatiotemporal control of rac activity in primary cells and tissues. *Cell Rep* (2014) 6:1153–64. doi: 10.1016/j.celrep.2014.02.024

40. Clark J, Anderson KE, Juvin V, Smith TS, Karpe F, Wakelam MJ, et al. Quantification of PtdInsP3 molecular species in cells and tissues by mass spectrometry. *Nat Methods* (2011) 8:267–72. doi: 10.1038/nmeth.1564

41. Rynkiewicz NK, Anderson KE, Suire S, Collins DM, Karanasios E, Vadas O, et al. Gbetagamma is a direct regulator of endogenous p101/p110gamma and p84/p110gamma PI3Kgamma complexes in mouse neutrophils. *Sci Signal* (2020) 13:eaaz4003. doi: 10.1126/scisignal.aaz4003

42. Dutta S, Sengupta P. Men and mice: Relating their ages. *Life Sci* (2016) 152:244–8. doi: 10.1016/j.lfs.2015.10.025

43. Vogt KL, Summers C, Chilvers ER, Condliffe AM. Priming and de-priming of neutrophil responses *in vitro* and *in vivo*. *Eur J Clin Invest* (2018) 48:e12967. doi: 10.1111/eci.12967

44. Pieterse E, Rother N, Yanginlar C, Hilbrands LB, van der Vlag J. Neutrophils discriminate between lipopolysaccharides of different bacterial sources and selectively release neutrophil extracellular traps. *Front Immunol* (2016) 7:484. doi: 10.3389/fimmu.2016.00484

45. Pioli PD, Casero D, Montecino-Rodriguez E, Morrison SL, Dorshkind K. Plasma cells are obligate effectors of enhanced myelopoiesis in aging bone marrow. *Immunity* (2019) 51:351–366.e356. doi: 10.1016/j.immuni.2019.06.006

46. Borregaard N, Cowland JB. Granules of the human neutrophilic polymorphonuclear leukocyte. *Blood* (1997) 89:3503–21. doi: 10.1182/blood.V89.10.3503

47. Rorvig S, Ostergaard O, Heegaard NH, Borregaard N. Proteome profiling of human neutrophil granule subsets, secretory vesicles, and cell membrane: correlation with transcriptome profiling of neutrophil precursors. *J Leuk Biol* (2013) 94:711–21. doi: 10.1189/jlb.1212619

48. Cassatella MA, Ostberg NK, Tamassia N, Soehnlein O. Biological roles of neutrophil-derived granule proteins and cytokines. *Trends Immunol* (2019) 40:648–64. doi: 10.1016/j.it.2019.05.003

49. Gavin AL, Huang D, Huber C, Martensson A, Tardif V, Skog PD, et al. PLD3 and PLD4 are single-stranded acid exonucleases that regulate endosomal nucleic-acid sensing. *Nat Immunol* (2018) 19:942–53. doi: 10.1038/s41590-018-0179-y

50. Yang Y, Wang C, Cheng P, Zhang X, Li X, Hu Y, et al. CD180 ligation inhibits TLR7- and TLR9-mediated activation of macrophages and dendritic cells through the Lyn-SHP-1/2 axis in murine lupus. *Front Immunol* (2018) 9:2643. doi: 10.3389/fimmu.2018.02643

51. Guo X, Jiang H, Chen J, Zhang BF, Hu Q, Yang S, et al. RP105 ameliorates hypoxiareoxygenation injury in cardiac microvascular endothelial cells by suppressing TLR4MAPKsNF-kappaB signaling. *Int J Mol Med* (2018) 42:505–13. doi: 10.3892/ijmm.2018.3621

52. Hawkins PT, Stephens LR, Suire S, Wilson M. PI3K signaling in neutrophils. *Curr Top Microbiol Immunol* (2010) 346:183–202. doi: 10.1007/82_2010_40

53. Pantarelli C, Welch HCE. Rac-GTPases and rac-GEFs in neutrophil adhesion, migration and recruitment. *Eur J Clin Invest* (2018) 48:e12939. doi: 10.1111/eci.12939

54. Swift ME, Burns AL, Gray KL, DiPietro LA. Age-related alterations in the inflammatory response to dermal injury. *J Invest Dermatol* (2001) 117:1027–35. doi: 10.1046/j.0022-202x.2001.01539.x

55. Frisch BJ, Hoffman CM, Latchney SE, LaMere MW, Myers J, Ashton J, et al. Aged marrow macrophages expand platelet-biased hematopoietic stem cells *via* Interleukin1B. *JCI Insight* (2019) 5:e124213. doi: 10.1172/jci.insight.124213

56. Sauce D, Dong Y, Campillo-Gimenez L, Casulli S, Bayard C, Autran B, et al. Reduced oxidative burst by primed neutrophils in the elderly individuals is associated with increased levels of the CD16bright/CD62Ldim immunosuppressive subset. *J Gerontol A Biol Sci Med Sci* (2017) 72:163–72. doi: 10.1093/gerona/glw062

57. Bou Ghanem EN, Lee JN, Joma BH, Meydani SN, Leong JM, Panda A. The alpha-tocopherol form of vitamin e boosts elastase activity of human PMNs and their ability to kill streptococcus pneumoniae. *Front Cell Infect Microbiol* (2017) 7:161. doi: 10.3389/fcimb.2017.00161

58. Ortmann W, Kolaczkowska E. Age is the work of art? impact of neutrophil and organism age on neutrophil extracellular trap formation. *Cell Tissue Res* (2018) 371:473–88. doi: 10.1007/s00441-017-2751-4

59. McLeish KR, Merchant ML, Klein JB, Ward RA. Technical note: proteomic approaches to fundamental questions about neutrophil biology. *J Leuk Biol* (2013) 94:683–92. doi: 10.1189/jlb.1112591

60. Adrover JM, Aroca-Crevillen A, Crainiciuc G, Ostos F, Rojas-Vega Y, Rubio-Ponce A, et al. Programmed 'disarming' of the neutrophil proteome reduces the magnitude of inflammation. *Nat Immunol* (2020) 21:135–44. doi: 10.1038/s41590-019-0571-2

61. Zhu J, Zhang H, Guo T, Li W, Li H, Zhu Y, et al. Quantitative proteomics reveals differential biological processes in healthy neonatal cord neutrophils and adult neutrophils. *Proteomics* (2014) 14:1688–97. doi: 10.1002/pmic.201400009

62. Kawasaki T, Kawai T. Toll-like receptor signaling pathways. *Front Immunol* (2014) 5:461. doi: 10.3389/fimmu.2014.00461

63. Laird MH, Rhee SH, Perkins DJ, Medvedev AE, Piao W, Fenton MJ, et al. TLR4/MyD88/PI3K interactions regulate TLR4 signaling. *J Leuk Biol* (2009) 85:966–77. doi: 10.1189/jlb.1208763

64. Ferguson GJ, Milne L, Kulkarni S, Sasaki T, Walker S, Andrews S, et al. PI(3)Kγ has an important context-dependent role in neutrophil chemokinesis. *Nat Cell Biol* (2007) 9:86–91. doi: 10.1038/ncb1517

65. Chelvarajan RL, Liu Y, Popa D, Getchell ML, Getchell TV, Stromberg AJ, et al. Molecular basis of age-associated cytokine dysregulation in LPS-stimulated macrophages. *J Leuk Biol* (2006) 79:1314–27. doi: 10.1189/jlb.0106024

66. Boehmer ED, Goral J, Faunce DE, Kovacs EJ. Age-dependent decrease in toll-like receptor 4-mediated proinflammatory cytokine production and mitogen-activated protein kinase expression. *J Leuk Biol* (2004) 75:342–9. doi: 10.1189/jlb.0803389

67. Wong CP, Magnusson KR, Ho E. Aging is associated with altered dendritic cells subset distribution and impaired proinflammatory cytokine production. *Exp Gerontol* (2010) 45:163–9. doi: 10.1016/j.exger.2009.11.005

68. Paula C, Motta A, Schmitz C, Nunes CP, Souza AP, Bonorino C. Alterations in dendritic cell function in aged mice: potential implications for immunotherapy design. *Biogerontology* (2009) 10:13–25. doi: 10.1007/s10522-008-9150-x

69. van Duin D, Mohanty S, Thomas V, Ginter S, Montgomery RR, Fikrig E, et al. Age-associated defect in human TLR-1/2 function. *J Immunol* (2007) 178:970–5. doi: 10.4049/jimmunol.178.2.970

70. Qian F, Wang X, Zhang L, Chen S, Piecychna M, Allore H, et al. Age-associated elevation in TLR5 leads to increased inflammatory responses in the elderly. *Aging Cell* (2012) 11:104–10. doi: 10.1111/j.1474-9726.2011.00759.x

frontiers | Frontiers in Immunology

TYPE Original Research
PUBLISHED 25 August 2022
DOI 10.3389/fimmu.2022.927215

OPEN ACCESS

EDITED BY
Natalia Elguezabal,
NEIKER-Instituto Vasco de Investigación y Desarrollo Agrario, Spain

REVIEWED BY
Gina Pighetti,
Retired, Howard, PA, United States
Tabaran Alexandru Flaviu,
University of Agricultural Sciences and Veterinary Medicine of Cluj-Napoca, Romania

*CORRESPONDENCE
Jinfeng Miao
miaojinfeng@njau.edu.cn

SPECIALTY SECTION
This article was submitted to Comparative Immunology, a section of the journal Frontiers in Immunology

RECEIVED 24 April 2022
ACCEPTED 08 August 2022
PUBLISHED 25 August 2022

CITATION
Li M, Gao Y, Wang Z, Wu B, Zhang J, Xu Y, Han X, Phouthapane V and Miao J (2022) Taurine inhibits *Streptococcus uberis*-induced NADPH oxidase-dependent neutrophil extracellular traps *via* TAK1/MAPK signaling pathways. *Front. Immunol.* 13:927215. doi: 10.3389/fimmu.2022.927215

Taurine inhibits *Streptococcus uberis*-induced NADPH oxidase-dependent neutrophil extracellular traps *via* TAK1/MAPK signaling pathways

Ming Li[1], Yabing Gao[1], Zhenglei Wang[1], Binfeng Wu[1], Jinqiu Zhang[2], Yuanyuan Xu[1], Xiangan Han[3], Vanhnaseng Phouthapane[4] and Jinfeng Miao[1]*

[1]Ministry of Education Joint International Research Laboratory of Animal Health and Food Safety, Key Laboratory of Animal Physiology & Biochemistry, College of Veterinary Medicine, Nanjing Agricultural University, Nanjing, China, [2]National Research Center for Veterinary Vaccine Engineering and Technology of China, Jiangsu Academy of Agricultural Sciences, Nanjing, China, [3]Shanghai Veterinary Research Institute, Chinese Academy of Agricultural Sciences, Shanghai, China, [4]Department of Livestock and Fisheries, Ministry of Agriculture and Forestry, Vientiane, Laos

Neutrophil extracellular traps (NETs) are produced by neutrophil activation and usually have both anti-infective and pro-damage effects. *Streptococcus uberis* (*S. uberis*), one of the common causative organisms of mastitis, can lead to the production of NETs. Taurine, a free amino acid abundant in the organism, has been shown to have immunomodulatory effects. In this study, we investigated the molecular mechanisms of *S. uberis*-induced NETs formation and the regulatory role of taurine. The results showed that NETs had a disruptive effect on mammary epithelial cells and barriers, but do not significantly inhibit the proliferation of *S. uberis*. *S. uberis* induced NADPH oxidase-dependent NETs. TLR2-mediated activation of the MAPK signaling pathway was involved in this process. Taurine could inhibit the activation of MAPK signaling pathway and NADPH oxidase by modulating the activity of TAK1, thereby inhibiting the production of ROS and NETs. The effects of taurine on NADPH oxidase and NETs in *S. uberis* infection were also demonstrated *in vivo*. These results suggest that taurine can protect mammary epithelial cells and barriers from damage by reducing *S. uberis*-induced NETs. These data provide new insights and strategies for the prevention and control of mastitis.

KEYWORDS

taurine, *Streptococcus uberis*, neutrophil extracellular traps, NADPH oxidase, TAK1/MAPK

Introduction

Neutrophil extracellular traps (NETs) are extracellular web-like structures released by neutrophils after specific stimulation and are made up of a combination of DNA, histones, granule proteins, antimicrobial peptides and so on. The process of their release is called NETosis (1). It has been a hot topic of research in neutrophil biology due to its close association with pathological phenomena such as infectious inflammation, tumor behavior and tissue damage. In recent years, research on the link between NETs and mastitis has been gaining attention. Swain et al. found NETs only was detected in the milk of cows with clinical mastitis, but not subclinical mastitis (2, 3). The milk can affect the phagocytosis of pathogenic bacteria by neutrophils, but has no inhibitory effect on the formation of NETs (4). In addition, it has been suggested that NETs and their histone components can cause damage to mammary epithelial cells (5). These studies suggest that NETs may be related to the severity of mastitis. Therefore, understanding the mechanism of neutrophil NETosis and regulating it appropriately could help in the prevention and control of mastitis.

Different stimuli can induce NETs by different molecular mechanisms (6). NADPH oxidase, a key enzyme in redox signaling, is a major generator of reactive oxygen species (ROS) *in vivo*. ROS generation by NADPH oxidases have been shown to be involved in most of the mechanisms underlying NET induction. MAPK is an important cellular signal that regulates cellular immune defense, including extracellular signal-regulated kinase (ERK), p38 family of kinases, and c-Jun N-terminal kinases (JNK) (7). The MAPK signaling pathway has been reported to be associated with the formation of NADPH oxidase-mediated NETs induced by *Escherichia coli* (*E. coli*), *Streptococcus lactis* and *Streptococcus suis* (8–10). These studies suggest that the extent to which p38, ERK and JNK affect the formation of NETs is pathogen-specific. *Streptococcus uberis* (*S. uberis*) is by far the most common causative agent of *Streptococcus* mastitis, with increasing prevalence worldwide (11, 12). Reinhardt et al. reported the observation of NETs formation in *S. uberis*-infected mammary glands (13). However, it is unclear whether MAPK signaling pathway and NADPH oxidase are involved in the mechanisms underlying *S. uberis*-induced NETs.

Nutritional modulation has been shown to be a viable strategy for mastitis prevention and control. Taurine, as the most abundant free amino acid in the body, has anti-inflammatory, antioxidant, ion homeostasis and metabolic regulating functions (14). Neutrophils are important effector cells in the mammary gland inflammatory response. Taurine, present in neutrophils at levels of up to 20-50 mM, has a regulatory effect on the immune function of neutrophils (15). For example, taurine supplementation *in vitro* has been shown to down-regulate pro-inflammatory-related gene expression in bovine PMN and to improve cellular antioxidant properties (16). Our group has shown that taurine can alleviate mammary inflammation and protect the integrity of the blood-milk barrier in mice infected with *S. uberis*, indicating the regulatory effect of taurine on the mammary inflammatory response (17). Based on this, understanding the regulatory effect of taurine on NETosis will contribute to furthering reveal the protective effect of taurine on the mammary gland in *S. uberis* infection.

In the present study, we aimed to explore the molecular mechanisms of NETosis in *S. uberis* infection and the role of taurine. The data clearly demonstrated that *S. uberis* induced NADPH oxidase-dependent NETs *via* TLR2/TAK1/MAPK signaling pathway. Taurine was able to limit NETs formation by inhibiting TAK1 activity. This helps to reduce the disruption of the mammary epithelial barrier by NETs. These data provide new scientific basis for the use of taurine in the prevention and control of mastitis.

Materials and methods

Bacterial culture

S. uberis 0140J (ATCC, Manassas, USA) were inoculated into Todd-Hewitt broth (THB) supplemented with 2% fetal bovine serum in an orbital shaker at 37°C for 3-4 h until grown at an OD_{600} of 0.5-0.6 (about 1×10^9 CFU/mL).

Animals and model of mammary infection

Specific pathogen-free (SPF) C57BL/6 mice(WT-B6) were purchased from Nanjing Qinglongshan Animal Farm (Nanjing, China) and bred under specific pathogen-free conditions in the Nanjing Agricultural University Laboratory Anima Center. All procedures involving animals were approved by the committee on the Use and Care of Animals of Nanjing Agricultural University (Nanjing, China).

24 pregnant mice aged 8-10 weeks were randomly divided into 4 groups. Two groups (Taurine, Taurine+*S. uberis*) were treated with taurine. Mice received 200 mg/kg of taurine daily, suspended in physiological saline by intragastric gavage from gestation day 14 until parturition. The other groups (Control, *S. uberis*) were given only the equal volume of physiological saline. At 48 h after parturition, mice in the *S. uberis* and taurine+*S. uberis* groups were infused with approximately 1×10^7 CFU/mL *S. uberis* in 50 μL of sterile pyrogen-free saline into the L4 and R4 teats and 50 μL of saline was given to the control and taurine group. In detail, after administration of ether anesthesia, the L4

and R4 teats of mice were moistened with 75% ethanol, and a 33-gauge needle fitted to a 1 mL syringe was gently inserted into the mammary duct, then 50 μL of *S. uberis* or physiological saline was injected. At 24 h post infection, all mice in the 4 groups were euthanized, and the mammary gland and blood serum were collected and stored at -80°C until analyzed.

EpH4-Ev cells culture

EpH4-Ev cells (ATCC, Manassas, USA) were grown in Dulbecco's modified Eagle's medium (DMEM, Gibco, NY, USA) with 10% fetal bovine serum (FBS, Gibco, NY, USA) in 6-well plates until the confluence reached 70–80%.

Bone marrow neutrophil extraction and treatment

Neutrophils were isolated from 6-8 week old C57BL/6 mice (WT-B6) bone marrow as previously described (18). Tibias and femurs were collected from euthanized mice. Bone marrow were suspended in PBS buffer before overlaid on discontinuous percoll gradients (55%, 62%, and 81% in the order from top to bottom) (Solarbio, Beijing, China). After centrifugation at 1,000× g for 30 min, cells at the interface between 62% and 81% gradients were harvested and washed by 1640 medium. The cells were cultured in 1640 medium (Gibco, NY, USA) with 5% heat-inactivated FBS in a constant temperature cell incubator at 37°C and 5% CO_2. Cells were used in subsequent experiments when they reached more than 85% $Ly6G^+$ analyzed flow cytometry.

In the challenge experiments, the *S. uberis* grown at an OD_{600} of 0.5–0.6 was centrifuged for 10 min at 3,000× g and resuspended in an equal volume of PBS. Then this suspension was added to cells (MOI = 10). For the treatment experiments, neutrophils were pre-treated with taurine (Sigma, MO, USA), NAC (ROS scavenger, Beyotime, Nantong, China), DPI (NADPH oxidase inhibitor, Sellcek, TX, USA), mitoTEMPO (Mitochondria ROS scavenger, Cayman, MI, USA), Losmapimod (p38 inhibitor, TargetMOL, Shanghai, China), SCH772984 (ERK inhibitor, TargetMOL, Shanghai, China), SP600125 (JNK inhibitor, TargetMOL, Shanghai, China), NG25 (TAK1 inhibitor, Invitrogen, CA, USA) and TLR2 antibody (Affinity, OH, USA) 1 h before addition of *S. uberis*.

Cell viability assay

The effect of taurine on neutrophils viability was determined by CCK-8 assay (Solarbio, Beijing, China). Briefly, the cells were seeded at 1×10^4 cells/well in a 96-well plate and treated with different doses of taurine for 5 h. Then 10 μL of CCK-8 was added into each well and incubated for another 1 h. The optical density was measured at OD_{450}.

Fluorescent staining of NETs

The concentration of extracted neutrophils was adjusted to 5×10^6/mL using 1640 medium containing 5% heat-inactivated FBS, and 500 μL of cell suspension was added to each well of a 24-well plate. After adding *S. uberis* (MOI = 10), mix thoroughly and then centrifuge using 1,000× g for 10 min to spin down cells. Neutrophils were incubated at 37°C, 5% CO2 for 4 h. After incubation, adding SYTOX GREEN (1 μM) staining solution to treat for 10 min and observe directly under a fluorescent microscope.

NETs induction and quantification

The concentration of extracted neutrophils was adjusted to 5×10^6/mL using 1640 medium containing 5% heat-inactivated FBS, and 500 μL of cell suspension was added to each well of a 24-well plate. After stimulation by *S. uberis* (MOI = 10), the medium was removed and then 0.5 mL of 1640 medium was added to the well plate. Wells were treated with 0.1 mg/mL DNase I (Solarbio, Beijing, China) and incubated at 37°C for 10 min to partially digest NETs. The cell suspension was transferred to a sterile centrifuge tube by centrifugation at 500× g for 10 min and the cell free dsDNA supernatant was collected.

NETs in the supernatant and blood serum were quantified by measuring the dsDNA content in the supernatant according to the Quant-iT™ PicoGreen ® dsDNA kit instructions (Invitrogen, CA, USA).

Collection of NETs

To perform induction and isolation of the NETs, 5×10^6 neutrophils were stimulated for 4 h using 100 nM PMA (Solarbio, Beijing, China). The medium was removed and then 0.2 mL of DMEM was added to the well plate. Wells were treated with 0.1 mg/mL of DNase I and incubated at 37°C for 10 min to partially digest NETs. The cell suspension was transferred to a sterile centrifuge tube by centrifugation at 500× g for 10 min and the cell free dsDNA supernatant was collected. NETs in the supernatant were quantified by measuring the dsDNA content in the supernatant according to the Quant-iT™ PicoGreen ® dsDNA kit instructions.

LDH assays of EpH4-Ev cells

The lactate dehydrogenase (LDH) activity in EpH4-Ev cell supernatants were determined using commercial kits (Solarbio, Beijing, China) according to the manufacturer's instructions.

Measurement of mammary epithelial barrier permeability

EpH4-Ev cells were inoculated in the upper chamber of the Transwell (Millipore, MA, USA). The culture medium was changed 24 h after inoculation and every other day thereafter. The trans-epithelial cell resistance was measured using a Millicell resistivity meter. TEER value = (actual value - blank control assay)/bottom area of the chamber. The TEER increased significantly after about 5-7 d of cell culture, demonstrating the formation of a somatic mammary epithelial barrier model, and could be used for subsequent experimental studies when the TEER was > 1500 Ω/cm^2. Then NETs or DNase I (3 mg/mL) were added in the upper chamber. FITC-dextran (FITC-D, Sigma, MO, USA) was selected as a marker for paracellular transport. After stimulated for 12 h, the monolayer was washed and 200 μL of 1 mg/mL FITC-D was added to the upper chamber. After incubation for 1 h at 37°C and 5% CO_2, the sample from the lower chamber was collected. The fluorescence intensity of FITC-D in the samples (excitation wavelength 490 nm, emission wavelength 520 nm) was measured using a fluorescent enzyme marker.

Determination of the antibacterial effect of NETs

About 1×10^3 CFU/mL *S. uberis* 0140J was in sterilized DMEM medium containing 400 ng/mL NETs or DNase I (3 mg/mL) and incubated at 37°C for 4 h. Then the bacteria solution was diluted 10-fold with sterile saline in a gradient manner. The mixed dilution was evenly applied to a solid THB dish and incubated at 37°C for 24 h. Plates with CFU in the range of 30-300 were selected for counting and the number of viable colonies was calculated according to the dilution.

ROS determination

Intracellular ROS of neutrophils was stained by DCFH-DA according to the instructions (Beyotime, Nantong, China). Briefly, 1×10^6 neutrophils were infected with *S. uberis* 0140J at a MOI of 10 for 2 h, and then the cells were loaded with 10 μM DCFH-DA for 30 min at 37°C. Cells were washed 3 times with PBS. Next, they were collected at 1,000× g for 5 min and resuspended in PBS. The cell samples were immediately analyzed by flow cytometry using a FACSCanto instrument; 10 000 cells per sample were analyzed using CellQuest Pro acquisition software and FlowJo software.

Western blot

Total proteins were isolated from mouse mammary gland and neutrophils with RIPA lysis buffe (Solarbio, Beijing, China) with added 1 mM phenylmethylsulfonyl fluoride (PMSF, Solarbio, Beijing, China). The supernatants were collected by centrifuging at 12,000 rpm for 10 min at 4°C. Protein concentration was measured by bicinchoninic acid assay (BCA) (Beyotime, Nantong, China). About 30 μg protein lysates were separated on polyacrylamide gel by electrophoresis and transferred onto polyvinylidene difluoride (PVDF) membranes (Millipore, MA, USA). The membranes were blocked with 5% bovine serum albumin diluted in Tris buffered saline with Tween-20 (TBST) for 2 h at room temperature and hybridized overnight with primary antibody (1:1000) at 4°C. Before and after incubation with the HRP-linked anti-rabbit IgG (1:10000, CST, MA, USA) at room temperature for 2 h, the membranes were washed 3 times with TBST. The signals were detected by an ECL Western blot analysis system (Tanon, Shanghai, China). Analysis of bands was quantifed with ImageJ software (NIH, USA). The primary antibodies were listed as follows: β-actin (ABclonal, Wuhan, China), TAK1, p-TAK1 (CST, MA, USA), p38, p-p38, ERK, p-ERK, JNK, p-JNK, $p47^{phox}$, p-$p47^{phox}$ and TLR2 (Affinity, OH, USA).

Statistical analysis

All experiments were repeated at least 3 times. Results were analyzed using the GraphPad Prism 8.0 software (La Jolla, CA, USA). Data were expressed as means ± standard error of the mean (SEM). Differences were evaluated by one-way analysis of variance (ANOVA) followed by Tukey's tests and Student–Newman–Keuls test. Significant differences were $P < 0.05$.

Results

S. uberis induces NETs that cause damage to EpH4-Ev cells and mammary epithelial barrier damage

First, we found that *S. uberis* challenge of neutrophils for more than 2 h resulted in a significant increase in extracellular

dsDNA (Figure 1A). By STYOX Green fluorescence staining, we observed the reticulated DNA backbone of NETs (Figure 1B). So the extracellular DNA levels were quantified to evaluate the NET formation. This suggests that *S. uberis* could induce NETs formation. Next, we treated mammary epithelial cells and mammary epithelial barriers with NETs for 12 h. Treatment with NETs at 200 ng/mL and 400 ng/mL resulted in a significant increase on LDH activity of EpH4-Ev cell supernatants as well as mammary epithelial barrier permeability compared to controls. In contrast, pretreatment with DNase I enzyme significantly reduced the damage to cells and barrier by NETs (Figures 1C, D). In addition, we also found that 400 ng/mL of NETs had no significant effect on the proliferation of *S. uberis* (Figure 1E). These results suggest that NETs cause EpH4-Ev cell damage and disrupt mammary epithelial barrier integrity, but may have no effect on *S. uberis* proliferation.

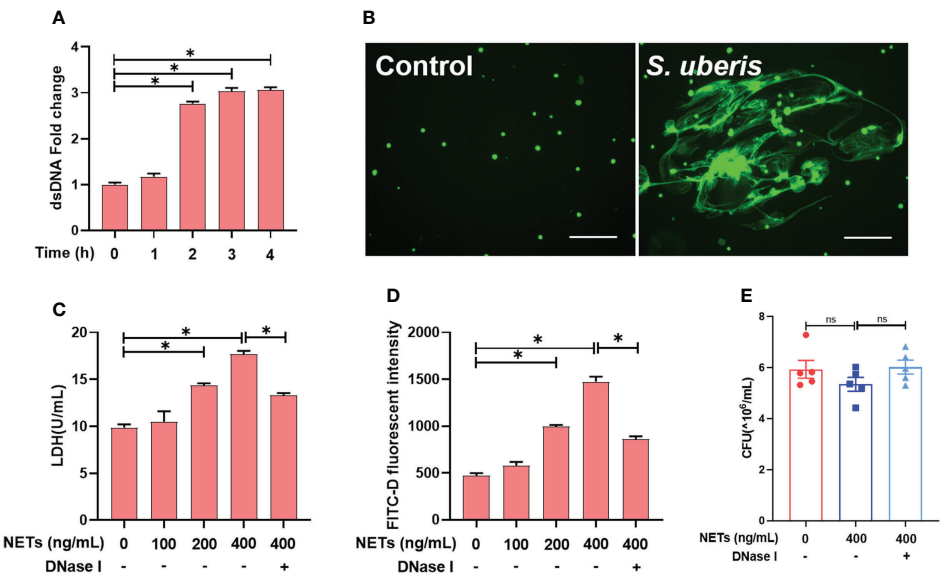

FIGURE 1
S. uberis induce NETs that cause damage to EpH4-Ev cells and mammary epithelial barrier damage. **(A, B)** Neutrophils were infected with *S. uberis* at MOI of 10. **(A)** The extracellular dsDNA content of neutrophils (n = 3). **(B)** SYTOX Green fluorescence staining of neutrophil extracellular dsDNA at 4 h after *S. uberis* stimulation (green) (n = 3). **(C, D)** EpH4-Ev cell and mammary epithelial barrier were treatment with NETs or DNase I (1.5 mg/mL) for 12 h. **(C)** LDH activity in EpH4-Ev cells supernatant (n = 3). **(D)** FITC-dextran (FITC-D) flux of mammary epithelial barrier (n = 3). **(E)** CFU of *S. uberis* (n = 5). Data are presented as mean ± SEM. **P* > 0.05. ns, not significant (P > 0.05).

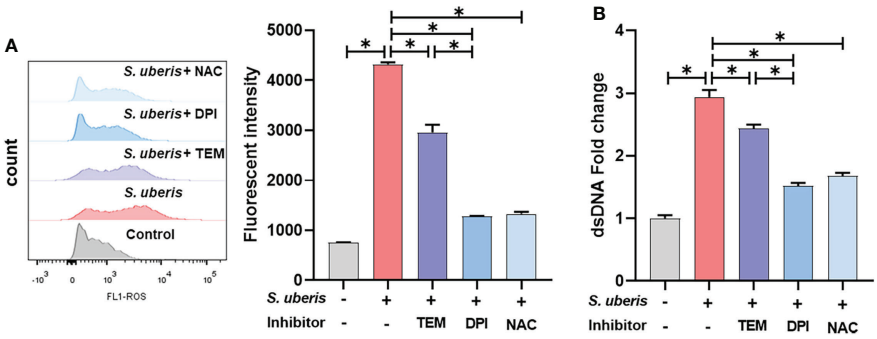

FIGURE 2
NADPH oxidase-mediated ROS dominate the production of NETs in *S. uberis* infection. The neutrophils were pretreated with NAC (5 mM), DPI (2 μM) and mitoTEMPO (TEM, 10 μM) for 1 h before infected with *S. uberis* at MOI of 10 for 2 h at 37°C. **(A)** The intracellular ROS level evaluated by Flow Cytometry. **(B)** The dsDNA content in supernatant. Data are presented as mean ± SEM (n = 3). **P* < 0.05.

NADPH oxidase-mediated ROS dominate the production of NETs in *S. uberis* infection

To investigate whether there is a link between *S. uberis*-induced NETs and ROS, NAC, DPI and mitoTEMPO were used to pretreat the cells. As shown, *S. uberis* significantly increased intracellular ROS levels compared to controls (Figure 2A). Pretreatment with NAC, mitoTEMPO or DPI significantly inhibited the *S. uberis*-induced rise in intracellular ROS and also significantly reduced the level of NETs in the supernatant. Moreover, DPI was significantly more effective than mitoTEMPO (Figures 2A, B). The results imply that NADPH oxidase-mediated ROS production in *S. uberis* infection is an important factor driving the formation of neutrophil NETs.

MAPK signaling pathway is involved in *S. uberis*-induced NADPH oxidase activation and ROS production

To further clarify the upstream signals mediating NADPH oxidase activation, we examined the effect of *S. uberis* on MAPK signaling activation. We found that *S. uberis* caused a significant increase in the phosphorylation levels of p38, ERK and JNK in neutrophils (Figure 3A). Moreover, pretreatment with Losmapimod, SCH772945 or SP6001255 significantly reduced the levels of $p47^{phox}$ phosphorylation and ROS (Figures 3B, C) and significantly downregulated the levels of NETs (Figure 3D). The results show that *S. uberis* induces NETs by activating NADPH oxidase production into ROS through the MAPK signaling pathway.

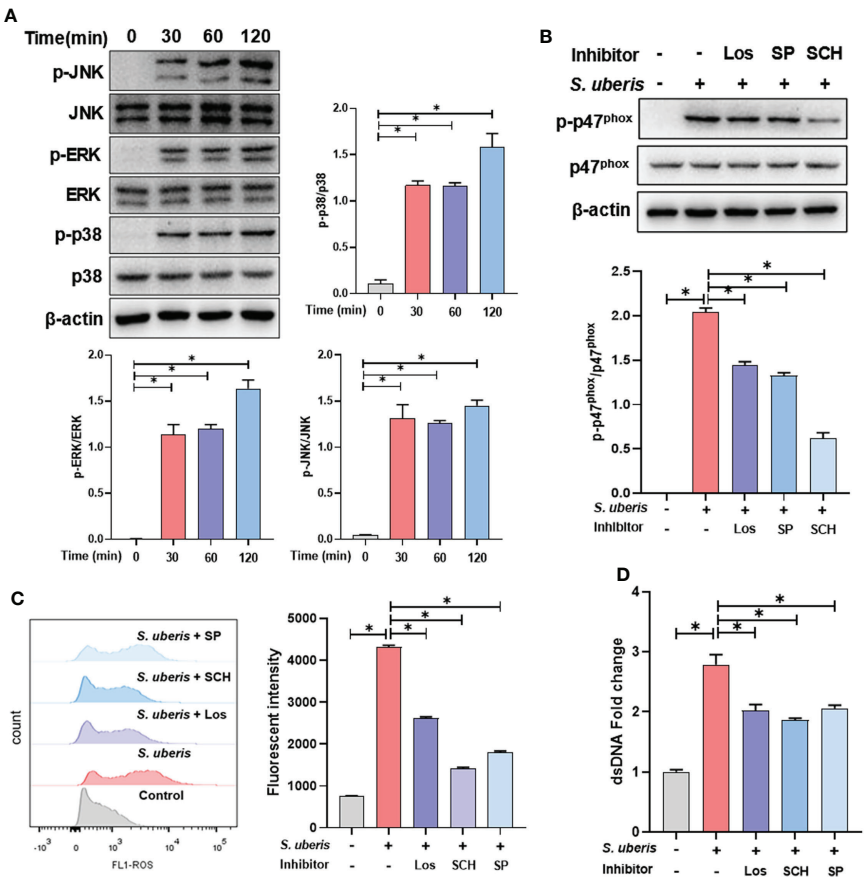

FIGURE 3
MAPK signaling pathway is involved in *S. uberis*-induced NADPH oxidase activation and ROS production. The neutrophils were pretreated with Losmapimod (Los, 20 μM), SCH772945 (SCH, 0.5 μM) and SP6001255 (SP, 10 μM) for 1 h before infected with *S. uberis* at MOI of 10. **(A)** Immunoblot and statistical analysis of neutrophil p38, ERK and JNK proteins and phosphorylated proteins. **(B)** Immunoblot and statistical analysis of neutrophil $p47^{phox}$ proteins and phosphorylated proteins at 2 h. **(C)** The Intracellular ROS level evaluated by Flow Cytometry at 2 h. **(D)** The dsDNA content in supernatant at 4 h. Data are presented as mean ± SEM (n = 3). *$P > 0.05$.

TLR2 mediates the activation of MAPK signaling pathways in *S. uberis* infection

To clarify whether TLR2 is involved in infection-induced MAPK signaling activation and NETosis, TLR2 antibodies were used to pretreat cells to block ligands from binding to TLR2. As shown in the figure, pretreatment with TLR2-containing antibodies significantly inhibited infection-induced increases in cellular p38, ERK, JNK and $p47^{phox}$ protein phosphorylation levels (Figure 4A). At the same time, TLR2 antibody also caused a significant down-regulation of neutrophil intracellular ROS and supernatant NETs levels in infection (Figures 4B, C). This suggests that TLR2 mediates the activation of MAPK signaling and NADPH oxidase in neutrophils stimulated by *S. uberis*, contributing to NETs production.

Taurine inhibits *S. uberis*-induced NETs production and MAPK signaling activation

Next, we explored the role of taurine in regulating the release of neutrophil NETs in infection. Taurine treatment for 5 h had no significant effect on cell viability compared to the control group (Figure 5A). Compared to the *S. uberis* group, pretreatment with 15 mM and 45 mM taurine resulted in a significant reduction in NETs levels in supernatants (Figure 5B), and also significantly reduced cellular p38, ERK and JNK protein phosphorylation levels (Figure 5C). This suggests that MAPK signaling pathway is involved in the inhibitory effect of taurine on neutrophil NETosis in *S. uberis* infection.

TAK1 is critical for the inhibition of MAPK signaling activation and NETs production by taurine in *S. uberis* infection

We further explored the regulatory mechanism of taurine on MAPK signaling pathway. Compared with the control group, TAK1 phosphorylation levels were significantly increased in the *S. uberis*-infected neutrophils. Taurine pretreatment significantly inhibited the phosphorylation level of neutrophil TAK1 in infection (Figure 6A). NG25, a TAK1 inhibitor, significantly inhibited the phosphorylation levels of p38, ERK, JNK and p47phox proteins, consistent with the effect of taurine (Figure 6B). Also, taurine and NG25 had a similar inhibitory effect on the production of neutrophil ROS and NETs (Figures 6C, D). These results suggest that taurine inhibits MAPK signaling pathway and NADPH oxidase activation by modulating TAK1 activity, thereby reducing the production of neutrophil ROS and NETs.

Taurine inhibits NAPDH oxidase activity and NETs production in *S. uberis*-induced mastitis in mice

Finally, we demonstrated the effect of taurine on neutrophil NETs production *in vivo* through a *S. uberis*-induced mice mastitis model. Taurine treatment significantly inhibited the increase in $p47^{phox}$ protein expression and phosphorylation levels in mammary tissue resulting from *S. uberis* infection (Figure 7A). This is consistent with the results of the *in vitro* assay. At the same time, *S. uberis* caused a significant upward

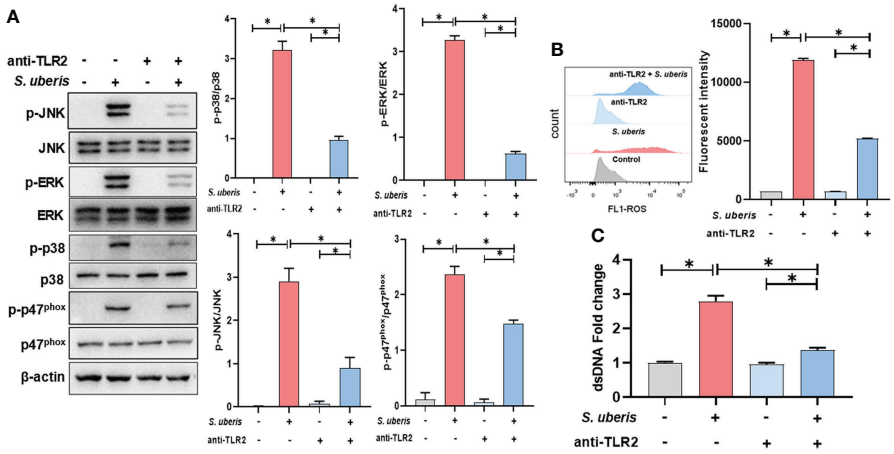

FIGURE 4
TLR2 mediates the activation of MAPK signaling pathways in *S. uberis* infection. The neutrophils were pretreated with TLR2-antibody (anti-TLR2, 100 ng/mL) for 1 h before infected with *S. uberis* at MOI of 10. **(A)** Immunoblot and statistical analysis of neutrophil p38, ERK, JNK and $p47^{phox}$ proteins and phosphorylated proteins at 2 h. **(B)** The Intracellular ROS level evaluated by Flow Cytometry at 2 h. **(C)** The dsDNA content in supernatant at 4 h. Data are presented as mean ± SEM (n = 3). $^*P < 0.05$.

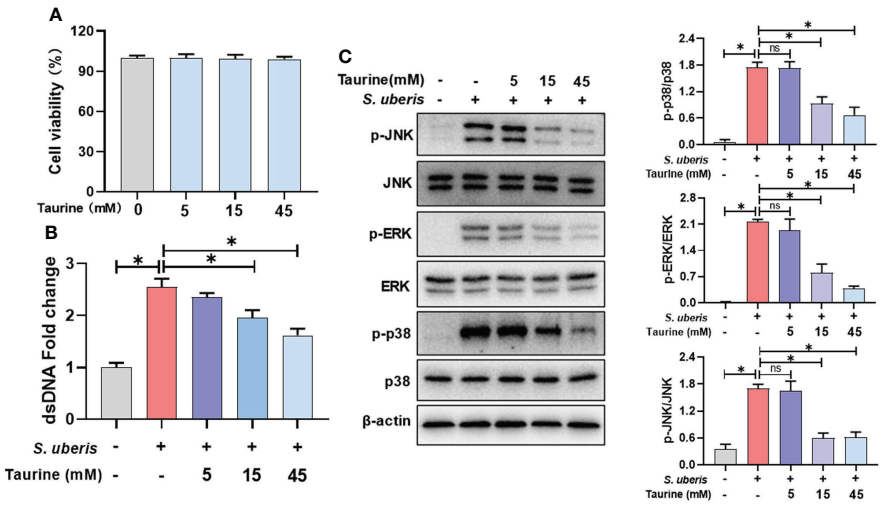

FIGURE 5
Taurine inhibits *S. uberis*-induced NETs production and MAPK signaling activation. The neutrophils were pretreated with taurine for 1 h before infected with *S. uberis* at MOI of 10. **(A)** The cell viabilities treated with taurine for 5 h detected by CCK-8 assay. **(B)** The dsDNA content in supernatant at 4 h. **(C)** Immunoblot and statistical analysis of p38, ERK and JNK proteins and phosphorylated proteins at 2 h. Data are presented as mean ± SEM (n = 3). **P* > 0.05. ns, not significant (P > 0.05).

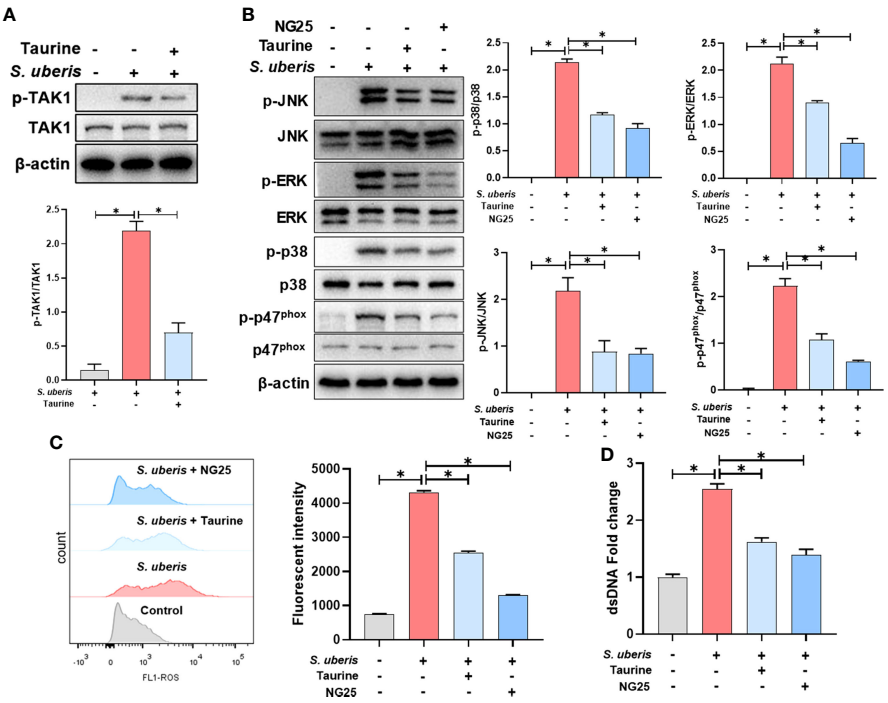

FIGURE 6
TAK1 is critical for the inhibition of MAPK signaling activation and NETs production by taurine in *S. uberis* infection. The neutrophils were pretreated with taurine (45 mM) or NG25 (40 nM) for 1 h before infected with *S. uberis* at MOI of 10. **(A)** Immunoblot and statistical analysis of TAK1 proteins and phosphorylated proteins. **(B)** Immunoblot and statistical analysis of p38, ERK, JNK and $p47^{phox}$ proteins and phosphorylated proteins. **(C)** The Intracellular ROS level evaluated by Flow Cytometry. **(D)** The dsDNA content in supernatant. Data are presented as mean ± SEM (n = 3). **P* < 0.05.

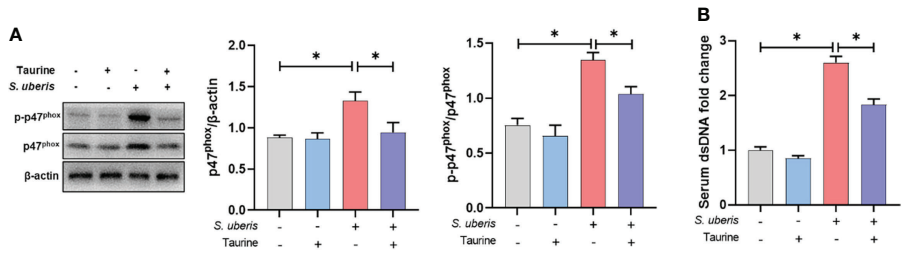

FIGURE 7
Taurine inhibits NAPDH oxidase activity and NETs production in *S. uberis*-induced mastitis in mice. **(A)** Immunoblot and statistical analysis of $p47^{phox}$ proteins and phosphorylated proteins. **(B)** The dsDNA change in serum. Data are presented as mean ± SEM (n = 6). *$P < 0.05$.

shift in the concentration of NETs in the serum of mice compared to the control group, while taurine significantly reduced the level of NETs (Figure 7B). This indicates that taurine has the same inhibitory effect on the production of NETs *in vivo*.

Discussion

Mastitis is an important disease that threatens the development of dairy farming. *S. uberis* is a common causative agent of mastitis and is capable of inducing NETs formation. In this study, we found that *S. uberis* induced NADPH oxidase-dependent NETs *via* TLR2/MAPK signaling. NETs are a double-edged sword for the host's immune defense system, which have been shown to cause damage to mammary epithelial cells. Here, the resultant data demonstrate taurine, a well-known nutrient, was able to inhibit NETosis by modulating the activity of TAK1 in *S. uberis* challenge. These data bring new insights into the prevention and control of mastitis.

Previous studies have found that most mammary pathogenic bacteria could induce NETosis (19). Such as *E. coli*, *Staphylococcus aureus* (*S. aureus*) and *Klebsiella pneumoniae* (19). Pisanu et al. detected NETs in the mammary gland alveoli and milk from *S. uberis*-infected sheep (20). In this study, we found that *in vitro S. uberis* stimulation of neutrophils induced NETs. It is well known that NETs usually have a dual role of being anti-infective and causing damage (1). The results of the present study showed that NETs at 200 and 400 ng/mL were able to cause damage to mammary epithelial cells, which is consistent with the findings of Wei et al (5). Moreover, we further found that NETs were able to disrupt the integrity of the mammary epithelial barrier, leading to increased permeability. However, the inhibitory effect of 400 ng/mL of NETs on *S. uberis* proliferation was not significant, suggesting that *S. uberis* may escape killing by NETs. It is not uncommon for pathogenic bacteria to escape killing by NETs. Many pathogenic bacteria have developed strategies to evade neutrophil immune defense mechanisms. For example, *S. aureus* can escape by secreting micrococcal nucleases to degrade NETs (21). Group A *Streptococci* have developed several strategies to evade NETs-dependent host defenses, including the expression of nucleases to degrade NETs (22, 23) and the inhibition of MPO release *via* M1T1 serotype *Streptococcal collagen*-like proteins (24). Indeed, it has been shown earlier that neutrophils have a limited role in host resistance to *S. uberis* infection and that the rise in neutrophil numbers induced by *S. uberis* infection failed to reduce CFU of bacteria in milk (25, 26). However, studies on the escape of *S. uberis* from killing by NETs have not been reported and the mechanism needs to be further investigated. In conclusion, the above results suggest that *S. uberis* is able to stimulate NETosis and may escape killing by NETs, implying that NETs may not play a role in the clearance of pathogenic bacteria in *S. uberis*-infected mastitis, but still cause damage to the mammary epithelial barrier. Therefore, limiting the formation of NETs is beneficial in alleviating the blood-milk barrier damage caused by *S. uberis* infection.

There are multiple ways in which neutrophils are affected by different stimuli to trigger NETosis, of which the typical triggering mechanisms can be categorized as NADPH oxidase-independent and NADPH-dependent pathways (6). The former is due to the transfer of large amounts of peptidylarginine deiminase 4 from the cytoplasm of neutrophils to the nucleus after binding to calcium ions, mediating histone periguanylation and subsequently promoting chromatin relaxation and release. The process is not dependent on the activation of NADPH oxidases. For example, *S. aureus*, *Candida albicans*, MIP-2, A23187 and ionomycin can induce NETosis through this mechanism (18, 27–29). The NADPH-dependent pathway is attributed to the activation of NADPH oxidase in neutrophils followed by the production of ROS, which then disassemble the nuclear membrane, allowing elastin and MPO to interact with the nucleus, thereby cleaving histones and promoting chromatin depolymerization. Eventually the neutrophil membrane is completely lost and the granular contents of the depolymerized DNA are released into the extracellular

environment. Stimuli that trigger this mechanism include PMA, Oxidized LDL, *Pseudomonas aeruginosa* and so on (30–32). Here, DPI, mitoTEMPO and NAC all significantly reduced the *S. uberis*-induced increase in ROS levels and NETs release. Notably, NADPH oxidase inhibitors (DPI) were significantly more effective than mitochondrial ROS scavengers (mitoTEMPO), implyting that NADPH oxidase-mediated ROS play a dominant role in *S. uberis*-induced NETs. This suggests that *S. uberis* is capable of inducing NADPH oxidase-dependent NETs.

Our previous experiments showed that *S. uberis* induced neutrophil infiltration and MAPK signaling pathway activation in mammary tissue (17). Here, we also found that *S. uberis* stimulated JNK, p38 and ERK signaling activation in neutrophils. NADPH oxidase is a multi-component enzyme system that is active only after the assembly of four cytoplasmic proteins, $p47^{phox}$, $p67^{phox}$, $p40^{phox}$ and Rac2, with the transmembrane proteins $p22^{phox}$ and $gp91^{phox}$. Phosphorylation of $p47^{phox}$ at Ser379 is required for its activation (33). MAPK signaling pathway is one of the important pathways that induce NADPH oxidase activation and NETs formation (34). For example, JNK activation turns on LPS and *E. coli*-induced NADPH oxidase-dependent suicidal NETosis (10). NADPH oxidase-derived reactive oxygen species production activates the ERK1/2 pathway in *Streptococcus agalactiae*-induced NETs formation (8). *Streptococcus Suis* serotype 2 stimulates NETs formation *via* activation of both p38 and ERK1/2 (9). In this study, inhibition of p38, ERK and JNK all prevented *S. uberis*-induced phosphorylation levels of the $p47^{phox}$ and reduced the production of ROS and NETs. In addition, TLR2 has an important role in the innate immune response of mammary tissue and mammary epithelial cells induced in *S. uberis* infection (7, 35). Here, the use of neutralizing antibodies to block TLR2 was able to reduce MAPK signaling and NADPH oxidase activation levels and decrease NETs formations. These results suggest that TLR2-mediated activation of the MAPK signaling pathway and NADPH oxidase leads to NETosis in *S. uberis* infection.

Because of the damaging effects of NETs, a growing number of studies have identified NETs as a therapeutic target for inflammatory diseases (36). Wang et al. showed that treatment with the peptidyl arginine deiminase inhibitor Cl-amidine could inhibit the release of NETs to reduce LPS-induced pathological damage in mouse mammary glands (37). Antioxidants are often used as NETosis modulators due to the close association of ROS with NETosis (33). Taurine is involved in the maintenance of neutrophil redox homeostasis (15). It has been reported taurine has prorotective effect on respiratory burst activity of polymorphonuclear leukocytes in endotoxemia (27). Abdelmegeid et al. showed that taurine supplementation down-regulated the expression of inflammation-related genes in bovine neutrophils (16). *In vitro* taurine exogenous taurine reduced the production of NETs stimulated by PMA and HOCl (38). Moreover, its derivative TauCl could also inhibit the production of NETs under PMA stimulation (39). We found 15 mM and 45 mM taurine pretreatment significantly inhibited *S. uberis*-induced NETs. At the same time, taurine also inhibited MAPK signaling pathway activation, consistent with the results of previous animal experiments (17). TAK1 is a member of the mitogen-activated protein kinase kinase family and is functionally located downstream of TLR2 (40). Further studies revealed that taurine was able to reduce the activation of TAK1. The inhibitory effects of TAK1 inhibitor (NG25) on MAPK signaling and NADPH oxidase activation were similar to those of taurine. These results suggest that taurine is able to inhibit MAPK/NADPH oxidase activation by modulating TAK1 activity in neutrophils, thereby limiting of NETs formation.

Our previous studies have demonstrated the ability of taurine to inhibit MAPK signaling activation in mice mammary tissue caused by *S. uberis* infection and to protect the blood-milk barrier (17). Here, taurine inhibited the expression of the $p47^{phox}$ in *S. uberis*-infected mammary tissue, consistent with previous findings in a rat animal model (41). As a brief addition, we further found that taurine also had an inhibitory effect on the phosphorylation of the $p47^{phox}$ which reflect NADPH oxidase activity and was able to significantly reduce the concentration of NETs in serum. It is important to note that these data do not prove that taurine has a direct effect on neutrophil NADPH activation and NETosis *in vivo*. Because a reduction in neutrophil trafficking to the gland, which has been shown by our previous studies (17), would also contribute to this result. However, it is sufficient to suggests that taurine may protect the blood-milk barrier from disruption by reducing NADPH oxidase activity and NETs formation.

In summary, *S. uberis* induced the formation of NETs by activating the neutrophil TLR2/TAK1/MAPK signaling pathway to drive NADPH oxidase production of ROS. Taurine was able to inhibit MAPK/NADPH oxidase activation by regulating TAK1 activity. Limiting effect of taurine on NETs contributes to reducing the disruption of the mammary epithelial barrier.

Data availability statement

The original contributions presented in the study are included in the article/Supplementary Material. Further inquiries can be directed to the corresponding author.

Ethics statement

All procedures involving animals were approved by the committee on the Use and Care of Animals of Nanjing Agricultural University (Nanjing, China).

Author contributions

ML performed the whole experiments and wrote the manuscript. YG and ZW participated in the design of this study. BW and JZ provided assistance for data acquisition, data analysis, and statistical analysis. YX collected important background information. XH provided the support platform and funding. VP performed manuscript review. JM carried out the definition of intellectual content and provided the support platform and funding. All authors read and approved the final manuscript.

Funding

This project was supported by grants from the Shanghai Agriculture Applied Technology Development Program, China (No. 2020-02-08-00-08-F01489); the National Natural Science Foundation of China (No. 32072867 and 31772701), the Special Fund for Independent Innovation of Agricultural Science and Technology in Jiangsu Province of China (No. cx (20) 3157), Key Scientific and Technological Project of XPCC (No. 2020AB025), the Key Project of Inter-governmental International Scientific and Technological Innovation Cooperation (No. 2018YFE0102200), Postgraduate Research & Practice Innovation Program of Jiangsu Province (KYCX22-0781, SJCX21-0240) and the Project Funded by the Priority Academic Program Development of Jiangsu Higher Education Institutions.

Acknowledgments

The authors express their thanks to Dr. Howard Gelberg (Oregon State University) for manuscript editing.

Conflict of interest

The authors declare that the research was conducted in the absence of any commercial or financial relationships that could be construed as a potential conflict of interest.

Publisher's note

References

1. Burgener SS, Schroder K. Neutrophil extracellular traps in host defense. *Cold Spring Harb Perspect Biol* (2020) 12:1–15. doi: 10.1101/cshperspect.a037028

2. Swain DK, Kushwah MS, Kaur M, Dang AK. Neutrophil dynamics in the blood and milk of crossbred cows naturally infected with staphylococcus aureus. *Vet World* (2015) 8:336–45. doi: 10.14202/vetworld.2015.336-345

3. Swain DK, Kushwah MS, Kaur M, Patbandha TK, Mohanty AK, Dang AK. Formation of NET, phagocytic activity, surface architecture, apoptosis and expression of toll like receptors 2 and 4 (TLR2 and TLR4) in neutrophils of mastitic cows. *Vet Res Commun* (2014) 38:209–19. doi: 10.1007/s11259-014-9606-1

4. Lippolis JD, Reinhardt TA, Goff JP, Horst RL. Neutrophil extracellular trap formation by bovine neutrophils is not inhibited by milk. *Vet Immunol Immunopathol* (2006) 113:248–55. doi: 10.1016/j.vetimm.2006.05.004

5. Wei Z, Wang J, Wang Y, Wang C, Liu X, Han Z, et al. Effects of neutrophil extracellular traps on bovine mammary epithelial cells *in vitro*. *Front Immunol* (2019) 10:1003. doi: 10.3389/fimmu.2019.01003

6. Ravindran M, Khan MA, Palaniyar N. Neutrophil extracellular trap formation: Physiology, pathology, and pharmacology. *Biomolecules* (2019) 4:1–15. doi: 10.3390/biom9080365

7. Li B, Wan Z, Wang Z, Zuo J, Xu Y, Han X, et al. TLR2 signaling pathway combats streptococcus uberis infection by inducing mitochondrial reactive oxygen species production. *Cells* (2020) 9:494. doi: 10.3390/cells9020494

8. Ma F, Yang S, Zhou M, Lu Y, Deng B, Zhang J, et al. NADPH oxidase-derived reactive oxygen species production activates the ERK1/2 pathway in neutrophil extracellular traps formation by streptococcus agalactiae isolated from clinical mastitis bovine. *Vet Microbiol* (2022) 268:109427. doi: 10.1016/j.vetmic.2022.109427

9. Ma F, Chang X, Wang G, Zhou H, Ma Z, Lin H, et al. Streptococcus suis serotype 2 stimulates neutrophil extracellular traps formation *via* activation of p38 MAPK and ERK1/2. *Front Immunol* (2018) 9:2854. doi: 10.3389/fimmu.2018.02854

10. Khan MA, Farahvash A, Douda DN, Licht JC, Grasemann H, Sweezey N, et al. JNK activation turns on LPS-and gram-negative bacteria-induced NADPH oxidase-dependent suicidal NETosis. *Sci Rep* (2017) 7(1):3409. doi: 10.1038/s41598-017-03257-z

11. Cvetnic L, Samardžija M, Habrun B, Kompes G, Benic M. Microbiological monitoring of mastitis pathogens in the control of udder health in dairy cows. *Slov Vet Res* (2016) 53:131–40.

12. Phuektes P, Mansell PD, Dyson RS, Hopper ND, Dick JS, Browning GF. Molecular epidemiology of streptococcus uberis isolates from dairy cows with mastitis. *J Clin Microbiol* (2001) 39:1460–6. doi: 10.1128/JCM.39.4.1460-1466.2001

13. Reinhardt TA, Sacco RE, Nonnecke BJ, Lippolis JD. Bovine milk proteome: Quantitative changes in normal milk exosomes, milk fat globule membranes and whey proteomes resulting from staphylococcus aureus mastitis. *J Proteomics* (2013) 82:141–54. doi: 10.1016/j.jprot.2013.02.013

14. Schuller-Levis GB, Park E. Taurine: new implications for an old amino acid. *FEMS Microbiol Lett* (2003) 226:195–202. doi: 10.1016/S0378-1097(03)00611-6

15. Surai PF, Earle-payne K, Kidd MT. Taurine as a natural antioxidant: From direct antioxidant effects to protective action in various toxicological models. *Antioxidants* (2021) 10:1876. doi: 10.3390/antiox10121876

16. Abdelmegeid MK, Vailati-Riboni M, Alharthi A, Batistel F, Loor JJ. Supplemental methionine, choline, or taurine alter *in vitro* gene network expression of polymorphonuclear leukocytes from neonatal Holstein calves. *J Dairy Sci* (2017) 100:3155–65. doi: 10.3168/jds.2016-12025

17. Li M, Wang Z, Qiu Y, Fu S, Xu Y, Han X, et al. Taurine protects blood-milk barrier integrity *via* limiting inflammatory response in streptococcus uberis infections. *Int Immunopharmacol* (2021) 101(Pt B):108371. doi: 10.1016/j.intimp.2021.108371

18. Wu SY, Weng CL, Jheng MJ, Kan HW, Hsieh ST, Liu FT, et al. Candida albicans triggers NADPH oxidase-independent neutrophil extracellular traps through dectin-2. *PloS Pathog* (2019) 15:e1008096. doi: 10.1371/journal.ppat.1008096

19. Worku M, Rehrah D, Ismail HD, Asiamah E, Adjei-Fremah S. A review of the neutrophil extracellular traps (Nets) from cow, sheep and goat models. *Int J Mol Sci* (2021) 22:8046. doi: 10.3390/ijms22158046

20. Pisanu S, Cubeddu T, Pagnozzi D, Rocca S, Cacciotto C, Alberti A, et al. Neutrophil extracellular traps in sheep mastitis. *Vet Res* (2015) 46:59. doi: 10.1186/s13567-015-0196-x

21. von Köckritz-Blickwede M, Winstel V. Molecular prerequisites for neutrophil extracellular trap formation and evasion mechanisms of staphylococcus aureus. *Front Immunol* (2022) 13:836278. doi: 10.3389/fimmu.2022.836278

22. Walker MJ, Hollands A, Sanderson-Smith ML, Cole JN, Kirk JK, Henningham A, et al. DNase Sda1 provides selection pressure for a switch to invasive group a streptococcal infection. *Nat Med* (2007) 13:981–5. doi: 10.1038/nm1612

23. Sumby P, Barbian KD, Gardner DJ, Whitney AR, Welty DM, Long RD, et al. Extracellular deoxyribonuclease made by group a streptococcus assists pathogenesis by enhancing evasion of the innate immune response. *Proc Natl Acad Sci U.S.A.* (2005) 102:1679–84. doi: 10.1073/pnas.0406641102

24. Döhrmann S, Anik S, Olson J, Anderson EL, Etesami N, No H, et al. Role for streptococcal collagen-like protein 1 in M1T1 group a streptococcus resistance to neutrophil extracellular traps. *Infect Immun* (2014) 82:4011–20. doi: 10.1128/IAI.01921-14

25. Thomas LH, Haider W, Hill AW, Cook RS. Pathologic findings of experimentally induced streptococcus uberis infection in the mammary gland of cows. *Am J Vet Res* (1994) 55:1723–8.

26. Leigh JA, Field TR, Williams MR. Two strains of streptococcus uberis, of differing ability to cause clinical mastitis, differ in their ability to resist some host defence factors. *Res Vet Sci* (1990) 49:85–7. doi: 10.1016/s0034-5288(18)31052-x

27. Ekremoğlu M, Türközkan N, Erdamar H, Kurt Y, Yaman H. Protective effect of taurine on respiratory burst activity of polymorphonuclear leukocytes in endotoxemia. *Amino Acids* (2007) 32:413–7. doi: 10.1007/s00726-006-0382-2

28. Pilsczek FH, Salina D, Poon KKH, Fahey C, Yipp BG, Sibley CD, et al. A novel mechanism of rapid nuclear neutrophil extracellular trap formation in response to staphylococcus aureus. *J Immunol* (2010) 185(12):7413–25. doi: 10.4049/jimmunol.1000675

29. Farley K, Stolley JM, Zhao P, Cooley J, Remold-O'Donnell E. A SerpinB1 regulatory mechanism is essential for restricting neutrophil extracellular trap generation. *J Immunol* (2012) 189(9):4574–81. doi: 10.4049/jimmunol.1201167

30. Awasthi D, Nagarkoti S, Sadaf S, Chandra T, Kumar S, Dikshit M. Glycolysis dependent lactate formation in neutrophils: A metabolic link between NOX-dependent and independent NETosis. *Biochim Biophys Acta - Mol Basis Dis* (2019) 1865(12):165542. doi: 10.1016/j.bbadis.2019.165542

31. Awasthi D, Nagarkoti S, Kumar A, Dubey M, Singh AK, Pathak P, et al. Oxidized LDL induced extracellular trap formation in human neutrophils *via* TLR-PKC-IRAK-MAPK and NADPH-oxidase activation. *Free Radic Biol Med* (2016) 93:190–203. doi: 10.1016/j.freeradbiomed.2016.01.004

32. Yoo D, Winn M, Pang L, Moskowitz SM, Malech HL, Leto TL, et al. Release of cystic fibrosis airway inflammatory markers from pseudomonas aeruginosa – stimulated human neutrophils involves NADPH oxidase-dependent extracellular DNA trap formation. *J Immunol* (2014) 192(10):4728–38. doi: 10.4049/jimmunol.1301589

33. Nguyen GT, Green ER, Mecsas J. Neutrophils to the ROScue: Mechanisms of NADPH oxidase activation and bacterial resistance. *Front Cell Infect Microbiol* (2017) 7:373. doi: 10.3389/fcimb.2017.00373

34. Belambri SA, Rolas L, Raad H, Hurtado-Nedelec M, Dang PMC, El-Benna J. NADPH oxidase activation in neutrophils: Role of the phosphorylation of its subunits. *Eur J Clin Invest* (2018) 48:e12951. doi: 10.1111/eci.12951

35. Wan Z, Wang X, Liu M, Zuo J, Xu Y, Han X, et al. Role of toll-like receptor 2 against streptococcus uberis infection in primary mouse mammary epithelial cells. *Int Immunopharmacol* (2020) 79:106142. doi: 10.1016/j.intimp.2019.106142

36. McCarthy CG, Saha P, Golonka RM, Wenceslau CF, Joe B, Vijay-Kumar M. Innate immune cells and hypertension: Neutrophils and neutrophil extracellular traps (nets). *Compr Physiol* (2021) 11:1575–89. doi: 10.1002/cphy.c200020

37. Wang C, Wang J, Liu X, Han Z, Jiang A, Wei Z, et al. Cl-amidine attenuates lipopolysaccharide-induced mouse mastitis by inhibiting NF-κB, MAPK, NLRP3 signaling pathway and neutrophils extracellular traps release. *Microb Pathog* (2020) 149:104530. doi: 10.1016/j.micpath.2020.104530

38. Palmer LJ, Cooper PR, Ling MR, Wright HJ, Huissoon A, Chapple ILC. Hypochlorous acid regulates neutrophil extracellular trap release in humans. *Clin Exp Immunol* (2012) 167:261–8. doi: 10.1111/j.1365-2249.2011.04518.x

39. Kim DG, Kwon YM, Kang IS, Kim C. Taurine chloramine selectively regulates neutrophil degranulation through the inhibition of myeloperoxidase and upregulation of lactoferrin. *Amino Acids* (2020) 52:1191–9. doi: 10.1007/s00726-020-02886-5

40. Cohen P, Strickson S. The role of hybrid ubiquitin chains in the MyD88 and other innate immune signalling pathways. *Cell Death Differ* (2017) 24:1153–9. doi: 10.1038/cdd.2017.17

41. Miao J, Zhang J, Ma Z, Zheng L. The role of NADPH oxidase in taurine attenuation of streptococcus uberis-induced mastitis in rats. *Int Immunopharmacol* (2013) 16:429–35. doi: 10.1016/j.intimp.2013.05.007

frontiers | Frontiers in Immunology

TYPE Original Research
PUBLISHED 29 September 2022
DOI 10.3389/fimmu.2022.1014296

OPEN ACCESS

EDITED BY
Guoshun Wang,
Louisiana State University Health Sciences Center, United States

REVIEWED BY
Andre Luis Lacerda Bachi,
Universidade Santo Amaro, Brazil
Huaping Zheng,
Sichuan University, China

*CORRESPONDENCE
Li Kang
kang0724@163.com
Hao He
hehao3000@qq.com

†These authors have contributed equally to this work

SPECIALTY SECTION
This article was submitted to Inflammation, a section of the journal Frontiers in Immunology

RECEIVED 08 August 2022
ACCEPTED 15 September 2022
PUBLISHED 29 September 2022

CITATION
Tang L, Cai N, Zhou Y, Liu Y, Hu J, Li Y, Yi S, Song W, Kang L and He H (2022) Acute stress induces an inflammation dominated by innate immunity represented by neutrophils in mice. *Front. Immunol.* 13:1014296. doi: 10.3389/fimmu.2022.1014296

Acute stress induces an inflammation dominated by innate immunity represented by neutrophils in mice

Lanjing Tang[1,2†], Nannan Cai[3†], Yao Zhou[1], Yi Liu[4], Jingxia Hu[1], Yalin Li[1], Shuying Yi[1], Wengang Song[2], Li Kang[1*] and Hao He[1,2*]

[1]Department of Immunology, Shandong First Medical University & Shandong Academy of Medical Sciences, Jinan, China, [2]Shandong Provincial Key Laboratory for Rheumatic Disease and Translational Medicine, The First Affiliated Hospital of Shandong First Medical University & Shandong Provincial Qianfoshan Hospital, Jinan, China, [3]Department of Ophthalmology, Taian Maternity and Child Health Hospital, Taian, China, [4]Department of Pediatrics, Taian Maternity and Child Health Hospital, Taian, China

It is well known that psychological stress could affect the immune system and then regulate the disease process. Previous studies mostly focused on the effects of chronic stress on diseases and immune cells. How acute stress affects the immune system remains poorly understood. In this study, after 6 hours of restraint stress or no stress, RNA was extracted from mouse peripheral blood followed by sequencing. Through bioinformatics analysis, we found that when compared with the control group, differentially expressed genes in the stress group mainly displayed up-regulated expression. Gene set enrichment analysis results showed that the enriched gene terms were mainly related to inflammatory response, defense response, wounding response, wound healing, complement activation and pro-inflammatory cytokine production. In terms of cell activation, differentiation and chemotaxis, the enriched gene terms were related to a variety of immune cells, among which neutrophils seemed more active in stress response. The results of gene set variation analysis showed that under acute stress, the inflammatory reaction dominated by innate immunity was forming. Additionally, the concentration of serum IL-1β and IL-6 increased significantly after acute stress, indicating that the body was in an inflammatory state. Importantly, we found that acute stress led to a significant increase in the number of neutrophils in peripheral blood, while the number of T cells and B cells decreased significantly through flow cytometric analysis. Through protein-protein interaction network analysis, we screened 10 hub genes, which mainly related to inflammation and neutrophils. We also found acute stress led to an up-regulation of *Ccr1, Ccr2, Xcr1* and *Cxcr2* genes, which were involved in cell migration and chemotaxis. Our data suggested that immune cells were ready to infiltrate into tissues in emergency through blood vessels under acute stress. This hypothesis was supported in LPS-induced acute inflammatory models. After 48 hours of LPS treatment, flow cytometric analysis showed that the lungs of mice with acute stress were characterized by increased neutrophil infiltration, decreased T cell and B cell

infiltration. Immunohistochemical analysis also showed that acute stress led to more severe lung inflammation. If mice received repeat acute stress and LPS stimulation, the survival rate was significantly lower than that of mice only stimulated by LPS. Altogether, acute stress led to rapid mobilization of the immune system, and the body presented an inflammatory state dominated by innate immune response represented by neutrophils.

KEYWORDS

acute stress, bioinformatics, inflammation, neutrophils, peripheral blood

Introduction

Psychological stress is the process of psychological and physiological changes caused by the body's awareness of the threat of stressors through cognition and evaluation (1, 2). Psychological stress beyond individual tolerance is often the source of many diseases. Depression, cardiovascular diseases, tumors, inflammatory bowel diseases and autoimmune diseases are closely related to psychological stress (3–8). With the transformation from traditional medical model to biopsychosocial model (9), the role of psychological stress in the occurrence and development of diseases has drawn increasing attention.

Stress is usually be regarded as the experience of anticipating or encountering adversity, while stress response is the non-specific response of the body to stressors. According to the duration of stimulation, stress can be divided into acute stress and chronic stress (10). The effects of acute stress and chronic stress are different. It is generally believed that chronic stress is harmful to health (11–13), while acute stress is conducive to life survival (14). Current evidence supports that stress regulates the process of disease by affecting the immune system (15–17). At present, most studies focused on the effects of chronic stress on diseases and immune cells. However, acute stress is the basis of chronic stress and may determine the direction of chronic stress-induced response. How acute stress affects the immune system remains poorly understood. Here, we studied the effects of acute stress on gene transcription in peripheral blood cells of mice through bioinformatics analysis, and detected the changes of blood cell populations under acute stress. We further explored the effect of acute stress on the pathological state of the body. Given that the effect of acute stress gradually attenuates with the removal of stressor, it is a good choice to verify in the acute inflammation model. Therefore, LPS-induced acute inflammation model widely used in medical research was selected as the verifier. Our data showed that acute stress led to rapid mobilization of the immune system, and the body presented an inflammatory state dominated by innate immune response represented by neutrophils.

Materials and methods

Mice

Female C57BL/6 (B6; H-2 Kb) mice, aged 6-8 weeks, were purchased from Charles River (Beijing, China). All mice were maintained in specific pathogen–free (SPF) conditions. All protocols involving animals were in compliance with the experimental guidelines approved by the Laboratory Animal Care Committee of Shandong First Medical University & Shandong Academy of Medical Sciences.

Stress model and LPS administration

Stress model was prepared as described previously (18). Briefly, mice were placed in a 50-ml conical centrifuge tube filled with multiple punctures to allow ventilation without food and water supply. The control littermates were kept in normal cage and were not supplied with food and water during the stress. After 6 hours of restrain stress, peripheral blood cells were obtained for flow cytometric analysis. In other experiments, mice received restrain stress followed by intraperitoneal injection with 2 mg/kg LPS diluted in PBS (E.coli, serotype 0111:b4; Sigma-Aldrich) or the same volume of PBS. 48 hours later, mice were killed and the lung tissues were taken for flow cytometric analysis and H&E staining. In other cases, mice received daily restraint stress and LPS injection, and their mortality was monitored.

ELISA assay

After mice received restraint stress or no stress for 6 hours, mouse serum was collected. Concentration of IL-1β, IL-6 and TNF-α in the serum were determined by ELISA Ready-SET-Go Kit (eBioscience) according to the manufacturers' protocol.

Bulk RNA-seq

Peripheral blood was obtained from mice with or without stress. RNA were extracted by using Illumina TruSeq RNA Sample Prep Kit (Illumina) according to the manufacturer's instructions. RNA-seq libraries were prepared using standard Illumina protocols, followed by sequencing on an Illumina NovaSeq6000 instrument. RNA sequencing data have been saved in the NCBI GEO database for public access. GEO accession number is GSE210252.

DEG identification

Dimension reduction analysis of RNA-seq was performed using R package Rtsne (19). R package DESeq2 was used to identify differentially expressed genes (DEG). Log2 fold change (FC) was used to evaluate the degree of gene expression difference. The adjusted p value (adj.P.Val) was used to avoid the occurrence of false-positive results. Compared with control group, genes with | log2FC | >1 and adj.P.Val < 0.01 were regarded as DEG in stress group. R package ggplot2 and pheatmap were used to visualize the identified DEG by generating volcano plot and heat maps respectively.

PPI construction and hub gene identification

Based on the selected DEG, we used an online tool for searching of interacting genes (string; http://string.embl.de/) to predict the functional interactions between proteins (20). Based on the STRING database, a protein-protein interaction (PPI) network was constructed by using genes with confidence score ≥ 0.4. Subsequently, the network data were input into Cytoscape (v3.7.2) software. The Molecular Complex Detection (MCODE) was performed to screen modules of PPI network (degree cutoff=2, node cutoff=0.2, k-core=2, max.depth=100). Ten hub genes were identified by maximum clique centrality (MCC) algorithm.

Functional analyses

Gene set enrichment analysis (GSEA) and gene set variation analysis (GSVA) were used for functional analyses (21, 22). Briefly, GSEA was performed on the whole transcriptome by using R package clusterprofiler (23). Gene Ontology (GO) enrichment analysis included cellular component (CC) analysis, molecular function (MF) analysis and biological process (BP) analysis. GOplot packages of R was used to visualize the enriched gene terms (24). "GO BP" gene terms were downloaded from the molecular signature database, and GSVA was performed by using R package GSVA to reveal the functional changes between the stress group and the control group. For GSEA and GSVA, adj.P.Value < 0.05 was considered statistically significant.

Preparation of single cell suspensions

Single cell suspensions were prepared as described previously (25). Briefly, blood leukocytes were purified by lysing erythrocytes with ACK Lysing buffer. Lung parenchyma was collected from mice and digested with collagenase IV (1mg per ml) for 1h at 37°C followed by resuspension in 30% Percoll (GE Healthcare, Uppsala, Sweden)for centrifugation at 1200g for 20 min at room temperature. Then cells were incubated with ACK Lysing buffer to remove erythrocytes.

Flow cytometry

Single cell suspensions were first blocked with anti-Fcr III/II receptor mAb (2.4G2) followed by staining with fluorescence-conjugated mAb for CD45 (30-F11), CD19 (1D3), CD3 (145-2C11), CD11b (M1/70), Ly6G (1A8), Ly6C (HK1.4), NK1.1 (PK136). All mAbs were obtained from Thermo Fisher (Thermo Fisher Scientific Inc., Waltham, MA, USA). $CD45^+$ cells were gated to analyze the $CD3^-CD19^+$ B cells, $CD3^+NK1.1^-$ T cells and $CD3^-NK1.1^-$ NK cells. $CD45^+CD11b^+$ cells were gated to analyze $Ly6C^+Ly6G^{high}$ neutrophils and $Ly6C^{high}Ly6G^-$ monocytes. Flow cytometry gating strategy was shown in Supplementary Figure 1. For cell count, stained cells were collected at high speed for 50 seconds and counted by flow cytometry using the Aria II Flow Cytometer (BD Bioscience).

Statistical analysis

Statistical significance of differences was determined by Student's t tests (2 groups) or ANOVA (at least 3 groups). Data were presented as mean ± SD, and $P < 0.05$ was considered statistically significant. GraphPad Prism 5 software (Graphpad, software, Inc, LaJolla, CA, USA) was used for statistical analysis.

Results

Acute stress changes the gene expression profile of peripheral blood cells

RNA sequencing was performed on the peripheral blood of 6-hour stressed mice and control mice, and the samples were

clustered according to the gene expression profile. As shown in Figure 1A, 8 samples could be classified into two groups, which was completely consistent with the experimental design. Dimension reduction analysis of RNA-seq was also performed using t-SNE method. We constructed a low dimensional embedding of high-dimensional gene expression data, and obtained two-dimensional analogues of clusters. As shown in Figure 1B, these two clusters just responded to the stress group and the control group. Our data indicated that the quality control of RNA-seq was good. Gene differential expression analysis was subsequently carried out on the two groups of samples. Taking | log2FC | >1 & adj.P.Val < 0.01 as the threshold, our data showed that there were significant differences in the gene expression profiles between the stress group and the control group. Compared with the control group, 307 genes displayed up-regulated expression and 12 genes displayed down-regulated expression in the stress group (Figure 1C, D). All the DEG were listed in Supplementary data.

Acute stress affect the gene expression at immune response level

Through the GO enrichment analysis of the whole transcriptome by GSEA, there enriched many gene terms under acute stress. At the level of immune response, the biological processes represented by gene terms mainly involved inflammatory response to wounding, wound healing, defense response to bacterium, acute inflammatory response, chronic inflammatory response, humoral immune response, regulation of inflammation and immune response (Figure 2A). The molecules corresponding to these gene terms were mainly

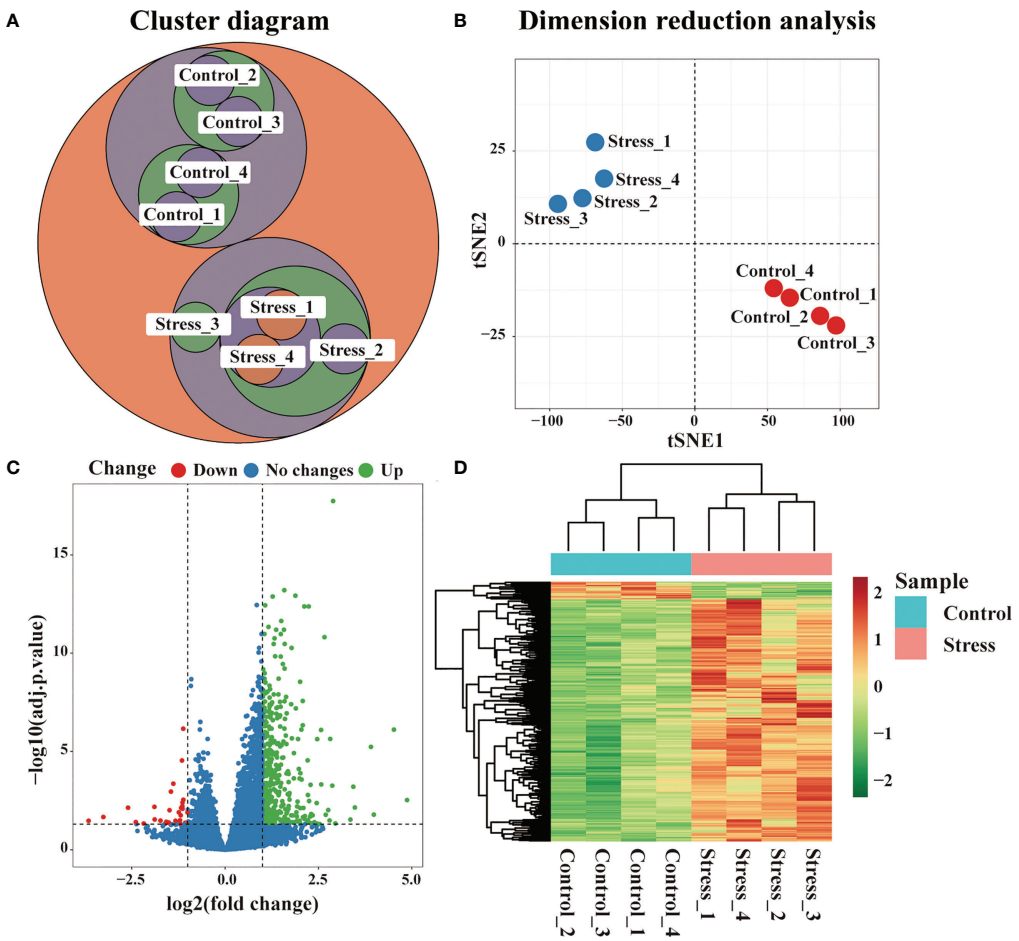

FIGURE 1
Changes of gene expression profile in peripheral blood of mice under acute stress. After 6 hours of restraint stress (n=4) or no stress (n=4), RNA of peripheral blood was extracted and sequenced, and DEG were further screened. **(A)** Cluster analysis of all samples. **(B)** Dimension reduction analysis of all samples by t-SNE method. **(C)** Difference of gene expression between the stress group and the control group displayed by volcano graph. **(D)** Difference of gene expression between the stress group and the control group displayed by heatmap graph.

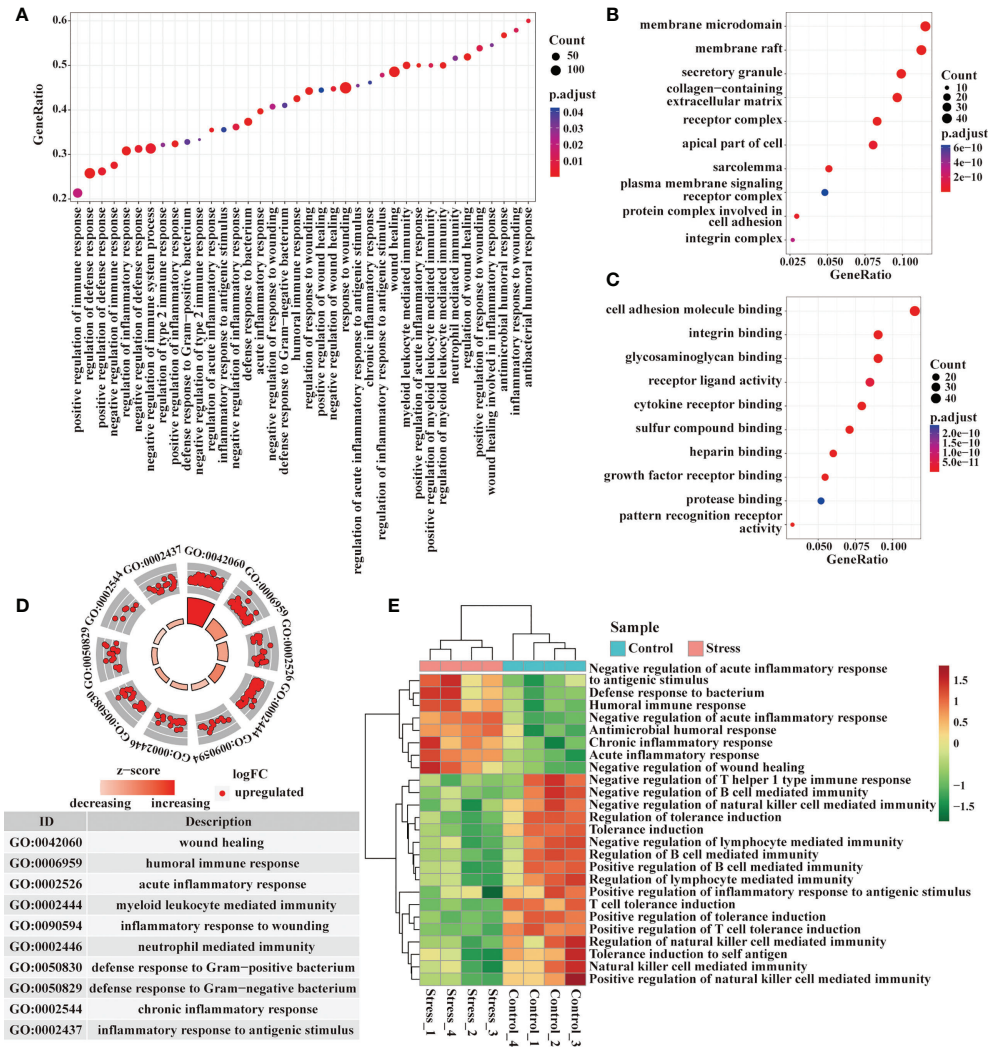

FIGURE 2
Analysis of gene expression at immune response level by GSEA and GSVA. **(A)** GO enrichment analysis of the whole transcriptome was performed by GSEA, and the biological processes represented by the gene terms were visualized at the immune response level. **(B, C)** Genes from these gene terms were selected for another GO enrichment analysis, and the top 10 CC and MF were visualized. **(D)** Select some important gene terms related to immune response, and then visualize the gene expression. **(E)** Meanwhile, GSVA was performed on RNA-seq, and the differentially expressed gene terms were visualized at the immune response level.

distributed in cell membrane, secretory granule, receptor complex, integrin complex and so on (Figure 2B), and their functions were mainly related to cell adhesion, integrin binding, glycosaminoglycan binding, receptor ligand activity, cytokine receptor binding, pattern recognition receptor activity, etc. (Figure 2C). We selected some important gene terms related to immune response and found that all genes in these gene terms showed up-regulated expression (Figure 2D). The results of GSVA showed that when compared with control group, some gene terms such as defense response to bacterium, acute/chronic inflammatory response displayed up-regulated expression, while other gene terms such as tolerance induction displayed down-regulated expression in the stress group (Figure 2E). Our data suggested that acute stress might trigger inflammatory response to cope with the upcoming unknown threat.

Acute stress affect the gene expression at immune molecular level

Immune molecules are usually used by immunocytes to interact with each other and exert effects, so we analyzed the enriched gene terms by GSEA at the immune molecular level. The biological processes represented by the enriched gene terms

10.3389/fimmu.2022.1014296

mainly involved cytokine-mediated signal pathway, production of IL-1, IL-6, IL-8, TNF, responses to IL-1, IFN-γ and chemokines, as well as complement activation (Figure 3A). The molecules corresponding to these gene terms were mainly distributed in cell membrane, receptor complex, secretory granule, endocytic vesicle, phagocytic vesicle and so on (Figure 3B), and their functions were mainly related to the cytokine receptor binding, immune receptor activity, cytokine activity, cell adhesion, glycosaminoglycan binding, cytokine receptor activity, cytokine binding, pattern recognition receptor activation, etc. (Figure 3C). In some important gene terms related to immune molecules, all genes showed up-regulated expression (Figure 3D), suggesting that acute stress might trigger the mobilization of immune molecules. We further detected the serum proinflammatory cytokines in mice by ELISA. Our data showed that IL-1β and IL-6 increased significantly in the circulation after acute stress, but TNF-α did not change significantly. The promoting effect of acute stress on serum IL-6 was much stronger than that on IL-1β (Figure 3E). The results of GSVA showed that when compared

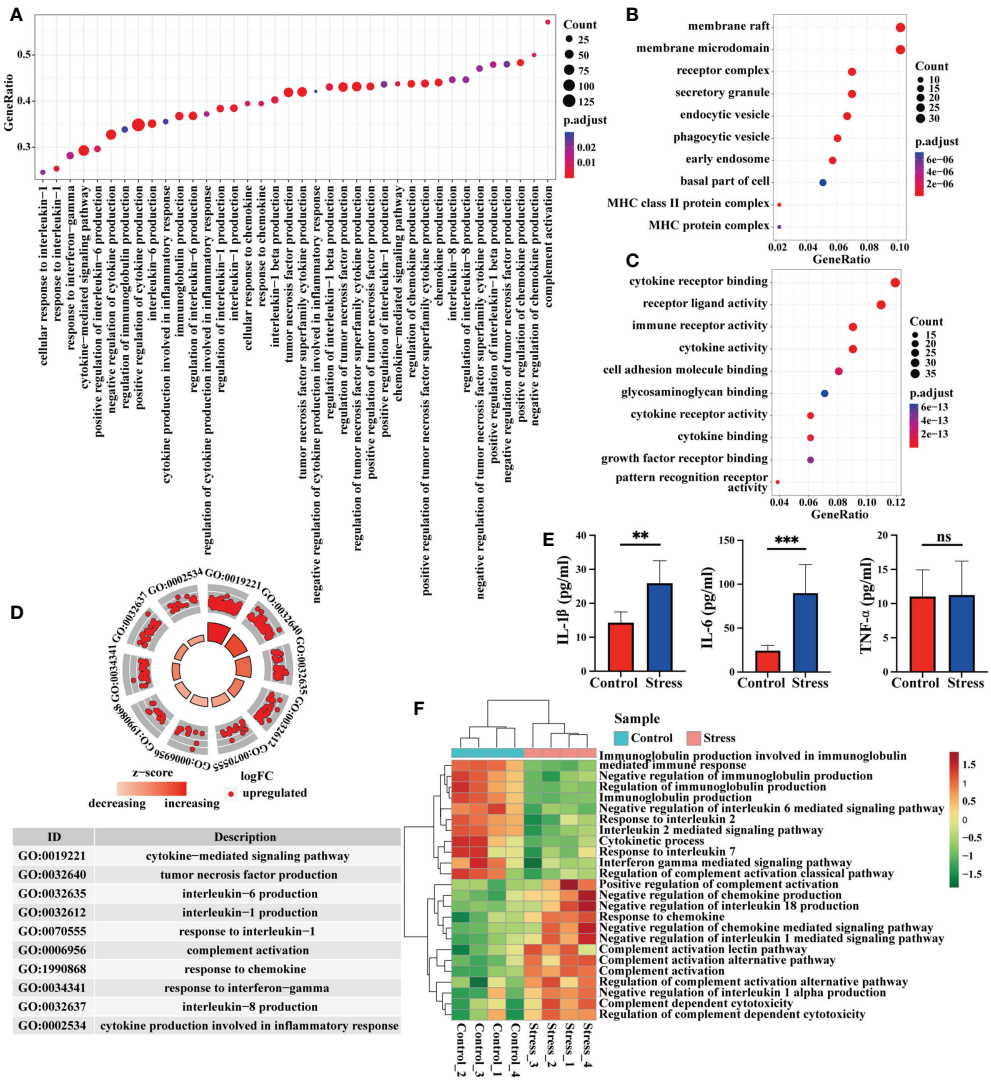

ID	Description
GO:0019221	cytokine−mediated signaling pathway
GO:0032640	tumor necrosis factor production
GO:0032635	interleukin−6 production
GO:0032612	interleukin−1 production
GO:0070555	response to interleukin−1
GO:0006956	complement activation
GO:1990868	response to chemokine
GO:0034341	response to interferon−gamma
GO:0032637	interleukin−8 production
GO:0002534	cytokine production involved in inflammatory response

FIGURE 3
Analysis of gene expression at immune molecular level by GSEA and GSVA. **(A)** GO enrichment analysis of the whole transcriptome was performed by GSEA, and the biological processes represented by the gene terms were visualized at the immune molecular level. **(B, C)** Genes from these gene terms were selected for another GO enrichment analysis, and the top 10 CC and MF were visualized. **(D)** Select some important gene terms related to immune molecules, and then visualize the gene expression. **(E)** Concentration of serum proinflammatory cytokines IL-6, TNF-α and IL-1β were detected by ELISA in mice with or without stress (n=5, per group). **P < 0.01, ***P < 0.001. Means ± SD are shown. Data shown are representative of 2 independent experiments. **(F)** Meanwhile, GSVA was performed on RNA-seq, and the differentially expressed gene terms were visualized at the immune molecular level.

with control group, some gene terms such as complement activation and response to chemokine displayed up-regulated expression, while other gene terms such as immunoglobulin production, response to IL-2 and IL-7 displayed down-regulated expression in the stress group (Figure 3F).

Acute stress affect the gene expression at the cellular level and the number of blood cells

Immune cells are the core components that reflect the immune function of the body, we thus analyzed the enriched gene terms by GSEA at the cellular level (Figure 4A). In terms of cell activation, the biological processes represented by the enriched gene terms mainly involved granulocyte activation, neutrophil activation, neutrophil degranulation, B cell activation, $CD4^+$ αβT cell activation, platelet activation and the regulation of cell activation. In terms of cell development and differentiation, the biological processes represented by the enriched gene terms mainly involved leukocyte differentiation, granulocyte differentiation, regulation of T cell proliferation and regulation of cell differentiation. In terms of cell chemotaxis or migration, the biological processes represented by the enriched gene terms mainly involved granulocyte migration, neutrophil migration, monocyte chemotaxis, mononuclear cell migration and regulation of cell chemotaxis or migration (Figure 4B). It was worth noting that genes in the gene terms related to B cell activation and T cell activation showed down-regulated expression (Figure 4B). The results of GSVA showed that when compared with control group, some gene terms such as neutrophil mediated killing, monocyte activation and chemotaxis displayed up-regulated expression, while other gene terms such as B cell activation and differentiation, T cell activation, differentiation and function, NK cell degranulation, NKT cell differentiation displayed down-regulated expression in the stress group (Figure 4C). Flow cytometric analysis showed that acute stress led to a sharp reduction of T cells, B cells, NK cells and monocytes as well as significant increment of neutrophils in peripheral blood (Figure 4D, E).

Identifying the hub genes and analyzing migration-related genes from DEG

To further predict the interaction network among the molecules corresponding to the DEG, we performed PPI network analysis online and visualized it using R package ggraph. As predicted, PPI network was full of complex molecular communication (Figure 5A). We next imported the PPI network data into Cytoscape software and identified 10 major hub genes containing *Il1b*, *Tlr2*, *Fn1*, *Cd14*, *Lgals3*, *Clec7a*, *Vegfa*, *Nlrp3*, *Ly6g and Fcgr3* (Figure 5B). *Il1b* got the highest score among hub genes, and the cytokine encoded by it is crucial for the occurrence of inflammation. We further used the MCODE plug-in to calculate and screen the co-expression module containing *Il1b*. As shown in Figure 6C, there were 8 up-regulated genes in the module including *Il1b*, *Il1rn*, *Ccr1*, *Cxcr2*, *Mefv*, *Cd80*, *Fpr1* and *Fpr2* (Figure 5C). *Ccr1* and *Ccr2* have been known to be related to cell migration and chemotaxis. Considering the fact that peripheral blood immune cells need to cross blood vessels to play a role in tissues, we analyzed the differential expression of known genes related to cell migration. As shown in Figure 5D and Figure 5E, the expression of *Ccr1*, *Ccr2*, *Xcr1* and *Cxcr2* was up-regulated in the stress group as compared to the control group, suggesting that they played an important role in the migration of immune cells to tissues with emergency under acute stress.

Acute stress leads to excessive lung inflammation in LPS-treated mice

The above bioinformatics analysis showed that acute stress could affect the gene expression profile of peripheral blood cells. Among these cells, myeloid cells other than lymphoid cells seemed to be ready to migrate from blood vessels to tissues to participate in inflammation. We tested this hypothesis. As shown in Figure 6A, LPS was injected intraperitoneally into mice to simulate microbial infection. 48 hours later, a lot of neutrophils and monocytes infiltrated into the lungs, but this phenomenon was not found in mice with simple acute stress. If LPS stimulation was performed after restrain stress, only neutrophil infiltration into the lung was further enhanced, while T cells and B cells showed a trend of decreased infiltration. We also performed H&E staining on lung tissue to assess the severity of pneumonia. The results showed that lungs of mice with LPS stimulation were characterized by inflammatory cell infiltration into alveolar interstitium, thickened alveolar walls and fluid exudation into alveoli. Such pathological changes were not found in the control group and stress group. Surprisingly, acute stress followed by LPS stimulation caused more serious pneumonia (Figure 6B). If mice received daily LPS stimulation, they would die occasionally. If LPS stimulation was performed after stress, the mortality of mice began to increase significantly after 4 days. The hazard ratio of mouse mortality under stress was 8.6 (Figure 6C). These data showed that acute stress led to an inflammatory state characterized by neutrophil mediated reaction, and repeated acute stress was harmful to the health of mice.

Discussion

As we all know, chronic or long-term stress has many adverse effects on health (4, 5, 26). Acute or short-term stress

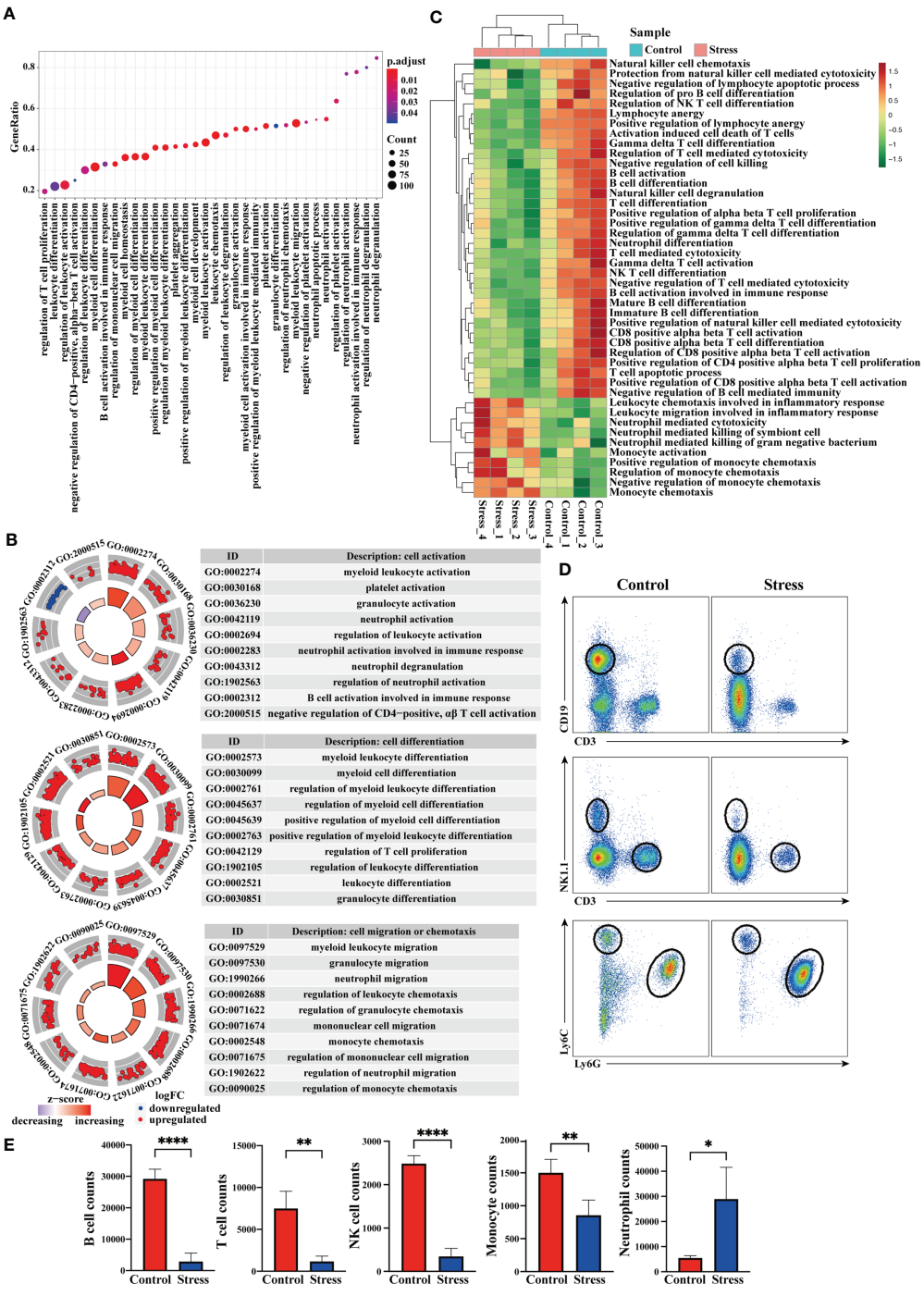

FIGURE 4
Analysis of gene expression at the cellular level and cell number in peripheral blood. **(A)** GO enrichment analysis of the whole transcriptome was performed through GSEA, and the biological processes represented by enriched gene terms were visualized at the cellular level. **(B)** Select some important gene terms related to cell activation, differentiation and migration, and then visualize the gene expression. **(C)** GSVA was performed on RNA-seq, and the differentially expressed gene terms were visualized at the cellular level. **(D)** At the same time, flow cytometry was used to analyze the changes of immunocytes in the peripheral blood between stress group and control group (n=4, per group). **(E)** Histograms represent the cell number counted by flow cytometry. Data are representative of 3 independent experiments. *P < 0.05, **P < 0.01, ****P < 0.0001. Means ± SD are shown.

10.3389/fimmu.2022.1014296

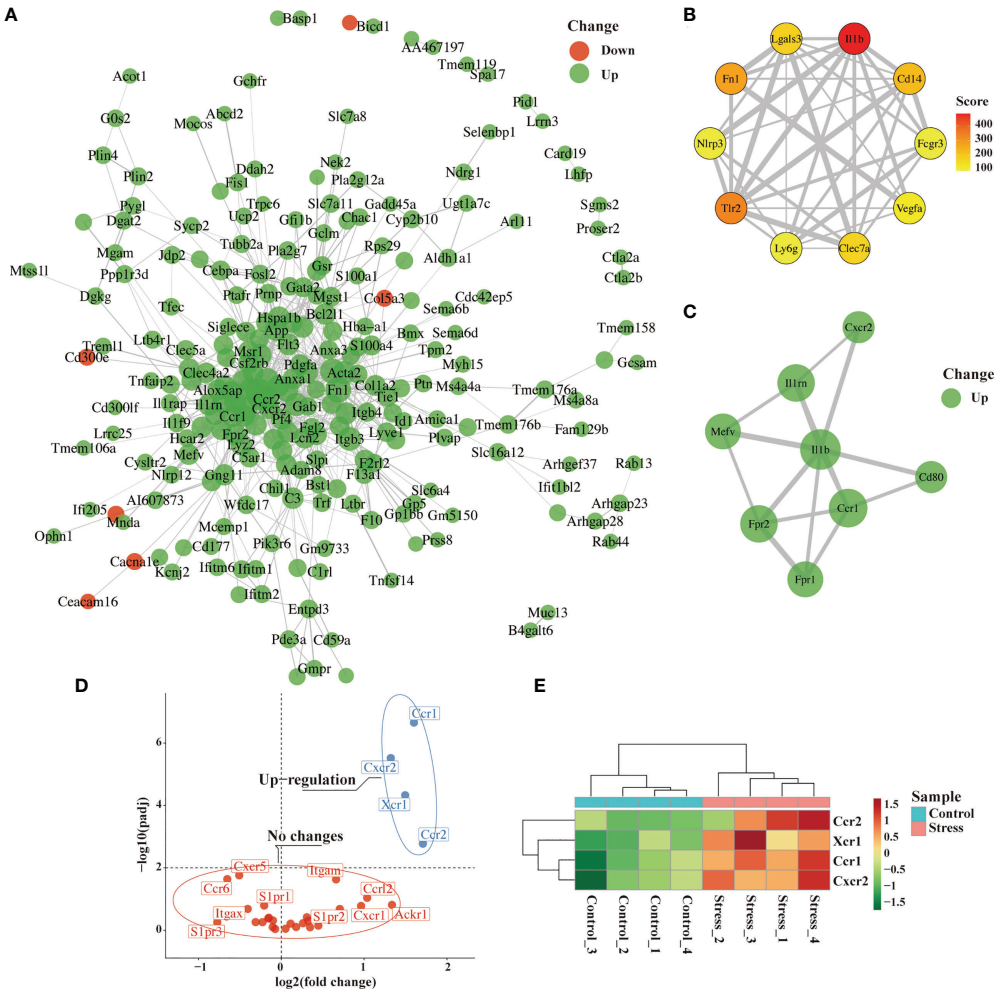

FIGURE 5
Identification of hub genes and analysis of migration-related genes from DEG. After 6 hours of restraint stress or no stress (n=4, per group), RNA extracted from peripheral blood was sequenced and analyzed. **(A)** The selected DEG were used for PPI network analysis online. **(B, C)** Hub gene and modules were screened from PPI network through Cytoscape software. **(D, E)** Genes related to cell migration or chemotaxis were analyzed and visualized by volcano graph and heatmap graph.

could improve mobility and responsiveness for battle or flight, so as to promote the survival of life (14). Both acute and chronic stress affect the occurrence, progression, and outcome of diseases through the neuroendocrine-immune axis (15, 27). Although chronic stress seems to be more closely related to disease, immune changes caused by acute stress are often the basis of biological effects caused by chronic stress. Exploring the regulation of acute stress on the immune system not only helps to deeply understand the initiation of stress response, but also helps to explain how chronic stress affects the progress of disease. Previous studies have reported that acute stress could enhance the body's immune response (16, 28, 29), but the characteristics of the immune response have not been described in detail.

Most immune cells are transported to tissues and organs through the circulatory system after they mature from bone marrow or thymus. Therefore, detecting the changes of peripheral blood immune cells could better reflect the impact of acute stress on the immune system. To avoid the problem of insufficient information obtained by traditional detection methods, we sequenced RNA extracted from peripheral blood to obtain biological big data, and then performed bioinformatics analysis. We found that 6 hours of restraint stress was enough to change the gene expression profile of peripheral blood immune cells, and most of DEG displayed up-regulated expression. The gene terms enriched by GSEA and GSVA were mainly related to inflammation, defense response, inflammatory response to wounding, pro-inflammatory cytokine production and so on.

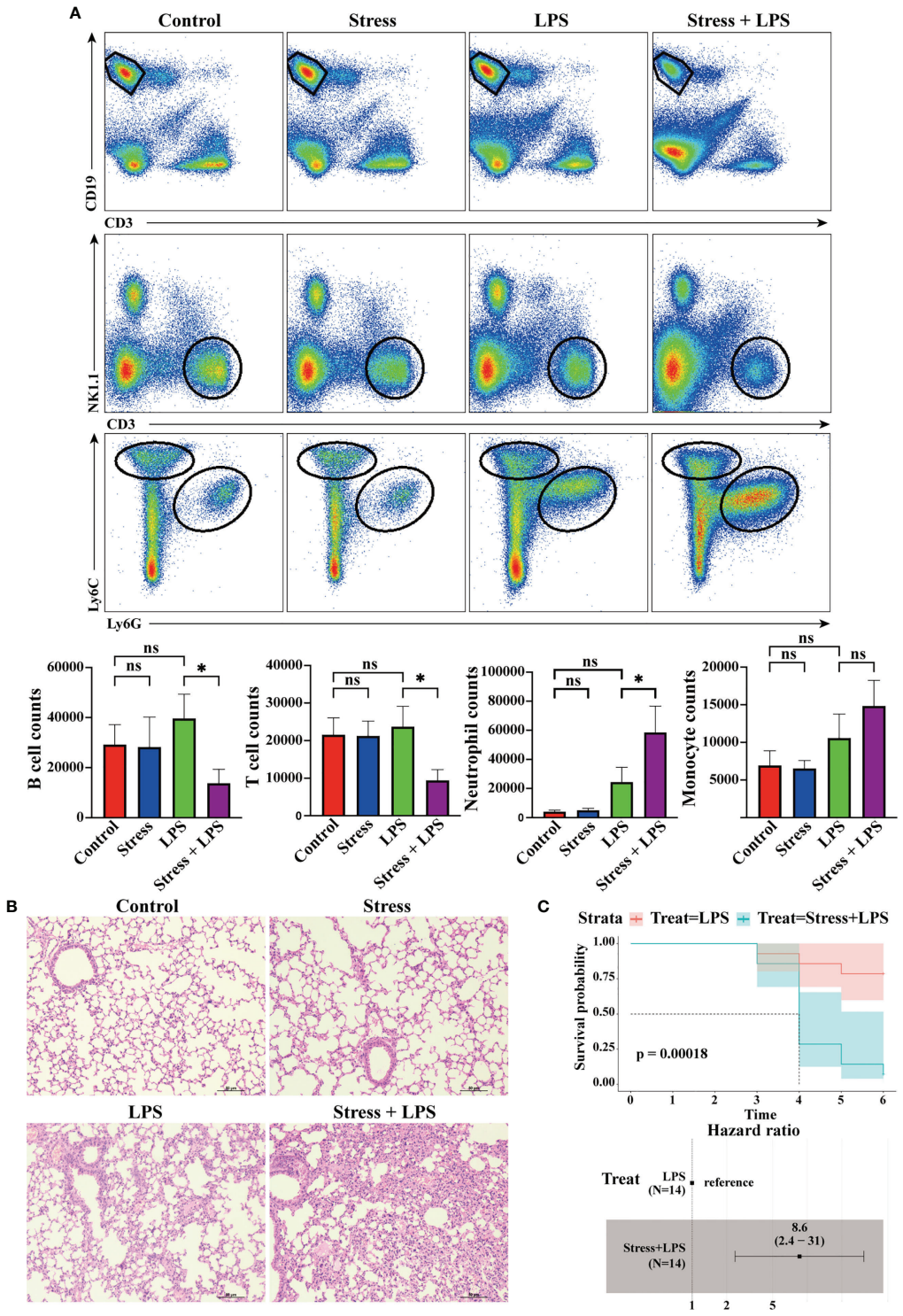

FIGURE 6
Acute stress caused excessive lung inflammation in LPS-treated mice. Mice were intraperitoneally injected with LPS after 6 hours of restraint stress or no stress. **(A)** 48 hours later, the inflammatory cells infiltrated in the lungs were detected by flow cytometry (n=4, per group). Histograms represent the cell number counted by flow cytometry. **(B)** Meanwhile, lungs were sectioned and stained with H&E to observe the pathological changes. **(C)** Mice received LPS stimulation with or without restraint stress every day, and the mortality and hazard ratio were calculated (n=4, per group). *P < 0.05, Means ± SD are shown. Data are representative of 3 independent experiments. ns, no significance.

The core of these data was that acute stress may trigger an inflammatory state. This opinion was supported by the increase of serum proinflammatory cytokines after acute stress. Our results are consistent with previous literature that IL-6 is the dominant cytokine induced by acute stress in mice in the circulation (30). Similarly, a meta-analysis of several studies also showed that IL-6, TNF-α, and IL-1-β secretion were increased in response to acute stress in human (29). Among the 10 hub genes screened from PPI network, *Ilb* encodes one important pro-inflammatory cytokine, which is crucial for the occurrence of inflammation (31). *Tlr2*, *Cd14*, *Nlrp3* and *Clec7a* are involved in the signal pathways mediated by pattern recognition receptors, thus participating in the recognition of pathogenic microorganisms (32–35). *Fn1* is a fibrinogen-encoding gene and *Vegfa* is a growth factor-encoding gene, they are involved in the wound healing (36). *Lgals3* is a gene encoding Galectin-3, which has been considered as a modifier of anti-microbial immunity (37). *Ly6g*-encoded Ly6G has been regarded as neutrophil-specific marker in mice (38), suggesting an important participant of neutrophils in acute stress-induced response. *Fcgr3* is a gene encoding a receptor that binds IgG with high affinity and participates in IgG-mediated biological activity (39). Our results supported the previous hypothesis that acute or short-term stress prepares the immune system to respond to possible challenges such as injury or infection caused by stressors (such as predators, or modern medical/surgical procedures) (28, 40).

We evaluated the gene terms enriched by GSEA and GSVA in three aspects including cell activation, differentiation and chemotaxis. Obviously, acute stress enhanced the activation, differentiation and migration of granulocytes, especially neutrophils. However, the activation and differentiation of B cells and T cells were weakened under acute stress. Our data suggested that granulocytes were more active in the response induced by acute stress. Correspondingly, acute stress led to a significant decrease of T cells and B cells and a significant increase of neutrophils in peripheral blood, which supported our hypothesis. This phenomenon did not depend on the gender of mice (data not shown). Even in humans, the changes of immune cell populations in peripheral blood caused by acute stress are similar to those in mice (41). We agree with the opinion that stress response is a non-specific response of the body to stressors. In addition, previous studies have shown that acute stress could trigger the redistribution of immune cells in the body, in which hormones played an important regulatory role (42, 43). Our results showed that some DEG were involved in the process of granulocyte differentiation, which suggested that modifying the development and differentiation of different cell populations may be one of the reasons for the changes of peripheral blood cells under acute stress. This conjecture was supported by the analysis of hematopoietic stem and progenitor cells in the bone marrow under acute stress. We found that granulocyte-macrophage progenitor cells (GMP) increased in the bone marrow during acute stress (Supplementary Figure 2). Since GMP is the progenitor of granulocytes, the increase in its number under acute stress may lead to the generation of more neutrophils, which are then released into the peripheral blood.

The terminal site where immune cells play a role are usually tissues and organs. After infection or injury, tissues will release chemokines, which quickly attract and recruit immune cells from adjacent blood vessels (44). Under acute stress, we found that the enriched gene terms involved in cell chemotaxis or migration were mainly related to granulocytes and monocytes but not T cells and B cells. This highly suggested that acute stress prepares innate immune cells in peripheral blood to infiltrate into tissues with emergency. For cell migration, chemokines released by infected or damaged tissues determine the destination of cell migration, while the expression of chemokine receptors determines which cell types need to migrate (45). Our data showed that the expression of chemokine receptor-encoding genes including *Ccr1*, *Ccr2*, *Cxcr2* and *Xcr1* in the stress group was significantly higher than that in the control group. *Ccr1*-encoded CCR1 and *Cxcr2*-encoded CXCR2 are mainly expressed in neutrophils, and *Ccr2*-encoded CCR2 is mainly expressed in monocytes in the blood (46–48). This suggested that acute stress will mobilize peripheral blood neutrophils and monocytes to migrate to infected or injured tissues. To test the hypothesis, it is a good choice to take the inflammatory model as an amplifier. It was well known that peritoneal injection of LPS could induced system inflammation. Considering that the effect of acute stress gradually attenuates with the removal of the stressor, we detected the pathological status and immune cell infiltration of lung tissue on day 2 after LPS administration. Not surprisingly, LPS treatment led to obvious inflammatory pathological changes in the lungs of mice, and myeloid cells rather than lymphocytes were mainly accumulated in the lungs. Our data was consistent with previous studies that lymphocytes obviously infiltrated into lung tissue on day 4 after LPS treatment, while neutrophils and monocytes migrated to the lung earlier than lymphocytes (49, 50). This reflected the different migration speeds of different immune cell populations to inflammatory tissues. The opinion was supported in our previous study on LPS-induced neuroinflammation (51). Interestingly, if mice with acute inflammation were under acute stress, only neutrophil infiltration into lung tissue was enhanced. So, it was obvious that innate immune cells dominated by neutrophils played a central role in the inflammatory state caused by acute stress.

Although bioinformatics analysis has many advantages, its results need to be verified by experiments. Through a series of analysis strategies, we gradually guided the analysis results to the immune cell populations. Therefore, our validations were not for some genes, but for certain cell populations and pathological states. The reason why we did not pay attention to T cells and B cells was that their numbers in the peripheral blood are decreasing. In fact, lymphocytes in multiple organs showed a decreasing trend, and many of them migrated to the bone marrow (Supplementary Figure 3).

In LPS-induced systemic inflammation, repeated acute stress and LPS injection increased the risk of death in mice, which was consistent with the understanding that chronic stress was usually harmful to health. But what is the significance of acute stress-aggravated pneumonia? We could explain that excessive inflammation may be an important factor in promoting the death of mice, or we think that enhanced inflammation is a powerful tool against infection. Under acute stress, LPS-induced pneumonia seemed to be dominated by innate immunity represented by neutrophils, while adaptive immunity represented by T cells and B cells was in a contracting state. Previous data have shown that chronic restraint stress promoted lymphocyte apoptosis (18) and even weakened autoimmune diseases such as EAE (42). These data were consistent with our findings that acute restraint stress led to the reduction of peripheral blood lymphocytes. So, chronic stress effects may be the continuation and accumulation of acute stress effects. However, in other stress models, chronic stress could aggravate autoimmune diseases such as inflammatory bowel disease (52, 53). The regulation of immune system by chronic stress and acute stress may be very different. So, there is a significant gap in our understanding of the transitional phase between acute and chronic stress, studies on repeated acute stress might help fill this gap (54).

Altogether, our data showed that acute stress led to rapid mobilization of the immune system, and the body presented an inflammatory state dominated by innate immune response represented by neutrophils.

Data availability statement

The datasets presented in this study can be found in online repositories. The names of the repository/repositories and accession number(s) can be found in the article/Supplementary Material.

Ethics statement

The animal study was reviewed and approved by the Laboratory Animal Care Committee of Shandong First Medical University & Shandong Academy of Medical Sciences.

Author contributions

HH designed the experiments; HH and LK wrote the manuscript and WS revised the manuscript. LT and NC performed bioinformatics analysis. YZ, JH and YL made animal model of disease and extracted RNA from blood. SY and YL performed flow cytometric analysis. All authors contributed to the article and approved the submitted version.

Funding

This work was supported by grants from the National Natural Science Foundation of China (81971553, 82271803, 81971512), Shandong Introduction and Education Program of Yong Innovative Talents (rcjf005), Shandong Provincial key research and development program (2019GSF108256) and Shandong medical and health science and technology development project (2016WS0594).

Conflict of interest

The authors declare that the research was conducted in the absence of any commercial or financial relationships that could be construed as a potential conflict of interest.

Publisher's note

Supplementary material

The Supplementary Material for this article can be found online at: https://www.frontiersin.org/articles/10.3389/fimmu.2022.1014296/full#supplementary-material

References

1. Russell G, Lightman S. The human stress response. *Nat Rev Endocrinol* (2019) 15(9):525–34. doi: 10.1038/s41574-019-0228-0

2. Nagaraja AS, Sadaoui NC, Dorniak PL, Lutgendorf SK, Sood AK. SnapShot: Stress and disease. *Cell Metab* (2016) 23(2):388–e1. doi: 10.1016/j.cmet.2016.01.015

3. Hong H, Ji M, Lai D. Chronic stress effects on tumor: Pathway and mechanism. *Front Oncol* (2021) 11:738252. doi: 10.3389/fonc.2021.738252

4. Dai S, Mo Y, Wang Y, Xiang B, Liao Q, Zhou M, et al. Chronic stress promotes cancer development. *Front Oncol* (2020) 10:1492. doi: 10.3389/fonc.2020.01492

5. Ilchmann-Diounou H, Menard S. Psychological stress, intestinal barrier dysfunctions, and autoimmune disorders: An overview. *Front Immunol* (2020) 11:1823. doi: 10.3389/fimmu.2020.01823

6. Peppas S, Pansieri C, Piovani D, Danese S, Peyrin-Biroulet L, Tsantes AG, et al. The brain-gut axis: Psychological functioning and inflammatory bowel diseases. *J Clin Med* (2021) 10(3):377. doi: 10.3390/jcm10030377

7. Fishta A, Backe EM. Psychosocial stress at work and cardiovascular diseases: an overview of systematic reviews. *Int Arch Occup Environ Health* (2015) 88 (8):997–1014. doi: 10.1007/s00420-015-1019-0

8. Nasilowska-Barud A, Barud M. Psychological risk factors for cardiovascular diseases. *Wiad Lek* (2020) 73(9 cz. 1):1829–34. doi: 10.36740/WLek202009104

9. Bolton D. Looking forward to a decade of the biopsychosocial model. *BJPsych Bull* (2022) 46:228–32. doi: 10.1192/bjb.2022.34

10. McEwen BS. Physiology and neurobiology of stress and adaptation: central role of the brain. *Physiol Rev* (2007) 87(3):873–904. doi: 10.1152/physrev.00041.2006

11. Zhang L, Pan J, Chen W, Jiang J, Huang J. Chronic stress-induced immune dysregulation in cancer: implications for initiation, progression, metastasis, and treatment. *Am J Cancer Res* (2020) 10(5):1294–307. doi: 10.3410/f.738145282.793589789

12. Palumbo ML, Prochnik A, Wald MR, Genaro AM. Chronic stress and glucocorticoid receptor resistance in asthma. *Clin Ther* (2020) 42(6):993–1006. doi: 10.1016/j.clinthera.2020.03.002

13. Wozniak E, Owczarczyk-Saczonek A, Placek W. Psychological stress, mast cells, and psoriasis-is there any relationship? *Int J Mol Sci* (2021) 22(24):13252. doi: 10.3390/ijms222413252

14. McEwen BS. Protective and damaging effects of stress mediators. *N Engl J Med* (1998) 338(3):171–9. doi: 10.1056/NEJM199801153380307

15. Zefferino R, Di Gioia S, Conese M. Molecular links between endocrine, nervous and immune system during chronic stress. *Brain Behav* (2021) 11(2): e01960. doi: 10.1002/brb3.1960

16. Dhabhar FS. Effects of stress on immune function: the good, the bad, and the beautiful. *Immunol Res* (2014) 58(2-3):193–210. doi: 10.1007/s12026-014-8517-0

17. Glaser R, Kiecolt-Glaser JK. Stress-induced immune dysfunction: implications for health. *Nat Rev Immunol* (2005) 5(3):243–51. doi: 10.1038/nri1571

18. Yin D, Tuthill D, Mufson RA, Shi Y. Chronic restraint stress promotes lymphocyte apoptosis by modulating CD95 expression. *J Exp Med* (2000) 191 (8):1423–8. doi: 10.1084/jem.191.8.1423

19. Laurens V. Accelerating t-SNE using tree-based algorithms. *J Mach Learn* (2014) 15:3221–45. doi: 10.5555/2627435.2697068

20. Szklarczyk D, Franceschini A, Wyder S, Forslund K, Heller D, Huerta-Cepas J, et al. STRING v10: protein-protein interaction networks, integrated over the tree of life. *Nucleic Acids Res* (2015) 43(Database issue):D447–52. doi: 10.1093/nar/gku1003

21. Subramanian A, Tamayo P, Mootha VK, Mukherjee S, Ebert BL, Gillette MA, et al. Gene set enrichment analysis: a knowledge-based approach for interpreting genome-wide expression profiles. *Proc Natl Acad Sci U.S.A.* (2005) 102(43):15545–50. doi: 10.1073/pnas.0506580102

22. Hanzelmann S, Castelo R, Guinney J. GSVA: gene set variation analysis for microarray and RNA-seq data. *BMC Bioinf* (2013) 14:7. doi: 10.1186/1471-2105-14-7

23. Yu G, Wang LG, Han Y, He QY. clusterProfiler: an r package for comparing biological themes among gene clusters. *OMICS* (2012) 16(5):284–7. doi: 10.1089/omi.2011.0118

24. Walter W, Sanchez-Cabo F, Ricote M. GOplot: an r package for visually combining expression data with functional analysis. *Bioinformatics* (2015) 31 (17):2912–4. doi: 10.1093/bioinformatics/btv300

25. Yi S, Zhai J, Niu R, Zhu G, Wang M, Liu J, et al. Eosinophil recruitment is dynamically regulated by interplay among lung dendritic cell subsets after allergen challenge. *Nat Commun* (2018) 9(1):3879. doi: 10.1038/s41467-018-06316-9

26. Evers AW, Zautra A, Thieme K. Stress and resilience in rheumatic diseases: a review and glimpse into the future. *Nat Rev Rheumatol* (2011) 7(7):409–15. doi: 10.1038/nrrheum.2011.80

27. Haykin H, Rolls A. The neuroimmune response during stress: A physiological perspective. *Immunity* (2021) 54(9):1933–47. doi: 10.1016/j.immuni.2021.08.023

28. Dhabhar FS. Enhancing versus suppressive effects of stress on immune function: implications for immunoprotection and immunopathology. *Neuroimmunomodulation* (2009) 16(5):300–17. doi: 10.1159/000216188

29. Marsland AL, Walsh C, Lockwood K, John-Henderson NA. The effects of acute psychological stress on circulating and stimulated inflammatory markers: A systematic review and meta-analysis. *Brain Behav Immun* (2017) 64:208–19. doi: 10.1016/j.bbi.2017.01.011

30. Qing H, Desrouleaux R, Israni-Winger K, Mineur YS, Fogelman N, Zhang C, et al. Origin and function of stress-induced IL-6 in murine models. *Cell* (2020) 182(6):1660. doi: 10.1016/j.cell.2020.08.044

31. Dinarello CA. Overview of the IL-1 family in innate inflammation and acquired immunity. *Immunol Rev* (2018) 281(1):8–27. doi: 10.1111/imr.12621

32. Brubaker SW, Bonham KS, Zanoni I, Kagan JC. Innate immune pattern recognition: a cell biological perspective. *Annu Rev Immunol* (2015) 33:257–90. doi: 10.1146/annurev-immunol-032414-112240

33. Takeuchi O, Akira S. Pattern recognition receptors and inflammation. *Cell* (2010) 140(6):805–20. doi: 10.1016/j.cell.2010.01.022

34. Kalia N, Singh J, Kaur M. The role of dectin-1 in health and disease. *Immunobiology* (2021) 226(2):152071. doi: 10.1016/j.imbio.2021.152071

35. Lu X, Nagata M, Yamasaki S. Mincle: 20 years of a versatile sensor of insults. *Int Immunol* (2018) 30(6):233–9. doi: 10.1093/intimm/dxy028

36. Tonnesen MG, Feng X, Clark RA. Angiogenesis in wound healing. *J Investig Dermatol Symp Proc* (2000) 5(1):40–6. doi: 10.1046/j.1087-0024.2000.00014.x

37. Sehrawat S, Kaur M. Galectin-3 as a modifier of anti-microbial immunity: Unraveling the unknowns. *Glycobiology* (2020) 30(7):418–26. doi: 10.1093/glycob/cwaa005

38. Lee PY, Wang JX, Parisini E, Dascher CC, Nigrovic PA. Ly6 family proteins in neutrophil biology. *J Leukoc Biol* (2013) 94(4):585–94. doi: 10.1189/jlb.0113014

39. van der Poel CE, Spaapen RM, van de Winkel JG, Leusen JH. Functional characteristics of the high affinity IgG receptor, FcgammaRI. *J Immunol* (2011) 186 (5):2699–704. doi: 10.4049/jimmunol.1003526

40. Dhabhar FS, McEwen BS. Acute stress enhances while chronic stress suppresses cell-mediated immunity *in vivo*: a potential role for leukocyte trafficking. *Brain Behav Immun* (1997) 11(4):286–306. doi: 10.1006/brbi.1997.0508

41. Breen MS, Beliakova-Bethell N, Mujica-Parodi LR, Carlson JM, Ensign WY, Woelk CH, et al. Acute psychological stress induces short-term variable immune response. *Brain Behav Immun* (2016) 53:172–82. doi: 10.1016/j.bbi.2015.10.008

42. Poller WC, Downey J, Mooslechner AA, Khan N, Li L, Chan CT, et al. Brain motor and fear circuits regulate leukocytes during acute stress. *Nature* (2022) 607 (7919):578–84. doi: 10.1038/s41586-022-04890-z

43. Dhabhar FS, Malarkey WB, Neri E, McEwen BS. Stress-induced redistribution of immune cells–from barracks to boulevards to battlefields: a tale of three hormones–curt Richter award winner. *Psychoneuroendocrinology* (2012) 37(9):1345–68. doi: 10.1016/j.psyneuen.2012.05.008

44. Charo IF, Ransohoff RM. The many roles of chemokines and chemokine receptors in inflammation. *N Engl J Med* (2006) 354(6):610–21. doi: 10.1056/NEJMra052723

45. Zlotnik A, Yoshie O. The chemokine superfamily revisited. *Immunity* (2012) 36(5):705–16. doi: 10.1016/j.immuni.2012.05.008

46. Zimmermann HW, Sterzer V, Sahin H. CCR1 and CCR2 antagonists. *Curr Top Med Chem* (2014) 14(13):1539–52. doi: 10.2174/1568026614666140827144115

47. Hughes CE, Nibbs RJB. A guide to chemokines and their receptors. *FEBS J* (2018) 285(16):2944–71. doi: 10.1111/febs.14466

48. Sokol CL, Luster AD. The chemokine system in innate immunity. *Cold Spring Harb Perspect Biol* (2015) 7(5):a016303. doi: 10.1101/cshperspect.a016303

49. Nakajima T, Suarez CJ, Lin KW, Jen KY, Schnitzer JE, Makani SS, et al. T Cell pathways involving CTLA4 contribute to a model of acute lung injury. *J Immunol* (2010) 184(10):5835–41. doi: 10.4049/jimmunol.0903238

50. Maus UA, Wellmann S, Hampl C, Kuziel WA, Srivastava M, Mack M, et al. CCR2-positive monocytes recruited to inflamed lungs downregulate local CCL2 chemokine levels. *Am J Physiol Lung Cell Mol Physiol* (2005) 288(2):L350–8. doi: 10.1152/ajplung.00061.2004

51. He H, Geng T, Chen P, Wang M, Hu J, Kang L, et al. NK cells promote neutrophil recruitment in the brain during sepsis-induced neuroinflammation. *Sci Rep* (2016) 6:27711. doi: 10.1038/srep27711

52. Sgambato D, Miranda A, Ranaldo R, Federico A, Romano M. The role of stress in inflammatory bowel diseases. *Curr Pharm Des* (2017) 23(27):3997–4002. doi: 10.2174/1381612823666170228123357

53. Rousset L, Halioua B. Stress and psoriasis. *Int J Dermatol* (2018) 57 (10):1165–72. doi: 10.1111/ijd.14032

54. Rohleder N. Stress and inflammation - the need to address the gap in the transition between acute and chronic stress effects. *Psychoneuroendocrinology* (2019) 105:164–71. doi: 10.1016/j.psyneuen.2019.02.021

frontiers | Frontiers in Immunology

TYPE Original Research
PUBLISHED 29 September 2022
DOI 10.3389/fimmu.2022.969336

OPEN ACCESS

EDITED BY
Kenneth Beaman,
Rosalind Franklin University of Medicine and Science, United States

REVIEWED BY
Shanmuga Priyaa Madhukaran,
University of Texas Southwestern Medical Center, United States
Agnieszka Waclawik,
Institute of Animal Reproduction and Food Research (PAS), Poland

*CORRESPONDENCE
Silvana Sandri
ssandri@usp.br

SPECIALTY SECTION
This article was submitted to Immunological Tolerance and Regulation, a section of the journal Frontiers in Immunology

RECEIVED 14 June 2022
ACCEPTED 29 August 2022
PUBLISHED 29 September 2022

CITATION
Hebeda CB, Savioli AC, Scharf P, de Paula-Silva M, Gil CD, Farsky SHP and Sandri S (2022) Neutrophil depletion in the pre-implantation phase impairs pregnancy index, placenta and fetus development. *Front. Immunol.* 13:969336. doi: 10.3389/fimmu.2022.969336

Neutrophil depletion in the pre-implantation phase impairs pregnancy index, placenta and fetus development

Cristina Bichels Hebeda[1,2], Anna Carolina Savioli[1], Pablo Scharf[1], Marina de Paula-Silva[3], Cristiane Damas Gil[4], Sandra Helena Poliselli Farsky[1] and Silvana Sandri[1]*

[1]Department of Clinical and Toxicological Analyses, School of Pharmaceutical Sciences, University of São Paulo, SP, São Paulo, Brazil, [2]Núcleo de Pesquisa em Ciências Médicas, Fundação Universidade para o Desenvolvimento do Alto Vale do Itajaí – UNIDAVI, Rio do Sul, SC, Brazil, [3]Center for Stem Cells and Regenerative Medicine, King's College London, London, United Kingdom, [4]Department of Morphology and Genetics, Federal University of São Paulo, São Paulo, SP, Brazil

Maternal neutrophils cells are players in gestational tolerance and fetus delivery. Nonetheless, their actions in each phase of the pregnancy are unknown. We here investigated the role of maternal neutrophil depletion before the blastocyst implantation phase and outcomes in the pregnancy index, placenta, and fetus development. Neutrophils were pharmacologically depleted by i.p. injection of anti-Gr1 (anti-neutrophils; 200 µg) 24 hours after plug visualization in allogeneic-mated C57BL/6/BALB/c mice. Depletion of peripheral neutrophils lasted until 48 hours after anti-Gr1 injection (gestational day 1.5-3.5). On gestational day 5.5, neutrophil depletion impaired the blastocyst implantation, as 50% of pregnant mice presented reduced implantation sites. On gestational day 18.5, neutrophil depletion reduced the pregnancy rate and index, altered the placenta disposition in the uterine horns, and modified the structure of the placenta, detected by reduced junctional zone, associated with decreased numbers of giant trophoblast cells, spongiotrophoblast. Reduced number of placenta cells labeled for vascular endothelial growth factor (VEGF), platelet-endothelial cell adhesion molecule (PECAM-1), and intercellular cell adhesion molecule (ICAM-1), important markers of angiogenesis and adhesiveness, were detected in neutrophil depleted mice. Furthermore, neutrophil depletion promoted a higher frequency of monocytes, *natural killers*, and T regulatory cells, and lower frequency of cytotoxic T cells in the blood, and abnormal development of offspring. Associated data obtained herein highlight the pivotal role of neutrophils actions in the early stages of pregnancy, and address further investigations on the imbricating signaling evoked by neutrophils in the trophoblastic interaction with uterine epithelium.

KEYWORDS

anti-granulocytes, pregnancy index, abnormal fetal development, maternal immune system, placenta morphology, window of implantation

Introduction

Mammalian reproduction is a complex phenomenon, which generally leads to inefficient outcomes. The majority of conceptions do not evolve, especially by losses before the blastocyst implantation (1, 2), which takes place in a very short period of gestation named window of implantation (WOI). During WOI occurs the synchronization of embryonic development and uterine differentiation into a receptive status (3). WOI is characterized by pre-receptive and receptive periods followed by refractory no receptive phases. In humans and rodents, implantation of blastocysts begins with apposition, followed by attachment to trophoblast outgrowth and decidualization, which are spatiotemporally regulated by many players, such as endocrine/growth factors/immune mediators of cell-cell and cell-matrix interactions (3, 4). Disruptions to the implantation process are also considered causes of pregnancy-associated complications, such as preeclampsia, intrauterine growth restriction, and preterm birth (5, 6).

The maternal immune response in the endometrium is pivotal to the establishment of WOI. The fetal antigen contact with the maternal endometrium modifies the local repertoire of immune cells, which display a fundamental role in trophoblast invasion, vascular remodeling by extravillous trophoblast, embryo invasion, and maternal tolerance (7, 8). The innate immune response in the blastocyst implantation period is not characterized as classical inflammation, as it occurs to enhance the adhesiveness of the uterine epithelium and the formation of new vessels for the blood supply. Therefore, innate-mediated inflammation must be local and adjustable to the process, as both impaired and exacerbated innate response leads to failure in the blastocyst-endometrium interactions (9).

Neutrophils are the predominant circulating innate immune cells in humans prompted to migrate into the site of inflammation to eliminate insulting agents. More recently, the role of neutrophils in host defense and homeostasis has been outspread by identifying neutrophil phenotypes, which display pro or anti-inflammatory properties and influence the resolution of inflammation and tissue repair (10). Neutrophil switching to distinct subtypes is dependent on the phase of the inflammatory process and modulated by the chemical and cellular composition of the surrounding inflammatory microenvironment (11).

In this context, it has been highlighted that neutrophils acquire different phenotypes during pregnancy, with fundamental roles in each phase. Studies describing neutrophils phenotype in the placental microenvironment are scarce. However, all studies corroborate that neutrophils display a proangiogenic phenotype. In the first trimester, neutrophils are found in the human decidua, in an area mainly involved in tissue remodeling and physiological decidual implant reaction, displaying high resistance to apoptosis, do not exerting a suppressive activity, and expressing fibro/angiogenic factors (12) In the second trimester, the number of neutrophils at decidua basalis is increased and high levels of activation markers and angiogenesis-related proteins, such as vascular endothelial growth factor-A (VEGF) are detected (13). In pregnant mice, the augmented neutrophils numbers were observed on gestational days 8 – 10, which coincides with the period of spiral arterial angiogenesis (13).

Several chemical mediators in the uterine microenvironment modulate neutrophil recruitment and functional phenotypes in normal pregnancy (14–16). Studies have demonstrated that placental cell debris and IL-8 are involved in the neutrophil migration to decidua (17). During coitus, inflammatory neutrophils are recruited for the elimination of excessive sperm through phagocytosis; nevertheless, in the following phases, they are inhibited to allow the healthy motile sperm to reach the oviduct (18). Moreover, neutrophils are found in the uterine stroma at the early phase of WOI and proangiogenic neutrophils were identified in the second-trimester decidua of normal pregnancy, displaying the ability to perform transendothelial invasion and induce endothelial tube formation *in vitro* in comparison to resting circulating neutrophil (13, 15). During maternal tolerance mediated by T cells, mice neutrophils in the pregnant uterus acquire an anti-inflammatory phenotype, undergo apoptosis, and release intracellular granules into T cells, favoring the Treg maternal tolerance, and placenta angiogenesis; the frequency of anti-inflammatory neutrophils is reduced in the blood of pre-eclampsia mothers (19). During childbirth, local neutrophils are classical pro-inflammatory cells, which contribute to fetus expulsion (20). Moreover, it is evident that pro-inflammatory activated neutrophils are involved in the pre-eclampsia pathogenesis, and a higher neutrophil-lymphocyte ratio is related to preterm labor (7, 18, 19, 21).

Some studies using antibody-mediated circulating neutrophil depletion approaches have highlighted the role of these cells in the placenta and fetus development. In this context, Higashisaka and collaborators showed that neutrophil depletion in mice on gestational day 15 just exacerbated the pregnancy complications induced by the silica nanoparticles, being that neutrophil depletion per se was not able to impair the pregnancy outcomes (22). On the other hand, Nadkarni and collaborators showed that neutrophil depletion on gestational days 5 and 8 promoted abnormal placentation and fetus alterations (19). These studies suggest that the effects of neutrophil depletion can be associated with the earlier stages of placentation. Indeed, we show that circulating neutrophils are required for efficient placentation and fetal development.

Material and methods

Animals and allogenic pregnancy

Mice were maintained and reproduced at Animal House at the School of Pharmaceutical Sciences, University of Sao Paulo

(Brazil) with chow and water *ad libitum* in a temperature-controlled room (22–25°C and 70% humidity) with a 12-hr light-dark cycle. Allogeneic pregnancy was performed by mating male Balb/C with female C57Bl/6 mice (both 5–6 weeks old). Females were caged overnight with males (3:1), and successful mating was verified the following morning by the presence of a vaginal plug. All procedures were performed according to the Brazilian Society for the Science of Laboratory Animals (SBCAL) and approved by the Institutional Animal Care and Use Committee from the Faculty of Pharmaceutical Sciences of the University of Sao Paulo (Protocol number 557).

Peripheral maternal neutrophil depletion

Neutrophil depletion was achieved by intraperitoneal injection of 200 µg anti-Gr1 antibody (clone RB6-8C5; e-Bioscience/Invitrogen, Waltham, Massachusetts, USA), isotype-matched control antibody (clone eB149/10H5; Rt IgG2b k; e-Bioscience/Invitrogen), or phosphate-buffered saline (Control) into C57Bl/6 pregnant at 24 h after vaginal plug visualization (reported as gestational day 0.5). Maternal blood was collected from the abdominal aorta and used to perform leukogram and flow cytometry.

Peripheral leukocyte profile and immunophenotyping by flow cytometry

The effectiveness of maternal peripheral neutrophil depletion and peripheral leukocyte profile was evaluated by total and differential leukogram, and flow cytometry. For the evaluation of maternal peripheral neutrophil depletion, peripheral blood was collected by aortic puncture in tubes containing heparin on gestational day 3.5. The leukogram was performed under optical microscopy by manual counting in the Neubauer chamber using Turk's solution. The morphological evaluation was performed using Panotico staining smears (peripheral blood mononuclear cells - MNs and peripheral polymorphonuclear cells - PMNs).

Flow cytometry was employed to confirm the efficacy of anti-Gr1 injection using peripheral blood collected by aortic puncture in tubes containing heparin. Leukocyte population, PMNs and MNs were isolated using forward versus side scatter channels.

Peripheral leukocyte profile was investigated by flow cytometry. Leukocytes were obtained from abdominal aorta on gestational day 18.5. Whole blood was lysed with an ammonium lysis buffer. Isolated leukocytes were incubated with PE-anti-mouse CD3; FITC anti-mouse CD4, APC anti-mouse CD8, APC anti-mouse FoxP3, PE anti-mouse B220; FITC anti-mouse F4/80; PerCP Cy5 anti-mouse-Gr1, and FITC anti-NK1.1 (BD-Bioscience or Invitrogen) for 50 minutes at room temperature and in the dark. In sequence, the labeling cells were acquired in an Accuri C6 flow cytometer (BD Biosciences), and 10,000 events were considered for analysis. The data were expressed as the frequency of positive cells.

Cesarean section procedure

C-sections were performed under aseptic conditions on gestational days 5.5 to count the number of implantation sites and on 18.5 to investigate the reproductive and pregnancy outcomes and to collect the fetus and placentas for posterior analysis. C-sections were performed after mice were anesthetized with xylazine and ketamine (7 mg/kg and 77 mg/kg, respectively; i.p; Vetbrands, Jacarei, SP, Brazil). In addition, on gestational day 18.5, maternal blood was collected from the abdominal aorta and used to identify the leukocyte profile by flow cytometry.

Reproductive and pregnancy outcomes calculation

On gestational day 5.5, the uterus was surgically removed for implantation points count. The pregnancy index and outcomes were performed as previously described (23, 24). Briefly, the successful pregnancy index was calculated considering the ratio of mice that presented vaginal plugs and the presence of live fetuses at C-section performed on gestational day 18.5. Also, the uterus and ovary were removed followed by the count of fetuses and resorption points. The uterus, placenta, and fetus were also weighted, and a placenta index was calculated by considering the ratio between the weight of the fetus and the weight of their respective placentas.

Histological procedures and analyses

Placentas were fixed in 4% buffered paraformaldehyde and histologically processed for inclusion in paraffin. Sections of 4 µm were stained according to analyses performed. The photomicrographs were obtained by optical microscopy using high-power objectives on the Imager.A2 Zeiss microscope (Zeiss, Oberkochen, Germany). The quantification of all the parameters cited below was carried out using ImageJ software by analyzing 5 fields of each section.

Placenta morphometric analysis

Placenta morphometry (total size, decidua, junctional zone, and labyrinth area) was measured in hematoxylin and eosin-stained (H&E) sections using the Axiovision software (Zeiss,

Oberkochen, Germany). Periodic Acid Schiff (PAS) staining was performed using a commercial kit and following the manufacturer's instructions (EasyPath; São Paulo, Brazil) to count the glycogen-positive cells. Also, the giant trophoblast cells and spongiotrophoblast were counted based on morphologic characteristics. The cell count was performed using the Cell counter tool from Image J software (National Institutes of Health, Bethesda, USA). Five fields were analyzed in the junctional zone from each placenta section by two independent observers.

Immunohistochemistry

After placenta section permeabilization (0.01% Triton X; Sigma) (Sigma-Aldrich, Burlington, USA) and antigen retrieval (sodium citrate buffer, 10 mM, pH 6.0, 30 minutes in 96°C), endogenous peroxidase was blocked with three rounds of 3% hydrogen peroxide. Slides were incubated with blocking buffer (5% Tris-buffered saline–bovine serum albumin; 1 h) and incubated overnight with purified rabbit anti-VEGF (1:200; Invitrogen) goat anti-ICAM, or anti-PECAM antibodies (both 1:25; Santa Cruz Biotechnology, Dallas, USA). Thus, the slides were washed with tris-buffered saline three times and then incubated with anti-rabbit (1:250; Abcam, Cambridge, UK) or anti-goat (1:100; R&D System, Minneapolis, USA) horseradish peroxidase (HRP) antibody, followed by 3,3-diaminobenzidine (DAB; DAKO, Glostrup, DEN), and hematoxylin counterstaining. As negative control of reactions, slides were incubated only with anti-rabbit or anti-goat HRP antibodies.

Statistical analysis

Data were analyzed using Student's t-test or one-factor analysis of variance (One-Way ANOVA) followed by Tukey *post-hoc* test using GraphPad software version 7. Differences between assessed means were considered statistically significant assuming $p < 0.05$. All results are shown as mean ± standard error of the mean. When needed, nominal data were statistically evaluated using the Fischer Exact Test and $p < 0.05$ was considered statistically significant.

Results

Neutrophils depletion before the implantation phase reduced the pregnancy index

Neutrophil depletion at the pre-receptive phase of implantation, was carried out by i.p. of anti-Gr1 24 hours after vaginal plug visualization (Figure 1A). In this experimental approach, a decrease in the circulating neutrophils number was observed up to 48 hours after anti-Gr1 i.p injection, while the mononuclear cells population was not affected (Figures 1B and b'). The depletion of circulating neutrophils abrogated implantation points in 50% of the pregnant mice, as observed by laparotomy performed on gestational day 5.5. Differently, all control animals (100%) presented around ten points of implantation. It is important to mention that the remaining 50% of mice treated with anti-Gr1, presented around eight and just one had almost twenty points of implantation (Figures 1C, D). On gestational day 18.5, pregnant mice were submitted for cesarean section and reproductive parameters were analyzed. Herein, it was observed that the number of resorption sites in neutrophil-depleted mice was similar to those found in the control/isotype groups (Figure 1E) Ilustrative image of the absence of resorption sites is exhibited in the Figure 1F - f'. Only one anti-Gr1 animal presented higher resorption sites as shown in Figure 1 - f'. Nonetheless, the pregnancy failure rate was around 60% in the neutrophil-depleted group. On the other hand, the control/isotype group showed a rate of pregnancy success of around 86% (Supplementary Table 1). Furthermore, in the neutrophil-depleted mice that had a successful pregnancy, the number of the fetuses was similar to the control group (Figure 1G), and the weight gain of pregnant mice and the weight of the pregnancy uterus were not altered (Supplementary Figures 1A, B). The gross analysis of the uterus showed that neutrophil depletion altered the placenta's disposition inside of uterine horns. As shown in Figure 1H, the control/isotype mice showed the same number of placenta on both uterine horns (four fetuses on each horn - left/right). On the other hand, neutrophil-depleted mice presented three and five placentas on the right and left horns, respectively, showing no equidistant pattern as observed for the control/isotype group. Moreover, the placental weight and index were not changed (Supplementary Figures 1C, D).

Neutrophils depletion impaired the development of the junctional zone

Macroscopic analysis of the placenta from neutrophil-depleted mice showed a reduced size and altered macrostructure compared to the control/isotype group (Figures 2A–C). Thus, morphometric analyses were performed. Placenta sections stained with H&E were used to measure the total area and the three main placental layers: the labyrinth (Lb), the junctional zone (JZ), and the maternal decidua (Dc) (Figures 2D–F). As shown in Figure 2G, the neutrophil-depleted mice showed a reduced total area in comparison to control/isotype groups. The labyrinth and decidua areas were not altered by neutrophil depletion (Figures 2H, I). However, it was verified that anti-Gr1 treatment decreased the junctional zone area (Figure 2J). Considering the role of the junctional zone as an endocrine

10.3389/fimmu.2022.969336

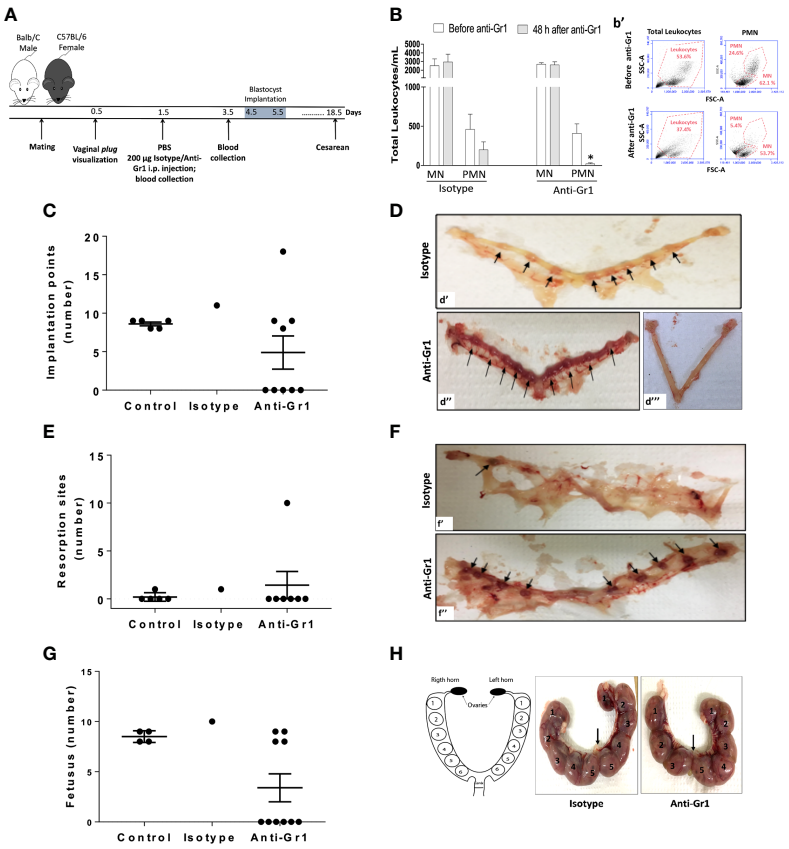

FIGURE 1
Neutrophil depletion before the implantation phase of pregnancy reduces pregnancy index and reproductive outcomes. Anti-Gr1/isotype injection and the subsequent endpoints were illustrated in the experimental workflow **(A)**. The total number of mononuclear cells (MN) and polymorphonuclear (PMN) was monitored before and after 48h of anti-Gr1/isotype i.p. injection by manual count **(B)** and flow cytometry **(b')**, respectively. On gestational day 5.5, mice were euthanized for implantation points count **(C)**. Representative images of implantation points **(D** - arrows**)** in the isotype **(d')**, and in the Anti-Gr1 **(d'')** groups are shown. The lack of implantation points observed in anti-Gr1 treated mice is also depicted **(d''')**. On gestational day 18.5, pregnant mice were submitted for cesarean and the number of resorption points **(E)**, fetuses **(G)**, and disposition of fetuses in the uterine horns **(H)** was analyzed. Representative images of resorption sites **(F)** in the isotype **(f')** and Anti-Gr1 **(f'')** are shown. Schematic diagram, isotype, and Anti-Gr1 placenta distribution into the uterine horns are demonstrated **(H)**. Each number indicates a fetus inside of the placenta. Arrow indicates cervix location. Data were statistically analyzed using One-Way ANOVA followed by Tukey's post-test (n= 5 – 9 animals/group) and $p < 0.05$ was considered statistically significant. * $p < 0.05$ versus respective control before Anti-Gr1 injection **(B)**. No significant difference was observed **(C, E, G)**.

compartment and potential energy source (25, 26), we evaluated whether the number of cell types that comprise this layer (glycogen trophoblast cells - GlyTCs; spongiotrophoblast - SpT; and trophoblast giant cells - TGCs) was altered. As shown in Figures 2K–M, at the junctional zone, it was verified the presence of GlyTC (arrow) exhibiting vacuoles containing particles of glycogen (PAS positive); TGCs (*) characterized by the largest cytoplasm and located at the boundary between JZ and Dc zones; and SpTs (arrowhead) identified as clusters of tightly packed polygonal cells that comprise the middle layer of the placenta sandwiched between the outer secondary TGCs and the Lb layer. Further, we observed that the number of GlyTC was not significantly altered by neutrophil depletion (Figure 2N). However, we verified that the counting of TGCs and SpT was decreased in neutrophil-depleted mice (Figures 2O, P).

The angiogenesis and adhesiveness markers in the junctional zone were altered by neutrophils depletion

Since VEGF, PECAM-1, and ICAM-1 are important for angiogenesis and placentation, their expression was assessed in the junctional zone by immunohistochemistry. We verified that

10.3389/fimmu.2022.969336

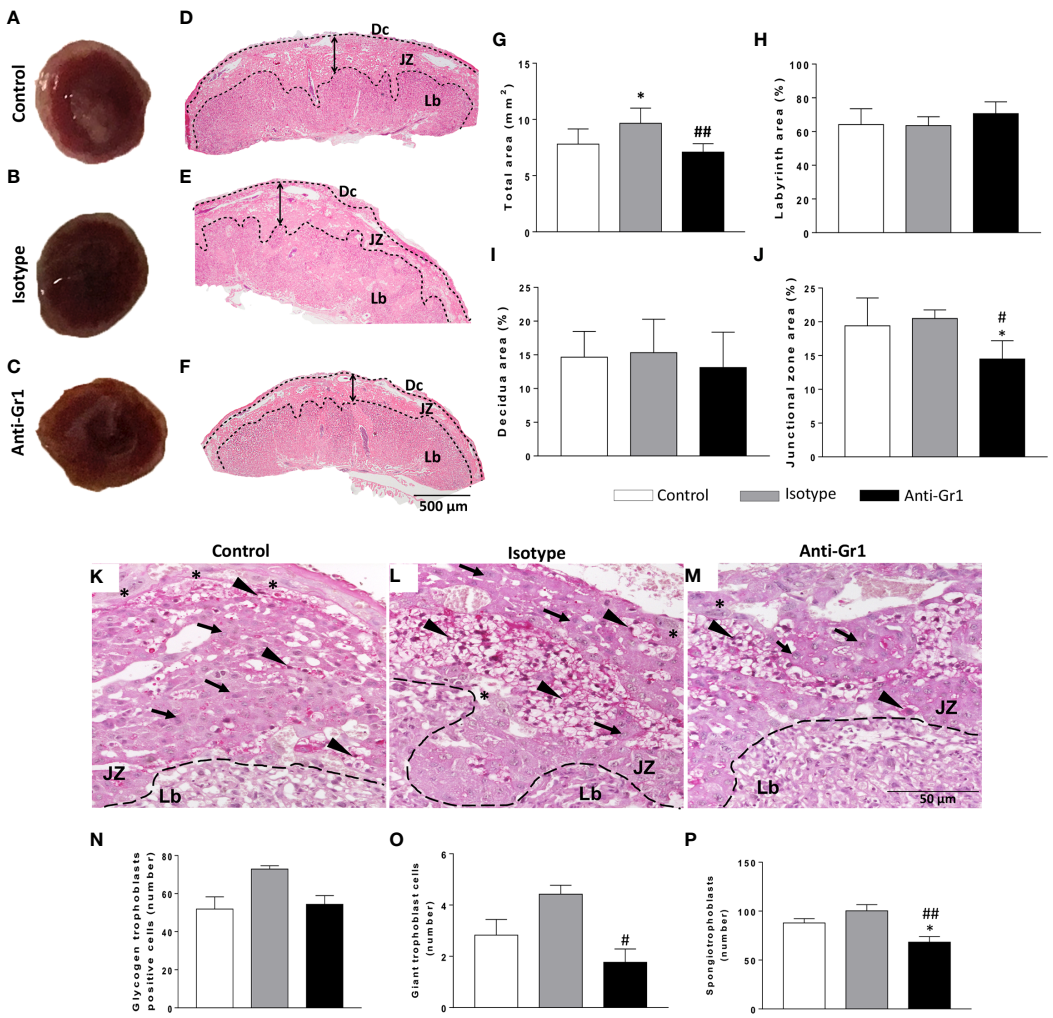

FIGURE 2
Neutrophil depletion altered placenta morphology and reduced the number of specialized cells in the junctional zone. On gestational day 18.5, placentas were removed for gross analyses **(A-C)** and then submitted for histology evaluation with H&E staining **(D-F)**. Morphometrical analysis was employed to measure the total area **(G)**, the Lb- labyrinth **(H)**, Dc - decidua **(I)**, and JZ - junctional zone **(J)** using PAS staining. The count of the types of cells in the junctional zone and the presence of glycogen trophoblast-positive cells was performed by analyzing five fields **(M)**. The trophoblast subtypes were quantified and indicated in the sections as glycogen-trophoblast cells **(N)**, giant trophoblast cells **(O)**, and spongiotrophoblast **(P)**. * < 0.05 in comparison to control group; #p < 0.05; ##p < 0.01 in comparison to isotype control. Data were statistically analyzed using One-Way ANOVA followed by Tukey's post-test (n = 6 – 9). Results were expressed as mean ± SEM. Arrowheads in PAS staining **(K-M)** indicate spongiotrophoblast (SpTs); arrows indicate glycogen trophoblasts (GlyTCs), and asterisks indicate giant trophoblast cells (TGCs). Embedding paraffin; sections thickness 4 µm. Bars 50 µm.

VEGF protein was expressed by TGCs and SpTs (Figures 3A–C). However, the neutrophil depletion reduced the number of VEGF-positive cells when compared to control/isotype groups (Figure 3L). The expression of PECAM- 1 (Figures 3D–F) and ICAM-1 (Figures 3G–I) was located especially in cells next to maternal vessels, being this pattern was observed for all studied groups (Figures 3J, K show the negative control). Nonetheless, the number of positive cells for the adhesion markers decreased in the neutrophil-depleted compared to the control/isotype groups (Figures 3M, N).

Neutrophils depletion modified the circulating leukocytes profile and promoted morphologic alterations in the offspring

The analysis of circulating leukocytes performed at the end of pregnancy showed the frequency of monocytes (F4/80+) and *natural killers*' cells (NK.1+), which were higher in neutrophil-depleted mice in comparison to control/isotype groups. The frequency of neutrophils (Ly6G+) and B lymphocytes (B220+)

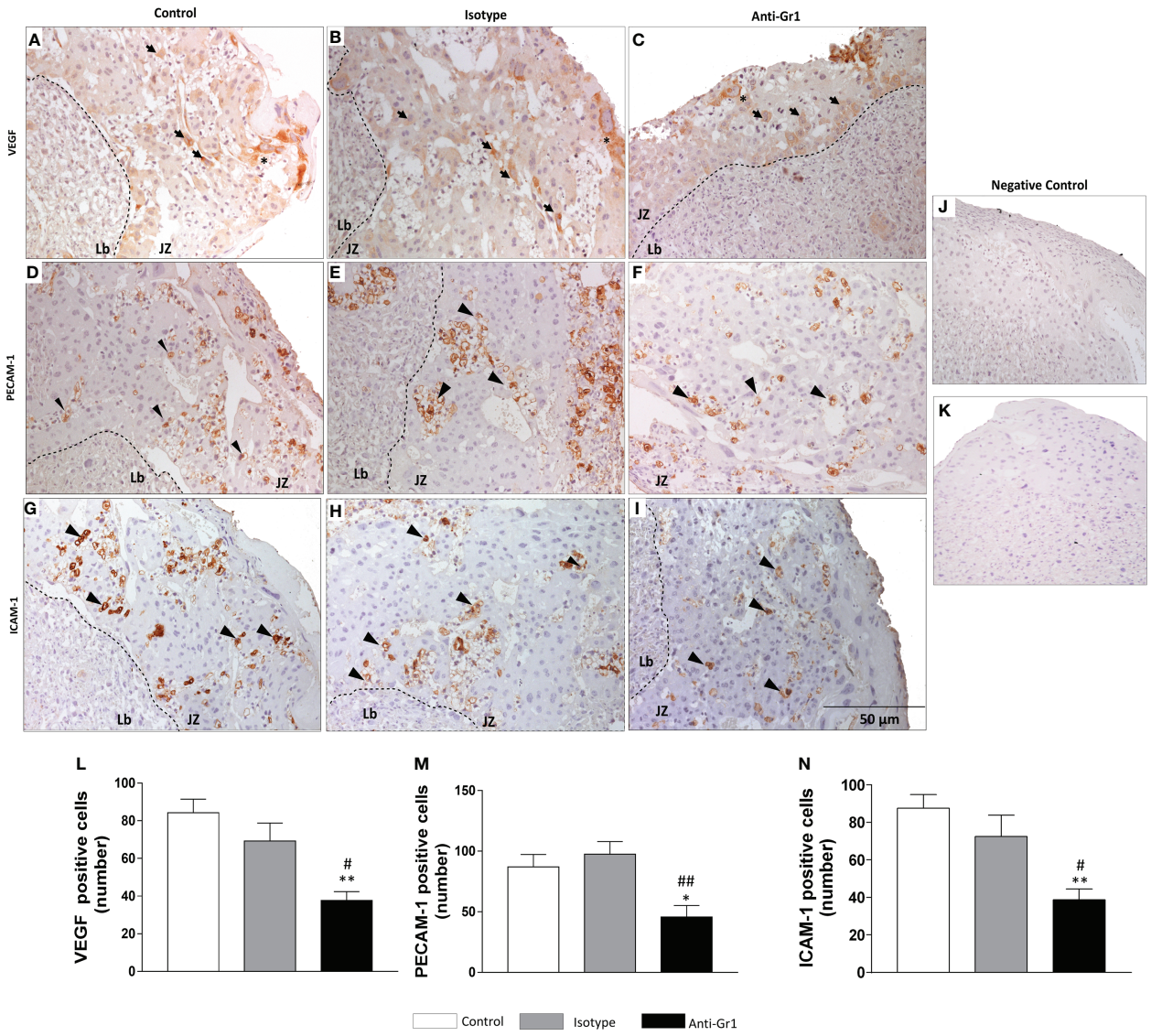

FIGURE 3
Neutrophil depletion altered angiogenesis and adhesiveness markers in the placenta. Expression and distribution of VEGF **(A-C)**, PECAM-1 **(D-F)**, and ICAM-1 **(G-I)** in the junctional zone of placenta were evaluated by immunohistochemistry. Negative control sections labeled with anti-rabbit **(J)** and anti-goat **(K)** HRP-conjugated antibodies. Count of VEGF **(L)**, PECAM-1 **(M)** and ICAM-1 **(N)** positive cells. *, **p < 0.05; 0.01 in comparison to control group; #, ##p <0.05, 0.01 in comparison to isotype. Data were statistically analyzed using One-Way ANOVA followed by Tukey's post-test (n= 4 – 6 placentas). Results were expressed as mean ± SEM. Immunoreactive cells for adhesiveness markers are indicated as arrowheads. Asterisks - giant trophoblast cells; TGCs. Arrows - spongiotrophoblast – SpTs. Counterstaining with hematoxylin; embedding paraffin; sections thickness 4 µm. Bars 50 µm.

was similar for both groups (Figure 4A). Furthermore, the circulating CD4+ and CD8+ cells were reduced in the neutrophil-depleted group (Figure 4B). However, in the CD4+ population, the frequency of T regulatory cells (FoxP3+) was increased in the neutrophil-depleted group (Figure 4C).

Considering that neutrophil depletion affected the placenta structure, we performed a gross evaluation of the offspring. Indeed, neutrophil depletion promoted significant abnormalities, as offspring presented an overall swollen appearance, indicative of generalized edema, and the limbs remained attached to the body (Figure 4D). It was also observed that the alterations displayed a pattern among the fetuses (Supplementary Figure 2A). The fetal weight was not changed (Supplementary Figure 2B). Altogether the gross analyses may indicate that neutrophil depletion evokes delayed fetal development.

10.3389/fimmu.2022.969336

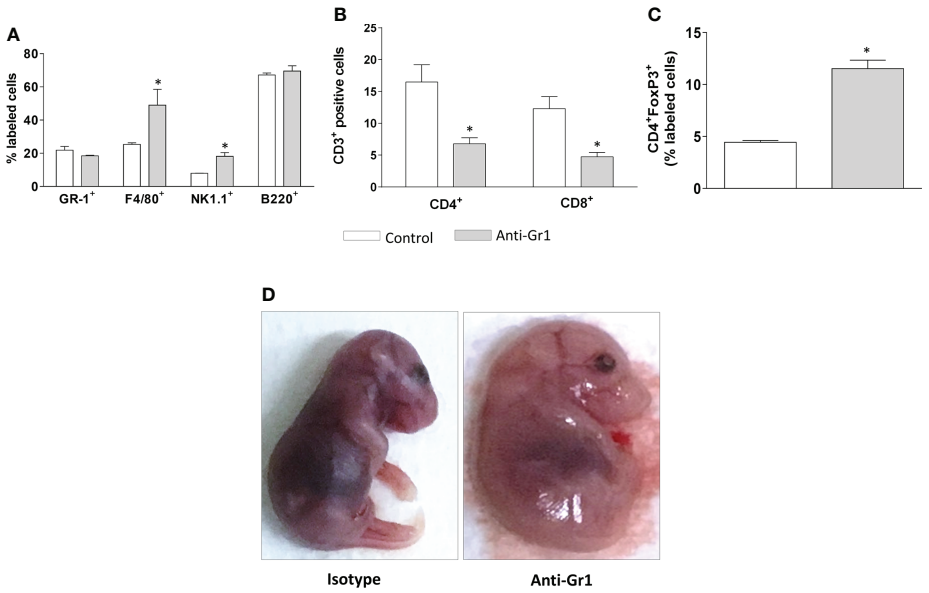

FIGURE 4
Neutrophil depletion altered the peripheral leukocyte profile and offspring development. On gestational day 18.5, peripheral leukocytes from mice were collected for immunophenotyping of granulocytes (Gr-1), monocytes (F4/80), *natural killers* cells (NK1.1), and mature B cells (B220) **(A)**. T lymphocyte subtypes were divided into CD3+ CD4/CD8 positive cells **(B)** and T regulatory cells, characterized as CD3+CD4+FoxP3+ positive cells **(C)**. The fetuses were carefully removed for gross analyses **(D)**. *p < 0.05 in comparison to the control group. Data were statistically analyzed using One-Way ANOVA followed by Tukey's post-test (n= 3 – 4 animals/group). Results were expressed as mean ± SEM.

Discussion

Pre-implantation embryos are highly sensitive to environmental conditions during the early development process (27), which includes embryonic epigenome remodeling, and the first cell differentiation. In this phase, blastocyst differentiates into inner cell mass which gives rise to the embryo, and trophectoderm will form the placenta (28).

It is well known that the implantation site resembles an inflammatory response, with a profusion of recruited immune cells (29) into the endometrial stroma and lumen from the blood (30–32). Innate immune cells are the significant population of leukocytes in the uterus at the time of blastocyst implantation. Uterine NK (uNK) cells are the most abundant population, although DCs, macrophages, neutrophils, and mast cells are also present (33). Even though the role of immune cells in pregnancy has been extensively investigated, many questions remain open. Thus, approaches such as immune cell depletion have been applied to better understand the role of the immune system at different phases of pregnancy. In this context, it has been shown the depletion of T regulatory cells in the early phase of pregnancy causes increased fetal resorption, maternal systemic inflammation, enhanced uterine artery resistance to flow and increased nitric oxide modulation of blood pressure (34). Furthermore, macrophages depletion evokes blastocyst implantation failure due to disruption of the luteal microvascular network associated with the decreased production of progesterone, which is essential for establishing pregnancy (35). Recently, the neutrophil's role in the placenta has been also discussed, as they address their role in the earliest phases of gestation (19, 22). Indeed, we here observed the depletion of neutrophils sustained at the beginning of WOI promoted a reduction of implantation points and compromised the placenta architecture and fetal development, reinforcing the signaling induced by neutrophils is necessary to the implantation of the blastocyst.

Implantation depends on a genetically healthy blastocyst and uterine receptivity (36). However, the immune cells' repertoire decides whether the uterine endometrium will be receptive or refractive. An immune-competent and receptive endometrium will tolerate and support the trophoblast invasion to initiate the placentation (33). Mouse placenta is organized in the maternal decidua, junctional zone, and labyrinth. The trophoblast giant cells (TGC) and spongiotrophoblast (SpT) are found in the junctional zone and the syncytiotrophoblast in the labyrinth (37). The TGCs help the embryo invade the uterine epithelium and implant it into the endometrium (38). These cells also acquire an invasive phenotype, penetrating deeply into the endometrial stroma and contacting maternal arteries, promoting vascular remodeling, the crucial step that supports the anatomical foundations for placenta development (39). While SpT probably has a structural function and produces

several layer-specific secreted factors that may prevent the growth of maternal blood vessels into the fetal placenta (40). Here, morphometric analyses showed the lack of maternal peripheral neutrophils decreased the placenta area due to junctional zone reduction, which presented a decreased TGC and SpT cells number. The reduced junctional zone observed in different experimental conditions has been associated with changing the endocrine environment in the placenta locally and with systemic effects on both fetus and mother (41–43). Also, the control of invasion of trophoblast cells depends on their interaction with immune cells (44, 45). Herein, the neutrophils depletion at the beginning of pregnancy seems to alter the invasion of trophoblast, and consequently impairs the proper placenta development.

Besides morphometric analyses, angiogenic and adhesiveness markers were assessed in the junctional zone. The VEGF-induced signaling controls the angiogenesis-vascularization during placentation. It is expressed in arteriolar smooth muscle, endothelium, trophoblast, uNKs, and decidual cells (46–49). The VEGF expression in the placenta microenvironment has been associated with the modulation of the TGC development and differentiation, and consequent maintenance of the homeostasis of the maternal vascular space in the mouse placenta (50). Additionally, placental VEGF has related to the modulation of metalloproteinase 2 and 9, which play a role in the endometrial tissue remodeling at implantation (51), decidualization (52), and trophoblast invasiveness (53, 54). The imbalance in the VEGF expression is associated with the abnormal placenta and its pathologies such as pre-eclampsia (55). Furthermore, it has been demonstrated that neutrophils at decidua basalis adopt a unique phenotype, expressing high levels of activation markers and angiogenesis-related proteins such as VEGF (13). Although immunohistochemical staining is not the most accurate for quantitative determination, here, we found a reduced number of VEGF-positive trophoblast cells associated with neutrophil depletion during the pre-receptive phase of embryo implantation.

Homotypic and heterotypic cell adhesions are pivotal to blastocyst implantation, and deficiencies in cell-cell interactions impair this process. Immunoglobulins cell adhesions, such as ICAM-1 and PECAM-1, display pivotal roles in immune response and tissue structure, as they are adhesion membrane proteins that cross-link with actin filaments. Also, they are relevant players in intracellular signaling during cell adhesions (56, 57). In pregnancy, ICAM-1 expression on the apical membrane of uterine epithelial cells and on the inner cells of trophoblast formation is enhanced at the time of implantation, which seems to be induced by progesterone secretion (58, 59). Furthermore, ICAM-1 is involved in maternal tolerance maintenance by controlling the secretion of Th2 cytokines (60). By being expressed on endothelial cells, PECAM-1 is highly involved in the angiogenesis process and its up-regulation on the placenta is expected, as novel vessels are required to irrigate the growing fetus. Several pieces of evidence support the role of PECAM-1 on pregnancy failures, as in preeclampsia, cytotrophoblasts fail to express PECAM-1 (54, 61). Mothers down expressing PECAM-1 suffer recurrent implantation failures, in a mechanism depending on the secretion of transforming growth factor β1 induced by PECAM-1 (62), and the impairment of PECAM-1 expression on blastocyst has been pointed out as an emerging marker to successfully assisted transfer embryo (63). Furthermore, PECAM-1 is detected early in the pluripotent inner cell mass of mouse blastocyst, which contains no vascular cells (64) (61), suggesting that it may exert additional roles on blastocyst implantation beyond angiogenesis. Despite the mechanisms displayed by neutrophils needing to be further evaluated, it is possible to infer that the impairment of VEGF, ICAM-1, and PECAM-1 positive cells associated with neutrophil depletion at the earlier phase of pregnancy contributes to placenta and fetus deficiencies shown here.

Many factors are involved in fetal malformation that includes specific genetic defects or congenital abnormalities in the embryo itself, intrauterine infections, and defects in placentation (39, 65). The association between placental dysfunction and fetus alterations has been explored in different contexts. It was shown that the majority of animal lethality found during genetic manipulation was associated with placental dysmorphologies, which were correlated with abnormalities, such as forebrain development, heart chamber, and septum morphology, subcutaneous edema, and overall artery or vein topology (66). Furthermore, alterations in the placenta during preeclampsia cause defective trophoblast invasion, spiral arterial impairment, and maternal decidua remodeling, leading to maternal and fetal complications or diseases (67, 68). Moreover, impairment in the development of the junctional, zone promotes endocrine changes in the placenta environment leading to reduced fetal growth (41, 43). Hence, the placental alterations promoted by neutrophil depletion during the pre-receptive phase of embryo implantation may be associated with the morphological alterations found in the offspring.

Altogether, the data obtained here highlight the relevance of maternal neutrophils in the earliest phase of pregnancy and to sustain placentation and fetus development. The reduced number of neutrophils in the pre-receptive phase led to fetal morphological alterations and an imbalance in the maternal peripheral leukocyte profile. The present data shed light on the intrinsic communication between neutrophils and pregnancy successful; further investigations will provide data to elucidate the fine-tuning mechanisms and signaling triggered by neutrophils during blastocyst implantation.

Data availability statement

The raw data supporting the conclusions of this article will be made available by the authors, without undue reservation.

Ethics statement

The animal study was reviewed and approved by Institutional Animal Care and Use Committee from the Faculty of Pharmaceutical Sciences of the University of Sao Paulo.

Author contributions

Conceptualization, CH, SF, and SS; Data curation, PS and SS; Funding acquisition, SF; Investigation, CH, PS, CG, and SS; Experiments, CH, AS, PS, and SS; Statistical analysis, CH, and SS; Supervision, SF, and SS; Validation, SF, and SS; Writing—original draft, CH, PS, SF, and SS; Writing—review and editing, CH, PS, SF, and SS. All authors contributed to the article and approved the submitted version.

Funding

This work was supported by FAPESP (Fundação de Amparo á Pesquisa do Estado de São Paulo), grant number 2014/07328-4; SF is a fellow researcher of CNPq (Conselho Nacional de Pesquisa); CH and SS were post-doctoral fellows of CAPES (Coordenação de Aperfeiçoamento de Pessoal de Nível Superior); PS is a PhD fellow of the FAPESP, grant number 2020/14368-3. AS is a Msc fellow of the CAPES.

Acknowledgments

The authors thank Franciani Rodrigues da Rocha from Núcleo de Pesquisa em Ciências Médicas, Fundação Universidade para o Desenvolvimento do Alto Vale do Itajaí – UNIDAVI; Rio do Sul, SC, Brazil for the statistical analysis support.

Conflict of interest

The authors declare that the research was conducted in the absence of any commercial or financial relationships that could be construed as a potential conflict of interest.

Publisher's note

All claims expressed in this article are solely those of the authors and do not necessarily represent those of their affiliated organizations, or those of the publisher, the editors and the reviewers. Any product that may be evaluated in this article, or claim that may be made by its manufacturer, is not guaranteed or endorsed by the publisher.

Supplementary material

The Supplementary Material for this article can be found online at: https://www.frontiersin.org/articles/10.3389/fimmu.2022.969336/full#supplementary-material

SUPPLEMENTARY FIGURE 1
Effects of neutrophil depletion on maternal weight gain, fetuses, and placental weight and index. Pregnant mice were weight on gestational day 1 and before euthanasia on day 18.5 **(A)**. After the cesarean, placenta **(B)** and pregnant utero **(C)** were weighted. The placenta index was based on the ratio of fetus weight in relation to its respective placenta **(D)**. Data were statistically analyzed using test "t" (n = 3 - 6). No significant difference was observed.

SUPPLEMENTARY FIGURE 2
Effects of neutrophil depletion on the offspring development. Representative image of offspring from control/isotype and anti-Gr1 groups **(A)**. Fetus weight **(B)**.

SUPPLEMENTARY TABLE 1
Pregnancy index (PI) was calculated considering the of number of females delivering live pups/number of females with evidence of pregnancy*100. Data was statistically evaluated using Fischer Exact Test and results obtained showed there was no statistical association between Isotype/PBS and anti-Gr1 (0.13) as $p < 0.05$ was considered statistically significant.

References

1. Norwitz ER, Schust DJ, Fisher SJ. Implantation and the survival of early pregnancy. *N Engl J Med* (2001) 345: 1400–8. doi: 10.1056/nejmra000763

2. Ng SW, Norwitz GA, Pavlicev M, Tilburgs T, Simón C, Norwitz ER. Endometrial decidualization: The primary driver of pregnancy health. *Int J Mol Sci* (2020) 21: 4092. doi: 10.3390/ijms21114092

3. Governini L, Luongo FP, Haxhiu A, Piomboni P, Luddi A. Main actors behind the endometrial receptivity and successful implantation. *Tissue Cell* (2021) 73:101656. doi: 10.1016/j.tice.2021.101656

4. Guo X, Yi H, Li TC, Wang Y, Wang H, Chen X. Role of vascular endothelial growth factor (Vegf) in human embryo implantation: Clinical implications. *Biomolecules* (2021) 11: 253. doi: 10.3390/biom11020253

5. Boeldt DS, Bird IM. Vascular adaptation in pregnancy and endothelial dysfunction in preeclampsia. *J Endocrinol* (2017) 232: R27–R44. doi: 10.1530/JOE-16-0340

6. Ball E, Bulmer JN, Ayis S, Lyall F, Robson SC. Late sporadic miscarriage is associated with abnormalities in spiral artery transformation and trophoblast invasion. *J Pathol* (2006) 208: 535–42. doi: 10.1002/path.1927

7. Bert S, Ward EJ, Nadkarni S. Neutrophils in pregnancy: New insights into innate and adaptive immune regulation. *Immunology* (2021) 164: 665–676. doi: 10.1111/imm.13392

8. Liu Y, Gao S, Zhao Y, Wang H, Pan Q, Shao Q. Decidual natural killer cells: A good nanny at the maternal-fetal interface during early pregnancy. *Front Immunol* (2021) 12:663660. doi: 10.3389/fimmu.2021.663660

9. Schjenken JE, Green ES, Overduin TS, Mah CY, Russell DL, Robertson SA. Endocrine disruptor compounds–a cause of impaired immune tolerance driving inflammatory disorders of pregnancy? *Front Endocrinol (Lausanne)* (2021) 12:607539. doi: 10.3389/fendo.2021.607539

10. Hellebrekers P, Vrisekoop N, Koenderman L. Neutrophil phenotypes in health and disease. *Eur J Clin Invest* (2018) 48: e12943. doi: 10.1111/eci.12943

11. Kim HR, Kim YS, Yoon JA, Yang SC, Park M, Seol DW, et al. Estrogen induces EGR1 to fine-tune its actions on uterine epithelium by controlling PR signaling for successful embryo implantation. *FASEB J* (2018) 32:1184–95. doi: 10.1096/fj.201700854RR

12. Croxatto D, Micheletti A, Montaldo E, Orecchia P, Loiacono F, Canegallo F, et al. Group 3 innate lymphoid cells regulate neutrophil migration and function in human decidua. *Mucosal Immunol* (2016) 9: 1372–1383. doi: 10.1038/mi.2016.10

13. Amsalem H, Kwan M, Hazan A, Zhang J, Jones RL, Whittle W, et al. Identification of a novel neutrophil population: Proangiogenic granulocytes in second-trimester human decidua. *J Immunol* (2014) 193:3070–9. doi: 10.4049/jimmunol.1303117

14. Giaglis S, Stoikou M, Grimolizzi F, Subramanian BY, van Breda SV, Hoesli I, et al. Neutrophil migration into the placenta: Good, bad or deadly? *Cell Adhes Migr* (2016) 10:208–25. doi: 10.1080/19336918.2016.1148866

15. Giaglis S, Stoikou M, Chowdhury CS, Schaefer G, Grimolizzi F, Rossi SW, et al. Multimodal regulation of NET formation in pregnancy: Progesterone antagonizes the pro-NETotic effect of estrogen and G-CSF. *Front Immunol* (2016) 7:565. doi: 10.3389/fimmu.2016.00565

16. Calo G, Sabbione F, Vota D, Paparini D, Ramhorst R, Trevani A, et al. Trophoblast cells inhibit neutrophil extracellular trap formation and enhance apoptosis through vasoactive intestinal peptide-mediated pathways. *Hum Reprod* (2017) 32:55–64. doi: 10.1093/humrep/dew292

17. Gupta AK, Hasler P, Holzgreve W, Gebhardt S, Hahn S. Induction of neutrophil extracellular DNA lattices by placental microparticles and IL-8 and their presence in preeclampsia. *Hum Immunol* (2005) 66:1146–54. doi: 10.1016/j.humimm.2005.11.003

18. Hahn S, Giaglis S, Hoesli I, Hasler P. Neutrophil NETs in reproduction: From infertility to preeclampsia and the possibility of fetal loss. *Front Immunol* (2012) 3:362. doi: 10.3389/fimmu.2012.00362

19. Nadkarni S, Smith J, Sferruzzi-Perri AN, Ledwozyw A, Kishore M, Haas R, et al. Neutrophils induce proangiogenic T cells with a regulatory phenotype in pregnancy. *Proc Natl Acad Sci U.S.A.* (2016) 113:E8415-E8424. doi: 10.1073/pnas.1611944114

20. Gomez-Lopez N, StLouis D, Lehr MA, Sanchez-Rodriguez EN, Arenas-Hernandez M. Immune cells in term and preterm labor. *Cell Mol Immunol* (2014) 11:571-81. doi: 10.1038/cmi.2014.46

21. Vakili S, Torabinavid P, Tabrizi R, Shojazadeh A, Asadi N, Hessami K. The association of inflammatory biomarker of neutrophil-to-Lymphocyte ratio with spontaneous preterm delivery: A systematic review and meta-analysis. *Mediators Inflammation* (2021) 2021:6668381. doi: 10.1155/2021/6668381

22. Higashisaka K, Nakashima A, Iwahara Y, Aoki A, Nakayama M, Yanagihara I, et al. Neutrophil depletion exacerbates pregnancy complications, including placental damage, induced by silica nanoparticles in mice. *Front Immunol* (2018) 9:1850. doi: 10.3389/fimmu.2018.01850

23. Hurt B, Schulick R, Edil B, El KC, Barnett C. The American journal of surgery cancer-promoting mechanisms of tumor-associated neutrophils. *Am J Surg* (2017); 214: 1–7. doi: 10.1016/j.amjsurg.2017.08.003

24. Hebeda CB, Machado ID, Reif-Silva I, Moreli JB, Oliani SM, Nadkarni S, et al. Endogenous annexin A1 (AnxA1) modulates early-phase gestation and offspring sex-ratio skewing. *J Cell Physiol* (2018) 233:6591–603. doi: 10.1002/jcp.26258

25. Coan PM, Conroy N, Burton GJ, Ferguson-Smith AC. Origin and characteristics of glycogen cells in the developing murine placenta. *Dev Dyn* (2006) 235:3280–94. doi: 10.1002/dvdy.20981

26. Simmons DG, Cross JC. Determinants of trophoblast lineage and cell subtype specification in the mouse placenta. *Dev Biol* (2005) 284:12–24. doi: 10.1016/j.ydbio.2005.05.010

27. Monk D, Mackay DJG, Eggermann T, Maher ER, Riccio A. Genomic imprinting disorders: lessons on how genome, epigenome and environment interact. *Nat Rev Genet* (2019) 20: 235–248. doi: 10.1038/s41576-018-0092-0

28. Marikawa Y, Alarcón VB. Establishment of trophectoderm and inner cell mass lineages in the mouse embryo. *Mol Reprod Dev* (2009) 76: 1019–32. doi: 10.1002/mrd.21057

29. Griffith OW, Chavan AR, Protopapas S, Maziarz J, Romero R, Wagner GP. Embryo implantation evolved from an ancestral inflammatory attachment reaction. *Proc Natl Acad Sci U.S.A.* (2017) 114:E6566–E6575. doi: 10.1073/pnas.1701129114

30. Schjenken JE, Glynn DJ, Sharkey DJ, Robertson SA. TLR4 signaling is a major mediator of the female tract response to seminal fluid in mice. *Biol Reprod* (2015) 93:68. doi: 10.1095/biolreprod.114.125740

31. De M, Choudhuri R, Wood GW. Determination of the number and distribution of macrophages, lymphocytes, and granulocytes in the mouse uterus from mating through implantation. *J Leukoc Biol* (1991) 50: 252–62. doi: 10.1002/jlb.50.3.252

32. Robertson SA, Mau VJ, Tremellen KP, Seamark RF. Role of high molecular weight seminal vesicle proteins in eliciting the uterine inflammatory response to semen in mice. *J Reprod Fertil* (1996) 107: 265–77. doi: 10.1530/jrf.0.1070265

33. Schumacher A, Sharkey DJ, Robertson SA, Zenclussen AC. Immune cells at the fetomaternal interface: How the microenvironment modulates immune cells to foster fetal development. *J Immunol* (2018) 201:325–334. doi: 10.4049/jimmunol.1800058

34. Care AS, Bourque SL, Morton JS, Hjartarson EP, Robertson SA, Davidge ST. Reduction in regulatory t cells in early pregnancy causes uterine artery dysfunction in mice. *Hypertension* (2018) 72: 177–187. doi: 10.1161/HYPERTENSIONAHA.118.10858

35. Care AS, Diener KR, Jasper MJ, Brown HM, Ingman WV, Robertson SA. Macrophages regulate corpus luteum development during embryo implantation in mice. *J Clin Invest* (2013) 123:3472–87. doi: 10.1172/JCI60561

36. Paria BC, Reese J, Das SK, Dey SK. Deciphering the cross-talk of implantation: Advances and challenges. *Science* (2002) 296:2185–8. doi: 10.1126/science.1071601

37. Watson ED, Cross JC. Development of structures and transport functions in the mouse placenta. *Physiology* (2005) 20:180–93. doi: 10.1152/physiol.00001.2005

38. Latos PA, Hemberger M. From the stem of the placental tree: Trophoblast stem cells and their progeny. *Dev* (2016) 143:3650–66. doi: 10.1242/dev.133462

39. Woods L, Perez-Garcia V, Hemberger M. Regulation of placental development and its impact on fetal growth–new insights from mouse models. *Front Endocrinol (Lausanne)* (2018) 9:570. doi: 10.3389/fendo.2018.00570

40. Cross JC, Hemberger M, Lu Y, Nozaki T, Whiteley K, Masutani M, et al. Trophoblast functions, angiogenesis and remodeling of the maternal vasculature in the placenta. *Mol Cell Endocrinol* (2002); 187: 207–12. doi: 10.1016/S0303-7207(01)00703-1

41. Salas M, John R, Saxena A, Barton S, Frank D, Fitzpatrick G, et al. Placental growth retardation due to loss of imprinting of Phlda2. *Mech Dev* (2004) 121:1199–210. doi: 10.1016/j.mod.2004.05.017

42. Tunster SJ, Van De Pette M, John RM. Impact of genetic background on placental glycogen storage in mice. *Placenta* (2012) 33:124–7. doi: 10.1016/j.placenta.2011.11.011

43. Fowden AL, Moore T. Maternal-fetal resource allocation: Co-operation and conflict. *Placenta* (2012) 33:e11-5. doi: 10.1016/j.placenta.2012.05.002

44. Stieglitz F, Celik AA, von Kaisenberg C, Camps MA, Blasczyk R, Bade-Döding C. The microstructure in the placenta is influenced by the functional diversity of HLA-G allelic variants. *Immunogenetics* (2019) 71:455–46. doi: 10.1007/s00251-019-01121-0

45. Fu B, Zhou Y, Ni X, Tong X, Xu X, Dong Z, et al. Natural killer cells promote fetal development through the secretion of growth-promoting factors. *Immunity* (2017) 47:1100–13. doi: 10.1016/j.immuni.2017.11.018

46. Hoffmann P, Feige JJ, Alfaidy N. Placental expression of EG-VEGF and its receptors PKR1 (Prokineticin receptor-1) and PKR2 throughout mouse gestation. *Placenta* (2007) 28:1049–58. doi: 10.1016/j.placenta.2007.03.008

47. Zhang J, Chen Z, Smith GN, Croy BA. Natural killer cell-triggered vascular transformation: Maternal care before birth? *Cell Mol Immunol* (2011) 8:1–11. doi: 10.1038/cmi.2010.38

48. Hofmann AP, Gerber SA, Croy BA. Uterine natural killer cells pace early development of mouse decidua basalis. *Mol Hum Reprod* (2014) 20:66–76. doi: 10.1093/molehr/gat060

49. Ventureira MR, Sobarzo C, Argandoña F, Palomino WA, Barbeito C, Cebral E. Decidual vascularization during organogenesis after perigestational alcohol ingestion. *Reproduction* (2019) 158:109–22. doi: 10.1530/REP-18-0230

50. Fan X, Muruganandan S, Shallie PD, Dhal S, Petitt M, Nayak NR. Vegf maintains maternal vascular space homeostasis in the mouse placenta through modulation of trophoblast giant cell functions. *Biomolecules* (2021) 11:1062. doi: 10.3390/biom11071062

51. Novaro V, Pustovrh C, Colman-Lerner A, Radisky D, Lo Nostro F, Paz D, et al. Nitric oxide induces gelatinase a (matrix metalloproteinase 2) during rat embryo implantation. *Fertil Steril* (2002) 78:487–96. doi: 10.1016/S0015-0282(02)04240-1

52. Fontana V, Coll TA, Sobarzo CMA, Tito LP, Calvo JC, Cebral E. Matrix metalloproteinase expression and activity in trophoblastdecidual tissues at

organogenesis in CF-1 mouse. *J Mol Histol* (2012) 78:487–96. doi: 10.1007/s10735-012-9429-8

53. Staun-Ram E, Goldman S, Gabarin D, Shalev E. Expression and importance of matrix metalloproteinase 2 and 9 (MMP-2 and -9) in human trophoblast invasion. *Reprod Biol Endocrinol* (2004) 2:59. doi: 10.1186/1477-7827-2-59

54. Gualdoni G, Gomez Castro G, Hernández R, Barbeito C, Cebral E. Comparative matrix metalloproteinase-2 and -9 expression and activity during endotheliochorial and hemochorial trophoblastic invasiveness. *Tissue Cell* (2022) 74:101698. doi: 10.1016/j.tice.2021.101698

55. Cerdeira AS, Karumanchi SA. Angiogenic factors in preeclampsia and related disorders. *Cold Spring Harb Perspect Med* (2012) 2:a006585. doi: 10.1101/cshperspect.a006585

56. Yonemura S, Tsukita S, Tsukita S. Direct involvement of ezrin/radixin/moesin (ERM)-binding membrane proteins in the organization of microvilli in collaboration with activated ERM proteins. *J Cell Biol* (1999) 145:1497–509. doi: 10.1083/jcb.145.7.1497

57. Ley K, Laudanna C, Cybulsky MI, Nourshargh S. Getting to the site of inflammation: The leukocyte adhesion cascade updated. *Nat Rev Immunol* (2007) 7:678–89. doi: 10.1038/nri2156

58. Lecce L, Kaneko Y, Madawala RJ, Murphy CR. ICAM1 and fibrinogen-γ are increased in uterine epithelial cells at the time of implantation in rats. *Mol Reprod Dev* (2011) 78:318–27. doi: 10.1002/mrd.21307

59. Matsumoto H, Daikoku T, Wang H, Sato E, Dey SK. Differential expression of Ezrin/Radixin/Moesin (ERM) and ERM-associated adhesion molecules in the blastocyst and uterus suggests their functions during implantation. *Biol Reprod* (2004) 70:729–36. doi: 10.1095/biolreprod.103.022764

60. Takeshita T, Satomi M, Akira S, Nakagawa Y, Takahashi H, Araki T. Preventive effect of monoclonal antibodies to intercellular adhesion molecule-1 and leukocyte function-associate antigen-1 on murine spontaneous fetal resorption. *Am J Reprod Immunol* (2000) 43:80–5. doi: 10.1111/j.8755-8920.2000.430308.x

61. Cho S, Sohn YD, Kim S, Rajakumar A, Badell ML, Sidell N, et al. Reduced angiovasculogenic and increased inflammatory profiles of cord blood cells in severe but not mild preeclampsia. *Sci Rep* (2021) 11:3630. doi: 10.1038/s41598-021-83146-8

62. Guo F, Si C, Zhou M, Wang J, Zhang D, Leung PCK, et al. Decreased PECAM1-mediated TGF-β1 expression in the mid-secretory endometrium in women with recurrent implantation failure. *Hum Reprod* (2018) 33:832–843. doi: 10.1093/humrep/dey022

63. Freis A, Roesner S, Marshall A, Rehnitz J, von Horn K, Capp E, et al. Non-invasive embryo assessment: Altered individual protein profile in spent culture media from embryos transferred at day 5. *Reprod Sci* (2021) 28:1866–1873. doi: 10.1007/s43032-020-00362-9

64. Robson P, Stein P, Zhou B, Schultz RM, Baldwin HS. Inner cell mass-specific expression of a cell adhesion molecule (PECAM-1/CD31) in the mouse blastocyst. *Dev Biol* (2001) 234:317–29. doi: 10.1006/dbio.2001.0274

65. Sharma D, Shastri S, Sharma P. Intrauterine growth restriction: Antenatal and postnatal aspects. *Clin Med Insights Pediatr* (2016) 10:67–83. doi: 10.4137/cmped.s40070

66. Perez-Garcia V, Fineberg E, Wilson R, Murray A, Mazzeo CI, Tudor C, et al. Placentation defects are highly prevalent in embryonic lethal mouse mutants. *Nature* (2018) 555:463–8. doi: 10.1038/nature26002

67. Roberts JM, Escudero C. The placenta in preeclampsia. *Pregnancy Hypertens* (2012) 2:72–83. doi: 10.1016/j.preghy.2012.01.001

68. Lyall F, Robson SC, Bulmer JN. Spiral artery remodeling and trophoblast invasion in preeclampsia and fetal growth restriction relationship to clinical outcome. *Hypertension* (2013) 62:1046–5. doi: 10.1161/HYPERTENSIONAHA.113.01892

frontiers | Frontiers in Immunology

TYPE Original Research
PUBLISHED 13 October 2022
DOI 10.3389/fimmu.2022.1005551

OPEN ACCESS

EDITED BY
Krishna Rajarathnam,
University of Texas Medical Branch at Galveston, United States

REVIEWED BY
Shuvasree Sengupta,
University of Michigan, United States
Sudarshan Rajagopal,
Duke University Health System, United States

*CORRESPONDENCE
Gwendal Lazennec
Gwendal.lazennec@sys2diag.cnrs.fr

SPECIALTY SECTION
This article was submitted to Inflammation, a section of the journal Frontiers in Immunology

RECEIVED 29 July 2022
ACCEPTED 23 September 2022
PUBLISHED 13 October 2022

CITATION
Delobel P, Ginter B, Rubio E, Balabanian K and Lazennec G (2022) CXCR2 intrinsically drives the maturation and function of neutrophils in mice.
Front. Immunol. 13:1005551.
doi: 10.3389/fimmu.2022.1005551

CXCR2 intrinsically drives the maturation and function of neutrophils in mice

Pauline Delobel[1], Benjamin Ginter[1], Eliane Rubio[1], Karl Balabanian[2,3] and Gwendal Lazennec[1,2]*

[1]CNRS, UMR9005, Sys2Diag-ALCEN, Cap delta, Montpellier, France, [2]CNRS, GDR 3697 "Microenvironment of tumor niches", Micronit, France, [3]Université Paris-Cité, Institut de Recherche Saint-Louis, INSERM U1160, Paris, France

Neutrophils play a major role in the protection from infections but also in inflammation related to tumor microenvironment. However, cell-extrinsic and -intrinsic cues driving their function at steady state is still fragmentary. Using *Cxcr2* knock-out mice, we have evaluated the function of the chemokine receptor Cxcr2 in neutrophil physiology. We show here that Cxcr2 deficiency decreases the percentage of mature neutrophils in the spleen, but not in the bone marrow (BM). There is also an increase of aged CD62L^{lo} CXCR4^{hi} neutrophils in the spleen of KO animals. Spleen *Cxcr2*$^{-/-}$ neutrophils display a reduced phagocytic ability, whereas BM neutrophils show an enhanced phagocytic ability compared to WT neutrophils. Spleen *Cxcr2*$^{-/-}$ neutrophils show reduced reactive oxygen species production, F-actin and α-tubulin levels. Moreover, spleen *Cxcr2*$^{-/-}$ neutrophils display an altered signaling with reduced phosphorylation of ERK1/2 and p38 MAPK, impaired PI3K-AKT, NF-κB, TGFβ and IFNγ pathways. Altogether, these results suggest that Cxcr2 is essential for neutrophil physiology.

KEYWORDS

chemokine receptors, Cxcr2, neutrophils, inflammation, tumor microenvironment

Introduction

One of the first line of defense against pathogens such as bacteria, fungi, or parasites involves neutrophils, which are key mediator of innate immunity and inflammation. Neutrophils use different ways to clear the infection, including bacterial uptake (phagocytosis), phagolysosomal degradation of bacteria with a cocktail of antimicrobial factors and reactive oxygen species (ROS) (oxidative burst) or release of granules to neutralize extracellular pathogens (degranulation) (1). In addition, when intruders are too large or have escaped the other microbial killing processes, neutrophils can extrude a physical barrier to pathogen dissemination, called a neutrophil extracellular trap (NET), containing DNA, histones and granule proteases (2).

10.3389/fimmu.2022.1005551

Neutrophils are the most abundant circulating leukocytes, representing 50% to 70% of all circulating leukocytes in humans and about 10 to 25% in mice (3). Neutrophils are relatively short lived cells (4), even if recent studies have questioned this aspect and it is now believed that human and murine neutrophils could have a half-life of 5 days or 18h, respectively (5).

Neutrophils arise from granulocyte–monocyte progenitors (GMPs), mostly within the bone marrow (BM) during hematopoiesis in response to several cytokines, principally granulocyte colony–stimulating factor (G-CSF) (6), but also from extramedullary tissues such as spleen (7–9). The first progenitor that is 'neutrophil committed' is the neutrophil promyelocyte (10), which then maturates through granulocyte-committed precursors comprising myeloblasts, promeylocytes and myelocytes, to a post-mitotic or transition pool of metamyelocytes, band cells and segmented neutrophils (11). Mature post-mitotic neutrophils are released from the BM into the peripheral blood, extravasate from circulation into the tissues under the coordinate regulation of various adhesion molecules and chemokines (12). They are involved not only in the control of inflammation following infections or injuries but have also pro or anti-tumoral actions as tumor associated neutrophils (TANs) (13–15). In inflammatory sites, neutrophils fight the injury or infection and undergo apoptosis and are phagocyted by macrophages, once inflammation has been resolved (16). Senescent neutrophils can also home back to the BM in a Cxcr4-dependent mechanism (17). The terminal differentiation of neutrophils in the BM, before release into the bloodstream, is still a subject of debate, as some steps of maturation could occur in other organs such as the spleen (9) and in the same line, neutrophil progenitors have been found in the spleen (18). Maturation markers of neutrophils are also currently discussed, but classically Ly6G, Cd101, Cxcr4 and Cxcr2 are used in mice (8, 12).

Cxcr2 appears as one of the key chemokine receptor expressed by neutrophils both in mice and humans (19, 20). Cxcr2 binds the chemokines Cxcl1, 2, 3, 5, 6, 7 and 8 in human, which all have pro-angiogenic properties and are located in a short cluster of chromosome 4 (21–23). Cxcr2 ligand action is conditioned by its interaction with proteoglycans (24) and Cxcr2 signals through multiple pathways including PI3K and Src (25). In addition, recent work has highlighted the role of Cxcr2 in tumorigenesis, in particular through tumor-associated neutrophils (14, 23, 26, 27), but also in the effects microbiota on pituitary function (28). *Cxcr2* knockout mice have been generated and are characterized by a splenomegaly due to an increase of metamyelocytes, mature neutrophils and B lymphocytes (29). These mice also display a defect in neutrophil recruitment after infection (30).

So far, the mechanism of Cxcr2 action in neutrophils remains poorly understood. In this study, we have investigated the role of Cxcr2 in mouse neutrophils in the spleen and the BM, taking advantage of *Cxcr2*$^{-/-}$ mice. Our data show that Cxcr2 impairment in neutrophils affects differently spleen and BM neutrophils in terms of maturation, phagocytosis and ROS production. Moreover, we analyzed at the transcriptomic level the pathways that were altered by *Cxcr2* deletion in neutrophils. Altogether, these results suggest that proper Cxcr2 expression and function is required for maturation and effector functions of peripheral neutrophils.

Materials and methods

Animal models and housing

All animal experiments conformed to our animal protocols that were reviewed and approved by the Institutional Animal Care and Use Committee. *Cxcr2*$^{-/-}$ mice (29) were obtained from the Jackson Laboratory. *Cxcr2*$^{-/-}$ mice were backcrossed in FVB genetic background for more than 12 generations. Control (WT) mice were also in a FVB background. All mice were housed in a SOPF (Specific and Opportunistic Pathogen Free) animal facility.

Isolation of cells

Cells from the BM were isolated by centrifugation from the femurs and tibias of the animals, whereas spleens were mashed on 100 µm nylon cell strainer. After centrifugation, red blood cells were eliminated by treatment with ACK buffer (0.155 mM NH4Cl, 1 mM KHCO3, 0.1 mM EDTA) and filtered on a 40 µm nylon cell strainer. After ACK treatment, cells were filtered on a 40 µm nylon cell strainer. For neutrophil isolation, a first enrichment with EasySep™ Mouse CD11b Positive Selection kit (StemCell technologies, Grenoble, France) was performed followed by cell sorting of CD45+ CD11b+ Ly6G+ F4/80- cells on an ARIA IIu FACS sorter (Becton Dickinson, Le Pont-de-Claix, France).

Flow cytometry

Flow cytometry experiments were performed with the following conjugated antibodies from Biolegend (London, United Kingdom): anti-mouse CD11b (clone M1/70), CD45 (clone 30-F11), Cxcr2 (clone SA044G4), Ly6G (clone 1A8), CD62L (clone MEL-14) or BD Biosciences (BD Biosciences, Le Pont-de-Claix, France): Cxcr4 (clone 2B11), or Ebiosciences (Fisher Scientific, Illkirch, France): CD101 (clone Moushi101), Fixable viability dye (65-0866). Flow analysis was performed on live singlets with a LSR II Fortessa flow cytometer (Becton Dickinson, Le Pont-de-Claix, France). Data were analyzed using FlowJo (Tree Star).

Intracellular flow cytometry

Cells were first stained with antibodies directed against extracellular markers (CD45, CD11b, Ly6G) and then permeabilized with Cytofix/Cytoperm and Permwash buffer (BD Biosciences). Intracellular staining of F-actin was performed with Phalloidin, Fluorescein Isothiocyanate Labeled (Sigma-Aldrich, ref P5282), whereas α-tubulin was labeled with α-Tubulin antibody (clone 11H10, Cell Signaling, ref 2125) followed by secondary an anti-rabbit IgG antibody coupled to Alexa Fluor 555 (ThermoFisher, ref A27039). Phospho-p42/44 MAPK ERK1/2 (Thr 202/Tyr 204) (Cell signaling, ref 4370) followed by secondary an anti-rabbit IgG antibody coupled to Alexa Fluor 555 (ThermoFisher, ref A27039) was used to detect Phospho-p42/44 MAPK ERK1/2. p-p38 MAPK (Thr 180/Tyr 182) coupled to PE (cell Signaling 6908), was used to detect phospho-p38 MAPK.

Annexin V staining and measure of mortality

To determine the proportion of apoptotic and dead cells, fresh neutrophils were stained with Annexin-FITC and propidium iodide (PI) according to manufacturer instruction (Invitrogen, ref V13242).

Phagocytosis assay

CD45+ CD11b+ Ly6G+ neutrophils were incubated for various times at 37°C with E. coli Red Phrodo bioparticles (ThermoFisher, Illkirch, France) at a concentration of 15 µg/ml and analyzed in a kinetic manner by flow cytometry with a LSR II Fortessa flow cytometer (Becton Dickinson, Le Pont-de-Claix, France). Data were analyzed using FlowJo (Tree Star). When opsonized particles were used, they were opsonized for 1h at 37°C with opsonizing reagent (E2870, ThermoFisher, Illkirch, France), according to manufacturer instructions.

Reactive oxygen species and mitochondrial superoxide quantification

Reactive oxygen species and mitochondrial quantification was performed by labelling fresh CD45+ CD11b+ Ly6G+ neutrophils for 20 min at 37°C, using CellRox Orange reagent (ref. C10443) and Mitosox reagent (ref. M36008) respectively, following the manufacturer's instructions (Molecular Probes, ThermoFisher Scientific).

RNA extraction and RNA-seq data processing

Total RNA was isolated using TRIzol reagent (Fisher Scientific, Illkirch, France), as described by the manufacturer. RNA integrity and quality were verified using RNA ScreenTape kit and Tapestation 2200 apparatus from AGILENT (Les Ulis, France). cDNA libraries were synthesized using NEBNext® rRNA Depletion and Ultra™ II Directional RNA Library Prep Kit (New England Biolabs, Evry-Courcouronnes, France). Library quality was checked on Tapestation 2200 apparatus from AGILENT (Les Ulis, France) with DNA 1000 ScreenTape. Samples were sequenced on Novaseq 6000 (Illumina) with an average sequencing depth of 30 million of paired-end reads. Length of the reads was 150 bp. Each 24 Plex Samples was sequenced on one Illumina SP FlowCell (2*800 million of 150bases reads). Raw sequencing data was quality-controlled with the FastQC program. Low quality reads were trimmed or removed using Trimmer (minimum length: 120 bp). Reads were aligned to the mouse reference genome (mm10 build) with the Star tool. Gene counts were obtained by read counting software Htseq. Normalization and differential analysis were performed with the DESeq2 package with Benjamini-Hochberg FDR multiple testing correction ($p < 0.05$; 1.5-fold or higher change) comparing WT and KO animals. The data discussed in this publication have been deposited in NCBI's Gene Expression Omnibus (31) and are accessible through GEO Series accession number GSE209860 (https://www.ncbi.nlm.nih.gov/geo/query/acc.cgi?acc=GSE209860).

Bioinformatic analysis

To assess biological interpretation of the most differentially expressed genes, we used Gene ontology (GO) enrichment analysis. A gene set enrichment analysis (GSEA) was performed using signatures from GSEA collections. A normalized enrichment score (NES) was calculated for each gene set and only gene sets with an adjusted p value < 0.05 were selected.

Statistics

Statistical analyses were carried out using unpaired Mann-Whitney test.

Results

Cxcr2 invalidation affects the maturation of neutrophils

To evaluate the impact of *Cxcr2* knockout on neutrophil distribution and function, we first measured the presence of

10.3389/fimmu.2022.1005551

CD45+ CD11b+ Ly6G+ neutrophils in the BM and the spleen by flow cytometry (Figure 1A). Ly6G+ neutrophils were composed of two subpopulations with high ($Ly6G^{hi}$) or low ($Ly6G^{lo}$) levels of Ly6 (Figure 1A). In BM, the percentage of total Ly6G+ ($Ly6G^{hi}$ + $Ly6G^{lo}$) neutrophils was increased by about 30% in *Cxcr2-/-* compared to WT animals, and this was much more pronounced in the spleen, with more than 8 - fold more neutrophils in *Cxcr2-/-* animals (Figure 1B). Of particular note, the percentage of CD45+ cells was not different in WT and KO spleens, whereas it slightly increased (88.7% vs 95.2%) in KO BM compared to WT BM (Supplemental Figure 1). No major change in FSC and SSC distribution was observed for Ly6G+ neutrophils (Supplemental Figure 2). In terms of absolute numbers, we observed a 5-fold increase of the total number of CD45+ cells and CD45+ CD11b+ Ly6G+ neutrophils in the spleen of Cxcr2-/- animals, whereas minimal differences between and Cxcr2-/- and WT animals was seen in BM (no change of the number of CD45+ cells and less than 30% increase for CD45+ CD11b+ Ly6G+) (Supplemental Figure 3). This obviously creates a bias in the analysis of any type of subpopulation and for this reason, we decided to continue to look at percentage of subpopulations of neutrophils among neutrophils, to avoid this.

The level of Ly6G expression has been correlated with the degree of maturation of neutrophils with $Ly6G^{hi}$ neutrophils being the most mature (32). In BM, there was a slight reduction of the percentage of immature $Ly6G^{lo}$ neutrophils among total Ly6G+ in *Cxcr2-/-* animals, whereas there was an increase by 2-fold of immature $Ly6G^{lo}$ neutrophils in *Cxcr2-/-* spleen (Figure 1C). To strengthen these results, we used the CD101 marker, which characterizes mature neutrophils (8). Among neutrophils, we observed a reduction of CD101+ mature neutrophils in the spleen, but an increase of mature neutrophils in BM (Figures 1D, F). Next, we also looked at Cxcr4 expression in neutrophils, which is correlated not only to immaturity of neutrophils (8), but also to aged neutrophils (33). The percentage of Cxcr4+ neutrophils increased twice in the spleen, but was unaffected in the BM (Figures 1E, G), confirming the increase of the proportion of immature neutrophils in the neutrophil fraction of the spleen. To assess more precisely whether these neutrophils corresponded to immature or aged neutrophils in the spleen of KO animals, we used the marker CD62L (L-Selectin), in addition to CXCR4 to identify "aged" $CD62L^{lo}$- $CXCR4^{hi}$ neutrophils, as previously described (33). We observed that the proportion of aged $CD62L^{lo}$- $CXCR4^{hi}$ cells among neutrophils increased in KO spleen compared to WT, but there was no significant change in BM (Supplemental Figure 4).

To further assess the nature of neutrophils, we isolated by cell sorting CD45+ CD11b+ Ly6G+ neutrophils from WT and KO BM and spleen and colored them with Giemsa (Supplemental Figure 9). WT BM neutrophils displayed a condensed round nucleus, with a small cytoplasm, whereas KO BM neutrophils seem to have a larger ring-shaped nucleus, which could suggest that they are more mature. In the spleen, WT neutrophils had a strongly colored ring-shaped nucleus. Spleen KO neutrophils exhibited a larger nucleus with a less pronounced staining and also a cytoplasmic center, which could be reminiscent of band neutrophils (34). These morphological differences suggest that WT and KO neutrophils might have distinct features.

Cxcr2-/- neutrophils display altered phagocytic ability

Phagocytosis is one of the major function of neutrophils to eliminate infections. Thus, we analyzed the phagocytic abilities of BM and spleen neutrophils. Kinetics of phagocytosis showed that BM *Cxcr2-/-* neutrophils had an enhanced phagocytic ability compared to WT neutrophils (Figure 2A), whereas spleen *Cxcr2-/-* neutrophils were less phagocytic than spleen WT neutrophils (Figure 2B). We have also performed an additional analysis, by separating $Ly6G^{hi}$ and $Ly6G^{lo}$ neutrophils (Supplemental Figure 5). Similar results were obtained for $Ly6G^{hi}$ neutrophils as for Ly6G+ neutrophils, which is an increase of phagocytosis for BM KO neutrophils and a decrease of phagocytosis for spleen KO neutrophils. Concerning $Ly6G^{lo}$ neutrophils, they were less phagocytic than $Ly6G^{hi}$ neutrophils, both in the spleen and BM. Moreover, BM KO $Ly6G^{lo}$ were also more phagocytic than BM WT $Ly6G^{lo}$ neutrophils. On the other hand, no difference was seen for spleen $Ly6G^{lo}$ neutrophils between WT and KO animals. In addition, when using opsonized bioparticles (Supplemental Figure 6), we obtained the same trend of difference between WT and KO neutrophils as for non-opsonized particles.

To better understand the mechanisms underlying these changes in phagocytic ability, we looked at ROS production and to actin-tubulin cytoskeleton organization of neutrophils, which are essential for phagocytosis (35). We observed a strong reduction in the production of cytoplasmic ROS (Figures 3A, B) and mitochondrial superoxide (Figures 3C, D) of spleen *Cxcr2-/-* neutrophils, whereas no difference could be measured between BM WT and *Cxcr2-/-* neutrophils. Spleen *Cxcr2-/-* neutrophils had also lower levels of F-Actin (Figures 4A, B) as well as tubulin (Figures 4C, D) compared to WT, but BM neutrophils were unaffected by *Cxcr2* impairment. These results of decreased levels of F-actin and tubulin were also confirmed, when comparing MFI values for F-actin and tubulin for the different types of neutrophils (Supplemental Figure 7). Altogether, these results could account for the lower phagocytic ability of spleen *Cxcr2-/-* neutrophils, which is in agreement with a lower maturity.

Spleen *Cxcr2-/-* neutrophils have a higher viability

Neutrophil are short term living cells, so we wondered whether Cxcr2 could modulate their survival ability. We

10.3389/fimmu.2022.1005551

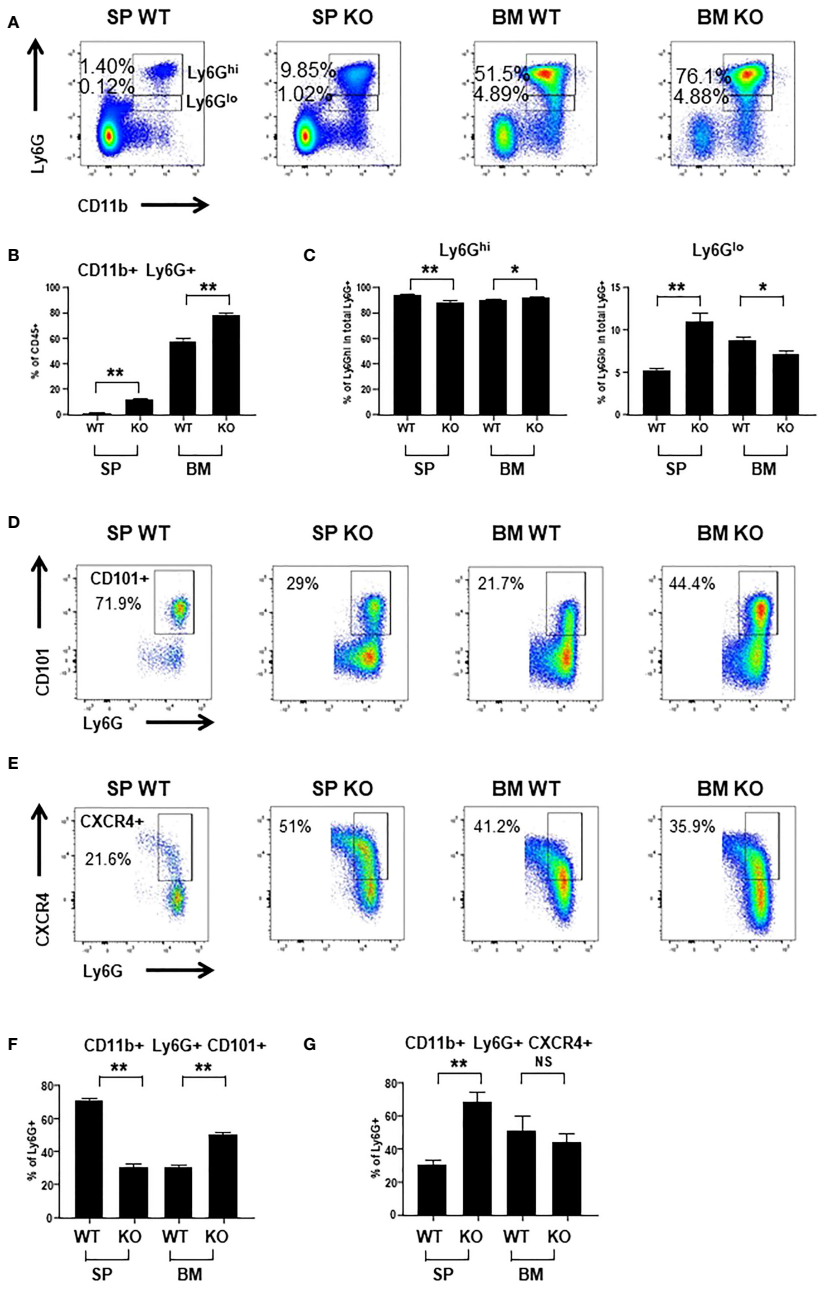

FIGURE 1
Cxcr2 knock-out decreases the percentage of mature neutrophils in the spleen. **(A)** Representative dot plots of the gating strategy of CD45+ CD11b + Ly6G^{hi} and CD45+ CD11b+ Ly6G^{lo} neutrophils among CD45+ cells in WT and *Cxcr2-/-* bone marrow (BM) and spleen (SP). **(B)** Quantification of the percentage of the total neutrophils (CD11b+ Ly6G+: sum of Ly6G^{hi} and Ly6G^{lo}) in the CD45+ fraction. **(C)** Quantification of CD11b+ Ly6G^{hi} cells (left panel) and CD11b Ly6G^{lo} (right panel) in the CD11b+ Ly6G+ (Ly6G^{hi} and Ly6G^{lo} fractions) population. **(D)** Gating strategy to identify CD101+ neutrophils in the CD45+ CD11b+ Ly6G+ fraction. **(E)** Gating strategy to identify CXCR4+ neutrophils in the CD45+ CD11b+ Ly6G+ fraction. **(F)** Percentage of mature CD101+ neutrophils in the CD11b+ Ly6G+ fraction. **(G)** Percentage of CXCR4+ neutrophils in the CD11b+ Ly6G+ fraction. Data represent the mean ± SEM of at least 6 animals (Mann-Whitney test, NS: non-significant, *p < 0.05, **p < 0.01).

observed that the percentages of apoptotic or dead cells were reduced for spleen *Cxcr2-/-* neutrophils (Figures 5A–C, respectively), whereas it was similar for WT and *Cxcr2-/-* BM neutrophils. So, this suggests that the reduced phagocytic ability of spleen *Cxcr2-/-* neutrophils is not a consequence of an impaired survival. We have also measured apoptosis and death after a 2h incubation at 37°C, and obtained similar results (Supplemental Figure 8), which suggests that an increased

10.3389/fimmu.2022.1005551

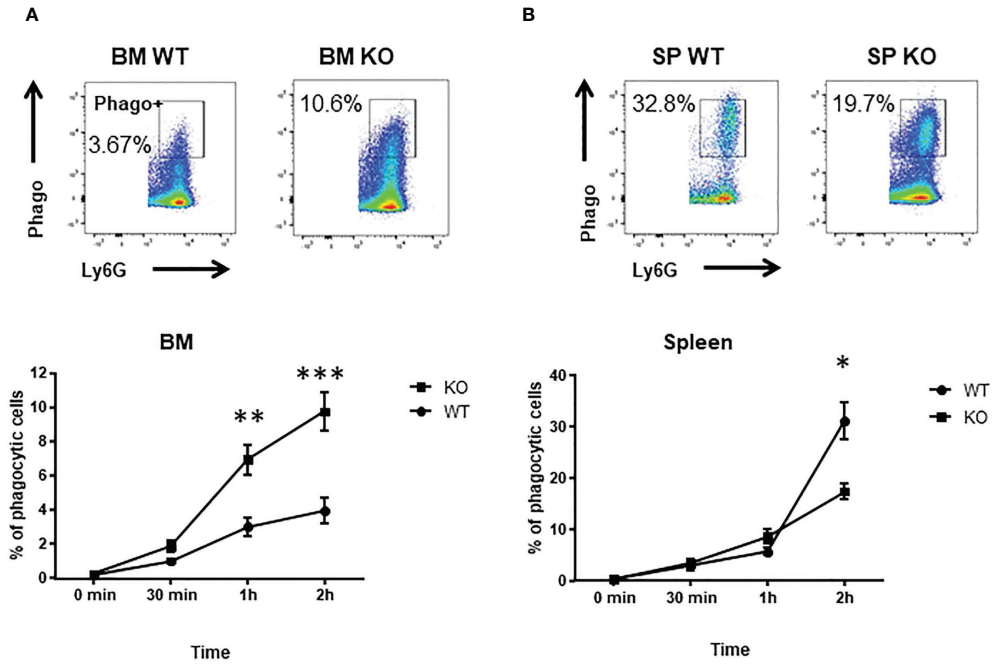

FIGURE 2
spleen *Cxcr2-/-* neutrophils have an impaired phagocytosis ability. **(A)** To measure phagocytosis, BM CD11b+ Ly6G+ neutrophils were incubated with Red *E. coli* Phrodo bioparticles at 37°C for 0, 30 min, 1h or 2h and analyzed by flow cytometry. Upper panel: Gating strategy to identify phagocytic neutrophils (Phago+) in the CD11b+ Ly6G+ fraction at 2h time. Lower panel: Percentage of phagocytic Ly6G+ neutrophils. **(B)** Same experiment with spleen neutrophils. Results are expressed as the percentage of phagocytic neutrophils in the CD11b+ Ly6G+ population and represent the mean ± SEM of at least 6 animals (Mann-Whitney test, *p < 0.05, **p < 0.01, ***p < 0.001).

apoptosis or death after 2h incubation does not affect the phagocytosis ability of neutrophils.

Transcriptomic analysis confirms the impaired maturation of spleen *Cxcr2-/-* neutrophils

We next focused on spleen neutrophils to decipher whether and how Cxcr2 deficiency impacts their molecular identity. RNAseq analyses of WT and *Cxcr2-/-* spleen neutrophils showed that more than 2,500 transcripts were up-regulated and about the same number down-regulated in *Cxcr2-/-* spleen neutrophils (Figures 6A–C). We then focused on their maturation using the neutrophil maturation signature reported by Xie and collaborators (36). GSEA analysis confirmed that spleen *Cxcr2-/-* were less mature than their WT counterparts (Figures 6D, E), with down regulation of genes encoding Cathepsin D (Ctsd), JunB or IL-1β involved in Netosis (2), Arginase-2 (Arg2) controlling extra-urea cycle arginine metabolism and nitric oxide synthesis (12), C-type lectin receptor Clec4d crucial for bacteria elimination (37) or Selplg (CD162), important for the rolling of neutrophils (38).

In addition, there was a cluster of GSEA Biological process (BP) signatures showing a down-regulation of the chemotaxis and migration of spleen *Cxcr2-/-* neutrophils (Figure 6F), suggesting a decrease in the migration ability of these neutrophils.

ERK and p38 MAPK pathways are down-regulated in spleen *Cxcr2-/-* neutrophils

To look at the signaling that were affected in spleen *Cxcr2-/-* neutrophils, we first focused on ERK and p38 MAPK signaling, which are known to modulate the migration and adhesion of neutrophils (39, 40). RNAseq data showed that both ERK1 and ERK2 cascade (Figures 7A, C), as well as p38MAPK cascade (Figures 7B, D), were down regulated in spleen *Cxcr2-/-* neutrophils. Concerning ERK1/2 cascade, there is in particular a down-regulation of the AP-1 Transcription Factor Jun, of the Cyclic AMP-Dependent Transcription Factor Atf-3, IL1β, growth factors such as TGFβ1 and IGF1, multiple chemokines such as Ccl3, 4, 15, 18, 23 and of a number of kinases such as Ptk2b (Protein Tyrosine Kinase 2 Beta), the tyrosine-protein kinase Syk, Csk (C-Terminal Src Kinase) or the serine/threonine protein kinase BRAF (Figure 7C). For p38MAPK cascade, we observed in particular a down regulation of Mitogen-Activated Protein Kinase 14 (Mapk14), Mitogen-Activated Protein Kinase Kinase Kinase 3 (Map3k3), Map3k5, and cytokines such as IL1β, HGF.

10.3389/fimmu.2022.1005551

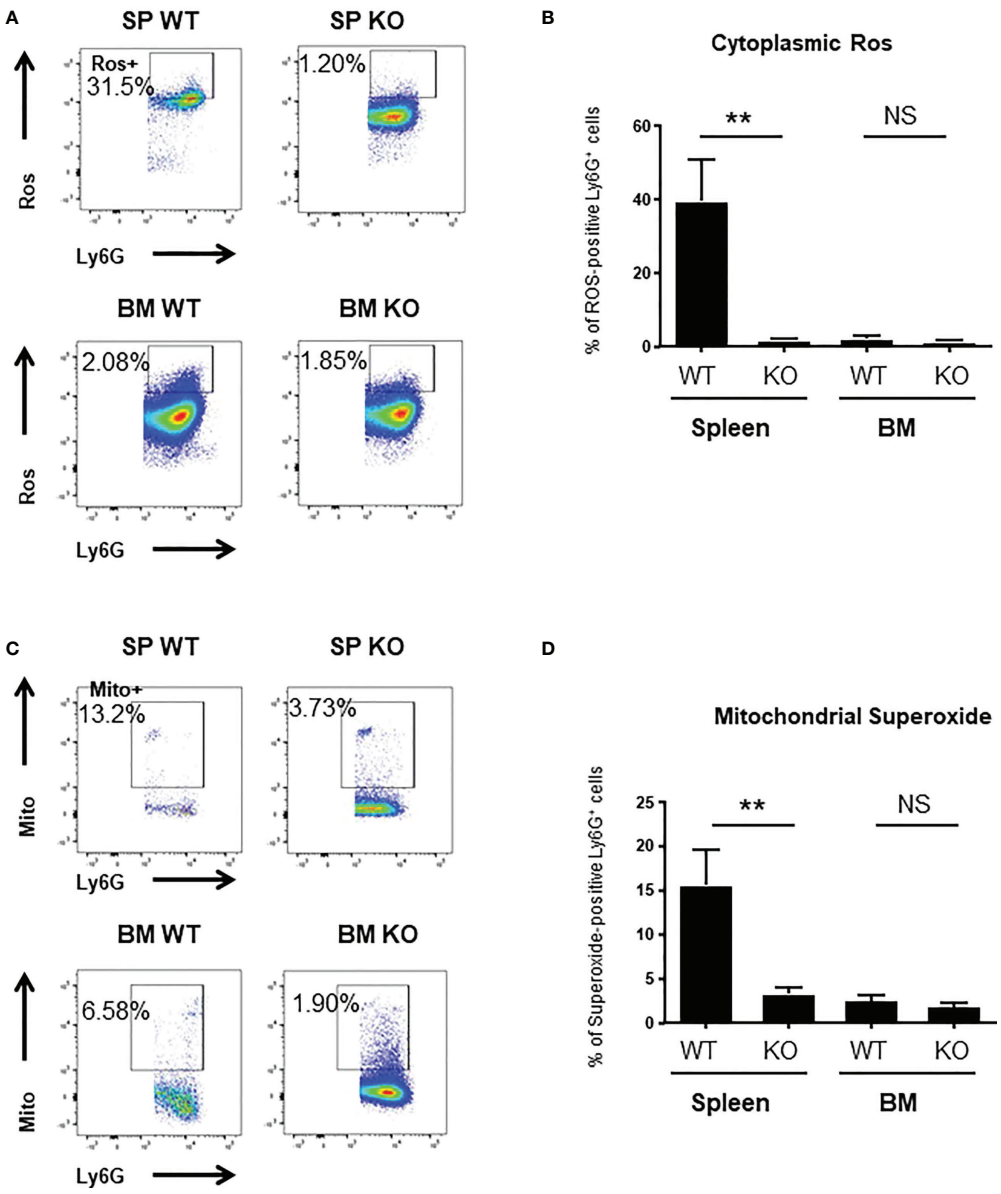

FIGURE 3
spleen *Cxcr2-/-* neutrophils display reduced ROS and superoxide levels. **(A)** Gating strategy to measure cytoplasmic Ros levels using CellRox Orange in CD11b+ Ly6G+ neutrophils. **(B)** ROS levels were quantified in spleen and BM CD11b+ Ly6G+ neutrophils using CellRox Orange probe. Results are expressed as the percentage of ROS-positive neutrophils in the CD11b+ Ly6G+ population and represent the mean ± SEM of at least 6 animals (Mann-Whitney test, NS: non-significant, **p < 0.01). **(C)** Gating strategy to measure Mitochondrial superoxide levels using Mitosox in CD11b+ Ly6G+ neutrophils. **(D)** Measure of the percentage of mitochondrial superoxide –positive CD11b+ Ly6G+ neutrophils using Mitosox reagent. Data represent the mean ± SEM of at least 6 animals (Mann-Whitney test, NS: non-significant, **p < 0.01).

To confirm these results, we measured by flow cytometry the intracellular content of Phospho-p42/44 MAPK ERK1/2 and phospho-p38 MAPK (Thr 180/Tyr 182). The mean of fluorescence (MFI) of p-ERK1/2 and p-p38 were down-regulated by about 50% in spleen *Cxcr2-/-* neutrophils compared to WT neutrophils (Figures 7E, F, respectively) confirming the alterations of these pathways.

Several pathways are impaired in spleen *Cxcr2-/-* neutrophils

To further investigate the mechanisms involved in the changes observed in spleen *Cxcr2-/-* neutrophils, we explored the main pathways that were affected at the transcriptomic level. GSEA analysis showed a reduction of PI3K-AKT signaling

10.3389/fimmu.2022.1005551

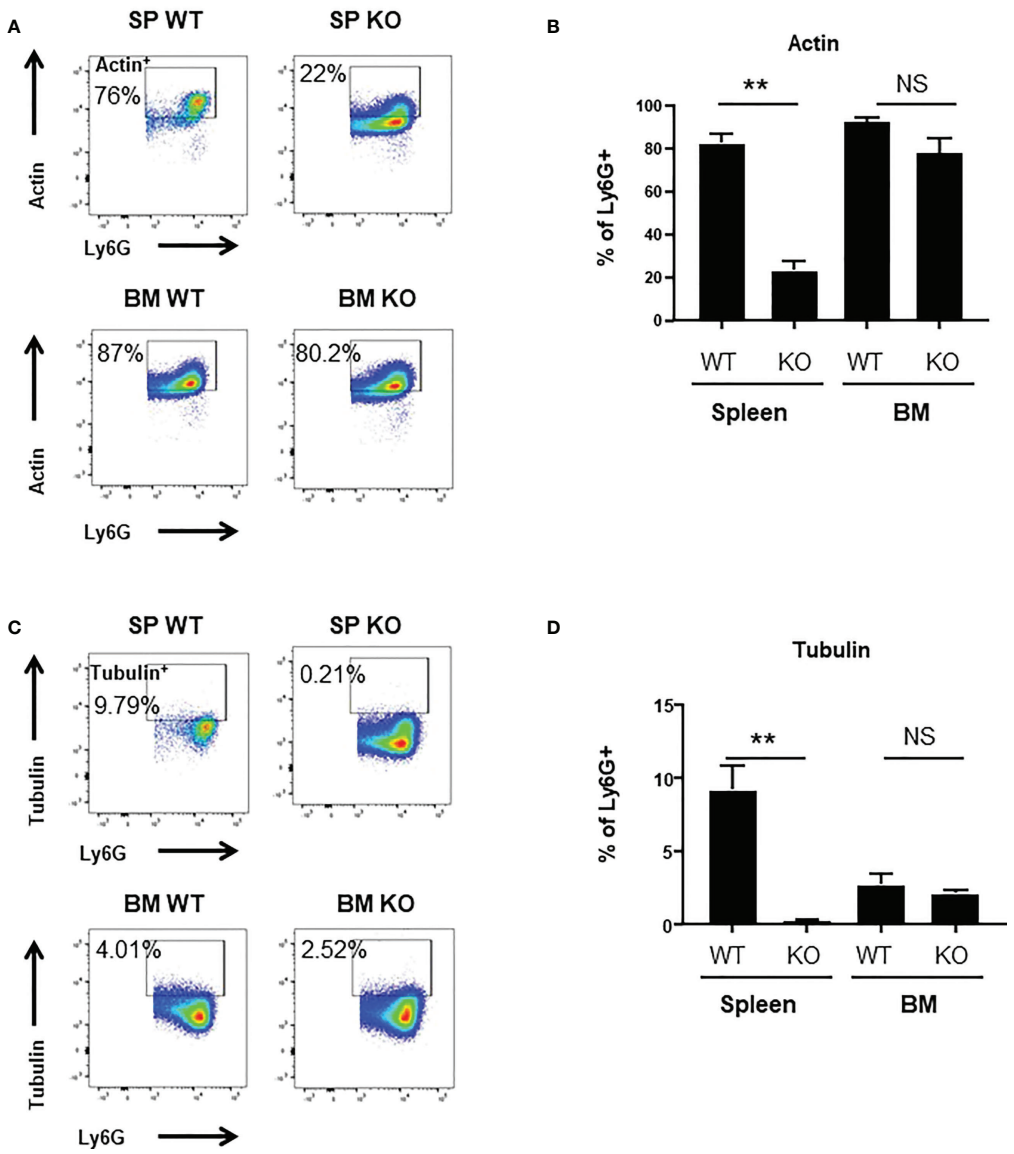

FIGURE 4
Decrease of Actin$^+$ and Tubulin$^+$ levels in spleen *Cxcr2-/-*. **(A)** Gating strategy to measure F-Actin levels (Actin$^+$) in CD11b+ Ly6G+ neutrophils. **(B)** Percentage of CD11b+ Ly6G+ expressing Actin (mean ± SEM of at least 6 animals; Mann-Whitney test, NS: non-significant, **p < 0.01). **(C)** Gating strategy to measure α-Tubulin levels (Tubulin$^+$) in CD11b+ Ly6G+ neutrophils. **(D)** Percentage of CD11b+ Ly6G+ expressing Tubulin. (mean ± SEM of at least 6 animals; Mann-Whitney test, NS: non-significant, **p < 0.01).

(Figure 8A), TNFα signaling *via* NFκB (Figure 8B), NIK-NFκB signaling (Figure 8C), as well of the cellular response to IL-1 (Figure 8D) and TGFβ signaling (Figure 8E) and signaling by IFNγ (Figure 8F) signatures in spleen *Cxcr2-/-* neutrophils compared to WT neutrophils. Among the genes involved in PI3K-AKT pathway, we observed a down-regulation of Phosphatidylinositol-4,5-Bisphosphate 3-Kinase Catalytic Subunit Alpha, Delta and Gamma (Pik3ca, Pik3cd and Pik3cg), and Phosphoinositide-3-Kinase Regulatory Subunit 1, 2 and 5 (Pik3r1, Pik3r2, Pik3r5), Janus Kinase 1 (Jak1), Glycogen Synthase Kinase 3 Beta (GSK3b), and Kras, which are crucial for this pathway.

NF-κB pathway was also impaired with in particular down-regulation of genes such as NF-κB Subunits p52 (Nfkb2), Relb, C-Rel (Rel), TNF Alpha Induced Protein 2 and 3 (Tnfaip2 and Tnfaip3), Tnfaip3 Interacting Protein 1 (Tnip1), TNF Receptor-Associated Factor 1, 3 and 5 (Traf1, Traf3, Traf5) or TNF Receptor Superfamily Member 10b (Tnfrsf10b).

Upstream of NF-κB activation, cellular response to IL-1 was also altered, with a down-regulation of IL-1 itself, but also of

10.3389/fimmu.2022.1005551

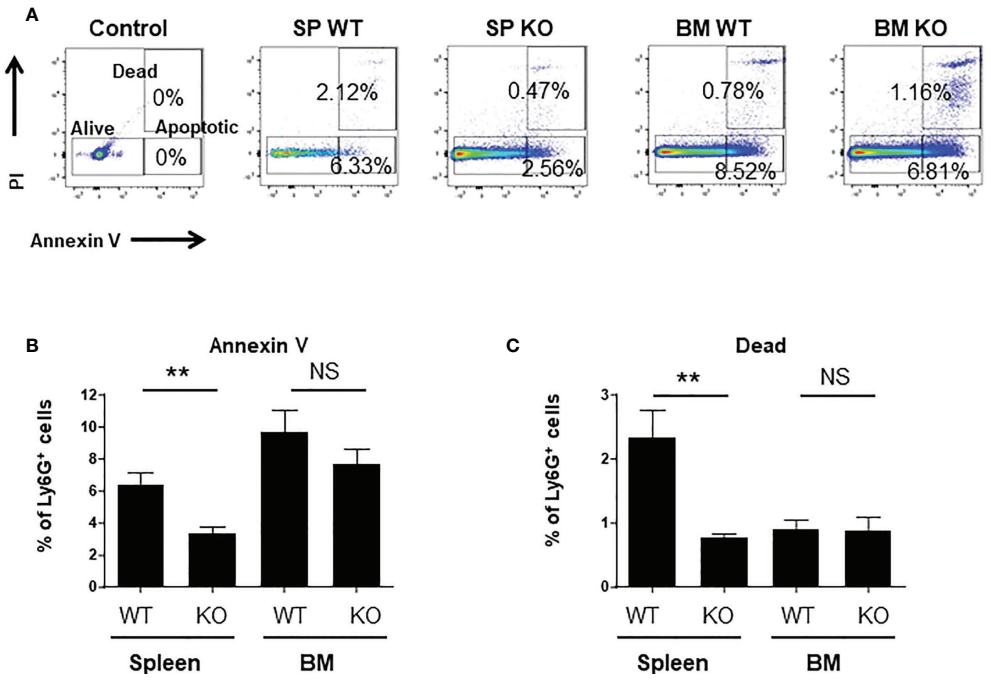

FIGURE 5
spleen *Cxcr2-/-* neutrophils exhibit a reduced apoptosis and mortality. **(A)** Gating strategy to identify alive, dead and apoptotic cells based on Annexin V and PI staining. Control plot corresponds to cells labelled with cell surface markers, but not with Annexin V and PI **(B)** Measure of the percentage of apoptotic neutrophils in the spleen and BM of WT and *Cxcr2-/-* animals by annexin V staining. **(C)** Same measure of dead cells by PI staining. Results are expressed as the percentage of CD11b+ Ly6G+ neutrophils and represent the mean ± SEM of 6 animals; Mann-Whitney test, NS: non-significant, **p < 0.01.

Interleukin 1 Receptor Type 1 (Il1r1). Two other pathways were also linked to PI3K/Akt, ERK, p38 and NF-κB signaling, namely TGFβ and IFNγ signaling. TGFβ signaling was impaired with a decrease in Transforming Growth Factor Beta 1 (Tgfb1), Transforming Growth Factor Beta Receptor 1 and 2 (Tgfbr1 and Tgfbr2), and Smad2, 3, and 4. IFNγ signaling is also acting through ERK and MAPK and PI3K signaling and exhibits in particular a down-regulation of Janus kinase 2 (Jak2), suppressor of cytokine signaling protein 1n and 3 (Socs1, Socs3), Signal transducer and activator of transcription 4 (Stat4), Intercellular adhesion molecule-1 (ICAM-1) and Integrin Subunit Beta 7 (ITGB7).

Discussion

Although the role of neutrophils in general inflammation but also tumor microenvironment inflammation is growing, the factors controlling their function are still not completely identified. In particular, the involvement of Cxcr2 in neutrophil physiology and features, as well as its impact on signalization in neutrophils is still a matter of debate. In this study, we report that impairment of *Cxcr2* leads to a modest increase of the percentage of neutrophils in the BM, but a strong one in the spleen, in agreement with previous studies (29). We also show that Cxcr2 differentially affects the maturation state of neutrophils in the spleen and the BM. More precisely, based on the maturation markers Ly6G (32) and Cd101 (8) expression, *Cxcr2* deletion led an increase of $Ly6G^{lo}$ or CD101- immature neutrophils in the spleen, but to a decrease of immature neutrophils in the BM. The presence of resident immature neutrophils in the spleen is thought to serve as a reservoir of neutrophils, which will undergo a rapid proliferation and mobilization in case of infection to increase the number of active mature neutrophils (18, 32). Spleen is also a site of accumulation and destruction of neutrophils in human (41), so the presence of a high number of immature neutrophils could correspond to both resident and recruited neutrophils. On the other hand, considering that the BM is the main site of production of neutrophils, this would suggest that Cxcr2 impairment does not alter the maturation process on neutrophils in the BM, or that there could be a retention of mature neutrophils in BM. This latter hypothesis is unlikely, as we did not see any difference in the percentage Cxcr4+ neutrophils in the BM. Cxcr4 is indeed crucial for the retention of neutrophils in the BM (17), even though other studies have shown that the CXCR4 antagonist plerixafor did not mobilize neutrophils from the BM, but rather enhanced the

10.3389/fimmu.2022.1005551

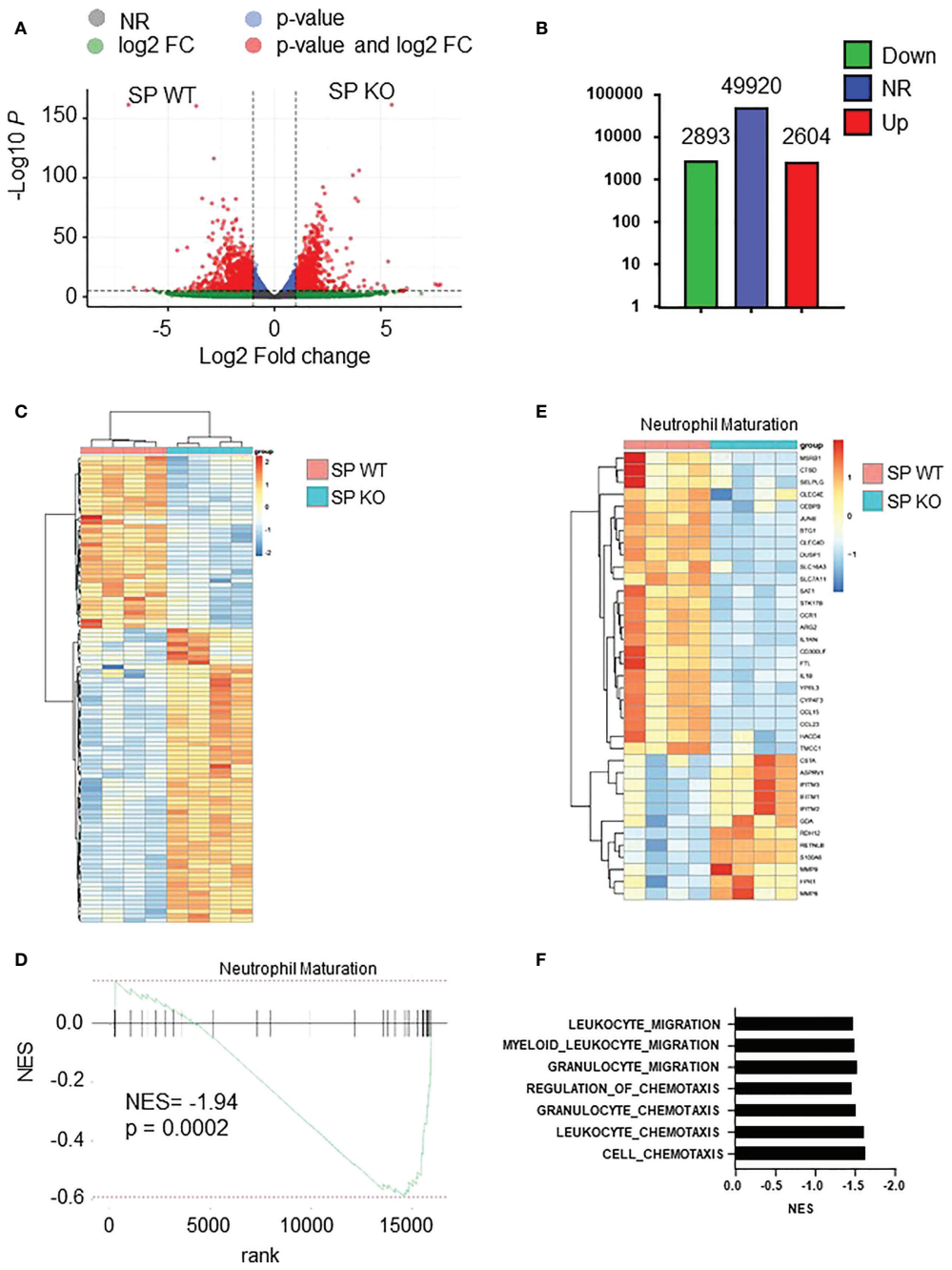

FIGURE 6
Cxcr2-/- neutrophils display decreased maturity at the transcriptomic level. **(A)** Volcano plot showing the global changes in RNA expression patterns for spleen neutrophils isolated from *Cxcr2-/-* (SP KO) versus WT (SP WT) animals. Data represent analysis of cpm estimates with a log of fold change of more than 1.5 fold and p< 0.05 of 4 animals per group. Grey dots: NR: non-regulated genes; Green dots: genes with a log of fold change of more than 1.5 fold; blue dots: genes with a p-value <0.05; red dots: genes with a log of fold change of more than 1.5 fold and p< 0.05. **(B)** Number of differentially regulated genes for the spleen neutrophils. Up: genes up-regulated in spleen isolated from *Cxcr2-/-* versus WT animals. Down: down-regulated genes. NR: non regulated genes. **(C)** Simplified Heatmap of spleen *Cxcr2-/-* versus WT neutrophils. **(D)** Normalized enrichment score (NES) after GSEA analysis of the transcriptome of spleen neutrophils isolated from *Cxcr2-/-* versus WT animals according to Neutrophil maturation of Xie et al. (36). **(E)** Heatmap of the significantly regulated genes (p<0.05) of Neutrophil maturation signature. **(F)** Cluster of chemotaxis and migration GSEA analysis from *Cxcr2-/-* versus WT animals according to Biologic process GO: Cell-chemotaxis (NES= -1.64; q= 0.0002), Leukocyte-chemotaxis (NES= -1.62; q= 0.001), Granulocyte chemotaxis (NES= -1.53; q= 0.029), Regulation of Chemotaxis (NES = -1.46; q = 0.013), Granulocyte migration (NES= -1.54; q=0.025), Myeloid-leukocyte-migration (NES= -1.50; q= 0.012), leukocyte-migration (NES = -1.48; q= 0.003).

10.3389/fimmu.2022.1005551

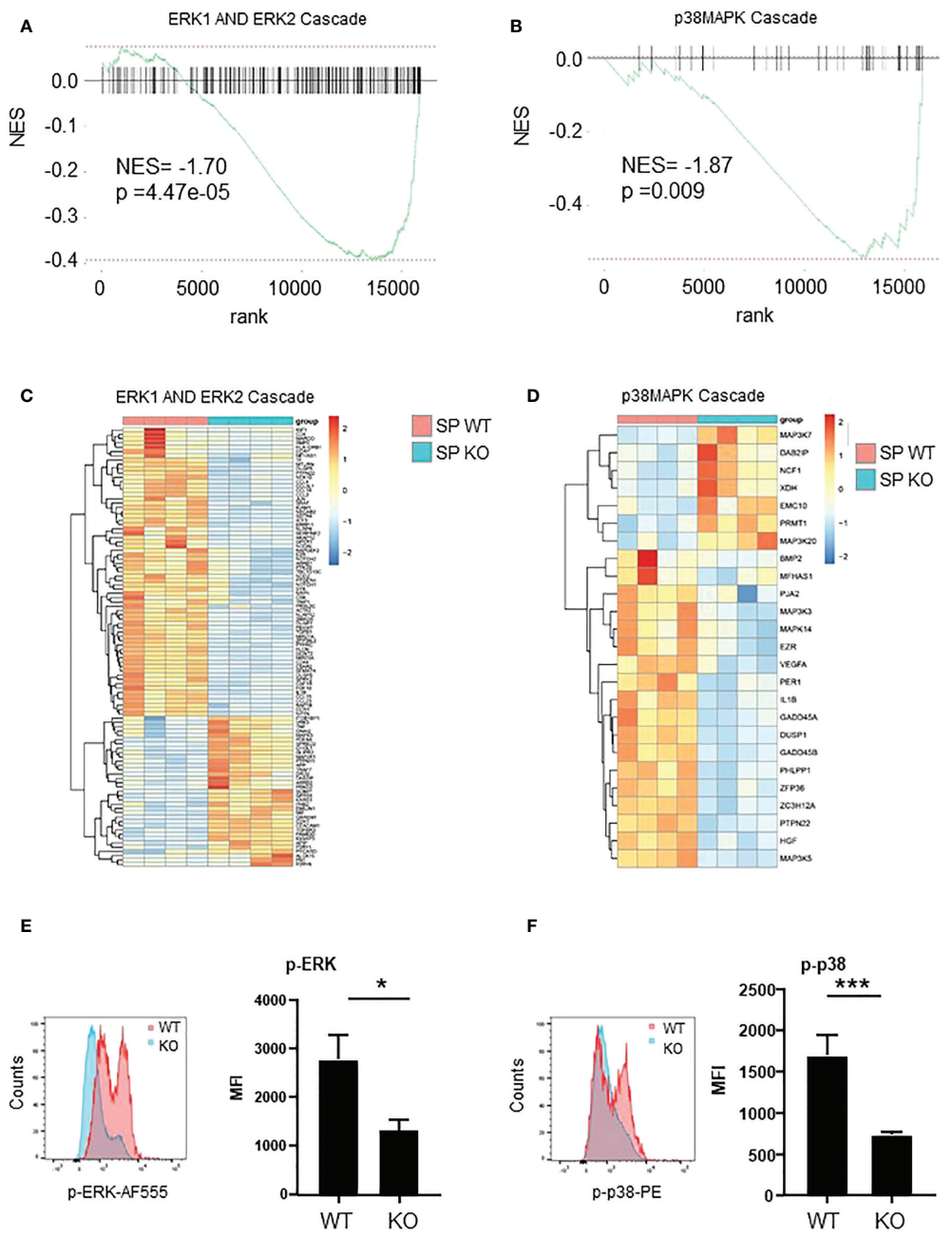

FIGURE 7
ERK and p38 pathways are down-regulated in Spleen *Cxcr2-/-* neutrophils. **(A)** NES after GSEA analysis of the transcriptome of spleen neutrophils isolated from *Cxcr2-/-* versus WT animals according to ERK1 and ERK2 cascade signature. **(B)** Same analysis for p38-MAPK signature. **(C)** Heatmap of the significantly regulated genes ($p<0.05$) of GO-BP ERK1 and ER2 cascade signature. **(D)** Heatmap of the significantly regulated genes ($p < 0.05$) of GO-BP p38 MAPK cascade signature. **(E)** Phospho-p42/44 MAPK ERK1/2 (Thr 202/Tyr 204) was analyzed by flow cytometry in spleen CD11b+ Ly6G+ neutrophils. Left panel: representative Mean of Fluorescence (MFI) of WT (red line) and KO (blue line) Ly6G+ neutrophils. Results are expressed as MFI of phospho-ERK positive neutrophils in the CD11b+ Ly6G+ population and represent the mean ± SEM of at least 6 animals (Mann-Whitney test, $*p < 0.05$). **(F)** Phosphorylation of p38MAPK on Thr180/Tyr182 was analyzed by flow cytometry in the same conditions (Mann-Whitney test, $***p < 0.001$).

10.3389/fimmu.2022.1005551

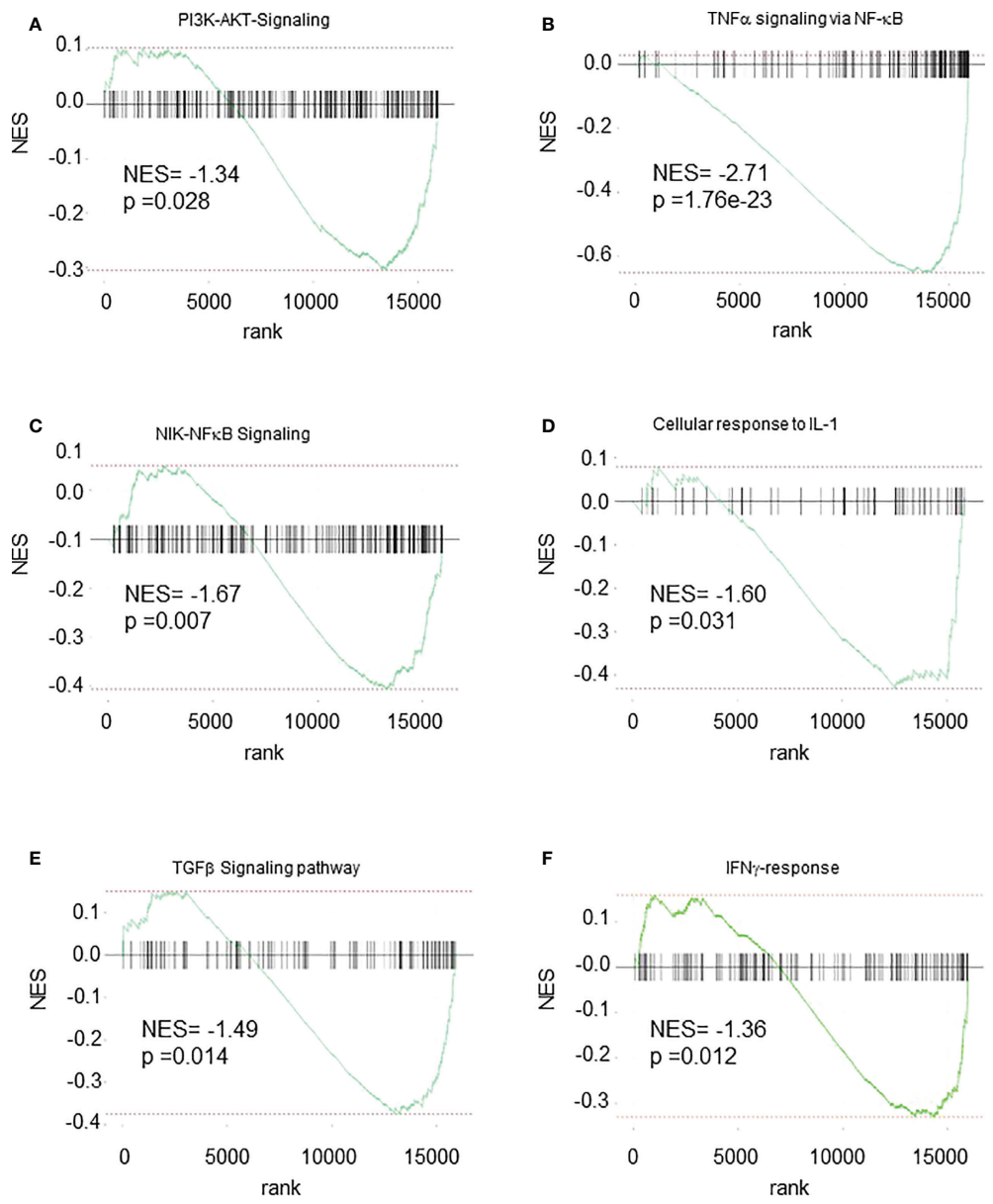

FIGURE 8
Multiple pathways are down-regulated in Spleen *Cxcr2-/-* neutrophils. GSEA analysis of the following signatures: **(A)** WIKI-PI3K-AKT signaling. **(B)** Hallmark-TNFα signaling *via* NFκB. **(C)** GO-BP NIK-NFκB Signaling **(D)** GO-BP Cellular response to IL-1 **(E)** WP-TGFβ signaling pathway **(F)** Hallmark IFNγ-response.

release of neutrophils in the circulation from the marginated pool present in the lung (42). In contrast, the percentage of Cxcr4+ neutrophils was increased 2-fold in the spleen, which could account for several features: this could be the sign of more immature, since Cxcr4 expression is high in proliferating immature neutrophils (8). However, high levels of Cxcr4 can also be seen in senescent or aging neutrophils (17, 43). To clarify this point, we analyzed the presence of aged $CD62L^{lo}$ – $CXCR4^{hi}$ neutrophils as defined previously (33). This shows that there is an increase of aged $CD62L^{lo}$ – $CXCR4^{hi}$ neutrophils in the spleen of KO animals, but no change in BM. In addition, we also observed that the percentage of apoptotic or dead neutrophils was reduced among spleen *Cxcr2-/-* neutrophils compared to WT, whereas no difference was seen in BM. Overall, our data suggest that spleen *Cxcr2-/-* neutrophils are distinct from BM neutrophils, as they are healthier and have

more immature features (Ly6Glo Cd101- Cxcr4+) than their WT counterparts.

To go further in the understanding of the effects of Cxcr2 impairment, we have observed that spleen *Cxcr2-/-* neutrophils exhibited a reduced phagocytic ability than WT neutrophils. On the other hand, BM *Cxcr2-/-* neutrophils had a higher phagocytic ability than the WT. This difference between spleen and BM neutrophils might be explained by their difference of maturation mentioned above. This is also true for basal phagocytic ability of WT neutrophils, which is higher in the spleen than in the BM. This might be due to a higher proportion of mature CD101+ neutrophils in WT spleen compared to WT BM (Figure 1F), as we have also shown that $Ly6G^{hi}$ neutrophils had a better phagocytic ability than $Ly6G^{lo}$ neutrophils (Supplemental Figure 5).

To explore the difference in phagocytic ability of WT and *Cxcr2-/-* neutrophils more thoroughly, we looked at ROS production and actin and tubulin cytoskeleton, which are key elements in phagocytosis (35, 44). The percentage of cells with high cytoplasmic ROS, mitochondrial superoxide, F-actin and α-tubulin was reduced among spleen *Cxcr2-/-* neutrophils compared to WT, but was not modified in BM neutrophils. This reduction could explain part of the reduced phagocytic ability of spleen *Cxcr2-/-* neutrophils, although one can also notice that decreased phagocytic ability of WT BM neutrophils compared to WT spleen neutrophils is not correlated to their actin levels, suggesting that other parameters might be involved. It is interesting to notice that aged neutrophils are resistant to infections and display also a reduction of actin levels (43). Moreover, it has also been shown that in some cases, immature neutrophils could produce less ROS (8).

It was essential to analyze the mechanisms underlying the differences between spleen *Cxcr2-/-* and WT neutrophils. RNAseq analysis of both types of isolated neutrophils confirmed the defect in maturation of spleen *Cxcr2-/-* neutrophils, with in particular a down regulation of genes involved in Netosis (Cathepsin D, JunB or IL-1β) (45), of Arginase-2 controlling extra-urea cycle arginine metabolism and nitric oxide synthesis, of Clec4d implicated in bacteria elimination (46) or Selplg (CD162), essential for the rolling of neutrophils (47). Several GO pathways of migration and chemotaxis constituted a down-regulated cluster, suggesting also an impairment of spleen *Cxcr2-/-* chemotaxis. This could explain an accumulation of neutrophils in the spleen, with a weak ability to migrate to other tissues. Earlier studies have shown that in inflammatory conditions, Cxcr2 was essential for the recruitment of neutrophils (48).

In terms of signaling, we report a down regulation of ERK and p38 MAPK pathways, both at the transcriptomic level, but also when assessing the phosphorylation of ERK and p38 at the protein level. The ERK and p38 MAP kinases are strongly stimulated in neutrophils upon activation by G-protein coupled receptors agonists. Moreover, p38 MAPK is critical for the release of primary and secondary granules, but not that of secretory vesicles by neutrophils (49). p38 inhibition has been shown to delay apoptosis of neutrophils (50), which is in agreement of the reduced rate of apoptosis that we observed in spleen *Cxcr2-/-* neutrophils. Moreover, p38 MAPK promotes chemotaxis towards fMLP by interfering with GRK2-mediated desensitization, whereas ERK MAPK is inhibiting it (51, 52). However, the role of ERK MAPK pathway in neutrophil functions remains unclear, due to contradictory studies (37).

In addition, PI3K-Akt, TNFα signaling and NF-κB signaling, were also altered. TNFα is essential to trigger neutrophil activation and phagocytic activity (53). It is interesting to note that in neutrophils, the production of ROS is dependent on PI3K and ERK (54). Moreover, PI3K, ERK and p38 are necessary for efficient phagocytosis (55). It has also been reported that PI3Kγ-/- neutrophils display a defect in migration towards fMLP, C5a, Cxcl8 or Ccl3 and respiratory burst upon activation by C5a or fMLP (56), but another study suggests that PI3K is not required for chemotaxis towards fMLP (51).

Cellular response to IL-1 was also reduced. IL1α and IL1β are very potent mediators of inflammation response, but their role in neutrophils remains poorly understood. Their main effect on neutrophils could be to increase their survival (37).

We also observed a down-regulation of TGFβ and IFNγ pathways. In the steady state situation, the role of TGFβ on neutrophil function is poorly understood. However, in cancer context, TGFβ is responsible for promoting the generation of pro-tumoral type N2 neutrophils (57), whereas type IFNβ and IFNγ might favor anti-tumoral type N2 neutrophils (58, 59). In non-cancerous situation, IFNγ has also been shown to enhance, or prime, increased ROS production in combination with a secondary stimulus and to promote phagocytosis (60), which could account for the decrease in ROS and phagocytosis that we observed in spleen *Cxcr2-/-* neutrophils. As treatment of PMNs with IFNγ increases the production of TNFα and IL-1β (61), this could also account for the down-regulation of TNFα and IL1β signaling that we report.

In conclusion, this work highlights the multiple roles played by the chemokine receptor Cxcr2 in neutrophils and reinforces the importance of localization of neutrophils in terms of action and features. The identification of the pathways that are dependent on Cxcr2 and their further investigation will be essential to understand the roles of Cxcr2 in neutrophils in the steady state or inflammatory situation but also in the tumoral context.

Data availability statement

The datasets presented in this study can be found in online repositories. The names of the repository/repositories and accession number(s) can be found in the article.

Ethics statement

The animal study was reviewed and approved by Ministère de l'enseignement supérieur, de la recherche et de l'innovation.

Author contributions

PD, BG, and ER and have contributed to the investigation. KB participated to writing review and editing. GL was in charge of the conceptualization, investigation and supervision of the project, funding acquisition and writing original draft preparation. All authors have read, revised and agreed to the published version of the manuscript.

Funding

This work was supported by la Ligue contre le Cancer to GL.

Acknowledgments

We acknowledge the PCEA, RAM, MRI facilities in Montpellier. We are grateful to Institut du cerveau et de la moëlle épinière in Paris for RNAseq experiments. We thank Vincent Rondeau and Marie-Laure Aknin for useful advices in protocols.

Conflict of interest

The authors declare that the research was conducted in the absence of any commercial or financial relationships that could be construed as a potential conflict of interest.

Publisher's note

All claims expressed in this article are solely those of the authors and do not necessarily represent those of their affiliated organizations, or those of the publisher, the editors and the reviewers. Any product that may be evaluated in this article, or claim that may be made by its manufacturer, is not guaranteed or endorsed by the publisher.

Supplementary material

The Supplementary Material for this article can be found online at: https://www.frontiersin.org/articles/10.3389/fimmu.2022.1005551/full#supplementary-material

References

1. Dohrmann S, Cole JN, Nizet V. Conquering neutrophils. *PLoS Pathog* (2016) 12(7):e1005682. doi: 10.1371/journal.ppat.1005682

2. Burgener SS, Schroder K. Neutrophil extracellular traps in host defense. *Cold Spring Harb Perspect Biol* (2020) 12(7):1–15. doi: 10.1101/cshperspect.a037028

3. Ng LG, Ostuni R, Hidalgo A. Heterogeneity of neutrophils. *Nat Rev Immunol* (2019) 19(4):255–65. doi: 10.1038/s41577-019-0141-8

4. Cronkite EP, Fliedner TM, Bond VP, Rubini JR. Dynamics of hemopoietic proliferation in man and mice studied by H3-thymidine incorporation into DNA. *Ann N Y Acad Sci* (1959) 77:803–20. doi: 10.1111/j.1749-6632.1959.tb36943.x

5. Pillay J, den Braber I, Vrisekoop N, Kwast LM, de Boer RJ, Borghans JA, et al. *In vivo* labeling with 2H2O reveals a human neutrophil lifespan of 5.4 days. *Blood* (2010) 116(4):625–7. doi: 10.1182/blood-2010-01-259028

6. Kim HK, de la Luz Sierra M, Williams CK, Gulino AV, Tosato G. G-CSF down-regulation of CXCR4 expression identified as a mechanism for mobilization of myeloid cells. *Blood* (2006) 108(3):812–20. doi: 10.1182/blood-2005-10-4162

7. Borregaard N. Neutrophils, from marrow to microbes. *Immunity* (2010) 33 (5):657–70. doi: 10.1016/j.immuni.2010.11.011

8. Evrard M, Kwok IWH, Chong SZ, Teng KWW, Becht E, Chen J, et al. Developmental analysis of bone marrow neutrophils reveals populations specialized in expansion, trafficking, and effector functions. *Immunity* (2018) 48 (2):364–79.e8. doi: 10.1016/j.immuni.2018.02.002

9. Hidalgo A, Chilvers ER, Summers C, Koenderman L. The neutrophil life cycle. *Trends Immunol* (2019) 40(7):584–97. doi: 10.1016/j.it.2019.04.013

10. Cowland JB, Borregaard N. Isolation of neutrophil precursors from bone marrow for biochemical and transcriptional analysis. *J Immunol Methods* (1999) 232(1-2):191–200. doi: 10.1016/s0022-1759(99)00176-3

11. Terstappen LW, Safford M, Loken MR. Flow cytometric analysis of human bone marrow. III. neutrophil maturation. *Leukemia* (1990) 4(9):657–63.

12. Capucetti A, Albano F, Bonecchi R. Multiple roles for chemokines in neutrophil biology. *Front Immunol* (2020) 11:1259. doi: 10.3389/fimmu.2020.01259

13. Jaillon S, Ponzetta A, Di Mitri D, Santoni A, Bonecchi R, Mantovani A. Neutrophil diversity and plasticity in tumour progression and therapy. *Nat Rev Cancer* (2020) 20(9):485–503. doi: 10.1038/s41568-020-0281-y

14. Timaxian C, Vogel CFA, Orcel C, Vetter D, Durochat C, Chinal C, et al. Pivotal role for Cxcr2 in regulating tumor-associated neutrophil in breast cancer. *Cancers (Basel)* (2021) 13(11):1–20. doi: 10.3390/cancers13112584

15. Mancini SJC, Balabanian K, Corre I, Gavard J, Lazennec G, Le Bousse-Kerdiles MC, et al. Deciphering tumor niches: Lessons from solid and hematological malignancies. *Front Immunol* (2021) 12:766275. doi: 10.3389/fimmu.2021.766275

16. Haslett C. Granulocyte apoptosis and its role in the resolution and control of lung inflammation. *Am J Respir Crit Care Med* (1999) 160(5 Pt 2):S5–11. doi: 10.1164/ajrccm.160.supplement_1.4

17. Martin C, Burdon PC, Bridger G, Gutierrez-Ramos JC, Williams TJ, Rankin SM. Chemokines acting *via* CXCR2 and CXCR4 control the release of neutrophils from the bone marrow and their return following senescence. *Immunity* (2003) 19 (4):583–93. doi: 10.1016/s1074-7613(03)00263-2

18. Jhunjhunwala S, Alvarez D, Aresta-DaSilva S, Tang K, Tang BC, Greiner DL, et al. Frontline science: Splenic progenitors aid in maintaining high neutrophil numbers at sites of sterile chronic inflammation. *J Leukoc Biol* (2016) 100(2):253–60. doi: 10.1189/jlb.1HI0615-248RR

19. Chuntharapai A, Lee J, Hebert CA, Kim KJ. Monoclonal antibodies detect different distribution patterns of IL-8 receptor a and IL-8 receptor b on human peripheral blood leukocytes. *J Immunol* (1994) 153(12):5682–8.

20. Marin-Esteban V, Youn J, Beaupain B, Jaracz-Ros A, Barlogis V, Fenneteau O, et al. Biallelic CXCR2 loss-of-function mutations define a distinct congenital neutropenia entity. *Haematologica* (2022) 107(3):765–9. doi: 10.3324/haematol.2021.279254

21. Addison CL, Daniel TO, Burdick MD, Liu H, Ehlert JE, Xue YY, et al. The CXC chemokine receptor 2, CXCR2, is the putative receptor for ELR+ CXC chemokine-induced angiogenic activity. *J Immunol* (2000) 165(9):5269–77. doi: 10.4049/jimmunol.165.9.5269

22. Bieche I, Chavey C, Andrieu C, Busson M, Vacher S, Le Corre L, et al. CXC chemokines located in the 4q21 region are up-regulated in breast cancer. *Endocr Relat Cancer* (2007) 14(4):1039–52. doi: 10.1677/erc.1.01301

23. Lazennec G, Richmond A. Chemokines and chemokine receptors: new insights into cancer-related inflammation. *Trends Mol Med* (2010) 16(3):133–44. doi: 10.1016/j.molmed.2010.01.003

24. Rajarathnam K, Desai UR. Structural insights into how proteoglycans determine chemokine-CXCR1/CXCR2 interactions: Progress and challenges. *Front Immunol* (2020) 11:660. doi: 10.3389/fimmu.2020.00660

25. Sai J, Raman D, Liu Y, Wikswo J, Richmond A. Parallel phosphatidylinositol 3-kinase (PI3K)-dependent and src-dependent pathways lead to CXCL8-mediated Rac2 activation and chemotaxis. *J Biol Chem* (2008) 283(39):26538–47. doi: 10.1074/jbc.M805611200

26. Boissiere-Michot F, Jacot W, Massol O, Mollevi C, Lazennec G. CXCR2 levels correlate with immune infiltration and a better prognosis of triple-negative breast cancers. *Cancers (Basel)* (2021) 13(10):1–16. doi: 10.3390/cancers13102328

27. Yang J, Yan C, Vilgelm AE, Chen SC, Ayers GD, Johnson CA, et al. Targeted deletion of CXCR2 in myeloid cells alters the tumor immune environment to improve antitumor immunity. *Cancer Immunol Res* (2020) 9:200–13. doi: 10.1158/2326-6066.CIR-20-0312

28. Timaxian C, Raymond-Letron I, Bouclier C, Gulliver L, Le Corre L, Chebli K, et al. The health status alters the pituitary function and reproduction of mice in a Cxcr2-dependent manner. *Life Sci Alliance* (2020) 3(3):1–28. doi: 10.26508/lsa.201900599

29. Cacalano G, Lee J, Kikly K, Ryan AM, Pitts-Meek S, Hultgren B, et al. Neutrophil and b cell expansion in mice that lack the murine IL-8 receptor homolog. *Science* (1994) 265(5172):682–4. doi: 10.1126/science.8036519

30. Del Rio L, Bennouna S, Salinas J, Denkers EY. CXCR2 deficiency confers impaired neutrophil recruitment and increased susceptibility during toxoplasma gondii infection. *J Immunol* (2001) 167(11):6503–9. doi: 10.4049/jimmunol.167.11.6503

31. Edgar R, Domrachev M, Lash AE. Gene expression omnibus: NCBI gene expression and hybridization array data repository. *Nucleic Acids Res* (2002) 30 (1):207–10. doi: 10.1093/nar/30.1.207

32. Deniset JF, Surewaard BG, Lee WY, Kubes P. Splenic Ly6G(high) mature and Ly6G(int) immature neutrophils contribute to eradication of s. *Pneumoniae J Exp Med* (2017) 214(5):1333–50. doi: 10.1084/jem.20161621

33. Casanova-Acebes M, Pitaval C, Weiss LA, Nombela-Arrieta C, Chevre R, Zhang D, et al. Rhythmic modulation of the hematopoietic niche through neutrophil clearance. *Cell* (2013) 153(5):1025–35. doi: 10.1016/j.cell.2013.04.040

34. MacCalman CD, Farookhi R, Blaschuk OW. Estradiol regulates n-cadherin mRNA levels in the mouse ovary. *Dev Genet* (1995) 16(1):20–4. doi: 10.1002/dvg.1020160106

35. Fine N, Khaliq S, Hassanpour S, Glogauer M. Role of the cytoskeleton in myeloid cell function. *Microbiol Spectr* (2016) 4(4):1–15. doi: 10.1128/microbiolspec.MCHD-0029-2016

36. Xie X, Shi Q, Wu P, Zhang X, Kambara H, Su J, et al. Single-cell transcriptome profiling reveals neutrophil heterogeneity in homeostasis and infection. *Nat Immunol* (2020) 21(9):1119–33. doi: 10.1038/s41590-020-0736-z

37. Futosi K, Fodor S, Mocsai A. Reprint of neutrophil cell surface receptors and their intracellular signal transduction pathways. *Int Immunopharmacol* (2013) 17 (4):1185–97. doi: 10.1016/j.intimp.2013.11.010

38. Zarbock A, Lowell CA, Ley K. Spleen tyrosine kinase syk is necessary for e-selectin-induced alpha(L)beta(2) integrin-mediated rolling on intercellular adhesion molecule-1. *Immunity* (2007) 26(6):773–83. doi: 10.1016/j.immuni.2007.04.011

39. Pillinger MH, Feoktistov AS, Capodici C, Solitar B, Levy J, Oei TT, et al. Mitogen-activated protein kinase in neutrophils and enucleate neutrophil cytoplasts: evidence for regulation of cell-cell adhesion. *J Biol Chem* (1996) 271 (20):12049–56. doi: 10.1074/jbc.271.20.12049

40. Kim D, Haynes CL. The role of p38 MAPK in neutrophil functions: single cell chemotaxis and surface marker expression. *Analyst* (2013) 138(22):6826–33. doi: 10.1039/c3an01076g

41. Saverymuttu SH, Peters AM, Keshavarzian A, Reavy HJ, Lavender JP. The kinetics of 111indium distribution following injection of 111indium labelled autologous granulocytes in man. *Br J Haematol* (1985) 61(4):675–85. doi: 10.1111/j.1365-2141.1985.tb02882.x

42. Devi S, Wang Y, Chew WK, Lima R, Chong SZ, Schlitzer A, et al. Neutrophil mobilization *via* plerixafor-mediated CXCR4 inhibition arises from lung demargination and blockade of neutrophil homing to the bone marrow. *J Exp Med* (2013) 210(11):2321–36. doi: 10.1084/jem.20130056

43. Adrover JM, Del Fresno C, Crainiciuc G, Cuartero MI, Casanova-Acebes M, Weiss LA, et al. A neutrophil timer coordinates immune defense and vascular protection. *Immunity* (2019) 50(2):390–402.e10. doi: 10.1016/j.immuni.2019.01.002

44. Dupre-Crochet S, Erard M, Nubetae O. ROS production in phagocytes: why, when, and where? *J Leukoc Biol* (2013) 94(4):657–70. doi: 10.1189/jlb.1012544

45. Garratt LW. Current understanding of the neutrophil transcriptome in health and disease. *Cells* (2021) 10(9). doi: 10.3390/cells10092406

46. Steichen AL, Binstock BJ, Mishra BB, Sharma J. C-type lectin receptor Clec4d plays a protective role in resolution of gram-negative pneumonia. *J Leukoc Biol* (2013) 94(3):393–8. doi: 10.1189/jlb.1212622

47. Ma YQ, Plow EF, Geng JG. P-selectin binding to p-selectin glycoprotein ligand-1 induces an intermediate state of alphaMbeta2 activation and acts cooperatively with extracellular stimuli to support maximal adhesion of human neutrophils. *Blood* (2004) 104(8):2549–56. doi: 10.1182/blood-2004-03-1108

48. de Oliveira THC, Marques PE, Poosti F, Ruytinx P, Amaral FA, Brandolini L, et al. Intravital microscopic evaluation of the effects of a CXCR2 antagonist in a model of liver ischemia reperfusion injury in mice. *Front Immunol* (2017) 8:1917. doi: 10.3389/fimmu.2017.01917

49. Mocsai A, Jakus Z, Vantus T, Berton G, Lowell CA, Ligeti E. Kinase pathways in chemoattractant-induced degranulation of neutrophils: the role of p38 mitogen-activated protein kinase activated by src family kinases. *J Immunol* (2000) 164(8):4321–31. doi: 10.4049/jimmunol.164.8.4321

50. Aoshiba K, Yasui S, Hayashi M, Tamaoki J, Nagai A. Role of p38-mitogen-activated protein kinase in spontaneous apoptosis of human neutrophils. *J Immunol* (1999) 162(3):1692–700.

51. Heit B, Liu L, Colarusso P, Puri KD, Kubes P. PI3K accelerates, but is not required for, neutrophil chemotaxis to fMLP. *J Cell Sci* (2008) 121(Pt 2):205–14. doi: 10.1242/jcs.020412

52. Liu X, Ma B, Malik AB, Tang H, Yang T, Sun B, et al. Bidirectional regulation of neutrophil migration by mitogen-activated protein kinases. *Nat Immunol* (2012) 13(5):457–64. doi: 10.1038/ni.2258

53. Klebanoff SJ, Vadas MA, Harlan JM, Sparks LH, Gamble JR, Agosti JM, et al. Stimulation of neutrophils by tumor necrosis factor. *J Immunol* (1986) 136 (11):4220–5.

54. Bei L, Hu T, Qian ZM, Shen X. Extracellular Ca2+ regulates the respiratory burst of human neutrophils. *Biochim Biophys Acta* (1998) 1404(3):475–83. doi: 10.1016/s0167-4889(98)00081-0

55. Uribe-Querol E, Rosales C. Phagocytosis: Our current understanding of a universal biological process. *Front Immunol* (2020) 11:1066. doi: 10.3389/fimmu.2020.01066

56. Li Z, Jiang H, Xie W, Zhang Z, Smrcka AV, Wu D. Roles of PLC-beta2 and -beta3 and PI3Kgamma in chemoattractant-mediated signal transduction. *Science* (2000) 287(5455):1046–9. doi: 10.1126/science.287.5455.1046

57. Fridlender ZG, Sun J, Kim S, Kapoor V, Cheng G, Ling L, et al. Polarization of tumor-associated neutrophil phenotype by TGF-beta: "N1" versus "N2" TAN. *Cancer Cell* (2009) 16(3):183–94. doi: 10.1016/j.ccr.2009.06.017

58. Andzinski L, Kasnitz N, Stahnke S, Wu CF, Gereke M, von Kockritz-Blickwede M, et al. Type I IFNs induce anti-tumor polarization of tumor associated neutrophils in mice and human. *Int J Cancer* (2016) 138(8):1982–93. doi: 10.1002/ijc.29945

59. Stoppacciaro A, Melani C, Parenza M, Mastracchio A, Bassi C, Baroni C, et al. Regression of an established tumor genetically modified to release granulocyte colony-stimulating factor requires granulocyte-T cell cooperation and T cell-produced interferon gamma. *J Exp Med* (1993) 178(1):151–61. doi: 10.1084/jem.178.1.151

60. Ellis TN, Beaman BL. Interferon-gamma activation of polymorphonuclear neutrophil function. *Immunology* (2004) 112(1):2–12. doi: 10.1111/j.1365-2567.2004.01849.x

61. Meda L, Gasperini S, Ceska M, Cassatella MA. Modulation of proinflammatory cytokine release from human polymorphonuclear leukocytes by gamma interferon. *Cell Immunol* (1994) 157(2):448–61. doi: 10.1006/cimm.1994.1241

frontiers | Frontiers in Immunology

TYPE Original Research
PUBLISHED 16 November 2022
DOI 10.3389/fimmu.2022.970287

OPEN ACCESS

EDITED BY
Shailendra Saxena,
King George's Medical University, India

REVIEWED BY
Luis Diambra,
National University of La Plata, Argentina
Pier Maria Fornasari,
Regen Health Solutions, Italy

*CORRESPONDENCE
Lana X. Garmire
lgarmire@med.umich.edu
Michal A. Olszewski
olszewsm@med.umich.edu
Jane C. Deng
jcdeng@med.umich.edu

†The authors have contributed equally to this work

SPECIALTY SECTION
This article was submitted to Viral Immunology, a section of the journal Frontiers in Immunology

RECEIVED 15 June 2022
ACCEPTED 27 October 2022
PUBLISHED 16 November 2022

CITATION
Xu J, He B, Carver K, Vanheyningen D, Parkin B, Garmire LX, Olszewski MA and Deng JC (2022) Heterogeneity of neutrophils and inflammatory responses in patients with COVID-19 and healthy controls.
Front. Immunol. 13:970287.
doi: 10.3389/fimmu.2022.970287

Heterogeneity of neutrophils and inflammatory responses in patients with COVID-19 and healthy controls

Jintao Xu[1,2†], Bing He[3†], Kyle Carver[1,2], Debora Vanheyningen[1,2], Brian Parkin[1,4], Lana X. Garmire[3*], Michal A. Olszewski[1,2*] and Jane C. Deng[1,2*]

[1]Research Service, LTC Charles S. Kettles Veterans Affairs Medical Center, Department of Veterans Affairs Health System, Ann Arbor, MI, United States, [2]Division of Pulmonary and Critical Care Medicine, Department of Internal Medicine, University of Michigan Medical School, Ann Arbor, MI, United States, [3]Department of Computational Medicine and Bioinformatics, University of Michigan, Ann Arbor, MI, United States, [4]Division of Hematology and Oncology, Department of Internal Medicine, University of Michigan Health System, Ann Arbor, MI, United States

Severe respiratory viral infections, including SARS-CoV-2, have resulted in high mortality rates despite corticosteroids and other immunomodulatory therapies. Despite recognition of the pathogenic role of neutrophils, in-depth analyses of this cell population have been limited, due to technical challenges of working with neutrophils. We undertook an unbiased, detailed analysis of neutrophil responses in adult patients with COVID-19 and healthy controls, to determine whether distinct neutrophil phenotypes could be identified during infections compared to the healthy state. Single-cell RNA sequencing analysis of peripheral blood neutrophils from hospitalized patients with mild or severe COVID-19 disease and healthy controls revealed distinct mature neutrophil subpopulations, with relative proportions linked to disease severity. Disruption of predicted cell-cell interactions, activated oxidative phosphorylation genes, and downregulated antiviral and host defense pathway genes were observed in neutrophils obtained during severe compared to mild infections. Our findings suggest that during severe infections, there is a loss of normal regulatory neutrophil phenotypes seen in healthy subjects, coupled with the dropout of appropriate cellular interactions. Given that neutrophils are the most abundant circulating leukocytes with highly pathogenic potential, current immunotherapies for severe infections may be optimized by determining whether they aid in restoring an appropriate balance of neutrophil subpopulations.

KEYWORDS

COVID-19, immune response, single-cell sequencing, neutrophil heterogeneity, SARS – CoV – 2

Introduction

Severe lung injury and systemic inflammation are the main hallmarks of severe respiratory viral infections, including SARS-CoV-2 (1). Neutrophils, or polymorphonuclear leukocytes, are the most abundant leukocyte population in the blood and found in high numbers in the lung during severe respiratory viral infections (2). During viral infections, neutrophils can contribute to viral clearance through mechanisms such as phagocytosis, and release of neutrophil extracellular traps, secretion of cytokines and activation of the adaptive immune response (2–4). However, the overactivation of neutrophils may cause bystander damage to host tissues and lead to poor outcomes (2–4). Although neutrophils are considered as a primary cellular driver of the pathogenesis of acute respiratory distress syndrome (ARDS) and have been implicated in the pathophysiology of severe COVID-19 (5–9), the challenges of isolating neutrophils for analysis and their inability to survive cryopreservation have resulted in poor understanding of their function in disease progression (10). Additionally, neutrophils are still largely considered to be a homogenous effector cell population with clearly established roles in combatting bacterial and fungal infections, but their mechanistic contributions to the immunopathogenesis or clearance of viral infections remain unclear. While recent studies have started to recognize the heterogeneity of neutrophils during cancer and other chronic diseases (11, 12), whether different neutrophil subtypes exist beyond "immature," "mature," and "senescent" is uncertain during an acute infection. The goal of our study, therefore, was to test the hypothesis that different phenotypes of mature neutrophils exist under basal healthy conditions, with subsequent changes in relative abundance during acute respiratory viral infections depending on the severity of immunopathology of COVID-19 disease.

To investigate this, we employed single-cell RNA sequencing (scRNA-seq) analysis of the peripheral immune response to SARS-CoV-2, a technique that has provided novel insights into immune cell heterogeneity and dysregulation during COVID-19 (7, 10, 13–18). Most of the studies to date have utilized preserved peripheral blood mononuclear cells (PBMC), which are mainly comprised of monocyte and lymphocyte populations. As a result, the literature largely reflects an incomplete and possibly biased picture of increased immature and dysfunctional neutrophils – largely reflecting low-density neutrophils that are captured in the PBMC fraction (15, 19, 20). Given that neutrophils are the most abundant leukocyte in peripheral blood during both health and infection, a comprehensive analysis of unpreserved, fresh neutrophils from human subjects is needed in order to determine whether mature neutrophils have the ability to adopt distinct phenotypes, and how these phenotypes change during clinically significant respiratory infections such as SARS-CoV-2.

In this study, we recruited adult subjects hospitalized with mild or severe SARS-CoV-2 infections, in order to examine how neutrophil phenotypes changed based upon the severity of infection over time, compared to healthy adults. We took care only to include adult patients who were without significant co-morbidities or underlying immunosuppressive conditions that might confound neutrophil phenotypes. Our analysis resulted in the identification of 7 mature and 2 immature neutrophil clusters, which had differential pathway activation patterns. Our results also demonstrated that quantitatively and qualitatively, neutrophils are a potentially more robust cellular regulator of inflammatory responses than monocytes, further underscoring the importance of investigating the considerable heterogeneity of responses in the neutrophil population.

Methods

Patient cohort, biological samples, and preparation of single-cell suspensions

A total of 11 patients admitted with SARS-CoV-2 infections and 5 healthy control subjects (all outpatients) were enrolled from the Veterans Affairs Ann Arbor Healthcare System and Michigan Medicine University Hospital. Between June, 2020 and June, 2021, all adult patients admitted with COVID-19 disease to these two facilities were screened and recruited if they had no evidence of baseline immunosuppression (e.g., chronic prednisone use of 15 mg or more daily, other immunosuppressive medications, HIV infection, neutropenia), active or recent malignancy within past 5 years, immunomodulatory therapies (e.g., biologics), chronic infection (e.g., hepatitis viral infection), significant systemic autoimmune disease, chronic malnutrition or debility, significant chronic organ dysfunction (e.g., chronic liver disease, poorly controlled diabetes, severe COPD or lung disease, heart failure with EF<40%), chronic alcohol consumption of >5 drinks a day, or active co-infection other than SARS-CoV-2. 11 patients with COVID-19 were classified into two groups based upon severity – "mild" (n = 4, hospitalized but needing <50% O2), or "severe" (n = 7, hospitalized but needing > 50% O2 or in Intensive Care Unit). Out of seven patients with severe symptoms, 4 patients deteriorated clinically and passed away. The demographic and disease characteristics of the prospectively recruited patients studied by scRNA-seq are listed in Supplementary Figure 1. All participants had to be capable of providing written informed consent for sample collection and subsequent analyses.

Within 72 hours of hospital admission ("T1") and 5-7 days later ("T2), blood was collected into lavender top tubes (EDTA) and processed immediately after collection except that one patient was sampled day 15 days later. Data from this patient passed our strict quality control and clustered with the other patients within the same group. Healthy control subjects and 2 Veterans who were discharged did not get a second sample. For

PMBC and granulocyte isolation from patient blood, 5ml of blood was carefully layered on 5ml of Lymphocyte-poly isolation media (NC9950836, Fisher) in a 15ml conical tube in a biosafety cabinet. The sample was spun in a sealed bucket at room temperature, 500g, 35 minutes. After centrifuge, leukocyte bands containing mononuclear cells and granulocytes were transferred to another 50 ml conical tube. Cells were diluted with an equal volume of HBSS without Calcium and Magnesium and spun at room temperature, 350g for 10min. The supernatant was removed from each pellet and suspended in 5ml 1x ACK lysis buffer for 2 minutes. Pellets were suspended with PBS containing 0.04% BSA and then counted. An aliquot of mononuclear and granulocyte cells was processed in a cytospin and stained using Diff Quick (26096-25, Electron Microscopy Sciences). Cell differentials were counted, and the mononuclear and granulocyte populations were combined to achieve a 1:1 ratio. Cells were immediately processed for the single-cell RNA library. For all samples, cell viability exceeded 90%.

Single-cell RNA library preparation and sequencing

The scRNA-seq libraries were constructed using a Chromium Next GEM Single Cell 3′ Reagent Kit v3.1 (10X Genomics) according to the manufacturer's introduction. In brief, the cell suspension (700-1,200 cells per ul) was loaded onto a Chromium single cell controller to generate single-cell gel beads in the emulsion (GEMs). Following this, scRNA-seq libraries were constructed according to the manufacturer's instructions. The libraries were sequenced using an Illumina Novaseq sequencer at Advanced Genomics Core of the University of Michigan using the suggested cycling from 10X Genomics.

Single-cell RNA-seq data processing

We aligned single-cell RNA sequencing data against the GRCh38 human reference genome and preprocessed using cellranger pipeline (version 6.0.0). A preliminary single-cell gene expression matrix was then exported from cellranger for further analysis. Quality control was applied to cells based on three metrics - the total UMI counts, number of detected genes, and proportion of mitochondrial gene counts per cell. Specifically, cells with less than 500 UMI counts and 200 detected genes were filtered out, as well as cells with more than 20% mitochondrial gene counts. Thereafter, we applied DoubletFinder, which identifies doublets formed from transcriptionally distinct cells (21), to remove potential doublets. The expected doublet rate was set to be 0.075, and cells predicted to be doublets were filtered out. After quality control, a total of 108,597 cells were collected for further analysis.

Clustering and cell-type annotation

We used Seurat (22) to integrate and cluster the collected single cells from COVID19 patients and healthy controls. The gene counts for each cell were normalized by LogNormalize method, which divides gene counts by the total counts for that cell and multiplied by the scale.factor. The normalized gene counts were then natural-log transformed using log1p function. The top 2000 most variable genes were selected using FindVariableFeatures functions for the clustering of single cells. We used dimensions of reduction 30 and resolution 0.3 for the cluster analysis. We used SingleR (23) and human primary cell atlas reference (24) to annotate cell types of single cells. The cell type of the cluster was determined by the dominant cell type in each cluster. The proportion of B cells, T cells, and NK cells in every sample was further calculated to determine the consistency between our data and observed in other published data (25, 26) in the cell type composition difference between severe COVID19 patients and healthy controls.

Cellular crosstalk analysis

We used iTALK (27) to identify and visualize the possible cellular crosstalk mediated by up-regulated ligand-receptor pairs between each cell type in COVID19 patients. We used the cytokine/chemokine category in the ligand-receptor database for this analysis. We used Wilcoxon rank-sum test to identify the significantly up-regulated genes (adjusted P-value <0.05 & average log fold change >0.1) for every cell type in the severe and mild COVID19 patients, respectively, compared with healthy controls at day 0. We also identified up-regulated genes (adjusted P-value <0.05 & average log fold change >0.1) between day 5 and day 0 in recovered mild COVID19 patients and deceased severe COVID19 patients, respectively. We then matched and paired the up-regulated genes against the ligand-receptor database to construct a putative cell-cell communication network using iTALK. The iTALK defines an interaction score using the log fold change of ligand and receptor to rank these interactions.

Feature genes and pathways for neutrophils

We collected neutrophil cells from mild and severe COVID19 patients within 72 hours of hospital admission ("T1"), as well as healthy controls to identify significantly up-regulated feature genes (adjusted P-value <0.05 & average log fold change >0.1) by comparing neutrophils from one type

(healthy, mild, or severe) to the rest of neutrophils from other types, using cells as biological replicates. The overlap among feature genes identified in healthy, mild, and severe groups was presented in the Venn plot using the Venn package. The top 10 feature genes for each type of neutrophil were presented in a bubble plot using the DotPlot function from the Seurat package. These feature genes were then mapped to human protein-protein interactions (PPIs) downloaded from the BioGRID database (version 4.4.197) using R. The KEGG pathways significantly enriched (adjusted P-value <0.05) in feature genes that connected by PPIs were identified using enrichKEGG function from clusterProfiler package (28). The GSEA analysis was performed using clusterProfiler package (28). The bipartite plot of significant pathways, genes, and PPIs was presented using the Cytoscape tool (29).

Neutrophil cluster analysis

We integrated neutrophils from mild and severe COVID19 patients, as well as healthy controls to identify neutrophil clusters using resolution 0.5 in Seurat. The significantly up-regulated (adjusted P-value <0.05 & average log fold change >0.1) feature genes for each neutrophil cluster were identified by comparing one cluster to all other clusters. The top 5 feature genes for each cluster were shown in a bubble plot using DotPlot function from the Seurat package. The KEGG and GO pathways significantly enriched (adjusted P-value <0.05) in feature genes were identified for each cluster using clusterProfiler package. The top 3 significant pathways (KEGG) and all significant pathways (GO) were shown in the bubble plot using ggplot2 package. The composition changes of each cluster among healthy control, mild and severe COVID19 were identified using student's t-test and presented using ggpubr package. We define the severity of COVID19 from 1 to 4, in which 1 means healthy, 2 means mild, 3 means severe but recovered, and 4 means severe patient that deteriorated clinically and later passed away. The association between composition changes of each cluster and severity of COVID19 were identified using spearman's correlation and the Hmisc package. The significant associations were shown using corrplot package. We further identified differentially expressed genes (DEGs) between severe and mild, mild and healthy respectively, for each cluster that associated with the severity of COVID19. The KEGG pathways significantly enriched (adjusted P-value <0.05) in DEGs were identified using the gseKEGG function from clusterProfiler package. The normalized enrichment score (NES) of significant pathways indicates the activation status of the pathway.

Statistics

Statistical analysis was performed using R with Student's t test or analysis of variance (ANOVA). Asterisks on figures indicate statistical significance as follows: *P < 0.05, **P < 0.01, ***P < 0.001, and ****P < 0.0001.

Study approval and ethics

This study was approved by the Veterans Affairs Ann Arbor Institutional Review Board (IRB) and University of Michigan IRB (IRB-2020-1228 and HUM00181804, respectively). All participants provided written informed consent for sample collection and subsequent analyses. Study procedures adhered to full ethical and safety standards.

Results

Neutrophils are major contributors to the inflammatory response relative to other leukocytes during COVID

Activated monocytes and T cells have been portrayed as the primary cellular drivers of inflammation during severe COVID-19. Despite being the predominant leukocyte population in terms of numbers (30), neutrophils have been largely overlooked in human studies due to the inability of these cells to survive long-term storage and cryopreservation. Thus, we performed droplet-based scRNA-seq to examine the transcriptomic profiles of freshly isolated peripheral neutrophils and other leukocytes from hospitalized adult patients with COVID-19 disease and healthy donors (HD) (Figures S1A,B). To reduce confounding, we excluded subjects with conditions are known to impact immune responses (Methods). The 11 patients with COVID-19 who met our stringent selection criteria were classified into two groups based upon severity – "mild" (n = 4, hospitalized but needing ≤50% O_2), or "severe" (n = 7, hospitalized but needing > 50% O_2 or in the intensive care unit, or ICU). The clinical characteristics of enrolled patients are detailed in Figure S1B. Neutrophils and other leukocytes were isolated from peripheral blood samples. Since neutrophils are particularly sensitive to degradation, isolated cells were immediately processed for scRNA-seq experiments (see Methods). Non-neutrophil leukocytes from peripheral blood were included at approximately equal proportions in the scRNA seq analysis to dissect cell-cell interactions.

A unified single-cell analysis pipeline was employed, including preprocessing involving batch removal and quality control steps (see Methods). A total of 108,597 high-quality cells from all samples proceeded to downstream analysis. Among these cells, 30,429 cells (28%) were from the healthy donor group, 22,188 cells (20%) were from the mild group, and 55,980 cells (52%) were from the severe group. Using Seurat (22) and SingleR (23), we identified 15 major cell types or subtypes

according to the expression of canonical gene transcripts in the peripheral blood (Figures 1A, B). Among them, 45,463 cells are classified as mature ($CXCR2^+$ $FCGR3B^+$) or immature ($CD24^+PGLYRP1^+CEACAM8^+$) neutrophils (Figures 1A, B) (7, 31).

Next, we analyzed the transcriptional profiles of the main myeloid (i.e., monocyte and neutrophil) cell populations to determine the differential contributions of each cell type towards the inflammatory landscape during COVID-19. First, to validate the compatibility of our approach with previous studies, we examined transcriptional expression of two monocyte markers most consistently reported to change with COVID-19 severity. Monocytes from severe COVID-19 patients displayed decreased HLA-DRA and increased CD163 expression compared to healthy donors and mild COVID-19 patients (Figures S2A, B), consistent with prior reports (10, 15). We next sought to investigate if neutrophils contribute to cytokine storm during COVID-19 disease. To capture a global snapshot

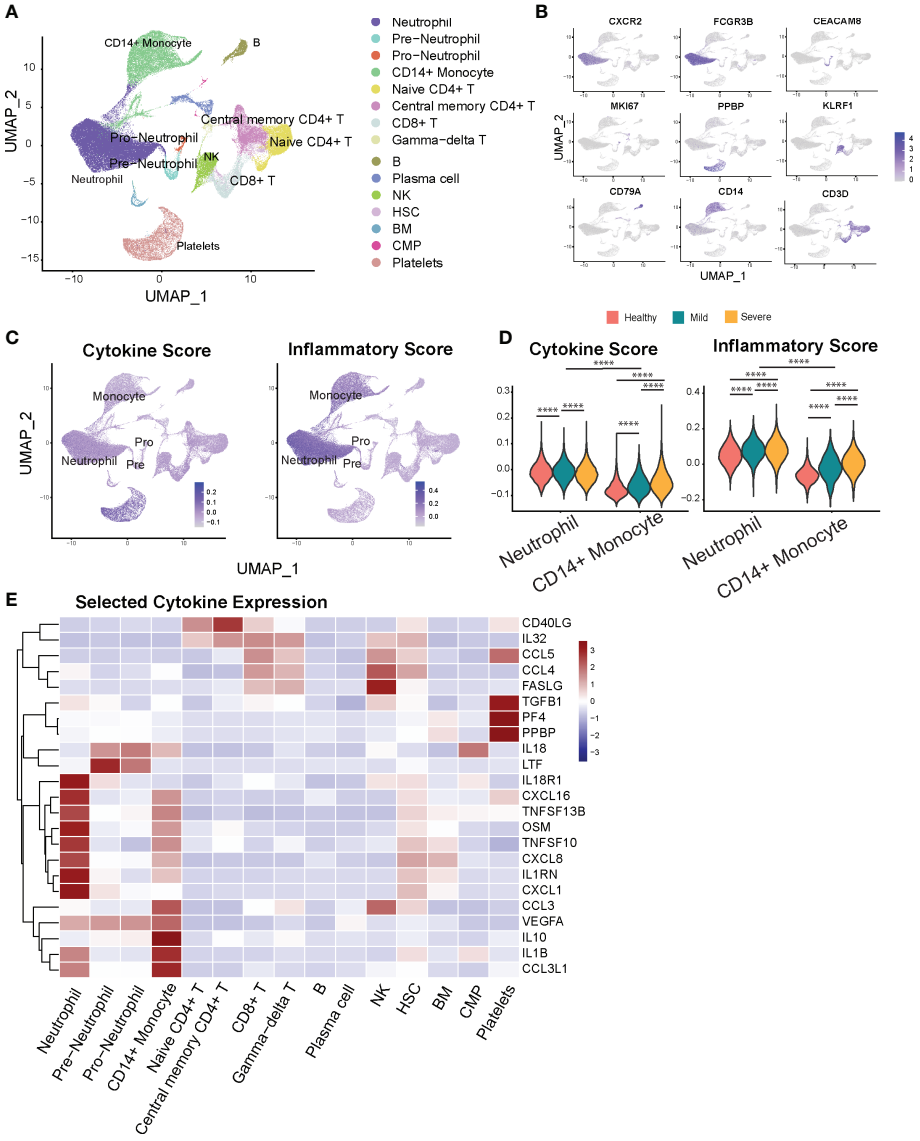

FIGURE 1
Neutrophils display marked inflammatory signatures relative to other leukocyte populations. **(A)** Cellular populations identified by scRNA seq. The UMAP projection from HD (n = 5), Mild (n = 4), severe (n = 6) samples. **(B)** Canonical cell-defining transcripts were used to label clusters by cell identity as represented in the UMAP plot. Data are colored according to expression levels and the legend is labeled in log scale. **(C)** UMAP plots of cells colored by cytokine score (left) and inflammatory score (right panel). **(D)** Violin plots indicate progression of cytokine (left) and inflammatory scores (right panel) for neutrophils and monocytes with increased severity of infection. **(E)** Heatmap of selected cytokine genes in different subsets of cells. ****p < 0.0001.

of the inflammatory state of different cell populations, we analyzed the cytokine and inflammatory pathways scores in different cell types based on the overall expression of cytokine and inflammatory response genes (Figures 1C, D, Supplementary Table 1), adapted from (26, 32). Monocytes and megakaryocytes have previously been shown to be major sources of systemic cytokine production based upon this scoring system in COVID-19 patients (26), which we also found in our results. Additionally, we observed that neutrophils have greater potential to contribute to the magnitude of the systemic inflammatory response, indicated by their high cytokine and inflammatory pathway scores (Figures 1C, D). In addition, neutrophils outnumber monocytes by 10 to 40-fold in infected subjects (Figure S2C). Altogether, the substantially higher numbers and the high inflammatory scores of neutrophils underscore the importance of regulating neutrophil-mediated systemic inflammatory responses in COVID-19.

We then investigated the main inflammatory gene signatures for each leukocyte population and found that neutrophils have a distinct inflammatory cytokine/receptor profile with enrichment of *CXCL1*, *IL1RN*, *CXCL8*, *TNFSF10*, *TNFSF13B*, *CXCL16*, and *IL8R1* (Figure 1E). Immature neutrophils express markedly higher levels of lactoferrin (*Ltf*) and *Il18*. Furthermore, we found strong transcriptional upregulation of *S100A9* and *S100A8* alarmins in neutrophils from COVID-19 patients (Figure S2D), previously reported to correlate with disease severity (16, 33). This increase persists over time for *S100A8* in the severe compared to the mild COVID-19 group (Figure S2E). Together, our data show that relative to other peripheral leukocytes, neutrophils are capable of being a major regulatory cell population that governs the severity and magnitude of the inflammatory response during COVID.

Identification of dysregulated neutrophil phenotypes in severe COVID-19 patients

We next analyzed transcriptional changes within the overall neutrophil population associated with the severity of the disease. Neutrophils from healthy, mild, and severe patient groups show distinct gene expression profiles (Figure 2A), reflecting significant transcriptomic changes during disease progression. Neutrophil transcripts which are robustly expressed in the uninfected state, including anti-proliferation and pro-apoptotic genes (*LST1, G0S2, CPPED1, BTG2, PMAIP1*) and anti-inflammatory genes (*AMPD2, SEC14L1, ZFP36*), are significantly downregulated in COVID-19 patients (Figure 2B). Neutrophils from mild patients have increased expression of genes associated with anti-viral responses, including Interferon stimulated genes (ISGs) and TRAIL (*TNFSF10*) (Figure 2B). Remarkably, expression of these genes is attenuated in neutrophils from the severe patients, whose neutrophils displayed increased activation markers including *GBP5* (activator of NLRP3 inflammasome assembly) (34), *FCER1G* (implicated in IL-1b production by neutrophils) (35), and *CD177*, previously associated with COVID-19 severity and death (36), as well as stress-related genes such as *IRAK3, FKBP5, IL1R2* (Figure 2B).

To further investigate how neutrophils may functionally differ during infection as compared to healthy controls, we performed pathway analysis of neutrophil transcriptomes. In hospitalized patients with milder COVID-19 disease, we observed broad activation of multiple pathways involved with immune responses to various viral infections, including COVID-19 related pathways (mostly antiviral genes), NOD-like receptor signaling, Toll-like receptor (TLR) signaling, and immune responses to both viral and intracellular pathogens (e.g., influenza A, Salmonella, Epstein-Barr) (Figure S3). Thus, upregulated pathways highlight a pronounced diversity of antiviral neutrophil response in hospitalized patients with milder COVID-19. Conversely, in neutrophils from patients with severe disease, we observed significant activation of NF-kB signaling, and TNF signaling pathways, as well as oxidative stress response pathways (e.g., cyclooxygenase genes, glutathione metabolism, and oxidative phosphorylation), compared to those from mild COVID-19 patients (Figure 2C). This suggests stress response phenotype in severe patients, rather than a protective-antiviral phenotype seen in the mild disease. Notably, unlike patients with mild disease, severe patients show marked induction of ribosomal genes, suggesting an increase of cellular protein production capacity beyond the observed increase in active gene transcription.

Neutrophil cell-cell interactions become progressively dysregulated in patients with severe COVID-19

To provide immunologic context for how neutrophils interact with other cell types, we conducted an analysis on the intercellular crosstalk between cytokines and receptors on immune cells. To identify how cytokine-receptor-mediated cell-cell interactions (CCI) evolve across disease severity, we counted the CCIs that represent the active intercellular communication probabilities between up-regulated cytokines and receptors on all cell types in mild versus severe COVID-19 disease. We found that during mild disease, there are overall more active CCIs among all of the different cell populations than that in severe disease (Figures 3A, B). Conversely, during severe disease, the number of unique CCIs drop out, resulting in potential degradation of cell-cell cross-regulatory mechanisms. Cell-cell interactions become concentrated and are dominated by interactions between 4 major cell types - neutrophils, monocytes, gamma-delta T cells, and hematopoietic stem cells (HSC), which accounts for more than 60% of the cell-cell interactions in severe disease (Figure 3C). As the illness

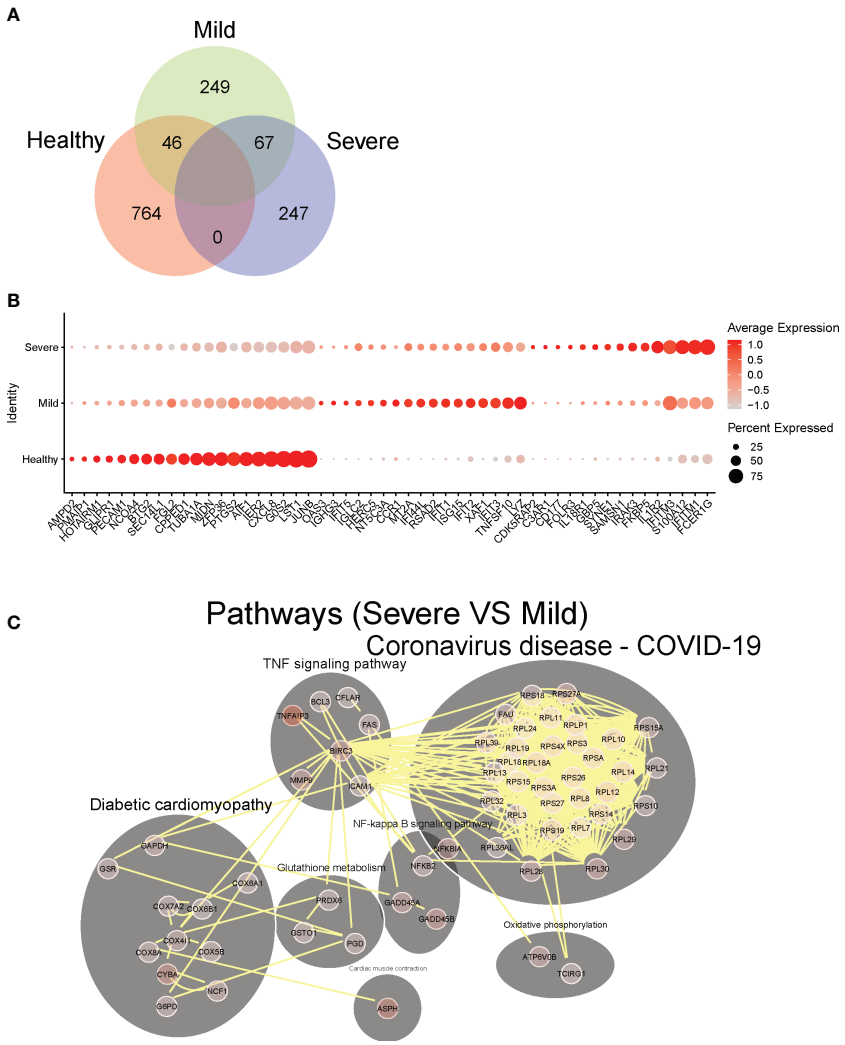

FIGURE 2
Identification of dysregulated neutrophil phenotypes in severe COVID-19 patients. **(A)** Venn plot of significantly up-regulated genes (adjusted P-value <0.05) in neutrophils from healthy controls, mild and severe COVID19 patients. **(B)** Top 10 differentially expressed upregulated genes in neutrophils from healthy controls, mild and severe COVID19 patients, respectively. **(C)** Predicted cell-cell interaction networks of significantly up-regulated pathways (adjusted P-value <0.05) in neutrophils from severe COVID19 patients compared with that from the mild group.

proceeds, we found that in mild patients who recovered from the disease, diverse cell-cell interactions remain preserved at later timepoints, while severe patients who eventually succumb have progressive loss of cell-cell interaction diversity compared to earlier timepoints (Figure 3D). These data support a framework where neutrophil cell-cell interactions become progressively dysregulated in patients with severe COVID-19. Additionally, a potential mechanism by which neutrophils contribute to severe inflammation may be reinforcement of activation pathways for specific cell populations such as monocytes and gamma-delta T cells, which have been reported to be robustly pro-inflammatory cell populations during viral infections.

COVID-19 resulted in alterations of neutrophil subset compositions and their transcription profiles across the levels of the disease severity

We next examined whether different phenotypes of neutrophil populations could be identified by scRNA-Seq. We performed cluster analysis of neutrophil scRNA data using the SNN modularity optimization-based clustering algorithm. In total, 9 distinct clusters of neutrophils could be identified based on specific patterns of gene expression. Cluster 9 represents pro-neutrophils (*DEFA3*$^+$*DEFA44*$^+$*MPO*$^+$*ELANE*$^+$

10.3389/fimmu.2022.970287

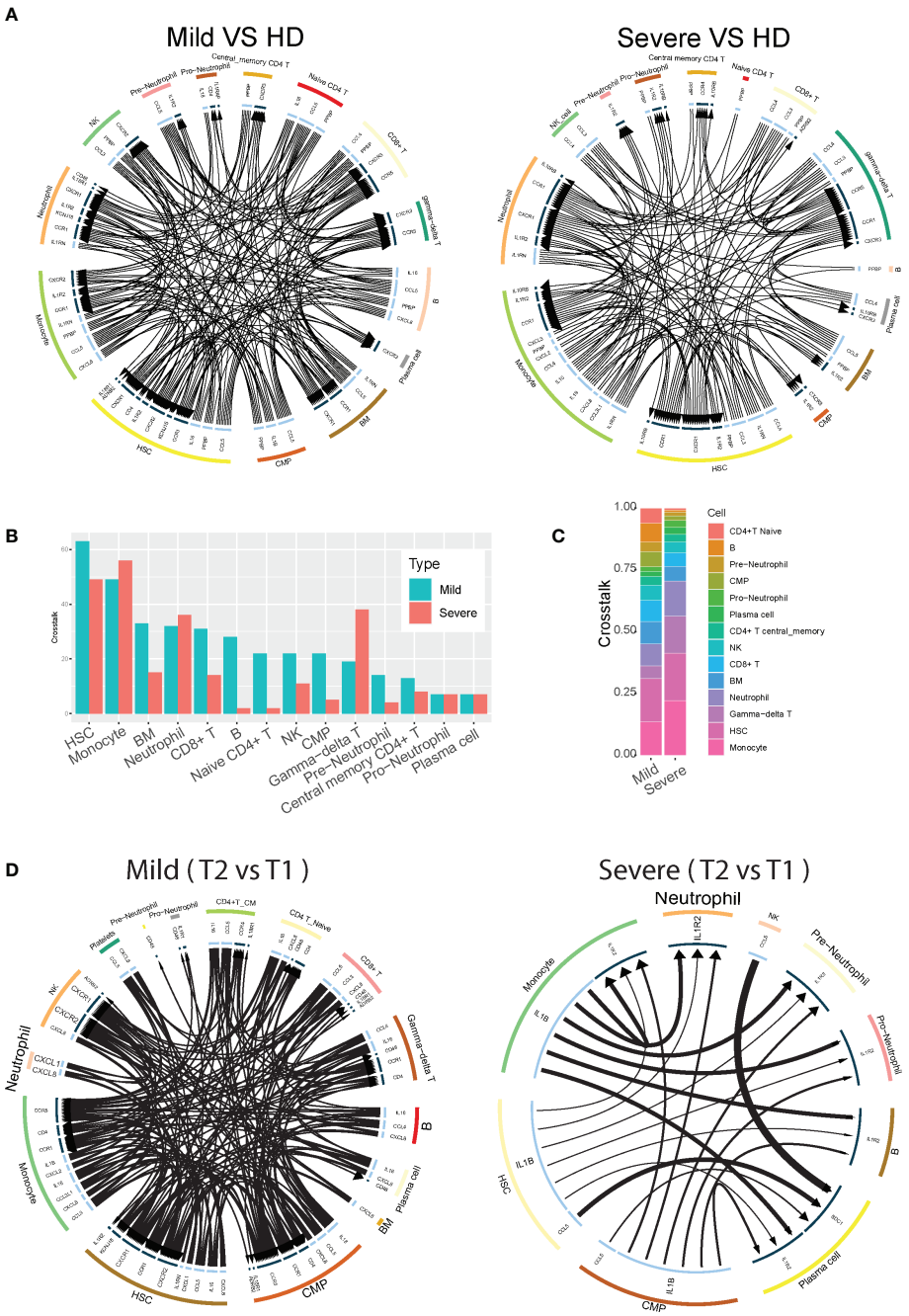

FIGURE 3
Neutrophil cell-cell interactions become progressively dysregulated in patients with severe COVID-19. **(A)** Circos plot showing the up-regulated cellular crosstalk mediated by significantly (adjusted P-value <0.05) up-regulated ligand-receptor pairs between inflammation-related cell types from mild or severe COVID19 patients compared with that from healthy controls. **(B)** Count of the up-regulated cellular crosstalk for every cell type in mild and severe COVID19 patients, respectively. **(C)** Composition of the up-regulated cellular crosstalk in mild and severe COVID19 patients, respectively. **(D)** Circos plot showing the cellular crosstalk mediated by up-regulated (2nd timepoint versus 1st timepoint, or T2 vs T1) ligand-receptor pairs between inflammation-related cell types from recovered mild (left) and deceased severe (right) COVID19 patients, respectively.

AZU$^+$; azurophilic granule content genes), cluster 7 represents pre-neutrophils (*LTG*$^+$*LCN2*$^+$*CAMP*$^+$*MMP8*$^+$; specific and gelatinase granule content genes), and the remaining 7 clusters represent mature neutrophils (all *CXCR2*$^+$) (Figures 4A, B). The two immature neutrophil clusters (clusters 7 and 9) exhibit robust gene expression of their respective granule content proteins but relative suppression of all of the other genes (Figure 4C). Conversely, the mature neutrophil clusters had suppression of granule content genes, but distinct patterns of gene activation that were relatively low in the immature populations (Figure 4C). Clusters 2 and 8 displayed upregulation of MMP9, several S100A genes including S100A12, and *MME* (i.e., Neprilysin), which have been implicated in the pathogenesis of COVID-19 (37, 38). Clusters 3, 5, and 6 had high levels of expression of regulatory genes for transcription and apoptosis (Figure 4C). Notably, cluster 4 was significantly enriched in interferon (IFN) stimulated genes (ISGs, e.g., *ISG15*, *IFIT* genes, *MX1*, *GBP*, *GBP5*, *HERC5*, and *RSAD2*). Thus, contrary to the assumption that they are a homogenous and transcriptionally quiescent cell population, mature neutrophils display transcriptional diversity with the ability to activate gene expression programs, ranging from immuno-regulatory types to a preferentially antiviral subtype with induction of IFN-stimulated genes.

Subsequent pathway analysis provided insights about possible biological functions of each neutrophil subset (Figure 4D and Figure S4). Pathway analysis using KEGG and GO of cluster 4 revealed significant activation of viral response pathways as well as NOD-like receptor signaling pathway, supporting its distinct role in anti-viral responses. Other clusters also show specific pathway enrichment; for example, cluster 1 exhibited pathways involved in ferroptosis, cluster 3 and 5 in NF-kappa B signaling, and cluster 7 with activated Ribosome and Coronavirus disease-COVID-19, which is

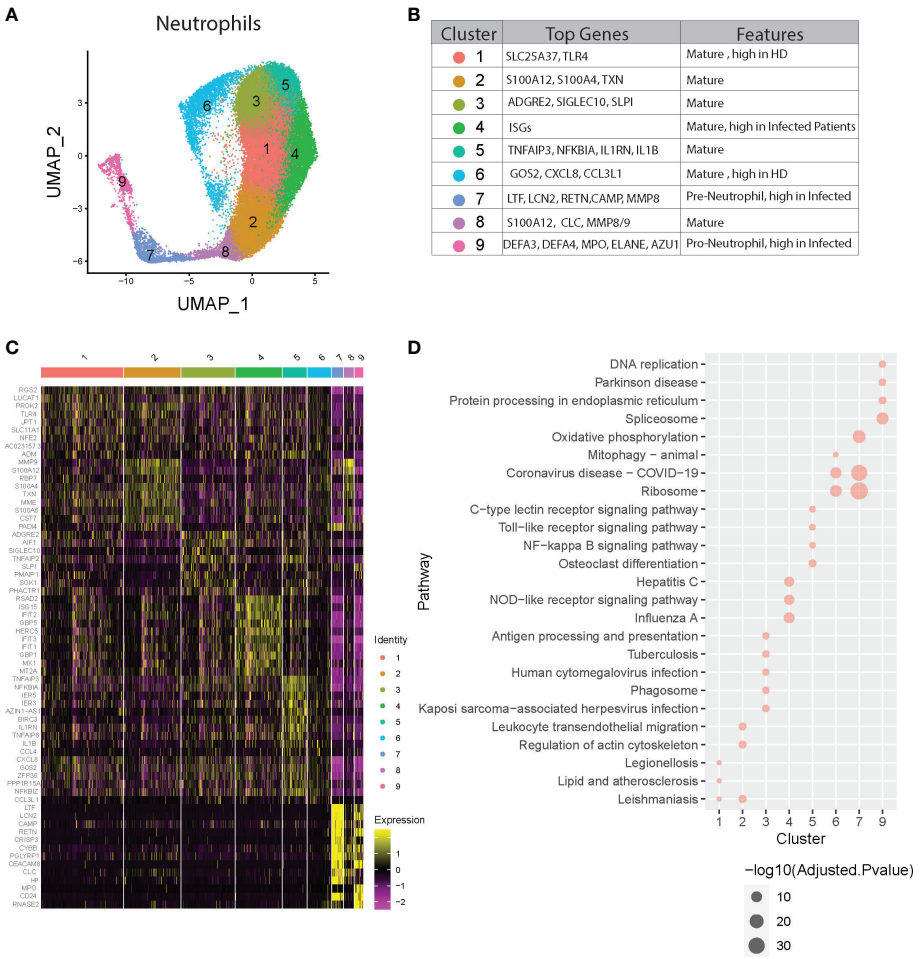

FIGURE 4
Neutrophil heterogeneity in COVID-19 patients. **(A)** UMAP plot of neutrophil clusters. **(B)** Nomenclature and marker genes for each neutrophil cluster. **(C)** Top5 up-regulated genes in every neutrophil cluster. **(D)** Top3 KEGG pathways significantly enriched in up-regulated genes in every neutrophil cluster.

consistent with the concept of "pre-neutrophils" being robustly activated during acute infection with SARS-CoV-2.

Next, we determined whether all of these clusters exist at baseline and whether specific neutrophil subsets were augmented depending on the presence or severity of infection. We found higher proportions of clusters 1 and 6 in healthy compared to infected subjects, while clusters 4, 7, and 9 were increased in COVID-19 patients, especially in the severe group (Figure 5A, Figures S5A, B). Since clusters 7 and 9 are immature neutrophils, their increase provides evidence of emergency myelopoiesis in severe COVID-19 patients, also supported by previous reports (15, 33). Overall, cluster 4 was significantly associated with disease severity, while cluster 6 was negatively associated with the severity of the disease (Figure 5B). Within each cluster, we also observed the neutrophils up-or down-regulating gene groups and pathways based upon disease state (Figure 5C, Figures S6, S7). For example, compared to healthy controls, cluster 7 neutrophils (immature neutrophils) from infected subjects upregulated genes involved in multiple pathways associated with host defense, including neutrophil extracellular trap formation, cytokine signaling, and NF-kB signaling (Figure 5C, Figure S6). Cluster 4 neutrophils, which are enriched with anti-viral responses, displayed activation of the ribosome and COVID-19 pathways in patients with mild disease, as compared to healthy controls, with further activation in subjects with severe disease (Figure 5D, Figure S7). Some pathways involved in anti-viral responses are down-regulated in cluster 4 from severe patients compared with mild patients, consistent with what we discovered in Figure 2B. Oxidative phosphorylation pathways were activated in multiple neutrophil clusters in subjects with severe infection compared to those with mild disease (Figure 5D). Cluster 6 displayed striking downregulation of multiple pathways during severe disease, including those related to IL-17 signaling, NF-kB, and cAMP signaling (Figure 5D). Strikingly, neutrophils displayed progressively decreased activation of hepatitis, influenza, and other viral pathways with increasing COVID-19 disease severity (Figures 5C, D). Together, neutrophils heterogeneity and their changes in proportion or transcription are strongly related to the severity of the COVID-19 disease.

Discussion

Since the start of the SARS-CoV-2 pandemic, a variety of "omic"-based analyses have been utilized to understand the pathogenesis of severe COVID-19 associated infection (7, 31, 39). Notably underrepresented in these studies is a comprehensive analysis of neutrophils, which despite being abundant and widely considered as integral cellular contributors to immune dysregulation, have been largely overlooked for a variety of reasons, including the technical difficulty of isolating neutrophils and preserving them for downstream studies such as single-cell sequencing analyses. Only recently have two groups put forth papers that have explicitly used neutrophil-preserving methods in studying human samples - one using scRNA sequencing-based phenotyping of healthy human subjects, and another examining neutrophil phenotypes from patients with acute respiratory distress syndrome (ARDS) from severe COVID-19 disease or bacterial pneumonia (40, 41). Our work builds upon their findings in that we examined how neutrophil phenotypes differ in relative abundance and pathway activation in patients with mild versus severe COVID-19 disease. We also determined whether all phenotypes exist at baseline, or if new subpopulations of neutrophils emerge during infections, based upon the severity of the infectious insult. Our results suggest that discrete clusters of mature neutrophils exist even under basal uninfected conditions, as reflected by distinct transcriptional profiles and activated pathways. We furthermore observed that the relative proportions of each cluster change during infection and with increasing severity.

Additionally, most scRNA seq studies of patients with COVID have utilized samples collected from subjects that span a large age range (children to elderly) and the full spectrum of co-morbid conditions, which may introduce bias and confounding factors when identifying what mechanisms underlie severe SARS-CoV-2 infections, particularly given the small sample sizes. Our study focused exclusively on human adult patients hospitalized with respiratory manifestations of COVID-19 disease, taking care to exclude subjects with chronic immunosuppression, active malignancy, autoimmune conditions, poorly controlled diabetes, chronic infections, and other advanced co-morbidities that could influence immune responses at baseline. Due to our cohort being mainly Veterans, all of our subjects were males and mostly White. Although the total number of subjects was small, our study was actually one of the largest studies to examine neutrophil responses by scRNA seq. Thus, by controlling for the variability in neutrophil responses that might be introduced by severe chronic comorbidities, sex, age, or race, our results can be considered to reflect the intrinsic heterogeneity of neutrophil responses during health and SARS-CoV-2 infections.

Upon SARS-CoV-2 infection, altered neutrophil abundance and functionality have been linked with the pathophysiology of severe COVID-19 disease (5, 7, 42, 43). We show that neutrophils are a potentially important cellular source of cytokines and can be major contributors to the inflammatory response upon SARS-CoV-2 infection. Importantly, neutrophils display dynamic responses, with evidence of increased oxidative stress and ribosomal pathway activation and suppression of multiple viral pathways (e.g., influenza and measles response pathways) during severe infections. Our results further contribute to our understanding of neutrophil biology, revealing vast heterogeneity and breadth of inflammatory responses in neutrophil subsets in COVID-19 patients (12), in

FIGURE 5
COVID-19 resulted in alterations of neutrophil subset compositions and their transcription profiles. **(A)** Neutrophil clusters that differed in proportions (% of neutrophils) between healthy controls and hospitalized patients with mild or severe COVID19. **(B)** Neutrophil clusters that significantly (adjusted P-value <0.05) associated with the severity of COVID19. Spearman's' correlations were used to determine the association between cluster proportion and the severity of COVID19 (healthy 1, mild 2, severe 3, decreased 4). Red: positive correlation; Blue: negative correlation. Depth of color increase with the absolute value of the association. Only significant associations (adjusted P-value <0.05) are shown in this graph. **(C)** GSEA analysis of significantly different KEGG pathway gene sets in selected neutrophil clusters from COVID19 patients compared with that from healthy controls. **(D)** GSEA analysis of significantly different KEGG gene sets in selected neutrophil clusters from severe COVID19 patients compared with that from mild COVID19 patients. *p < 0.05, **p < 0.01. NES, Normalized enrichment score.

contrast to the prevailing view that neutrophils are a homogeneous antimicrobial cell population.

Our computational clustering revealed extensive heterogeneity in neutrophils with the identification of seven transcriptionally distinctive mature and two immature neutrophil clusters. In particular, the identification of distinct mature neutrophil clusters is an important finding to our understanding of how neutrophils contribute to the pathogenesis of severe infections, as it underscores the importance of recognizing a broader spectrum of neutrophil functional phenotypes. We found those neutrophil subsets display the ability to activate differential gene expression programs, ranging from inhibitory/regulatory subsets to a preferentially antiviral subset

with activated IFN-regulated gene expression profile. The proportion of each phenotype correlated with severe disease course. For example, cluster 4 neutrophils showed significantly activated viral response pathways, suggesting a distinct subset of neutrophils in anti-viral responses. However, they also display progressively decreased activation of the viral pathways and increased stress response-related pathways with worsening COVID-19 disease severity. Our findings indicate that neutrophils are capable of mounting effective antiviral defenses but with disease progression, adopt a form of immune dysregulation characterized by excess cellular stress, thereby contributing to the immunopathology of severe SARS-CoV-2 infections.

The progression of ARDS during severe COVID-19 disease, as well as other severe respiratory viral infections, continues despite patients already having cleared the viral infection in the majority of cases, especially in immunocompetent hosts (44). It is during this period when the host is transitioning either to recovery or persistent inflammation that the outcome of infection is determined. The immune mechanisms governing resolution versus persistent inflammation are complex, with evidence of aberrant intercellular regulatory mechanisms that perpetuate inflammation (45). Our work builds upon this concept by examining how systemic neutrophil responses differ in COVID-19 patients, all of whom are sick enough to be hospitalized, but whose respiratory manifestations are milder versus severe. In patients with severe COVID-19, we find evidence of neutrophils no longer acting in concert with other cell types, as reflected by their loss of intensity and diversity of cell-cell interaction with other immune cell populations. To understand how neutrophils might impact systemic inflammatory responses, we found that neutrophils have higher inflammatory scores compared to monocytes, suggesting that they could be a key source of a diverse set of cytokines that are highly elevated in COVID-19 patients with severe disease progression. These findings complement prior reported findings that megakaryocytes and specific monocyte subsets were the primary producers of cytokines (26). Our results indicate that future investigations should identify ways to harness the regulatory capacities of neutrophils in a therapeutic manner, including how to promote antiviral functions early during infection, and perhaps more importantly, how to shift the balance towards a more restorative neutrophil profile as the human host attempts to recover after the infection has been cleared.

Altogether, our report presents details that help us better understand the vast heterogeneity and breadth of inflammatory responses in neutrophil subsets in COVID-19 patients.

Data availability statement

The datasets presented in this study can be found in online GEO repositories (access number GSE216020).

Ethics statement

The studies involving human participants were reviewed and approved by University of Michigan IRB. The patients/participants provided their written informed consent to participate in this study.

Author contributions

The overall project was conceived by MO and JD. JX and BH contributed equally to this work. Order for co-first author was determined by JX's primary role in manuscript preparation and formatting. Experiments were performed and data were analyzed by JX, BH, LG, and JD. Experimental support and methods: BH, JX, KC, DV, and JD. Substantive writing and revision: JX, BH, LG, MO, and JD. Project supervision: LG, MO, and JD. All authors contributed to the article and approved the submitted version.

Funding

LG is supported by NIH/NIGMS R01 LM012373, R01 LM012907 awarded by NLM, and R01 HD084633 awarded by NICHD. MO is supported by Veterans Affairs ORD RCS 1IK6 BX003615-01 and Merit BX000656Awards. JD is supported by NIH/NIA R01 AG028082, Veterans Affairs ORD I01BX004565, and I01BX005447.

Conflict of interest

The authors declare that the research was conducted in the absence of any commercial or financial relationships that could be construed as a potential conflict of interest.

Publisher's note

Supplementary material

The Supplementary Material for this article can be found online at: https://www.frontiersin.org/articles/10.3389/fimmu.2022.970287/full#supplementary-material

References

1. Xu Z, Shi L, Wang Y, Zhang J, Huang L, Zhang C, et al. Pathological findings of COVID-19 associated with acute respiratory distress syndrome. *Lancet Respir Med* (2020) 8:420–2. doi: 10.1016/S2213-2600(20)30076-X

2. Johansson C, Kirsebom FC. Neutrophils in respiratory viral infections. *Mucosal Immunol* (2021) 1-13:815-27. doi: 10.1038/s41385-021-00397-4

3. Galani IE, Andreakos E. Neutrophils in viral infections: current concepts and caveats. *J Leukocyte Biol* (2015) 98:557–64. doi: 10.1189/jlb.4VMR1114-555R

4. Ma Y, Zhang Y, Zhu L. Role of neutrophils in acute viral infection. *Immunity Inflamm Dis* (2021) 9:1186–96. doi: 10.1002/iid3.500

5. Giamarellos-Bourboulis EJ, Netea MG, Rovina N, Akinosoglou K, Antoniadou A, Antonakos N, et al. Complex immune dysregulation in COVID-19 patients with severe respiratory failure. *Cell Host Microbe* (2020) 27:992–1000. e1003. doi: 10.1016/j.chom.2020.04.009

6. Laforge M, Elbim C, Frère C, Hémadi M, Massaad C, Nuss P, et al. Tissue damage from neutrophil-induced oxidative stress in COVID-19. *Nat Rev Immunol* (2020) 20:515–6. doi: 10.1038/s41577-020-0407-1

7. Liao M, Liu Y, Yuan J, Wen Y, Xu G, Zhao J, et al. Single-cell landscape of bronchoalveolar immune cells in patients with COVID-19. *Nat Med* (2020) 26:842–4. doi: 10.1038/s41591-020-0901-9

8. Aschenbrenner AC, Mouktaroudi M, Kraemer B, Oestreich M, Antonakos N, Nuesch-Germano M, et al. Disease severity-specific neutrophil signatures in blood transcriptomes stratify COVID-19 patients. *Genome Med* (2021) 13:1–25. doi: 10.1186/s13073-020-00823-5

9. Meizlish ML, Pine AB, Bishai JD, Goshua G, Nadelmann ER, Simonov M, et al. A neutrophil activation signature predicts critical illness and mortality in COVID-19. *Blood Adv* (2021) 5:1164–77. doi: 10.1182/bloodadvances.2020003568

10. Reusch N, De Domenico E, Bonaguro L, Schulte-Schrepping J, Baßler K, Schultze JL, et al. Neutrophils in COVID-19. *Front Immunol* (2021) 12. doi: 10.3389/fimmu.2021.652470

11. Ng LG, Ostuni R, Hidalgo A. Heterogeneity of neutrophils. *Nat Rev Immunol* (2019) 19:255–65. doi: 10.1038/s41577-019-0141-8

12. Xie X, Shi Q, Wu P, Zhang X, Kambara H, Su J, et al. Single-cell transcriptome profiling reveals neutrophil heterogeneity in homeostasis and infection. *Nat Immunol* (2020) 21:1119–33. doi: 10.1038/s41590-020-0736-z

13. Cao Y, Su B, Guo X, Sun W, Deng Y, Bao L, et al. Potent neutralizing antibodies against SARS-CoV-2 identified by high-throughput single-cell sequencing of convalescent patients' b cells. *Cell* (2020) 182:73–84. e16. doi: 10.1016/j.cell.2020.05.025

14. Lee JS, Park S, Jeong HW, Ahn JY, Choi SJ, Lee H, et al. Immunophenotyping of COVID-19 and influenza highlights the role of type I interferons in development of severe COVID-19. *Sci Immunol* (2020) 5:eabd1554. doi: 10.1126/sciimmunol.abd1554

15. Schulte-Schrepping J, Reusch N, Paclik D, Baßler K, Schlickeiser S, Zhang B, et al. Severe COVID-19 is marked by a dysregulated myeloid cell compartment. *Cell* (2020) 182:1419–1440. e1423. doi: 10.1016/j.cell.2020.08.001

16. Silvin A, Chapuis N, Dunsmore G, Goubet A-G, Dubuisson A, Derosa L, et al. Elevated calprotectin and abnormal myeloid cell subsets discriminate severe from mild COVID-19. *Cell* (2020) 182:1401–1418. e1418. doi: 10.1016/j.cell.2020.08.002

17. Wilk AJ, Rustagi A, Zhao NQ, Roque J, Martínez-Colón GJ, Mckechnie JL, et al. A single-cell atlas of the peripheral immune response in patients with severe COVID-19. *Nat Med* (2020) 26:1070–6. doi: 10.1038/s41591-020-0944-y

18. Zhang JY, Wang XM, Xing X, Xu Z, Zhang C, Song JW, et al. Single-cell landscape of immunological responses in patients with COVID-19. *Nat Immunol* (2020) 21:1107–18. doi: 10.1038/s41590-020-0762-x

19. Carissimo G, Xu W, Kwok I, Abdad MY, Chan Y-H, Fong S-W, et al. Whole blood immunophenotyping uncovers immature neutrophil-to-VD2 T-cell ratio as an early marker for severe COVID-19. *Nat Commun* (2020) 11:1–12. doi: 10.1038/s41467-020-19080-6

20. Morrissey SM, Geller AE, Hu X, Tieri D, Ding C, Klaes CK, et al. A specific low-density neutrophil population correlates with hypercoagulation and disease severity in hospitalized COVID-19 patients. *JCI Insight* (2021) 6:e148435. doi: 10.1172/jci.insight.148435

21. Mcginnis CS, Murrow LM, Gartner ZJ. DoubletFinder: Doublet detection in single-cell RNA sequencing data using artificial nearest neighbors. *Cell Syst* (2019) 8:329–337 e324. doi: 10.1016/j.cels.2019.03.003

22. Stuart T, Butler A, Hoffman P, Hafemeister C, Papalexi E, Mauck WM3rd, et al. Comprehensive integration of single-cell data. *Cell* (2019) 177:1888–1902 e1821. doi: 10.1016/j.cell.2019.05.031

23. Aran D, Looney AP, Liu L, Wu E, Fong V, Hsu A, et al. Reference-based analysis of lung single-cell sequencing reveals a transitional profibrotic macrophage. *Nat Immunol* (2019) 20:163–72. doi: 10.1038/s41590-018-0276-y

24. Mabbott NA, Baillie JK, Brown H, Freeman TC, Hume DA. An expression atlas of human primary cells: Inference of gene function from coexpression networks. *BMC Genomics* (2013) 14:632. doi: 10.1186/1471-2164-14-632

25. Chen Z, John Wherry E. T Cell responses in patients with COVID-19. *Nat Rev Immunol* (2020) 20:529–36. doi: 10.1038/s41577-020-0402-6

26. Ren X, Wen W, Fan X, Hou W, Su B, Cai P, et al. COVID-19 immune features revealed by a large-scale single-cell transcriptome atlas. *Cell* (2021) 184:1895–1913. e1819. doi: 10.1016/j.cell.2021.01.053

27. Wang Y, Wang R, Zhang S, Song S, Jiang C, Han G, et al. iTALK: An r package to characterize and illustrate intercellular communication. *bioRxiv* (2019). doi: 10.1101/507871

28. Yu G, Wang LG, Han Y, He QY. clusterProfiler: an r package for comparing biological themes among gene clusters. *OMICS* (2012) 16:284–7. doi: 10.1089/omi.2011.0118

29. Shannon P, Markiel A, Ozier O, Baliga NS, Wang JT, Ramage D, et al. Cytoscape: a software environment for integrated models of biomolecular interaction networks. *Genome Res* (2003) 13:2498–504. doi: 10.1101/gr.1239303

30. Subrahmanyam YV, Yamaga S, Prashar Y, Lee HH, Hoe NP, Kluger Y, et al. RNA Expression patterns change dramatically in human neutrophils exposed to bacteria. *Blood J Am Soc Hematol* (2001) 97:2457–68. doi: 10.1182/blood.V97.8.2457

31. Chua RL, Lukassen S, Trump S, Hennig BP, Wendisch D, Pott F, et al. COVID-19 severity correlates with airway epithelium–immune cell interactions identified by single-cell analysis. *Nat Biotechnol* (2020) 38:970–9. doi: 10.1038/s41587-020-0602-4

32. Liberzon A, Birger C, Thorvaldsdóttir H, Ghandi M, Mesirov JP, Tamayo P. The molecular signatures database hallmark gene set collection. *Cell Syst* (2015) 1:417–25. doi: 10.1016/j.cels.2015.12.004

33. Guo Q, Zhao Y, Li J, Liu J, Yang X, Guo X, et al. Induction of alarmin S100A8/A9 mediates activation of aberrant neutrophils in the pathogenesis of COVID-19. *Cell Host Microbe* (2021) 29:222–235. e224. doi: 10.1016/j.chom.2020.12.016

34. Shenoy AR, Wellington DA, Kumar P, Kassa H, Booth CJ, Cresswell P, et al. GBP5 promotes NLRP3 inflammasome assembly and immunity in mammals. *Science* (2012) 336:481–5. doi: 10.1126/science.1217141

35. Sadik CD, Kim ND, Iwakura Y, Luster AD. Neutrophils orchestrate their own recruitment in murine arthritis through C5aR and FcgammaR signaling. *Proc Natl Acad Sci U.S.A.* (2012) 109:E3177–3185. doi: 10.1073/pnas.1213797109

36. Lévy Y, Wiedemann A, Hejblum BP, Durand M, Lefebvre C, Surénaud M, et al. CD177, a specific marker of neutrophil activation, is associated with coronavirus disease 2019 severity and death. *Iscience* (2021) 24:102711. doi: 10.1016/j.isci.2021.102711

37. Bellis A, Mauro C, Barbato E, Trimarco B, Morisco C. The rationale for angiotensin receptor neprilysin inhibitors in a multi-targeted therapeutic approach to COVID-19. *Int J Mol Sci* (2020) 21:8612. doi: 10.3390/ijms21228612

38. Rex D, Arun Kumar ST, Modi PK, Keshava Prasad TS. Broadening COVID-19 interventions to drug innovation: Neprilysin pathway as a friend, foe, or promising molecular target? *OMICS* (2021) 25:408–16. doi: 10.1089/omi.2021.0080

39. Wauters E, Van Mol P, Garg AD, Jansen S, Van Herck Y, Vanderbeke L, et al. Discriminating mild from critical COVID-19 by innate and adaptive immune single-cell profiling of bronchoalveolar lavages. *Cell Res* (2021) 31:272–90. doi: 10.1038/s41422-020-00455-9

40. Grieshaber-Bouyer R, Radtke FA, Cunin P, Stifano G, Levescot A, Vijaykumar B, et al. The neutrotime transcriptional signature defines a single continuum of neutrophils across biological compartments. *Nat Commun* (2021) 12:1–21. doi: 10.1038/s41467-021-22973-9

41. Sinha S, Rosin NL, Arora R, Labit E, Jaffer A, Cao L, et al. Dexamethasone modulates immature neutrophils and interferon programming in severe COVID-19. *Nat Med* (2022) 28:201–11. doi: 10.1038/s41591-021-01576-3

42. Guan W-J, Ni Z-Y, Hu Y, Liang W-H, Ou C-Q, He J-X, et al. Clinical characteristics of coronavirus disease 2019 in China. *New Engl J Med* (2020) 382:1708–20. doi: 10.1056/NEJMoa2002032

43. Qin C, Zhou L, Hu Z, Zhang S, Yang S, Tao Y, et al. Dysregulation of immune response in patients with coronavirus 2019 (COVID-19) in wuhan, China. *Clin Infect Dis* (2020) 71:762–8. doi: 10.1093/cid/ciaa248

44. Simons LM, Lorenzo-Redondo R, Gibson M, Kinch SL, Vandervaart JP, Reiser NL, et al. Assessment of virological contributions to COVID-19 outcomes in a longitudinal cohort of hospitalized adults. *Open Forum Infect Dis* (2022) 9:ofac027. doi: 10.1093/ofid/ofac027

45. Grant RA, Morales-Nebreda L, Markov NS, Swaminathan S, Querrey M, Guzman ER, et al. Circuits between infected macrophages and T cells in SARS-CoV-2 pneumonia. *Nature* (2021) 590:635–41. doi: 10.1038/s41586-020-03148-w

frontiers | Frontiers in Immunology

TYPE Review
PUBLISHED 17 November 2022
DOI 10.3389/fimmu.2022.1054753

OPEN ACCESS

EDITED BY
Rongqian Wu,
Xi'an Jiaotong University, China

REVIEWED BY
Hao Li,
Shanghai First People's Hospital, China
Monowar Aziz,
Feinstein Institute for Medical Research, United States

*CORRESPONDENCE
Zhongjun Wu
wzjtcy@126.com

SPECIALTY SECTION
This article was submitted to Alloimmunity and Transplantation, a section of the journal Frontiers in Immunology

RECEIVED 27 September 2022
ACCEPTED 26 October 2022
PUBLISHED 17 November 2022

CITATION
Liu Y, Yan P, Bin Y, Qin X and Wu Z (2022) Neutrophil extracellular traps and complications of liver transplantation.
Front. Immunol. 13:1054753.
doi: 10.3389/fimmu.2022.1054753

Neutrophil extracellular traps and complications of liver transplantation

Yanyao Liu[1], Ping Yan[1], Yue Bin[1], Xiaoyan Qin[2,3] and Zhongjun Wu[1*]

[1]Department of Hepatobiliary Surgery, The First Affiliated Hospital of Chongqing Medical University, Chongqing, China, [2]Department of General Surgery and Trauma Surgery, Children's Hospital of Chongqing Medical University, Ministry of Education Key Laboratory of Child Development and Disorders, Chongqing, China, [3]National Clinical Research Center for Child Health and Disorders, China International Science and Technology Cooperation Base of Child Development and Critical Disorders, Chongqing Key Laboratory of Pediatrics, Chongqing, China

Many end-stage liver disease etiologies are attributed to robust inflammatory cell recruitment. Neutrophils play an important role in inflammatory infiltration and neutrophil phagocytosis, oxidative burst, and degranulation. It has also been suggested that neutrophils may release neutrophil extracellular traps (NETs) to kill pathogens. It has been proven that neutrophil infiltration within the liver contributes to an inflammatory microenvironment and immune cell activation. Growing evidence implies that NETs are involved in the progression of numerous complications of liver transplantation, including ischemia-reperfusion injury, acute rejection, thrombosis, and hepatocellular carcinoma recurrence. NETs are discussed in this comprehensive review, focusing on their effects on liver transplantation complications. Furthermore, we discuss NETs as potential targets for liver transplantation therapy.

KEYWORDS

neutrophil extracellular traps, liver transplantation, ischemia-reperfusion injury, acute rejection, thrombosis, hepatocellular carcinoma recurrence, therapeutic targets

Introduction

Neutrophils play a major role in the innate immune response (1), and have a wide range of immune functions, including phagocytosis, reactive oxygen species (ROS) production, lytic enzyme activation, and neutrophil extracellular traps (NETs) production through a process called NETosis (2, 3). NETs comprise chromatin, DNA fibers, and granule proteins. Additionally, NETs are important in treating non-infectious diseases, such as cancer, diabetes, thrombosis, and autoimmune illnesses (4–6). Recent evidence suggests that NETs may contribute to pathological changes after liver transplantation, including liver ischemia-reperfusion injury (IRI), acute rejection, and recurrence of hepatocellular carcinoma (7–9). However, there is little knowledge of the

relationship between NET formation and complications of liver transplantation. Herein, we summarize the latest findings that associate NETs with liver IRI, acute rejection, thrombosis, and hepatocellular carcinoma recurrence. We also discuss the potential of NET as a potential therapeutic target in patients following liver transplantation. NET targeting and degradation could be novel promising therapeutic interventions in end-stage liver disease and complications of liver transplantation.

NET formation

A novel immune defense mechanism known as NETs was discovered in 2004. However, it is difficult to clearly define the specific function of NETs in immune defense (10, 11). With regards to neutrophil pathogenic stimulation, the activation of the signaling pathways, and membrane integrity, the formation of NETs can be classified into three types, namely, lytic, viable, and mitochondrial NET formation (12). Lytic NETs are formed within ten minutes from neutrophil stimulation with phorbol myristate acetate (PMA), lipopolysaccharide (LPS), or IL-8 (13). Several pathways lead to the formation of lytic NETs, including ROS generation in neutrophils that lead to the activation of the enzyme, peptidylarginine deiminase 4 (PAD4). Subsequently, PAD4 converts arginine residues on histones into citrulline, which results in chromatin decondensation (14, 15). In addition, neutrophil elastase (NE) and myeloperoxidase (MPO) are activated and translocated to the nucleus. NE and MPO are also synergistically involved in chromatin decondensation. Likewise, NE can also degrade actin filaments, and block the phagocytosis pathway (16). Single-stranded DNAs and histones are released in the cytoplasm, and form early NETs with antibacterial proteins (e.g., MPO, citH3, NE, and cathepsin G) (17). NET formation requires NADPH oxidase activity and downstream ROS formation (18). Lytic NET formation can be induced by bacteria, fungi and especially chemical stimuli, such as LPS, TNF-α and IL-8 (19). Several *in vitro* studies showed neutrophils formed NET-like structures in response to PMA, LPS, TNF-α and IL-8. In these cells, pretreatment with Cl-amidine or use of a PAD4-deficinet line reduced citrullination of histones and NET formation (20, 21).

In viable NET formation, PAD4 is activated by TLR-2 and TLR-4 receptors on neutrophils under different stimuli. For example, bacterial LPS results in the entry of PAD4 into the nucleus to citrullinate the histones, H3 and H4, and unwind DNA strands (22, 23). In contrast to the formation of lytic NET, the PAD4 gene is activated without ROS and does not rupture the cell or nuclear membrane. During the process, the neutrophils are not destroyed, and unwound DNA strands enter the cytoplasm to form early NETs with bacteriostatic proteins. As fascicles, they are exocytosed and released from the cell. Despite the absence of nuclear DNA, neutrophils are still capable of phagocytosing bacteria and killing them (24, 25).

The third mechanism describes the formation of NETs with mitochondrial DNA. A previous study demonstrated that eosinophils release mitochondrial DNA after the initial priming with IL-5 or INF-γ, and subsequent LPS stimulation (26). DNA release is ROS-dependent and independent of eosinophil apoptosis. In a subsequent study, mitochondrial NETs were reported to be damaged after the neutrophils were primed with GM-CSF for 20 minutes and then stimulated with LPS for another 15 minutes, which resulted in the release of DNA into the extracellular matrix (27). Neutrophil granular proteins, such as MPO and NE, were also detected in the extracellular matrix with the DNA, but nuclear proteins were not found. It was later reported that NETs contained mitochondrial DNA rather than nuclear DNA sequences (28). Unlike viable NETs, the formation of mitochondrial NETs is ROS-dependent, because the effects of ROS inhibitors and neutrophil deficiency inhibit the release of NETs (29). Recent studies further elucidated the importance of the post-translational modifications of histones, which has a biphasic impact on NETs formation (30). Another study found that the pre-forming protein gasdermin D (GSDMD) plays a key role in neutrophil membrane lysis, nuclear membrane development, and NETs formation (31). However, still unclear about the involvement of PAD4 activation and the presence of mitochondrial DNA in the formation and structure of NETs. To conclude, the mechanism behind the generation and release of NETs requires further investigation (Figure 1).

NETs function

Researchers have demonstrated that NETs have a wide range of efficacy against bacteria, viruses, fungi, and parasites. Several components in NETs, including histones, contain bactericidal and antimicrobial properties (32). NE, a granular protein, can also degrade certain bacterial virulence factors (33). According to prior studies, a fibrous NET structure enhances its bactericidal activity, by either concentrating the antimicrobial molecules into a small area or even serving as a physical barrier against microorganisms (34). Despite NETs' ability to fight infections, it was soon realized that they were also detrimental to gastrointestinal, liver, and lung inflammations (35, 36). Activated neutrophils co-cultured with enterocyte-like Caco-2 cells revealed that NETs might damage epithelial cells by directly binding to their proteases (37). The researchers also proposed that NETs could facilitate the attachment of enteropathogenic E. coli to the mucosa by causeing damage to the intestinal mucosal barrier (38). Inflammation-associated lung damage and fibrosis are linked to NETs. A recent study revealed postmortem that the four patients who died of COVID-19, each had NETs in their lungs. Airway compartments and neutrophil-rich inflammatory areas of the interstitium contained NETs, while the arteriolar microthrombi contained NET-prone primed neutrophils (39).

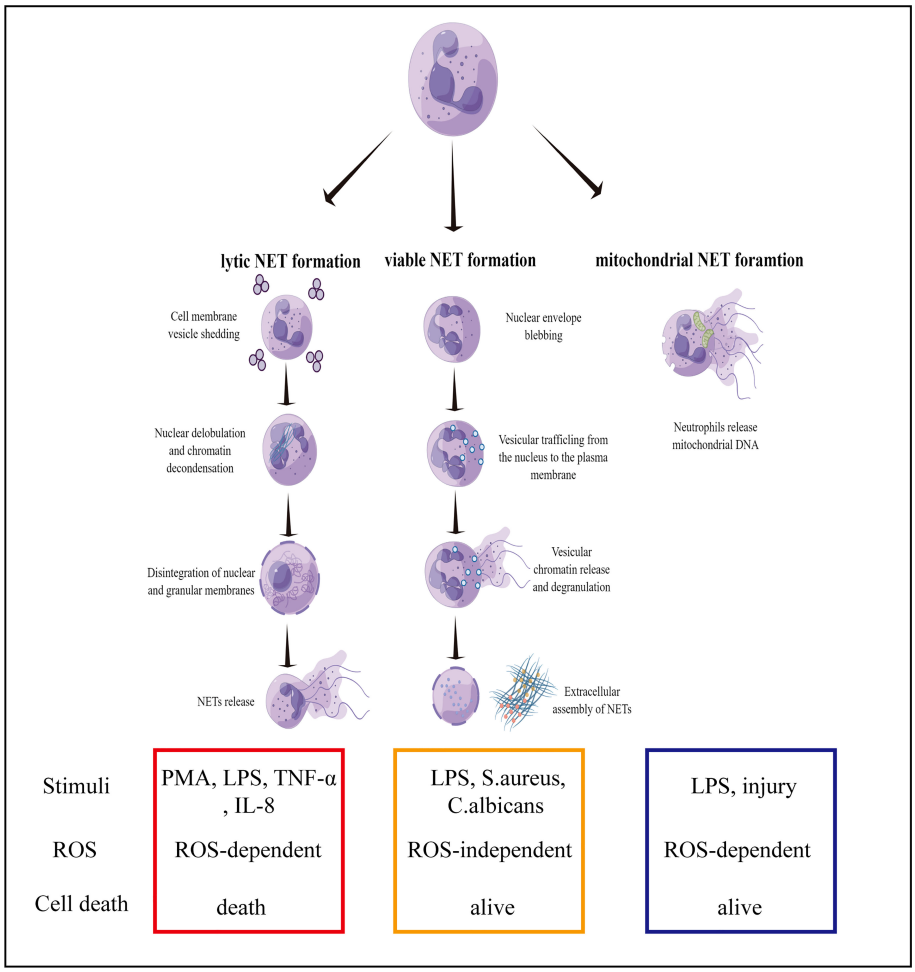

FIGURE 1
Mechanisms of NET formation. Three mechanisms of NET formation have been described: lytic NET formation, viable NET formation, and mitochondrial NET formation.

Murao A, et al. reported that the extracellular cold inducible RNA-binding protein (eCIRP)/TREM-1 interaction and Rho activation are expected to support the development of novel therapeutic molecules able to mitigate inflammation and sepsis by comtrolling NET formation (40).

NETs are considered to be double-edged swords in innate immunity. Because NETs play both an antibacterial and anti-infective role in the early stages of pathogenic microorganism invasion. However, excessive deposition and clearance disorder can lead to inflammation and immune damage to target organs (4, 16, 18, 41). Surgical stress, including liver resection and liver resection and liver transplantation that lead to NET formation. Yazdani et al. found that NET formation was decreased in IL-33 KO mice. IL-33 deficiency protected livers from I/R injury, whereas rIL-33 administration during I/R exacerbated hepatotoxicity and systemic inflammation. *In vitro*, IL-33 mainly released from liver sinusoidal endothelial cells, causes excessive sterile inflammation after hepatic I/R by inducing NET formation (42).

Thrombosis is the formation of a blood clot from the actions of platelets and coagulation factors in the events of vascular damage. A thrombus is formed when coagulation is activated, and fibrinolytic activity is decreased, thereby causing vasculitides to block and disrupt the blood supply to the tissues (43–45). Recent studies have reported the presence of neutrophils and NETs in the thrombus of humans and mice (46). In addition, NETs have been found to stimulate both internal and external coagulation pathways that promote thrombosisby providing a scaffold for the deposition of fibrinogen, platelets, von Willebrand factors, and erythrocytes (47). NETs also promote the deposition of thrombogenic substances. As platelets aggregate and become activated in NETs, the histones interact with fibrinogen, TLR2, and TLR4, to generate thrombin (48). In mouse models, DNase I can effectively prevent intravascular

microthrombosis, which suggests a key role of NETs in thrombosis (49). However, another study argued that NETs promote thrombosis through their DNA and histone components instead of the deposition approach (50). That said, further studies are required to fully understand the promoter role of NETs in thrombosis.

Over the past few years, NETs have attracted increasing attention due to their essential role in innate immunology and thrombosis. However, there is also evidence that NETs play a pro-tumorigenic role in cancer (51). A growing number of studies are looking into the potential diagnostic and prognostic values of circulating NETs (52). The deposition of NETs promotes tumor cell proliferation, immunosuppression, and cancer-associated thrombosis. In addition, NETs can accelerate metastasis by contributing to epithelial-to-mesenchymal transition. NETs collect and multiply circulating tumor cells, resulting in tumor cell intravasation and micrometastases (53). At the same time, post-operative infections can increase NETs deposition, which exacerbates the recurrence and progression of post-surgical cancer (54). Considering their integral role in cancer, NETs could be potential therapeutic targets to inhibit tumor cell proliferation, metastasis, and thrombosis.

With deepening research in the field of NETs in liver transplantation, multiple studies discovered that DAMPs, including HMGB1 and histones or superoxide released during liver IRI, related in NETs formation. TLR-4 and/or TLR-9-myeloid differentiation primary response protein signaling pathways stimulated by HMGB1 and histones, respectively, are thought to exacerbate liver IRI (7, 55, 56). Our study founded that NETs promote kupffer cell M1 polarization and intracellular translocation of HMGB1 aggravating liver IRI even cause acute graft rejection following liver transplantation (57).

NETs detection

Whilst the importance of NETs has been highlighted in innate immunity, it is a challenge to detect NETs due to their heterogenous and acellular structure (58). Moreover, primary human neutrophils cannot be transfected for mechanistic interrelation studies, further complicating NET-related studies (59). Besides that, NETs must be distinguished from cell-free DNA (cfDNA), which originates independently of necrosis and apoptosis (60). Hence, it is crucial to discover NETosis markers and develop quantitative detection strategies that are sensitive and specific, particularly towards lytic NETs. Immunoconfocal microscopes are commonly used to detect NETs *via* immunocytochemistry and immunohistochemistry. Several groups have recommended co-localizing at least three key NET components (i.e., extracellular DNA, NE, and histones) for the accurate detection of NETs. This co-localization helps to differentiate NETs from dead or dying cells that release DNA (61). SYTOX Green dye stain is more specific than DAPI for the detection of NETs in a mixture with extracellular DNA (62, 63). Despite the simple concept, the methodology is not well-developed. There are several challenges to this, such as the need for researchers to manually evaluate the presence of neutrophil-derived proteins and DNA, difficulty in quantifying the formation of NETs, and controversial reported analytical techniques (64). H3cit, MPO and NE are considered as NETs-specific biomarker. Thus, those markers can be used for the ELISA-based detection of NETs (65).

To improve the detection of NETs *in vitro*, two types of flow cytometry methods (i.e., image-based and cell-appendant) have been developed using antibodies against major NET components (66). For example, Zhao et al. used multispectral imaging flow cytometry to identify the swelling of the nuclei in NET-neutrophils as a potential marker for NETosis (67). According to Gavillet et al., NETs simultaneously express both MPO and citrullinated histones on their surface, and these molecules can be detected by flow cytometry (68). In another study, Cichon et al. introduced a novel method to detect NET formation *in vivo via* intravital microscopy (69). Recently, it was reported that CDr15 dye stain was impermeable to cell membranes and emitted strong fluorescent signals when bound to the extracellular DNA of NETs. When compared to SYTOX Green, CDr15 showed lower background fluorescence and higher specificity towards NETs. This was supported by the successful detection of NETs stained with CDr15 in formaldehyde-fixed tumor specimens (70). These novel approaches highlight the promising future developments of NET detection technologies. With advancing technology in NETs detection, accumulating evidence demonstrated that NETs may be a potential biomarker of inflammation and autoimmune diseases to reflect the degree of tissue damage and inflammatory conditions (71). A study reported that the serum levels of NETs changed dynamically during severe fever with thrombocytopenia syndrome (SFTS) progression. High NETs levels were strongly associated with multiple pathological processes and predicted severe illness in patients with SFTS (72). Another study found that serum levels of NETs can provide a picture of systemic inflammatory state and thereby estimate risk for HCC recurrence after surgery. The research of NETs detection technology have important clinical implications for both treatment and biomarker discovery (73).

NETs and end-stage liver disease

NETs can also play a pivotal role in liver diseases such as acute liver failure, alcohol-associated liver disease, non-alcoholic steatohepatitis (NASH), liver cirrhosis, and hepatocellular carcinoma (HCC) (59, 74, 75). Globally, liver cirrhosis ranks among the top ten leading causes of death (76). A recent study by Zenlander et al. suggests that the level of plasma markers for

NET formation correlates to the severity of liver dysfunction in patients with liver cirrhosis and HCC. A comparison between patients with liver cirrhosis and HCC showed that there was no significant increase in the plasma NET markers (77). Another study demonstrated that a higher rate of complications such as recurrent infections, may occur in liver cirrhosis patients with deficient NETs (78). NASH is becoming the most prevalent chronic liver disease in Western society due to its increasing prevalence (79). According to findings by Van der Windt et al., NETs may be involved in the protumorigenic inflammatory environment in NASH. The strategies used to eliminate NETs may also reduce the risk of HCC in NASH (78). Another study proved that NETs promote regulatory T cell activity through metabolic reprogramming in NASH. In other words, therapeutic targeting of NETs and regulatory T cells can prevent the development of HCC in NASH patients (80).

Acute liver failure (ALF) is a life-threatening condition, that is caused by a variety of factors, including viral infections and drug-induced liver damage (81). A clinical study involving 676 patients with ALF reported that patients with ALF had 7.1 folds higher levels of cfDNA and 2.5 folds higher levels of MPO-DNA complexes, as compared to healthy controls. The levels of cfDNA did not correlate with the 21-day transplant-free survival, but they were higher in more severe cases. This finding suggests that NET formation is a contributing factor to disease development (82). Another study of ALF in mice reported the pathogenic role of NETs in ALF. The management of ALF could be improved by regulating the levels of miR-223/NE and NETs (83).

There is also growing evidence that the presence of NETs in a cancer inflammatory microenvironment promotes HCC cell proliferation (53). Researchers found that neutrophils isolated from patients with HCC produced more NETs *in vitro*. The presence of elevated MPO-DNA was associated with increased mortality after liver surgery in HCC patients (84, 85). The oncogenic role of NETs in HCC has been preliminary confirmed. However, the specific mechanisms of NETs in portal vein tumor thrombus and HCC recurrence after surgical resection require further investigations (Figure 2).

NETs and IRI

End-stage liver disease patients benefit from liver transplantation. However, liver IRI is a major cause of liver failure and graft loss associated with liver transplantation (86, 87). In clinical studies, ischemia-reperfusion-related tissue injury accounts for approximately 10% of early graft failures and is a major contributor to both acute and chronic rejection (88). Ischemia livers produce lesser ATPs due to lower oxygen levels. As ATP is low, ROS cytokinesis, vasoactive agents, and adhesion molecules are produced, which can aggravate the damage (89).

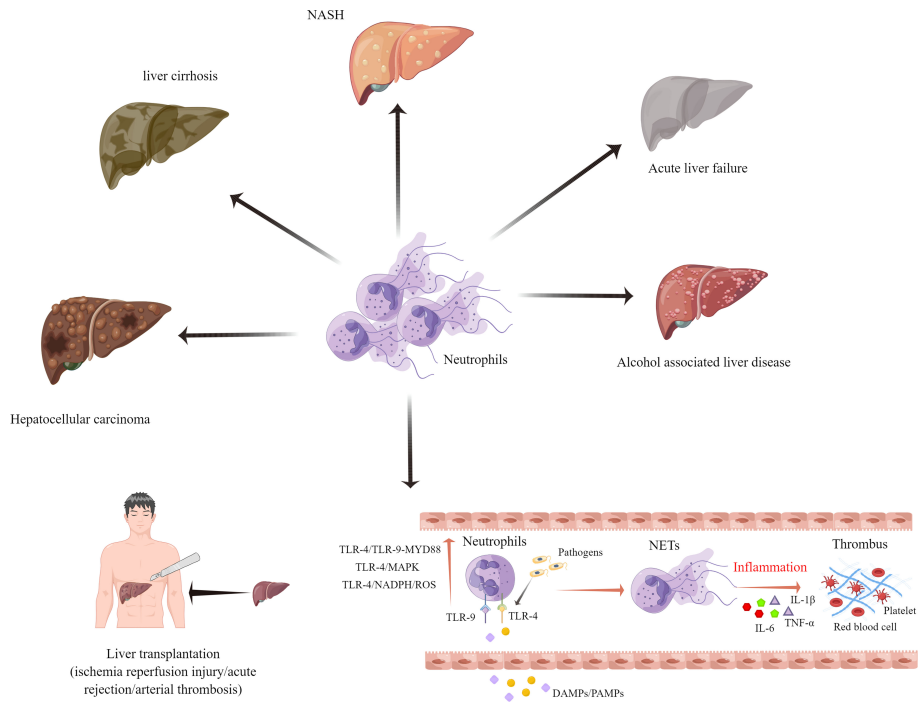

FIGURE 2
Neutrophil extracellular traps have been implicated in the pathophysiology of several different end-stage liver diseases.

As a result of ROS generation, the concentration of intracellular calcium increases, and the pH changes, leading to apoptosis and necrosis (90). An important component of liver IRI is inflammation, and neutrophils play an important role in the events leading to liver injury after reperfusion. The excessive activation and recruitment of neutrophils during reperfusion contribute significantly to the pathogenesis of IRI. A neutrophil induces liver injury through a multistep process that involves neutrophil activation, vasculature transport, and migration across the endothelium (91–93).

As more studies on the functions of NETs emerge, it is implicated that NETs may contribute to the pathogenesis of hepatic IRI. Histones and high mobility group box 1 (HMGB1) proteins, commonly associated with tissue damage, are released from damaged hepatocytes, and this activates TLR4 and TLR9 to induce NETs formation. A recent study suggested that NADPH-mediated superoxide production initiates NETs formation after IRI. Pretreatment with allopurinol and N-acetylcysteine was found to decrease NETs formation and liver injury after ischemia injury in mice (94). Neutrophils and NETs were found in the liver from ischemia-reperfusion mice models, and both were negatively correlated with histidine-rich glycoprotein (HRG) expression. Supplemental HRG treatment inhibited neutrophil infiltration and NETs formation in livers to alleviate liver IRI (95). Zhang et al. also correlated the presence of NETs with hepatic IRI, and hydroxychloroquine could alleviate hepatic IRI by inhibiting NETs formation in hepatic ischemia-reperfusion mice models (55). One study suggested that acrolein can cause the release of NETs in the liver during IRI and slow the recovery rate of a post-operative liver. In patients with chronic hepatic disorders, targeting NOX2 and P38MAPK signaling could inhibit the formation of NETs, and improve the survival and function of the post-operative liver (56). In our study, we found that tetramethylpyrazine (TMP), a compound extracted from *Ligusticum wallichii* Franchat, has the potential to improve liver functions and alleviate hepatic IRI. Furthermore, TMP inhibited NADPH oxidase activity, thus inhibiting the formation of NETs in rats after liver transplantation. We provide the first evidence of a synergistic effect between TMP and diphenyleneiodonium to alleviate hepatic IRI (96). We further examined the effect of recombinant human thrombomodulin (rTM) on liver transplantation in a rat model, focusing on the TLR-4/MAPK axis. Our data illustrated that NETs independently contribute to hepatic IRI, and rTM treatment mitigated neutrophil infiltration and suppressed NETs formation after liver transplantation (97). Although these results suggest that antioxidant treatment can protect against liver IRI *via* the attenuation of NETs formation, the therapeutic benefits of NETs inhibition should also take into account the possible complications in immunocompromised individuals after transplantation (Figure 3).

NETs and acute rejection

Many individuals with end-stage liver disease around the world benefit from liver transplantation (98). According to a recent publication, the 5-year survival rate of grafts and patients after a liver transplant was 72.8 and 76.1%, respectively. Acute rejection (AR) is a common complication after liver

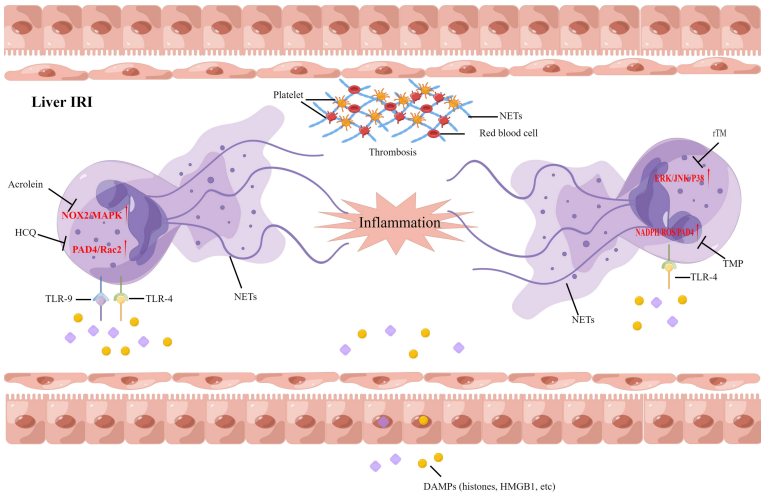

FIGURE 3
Neutrophil extracellular traps have been implicated in the pathophysiology of liver ischemia-reperfusion injury following liver transplantation. DAMPs, damage-associated molecular patterns; HCQ, Hydroxychloroquine; TMP; Tetramethylpyrazine, rTM; recombinant human thrombomodulin.

transplantation, that affects about 25 to 50% of patients (99). There is evidence that immunosuppressive agents can reduce the rates of acute rejection, but immunosuppressive treatments can also decrease the survival rate of patients (100, 101). Total bilirubin, alanine aminotransferase, and aspartate aminotransferase are commonly used clinically to monitor the liver function of liver grafts (102). Furthermore, the levels of immunosuppressive drugs in the blood can be monitored to predict the risk of AR (103). However, standard laboratory tests are inefficient for detecting AR, in terms of time and specificity (104, 105). Hence, the identification of therapeutic targets and early diagnostic strategies for AR should be the focus of future research (106). Recently, donor-derived cell-free DNA (dd-cfDNA) in AR is attracting increasing attention as a diagnostic biomarker (107). Allograft injury releases dd-cfDNA into the patient's serum, which makes it a good biomarker to evaluate the condition of allografts and the possibility of rejection (108). A study was conducted by Schutz et al. that measured the levels of dd-cfDNA in 107 patients with liver transplantation. Patients with AR had the highest percentage (29.6%) compared with those healthy controls (3.3%) (109). A more recent study suggested that dd-cfDNA is even more sensitive than conventional transaminases to detect AR (110).

Extracellular DNA is the most important component of NETs, and neutrophils are generally activated in the AR. However, there are insufficient studies to assess the correlation between NETs formation and AR after liver transplantation. As such, we have conducted some studies in this area (8, 15). Serum samples obtained from 13 liver transplant individuals were analyzed, and we found that the levels of NETs were elevated. During recovery, the levels of NETs decreased gradually and then stabilized. The levels of NETs increased following AR diagnosis, and decreased following treatment with oral rapamycin, in three patients. Next, the serum NETs were measured in liver transplant patients with AR. The levels of NETs in patients undergoing liver transplantation were positively correlated with liver enzymes and the incidence of AR. Our findings revealed that AR is influenced independently by NETs and that NETs subsequently induced kupffer cell M1 polarization and intracellular translocation of HMGB1. On the other hand, HMGB1 activates the TLR-4/MAPK signaling pathway, which causes NETs formation. This positive feedback loop between neutrophils and kupffer cells further amplifies the inflammatory signals and graft injury. Additionally, NET inhibitors combined with immunosuppressive agents may offer a novel treatment option for AR (57). NETs are a potential novel target for AR diagnosis and treatment (Figure 4).

NETs and arterial thrombosis

Hepatic artery thrombosis is the most common vascular complication, that may lead to non-functional liver graft and acute liver failure, following liver transplantation (111, 112). A significant proportion of this is seen in patients with recurrent biliary tract infection or asymptomatic biliary leakage with liver dysfunction (113). Thrombosis after liver transplantation has a high incidence rate and poor prognosis in children undergoing liver transplantation because it is difficult to diagnose in the early stages (114). It is well-recognized that neutrophils and platelets act as first responders to injuries and infections (115). As part of their host defense mechanisms, neutrophils promote blood coagulation by increasing fibrin deposition and limiting the spread of infections (32). NET-fibrin interactions prevent bacterial invasion into the surrounding tissues of the liver microvasculature, while their disruption promotes bacterial dissemination throughout the body (116). A dysregulation or

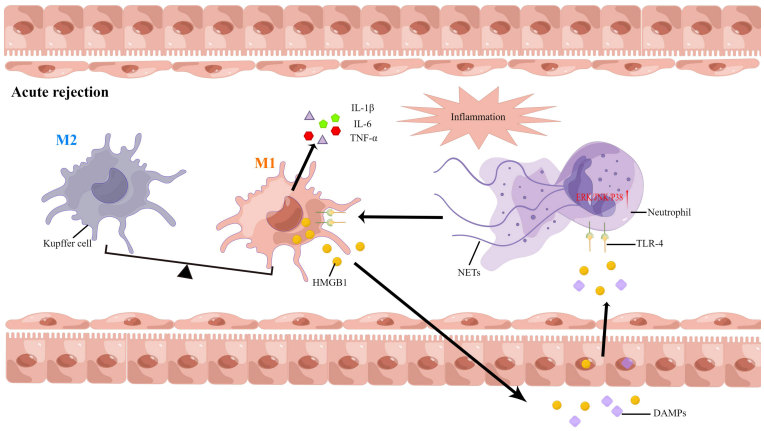

FIGURE 4
Neutrophil extracellular traps have been implicated in the pathophysiology of acute rejection following liver transplantation.

excessive stimulation of the vasculature may lead to pathological thrombosis. Therefore, neutrophils play a pivotal role in regulating thrombosis through several mechanisms (117).

NETs have been recently identified as new DNA-based components involved in the formation of blood clots and thrombosis (118). Platelets, red blood cells, and platelet adhesion molecules adhere to NETs *via* a scaffold, which promotes thrombosis (119). Additionally, many of the scaffold components can also stimulate platelet activation and blood coagulation (6). In addition, NETs can stimulate both intrinsic and extrinsic coagulation, primarily through the serine proteases in neutrophils. Endothelial cells are highly cytotoxic to the histones, H3 and H4, and that platelets can aggregate because of these histones (5). In comparison to venous thrombosis, arterial thrombosis is more common in acute events, as a result of thrombus shedding in acute myocardial infarction (AMI), ischemic stroke, and acute arterial embolism (120). According to Riegger et al., NETs were present in the thrombus of stroke patients and atherosclerotic plaques of patients with atrial fibrillation (121). Another study found that NETs were more prevalent in newly formed coronary thrombi than in older ones and that both myocardial infarction and ST-segment elevation were positively associated with the level of NETs in the coronary thrombi (122). The surgical stress response from liver resection and transplantation can aggravate the deposition of NETs in the liver, and platelets activated with NETs can produce a systemic procoagulant state, leading to immunothrombosis and remote organ injury (123). A mouse model with liver IRI was found to significantly increase both circulating platelet activation and platelet-neutrophil aggregation. NETs and platelet-rich microthrombi were found in the microvasculature of injured organs after liver surgery, and the inhibition of NETs with DNase reduced immune thrombosis and organ damage (124). Although the key role of NETs in immune thrombosis and its related mechanisms have been reported by a large number of studies, the findings on the regulation of coagulation and immune thrombosis after liver transplantation are still lacking. Hence, it is necessary to explore the role and specific mechanisms of NETs in immune thrombosis after liver transplantation, for better management of the condition.

NETs and hepatocellular carcinoma recurrence

Hepatocellular carcinoma (HCC) and end-stage liver diseases have widely benefited from liver transplantation (125, 126). However, HCC recurrence is one of the main causes of mortality in HCC patients who undergo liver transplantation (127, 128). It has been established that certain tumor characteristics can lead to the recurrence of HCC, including the concentration of alpha fetoproteins, tumor diameter, macrovascular invasion, and extended orthotopic liver transplantation criteria (129). A recent study found that both pre-operative serum hepatitis B viral DNA and pre-operative prognostic nutritional index can potentially be used to predict HCC recurrence after liver transplantation (130, 131). However, these studies all had small sample sizes or were conducted retrospectively and lack of molecular-biological investigations. Despite these advances, the mechanism behind the high HCC recurrence rates remains a mystery, and that these biomarkers have clear limitations.

Recently, NETs have been detected in various cancer samples (i.e., breast, liver, and gastric cancers) and metastatic tumors. In tumor development, NETs play an important role in cancer immunoediting and immune-cell interactions (132–134). Research suggests that NETs activate dormant cancer cells, which causes tumor recurrence (135). Furthermore, HMGB1 is also involved in NETs formation in TME by interacting with TLR4, and this releases excessive inflammatory cytokines (136). NETs also promote cancer invasion and migration, which exacerbates tumor aggressiveness (137). It is well known that the degradation of matrix proteins inhibits the immune system of the host, which is one of the mechanisms of tumor evasion (53). NETs-associated proteinases activate matrix metalloproteinases to induce tumor-associated macrophages, which stimulate the release of pro-inflammatory factors (i.e., IL-8, IL-1β, and TNF-α), eventually leading to immune escape and tumor metastasis (138).

Tumor metastasis is the main cause of cancer mortality, and neutrophils are involved in this process (139). Multiple studies reported that NETs trap circulating cancer cells and release proteases, which results in tumor metastasis and proliferation (35, 140). Najmeh et al. demonstrated that β1-integrin can induce NET-related entrapment of circulating lung carcinoma cells, resulting in cancer development and metastasis (141). These results were supported by Cools-Lartigue et al., where circulating lung carcinoma cells were found to be encapsulated in NET DNA conglomerates in a murine model. It was also shown that circulating "NETs-cancer cells packages" seeded in the liver, produced micrometastases within 48 hours and secondary hepatocellular carcinoma after two weeks (51). A retrospective analysis found that high level of NETs predicted shorter recurrence-free survival and overall survival. Serum levels of NETs as a biomarker pre-surgery can help identify patients with a higher risk for HCC recurrence (73). Another study showed that HCC is capable to stimulate NETs enriched in oxidized mitochondrial-DNA, which are highly pro-inflammatory and pro-metastatic (142). Cheng Y et al. demonstrated that combination of NK cell adoptive therapy and hydrogel-based delivery system can destruct NETs and prevent post-resection and post liver transplantation HCC recurrence (143). NETs play an integral role in cancer invasion, transport, and transendothelial migration according

to a multilevel model, especially in HCC recurrence should be further studied.

Potential therapeutic targets for NETs

In various diseases, NETs play the role of pathogenic drivers, thus making them attractive therapeutic targets. Studies have found that the levels of NETs correlated with the survival of cancer patients (142, 144). However, the risks of using NETs as therapeutic targets should also be evaluated. Targeting NETs would increase infection susceptibility, considering the protective role of NETs against severe infectious diseases (58). A study reported that mice with deletions of PAD4 were more vulnerable to bacterial infections (145). According to another study, PAD4 knockout may protect mice from polymicrobial sepsis-induced septic shock (146). Therefore, the potential risk of targeting NET formation may be determined by the type of disease and immune status of the organism. Another major risk of NETs degradation is the release of NETs-derived DNA and histones, which may trigger inflammation. Currently, therapies targeting NETs can be segmented into two categories: degradation/destabilization of NETs, and the inhibition of NETs formation.

The degradation of NETs has already been extensively studied. Research found that DNase I was capable of partially lysing NETs, and that tPA and DNase I could synergistically initiate thrombolysis (122). The use of DNase I as a treatment in mice suffering from thrombosis was also effective at preventing recurrent stroke, myocardial infarction, and deep vein thrombosis (49). However, further research is required to determine whether DNase I degradation of NETs would increase inflammation and risk for thrombosis. It has also been suggested that treatment with low molecular weight heparins (LMWH) can reduce NETs formation (5). Some researchers reported that histones could be dissociated from the chromatin backbone of NETs *via* heparin therapy and that LMWH can inhibit PMA-induced NETs formation (147). According to a study, the therapeutic use of heparin to treat NET-associated pathologies reported the opposite effect. Lelliott, et al. showed that heparin induced NETs formation *in vitro*, in the absence of PAD4 (148). Two independent studies reported that heparin-induced thrombocytopenia-related thrombosis was caused by NETs (149, 150). These contradictory results, as well as the potential side effects and risks, suggest the need for further investigations.

Another strategy to target already formed NETs is to interfere with their formation. Cloamidine, a pan PAD inhibitor, was found to inhibit the expression of PAD4, which subsequently prevents NETosis (151). Another potential advantage is that PAD4 deficiency in mice does not affect bacteremia during polymicrobial sepsis. The efficacy of GSK484 (developed by Glaxo Smith Kline) and BMS-P5

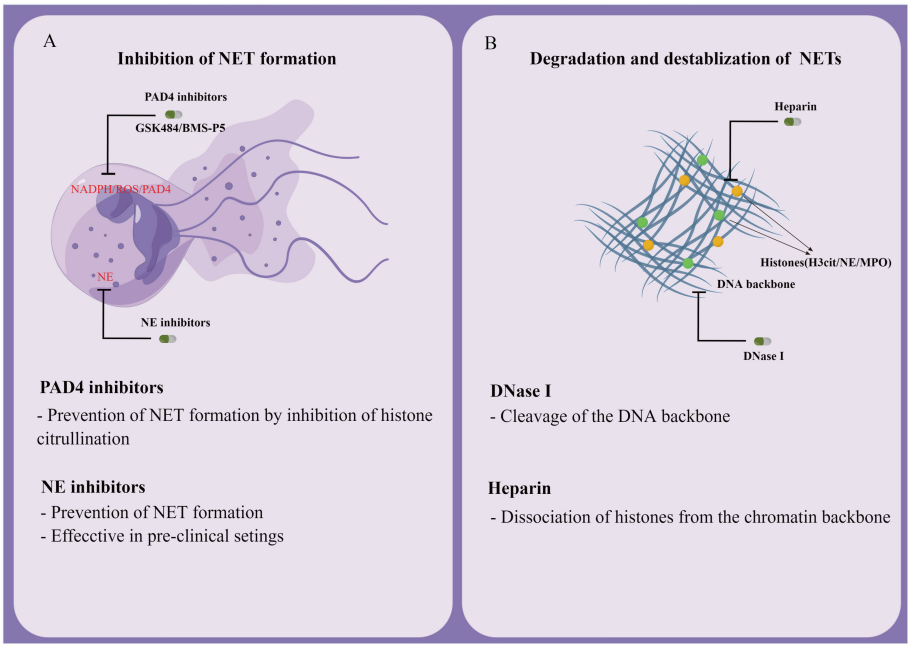

FIGURE 5
Potential therapeutic targets for NETs. **(A)** Inhibition of NET formation. **(B)** Degradation and destabilization of already formed NETs.

(developed by Bristol-Myers Squibb) in inhibiting NET development and suppressing associated diseases have now been confirmed by several *in vitro* and *in vivo* studies (152, 153). As a potential therapeutic target, NE inhibitors have proven effective in inhibiting NETs formation (51). For example, it was demonstrated that Sivelestat (an inhibitor of NE) inhibited NETs growth in mice with lung carcinoma (154). Antibodies are also known to prevent the formation and release of NETs in several inflammatory conditions, owing to their action toward citrullinated proteins (Figure 5) (155).

Conclusion and future perspectives

There is increasing evidence showing that NETs contribute to ischemia-reperfusion injury, acute rejection, thrombosis, and the recurrence of hepatocellular carcinoma. There is also potential for NET-related molecules as biomarkers and as targets for therapeutic intervention in complications of live transplantation. With further study, NETs is promising to provide a vast number of innovative applications in liver transplantation. There is an urgent need for the development of new methodologies to accurately detect NETs formation, considering the limitations of current methods. In addition, NETs detection should be standardized to ensure consistent results from comparative studies by different research groups. Thus far, strong evidence has shown that NETs might induce inflammation and tumor immune escape in ischemia-reperfusion injury and recurring hepatocellular carcinoma. Further research is required to understand the pathogenicity of NETs in liver transplantation. Neutrophils and NETs play a pivotal role in immune defense, and their potential as therapeutic targets warrants further study. A long-term safety assessment is also needed to assess the benefits and risks of NET-inhibition treatment. As an emerging field within liver transplantation, the relationship between NETs and the postoperative complication of liver transplantation also requires further investigation.

Author contributions

All authors listed have made a substantial, direct, and intellectual contribution to the work and approved it for publication. All authors contributed to the article and approved the submitted version.

Funding

This work was supported by the National Natural Science Foundation of China (No. 81873592 and No.82170666).

Conflict of interest

The authors declare that the research was conducted in the absence of any commercial or financial relationships that could be construed as a potential conflict of interest.

Publisher's note

References

1. Brinkmann V. Neutrophil extracellular traps in the second decade. *J Innate Immun* (2018) 10(5-6):414–21. doi: 10.1159/000489829

2. Wu L, Gao X, Guo Q, Li J, Yao J, Yan K, et al. The role of neutrophils in innate immunity–driven nonalcoholic steatohepatitis: Lessons learned and future promise. *Hepatol Int* (2020) 14(5):652–66. doi: 10.1007/s12072-020-10081-7

3. Bartneck M, Wang J. Therapeutic targeting of neutrophil granulocytes in inflammatory liver disease. *Front Immunol* (2019) 10:2257. doi: 10.3389/fimmu.2019.02257

4. Herre M, Cedervall J, Mackman N, Olsson AK. Neutrophil extracellular traps in the pathology of cancer and other inflammatory diseases. *Physiol Rev* (2023) 103 (1): 277–312. doi: 10.1152/physrev.00062.2021

5. Fuchs TA, Brill A, Duerschmied D, Schatzberg D, Monestier M, Jr DDM, et al. Extracellular DNA traps promote thrombosis. *Proc Natl Acad Sci USA* (2010) 107(36):15880–5. doi: 10.1073/pnas.1005743107

6. Zhou Y, Tao W, Shen F, Du W, Xu Z, LIu Z. The emerging role of neutrophil extracellular traps in arterial, venous, and cancer-associated thrombosis. *Front Cardiovasc Med* (2021) 2(8):786387. doi: 10.3389/fcvm.2021.786387

7. Huang H, Tohme S, AI-Khafaji AB, Tai S, Loughran P, Chen L, et al. Damage-associated molecular pattern-activated neutrophil extracellular trap exacerbates sterile inflammatory liver injury. *Hepatology* (2015) 62(2):600–14. doi: 10.1002/hep.27841

8. Liu Y, Qin X, Lei Z, Chai W, Wu Z. Diphenyleneiodonium ameliorates acute liver rejection during transplantation by inhibiting neutrophil extracellular traps formation *in vivo*. *Transpl Immunol* (2021) 68:101434. doi: 10.1016/j.trim.2021.101434

9. Erpenbeck L, Schön MP. Neutrophil extracellular traps: Protagonists of cancer progression? *Oncogene* (2017) 36(18):2483–90. doi: 10.1038/onc.2016.406

10. Brinkmann V, Reichard U, Goosmann C, Fauler B, Uhlemann Y, Weiss DS, et al. Neutrophil extracellular traps kill bacteria. *Science* (2004) 303(5663):1532–5. doi: 10.1126/science.1092385

11. Papayannopoulos V. Neutrophil extracellular traps in immunity and disease. *Nat Rev Immunol* (2018) 18(02):134–47. doi: 10.1038/nri.2017.105

12. Thiam HR, Wong SL, Qiu R, Kittisopikul M, Vahabikashi A, Goldman AE, et al. NETosis proceeds by cytoskeleton and endomembrane disassembly and PAD4-mediated chromatin decondensation and nuclear envelope rupture. *Proc Natl Acad Sci USA* (2020) 117(13):7326–37. doi: 10.1073/pnas.1909546117

13. Fuchs TA, Abed U, Goosmann C, Hurwitz R, Schulze I, Wahn V, et al. Novel cell death program leads to neutrophil extracellular traps. *J Cell Biol* (2007) 176(2):231–41. doi: 10.1083/jcb.200606027

14. Kapoor S, Opneja A, Nayak L. The role of neutrophils in thrombosis. *Thromb Res* (2018) 170:87–96. doi: 10.1016/j.thromres.2018.08.005

15. Avondt KV, Hartl D. Mechanisms and disease relevance of neutrophil extracellular trap formation. *Eur J Clin Invest.* (2018) 48Suppl2:e12919. doi: 10.1111/eci.12919

16. Jorch SK, Kubes P. An emerging role for neutrophil extracellular traps in noninfectious disease. *Nat Med* (2017) 23(3):279–87. doi: 10.1038/nm.4294

17. Kenny EF, Herzig A, Krüger R, Muth A, Mondal S, Thompson PR, et al. Diverse stimuli engage different neutrophil extracellular trap pathways. *Elife* (2017) 6:e24437. doi: 10.7554/eLife.24437

18. Denning NL, Aziz M, Gurien SD, Wang P. DAMPs and NETs in sepsis. *Front Immunol* (2019) 10:2536. doi: 10.3389/fimmu.2019.02536

19. Wang Y, Li M, Stadler S, Li P, Wang D, Hayama R, et al. Histone hypercitrullination mediates chromatin decondensation and neutrophil extracellular trap formation. *J Cell Biol* (2009) 184:205–13. doi: 10.1083/jcb.200806072

20. Shi L, Aymonnier K, Wagner DD. Neutrophil stimulation with citrullinate histone H4 slows down calcium influx and reduces NET formation compared with native histone H4. *PloS One* (2021) 16:e0251726. doi: 10.1371/journal.pone.0251726

21. Eghbalzadeh K, Georgi L, Louis T, Zhao H, Keser U, Weber C, et al. Compromised anti-inflammatory action of neutrophil extracellular traps in PAD4-deficient mice contributes to aggravated acute inflammation after myocardial infarction. *Front Immunol* (2019) 10:2313. doi: 10.3389/fimmu.2019.02313

22. Branzk N, Lubojemska A, Hardison SE, Wang Q, Gutierrez MG, Brown GD, et al. Neutrophils sense microbe size and selectively ReleaseNeutrophil extracellular traps in response to Large pathogens. *Nat Immunol* (2014) 15(11):1017–25. doi: 10.1038/ni.2987

23. Thålin C, Hisada Y, Lundström S, Mackman N, Wallén H. Neutrophil extracellular traps: Villains and targets in arterial, venous, and cancer-associated thrombosis. *Arterioscler Thromb Vasc Biol* (2019) 39(9):1724–38. doi: 10.1161/ATVBAHA.119.312463

24. Adrover JM, Aroca-Crevillén A, Crainiciuc G, Ostos F, Rojas-Vega Y, Rubio-Ponce A, et al. Programmed 'disarming' of the neutrophil proteome reduces the magnitude of inflammation. *Nat Immunol* (2020) 21(2):135–44. doi: 10.1038/s41590-019-0571-2

25. Altznauer F, Martinelli S, Yousefi S, Thürig C, Schmid, Conway EM, et al. Inflammation-associated cell cycle-independent block of apoptosis by survivin in terminally differentiated neutrophils. *J Exp Med* (2004) 199(10):1343–54. doi: 10.1084/jem.20032033

26. Yousefi S, Gold JA, Andina N, Lee JJ, Kelly AM, Kozlowski E, et al. Catapult-like release of mitochondrial DNA by eosinophils contributes to antibacterial defense. *Nat Med* (2008) 14(9):949–53. doi: 10.1038/nm.1855

27. Yousefi S, Mihalache C, Kozlowski E, Schmid I, Simon HU. Viable neutrophils release mitochondrial DNA to form neutrophil extracellular traps. *Cell Death Differ* (2009) 16(11):1438–44. doi: 10.1038/cdd.2009.96

28. Lood C, Blanco LP, Purmalek M, Carmona-Rivera C, Ravin SSD, Smith CK, et al. Neutrophil extracellular traps enriched in oxidized mitochondrial DNA are interferogenic and contribute to lupus-like disease. *Nat Med* (2016) 22(2):146–53. doi: 10.1038/nm.4027

29. Claushuis TAM, van der Donk LEH, Luitse AL, van Veen HA, van der Wel NN, van Vught AL, et al. Role of peptidylarginine deiminase 4 in neutrophil extracellular trap formation and host defense during klebsiella pneumoniae-induced pneumonia-derived sepsis. *J Immunol* (2018) 201(4):1241–52. doi: 10.4049/jimmunol.1800314

30. Hamam HJ, Palaniyar N. Post-translational modifications in NETosis and NETs-mediated diseases. *Biomolecules* (2019) 9(8):369. doi: 10.3390/biom9080369

31. Sollberger G, Choidas A, Burn GL, Habenberger P, Lucrezia RD, Kordes S, et al. Gasdermin d plays a vital role in the generation of neutrophil extracellular traps. *Sci Immunol* (2018) 3(26):eaar6689. doi: 10.1126/sciimmunol.aar6689

32. McDonald B, Urrutia R, Yipp BG, Jenne CN, Kubes P. Intravascular neutrophil extracellular traps capture bacteria from the blood-stream during sepsis. *Cell Host Microbe* (2012) 12(3):324–33. doi: 10.1016/j.chom.2012.06.011

33. Weinrauch Y, Drujan D, Shapiro SD, Weiss J, Zychlinsky A. Neutrophil elastase targets virulence factors of enterobacteria. *Nature* (2002) 417(6884):91–4. doi: 10.1038/417091a

34. Brinkmann V, Zychlinsky A. Beneficial suicide: why neutrophils die to make NETs. *Nat Rev Microbiol* (2007) 5(08):577–82. doi: 10.1038/nrmicro1710

35. Kolaczkowska E, Jenne CN, Surewaard BGJ, Thanabalasuriar A, Lee WY, Sanz MJ, et al. Molecular mechanisms of NET formation and degradation revealed by intravital imaging in the liver vasculature. *Nat Commun* (2015) 6:6673. doi: 10.1038/ncomms7673

36. Kubes P, Mehal WZ. Sterile inflammation in the liver. *Gastroenterology* (2012) 143(5):1158–72. doi: 10.1053/j.gastro.2012.09.008

37. Marin-Esteban V, Turbica I, Dufour G, Semiramoth N, Gleizes A, Gorges R, et al. Afa/Dr diffusely adhering escherichia coli strain C1845 induces neutrophil extracellular traps that kill bacteria and damage human enterocyte-like cells. *Infect Immun* (2012) 80(5):1891–9. doi: 10.1128/IAI.00050-12

38. Crane JK, Broome JE, Lis A. Biological activities of uric acid in infection due to enteropathogenic and shiga-toxigenic escherichia coli. *Infect Immun* (2016) 84(4):976–88. doi: 10.1128/IAI.01389-15

39. Radermecker C, Detrembleur N, Guiot J, Cavalier E, Henket M, d"mal C, et al. Neutrophil extracellular traps infiltrate the lung airway, interstitial, and vascular compartments in severe COVID-19. *J Exp Med* (2020) 217(12):e20201012. doi: 10.1084/jem.20201012

40. Murao A, A1 A, Brenner M, Denning NL, Jin H, Takizawa S, et al. Extracellular CIRP and TREM-1 axis promotes ICAM-1-Rho-mediated NETosis in sepsis. *FASEB J* (2020) 34(7):9771–86. doi: 10.1096/fj.202000482R

41. Bonaventura A, Liberale L, Carbone F, Vecchié A, Diaz-Cañestro C, Camici GG, et al. The pathophysiological role of neutrophil extracellular traps in inflammatory diseases. *Thromb Haemost.* (2018) 118(1):6–27. doi: 10.1160/TH17-09-0630

42. Yazdani HO, Chen HW, Tohme S, Tai S, van der Windt DJ, Loughran P, et al. IL-33 exacerbates liver sterile inflammation by amplifying neutrophil extracellular trap formation. *J Hepatol* (2017) S0168-8278(17):32291–2. doi: 10.1016/j.jhep.2017.09.010

43. Zhou Y, Xu Z, Liu Z. Impact of neutrophil extracellular traps on thrombosis formation: New findings and future perspective. *Front Cell Infect Microbiol* (2022) 12:910908. doi: 10.3389/fcimb.2022.910908

44. Kimball AS, Obi AT, Diaz JA, Henke PK. The emerging role of NETs in venous thrombosis and immunothrombosis. *Front Immunol* (2016) 7:236. doi: 10.3389/fimmu.2016.00236

45. Engelmann B, Massberg S. Thrombosis as an intravascular effector of innate immunity. *Nat Rev Immunol* (2013) 13:34–45. doi: 10.1038/nri3345

46. Kambas K, Mitroulis I, Apostolidou E, Girod A, Chrysanthopoulou A, Pneumatikos I, et al. Autophagy mediates the delivery of thrombogenic tissue factor to neutrophil extracellular traps in human sepsis. *PloS One* (2012) 7(9):e45427. doi: 10.1371/journal.pone.0045427

47. Nouboussie DF, Reeves BN, Strahl BD, Key NS. Neutrophils: Back in the thrombosis spotlight. *Blood* (2019) 133(20):2186–97. doi: 10.1182/blood-2018-10-862243

48. Yang X, Li L, Liu J, Lv B, Chen F. Extracellular histones induce tissue factor expression in vascular endothelial cells *via* TLR and activation of NF-kb and AP-1. *Thromb Res* (2016) 137:211–8. doi: 10.1016/j.thromres.2015.10.012

49. Ducroux C, Meglio LD, Loyau S, Delbosc S, Boisseau W, Deschildre C, et al. Thrombus neutrophil extracellular traps content impair tPA induced thrombolysis in acute ischemic stroke. *Stroke* (2018) 49(3):754–7. doi: 10.1161/STROKEAHA.117.019896

50. Nouboussie DF, Whelihan MF, Yu YB, Sparkenbaugh E, Pawlinski R, Monroe DM, et al. *In vitro* activation of coagulation by human neutrophil DNA and histone proteins but not neutrophil extracellular traps. *Blood* (2017) 129(8):1021–9. doi: 10.1182/blood-2016-06-722298

51. Cools-Lartigue J, Spicer J, McDonald B, Gowing S, Giannias B, et al. Neutrophil extracellular traps sequester circulating tumor cells and promote metastasis. *J Clin Invest.* (2013) 123(8):3446–58. doi: 10.1172/JCI67484

52. Zhang Y, Hu Y, Ma C, Sun H, Wei X, Li M, et al. Diagnostic, therapeutic predictive, and prognostic value of neutrophil extracellular traps in patients with gastric adenocarcinoma. *Front Oncol* (2020) 10:1036. doi: 10.3389/fonc.2020.01036

53. Meo MLD, Spicer JD. The role of neutrophil extracellular traps in cancer progression and metastasis. *Semin Immunol* (2021) 57:101595. doi: 10.1016/j.smim.2022.101595

54. Tohme S, Yazdani HO, Al-Khafaji AB, Chidi AP, Loughran P, Mowen K, et al. Neutrophil extracellular traps promote the development and progression of liver metastases after surgical stress. *Cancer Res* (2016) 76(6):1367–80. doi: 10.1158/0008-5472.CAN-15-1591

55. Zhang S, Zhang Q, Wang F, Guo X, Liu T, Zhao Y, et al. Hydroxychloroquine inhibiting neutrophil extracellular trap formation alleviates hepatic ischemia/reperfusion injury by blocking TLR9 in mice. *Clin Immunol* (2020) 216:108461. doi: 10.1016/j.clim.2020.108461

56. Arumugam S, Subbiah KG, Kemparaju K, Thirunavukkarasu C. Neutrophil extracellular traps in acrolein promoted hepatic ischemia-reperfusion injury: Therapeutic potential of NOX2 and p38MAPK inhibitors. *J Cell Physiol* (2018) 233(4):3244–61. doi: 10.1002/jcp.26167

57. Liu Y, Pu X, Qin X, Gong J, Huang Z, Lou Y, et al. Neutrophil extracellular traps regulate HMGB1 translocation and kupffer cell M1 polarization during acute liver transplantation rejection. *Front Immunol* (2022) 13:823511. doi: 10.3389/fimmu.2022.823511

58. Boeltz S, Amini P, Anders HJ, Andrade F, Billy R, Chatfield S, et al. To NET or not to NET: Current opinions and state of the science regarding the formation of neutrophil extracellular traps. *Cell Death Differ* (2019) 26(3):395–408. doi: 10.1038/s41418-018-0261-x

59. Honda M, Kubes P. Neutrophils and neutrophil extracellular traps in the liver and gastrointestinal system. *Nat Rev Gastroenterol Hepatol* (2018) 15(4):206–21. doi: 10.1038/nrgastro.2017.183

60. Breda SV, Vokalova L, Neugebauer C, Rossi SW, Hahn S, Hasler P, et al. Computational methodologies for the *in vitro* and *in situ* quantification of neutrophil extracellular traps. *Front Immunol* (2019) 10:1562. doi: 10.3389/fimmu.2019.01562

61. Seper A, Hosseinzadeh A, Gorkiewicz G, Lichtenegger S, Roier S, Lietner DR, et al. Vibrio cholerae evades neutrophil extracellular traps by the activity of two extracellular nucleases. *PloS Pathog* (2013) 9(9):e1003614. doi: 10.1371/journal.ppat.1003614

62. Metzler KD, Fuchs TA, Nauseef WM, Reumaux D, Roesler J, Schulze I, et al. Myeloperoxidase is required for neutrophil extracellular trap formation: Implications for innate immunity. *Blood* (2011) 117(3):953–9. doi: 10.1182/blood-2010-06-290171

63. Papayannopoulos V, Metzler KD, Hakkim A, Zychlinsky A. Neutrophil elastase and myeloperoxidase regulate the formation of neutrophil extracellular traps. *J Cell Biol* (2010) 191(3):677–91. doi: 10.1083/jcb.201006052

64. Carmona-Rivera C, Kaplan MJ. Induction and quantification of NETosis. *Curr Protoc Immunol* (2016) 115:14.41.1–14. doi: 10.1002/cpim.16

65. Tan C, Aziz M, Wang P. The vitals of NETs. *J Leukoc Biol* (2021) 110 (4):797–808. doi: 10.1002/JLB.3RU0620-375R

66. de Buhr N, von Kockritz-Blickwede M. How neutrophil extracellular traps become visible. *J Immunol Res* (2016) 2016:4604713. doi: 10.1155/2016/4604713

67. Zhao W, Fogg DK, Kaplan MJ. A novel image-based quantitative method for the characterization of NETosis. *J Immunol Methods* (2015) 423:104–10. doi: 10.1016/j.jim.2015.04.027

68. Gavillet M, Martinod K, Renella R, Harris C, Shapiro NI, Wagner DD, et al. Flow cytometric assay for direct quantification of neutrophil extracellular traps in blood samples. *Am J Hematol* (2015) 90(12):1155–8. doi: 10.1002/ajh.24185

69. Cichon I, Santocki M, Ortmann W, Kolaczkowska E, et al. Imaging of neutrophils and neutrophil extracellular traps (NETs) with intravital (*In vivo*) microscopy. *Methods Mol Biol* (2020) 2087:443–66. doi: 10.1007/978-1-0716-0154-9_26

70. Kim SJ, Kim J, Kim B, Lee WW, Liu X, Chang YT, et al. Validation of CDr15 as a new dye for detecting neutrophil extracellular trap. *Biochem Biophys Res Commun* (2020) 527(3):646–53. doi: 10.1016/j.bbrc.2020.04.153

71. Domerecka W, Homa-Mlak I, Mlak R, et al. Indicator of inflammation and NETosis-Low-Density granulocytes as a biomarker of autoimmune hepatitis. *J Clin Med* (2022) 11(8):2174. doi: 10.3390/jcm11082174

72. Zhang Y, Song R, Shen Y, Zhao Y, Zhao Z, Fan T, et al. High levels of circulating cell-free DNA are associated with a poor prognosis in patients with severe fever with thrombocytopenia syndrome. *Clin Infect Dis* (2020) 70(9):1941–9. doi: 10.1093/cid/ciz553

73. Kaltenmeier CT, Yazdani H, van der Windt D, Nolinari M, Geller D, Tsung A, et al. Neutrophil extracellular traps as a novel biomarker to predict recurrence-free and overall survival in patients with primary hepatic malignancies. *HPB (Oxford).* (2021) 23(2):309–20. doi: 10.1016/j.hpb.2020.06.012

74. Hilscher MB, Shah VH. Neutrophil extracellular traps and liver disease. *Semin Liver Dis* (2020) 40(2):171–9. doi: 10.1055/s-0039-3399562

75. Meijenfeldt FA, Jenne CN. Netting liver disease: Neutrophil extracellular traps in the initiation and exacerbation of liver pathology. *Semin Thromb Hemost.* (2020) 46(6):724–34. doi: 10.1055/s-0040-1715474

76. Bosetti C, Levi F, Lucchini F, Zatonski WA, Negri E, Vecchia CL. Worldwide mortality from cirrhosis: An update to 2002. *J Hepatol* (2007) 46:827–39. doi: 10.1016/j.jhep.2007.01.025

77. Zenlander R, Havervall S, Magnusson M, Engstrand J, Åren A, Thålin C, et al. Neutrophil extracellular traps in patients with liver cirrhosis and hepatocellular carcinoma. *Sci Rep* (2021) 11(1):18025. doi: 10.1038/s41598-021-97233-3

78. Van der Windt D, Sud V, Zhang H, Varley PR, Goswami J, Yazdani HO, et al. Neutrophil extracellular traps promote inflammation and development of hepatocellular carcinoma in nonalcoholic steatohepatitis. *Hepatology* (2018) 68 (4):1347–60. doi: 10.1002/hep.29914

79. Loomba R, Sanyal AJ. The global NAFLD epidemic. *Nat Rev Gastroenterol Hepatol* (2013) 10(11):686–90. doi: 10.1038/nrgastro.2013.171

80. Wang H, Zhang H, Wang Y, Brown ZJ, Xia Y, Huang Z, et al. Regulatory T cell and neutrophil extracellular trap interaction contributes to carcinogenesis in non-alcoholic steatohepatitis. *J Hepatol* (2021) 75(6):1271–83. doi: 10.1016/j.jhep.2021.07.032

81. Bernal W, Wendon J. Acute liver failure. *N Engl J Med* (2013) 369(26):2525–34. doi: 10.1056/NEJMra1208937

82. Meijenfeldt FA, Stravitz RT, Zhang J, Adelmeijer J, Zen Y, Durkalski V, et al. Generation of neutrophil extracellular traps in patients with acute liver failure is associated with poor outcome. *Hepatology* (2022) 75(3):623–33. doi: 10.1002/hep.32174

83. Ye D, Yao J, Du W, Chen C, Yang Y, Yan K, et al. Neutrophil extracellular traps mediate acute liver failure in regulation of miR-223/Neutrophil elastase signaling in mice. *Cell Mol Gastroenterol Hepatol* (2022) 14(3):587–607. doi: 10.1016/j.jcmgh.2022.05.012

84. Yang LY, Luo Q, Lu L, Zhu WW, Sun HT, Wei R, et al. Increased neutrophil extracellular traps promote metastasis potential of hepatocellular carcinoma *via* provoking tumorous inflammatory response. *J Hematol Oncol* (2020) 13(1):3. doi: 10.1186/s13045-019-0836-0

85. Velliou R, Mitroulis I, Chatzigeorgiou A. Neutrophil extracellular traps contribute to the development of hepatocellular carcinoma in NASH by promoting treg differentiation. *Hepatobiliary Surg Nutr* (2022) 11(3):415–8. doi: 10.21037/hbsn-21-557

86. Starzl TE, Fung JJ. Themes of liver transplantation. *Hepatology* (2010) 51 (6):1869–84. doi: 10.1002/hep.23595

87. Liu Y, Lu T, Zhang C, Xu J, Xue Z, Busuttil RW, et al. Activation of YAP attenuates hepatic damage and fibrosis in liver ischemia-reperfusion injury. *J Hepatol* (2019) 71(4):719–30. doi: 10.1016/j.jhep.2019.05.029

88. Uchida Y, Ke B, Freitas MCS, Yagita H, Akiba H, Busuttil RW, et al. T-Cell immunoglobulin mucin-3 determines severity of liver ischemia/reperfusion injury in mice in a TLR4-dependent manner. *Gastroenterology* (2010) 139(6):2195–206. doi: 10.1053/j.gastro.2010.07.003

89. Selzner M, Selzner N, Jochum W, Graf R, Clavien PA. Increased ischemic injury in old mouse liver: An ATP-dependent mechanism. *Liver Transpl* (2007) 13 (3):382–90. doi: 10.1002/lt.21100

90. Guan LY, Fu PY, Li PD, Li ZN, Li HY, Xin MG, et al. Mechanisms of hepatic ischemia-reperfusion injury and protective effects of nitric oxide. *World J Gastrointest Surg* (2014) 6(7):122–8. doi: 10.4240/wjgs.v6.i7.122

91. Oliveira THC, Marques PE, Proost P, Teixeira MMM. Neutrophils: A cornerstone of liver ischemia and reperfusion injury. *Lab Invest.* (2018) 98 (1):51–62. doi: 10.1038/labinvest.2017.90

92. Nakamura K, Kageyama S, Kupiec-Weglinski JW. The evolving role of neutrophils in liver transplant ischemia-reperfusion injury. *Curr Transplant Rep* (2019) 6(1):78–89. doi: 10.1007/s40472-019-0230-4

93. Imaeda AB, Watanabe A, Sohail MA, Mahmood S, Mohamadnejad M, Sutterwala FS, et al. Acetaminophen-induced hepatotoxicity in mice is dependent on Tlr9 and the Nalp3 inflammasome. *J Clin Invest.* (2009) 119(2):305–14. doi: 10.1172/JCI35958

94. Al-Khafaji AB, Tohme S, Yazdani HO, Miller D, Huang H, Tsung A. Superoxide induces neutrophil extracellular trap formation in a TLR-4 and NOX-dependent mechanism. *Mol Med* (2016) 22:621–31. doi: 10.2119/molmed.2016.00054

95. Guo J, Akahoshi T, MizutaAl Y, Murata M, Narahara S, Kawano T, et al. Histidine-rich glycoprotein alleviates liver Ischemia/Reperfusion injury in mice with nonalcoholic steatohepatitis. *Liver Transpl.* (2021) 27(6):840–53. doi: 10.1002/lt.25960

96. Liu Y, Qin X, Lei Z, Chai H, Huang Z, Wu Z. Tetramethylpyrazine inhibits neutrophil extracellular traps formation and alleviates hepatic ischemia/reperfusion injury in rat liver transplantation. *Exp Cell Res* (2021) 406(1):112719. doi: 10.1016/j.yexcr.2021.112719

97. Liu Y, Lei Z, Chai H, Xiang S, Wang Y, Yan P, et al. Thrombomodulin-mediated inhibition of neutrophil extracellular trap formation alleviates hepatic ischemia-reperfusion injury by blocking TLR4 in rats subjected to liver transplantation. *Transplantation* (2022) 106(2):e126–40. doi: 10.1097/TP.0000000000003954

98. Martinelli J, Habes D, Majed L, Guettier C, Gonzalès E, Linglart A, et al. Long-term outcome of liver transplantation in childhood: a study of 20-year survivors. *Am J Transplant.* (2018) 18(7):1680–9. doi: 10.1111/ajt.14626

99. Craig E, Heller M. Complications of liver transplant. *Abdom Radiol(NY)* (2021) 46(1):43–67. doi: 10.1007/s00261-019-02340-5

100. Dogan N, Husing-Kabar A, Schmidt HH, Cicinnati VR, Beckebaum S, Kabar I, et al. Acute allograft rejection in liver transplant recipients: Incidence, risk factors, treatment success, and impact on graft failure. *J Int Med Res* (2018) 46 (9):3979–90. doi: 10.1177/0300060518785543

101. Levitsky J, Goldberg D, Smith A, Mansfield SA, Gillespie BW, Merion RM, et al. Acute rejection increases risk of graft failure and death in recent liver transplant recipients. *Clin Gastroenterol Hepatol* (2017) 15(4):584–93. doi: 10.1016/j.cgh.2016.07.035

102. Florez MC, Bruner J, Zarrinpar A. Progress and challenges in diagnosis and treatment of rejection following liver transplantation. *Curr Opin Organ Transplant.* (2021) 26(6):669–74. doi: 10.1097/MOT.0000000000000924

103. Kawahara T, Asthana S, Kneteman NM. mTOR inhibitors: What role in liver transplantation? *J Hepatol* (2011) 55(6):1441–51. doi: 10.1016/j.jhep.2011.06.015

104. Perottino G, Harrington C, Levitsky J. Biomarkers of rejection in liver transplantation. *Curr Opin Organ Transplant.* (2022) 27(2):154–8. doi: 10.1097/MOT.0000000000000959

105. Sánchez-Fueyo A, Strom TB. Immunologic basis of graft rejection and tolerance following transplantation of liver or other solid organs. *Gastroenterology* (2011) 140(1):51–64. doi: 10.1053/j.gastro.2010.10.059

106. Krenzien F, Keshi E, Splith K, Griesel S, Kamali K, Sauer IM, et al. Diagnostic biomarkers to diagnose acute allograft rejection after liver transplantation: Systematic review and meta-analysis of diagnostic accuracy studies. *Front Immunol* (2019) 10:758. doi: 10.3389/fimmu.2019.00758

107. Taner T, Bruner J, Emamaullee J, Bonaccorsi-Riani E, Zarrinpar A. New approaches to the diagnosis of rejection and prediction of tolerance in liver transplantation. *Transplantation* (2022) 106(10):1952–62. doi: 10.1097/TP.0000000000004160

108. Grskovic M, Hiller DJ, Eubank LA, Sninsky JJ, Christopherson C, Collins JP, et al. Validation of a clinical-grade assay to measure donor-derived cell-free DNA in solid organ transplant recipients. *J Mol Diagn.* (2016) 18(6):890–902. doi: 10.1016/j.jmoldx.2016.07.003

109. Schütz E, Fischer A, Beck J, Harden M, Koch M, Wuensch T, et al. Graft-derived cell-free DNA, a noninvasive early rejection and graft damage marker in liver transplantation: A prospective, observational, multicenter cohort study. *PloS Med* (2017) 14(4):e1002286. doi: 10.1371/journal.pmed.1002286

110. Levitsky J, Kandpal M, Guo K, Kleiboeker S, Sinha R, Abecassis M, et al. Donor-derived cell-free DNA levels predict graft injury in liver transplant recipients. *Am J Transplant.* (2022) 22(2):532–40. doi: 10.1111/ajt.16835

111. Abdelaziz O, Osman AMA, Hosny KA, Emad-Eldin S, Serour 1DK, Mostafa M. Management of early hepatic artery thrombosis following living-donor liver transplantation: feasibility, efficacy and potential risks of endovascular therapy in the first 48 hours post-transplant-a retrospective cohort study. *Transpl Int* (2021) 34(6):1134–49. doi: 10.1111/tri.13839

112. Park J, Kim SH, Park SJ. Hepatic artery thrombosis following living donor liver transplantation: A 14-year experience at a single center. *J Hepatobiliary Pancreat Sci* (2020) 27(8):548–54. doi: 10.1002/jhbp.771

113. Duffy JP, Hong JC, Farmer DG, Ghobrial RM, Yersiz H, Hiatt JR, et al. Vascular complications of orthotopic liver transplantation: experience in more than 4,200 patients. *J Am Coll Surg* (2009) 208(5):896–903. doi: 10.1016/j.jamcollsurg.2008.12.032

114. Xu M, Dong C, Sun C, Wang K, Zhang W, Wu D, et al. Management and outcome of hepatic artery thrombosis with whole-liver transplantation using donors less than one year of age. *J Pediatr Surg* (2022), 54(11):656–65. doi: 10.1016/j.jpedsurg.2022.05.009

115. Massberg S, Grahl L, von Bruehl M-L, Manukyan D, Pfeiler S, Goosmann C, et al. Reciprocal coupling of coagulation and innate immunity *via* neutrophil serine proteases. *Nat Med* (2010) 16(8):887–96. doi: 10.1038/nm.2184

116. Shi C, Yang L, Braun A, Anders H. Extracellular DNA-a danger signal triggering immunothrombosis. *Front Immunol* (2020) 11:568513. doi: 10.3389/fimmu.2020.568513

117. Carminita E, Crescence L, Panicot-Dubois L, Dubois C. Role of neutrophils and NETs in animal models of thrombosis. *Int J Mol Sci* (2022) 23(3):1411. doi: 10.3390/ijms23031411

118. Gould TJ, Lysov Z, Liaw PC. Extracellular DNA and histones: double-edged swords in immunothrombosis. *J Thromb Haemost.* (2015) 13 Suppl 1:S82–91. doi: 10.1111/jth.12977

119. Xu J, Zhang X, Pelayo R, Monestier M, Ammollo CT, Semeraro F, et al. Extracellular histones are major mediators of death in sepsis. *Nat Med* (2009) 15 (11):1318–21. doi: 10.1038/nm.2053

120. Wendelboe AM, Raskob GE. Global burden of thrombosis: Epidemiologic aspects. *Circ Res* (2016) 118(9):1340–7. doi: 10.1161/CIRCRESAHA.115.306841

121. Riegger J, Byrne RA, Joner M, Chandraratne S, Gershlick AH, Ten Berg JM, et al. Histopathological evaluation of thrombus in patients presenting with stent thrombosis. A multicenter European study: A report of the prevention of late stent thrombosis by an interdisciplinary global European effort consortium. *Eur Heart J* (2016) 37(19):1538–49. doi: 10.1093/eurheartj/ehv419

122. Mangold A, Alias S, Scherz T, Hofbauer T, Jakowitsch J, Panzenböck A, et al. Coronary neutrophil extracellular trap burden and deoxyribonuclease activity in ST-elevation acute coronary syndrome are predictors of ST-segment resolution and infarct size. *Circ Res* (2015) 116(7):1182–92. doi: 10.1161/CIRCRESAHA.116.304944

123. Arshad F, Lisman T and Porte RJ. Hypercoagulability as a contributor to thrombotic complications in the liver transplant recipient. *Liver Int* (2013) 33 (6):820–7. doi: 10.1111/liv.12140

124. Zhang H, Goswami J, Varley P, van der Windt DJ, Ren J, Loughran P, et al. Hepatic surgical stress promotes systemic immunothrombosis that results in distant organ injury. *Front Immunol* (2020) 11:987. doi: 10.3389/fimmu.2020.00987

125. Sapisochin G, Bruix J. Liver transplantation for hepatocellular carcinoma: outcomes and novel surgical approaches. *Nat Rev Gastroenterol Hepatol* (2017) 14 (4):203–17. doi: 10.1038/nrgastro.2016.193

126. Costentin CE, Bababekov YJ, Zhu AX, Yeh H. Is it time to reconsider the Milan criteria for selecting patients with hepatocellular carcinoma for deceased-donor liver transplantation? *Hepatology* (2019) 69(3):1324–36. doi: 10.1002/hep.30278

127. Straś WA, Wasiak D, Łągiewska B, Tronina O, Hreńczuk M, Gotlib J, et al. Recurrence of hepatocellular carcinoma after liver transplantation: Risk factors and predictive models. *Ann Transplant.* (2022) 27:e934924. doi: 10.12659/AOT.934924

128. Kim SJ, Kim JM. Prediction models of hepatocellular carcinoma recurrence after liver transplantation: A comprehensive review. *Clin Mol Hepatol* (2022) 28(4): 739–753. doi: 10.3350/cmh.2022.0060

129. European Association for the study of the liver. EASL clinical practice guidelines:Management of hepatocellular carcinoma. *J Hepatol* (2022) 77(2):479–502. doi: 10.1016/j.jhep.2018.03.019

130. Kornberg A, Kaschny L, Kornberg J, Friess H. Preoperative prognostic nutritional index may be a strong predictor of hepatocellular carcinoma recurrence following liver transplantation. *J Hepatocell Carcinoma.* (2022) 9:649–60. doi: 10.2147/JHC.S366107

131. Zhang D, Feng D, Ren M, Bai Y, Lui Z, Wang H, et al. Preoperative serum hepatitis b virus DNA was a risk factor for hepatocellular carcinoma recurrence after liver transplantation. *Ann Med* (2022) 54(1):2213–21. doi: 10.1080/07853890.2022.2107233

132. Yang L, Liu Q, Zhang X, Liu X, Zhou B, Chen J, et al. DNA Of neutrophil extracellular traps promotes cancer metastasis *via* CCDC25. *Nature* (2020) 583 (7814):133–8. doi: 10.1038/s41586-020-2394-6

133. Park J, Wysocki RW, Amoozgar Z, Maiorino L, Fein MR, Jorn J, et al. Cancer cells induce metastasis-supporting neutrophil extracellular DNA traps. *Sci Transl Med* (2016) 8(361):361ra138. doi: 10.1126/scitranslmed.aag1711

134. Snoderly HT, Boone BA, Bennewitz MF. Neutrophil extracellular traps in breast cancer and beyond: current perspectives on NET stimuli, thrombosis and metastasis, and clinical utility for diagnosis and treatment. *Breast Cancer Res* (2019) 21(1):145. doi: 10.1186/s13058-019-1237-6

135. Albrengues J, Shields MA, Ng D, Park CG, Ambrico A, Poindexter ME, et al. Neutrophil extracellular traps produced during inflammation awaken dormant cancer cells in mice. *Science* (2018) 361(6409):eaao4227. doi: 10.1126/science.aao4227

136. Tadie JM, Bae HB, Jiang S, Park DW, Bell CP, Yang H, et al. HMGB1 promotes neutrophil extracellular trap formation through interactions with toll-like receptor 4. *Am J Physiol Lung Cell Mol Physiol* (2013) 304(5):L342–9. doi: 10.1152/ajplung.00151.2012

137. Leach J, Morton JP, Sansom OJ. Neutrophils: Homing in on the myeloid mechanisms of metastasis. *Mol Immunol* (2019) 11:69–76. doi: 10.1016/j.molimm.2017.12.013

138. Leal AC, Mizurini DM, Gomes T, Rochael NC, Saraiva EM, Dias MS, et al. Tumor-derived exosomes induce the formation of neutrophil extracellular traps: Implications for the establishment of cancer-associated thrombosis. *Sci Rep* (2017) 7(1):6438. doi: 10.1038/s41598-017-06893-7

139. Szczerba BM, Castro-Giner F, Vetter M, Krol I, Gkountela S, Landin J, et al. Neutrophils escort circulating tumour cells to enable cell cycle progression. *Nature* (2019) 566(7745):553–7. doi: 10.1038/s41586-019-0915-y

140. Wang H, Zhang Y, Wang Q, Wei X, Wang H, Gu K. The regulatory mechanism of neutrophil extracellular traps in cancer biological behavior. *Cell Biosci* (2021) 11(1):193. doi: 10.1186/s13578-021-00708-z

141. Najmeh S, Cools-Lartigue J, Rayes RF, Gowing S, Vourtzoumis P, Bourdeau F, et al. Neutrophil extracellular traps sequester circulating tumor cells *via* β1-integrin-mediated interactions. *Int J Cancer.* (2017) 140(10):2321–30. doi: 10.1002/ijc.30635

142. Yang LY, Shen XT, Sun HT, Zhu WW, Zhang JB, Lu L. Neutrophil extracellular traps in hepatocellular carcinoma are enriched in oxidized mitochondrial DNA which is highly pro-inflammatory and pro-metastatic. *J Cancer.* (2022) 13(4):1261–71. doi: 10.7150/jca.64170

143. Cheng Y, Gong Y, Chen X, Zhang Q, Zhang X, He Y, et al. Injectable adhesive hemostatic gel with tumor acidity neutralizer and neutrophil extracellular

traps lyase for enhancing adoptive NK cell therapy prevents post-resection recurrence of hepatocellular carcinoma. *Biomaterials* (2022) 284:121506. doi: 10.1016/j.biomaterials.2022.121506

144. Rosell A, Aguilera K, Hisada Y, Schmedes Y, Mackman N, Wallén H, et al. Prognostic value of circulating markers of neutrophil activation, neutrophil extracellular traps, coagulation and fibrinolysis in patients with terminal cancer. *Sci Rep* (2021) 11(1):5074. doi: 10.1038/s41598-021-84476-3

145. Li P, Li M, Lindberg MR, Kennett MJ, Xiong N, Wang Y, et al. PAD4 is essential for antibacterial innate immunity mediated by neutrophil extracellular traps. *J Exp Med* (2010) 207(9):1853–62. doi: 10.1084/jem.20100239

146. Martinod K, Fuchs TA, Zitomersky NL, Wong SL, Demers M, Gallant M, et al. PAD4-deficiency does not affect bacteremia in polymicrobial sepsis and ameliorates endotoxemic shock. *Blood* (2015) 125(12):1948–56. doi: 10.1182/blood-2014-07-587709

147. Manfredi AA, Rovere-Querini P, D'Angelo A, Maugeri N. Low molecular weight heparins prevent the induction of autophagy of activated neutrophils and the formation of neutrophil extracellular traps. *Pharmacol Res* (2017) 123:146–56. doi: 10.1016/j.phrs.2016.08.008

148. Lelliott PM, Momota M, Shibahara T, Lee MSJ, Smith NI, Ishii KJ, et al. Heparin induces neutrophil elastase-dependent vital and lytic NET formation. *Int Immunol* (2020) 32(5):359–68. doi: 10.1093/intimm/dxz084

149. Gollomp K, Kim M, Johnston I, Hayes V, Welsh J, Arepally GM, et al. Neutrophil accumulation and NET release contribute to thrombosis in HIT. *JCI Insight* (2018) 3(18):e99445. doi: 10.1172/jci.insight.99445

150. Perdomo J, Leung HHL, Ahmadi Z, Yan F, Chong JJH, Passam FH, et al. Neutrophil activation and NETosis are the major drivers of thrombosis in heparin-induced thrombocytopenia. *Nat Commun* (2019) 10(1):1322. doi: 10.1038/s41467-019-09160-7

151. Luo Y, Arita K, Bhatia M, Knuckley B, Lee YH, Stallcup MR, et al. Inhibitors and inactivators of protein arginine deiminase 4: functional and structural characterization. *Biochemistry* (2006) 45(39):11727–36. doi: 10.1021/bi061180d

152. Lewis HD, Liddle J, Coote JE, Atkinson SJ, Barker MD, Bax BD, et al. Inhibition of PAD4 activity is sufficient to disrupt mouse and human NET formation. *Nat Chem Biol* (2015) 11(3):189–91. doi: 10.1038/nchembio.1735

153. Li M, Lin C, Deng H, Strnad J, Bernabei L, Vogl DT, et al. A novel peptidylarginine deiminase 4 (PAD4) inhibitor BMS-P5 blocks formation of neutrophil extracellular traps and delays progression of multiple myeloma. *Mol Cancer Ther* (2020) 19(7):1530–8. doi: 10.1158/1535-7163.MCT-19-1020

154. Rayes RF, Mouhanna JG, Nicolau I, Bourdeau F, Giannias B, Rousseau S, et al. Primary tumors induce neutrophil extracellular traps with targetable metastasis promoting effects. *JCI Insight* (2019) 5(16):e128008. doi: 10.1172/jci.insight.128008

155. Chirivi RGS, van Rosmalen JWG, van der Linden M, Euler M, Schmets G, Bogatkevich G, et al. Therapeutic ACPA inhibits NET formation: A potential therapy for neutrophil-mediated inflammatory diseases. *Cell Mol Immunol* (2021) 18(6):1528–44. doi: 10.1038/s41423-020-0381-3

frontiers | Frontiers in Immunology

TYPE Original Research
PUBLISHED 14 April 2023
DOI 10.3389/fimmu.2023.1099017

OPEN ACCESS

EDITED BY
Ljubomir Vitkov,
University of Salzburg, Austria

REVIEWED BY
Violetta Borelli,
University of Trieste, Italy
M. Danilo Boada,
Wake Forest Baptist Medical Center,
United States

*CORRESPONDENCE
Man-Kyo Chung
mchung@umaryland.edu

†These authors have contributed equally to this work

SPECIALTY SECTION
This article was submitted to Molecular Innate Immunity, a section of the journal Frontiers in Immunology

RECEIVED 15 November 2022
ACCEPTED 23 March 2023
PUBLISHED 14 April 2023

CITATION
Siddiqui YD, Nie X, Wang S, Abbasi Y, Park L, Fan X, Thumbigere-Math V and Chung M-K (2023) Substance P aggravates ligature-induced periodontitis in mice. *Front. Immunol.* 14:1099017. doi: 10.3389/fimmu.2023.1099017

Substance P aggravates ligature-induced periodontitis in mice

Yasir Dilshad Siddiqui[1,2†], Xuguang Nie[1†], Sheng Wang[1†], Yasaman Abbasi[1], Lauren Park[1], Xiaoxuan Fan[3], Vivek Thumbigere-Math[4] and Man-Kyo Chung[1*]

[1]Program in Neuroscience, Center to Advance Chronic Pain Research, Department of Neural and Pain Sciences, School of Dentistry, University of Maryland, Baltimore, MD, United States, [2]Department of Preventive Dentistry, College of Dentistry, Jouf University, Sakaka, Saudi Arabia, [3]Department of Microbiology and Immunology, Flow Cytometry Shared Service, University of Maryland School of Medicine, Baltimore, MD, United States, [4]Department of Advanced Oral Sciences and Therapeutics, University of Maryland School of Dentistry, Baltimore, MD, United States

Periodontitis is one of the most common oral diseases in humans, affecting over 40% of adult Americans. Pain-sensing nerves, or nociceptors, sense local environmental changes and often contain neuropeptides. Recent studies have suggested that nociceptors magnify host response and regulate bone loss in the periodontium. A subset of nociceptors projected to periodontium contains neuropeptides, such as calcitonin gene-related peptide (CGRP) or substance P (SP). However, the specific roles of neuropeptides from nociceptive neural terminals in periodontitis remain to be determined. In this study, we investigated the roles of neuropeptides on host responses and bone loss in ligature-induced periodontitis. Deletion of tachykinin precursor 1 (*Tac1*), a gene that encodes SP, or treatment of gingiva with SP antagonist significantly reduced bone loss in ligature-induced periodontitis, whereas deletion of calcitonin related polypeptide alpha (*Calca*), a gene that encodes CGRP, showed a marginal role on bone loss. Ligature-induced recruitment of leukocytes, including neutrophils, and increase in cytokines leading to bone loss in periodontium was significantly less in *Tac1* knockout mice. Furthermore, intra-gingival injection of SP, but not neurokinin A, induced a vigorous inflammatory response and osteoclast activation in alveolar bone and facilitated bone loss in ligature-induced periodontitis. Altogether, our data suggest that SP plays significant roles in regulating host responses and bone resorption in ligature-induced periodontitis.

KEYWORDS

***Tac1*, substance P, periodontitis, mouse model, osteoclasts, cytokines, neutrophils**

1 Introduction

Periodontitis is a common oral disease affecting over 40% of the adult population in the United States (1). It is primarily due to the result of microbial dysbiosis and the dysregulation of host inflammatory responses (2, 3). Persistent and uncontrolled inflammation in periodontitis leads to a progressive loss of periodontal tissues, including

the alveolar bones that support the teeth. Alveolar bone is maintained by constant mechanical stimulation from the tooth and undergoes vigorous remodeling throughout life. Alveolar bone disruption that occurs in periodontitis is irreversible and is the primary cause of tooth loss.

The host inflammatory response to periodontal infection is regulated by a number of factors, including sensory neurons that innervate the periodontal tissues (4, 5). These sensory neurons transduce various noxious mechanical, thermal, and chemical stimuli. Among these, nociceptive afferents expressing transient receptor potential cation channel subfamily V member 1 (TRPV1), are largely peptidergic afferents that secrete a variety of neuropeptides to regulate the inflammatory process (6). Substance P (SP) and calcitonin gene-related peptide (CGRP) are the most abundant neuropeptides. Recent studies have suggested that nociceptors play a regulatory role in periodontitis (4, 5, 7). We have demonstrated that the activity of nociceptors exaggerates inflammatory tissue responses and facilitates bone loss in a mouse periodontitis model (4). Infection with pathogenic microbes leads to the activation of TRPV1 and transient receptor potential cation channel subfamily A member 1 (TRPA1), which are enriched in the peptidergic nerve terminals, and mediate the Ca^{2+}-dependent release of neuropeptides causing neurogenic inflammation (8–10). SP and CGRP are implicated in multiple biological processes including inflammation (11, 12); however, the specific role of these neuropeptides from these nociceptive terminals in periodontitis remains to be determined.

SP was identified as an early marker for gingival inflammation in experimental periodontitis in humans (13). SP has been detected at significantly higher levels in the gingival crevicular fluid of patients with periodontitis than normal, and its level decreases after effective treatment (14–17). In contrast, CGRP is present in human gingival crevicular fluid at lower levels at sites of periodontitis than at healthy sites (18–20). Given that CGRP and SP are known to affect bone remodeling, they may serve as neurogenic factors that contribute to the regulation of host responses and alveolar bone loss in the periodontium. Therefore, in this study, we used genetically engineered mouse models to investigate the roles of neuropeptides in ligature-induced periodontitis.

2 Materials and methods

2.1 Experimental mouse models

All animal procedures were performed in accordance with the NIH Guide for the Care and Use of Laboratory Animals (Publication 85–23, Revised 1996) and were performed according to the University of Maryland-approved Institutional Animal Care and Use Committee protocols and the ARRIVE guidelines. C57BL/6 mice, *Tac1*$^{-/-}$ (Jax, 004103), and *Calca*$^{Cre/Cre}$ mice (Jax, 033168) were obtained from the Jackson Laboratory. *Calca*^{Cre} is a knock-in/knock-out line in which Cre is targeted to the first coding exon of the mouse *Calca* gene, and therefore homozygote knock-in mice do not express *Calca*. Both *Tac1*$^{-/-}$ and *Calca*$^{Cre/Cre}$ mice procreate normally. Eight-week-old male and female mice were used in each experimental group. In all assays, the animals were randomly allocated to the experimental groups. Animals were group-housed under standard conditions with ad libitum access to water and food. The experimenters were blinded for the treatment groups during the analysis of the data in each assay.

2.2 Ligature-induced periodontitis

Mice were anesthetized using ketamine/xylazine (100-150 mg/kg of ketamine and 10-20 mg/kg of xylazine). A 5-0 silk ligature was placed around the second maxillary molar (M2), which remained in place in all mice throughout the experimental period. The suture was tied gently to prevent damage to the periodontal tissue. The ligatures remained in place in all mice throughout the indicated experimental period.

2.3 Micro-focus computed tomography

The animals were anesthetized with ketamine/xylazine and euthanized *via* transcardial perfusion using 4% PFA (4). Maxillae were hemisected and micro-focus computed tomography (μCT) images were obtained using a Siemens Inveon Micro-PET/SPECT/CT (Siemens, Ann Arbor, MI) at a 9 μm spatial resolution. Siemens Inveon Research Workplace 4.2 software was used for image acquisition and processing, 2-D and 3-D image viewing, and quantitative analysis. Unless otherwise indicated, bone loss was evaluated from the buccal side. To assess the levels of periodontal bone loss, four linear measurements were taken following 3-D reconstruction of the μCT scans. Bone loss was evaluated on the distal side of the distobuccal root of the first molar (M1), the mesial side of the mesiobuccal root of the second molar (M2), the distal side of the distobuccal root of M2, and the distal side of the distobuccal root of the third molar (M3). Unless otherwise indicated, distances from the cement-enamel junction (CEJ) to the most apical site of bone destruction were measured. Four measurements were averaged to obtain the distance from the CEJ.

2.4 Tissue processing and immunohistochemistry

Immunohistochemical assays of the trigeminal ganglion (TG) and maxillae were performed as previously described (4, 21–23). Maxillae were decalcified in 0.5M Ethylenediaminetetraacetic acid (EDTA) in PBS (pH 7.4) over the course of 14 days. Tissue processing was performed at the Histology Core at the University of Maryland School of Medicine for paraffin embedding and the tissues were sectioned at 5 μm. Some tissues were cryoprotected and cryosectioned at a thickness of 12 μm for TG and 30 μm for the decalcified maxillae. Immunohistochemical assays were performed using rat anti-substance P (Sigma-Aldrich, #MAB356), rabbit anti-TRPV1 (kindly provided by Dr. Michael Caterina at Johns Hopkins University), anti-CGRP (Millipore, #C7113, rabbit or Penninsula lab, guinea pig). pan-cytokeratin (BLD, #914204; mouse), and

rabbit anti-CD45 (abcam, #ab10558; rabbit). The specificity of the anti-TRPV1 and anti-CGRP was previously verified (24, 25). SP primary antibody was validated by using *Tac1*$^{-/-}$ mice. The sections were further incubated with appropriate secondary antibodies for two hours at room temperature. Tooth sections were stained with 4',6-diamidino-2-phenylindole (DAPI) to visualize the cellular nuclei.

2.5 Tartrate-resistant acid phosphatase (TRAP) staining

Maxillae were fixed overnight with 4% paraformaldehyde at 4°C and decalcified in 0.5M ethylenediaminetetraacetic acid (EDTA) for two weeks at room temperature. The decalcified tissues were dehydrated, embedded in paraffin, and sectioned into 5 µm slices. TRAP and alkaline phosphatase (ALP) staining was conducted using a commercial kit (#29467001; Fujifilm Wako Pure Chemical Corporation, Richmond, VA, USA), following the manufacturer's protocol, with some modifications. Briefly, deparaffinized and rehydrated sections were incubated in acetate-tartaric acid buffer containing naphthol ASMX phosphate and Fast Red TR (TRAP substrate). The staining process was monitored until the color reaction became distinct. After washing, tissues were counterstained with the nuclear staining solution. In an experiment, ALP staining was performed together with TRAP staining, but it was not quantified. Digital images were scanned using an Aperio scanning system (Leica, Wetzlar, Germany). To quantify the numbers of osteoclasts in the interradicular alveolar bone surface, we selected images showing the tooth roots of both the first and second molars and the second and third molars. Dense, purple-colored, TRAP-stained multinucleated osteoclasts on the surface of bone between the roots from two teeth were counted. The number of osteoclasts from each region was normalized to the perimeter of the bone surface assessed, to calculate the number of osteoclasts per millimeter (TRAP+ cells/mm) of each sample.

2.6 Retrograde labeling of periodontal afferents

In C57BL/6 mice anesthetized with ketamine/xylazine, fluoro-gold (FG) (Fluorochrome LLC, Denver, CO, USA) was injected into the gingiva around the maxillary first molar to retrogradely label the periodontal afferents in the TG as described previously (23). FG was dissolved in 0.9% saline at a concentration of 4%. A 50 µl Hamilton syringe was used to slowly inject 5 µl of tracer into five sites (1 µl per site) on the gingiva around the distobuccal groove, buccal groove, mesial groove, palatal groove, and the distopalatal groove of the first maxillary molar. On seven days after injection, the ligature was placed around the maxillary first molar. The unligatured side was used as control. After two weeks, the mice were euthanized by transcardial perfusion for further histological study. After performing IHC, the FG signal was identified under a gold filter (11006v2, Chroma, Bellows Falls, VT, USA). We used Image J to calculate the surface area of the cells. We followed the criteria for neuronal size classification (small, < 300 µm^2; medium, 300 to 600 µm^2; large, > 600 µm^2) (22, 26).

2.7 Flow cytometry

Mice were anesthetized using ketamine/xylazine and transcardial perfusion was performed using >20 ml PBS to flush out the immune cells from the vasculature. To dissect out the gingival blocks, vertical incisions were made immediately anterior to the maxillary M1 and posterior to the M3, and horizontal incisions were made at the border of the gingiva on both the buccal and palatal sides. Gingival tissues from the unligatured side were used as controls. The gingival tissues were processed as previously described (4, 27). The gingival tissues were digested in a mixture of 3.2 mg/ml type IV collagenase (Invitrogen, 17104019) and 0.15 µg/ml DNase (Sigma, DN25) in media for 25 min at 37°C with gentle shaking. Then EDTA was added to a final concentration of 2 mM, and the solution was incubated for 5 min. The enzymes were prepared in a complete media containing RPMI with 2 mM L-glutamine, 100 units/ml penicillin, 100 µg/ml streptomycin, and 10% fetal bovine serum. The enzyme-digested gingival tissues and media were mashed through a cell strainer with a pore size of 70 µm, and additional cold DNase media was added. The cell suspension was centrifuged at 4°C, at 314×g for 6 min, and the pellet was resuspended in 100 µl cold PBS containing 0.5% FBS. Gingival tissues and single cell suspensions obtained from two separate mice in the same experimental group were pooled for one flow cytometry experiment. Single cell suspensions obtained from two separate mice in the same experimental group were pooled for one flow cytometry experiment. CD45-PE, CD11b-BV421, and Ly6G-PE-Cy7 antibodies were used to identify neutrophils. Flow cytometry analysis was performed within 2 hours on Cytek Aurora flow cytometer (3 lasers: 405nm, 488nm, 640nm; Cytek Biosciences, San Jose, CA, USA). The spectral data were unmixed based on single color compensation beads controls and analyzed using FCS Express 7 software (*De Novo* Software, Pasadena, CA, USA). Neutrophils were defined by 7-AAD$^-$/CD45$^+$/Ly6G$^+$/CD11b$^+$. Percentages of each cell population in live, single cells were calculated for comparisons between groups.

2.8 Gingival injection of the drugs

Gingival injections of drugs were performed using an insulin syringe with a 31G needle under isoflurane anesthesia. SP (Sigma-Aldrich, # S6883; 1 µg/site), QWF (Tocris, #6645; 2 µg/site), neurokinin A (NKA; MilliporeSigma, # 86933746; 1 µg/site) or vehicles (PBS or dimethyl sulfoxide) were injected into the proximal and distal areas of the gingiva around M2.

2.9 Luminex multiplex assay

The mice were euthanized following anesthesia with ketamine/xylazine, and maxillae, including the gingiva, alveolar bone, and three molars, were dissected out. Whole tissues were ground in a

buffer (210 µl; 50 mM Tris, 2 mM EDTA pH 7.5) containing a protease/phosphatase inhibitor cocktail (5872S; Cell Signaling Technology, Danvers, MA, USA) using a tissue grinder (Pyrex PTFE Pestle Tissue Grinder with Steel Shaft). After spinning down for 5 min at 1000 g at 4°C, the supernatant was collected and frozen on dry ice. Luminex multiplex cytokine assays were performed using Mouse Luminex Discovery Assay Kits (R&D Systems, Minneapolis, MN, USA) and a Luminex 100 Multi-analyte System (Luminex, Chicago, IL, USA).

2.10 Quantification and statistical analysis

All data are presented as mean ± SEM. The data were analyzed using Student's t-tests, a one-way ANOVA, and a two-way ANOVA followed by *post hoc* assays, as indicated in the figure legends, using GraphPad Prism 7 (GraphPad Software, San Diego, California USA). Comparisons of distributions of neuronal sizes between two groups were performed using Mann-Whitney test. A value of $P< 0.05$ was considered statistically significant.

3 Results

3.1 *Tac1* knockout mice show reduced bone loss in periodontitis

A subset of TG neurons retrogradely labeled from gingiva expressed SP, CGRP, and TRPV1 (Figures 1A, B). The FG-labeled gingival TG neurons were largely small- (52.4%) or medium- (42.2%) sized neurons with only a few large-sized neurons (5.4%) (Figure 1C). We previously showed that 23% of TG neurons retrogradely labeled from gingiva expressed CGRP, which is highly co-expressed with TRPV1 (23). Approximately 15% of the FG-labeled neurons express SP or TRPV1, and approximately 10% of the labeled neurons co-express SP and TRPV1. The majority of SP+, CGRP+, or TRPV1+ neurons were small-sized neurons (Figure 1D). FG+/SP+ neurons were significantly larger than FG-negative SP+ neurons (red). FG+/TRPV1+ neurons were also significantly larger than FG-negative TRPV1+ neurons (blue). In contrast, FG+/CGRP+ neurons were not significantly different from FG-negative CGRP+ neurons (green). However, the size distribution of FG+/SP+ and FG+/CGRP+ neurons were not significantly different. SP+ nociceptive afferents abundantly project to the gingiva and periodontal ligaments (Figures 1E, F). In contrast, SP was undetectable in *Tac1* KO mice, confirming SP deficiency in this line. CGRP+ nociceptive terminals were also detected from periodontia (Figure 1G). These data suggest that SP + or CGRP+ afferents represent a subpopulation of sensory neurons innervating periodontal tissues.

To determine functional roles of SP and CGRP, encoded by *Tac1* and *Calca* gene respectively, we used *Tac1* and *Calca* knockout mice for ligature-induced periodontitis experiments. *Tac1* knockout (KO) mice ($Tac1^{-/-}$) were viable and exhibited a hypoalgesia phenotype (28). We first examined ligature-induced bone loss in the *Tac1* KO mice *via* µCT. Two weeks after placing the ligature, wild type (WT) mice showed remarkable alveolar bone loss in both the buccal and palatal sides as indicated by a decrease in alveolar bone height, as well as buccal bone plate disruption (Figures 2A–C). In contrast, *Tac1* KO mice exhibited an obviously reduced loss of the alveolar bones compared to WT controls. Specifically, alveolar bone height reduction and buccal bone disruption were less severe, and the buccal bone plate showed fenestration rather than complete resorption on the crest (Figures 2B, C). Consequently, the distance from CEJ to buccal alveolar bone crest (B-Crest) was significantly less in *Tac1* KO than WT, although the distance from CEJ to the most apical site of bone destruction (B-max) was not significantly different. Bone loss in palatal side was also significantly less in *Tac1* KO than WT. In histological sections, bone loss was more prominent in WT than in *Tac1* KO after ligature, whereas alveolar bone without ligature was comparable (Figure 2D). Different extent of bone loss between genotypes are unlikely due to the different extent of mucosal damage since cytokeratin-expressing gingival epithelia were comparable (Figure 2E).

We assessed if ligature-induced periodontitis produces changes in SP or TRPV1 expression in TG. The retrogradely labeled FG+ TG neurons from mice with ligature showed a slight but significant increase in neuronal sizes compared to controls (Figure 2F). The proportions of FG+/SP+ neurons, FG+/TRPV1+ neurons, or FG +/SP+/TRPV1+ neurons were not significantly different between the control and the ligature group (Figure 2G), suggesting that altered expressions of SP or TRPV1 in gingival afferents are not major contributors to the nociceptor regulation of periodontitis. Interestingly, the size distributions of FG+/SP+, FG+/TRPV1+, or FG+/SP+/TRPV1+ neurons were significantly larger in the ligature group than in controls, although the extent of such changes was modest (Figure 2H).

3.2 *Calca* deletion shows a marginal role in bone loss in periodontitis

Since CGRP is another type of neuropeptide abundantly expressed in nociceptors, we therefore also examined the involvement of CGRP in ligature-induced bone loss by using *Calca* KO mice that are deficient of CGRP (Figure 3). We found that ligature-induced bone loss in *Calca* KO mice was comparable to WT, suggesting that net effects of global knockout of CGRP may not significantly impact bone resorption in periodontitis.

3.3 *Tac1*-encoded neuropeptides modulate osteoclast activation and host immune responses in periodontitis

In agreement with reduced bone loss, TRAP staining revealed that osteoclast numbers outlining the bone surfaces were also decreased in *Tac1* KO mice in comparison to controls. These histological studies were conducted five days after ligature placement, when osteoclasts and bone resorption were more actively ongoing than at the two-week time point (Figures 4A–D). Osteoclasts activities were comparable between genotypes without

ligature (Figure 4E). In ligature groups, ALP activities were observed along the bone surfaces in both *Tac1* KO and WT mice in comparable extents, suggesting that *Tac1* KO did not substantially affect the bone formation process (Figure 4F).

Given that the regulation of host responses by neuropeptides underlies the neural regulation of barrier tissue functions, we further investigated the role of *Tac1* in the recruitment of immune cells to sites of periodontitis. We performed flow cytometry assays using cells collected from gingiva with and without ligature in WT and *Tac1* KO mice. The proportion of total CD45+ leukocytes (Figure 5A) and neutrophils (Figure 5B) were significantly greater in periodontia from the ligature side than from the control side in WT mice. In comparison, the proportion of ligature-induced total CD45+ leukocytes and neutrophils were significantly reduced in *Tac1* KO mice compared to WT (Figures 5C, D). Consistently, immunohistochemical labeling of CD45 in periodontia with ligatures also demonstrated limited recruitment of CD45+ cells in *Tac1* KO mice relative to controls (Figure 5). Furthermore, cytokines associated with inflammatory responses, such as tumor necrosis factor, interleukin 1β, and receptor activator of nuclear factor kappa- B ligand (RANKL), were significantly lower in the periodontia of *Tac1* KO mice than WT (Figure 6). Altogether, these results indicate that *Tac1* KO mice exhibit reduced host response in ligature-induced periodontitis and suggest that SP is a major neurogenic regulator of host immune responses and alveolar bone loss in periodontitis.

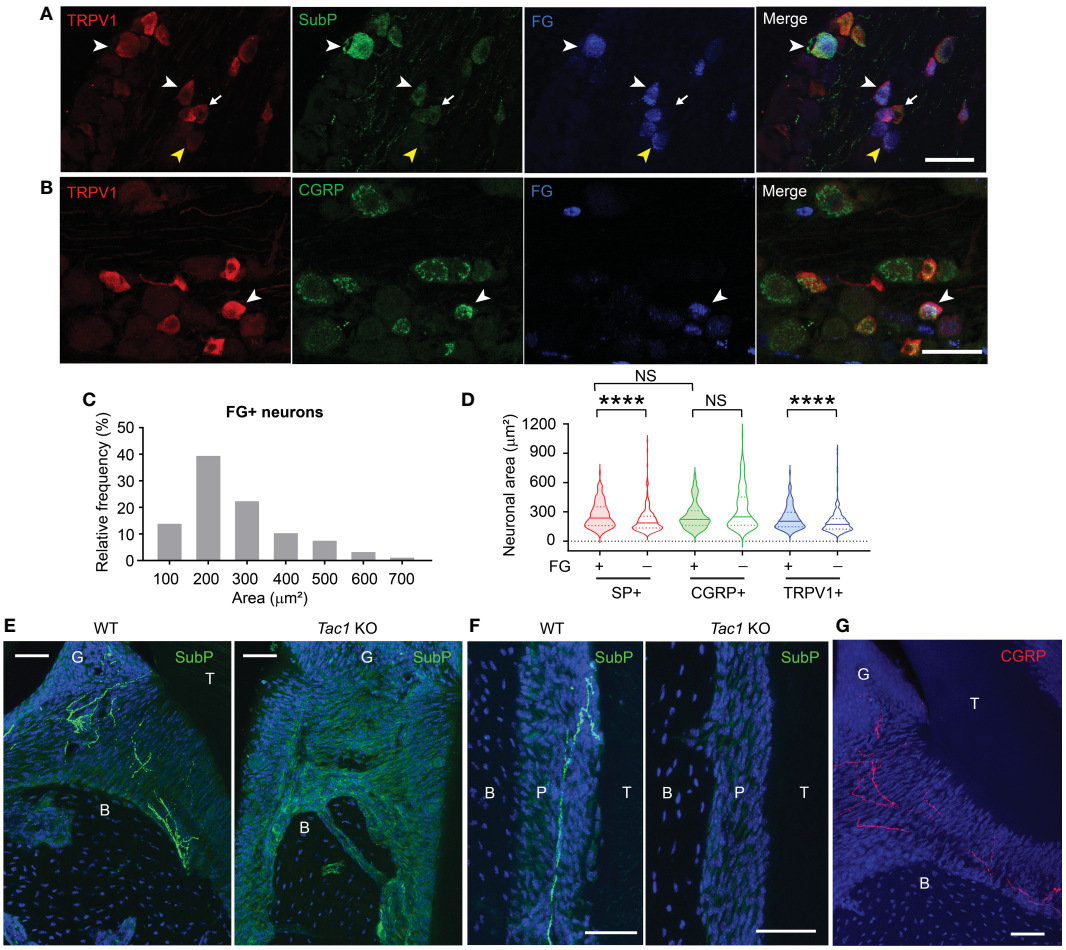

FIGURE 1
Substance P and CGRP is expressed in small to medium-sized gingival afferents. **(A)** Representative images of immunohistochemical labeling of TRPV1 (red) and substance P (SubP; green) in trigeminal ganglia (TG). Periodontal afferents were labeled by Fluoro-gold (FG), a retrograde tracer, injected into the gingiva around the maxillary second molar. White arrowheads indicate examples of FG+/TRPV1+/SP+ neurons in TG sections. The yellow arrowhead indicates an example of FG+/TRPV1+/SP-negative neuron. The arrow indicates FG-negative TRPV1+/SP+ neuron. Scale bar, 50 μm. **(B)** Representative images of immunohistochemical labeling of TRPV1 (red) and CGRP (green) in TG retrogradely labeled by FG from gingiva. The white arrowhead indicates an example of FG+/TRPV1+/CGRP+ neuron. Scale bar, 50 μm. **(C)** Size distribution of FG-labeled gingival afferents (1,234 neurons from five TG). **(D)** Violin plots comparing the size distribution of FG+ or FG-negative SP+ (red), CGRP+ (green), or TRPV1+ (blue) neurons. N=159, 231, 75, 219, 147, and 257 neurons. ****p<0.0001 in Mann-Whitney test. NS, not significant. **(E–G)** Immunohistochemical labeling of SP (green; **E, F**), CGRP (red; **G**) and DAPI (blue) in decalcified periodontia of *Tac1* KO or WT mice **(E, F)** or C57bl/6 **(G)** mice. B, bone; G, gingiva; P, periodontal ligament; T, tooth. Scale bar, 50 μm. NS, not significant.

10.3389/fimmu.2023.1099017

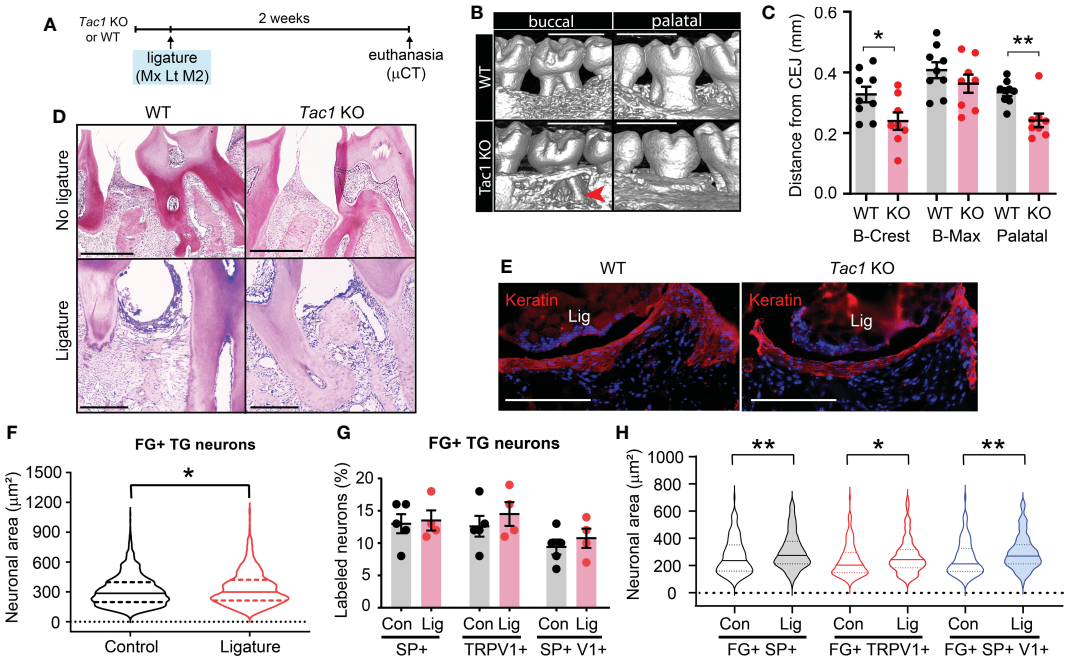

FIGURE 2
Knockout of *Tac1* reduces ligature-induced bone loss. **(A)** Time course of the experiments. Mx, Maxilla; Lt, left side ligature. **(B)** µCT examination of the effect of *Tac1* KO on bone loss two weeks after ligature placement. Arrowhead, fenestration of buccal alveolar bone on the distobuccal root of M2. Scale bar, 1 mm. **(C)** Quantification of bone loss. *p < 0.05, **p<0.01 in Student's t-tests. N=9 in WT and 8 in KO. **(D)** H&E staining of decalcified periodontia of WT and *Tac1* KO with (bottom) or without ligature (top). Scale bar, 200 µm. **(E)** Immunohistochemical labeling of pan-cytokeratin (red) in WT and *Tac1* KO 5 days after ligature. Blue, DAPI. Scale bar, 200 µm. Lig, ligature. **(F)** Violin plots comparing the frequency distribution of FG+ neuronal areas in TG from C57bl/6 mice in control and ligature side (N=1,234 neurons from five TG in control; N=779 from four TG in ligature group). Solid line within the plot, median; dotted lines, quartiles. *p<0.05 in Mann-Whitney test. **(G)** Proportions of SP+, TRPV1+, or SP+/TRPV1+ neurons among FG+ TG neurons in the control (Con) and the ligature (Lig) group. Each point indicates a proportion in a ganglion. N=5 in the control and 4 in the ligature group. 151 to 428 FG-labeled neurons per ganglia were quantified. **(H)** Violin plots comparing the size distribution of FG+/SP+ (black), FG+/TRPV1+ (red), or FG+/SP+/TRPV1+ (blue) neurons in the control (Con) or the ligature (Lig) group (N=159, 106, 147, 118, 111, and 85 neurons). Solid line within the plot, median; dotted lines, quartiles. * p<0.05; **p<0.01 in Mann-Whitney test.

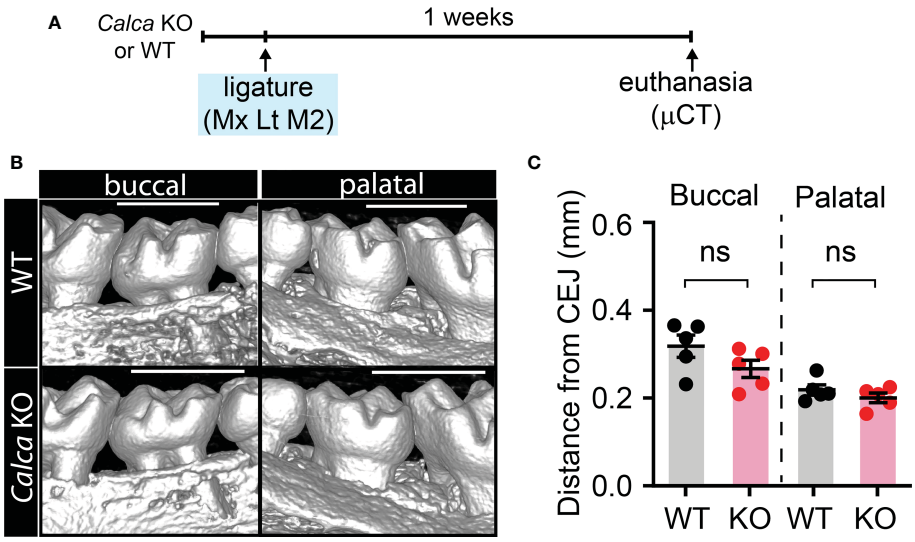

FIGURE 3
Knockout of *Calca* does not affect ligature-induced bone loss. **(A)** Time course of the experiments. **(B)** µCT analysis of bone loss one week after ligature placement in $Calca^{Cre/Cre}$, in which Cre is knocked into the locus of *Calca* without expression of *Calca*. Scale bar, 1 mm. **(C)** Quantification of bone loss. N=5 per group. ns, not significant.

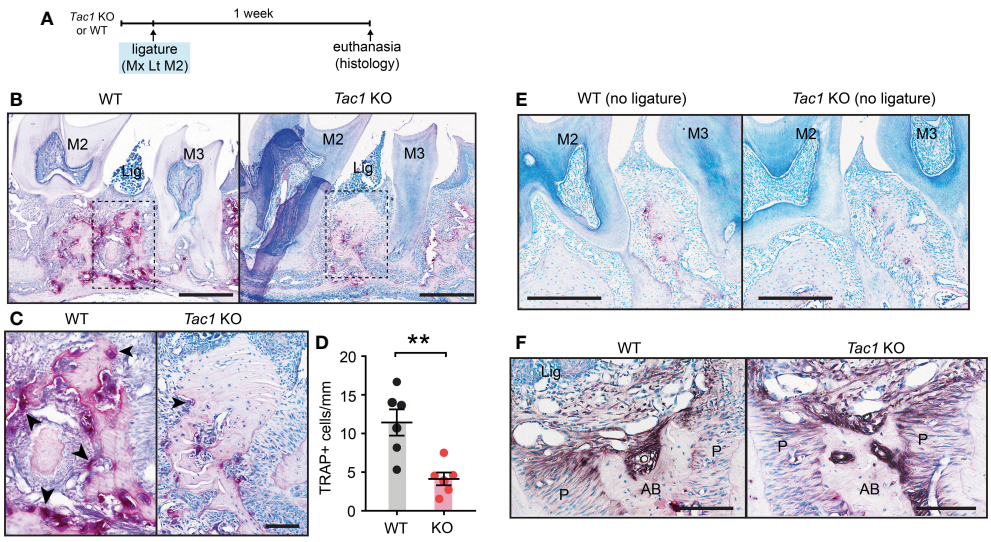

FIGURE 4
Knockout of *Tac1* reduces ligature-induced activation of osteoclasts. **(A)** Time course of the experiments. **(B)** TRAP staining five days after ligature placement in *Tac1* KO and WT mice. Lig, ligature; M2, second molar; M3, third molar. Scale bar, 500μm. **(C)** Magnified view of the insets in **(A)** Scale bar, 100μm. **(D)** Quantification of TRAP+ cells. **p < 0.01 in Student's t-tests. N=6 per group. **(E)** TRAP staining of periodontia without ligature in WT and *Tac1 KO* mice. Scale bar, 200μm. **(F)** Alkaline phosphatase staining in *Tac1* KO and WT mice. Scale bar, 100μm. AB, alveolar bone; Lig, ligature; P, periodontal ligament.

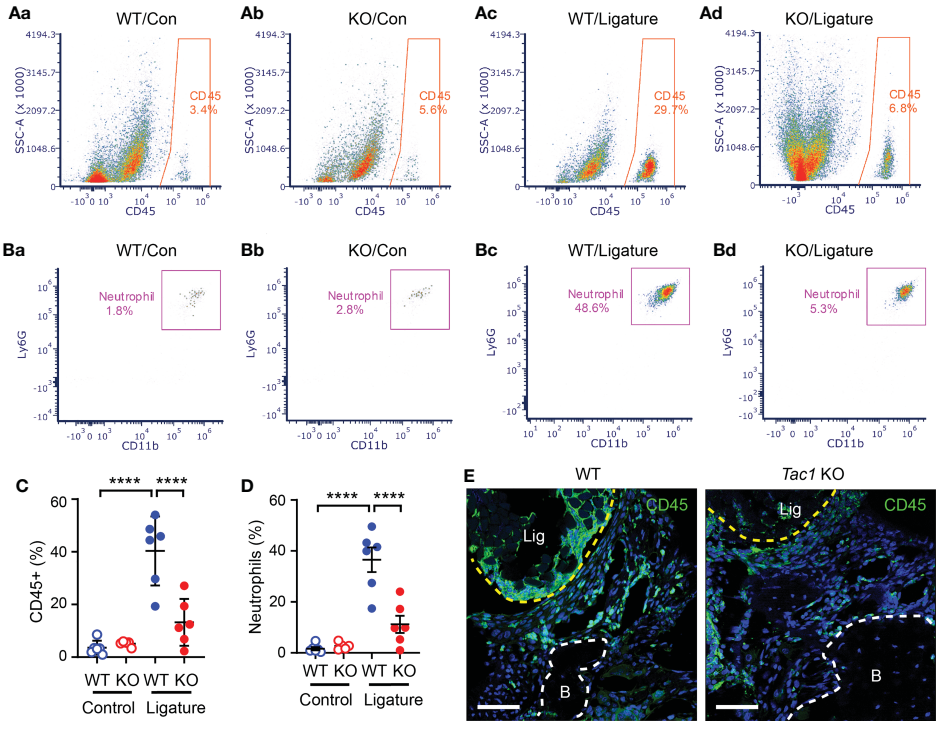

FIGURE 5
SP knockout reduces ligature-induced host responses at the site of periodontitis. **(A, B)** Flow cytometry was performed to identify the proportion of immune cells in single-cell suspensions from gingiva in control (Con; a-b) or ligature side (Ligature; c-d) in WT or *Tac1* KO mice two weeks after ligature placement. The percentage in each plot represents the fraction of the given cells out of live, single cells in each sample. Examples of total CD45+ leukocytes **(A)** and neutrophils **(B)** in WT/control, KO/control, WT/ligature, and KO/ligature groups are shown. **(C, D)** Proportions of CD45+ or neutrophils in live, single cells in each sample are plotted. ****p <0.0001 in Sidak *post hoc* tests following one-way ANOVA. N=6 per group. **(E)** Immunohistochemical labeling of CD45 in a periodontium under ligature (Lig; yellow dotted line) in WT or Tac1 KO mice two weeks after placing the ligature. Scale bar, 50 μm. B, alveolar bone; Lig, ligature.

3.4 Exogenous SP, but not NKA, induces inflammatory responses and promotes ligature-induced bone loss

Since *Tac1* encodes both SP and NKA and both are detected in human gingiva crevicular fluid (17, 29), we determined if local injection of exogenous SP or NKA into gingiva is sufficient to induce osteoclastic activities and gingival inflammation. Results showed that injections of SP alone without periodontal ligature increased the number of osteoclasts along the bone surfaces of the injected areas (Figures 7A–C). Moreover, infiltration of CD45+ cells was also increased in SP-injected areas compared to vehicle-injected areas (Figures 7D–F). In contrast, the injection of exogenous NKA did not induce the osteoclast activity (Figures 8A–C) or CD45+ cell infiltration (Figures 8D, E). These results support the idea that Tac1 KO phenotypes inducing the inflammatory responses and osteoclasts activation are dominantly mediated by SP, but not by NKA.

To further test the roles of exogenous SP in periodontitis, we examined ligature-induced bone loss in mice with local injections of SP or vehicle (Figure 9). Consistently, the SP-injected group demonstrated more vigorous bone resorption compared to the Veh-injected group.

3.5 Pharmacological inhibition of SP receptors decreases ligature-induced bone loss resembling *Tac1* KO mice

We also determined the effects of inhibiting SP receptors in the periodontium by performing gingival injections of QWF, a tripeptide SP antagonist, or vehicle with periodontal ligature (Figures 10A–D). Results showed that QWF injection significantly decreased bone loss compared to the vehicle injection, which is consistent with the effects of *Tac1* KO.

4 Discussion

It has been suggested that there are neural regulatory mechanisms for bone homeostasis, with sensory neurons playing an important role in regulating bone metabolism and remodeling (30, 31). Dysregulation of neural activity is involved in a number of pathological conditions affecting the skeletons. Recently, we showed that chemical ablation of nociceptors by resiniferatoxin (RTX) or chemogenetic silencing of TRPV1-lineage afferents reduced bone loss in a periodontitis mouse model (4). Here, we have further demonstrated that periodontal ligature applied to *Tac1* KO mice reduces alveolar bone loss, activation of osteoclasts, the recruitment of inflammatory cells to the periodontium, and cytokine levels. These results fully recapitulate the phenotype of mice with RTX induced-ablation or chemogenetic silencing of nociceptors. Moreover, we have shown that SP injections alone are sufficient to induce robust inflammation and bone resorption in the periodontium, while local pharmacological inhibition of SP receptors in gingiva decreases bone loss. Altogether, our data indicate that nociceptor Mediated SP signaling plays an important role in regulating bone resorption in periodontitis. In contrast, while CGRP has been suggested as an anabolic regulator of alveolar bone loss through *in vitro* assays (7), we found that *Calca* KO mice did not show significant differences in alveolar bone loss *in vivo*. We assume that CGRP-mediated anabolic effects are

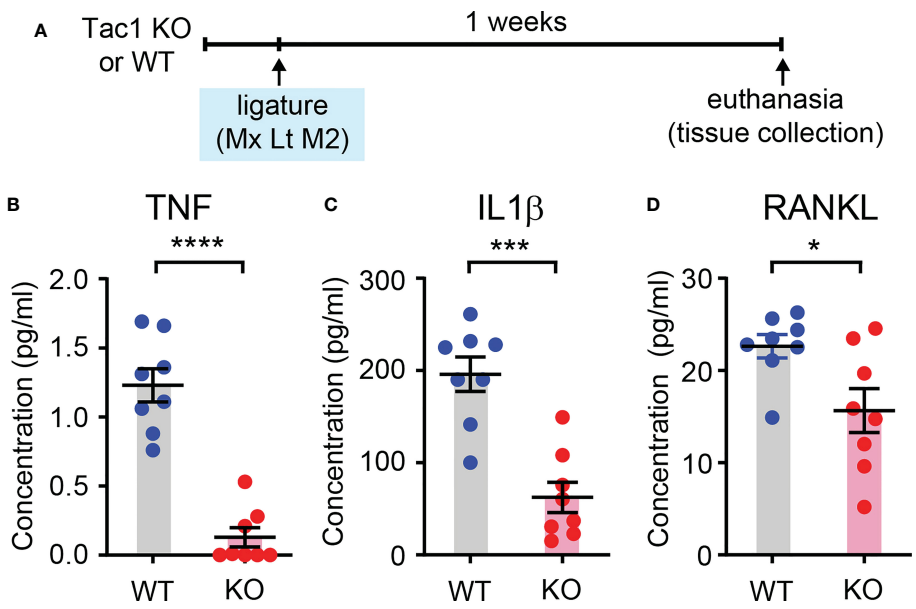

FIGURE 6
SP knockout decreases proinflammatory cytokines in periodontium. **(A)** Time course of the experiment. Luminex assay for measuring tumor necrosis factor (TNF; **B**), interleukin 1β (IL1βγ **C**) and receptor activator of nuclear factor kappa- B ligand (RANKL; **D**) in periodontia from WT or *Tac1* KO mice. The mice were euthanized two weeks after placing the ligature. *p<0.05; ***p<0.0005; ****p<0.0001. N=8 per group.

10.3389/fimmu.2023.1099017

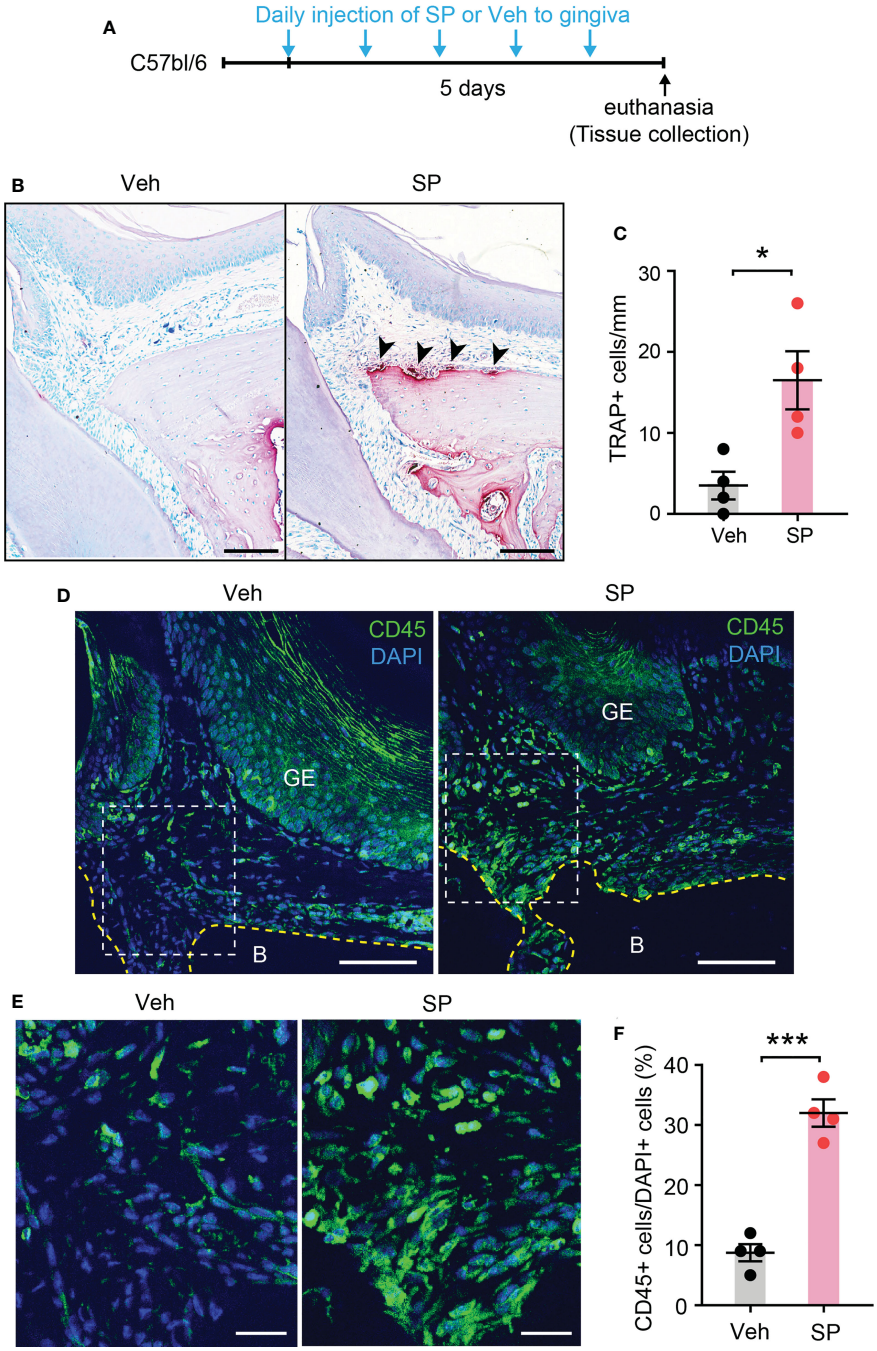

FIGURE 7
Exogenous injection of SP is sufficient to activate osteoclasts and to recruit immune cells in periodontium. **(A)** Time course of the experiment. **(B)** TRAP staining in substance P (SP; 1 µg/site)- or vehicle (Veh) injected into a periodontium. Scale bar, 100 µm. **(C)** Quantification of TRAP+ cells of the injected periodontia. *, p<0.05 in Student's t-test. N=4 mice per group. **(D)** Immunofluorescence for CD45 in a periodontium injected with Veh or SP. Scale bar, 100µm. B, bone; GE, gingival epithelium. **(E)** Magnified view of the insets in panel **(D)** Scale bar, 30µm. **(F)** Quantification of CD45+ cells. Percentage of the number of CD45+ cells among DAPI+ cells in gingival epithelium and connective tissues within 600 µm distance to tooth surface was calculated. ***p<0.0001 in Student's t-test. N=4 mice per group.

overwhelmed by the catabolic effects of SP, and the simultaneous release of SP and CGRP from nociceptor terminals induces a net increase in bone loss.

Retrograde labeling of gingival afferents showed that >90% of gingival afferents are small to medium-sized neurons. This is in contrast with pulpal afferents, in which large-sized neurons are highly enriched (49%) (22). Our previous (23) and the current study showed that 23% and 15% of gingival afferents express CGRP and SP, respectively. Therefore, it would be reasonable to estimate that approximately a quarter of gingival afferents are peptidergic afferents. The proportion of the SP+ or TRPV1+ gingival afferents was not changed after placing the ligature. Inflammation of masseter muscle produced by complete Freund's adjuvant upregulates the expression of SP and TRPV1 in TG whereas

10.3389/fimmu.2023.1099017

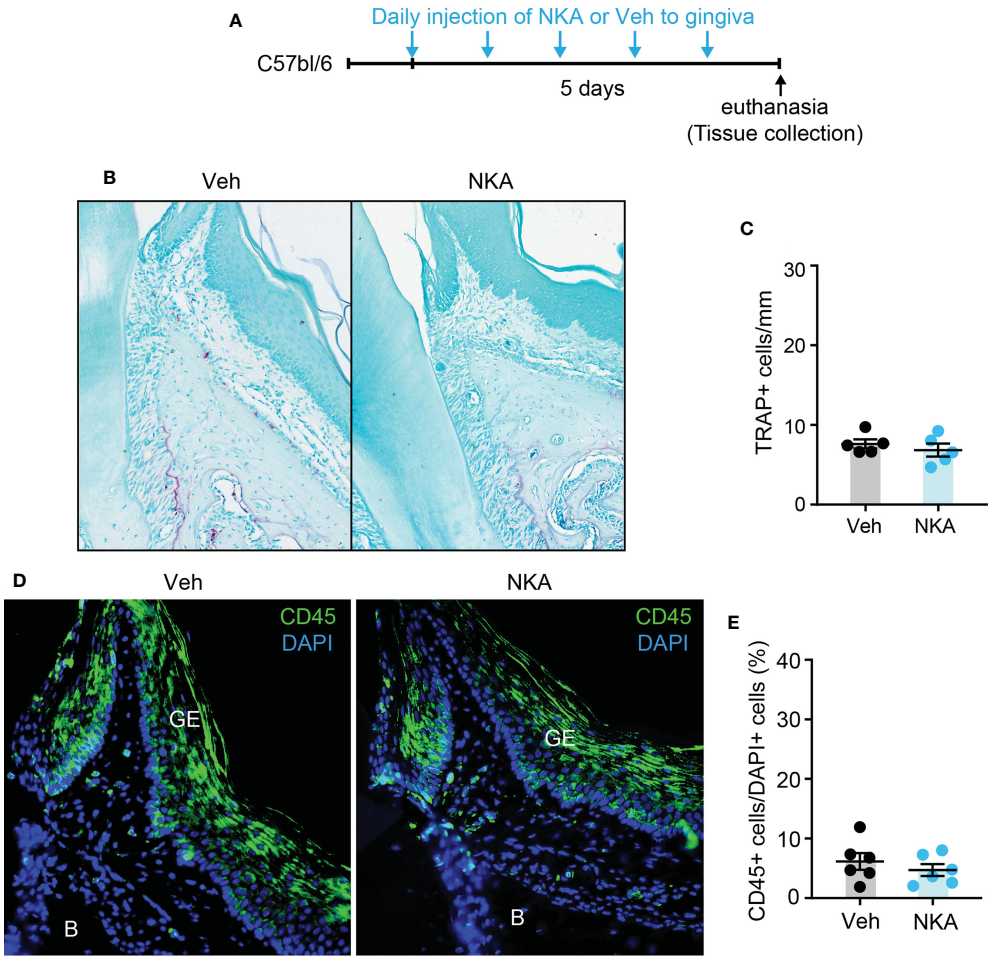

FIGURE 8
Exogenous injection of neurokinin A is not sufficient to activate osteoclasts and to recruit immune cells in periodontium. **(A)** Time course of the experiment. **(B)** TRAP staining in neurokinin A (NKA; 1 µg/site)- or vehicle (Veh) injected into a periodontium. Scale bar, 100 µm. **(C)** Quantification of TRAP+ cells of the injected periodontia. N=6 mice per group. P>0.4 in Student's t-test. N=6 mice per group. **(D)** Immunofluorescence for CD45 in periodontia injected with Veh or NKA. Scale bar, 100µm. B, bone; GE, gingival epithelium. **(E)** Quantification of CD45+ cells. Percentage of the number of CD45+ cells among DAPI+ cells in gingival epithelium and connective tissues within 600 µm distance to tooth surface was calculated. P>0.7 in Student's t-test. N=5 mice per group.

orthodontic tooth movement of the maxillary first molar does not induce such changes (32, 33). Therefore, upregulation of SP and TRPV1 in TG may be context dependent and the extent of tissue inflammation produced by ligature is not as strong as masseter inflammation. The analysis of size distribution showed that SP+ and TRPV1+ gingival afferents were larger than SP+ and TRPV1+ non-gingival (unlabeled) TG neurons, whereas CGRP+ gingival afferents were not different from CGRP+ non-gingival afferents. The size distributions of SP+ and CGRP+ peptidergic afferents were not significantly different. Comparing the size distributions between the control and the ligature group, SP+ or TRPV1+ gingival afferents were modestly shifted toward a larger range in the ligature group. These results suggest that gingival SP+ and TRPV1+, but not CGRP +, afferents are uniquely larger than non-gingival afferents, and the placement of ligature may upregulate SP and TRPV1 in medium-sized neurons. Alternatively, given the finding that the distribution of the entire FG+ neuronal sizes was also shifted in the ligature group, one possibility is that the harmful effects of retrograde labeling dye (e.g (34),) lead to the degeneration of a subset of small-sized TG neurons, which might be aggravated by the ligature-induced inflammation. Further studies using independent approaches (e.g., different chemical or viral tracers) may clarify it. Nonetheless, given the modest extent of changes, we presume that altered expressions of SP or TRPV1 in gingival afferents are not major contributors to the nociceptor regulation of periodontitis.

The *Tac1* gene (also known as *PPT-1* or *PPT-A*) encodes both SP and NKA (29). *Tac1* produces multiple isoforms of mRNA transcripts through alternative splicing, which further produces SP and NKA *via* post-translational modification. SP and NKA are co-synthesized and co-released from sensory neurons and are both implicated in periodontitis (14, 15). Therefore, our data using *Tac1* KO mice suggests that both SP and NKA are involved in the regulation of periodontal bone loss. Untangling the relative roles of *Tac1*-encoded SP and NKA in biological processes is challenging. As SP and NKA preferably bind to the G-protein linked NK1 receptor (NK1-R) and the NK2 receptor (NK2-R) respectively, and

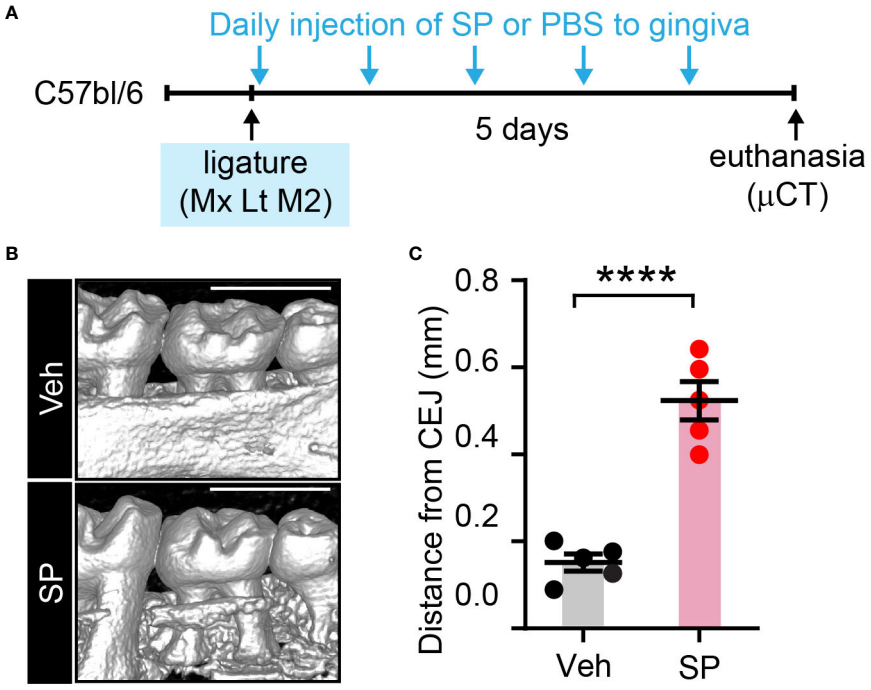

FIGURE 9
Exogenous substance P aggravates ligature-induced periodontitis. **(A)** Time course of the experiment. Under isoflurane anesthesia, SP (1 μg/site) or vehicle (PBS) was injected twice a day into two sites in the gingiva around the maxillary second molar; one site between the first and second molars, and the other site between the second and third molars) for five days after placing the ligature. **(B)** μCT examination of a periodontium five days after ligature placement with Veh or SP injection. Scale bar, 1 mm. **(C)** Quantification of bone height loss. ****p<0.0001 in Student's t-test. N=5 per group. CEJ, cement-enamel junction.

both receptors demonstrate broad expressions in periodontal tissues, specific inhibition of NK1-R and NK2-R may indicate the respective contributions of SP and NKA. Indeed, our data using QWF, an efficacious inhibitor of NK1-R, does suggest the dominant contribution of SP in periodontal bone loss. Furthermore, direct injection of SP, but not NKA, into gingiva was sufficient to produce immune cell recruitments and osteoclastic activation, which supports the dominant role of SP compared to NKA. These data suggest that specific NK1-R antagonists, such as FDA-approved anti-emetic Aprepitant (35), might be considered as a supplemental therapeutic approach to delay the development or progression of periodontitis.

NK1-R is broadly expressed in both immune and bone cells, and SP may, therefore, directly regulate the inflammatory process and bone remodeling under physiological and pathological conditions (36–38). SP enhances both osteogenesis and bone resorption *in vitro* (39–41). SP increases differentiation of osteoblasts and increases osteogenic activity at low concentration (39). Consistently, *Tac1* KO mice show reduced bone volume and trabecular number/thickness in femur (42). At the higher concentrations that are likely detected at the site of injury or inflammation, SP enhances differentiation and resorptive activity of osteoclasts (39, 43, 44). Our results suggest that *Tac1* deficiency does not globally influence alveolar bone without ligature but protects bone loss following ligature placement. Therefore, SP-induced osteoclast accumulation and differentiation may significantly contribute to the bone loss seen in periodontitis. In addition to NK1R, SP also binds to the mast cell surface receptor MRGPRB2 to activate mast cells, which play a significant role in the inflammatory process—including periodontitis (38, 45). Therefore, neural-mast cell interactions could lead to the regulation of the progression of periodontitis. In future studies, an analysis of the relative roles of NK1-R, NK2-R, and MRGPRB2 in periodontitis would be a rational approach to provide mechanistic insight into SP's regulation of periodontal bone loss.

Aside from nociceptors, SP expression has also been reported in many other tissues, including inflammatory cells in periodontitis models (12, 44). However, these results should be interpreted with caution, as many SP antibodies may also detect other members of the tachykinin family (36, 46). A study using RNA *in situ* hybridization has demonstrated that SP is only expressed in a highly restricted number of cells (aside from neurons) during the inflammatory process (46). Therefore, we believe nociceptors remain the primary source of SP release in periodontitis, particularly at an early stage of inflammation.

In the current study, we did not attempt to identify the upstream signal which trigger the release of SP from afferent terminals under periodontitis. TRPA1 and TRPV1 are largely co-expressed in nociceptors and are both involved in various inflammatory processes (5). Tissue inflammation generates putative endogenous agonists of TRPV1 and TRPA1, such as byproducts of oxidative stress (47, 48). Inflammatory mediators such as prostaglandin E2 or bacterial toxins such as *P. gingivalis*-derived lipopolysaccharides can activate or sensitize TRPV1 and TRPA1 (49–51). TRPA1 activation then evokes

10.3389/fimmu.2023.1099017

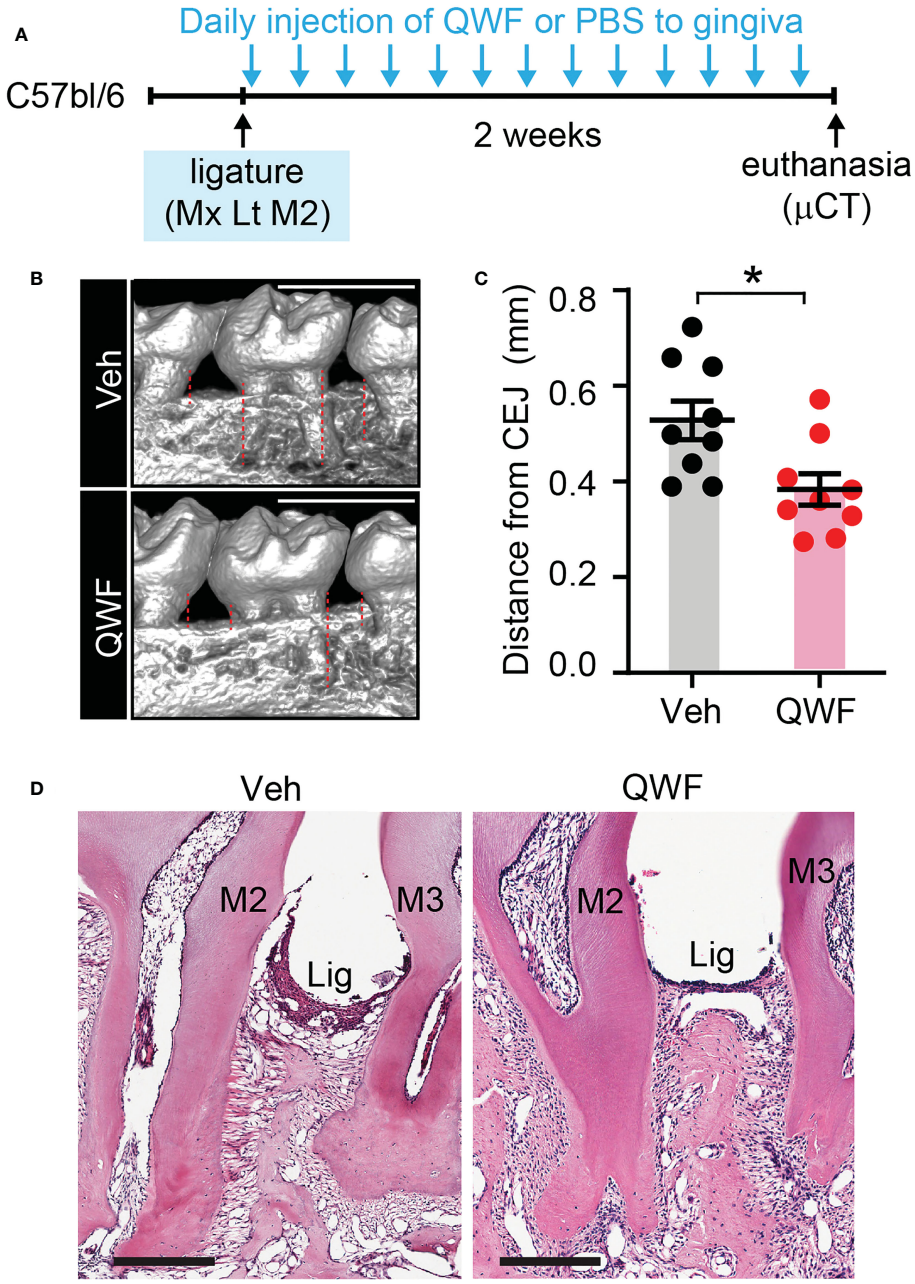

FIGURE 10
Substance P receptor antagonist reduces ligature-induced periodontitis. **(A)** Time course of the experiment. Under isoflurane anesthesia, QWF (2 μg/site) or vehicle (PBS) was injected twice a day into two sites in the gingiva around the maxillary second molar; one site between the first and second molars, and the other site between the second and third molars) for 14 days after placing the ligature. **(B)** μCT examination of a periodontium with vehicle or QWF injection. Scale bar, 1 mm. Dotted lines represent the measurements. **(C)** Quantification of bone loss. *p<0.05 in Student's t-test. **(D)** Representative images of H&E stained sagital sections. N=8 per group.

SP secretion in dorsal root ganglion neurons (52). Therefore, it is possible that periodontitis-induced TRPV1/TRPA1 signaling triggers SP secretion from nociceptors in ligature-induced periodontists. Interestingly, however, TRPV1 KO mice have previously been reported to increase ligature-induced bone loss (7). One possibility is that the global KO of TRPV1 affects the function of osteoclasts, which may express functional TRPV1 (53, 54). Conditional KOs of TRPV1 specific to sensory neurons should reveal the relative contributions of neuronal and osteoclastic TRPV1.

Despite the substantial contributions of the peptidergic nociceptive afferents to periodontitis, it is puzzling that chronic periodontitis is not usually accompanied by pain. The molecular mechanisms of such painless periodontitis are not well understood but might involve a multitude of unique bacteria-host responses in periodontitis (55, 56). For example, mechanical hyperalgesia in gingiva does not occur by inoculating *P. gingivalis*, which is due to the inhibition of macrophages by CXCR4 in gingiva (57). Interestingly, lipopolysaccharides from *P. gingivalis* increase interleukin-10, an anti-inflammatory cytokine, upon

injection into the skin (58). Further studies are warranted to determine the unique interactions of periodontal bacteria and the nociceptive system. Potential site-specific mechanisms of nociceptor regulation of local immunity and their contributions to the progression of alveolar bone pathology are also highly intriguing. While our data support the role of SP+ nociceptive afferents in aggravating marginal periodontitis, Nav1.8-expressing nociceptors, which include a substantial proportion of peptidergic nociceptors, show the opposite regulation of apical periodontitis (59). Besides nociceptive afferents, we do not exclude the potential roles of other neurochemically distinct subpopulations of gingival afferents in the alveolar bone remodeling in periodontitis. For example, glutamate is known to regulate bone homeostasis (60), and gingival afferents expressing glutamate, but not CGRP or SP, can regulate periodontal bone loss. These potential mechanisms of neural regulations of alveolar bone remodeling need to be further explored in the future.

In summary, we suggest that SP from nociceptors is a neuroimmune axis that modulates host responses and periodontitis-induced bone loss. Therefore, manipulating this axis, e.g., by localized inhibition of SP signaling in affected gums, could provide novel therapeutic approaches for treating periodontitis that supplement conventional therapies.

Data availability statement

The original contributions presented in the study are included in the article/supplementary materials. Further inquiries can be directed to the corresponding author.

Ethics statement

The animal study was reviewed and approved by University of Maryland Baltimore Institutional Animal Care and Use Committee.

Author contributions

SW, YS, XN, VT-M, and M-KC conceived the study. SW, XN, VT-M, XF, YA, and M-KC designed the experiments. SW, YS, XN, YA, LP, and XF collected and analyzed the data. SW, XN, YS, VT-M, XF, YA, LP, and M-KC interpreted the results. YS, XN, and M-KC prepared the manuscript, and other authors critically read and commented on the manuscript. M-KC supervised all aspects of the project. All authors contributed to the article and approved the submitted version.

Funding

This work was supported by the National Institutes of Health grants R01 DE027731 and R35 DE030045 to M-KC, R00 DE028439, R03 DE029258, R56 DK131277, start-up funds from the University of Maryland School of Dentistry to VT-M, and National Cancer Institute-Cancer Center Support Grant P30 CA134274 and the Maryland Department of Health's Cigarette Restitution Fund Program to XF.

Acknowledgments

The authors thank Ms. Sinu Kumari for her technical assistance and Dr. Sathish Kumar for help with the analysis of flow cytometry data.

Conflict of interest

The authors declare that the research was conducted in the absence of any commercial or financial relationships that could be construed as a potential conflict of interest.

Publisher's note

References

1. Eke PI, Dye BA, Wei L, Thornton-Evans GO, Genco RJ, Cdc Periodontal Disease Surveillance workgroup GDRP. James Beck, prevalence of periodontitis in adults in the united states: 2009 and 2010. *J Dent Res* (2012) 91:914–20. doi: 10.1177/0022034512457373

2. de Vries TJ, Andreotta S, Loos BG, Nicu EA. Genes critical for developing periodontitis: Lessons from mouse models. *Front Immunol* (2017) 8:1395. doi: 10.3389/fimmu.2017.01395

3. Lamont RJ, Koo H, Hajishengallis G. The oral microbiota: Dynamic communities and host interactions. *Nat Rev Microbiol* (2018) 16:745–59. doi: 10.1038/s41579-018-0089-x

4. Wang S, Nie X, Siddiqui Y, Wang X, Arora V, Fan X, et al. Nociceptor neurons magnify host responses to aggravate periodontitis. *J Dent Res* (2022) 101:812–20. doi: 10.1177/00220345211069956

5. Lundy FT, Linden GJ. Neuropeptides and neurogenic mechanisms in oral and periodontal inflammation. *Crit Rev Oral Biol Med* (2004) 15:82–98. doi: 10.1177/154411130401500203

6. Chung MK, Jung SJ, Oh SB. Role of TRP channels in pain sensation. *Adv Exp Med Biol* (2011) 704:615–36. doi: 10.1007/978-94-007-0265-3_33

7. Takahashi N, Matsuda Y, Sato K, de Jong PR, Bertin S, Tabeta K, et al. Neuronal TRPV1 activation regulates alveolar bone resorption by suppressing osteoclastogenesis via CGRP. *Sci Rep* (2016) 6:29294. doi: 10.1038/srep29294

8. Serhan N, Basso L, Sibilano R, Petitfils C, Meixiong J, Bonnart C, et al. House dust mites activate nociceptor-mast cell clusters to drive type 2 skin inflammation. *Nat Immunol* (2019) 20(11):1435–1443. doi: 10.1038/s41590-019-0493-z

9. Lai NY, Musser MA, Pinho-Ribeiro FA, Baral P, Jacobson A, Jacobson A, Ma P, et al. Gut-innervating nociceptor neurons regulate peyer's patch microfold cells and

SFB levels to mediate salmonella host defense. *Cell* (2020) 180:33–49 e22. doi: 10.1016/j.cell.2019.11.014

10. Pinho-Ribeiro FA, Baddal B, Haarsma R, O'Seaghdha M, Yang NJ, Blake KJ, et al. Blocking neuronal signaling to immune cells treats streptococcal invasive infection. *Cell* (2018) 173:1083–1097 e22. doi: 10.1016/j.cell.2018.04.006

11. Campos MM, Calixto JB. Neurokinin mediation of edema and inflammation. *Neuropeptides* (2000) 34:314–22. doi: 10.1054/npep.2000.0823

12. Suvas S. Role of substance p neuropeptide in inflammation, wound healing, and tissue homeostasis. *J Immunol* (2017) 199:1543–52. doi: 10.4049/jimmunol.1601751

13. Scott AE, Milward M, Linden GJ, Matthews JB, Carlile MJ, Lundy FT, et al. Mapping biological to clinical phenotypes during the development (21 days) and resolution (21 days) of experimental gingivitis. *J Clin Periodontol* (2012) 39:123–31. doi: 10.1111/j.1600-051X.2011.01825.x

14. Linden GJ, McKinnell J, Shaw C, Lundy FT. Substance p and neurokinin a in gingival crevicular fluid in periodontal health and disease. *J Clin Periodontol* (1997) 24:799–803. doi: 10.1111/j.1600-051X.1997.tb01192.x

15. Tuncer LI, Alacam T, Oral B. Substance p expression is elevated in inflamed human periradicular tissue. *J Endod* (2004) 30:329–32. doi: 10.1097/00004770-200405000-00006

16. Hanioka T, Takaya K, Matsumori Y, Matsuse R, Shizukuishi S. Relationship of the substance p to indicators of host response in human gingival crevicular fluid. *J Clin Periodontol* (2000) 27:262–6. doi: 10.1034/j.1600-051x.2000.027004262.x

17. Lundy FT, Mullally BH, Burden DJ, Lamey PJ, Shaw C, Linden GJ. Changes in substance p and neurokinin a in gingival crevicular fluid in response to periodontal treatment. *J Clin Periodontol* (2000) 27:526–30. doi: 10.1034/j.1600-051x.2000.027007526.x

18. Lundy FT, Shaw C, McKinnell J, Lamey PJ, Linden GJ. Calcitonin gene-related peptide in gingival crevicular fluid in periodontal health and disease. *J Clin Periodontol* (1999) 26:212–6. doi: 10.1034/j.1600-051X.1999.260403.x

19. Sert S, Sakallioglu U, Lutfioglu M, Aydogdu A, Acarel E, Gunaydin M. Neurogenic inflammation in periimplant and periodontal disease: A case-control split-mouth study. *Clin Oral Implants Res* (2019) 30:800–7. doi: 10.1111/clr.13486

20. Sakallioglu EE, Lutfioglu M, Sakallioglu U, Diraman E, Pamuk F, Odyakmaz S. Local peptidergic innervation of gingiva in smoking and non-smoking periodontitis patients. *J Periodontol* (2008) 79:1451–6. doi: 10.1902/jop.2008.070667

21. Chung MK, Jue SS, Dong X. Projection of non-peptidergic afferents to mouse tooth pulp. *J Dent Res* (2012) 91:777–82. doi: 10.1177/0022034512450298

22. Chung MK, Lee J, Duraes G, Ro JY. Lipopolysaccharide-induced pulpitis up-regulates TRPV1 in trigeminal ganglia. *J Dent Res* (2011) 90:1103–7. doi: 10.1177/0022034511413284

23. Wang S, Kim M, Ali Z, Ong K, Pae EK, Chung MK. TRPV1 and TRPV1-expressing nociceptors mediate orofacial pain behaviors in a mouse model of orthodontic tooth movement. *Front Physiol* (2019) 10:1207. doi: 10.3389/fphys.2019.01207

24. Caterina MJ, Leffler A, Malmberg AB, Martin WJ, Trafton J, Petersen-Zeitz KR, et al. Impaired nociception and pain sensation in mice lacking the capsaicin receptor. *Science* (2000) 288:306–13. doi: 10.1126/science.288.5464.306

25. Arora S, Wang XI, Keenan SM, Andaya C, Zhang Q, Peng Y, et al. Novel microtubule polymerization inhibitor with potent antiproliferative and antitumor activity. *Cancer Res* (2009) 69:1910–5. doi: 10.1158/0008-5472.CAN-08-0877

26. Ichikawa H, Matsuo S, Terayama R, Yamaai T, Sugimoto T. Aspartate-immunoreactive primary sensory neurons in the mouse trigeminal ganglion. *Brain Res* (2006) 1082:67–72. doi: 10.1016/j.brainres.2006.01.092

27. Dutzan N, Abusleme L, Konkel JE, Moutsopoulos NM. Isolation, characterization and functional examination of the gingival immune cell network. *J Vis Exp* (2016) (108):53736. doi: 10.3791/53736

28. Zimmer A, Zimmer AM, Baffi J, Usdin T, Reynolds K, Konig M, et al. Hypoalgesia in mice with a targeted deletion of the tachykinin 1 gene. *Proc Natl Acad Sci U.S.A.* (1998) 95:2630–5. doi: 10.1073/pnas.95.5.2630

29. Steinhoff MS, von Mentzer B, Geppetti C, Pothoulakis, Bunnett NW. Tachykinins and their receptors: Contributions to physiological control and the mechanisms of disease. *Physiol Rev* (2014) 94:265–301. doi: 10.1152/physrev.00031.2013

30. Nie X, Chung MK. Piezo channels for skeletal development and homeostasis: Insights from mouse genetic models. *Differentiation* (2022) 126:10–5. doi: 10.1016/j.diff.2022.06.001

31. Tomlinson RE, Christiansen BA, Giannone AA, Genetos DC. The role of nerves in skeletal development, adaptation, and aging. *Front Endocrinol (Lausanne)* (2020) 11:646. doi: 10.3389/fendo.2020.00646

32. Wang S, Chung MK. Orthodontic force induces nerve injury-like transcriptomic changes driven by TRPV1-expressing afferents in mouse trigeminal ganglia. *Mol Pain* (2020) 16:1744806920973141. doi: 10.1177/1744806920973141

33. Chung MK, Park J, Asgar J, Ro JY. Transcriptome analysis of trigeminal ganglia following masseter muscle inflammation in rats. *Mol Pain* (2016) 12. doi: 10.1177/1744806916668526

34. Mi D, Yuan Y, Zhang Y, Niu J, Wang Y, Yan J, et al. Injection of fluoro-gold into the tibial nerve leads to prolonged but reversible functional deficits in rats. *Sci Rep* (2019) 9:9906. doi: 10.1038/s41598-019-46285-7

35. Quartara L, Altamura M, Evangelista S, Maggi CA. Tachykinin receptor antagonists in clinical trials. *Expert Opin Investig Drugs* (2009) 18:1843–64. doi: 10.1517/13543780903379530

36. Niedermair T, Schirner S, Seebroker R, Straub RH, Grassel S. Substance p modulates bone remodeling properties of murine osteoblasts and osteoclasts. *Sci Rep* (2018) 8:9199. doi: 10.1038/s41598-018-27432-y

37. Mishra A, Lal G. Neurokinin receptors and their implications in various autoimmune diseases. *Curr Res Immunol* (2021) 2:66–78. doi: 10.1016/j.crimmu.2021.06.001

38. Green DP, Limjunyawong N, Gour N, Pundir, Dong X. A mast-Cell-Specific receptor mediates neurogenic inflammation and pain. *Neuron* (2019) 101:412–420 e3. doi: 10.1016/j.neuron.2019.01.012

39. Wang L, Zhao R, Shi X, Wei T, Halloran BP, Clark DJ, et al. Substance p stimulates bone marrow stromal cell osteogenic activity, osteoclast differentiation, and resorption activity *in vitro*. *Bone* (2009) 45:309–20. doi: 10.1016/j.bone.2009.04.203

40. Shih C, Bernard GW. Neurogenic substance p stimulates osteogenesis *in vitro*. *Peptides* (1997) 18:323–6. doi: 10.1016/S0196-9781(96)00280-X

41. Sohn SJ. Substance p upregulates osteoclastogenesis by activating nuclear factor kappa b in osteoclast precursors. *Acta Otolaryngol* (2005) 125:130–3. doi: 10.1080/00016480410017710

42. Niedermair T, Kuhn V, Doranehgard F, Stange R, Wieskotter B, Beckmann J, et al. Absence of substance p and the sympathetic nervous system impact on bone structure and chondrocyte differentiation in an adult model of endochondral ossification. *Matrix Biol* (2014) 38:22–35. doi: 10.1016/j.matbio.2014.06.007

43. Liu HJ, Yan H, Yan J, Li H, Chen L, Han LR, et al. Substance p promotes the proliferation, but inhibits differentiation and mineralization of osteoblasts from rats with spinal cord injury via RANKL/OPG system. *PloS One* (2016) 11:e0165063. doi: 10.1371/journal.pone.0165063

44. Yan K, Lin Q, Tang K, Liu S, Du Y, Yu X, et al. Substance p participates in periodontitis by upregulating HIF-1alpha and RANKL/OPG ratio. *BMC Oral Health* (2020) 20:27. doi: 10.1186/s12903-020-1017-9

45. Walsh LJ. Mast cells and oral inflammation. *Crit Rev Oral Biol Med* (2003) 14:188–98. doi: 10.1177/154411130301400304

46. Song Y, Stal PS, Yu JG, Forsgren S. Bilateral increase in expression and concentration of tachykinin in a unilateral rabbit muscle overuse model that leads to myositis. *BMC Musculoskelet Disord* (2013) 14:134. doi: 10.1186/1471-2474-14-134

47. Nassini R, Materazzi S, Benemei S, Geppetti. The TRPA1 channel in inflammatory and neuropathic pain and migraine. *Rev Physiol Biochem Pharmacol* (2014) 167:1–43. doi: 10.1007/112_2014_18

48. Hargreaves KM, Ruparel S. Role of oxidized lipids and TRP channels in orofacial pain and inflammation. *J Dent Res* (2016) 95:1117–23. doi: 10.1177/0022034516653751

49. Dall'Acqua MC, Bonet IJ, Zampronio AR, Tambeli CH, Parada CA, Fischer L. The contribution of transient receptor potential ankyrin 1 (TRPA1) to the *in vivo* nociceptive effects of prostaglandin E(2). *Life Sci* (2014) 105:7–13. doi: 10.1016/j.lfs.2014.02.031

50. Kaewpitak A, Bauer CS, Seward EP, Boissonade FM, Douglas CWI. Porphyromonas gingivalis lipopolysaccharide rapidly activates trigeminal sensory neurons and may contribute to pulpal pain. *Int Endod J* (2020) 53:846–58. doi: 10.1111/iej.13282

51. Ferraz CC, Henry MA, Hargreaves KM, Diogenes A. Lipopolysaccharide from porphyromonas gingivalis sensitizes capsaicin-sensitive nociceptors. *J Endod* (2011) 37:45–8. doi: 10.1016/j.joen.2007.07.001

52. Nakamura Y, Une Y, Miyano K, Abe H, Hisaoka K, Morioka N, et al. Activation of transient receptor potential ankyrin 1 evokes nociception through substance p release from primary sensory neurons. *J Neurochem* (2012) 120:1036–47. doi: 10.1111/j.1471-4159.2011.07628.x

53. Rossi F, Bellini G, Torella M, Tortora C, Manzo I, Giordano C, et al. The genetic ablation or pharmacological inhibition of TRPV1 signalling is beneficial for the restoration of quiescent osteoclast activity in ovariectomized mice. *Br J Pharmacol* (2014) 171:2621–30. doi: 10.1111/bph.12542

54. He LH, Liu M, He Y, Xiao E, Zhao L, Zhang T, et al. TRPV1 deletion impaired fracture healing and inhibited osteoclast and osteoblast differentiation. *Sci Rep* (2017) 7:42385. doi: 10.1038/srep42385

55. Gaurilcikaite E, Renton T, Grant AD. The paradox of painless periodontal disease. *Oral Dis* (2017) 23:451–63. doi: 10.1111/odi.12537

56. Chung MK, Wang S, Oh SL, Kim YS. Acute and chronic pain from facial skin and oral mucosa: Unique neurobiology and challenging treatment. *Int J Mol Sci* (2021) 22. doi: 10.3390/ijms22115810

57. Nagashima H, Shinoda M, Honda K, Kamio N, Watanabe M, Suzuki T, et al. CXCR4 signaling in macrophages contributes to periodontal mechanical hypersensitivity in porphyromonas gingivalis-induced periodontitis in mice. *Mol Pain* (2017) 13:1744806916689269. doi: 10.1177/1744806916689269

58. Khan J, Puchimada B, Kadouri D, Zusman T, Javed F, Eliav E. The anti-nociceptive effects of porphyromonas gingivalis lipopolysaccharide. *Arch Oral Biol* (2019) 102:193–8. doi: 10.1016/j.archoralbio.2019.04.012

59. Austah ON, Lillis KV, Akopian AN, Harris SE, Grinceviciute R, Diogenes A. Trigeminal neurons control immune-bone cell interaction and metabolism in apical periodontitis. *Cell Mol Life Sci* (2022) 79:330. doi: 10.1007/s00018-022-04335-w

60. Skerry TM. The role of glutamate in the regulation of bone mass and architecture. *J Musculoskelet Neuronal Interact* (2008) 8:166–73.

Frontiers in Immunology

Explores novel approaches and diagnoses to treat immune disorders.

The official journal of the International Union of Immunological Societies (IUIS) and the most cited in its field, leading the way for research across basic, translational and clinical immunology.

Discover the latest Research Topics

See more →

Frontiers

Avenue du Tribunal-Fédéral 34
1005 Lausanne, Switzerland
frontiersin.org

Contact us

+41 (0)21 510 17 00
frontiersin.org/about/contact